C21ORF91 as a Modulator of Oligodendroglial Lineage Fate and the Therapeutic Potential of Drug Repurposing for White Matter Restoration in Down Syndrome

Inaugural dissertation

to attain the academic degree
“ Doctor of Philosophy (PhD) “
in the Faculty of Mathematics and Natural Sciences
at the Heinrich Heine University Düsseldorf

presented by

Laura Reiche
from Erfurt, Germany

Düsseldorf, May 2025

from the Laboratory for Neuroregeneration,
Department of Neurology, Medical Faculty at the Heinrich Heine University Düsseldorf

Published by permission of the
Faculty of Mathematics and Natural Sciences at
Heinrich Heine University Düsseldorf

Reviewer 1:
Prof. Dr. Patrick Küry

Reviewer 2:
Prof. Dr. Christine R. Rose

Date of thesis defence: 25.09.2025

To My Family

and Friends Who Became Family

„Es liegt allein an uns,
ob wir aus den vielen Steinen,
die wir einander in den Weg legen,
Mauern oder Brücken bauen.“
- *E. Ferstl*

Abstract

Deciphering disease-specific functions of glial cells has become increasingly important in neuropathology. In particular, defective oligodendroglial differentiation and its impact on white matter abnormalities have been linked to cognitive impairments in various neurological disorders. Whereas myelin repair strategies have shown promise in demyelinating diseases such as multiple sclerosis (MS) and ischemic stroke, research addressing white matter abnormalities in Down syndrome (DS), the most common genetic cause of cognitive impairment and intellectual disability, has been limited. Despite an imbalanced cellular composition and hypomyelination found in DS brains, the molecular drivers behind these myelination deficits remain poorly understood. This dissertation aims to elucidate the role of *C21ORF91*, a chromosome 21-encoded gene, in oligodendrogenesis and to investigate pharmacological strategies to rescue aberrant oligodendroglial differentiation induced by C21orf91 orthologue overexpression, thus highlighting the potential of myelin restoration in DS.

In this thesis, the evaluation of primary rat cell cultures has shown that overexpression of C21orf91 indeed leads to profound disturbances of the oligodendroglial lineage progression. Its overexpression induced the formation of hybrid cells co-expressing astro- and oligodendroglial markers, accompanied by an induction of inflammatory properties characterised by elevated tumour necrosis factor (Tnf) α and lipocalin (Lcn) 2 secretion. Interestingly, this thesis provides the first description of similar abnormal glial phenotypes in human postmortem DS brains. By pharmacological screening in suitable *ex vivo* and *in vivo* models conducted in this thesis, new small molecules for myelin repair were identified. Among the identified molecules, danazol, parbendazole, and medrysone restored oligodendroglial differentiation and rescued the ability of C21orf91-overexpressed oligodendroglial precursor cells (OPCs) to mature to myelinating oligodendrocytes.

Data from this thesis suggest that targeting stabilisation of oligodendroglial lineage progression and reducing neurotoxic astrocytic features may be beneficial not only for classical demyelinating disorders but also for DS. Given the current lack of effective treatments for cognitive impairments in DS, our findings pave the way for future therapeutic interventions to enhance brain development and function in affected individuals. The repurposing of already existing drugs, potentially already investigated in demyelinating disease models, offers an attractive and timely strategy to address this unmet medical need.

Zusammenfassung

Die Verständnis krankheitsspezifischer Funktionen von Gliazellen hat in der Neuropathologie zunehmend an Bedeutung gewonnen. Insbesondere eine gestörte oligodendrogliale Differenzierung und deren Einfluss auf Anomalien der weißen Substanz werden mit kognitiven Beeinträchtigungen bei verschiedenen neurologischen Erkrankungen in Verbindung gebracht. Während Strategien zur Myelinreparatur in demyelinisierenden Erkrankungen wie Multiplen Sklerose (MS) und ischämischen Schlaganfall vielversprechend sind, ist die Forschung zu Anomalien der weißen Substanz bei Down-Syndrom (DS), der häufigsten genetischen Ursache für kognitive Beeinträchtigungen und geistige Behinderungen, bisher begrenzt. Trotz eines unausgeglichenen zellulären Zellverhältnisses und Hypomyelinisierung im DS-Gehirn sind die molekularen Ursachen der Myelinierungsdefizite weitgehend ungeklärt. Ziel dieser Dissertation ist es, die Rolle von C21ORF91, einem auf Chromosom 21 codierten Gen, in der Oligodendrogenese zu untersuchen und pharmakologische Strategien zur Rettung der durch Überexpression des C21orf91-Orthologs gestörten oligodendroglialen Differenzierung zu entwickeln, um so das Potenzial der Myelinrestauration bei DS aufzuzeigen.

Die Untersuchung primärer Rattenzellkulturen in dieser Thesis zeigte, dass die Überexpression von C21orf91 zu erheblichen Störungen der oligodendroglialen Entwicklung der Zelllinie führt. Seine Überexpression induzierte die Bildung von Hybridzellen, die sowohl astro- als auch oligodendrogliale Marker exprimieren, begleitet von einer Induktion inflammatorischer Eigenschaften wie erhöhte Tnfα- und Lcn2-Sekretion. Erstmals konnten ähnliche abnorme Glia-Phänotypen auch in postmortalen menschlichen DS-Gehirnen im Rahmen dieser Studie nachgewiesen werden. Durch pharmakologisches Screening in geeigneten *ex vivo* und *in vivo* Modellen wurden neue kleine Moleküle für die Myelinreparatur identifiziert. Von diesen konnten Danazol, Parbendazol und Medrysone die oligodendrogliale Differenzierung und ihre Funktion zu Myelinisieren in C21orf91-überexprimierten Vorläuferzellen (OVZ) wiederherstellen.

Die Ergebnisse dieser Arbeit deuten darauf hin, dass die Stabilisierung der oligodendroglialen Linienprogression und die Reduktion neurotoxischer astrozytärer Eigenschaften nicht nur für klassische Demyelinisierungserkrankungen, sondern auch für DS therapeutisches Potenzial bieten könnten. Angesichts des derzeitigen Mangels an wirksamen Therapien für kognitive Beeinträchtigungen bei DS ebnen diese Befunde den Weg für zukünftige Behandlungsansätze, um die Gehirnentwicklung und -funktion bei Betroffenen zu fördern. Die Nutzung bereits existierender Medikamente, die möglicherweise bereits in Modellen für demyelinisierende Krankheiten untersucht wurden, stellt dabei eine vielversprechende und zeitnahe Strategie dar, um diesen bislang ungedeckten medizinischen Bedarf zu adressieren.

Table of Contents

Abstract ..... **I**

Zusammenfassung ..... **III**

Table of Contents ..... **V**

List of Figures ..... **VII**

List of Abbreviations ..... **IX**

1 Introduction **1**

1.1 Central Nervous System Myelin and Its Creators 2

1.1.1 Oligodendroglial Lineage Cells – the Key Players in Myelin Formation 3

1.1.1.1 Oligodendrogenesis – Principles of Lineage Progression 4

1.1.1.2 Regulatory Mechanisms at a Glance 5

1.1.1.3 Oligodendroglial Precursor Cells – Designated Fate and Function? 6

1.1.2 Adult Neural Stem Cells and Their Contribution to Oligodendrogenesis 7

1.1.3 Schwann Cells – Unexpected Roles in Central Nervous System Repair 8

1.1.4 Astrocytes – Friend or Foe? 9

1.2 White Matter in Pathologies 9

1.2.1 Multiple Sclerosis – a Primary Demyelinating Disorder 10

1.2.2 Ischemic Stroke – Secondary White Matter Damage 11

1.2.3 Down Syndrome – Genetically Driven White Matter Malformation 12

1.3 C21ORF91 – A Novel Candidate Regulator of Neurodevelopment and Myelination? 13

1.4 Aims of the Thesis 14

2 Results – Publications at a Glance **17**

2.1 Aberrant Oligodendrogenesis in Down Syndrome: Shift in Gliogenesis? 18

2.2 C21orf91 Regulates Oligodendroglial Precursor Cell Fate – a Switch in the Glial Lineage? 37

2.3 Identification of Novel Myelin Repair Drugs by Modulation of Oligodendroglial Differentiation 55

2.4 Myelin Repair Is Fostered by the Corticosteroid Medrysone Specifically Acting on Astroglial Subpopulations 69

2.5 Teriflunomide as a Therapeutic Means for Myelin Repair 86

2.6 A Novel Ex Vivo Model to Study Therapeutic Treatments for Myelin Repair following Ischemic Damage 102

2.7 Star Power: Harnessing the Reactive Astrocyte Response to Promote Remyelination in Multiple Sclerosis 124

2.8 C21ORF91 Overexpression Leads to Glial Differentiation Misbalance in Down Syndrome to Be Rescued by Remyelination Drugs 129

3 Discussion 167

3.1 Oligodendroglial Cell Imbalance in DS and the Role of C21ORF91 168

3.2 The Role of C21orf91 in Shaping the Nervous System 173

3.3 Myelin Restoration – New Therapeutic Perspectives for Down Syndrome ... 177

3.4 Conclusion 181

3.5 Future Perspectives 181

4 Appendix 183

4.1 Additional Information and Figures 183

4.1.1 C21orf91 Modulation in Rat aNSCs 183

4.1.1.1 Experimental Procedure 183

4.1.1.2 Results 184

4.1.2 Changes in Transcript Levels in OPCs and aNSCs upon C21orf91 Modulation 186

4.1.2.1 Results 186

4.1.3 C21orf91 Modulation in Rat Schwann Cells 187

4.1.3.1 Experimental Procedure 187

4.1.3.2 Results 187

4.2 List of Author Contributions for this Thesis 190

4.3 List of Other Author Contributions 194

4.4 List of Co-Supervised Master Projects that Contributed to this Thesis 195

5 References 197

6 Danksagung XI

7 Eidesstattliche Erklärung XIII

List of Figures

Figure 1. Bibliometric analysis reveals trends in neuroscience over the past 40 years. ...1
Figure 2. Schematic illustration of a coronal frontal lobe section of a neonatal human brain depicting the cytoarchitectural alterations in DS (red) compared to euploid, typical development (blue). 170
Figure 3. C21orf91 modulation inhibits pro-oligodendroglial cues of mesenchymal stem cell-conditioned medium in rat SVZ-aNSCs *in vitro* and *ex vivo*. 185
Figure 4. Modulations of C21orf91 expression levels result in an overall dysregulated pattern for various important regulatory transcript levels in rat oligodendroglial precursor cells. 186
Figure 5. An overview of C21orf91's roles in rat Schwann cell mitosis, morphological presentation and transcript dynamics. 189

List of Abbreviations

AD	Alzheimer's disease
AKT	protein kinase B
ATP	adenosine triphosphate
BBB	blood-brain barrier
BCCIP	BRCA2 and CDKN1A interacting protein
BDNF	brain-derived neurotrophic factor
BF	brightfield
BMP	bone morphogenetic protein
CC	corpus callosum
CMT	Charcot-Marie-Tooth disease
CNP	2',3'-cyclic nucleotide 3'-phosphodiesterase
CNS	central nervous system
CNTF	ciliary neurotrophic factor
Ctnnb1	catenin beta 1
DS	Down syndrome
DSAD	DS with AD
DSCR	DS critical region
EAE	experimental autoimmune encephalomyelitis
EBV	Epstein–Barr virus
ECM	extracellular matrix
ERK	extracellular signal-regulated kinase
EURL	early undifferentiated retina and lens
FACS	fluorescence-activated cell sorting
FGF	fibroblast growth factor
GFAP	glial fibrillary acidic protein
Glast	glutamate aspartate transporter
GPR	G protein coupled receptor
HES	hairy and enhancer of split
HHV	human herpesvirus
ID	inhibitors of DNA binding
IGF	insulin growth factor
IL	interleukin
iNos	inducible NO synthetase
Lcn	lipocalin
Lrp	lipoprotein receptor related protein
MAG	myelin-associated glycoprotein
MAPK	mitogen-activated protein kinase
MBP	myelin basic protein
MOG	myelin oligodendrocyte glycoprotein
MS	multiple sclerosis
MSC-CM	mesenchymal stem cell-conditioned medium
mTor	mammalian target of rapamycin
NCAM	neural cell adhesion molecule
NG2	neuron-glia antigen 2
NKX	NK2 homeobox
NOM	non-organised Mbp-expressing
OCT	octamer-binding transcription factor
OLIG	oligodendrocyte transcription factor
OPC	oligodendrocyte precursor cells
PDGF	platelet-derived growth factor
PLP	proteolipid protein
PMP	peripheral myelin protein
PNS	peripheral nervous system
SGZ	subgranular zone
SHH	sonic hedgehog
SNX	sorting nexin
SOX	SRY-related HMG-box
SVZ	subventricular zone
Tcf	transcription factor
TNF	tumour necrosis factor
Wnt	wingless and integration site

1 Introduction

The human brain is one of the most complex and efficient biological systems. It regulates cognitive, emotional, and sensorimotor functions, facilitating a highly dynamic exchange of information. Although the first anatomical descriptions of the human brain date back to the 17th century, neuroscience remains a relatively young field that emerged as a distinct discipline in the 20th century. Traditionally, neuroscience has focused mainly on neurons, the fundamental units for transmitting electrical and chemical signals in the nervous system, while regarding glial cells solely as passive support. However, given that neurons constitute only approximately half of the cellular population in the human brain, a comprehensive understanding of neurodevelopment and dysfunction cannot neglect the critical role of neuroglia (astrocytes, oligodendrocytes, microglia, and ependymal cells). Indeed, in recent years, glial cells have gained increasing recognition and are now acknowledged as active regulators of neuronal health, signalling, and plasticity. Oligodendrocytes, the myelin-producing neuroglia of the central nervous system (CNS), are, however, still underrepresented in research, although they play a pivotal role in higher brain functions in humans. This underrepresentation is reflected by the rising but not evenly-matched number of published papers annually on oligodendrocytes in neurodegeneration or cognitive impairment compared to neurons or astrocytes (see Fig. 1A,B). Still, the growing appreciation for the role of glial cells – particularly in shaping brain development and functional connectivity – is also transforming our understanding of various neurological diseases and the diminished regenerative capacity of the CNS.

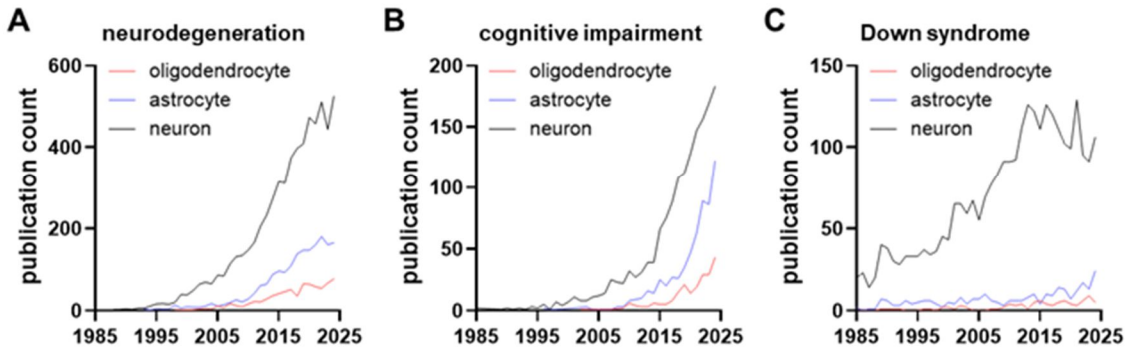

Figure 1. Bibliometric analysis reveals trends in neuroscience over the past 40 years. A literature search on PubMed (NCBI) was conducted using the keywords neurodegeneration (A), cognitive impairment (B), or Down syndrome (C) in combination with either oligodendrocytes (red), astrocytes (blue), or neurons (black) to demonstrate the annual publication count trends.

Neurodegenerative or ischemic conditions that lead to cognitive impairments were once considered mainly caused by neuronal dysfunction or damage, the old “neuroncentric” dogma. They are now increasingly recognised as involving glial dysfunction, glial–neuronal imbalance, and impaired (re-)myelination processes, leading to new approaches to

recovering a diseased or injured CNS. However, research on the most common genetic cause of cognitive impairment, Down syndrome (DS), still focuses almost exclusively on disrupted neurogenesis and neuronal dysfunction (see Fig. 1C).

Therefore, this thesis elucidates the relevance of oligodendrocytes and the impact of their aberrant development on the neuropathology of DS in light of a new therapeutic window to ameliorate cognitive impairments, including the identification and characterisation of a new modulatory driver for myelination and glial specification, C21ORF91.

1.1 Central Nervous System Myelin and Its Creators

Myelin is a multilamellar, lipid-rich membrane that ensheathes axons. It is organised in segments of alternating compact and non-compact concentric layers, also called internodes. This architecture allows the insulation of axons, enabling efficient saltatory nerve conduction along the nodes of Ranvier, small unmyelinated gaps between internodes (reviewed by Stadelmann et al., 2019).

Compared to other biological membranes, myelin exhibits a uniquely high lipid content (70–80%), primarily composed of saturated, long-chain fatty acids, and enriched in cholesterol and glycosphingolipids (Coetzee et al., 1996; O'Brien, 1965; Simons et al., 2024). This results in the characteristic and eponymous appearance of bundled myelinated nerve fibres: white matter tracts. Besides lipids, several proteins contribute to myelin architecture and function and therefore serve as suitable oligodendroglial maturation markers. These myelin-associated proteins, namely proteolipid protein (PLP), myelin basic protein (MBP), 2',3'-cyclic nucleotide 3'-phosphodiesterase (CNP), myelin-associated glycoprotein (MAG), and myelin oligodendrocyte glycoprotein (MOG), are involved in membrane compaction (Barradas et al., 2001; Boison et al., 1995; Roach et al., 1985), axo-glial adhesion, and signal transduction (Li et al., 1994; Trapp et al., 1989).

Myelination can be conceptually divided into an intrinsic, genetically predefined phase occurring until early childhood and an adaptive phase shaped by individual experience and activity within neural networks (Bechler et al., 2017; Stadelmann et al., 2019). The early postnatal brain is predominantly non-myelinated (Yeung et al., 2014), with a myelination peak in the first and second decades of life (Benes, 1994). As a dynamic and lifelong process, it extends into late adulthood up to age 50, although it gradually declines with age (Benes, 1994; Lebel et al., 2012; Miller et al., 2012). Myelinogenesis follows a complex spatiotemporal pattern, and myelin sheath properties exhibit context-dependent variations (for review see e.g. Purger et al., 2016; Simons et al., 2024).

A key conceptual shift in recent decades has been the realisation that myelination is not only responsible for (passive) signal insulation to accelerate transmission in the vertebrate nervous system, but due to its plasticity, is a prerequisite for higher brain functions,

including cognition, learning, and intelligence (Fields, 2008; Hill et al., 2019; Miller, 1994; Mount & Monje, 2017). It is now well-recognised that oligodendrocytes and their myelin additionally provide metabolic and trophic support, maintain axonal integrity, regulate the ionic environment, and modulate neuronal activity and plasticity – all of which are important functions for maintaining CNS homeostasis (Funfschilling et al., 2012; Monk et al., 2020; Saab & Nave, 2017; Simons et al., 2024; Stadelmann et al., 2019). This structural and functional variability reflects the underlying heterogeneity of oligodendroglial cells (Seeker and Williams 2021). The capacity for adaptive myelination and lifelong remodelling (Simons et al., 2024; Stadelmann et al., 2019) emphasises the importance of precise molecular regulation and coordinated cellular interactions via extrinsic and intrinsic cues in maintaining white matter integrity. Although neuronal signals (Pease-Raissi & Chan, 2021; Zhou & Zhang, 2023), as well as microglial-mediated mechanisms (Kent & Miron, 2023; Santos & Fields, 2021), play essential roles in (re-) myelination, this thesis will focus on the astroglial contribution and, in particular, the oligodendroglial lineage as such.

Disruption of myelin integrity – via inflammation, genetic mutations, ischemia, or other neurological disturbances – can result in significant deficits in neuronal connectivity and plasticity, even terminal neuron degradation, thereby contributing to cognitive impairments (Chen et al., 2021b; Wang et al., 2020) and diminished quality of life. A comprehensive understanding of the myelination process, particularly its cellular origin and potential regulatory developmental drivers, is therefore critical to identify therapeutic windows and approaches to stabilise and promote its accurate function or repair – a so far unmet medical need. The following chapter will, therefore, briefly emphasise the cellular sources and regulatory principles shaping the white matter landscape.

1.1.1 Oligodendroglial Lineage Cells – the Key Players in Myelin Formation

Oligodendrocytes are the mature, terminally differentiated cells along the oligodendroglial lineage and account for 45-75% of all neuroglial cells in the human brain, thereby outnumbering astrocytes (von Bartheld et al., 2016). They originate from a tightly regulated lineage progression that comprises proliferation, migration, and differentiation, ultimately leading to axonal myelination (Emery & Wood, 2024; Ma et al., 2024). A single oligodendrocyte can form between 20 to 60 segments of variable internodal lengths and thickness (Simons et al., 2024), depending on its regional origin and axon diameter (Bechler et al., 2015). The number of oligodendrocytes continuously expands until adulthood (Hill et al., 2018), and newly developed cells can successfully integrate into existing neural circuits, contributing to adaptive myelination (Franklin et al., 2021; Hughes et al., 2018; McKenzie et al., 2014; Sampaio-Baptista & Johansen-Berg, 2017; Yeung et al., 2014).

Traditionally considered a homogenous cell population due to their shared role in myelin formation, oligodendroglia are now recognised as morphologically and functionally highly diverse (Seeker & Williams, 2021). This heterogeneity is shaped by multiple factors, including their developmental origin, stage of maturation, anatomical and regional distribution, sex, age, and transcriptomic profile (Crawford et al., 2016; Jäkel et al., 2019; Leong et al., 2014; Long et al., 2021; Marques et al., 2016; Pérez-Cerdá et al., 2015; Rowitch & Kriegstein, 2010; Spitzer et al., 2019; Viganò et al., 2013). Notably, disease-related alterations can further exacerbate this diversity and affect function (Breton et al., 2021; Jäkel et al., 2019).

The CNS possesses a limited and insufficient yet clinically relevant potential to regenerate damaged myelin (reviewed by Franklin et al., 2024). The main source of newly formed, remyelinating oligodendrocytes is generated by oligodendrocyte precursor cells (OPCs) (Tripathi et al., 2010; Zawadzka et al., 2010). Emerging evidence also suggests that mature oligodendrocytes that survived demyelinating events may retain a limited ability to re-engage the myelination program, participating in remyelination by producing new myelin sheaths (Duncan et al., 2018; Kirby et al., 2019; Yeung et al., 2019). Nonetheless, their myelination capacity is considered markedly lower compared to the capacity of newly generated oligodendrocytes (Bacmeister et al., 2022; Mezydlo et al., 2023; Neely et al., 2022).

Therefore, oligodendrogenesis – the transition from progenitors to mature, myelinating oligodendrocytes, particularly deriving from OPCs – represents a critical regulatory process pivotal for myelination and CNS repair.

1.1.1.1 Oligodendrogenesis – Principles of Lineage Progression

OPCs are generated in multiple partially overlapping, spatiotemporal waves following a ventral-dorsal progression, initially originating from radial glial cells of the ventricular germinal zones in the embryonic brain (Bergles & Richardson, 2016; Emery & Wood, 2024). Once specified, OPCs migrate throughout the developing CNS using the vasculature as a scaffold (Tsai et al., 2016) and proliferate, evenly populating the CNS (Nishiyama et al., 2002) in a tiled distribution (Hill et al., 2024) that is balanced via local proliferation, programmed cell death, and differentiation (Raff et al., 1993; Trapp et al., 1997). Initiated during specification, OPCs express the transcription factor oligodendrocyte transcription factor (OLIG) 2 (Lu et al., 2002), which, downstream, when committed to oligodendroglial differentiation, results in the induction of SRY-related HMG-box (SOX) family member 10 (Küspert et al., 2011) among other important oligodendroglia-associated proteins. Both transcription factors serve as pan markers throughout lineage progression. During CNS development, dorsally derived OPCs progressively replace the earlier-generated, ventrally originated populations. Remarkably, despite this replacement, the

different OPC cohorts exhibit a high degree of functional redundancy. Elimination of one population results in the compensation of the remaining OPCs, ensuring the brain is populated with a physiological homeostatic density of OPCs and mature oligodendrocytes (Kessaris et al., 2005).

After cell cycle exit, OPCs differentiate into oligodendrocytes and initiate myelination, which is marked by a distinct expression pattern of markers and morphological changes (reviewed by e.g. Emery & Wood, 2024; Redwine & Evans, 2002; Snaidero & Simons, 2017). Briefly, bipolar shaped OPCs express markers such as platelet-derived growth factor (PDGFRα) and neuron-glia antigen 2 (NG2), which distinguish them from other progenitor populations (Nishiyama et al., 1996). As they transition into the pre-myelinating and myelinating stages, these markers are gradually downregulated in favour of markers such as the myelin-associated proteins CNPase, MBP, and MOG. This molecular progression is accompanied by extensive morphological changes, including process extension, enhancing complexity in branching, and axonal contact formation, which precede the wrapping of myelin membranes (Baumann & Pham-Dinh, 2001). Significant rearrangement of the actin cytoskeleton (Brown & Macklin, 2019) and microtubules (Weigel et al., 2020) is pivotal for these morphological changes and proper oligodendroglial function.

1.1.1.2 Regulatory Mechanisms at a Glance

The highly complex, spatiotemporal, and multistep-regulated progression of oligodendroglial lineage cells from progenitor specification, migration, proliferation, to terminal differentiation is tightly orchestrated by a multitude of signal cues that have been extensively reviewed in recent years (Bergles & Richardson, 2016; Domingues et al., 2016; El Waly et al., 2014; Elbaz & Popko, 2019; Emery & Wood, 2024; Hughes & Stockton, 2021; Ma et al., 2024; Zhu et al., 2024). Due to the diversity and specificity of these regulatory mechanisms and involved cell types, they are often further categorised based on their source or function, classifying extrinsic signals from CNS-resident cells (Baydyuk et al., 2020) or mediated via extracellular matrix (ECM) proteins (Yamada et al., 2022) and intrinsic regulatory programs (Gaesser & Fyffe-Maricich, 2016). These programs include, among others, the coordination of intracellular organelle trafficking by molecular motors (kinesins, dyneins, and myosins) (Barbosa et al., 2024), as well as hormonal modulations of e.g. amino acid-based (thyroid hormones, insulin-like growth factor (IGF) 1) or steroid hormones (Breton et al., 2021; Long et al., 2021). In parallel, transcriptional and epigenetic control cascades, including OLIG1/2, SOX10, NK2 homeobox (NKX) 2.2, inhibitors of DNA binding (ID) 2/4, and hairy and enhancer of split (HES) 1/5, guide lineage commitment and maturation (Fitzpatrick et al., 2015; Mitew et al., 2014; Tiane et al., 2019). Additionally,

metabolic regulation (Zhu et al., 2024), such as mitochondrial-mediated mechanisms (Gil & Gama, 2023), contributes to lineage progression.

The sophisticated balance between excitatory and inhibitory drivers (Kremer et al., 2011) is critical for guiding accurate maturation and myelin formation. Imbalances can result in detrimental malfunctions and impaired lineage specification and/or impaired maturation towards a functional, myelinating oligodendrocyte. This involves an array of conserved regulatory pathways such as sonic hedgehog (SHH), bone morphogenetic protein (BMP), Notch, wingless and integration site (Wnt)/β-catenin, protein kinase B (AKT) / mammalian target of rapamycin (mTOR), and extracellular signal-regulated kinase (ERK) / mitogen-activated protein kinase (MAPK) signalling cascades (Emery & Wood, 2024; Gaesser & Fyffe-Maricich, 2016; Nicolay et al., 2007). A focused analysis of selected key signalling pathways relevant for oligodendroglial specification and differentiation is provided in detail in section 2.1.

1.1.1.3 Oligodendroglial Precursor Cells – Designated Fate and Function?

Traditionally viewed as progenitors of myelinating oligodendrocytes, OPCs (also termed NG2-glia in this context (Nishiyama et al., 1999)) are now well-known as a multifunctional and distinct glial population within the CNS. A substantial pool of OPCs persists throughout life, comprising 2–8% of CNS cells, with a higher density in white matter (up to 9%) compared to grey matter (maximum 3%) (Dawson et al., 2003; Dimou et al., 2008; Rivers et al., 2008). While white matter-resident OPCs are mitotically active and contribute to oligodendrogenesis, OPCs of the grey matter are slowly proliferative or quiescent, remaining in an immature state (Dimou et al., 2008).

Functionally, OPCs display marked regional and morphological heterogeneity (Osorio et al., 2022), reflecting functional diversity beyond oligodendrogenesis. This has led to their classification as a distinct glial subtype, NG2-glia (Nishiyama et al., 1999; Nishiyama et al., 2009). Far from being passive precursors, they are involved in axon plasticity, regulating neuronal development and activity, engage in phagocytosis of axonal debris and synaptic terminals, contribute to apoptotic regulations, blood-brain barrier (BBB) integrity and astrocyte maturation, vascular formation, and immune signalling (Fang & Bai, 2023; Hill et al., 2024; Ma et al., 2024). Thus, genetic alterations of their intrinsic programmed function might also directly impair accurate CNS development and repair mechanisms and exacerbate disease progression or cognition.

Beyond maturation to oligodendrocytes, OPCs retain a latent astrocytic potential that can be reactivated under specific developmental or pathological conditions. *In vitro*, they give rise to process-bearing type-2 astrocytes in the presence of serum, a finding that led to their initial classification as oligodendrocyte-type-2 astrocyte (O–2A) progenitor cells (Raff et al., 1983). *In vivo* studies confirm this potential, although restricted to early

developmental stages and only resulting in the generation of astrocytes in the grey matter (protoplasmic), but never white matter astrocytes (fibrous) (Huang et al., 2019; Zhu et al., 2012). The astrocytic fate can also be activated in response to injury-induced environmental changes, such as stab wound, cerebral stroke or experimental autoimmune encephalomyelitis (EAE), a mouse model for the demyelinating disease multiple sclerosis (MS) (Akay et al., 2021; Hackett et al., 2018; Kirdajova et al., 2021; Komitova et al., 2011; Tanner et al., 2011). Additionally, this is not only a murine phenomenon, as foetal human OPCs have also been shown to differentiate into astrocytes when transplanted into postnatal mouse brains (Windrem et al., 2004). These observations suggest that while OPCs are at least bipotent, astrocyte differentiation is largely suppressed under physiological conditions and restricted to defined temporal or reactive contexts, here presumably contributing to repair and remyelination failures (Marangon et al., 2024).

1.1.2 Adult Neural Stem Cells and Their Contribution to Oligodendrogenesis

Adult neural stem cells (aNSCs) retain multipotency and potentially can generate neurons, astrocytes, and oligodendrocytes. They are primarily located in the subventricular zone (SVZ) of the lateral ventricles and the subgranular zone (SGZ) of the hippocampal dentate gyrus, (Davis & Temple, 1994). While their contribution to oligodendrogenesis under physiological conditions remains limited, their regenerative capacity becomes increasingly relevant in the context of CNS injury and demyelination (Xiao et al., 2017). Particularly, SVZ-NSCs were shown to restore myelination in response to demyelinating insults (reviewed by Akkermann et al., 2017; Akkermann et al., 2016).

As cell replacement therapies via NSC transplantation are well-studied approaches for the repair of injured or diseased CNS (Beyer et al., 2019), promoting and stabilising their progression towards oligodendroglial differentiation constitutes an important need. A significant boost to their oligodendroglial lineage progression is achieved by stimulation with bone marrow-derived mesenchymal stem cell-conditioned medium (MSC-CM, see Appendix, Fig. 3A) (Jadasz et al., 2018; Rivera et al., 2009; Samper Agrelo et al., 2020), attributed to mesenchymal stem cell-secreted tissue inhibitor of metalloproteinases (Timp) 1 (Samper Agrelo et al., 2020). Timp1 neutralisation significantly diminished the oligodendroglial response both *in vitro* and *in vivo*, establishing its role as a key factor in lineage specification (Schira-Heinen et al., 2022a) in line with findings by Nicaise et al. (Nicaise et al., 2018).

These findings emphasise the responsiveness of aNSCs to extrinsic cues, such as mesenchymal stem cell-derived secreted factors, which can promote oligodendrocyte fate specification and functional myelination. This offers a translationally relevant strategy not only to enhance myelin repair in acquired demyelinating diseases but possibly also to

support and stabilise oligodendrogenesis in neurodevelopmental contexts where myelination is delayed or dysregulated.

1.1.3 Schwann Cells – Unexpected Roles in Central Nervous System Repair

Schwann cells, the primary glial cells of the peripheral nervous system (PNS), fulfil functions broadly similar to those of oligodendrocytes in the CNS: they ensheath axons, provide metabolic support, and form myelin (reviewed by Salzer et al., 2024). Originating from neural crest cells, Schwann cells differentiate into either myelinating or non-myelinating phenotypes in response to axonal calibre and local signals. In contrast to oligodendrocytes, which can myelinate multiple axons, each Schwann cell wraps a single axon. While the functional principles of myelination are conserved between PNS and CNS, the molecular composition of myelin and regenerative capacity upon injury differ significantly (Scherer & Arroyo, 2009). PNS myelin is characterised by abundant proteins such as myelin protein zero (P0), peripheral myelin protein (PMP) 22, and periaxin – proteins absent or minimally expressed in CNS myelin. Schwann cells exhibit remarkable plasticity and can dedifferentiate into a repair phenotype following nerve injury. This process is regulated by factors such as c-JUN, octamer-binding transcription factor (OCT) 6, KROX20 (also early growth response protein; ERG2), and is accompanied by the downregulation of myelin-associated genes (Jessen & Mirsky, 2005; Jessen & Mirsky, 2016).

Their plasticity makes Schwann cells highly attractive for transplantation in PNS and CNS repair approaches. This is also due to their secretion of important neurotrophic factors (e.g., IGF, brain-derived neurotrophic factor (BDNF), and PDGF-BB) and ECM components (such as neural cell adhesion molecule (NCAM)), which support and promote axonal regrowth, myelination, and neuroprotection (for review, see e.g., Guest et al., 2025; Matsas et al., 2008; Xu, 2009). Unexpectedly, Schwann cells have also been implicated in CNS repair via endogenous mechanisms. For a long time, it was assumed that they invade the CNS after the breakdown of astroglial-guided limitations at demyelinating regions (for review see Franklin & Blakemore, 2003). However, two genetic lineage tracing studies in mice demonstrated that OPCs transdifferentiate into Schwann cells following toxin-induced demyelination or spinal cord injury and contribute to axonal remyelination within the CNS, though appearing to be restricted to the spinal cord (Assinck et al., 2017; Zawadzka et al., 2010). Whether CNS remyelination by Schwann cells is functionally equivalent to that performed by oligodendrocytes and why this transdifferentiation occurs remains an open question and subject of ongoing investigation (for review see Chen et al., 2021a).

1.1.4 Astrocytes – Friend or Foe?

Astrocytes are essential for maintaining CNS homeostasis, comprising approximately 30% of glial cells in the CNS (von Bartheld et al., 2016). They contribute to developmental patterning, neuronal and glial support, synaptic regulation, metabolic homeostasis, immune response, and blood–brain barrier integrity. Their diverse physiological functions have been reviewed elsewhere (e.g. Gradisnik & Velnar, 2023; Lee et al., 2022; Rupareliya et al., 2023). Increasing evidence points to their versatile role in direct and indirect regulation of myelination (reviewed by Kiray et al., 2016).

In the context of oligodendrogenesis, astrocytes influence OPC survival, proliferation, and maturation via multiple signalling mechanisms. Astroglial secreted PDGF and fibroblast growth factor (FGF) 2 support early OPC maintenance (Bögler et al., 1990; Ferrara et al., 1988; Pringle et al., 1989), while ciliary neurotrophic factor (CNTF) enhances OPC survival and maturation (Cao et al., 2010b; Stankoff et al., 2002; Stöckli et al., 1991) and protects against demyelination-associated apoptosis (Linker et al., 2002).

However, under pathological, inflammatory, or demyelinating conditions, astrocytes undergo reactive transformation and may acquire neurotoxic properties (for review see e.g. Gorter & Baron, 2022; Moulson et al., 2021; Sofroniew, 2020). These reactive astrocytes can release cytokines such as interleukin (IL) 1α, tumour necrosis factor (TNF) α and complement factors (C1q, C3), which impair OPC proliferation, migration, and differentiation and promote oxidative stress (Liddelow et al., 2017). Despite these detrimental effects, reactive astrocyte subtypes also exhibit neuroprotective features such as TIMP1 secretion (Saha et al., 2020), highlighting their context-dependent functional plasticity and that the balance between supportive vs. inhibitory roles is critical for regenerative success or failure in CNS pathologies (Escartin et al., 2021). As will be discussed in section 2.7, the dominant astrocytic response in demyelinating conditions such as MS often hinders repair. Thus, recent pharmacological approaches aim to shift or promote astrocyte phenotypes toward regeneration-permissive properties to reduce disease progression and foster repair (Silva Oliveira Junior et al., 2024).

1.2 White Matter in Pathologies

Myelin plays a critical role in neuronal plasticity, connectivity, and function, ensuring proper brain performance throughout life. Consequently, dysfunction or loss of oligodendrocytes and their myelin sheaths has emerged as a central pathogenic factor across a broad spectrum of neurological disorders. These include neurodegenerative conditions such as Alzheimer’s disease (AD) (Han et al., 2022) and Huntington’s disease (Back et al., 2024; Ferrari Bardile et al., 2023), or autoimmune demyelinating diseases like MS (Molina-Gonzalez et al., 2022; Stadelmann et al., 2019) or secondary demyelination following

acute CNS injury such as stroke (Marangon et al., 2024). Furthermore, psychiatric disorders, including depression (Zlomuzica et al., 2023) and schizophrenia (Valdés-Tovar et al., 2022), as well as cognitive and motor impairments (Chen et al., 2021b; Wang et al., 2020), have been linked to structural and functional abnormalities in white matter. However, white matter restoration remains an unmet medical need, although therapeutic strategies are rapidly advancing with promising approaches in pharmacology, cell therapy, and molecular targeting, as seen in MS (Bezukladova et al., 2022; Lubetzki et al., 2022). Thus, it can be beneficial to understand similarities or differences of white matter abnormalities in neurological disorders, to identify starting points for myelin restoration attempts.

Although less prevalent, inherited white matter disorders, collectively termed leukodystrophies, generally caused by single gene mutations, have significantly advanced our understanding of myelin pathology and the contributions of other glial cell types that should not be ignored (Perlman & Mar, 2012; Stadelmann et al., 2019). Despite its well-known association with intellectual disability and cognitive impairments, DS has rarely been examined in the context of white matter malformation. Yet, understanding these alterations could have significant implications for medical care, as insights from pharmacological, molecular, or cell transplantation therapies developed for demyelinating diseases may be transferable to – a gap this thesis intends to address.

1.2.1 Multiple Sclerosis – a Primary Demyelinating Disorder

MS is a chronic inflammatory, demyelinating, and neurodegenerative disease affecting approximately 2.8 million people worldwide (Walton et al., 2020). It typically manifests in young adults between 20 and 40 and shows a pronounced female predominance (2:1 ratio) (Koch-Henriksen et al., 2018; Kurtzke, 2000; Milo & Kahana, 2010). MS is characterised by autoimmune-driven responses targeting CNS myelin, resulting in focal demyelinating lesions within both white and grey matter of the brain and spinal cord (Filippi et al., 2018) and manifesting in different clinical forms (e.g. relapsing-remitting RRMS) (for review see Lassmann, 2019). MS lesions are spatially heterogeneous and widely disseminated across the CNS, leading to a broad range of clinical symptoms – from visual disturbances and sensory loss to motor dysfunction and cognitive decline (reviewed by e.g. Filippi et al., 2018; Lassmann, 2019).

The pathological hallmark of MS is the progressive loss of myelin due to oligodendroglial cell death which impairs metabolic and trophic support to neurons, disrupts ion channel organisation, and contributes to mitochondrial dysfunction and oxidative stress – ultimately promoting axonal damage and neuronal degeneration (Correale et al., 2019; Reich et al., 2018). While the immune response was traditionally viewed as being driven predominantly by peripheral immune cells (Dendrou et al., 2015; Prinz & Priller, 2017), accumulating

evidence highlights the pivotal contribution of CNS-resident glial cells. Activated microglia and astrocytes can independently mediate neurotoxicity and demyelination (for review see Muzio et al., 2021; Zhou et al., 2019). Also infectious agents have been implicated in MS pathogenesis. Strong epidemiological associations exist for Epstein–Barr virus (EBV) (Bjornevik et al., 2023; Wagner et al., 2004), while human herpesvirus (HHV) 6A (Álvarez-Lafuente et al., 2004) and human endogenous viruses (ERVs) (Gruchot et al., 2023a; Gruchot et al., 2023b; Küry et al., 2018) are emerging as additional viral contributors, although their exact mechanistic roles remain to be fully clarified.

Although OPCs and NSCs persist within the adult CNS, remyelination in MS remains inefficient, especially in chronic lesions, likely due to an inhibitory environment (astrogliosis and microgliosis) and insufficient OPC recruitment and differentiation (for review see Kotter et al., 2011; Tepavcevic & Lubetzki, 2022). The restoration of (re-)myelination can therefore be regarded as a central research focus for MS therapy.

1.2.2 Ischemic Stroke – Secondary White Matter Damage

Ischemic stroke occurs due to an acute disruption of cerebral blood flow, leading to deprivation of oxygen and glucose, which results in the death of neurons and oligodendroglial cells and ultimately causes disability (for review see Dewar et al., 2003). In 2021, the global age-standardised prevalence rate was around 820 cases per 100,000 individuals (Li et al., 2024). While clinical focus has long been on neuronal damage and degeneration, white matter injury, particularly the loss of oligodendrocytes and their myelin sheaths, has gained recognition as a significant contributor to post-stroke disability and long-term clinical outcome (Jia et al., 2019; Plemel et al., 2014; Zhou et al., 2013).

Oligodendrocytes are particularly susceptible to ischemia-induced necroptosis and apoptosis, triggered by excitotoxic mediators such as glutamate and adenosine triphosphate (ATP) (Xu et al., 2020). As early as three hours after middle cerebral artery occlusion, oligodendrocytes exhibit swelling and vacuolization, followed by process retraction and cell death within 24 hours (McIver et al., 2010; Pantoni et al., 2006). This acute demyelination compromises axonal integrity and structural stability, exacerbating neurological deficits.

Anatomically, the infarct core comprises the irreversibly damaged region where nearly all cells die within minutes. In contrast, the surrounding peri-infarct region (penumbra) contains partially viable tissue that may be preserved through reperfusion in short-term and regenerated with long-term remyelination strategies (Bonfanti et al., 2017; Lo, 2008; Sozmen et al., 2016). Indeed, OPCs are activated in response to ischemic injury and recruited to the lesion borders, particularly within the penumbra, where an increased number of oligodendroglial lineage cells have been detected (Kang et al., 2010). Although this OPC response may initially support axonal survival and myelin repair, their

differentiation into mature, myelinating oligodendrocytes is often insufficient, especially at later stages. This remyelination failure contributes to chronic white matter deficits and impedes functional recovery (for review see e.g. Hernández et al., 2021; Rosenzweig & Carmichael, 2015; Shi et al., 2015). Thus, approaches to foster OPC differentiation to support repair and long-term recovery of function are a relatively new research focus in stroke therapy.

1.2.3 Down Syndrome – Genetically Driven White Matter Malformation

DS, caused by trisomy of human chromosome 21 (HSA21), is the leading genetic reason for intellectual disability and cognitive impairments, affecting approximately 1 in 700–1000 live births worldwide (de Graaf et al., 2021). The condition is associated with a broad spectrum of systemic and neurological manifestations, most notably impairments in learning, memory, executive function, and age-related cognitive decline. Additionally, individuals with DS develop early-onset Alzheimer's disease concomitant with accelerated ageing of the brain (Lanfranchi et al., 2010; Lott & Head, 2019).

At the structural level, DS neuropathology is characterised by reduced brain volume, altered cortical organisation, and hypomyelination (Ábrahám et al., 2012; Golden & Hyman, 1994; Pinter et al., 2001). Cellularly, displacement and loss of cortical neurons have been reported (Golden & Hyman, 1994), alongside altered neuronal connectivity patterns emerging during foetal development (Marin-Padilla, 1976; Petit et al., 1984; Takashima et al., 1981; Weitzdoerfer et al., 2001). Furthermore, persistent reactive astrogliosis has been demonstrated in postmortem DS tissue (Murphy et al., 1992; Takashima & Becker, 1985), in line with findings of increased astrogliogenesis (Kurabayashi et al., 2015). A shift from neuro-to-gliogenic fate is thought to contribute to the observed cellular imbalance (Dossi et al., 2017; Haydar & Reeves, 2012; Kanaumi et al., 2013; Stagni et al., 2017).

For a long time, research has extensively focused on neuronal deficits and altered neurogenesis as major contributors to cognitive decline and intellectual disability in DS, while largely ignoring the role of white matter pathology and oligodendroglial dysfunction. However, emerging evidence suggests that the gliogenic fate shift may not only affect neuronal precursors but also influence oligodendroglial specification, potentially shifting them toward astrocytic differentiation and contributing to hypomyelination. Section 2.1 will explore these mechanisms, describing the altered oligodendroglial composition in DS and summarising key signalling pathways involved in fate regulation known to be altered in DS.

1.3 C21ORF91 – A Novel Candidate Regulator of Neurodevelopment and Myelination?

The triplication of HSA21 exerts genome-wide effects (Letourneau et al., 2014; Olmos-Serrano et al., 2016), causative to the various clinical presentations in DS and complicating the search for gene loci on HSA21 that may be sufficient to result in a specific DS phenotype. Nevertheless, investigating rare segmental HSA21 trisomies has proven valuable in narrowing down candidate regions and genes potentially responsible for distinct DS features, such as cognitive impairment (Korbel et al., 2009). In addition to the study of Korbel et al., two further independent reports described individuals with partial tetrasomy of HSA21 who exhibited remarkably strong cognitive impairment due to microcephaly (Slavotinek et al., 2000) and presented with intellectual disability and speech delay in the absence of other typical DS features (Rost et al., 2004). These findings highlight a subset of genes that may drive DS neuropathological phenotypes.

Among them, *C21ORF91*, also referred to as *early undifferentiated retina and lens* (*EURL*), has emerged as an interesting candidate. The protein was originally identified in chick embryos based on its expression in early retinal and lens precursor cells, suggesting a role in developmental processes prior to cell fate determination and differentiation (Godbout et al., 2003). In DS, C21ORF91 is overexpressed proportional to the gene dosage effect (1.5-fold increase observed in microarray analysis of DS lymphoblastoid cells), hence most likely contributing to DS phenotypes (Ait Yahya-Graison et al., 2007). Also, *C21ORF91* transcripts were among the most enriched transcripts in DS pluripotent stem cells (Chou et al., 2012). Analysis of euploid, healthy human brain tissues revealed spatiotemporal dynamics of *C21ORF91* expression during cortical development, following a characteristic pattern, decreasing toward birth, peaking in early postnatal stages, and declining again with age (Li et al., 2016). Notably, the highest transcript levels are observed in the corpus callosum, the largest white matter tract of the human brain. This expression profile strikingly coincides with the onset and progression of developmental myelination (Reiche et al., 2021, see section 2.2). Interestingly, *C21ORF91* transcript levels are elevated in foetal DS brains compared to euploid controls (Li et al., 2016).

In line with these findings, *C21orf91* was identified as part of a co-dysregulated gene module M43 in a developmental transcriptome analysis of DS patients, enriched for oligodendrocyte differentiation and myelin-associated genes such as *CNPase*, *Plp1*, *Sox10*, and *Gpr17* (Olmos-Serrano et al., 2016). Additionally, the mouse orthologue protein to C21ORF91, D16Ertd472e (encoded on chromosome 16 in mice) was enriched by a 5.5-fold in oligodendrocytes compared to astrocytes or neurons, similar to the level of other proteins associated and important for their development, such as Olig2 (Cahoy et

al., 2008). Both observations indicate an important role of C21ORF91 for the oligodendroglial lineage.

Independent bioinformatic analyses and data mining efforts conducted by Lydie Lane and Paula Duek (see section 2.2), along with yeast two-hybrid screening performed by Hybrigenics (France, unpublished), had further revealed a strong correlation between human *C21ORF91* and the oligodendroglial lineage and myelination. These converging observations led to the collaborative development of a research project aiming to investigate C21orf91 in primary rat oligodendroglia. The experimental validation of these predictions was subsequently carried out in our laboratory, demonstrating its involvement in rat brain development and OPC differentiation under both native and overexpression conditions (Reiche et al., 2021) and further extended to NSCs (Park, 2020) and Schwann cells (Schütte, 2022), and will be further discussed in this thesis.

In summary, *C21ORF91* emerges as a gene of high interest for CNS development (Godbout et al., 2003; Li et al., 2016). While its specific function in oligodendrogenesis is only beginning to be unravelled – inter alia within the work presented in this thesis – its inclusion in a myelination-relevant gene module and its phenotypic linkage to cognitive deficits in partial trisomic/tretrasomic cases support its candidacy as a critical regulator of glial development and white matter integrity, particularly in the context of DS.

1.4 Aims of the Thesis

Proper myelination in the CNS is crucial for maintaining neural circuit integrity and supporting higher brain functions. Oligodendrogenesis – whether occurring during development, learning or driven by repair mechanisms – relies on the precise and multi-faceted regulation of multiple signalling cues involving the cross-talk of all CNS-innate cell types. Disruptions within this process, whether of congenital origin or acquired through injury or disease, can impair white matter integrity, with detrimental consequences for cognition and life quality. In recent years, various neurological conditions, particularly demyelinating diseases such as MS, have recognised the therapeutic potential of stabilising OPC differentiation competence. In contrast, research on the neurobiology of DS has still predominantly focused on neuronal deficits as the leading cause of intellectual disability. Despite extensive investigations into neurogenesis and the possible neuro-to-gliogenic shift in DS, the role of oligodendroglia and hypomyelination remains largely descriptive rather than mechanistically explored. This thesis, therefore, aims to fill this gap and broaden our understanding of gliogenic dysregulation in DS, with a particular emphasis on the oligodendroglial lineage. By deepening our insight into these processes, novel strategies to ameliorate cognitive impairment in DS may become accessible.

In this context, the aims of this thesis are:

I.) To elucidate the extent of oligodendroglial imbalance in DS and to investigate the hypothesis that hypomyelination results from impaired lineage commitment rather than being secondary to altered neurogenesis.

II.) To characterise the gene *C21orf91* as a novel regulatory factor involved in oligodendroglial development and myelination, potentially contributing to hypomyelination in DS.

III.) To explore whether pharmacological approaches derived from remyelination research in demyelinating disorders can be translated to the context of *C21orf91*-related oligodendroglial dysfunction.

2 Results – Publications at a Glance

To address the first aim of this thesis, a literature review was conducted on hypomyelination and abnormalities in oligodendroglial cell composition in DS, focusing on signalling pathways that induce a neuro-to-astrogliogenic cell fate switch (see section 2.1). The review emphasises the dual role of these pathways, which are also essential for accurate oligodendrogenesis, indicating that switching progenitor specification to astrocytes may contribute to observed glial imbalances in DS. Finally, potential pharmacological strategies to correct this imbalance in DS, some of which have already shown a pro-oligodendroglial therapeutic effect in the context of demyelinating diseases such as MS, are presented.

Regarding the second aim, the predicted role of C21ORF91 in myelination and maturation of OPCs, evident by bioinformatic analysis, was proven by investigating the spatiotemporal expression dynamics in rat brain development and spontaneous differentiation of rat primary OPCs. Additional gene modulation via nucleofection demonstrated that elevated levels of the *C21orf91* rat ortholog indeed impaired accurate OPC differentiation, diminishing their myelination capacity, and resulted in the induction of astroglial properties, possibly resembling the suggested switch in glial specification observed in DS (see section 2.2 and section 2.8).

The third aim focused on the analysis of pharmacological approaches. In parallel to this DS-related project, our group was working on identifying small molecules to stabilise OPC differentiation competence and promote remyelination and repair in a demyelinating context (drug repurposing studies). By utilising primary cultures, organotypic slice cultures, and suitable experimental mouse models (cuprizone-mediated demyelination or photothrombotic ischemia), various promising candidates were determined during the last years (see sections 2.3-2.6). Interestingly, medrysone was shown to exert its restorative and beneficial features on remyelination primarily via promoting a repair phenotype in astrocytes (see section 2.4). This highlighted the role of astrocytes in a demyelinating context – a topic reviewed in section 2.7, including a discussion of biomedical strategies that may promote such a beneficial repair phenotype. Finally, all findings converged in demonstrating that the identified myelin repair compounds were indeed able to rescue *C21orf91*-induced defective OPC differentiation as well as the arising neurotoxic astroglial cues, thereby possibly paving the way for a novel therapeutic strategy for cognitive impairment in DS targeting myelin restoration (see section 2.8).

cells

MDPI

Review

Aberrant Oligodendrogenesis in Down Syndrome: Shift in Gliogenesis?

Laura Reiche, Patrick Küry † and Peter Göttle *,†

Department of Neurology, Medical Faculty, Heinrich-Heine-University, 40225 Düsseldorf, Germany; Laura.Reiche@hhu.de (L.R.); Patrick.kuery@uni-duesseldorf.de (P.K.)

* Correspondence: Peter.Goettle@uni-duesseldorf.de; Tel.: +49-211/81-08071; Fax: +49-(0211)-81-18469

† These authors contributed equally to this work.

Received: 31 October 2019; Accepted: 4 December 2019; Published: 7 December 2019

Abstract: Down syndrome (DS), or trisomy 21, is the most prevalent chromosomal anomaly accounting for cognitive impairment and intellectual disability (ID). Neuropathological changes of DS brains are characterized by a reduction in the number of neurons and oligodendrocytes, accompanied by hypomyelination and astrogliosis. Recent studies mainly focused on neuronal development in DS, but underestimated the role of glial cells as pathogenic players. Aberrant or impaired differentiation within the oligodendroglial lineage and altered white matter functionality are thought to contribute to central nervous system (CNS) malformations. Given that white matter, comprised of oligodendrocytes and their myelin sheaths, is vital for higher brain function, gathering knowledge about pathways and modulators challenging oligodendrogenesis and cell lineages within DS is essential. This review article discusses to what degree DS-related effects on oligodendroglial cells have been described and presents collected evidence regarding induced cell-fate switches, thereby resulting in an enhanced generation of astrocytes. Moreover, alterations in white matter formation observed in mouse and human post-mortem brains are described. Finally, the rationale for a better understanding of pathways and modulators responsible for the glial cell imbalance as a possible source for future therapeutic interventions is given based on current experience on pro-oligodendroglial treatment approaches developed for demyelinating diseases, such as multiple sclerosis.

Keywords: down syndrome; white matter; glial fate

1. Introduction

The majority of central nervous system (CNS) diseases are characterized by neuronal damage and white matter malfunctions, which can lead to detrimental motor and sensory effects. Trisomy 21, as an aneuploidy disorder, is characterized by an additional copy of human chromosome 21 (Hsa21) and causes Down syndrome (DS). DS is the most abundant human trisomy, affecting around 1 in 1100 neonates annually [1], making it the most common genetic cause for intellectual disability (ID) [2]. DS patients suffer from several cognitive impairments, accompanied by a low intelligence quotient (IQ) ranging from 30 to 70 [2], which can be attributed to brain abnormalities. In accordance with the neurocentric paradigm, brain research in DS has followed the concept that neuronal dysfunctions primarily lead to neurological diseases [3]. Therefore, much of the DS research aimed at identifying the underlying genetic interventions of altered neurogenesis. This information is essential for unraveling pharmacological approaches to ameliorate cognitive function (summarized in recent reviews [1,4–8]). Nevertheless, over the last few years consideration has been given to the re-evaluation of the role of astroglial and oligodendroglial lineage cells in CNS pathologies characterized by neurodegeneration [3,9]. Interestingly, several studies in DS indicated a neuro- to gliogenic shift, mainly focusing on the observed bias toward astrocytes [3,4,6,10]. Even though oligodendroglial

cells—as a source of CNS myelin sheaths—are essential for higher brain functions by assuring long-term axonal integrity, metabolic and trophic support, and accelerated electrical signal propagation, this crucial cell population has not attracted much attention in DS. The notion that aberrant oligodendrogenesis may contribute to cognitive impairments and ID in DS is supported by a recent developmental transcriptome analysis of post-mortem human DS brains [11]. Of note, the analysis of this study revealed a dysregulated gene cluster associated with oligodendroglial cell differentiation and myelination, showing that hypomyelination in DS is caused by a cell-autonomous phenomenon in oligodendrocyte development. To further highlight the importance of the oligodendroglial lineage in DS development, this review article summarizes the current knowledge regarding altered oligodendrogenesis and white matter malformations in human and rodent DS research. We show that signaling pathways assumed to lead to defective neurogenesis and to a neuro-to astrogenic shift also affect oligodendrogenesis. Such knowledge may help to devise new treatments that aim to improve brain development and ID by stabilization of the oligodendroglial lineage.

2. Down Syndrome: A Brief Neurological Profile

Associated with more than 80 clinical features affecting many organs, both the occurrence (penetrance) and severity (expressivity) of phenotypes vary across the DS population [4]. Nonetheless, certain characteristics, such as facial dysmorphology, reduced brain volume accompanied by ID, and an early-onset Alzheimer's disease (AD)-like pathology are common in all DS individuals. This neurological profile is distinctly marked by hypocellularity in the cerebral hemispheres, frontal lobe, temporal cortex, hippocampus, and cerebellum, most likely explained by a complex spatiotemporal perturbation in neurogenesis, resulting in a reduced neuronal cell population and a subsequently altered neuronal connectivity [1,4,6].

Moreover, aberrant astrogliogenesis and changes in several astrocytic marker expression patterns have been demonstrated in DS (reviewed in [3]). Notably, an over-population of astroglial cells in the frontal lobe of DS fetuses [12], as well as in the frontal cortex, calcarine cortex, and mainly hippocampus of infant and adult DS brains [13], has been observed. At an advanced age, astrogliosis in the amygdala [14], related to the occurrence of senile plaques and neurofibrillary tangles [13] and in areas of basal ganglia calcification [15], was shown to be implicated in DS.

Furthermore, DS brains of old adults are marked by reduced numbers of oligodendrocytes when compared to age-matched individuals [16]. More devastating is the observed hypomyelination in DS, pointing to an impaired myelination process which proceeds until adulthood, as demonstrated by myelin protein expression [11], histological [17,18], or magnetic resonance imaging (MRI) [19] examinations. Assessed by diffusion tensor imaging (DTI) fractional anisotropy (FA) analysis, white matter in DS patients showed lower fiber density, smaller axonal diameters, and a reduced myelination degree compared to healthy controls [20]. Decreased FA and early white matter damage were particularly observed in the region of the anterior thalamic radiation, the inferior fronto-occipital fasciculum, the inferior longitudinal fasciculum and the corticospinal tract, bilaterally, the corpus callosum (CC), and the anterior limb of the internal capsule [21–23]. Of note, diminished white matter integrity in DS was associated with poorer performance at neuropsychological assessments [20,23]. In this context, recent evidence in animal models suggests that ongoing myelin remodeling is important for behavior, cognition, and learning throughout adulthood [24,25]. Notably, the onset of cognitive deficits in DS is thought to occur in late infancy, becoming more obvious in adolescence [11,26–33]. This time course indeed correlates with the peak of myelination during the first years of life, continuing into young adulthood [34]. Moreover, immunohistochemical analysis for myelin basic protein (MBP) revealed a decreased density of myelinated axons and a generally delayed myelin formation in DS compared to age-matched controls [18], indicating that the oligodendroglial lineage was directly affected upon gene-dosage effects of Hsa21. Accordingly, a recent multi-region transcriptome analysis of DS and healthy brains spanning from fetal development to adulthood revealed that genes associated with oligodendroglial cell differentiation and myelination are dysregulated in trisomy 21 during late fetal

development and the first years of postnatal life [11]. Weighted-gene co-expression network analysis (WGCNA) within this study identified several modules of co-expressed genes, including the module number 43 (M43) which is related to oligodendrocyte development and myelination including, for example, 2′,3′-cyclic nucleotide-3′-phosphodiesterase (CNPase), proteolipid protein (PLP), Sox10, and G protein coupled receptor 17 (GPR17). This module exhibited a distinct downregulation throughout the DS neocortex and hippocampus during development [11]. Of note, GPR17, a modulator of oligodendroglial cell maturation [35], is linked to a significantly reduced expression of sorting nexin family member 27 (SNX27) in DS [36], which was demonstrated to impair oligodendroglial precursor cell (OPC) maturation, resulting in myelination deficits in Ts65Dn mice, a mouse model for DS [37]. However, there is much evidence on aberrant oligodendrogenesis correlating with or contributing to DS-related cognitive impairments, but the underlying mechanisms have so far not been investigated in detail.

3. Gliogenesis and Cell Types in Healthy CNS

The mammalian central nervous system (CNS) consists of neurons and glial cells, the latter of which make up at least 50% of human brain cells. Glial cell function is essential for the evolutionary increase in complexity of neurological function in mammals [38] and can be divided in macroglial cells deriving from the neuroepithelium and microglia with a hematopoietic (mesodermal) origin [38]. Despite their crucial importance for various physiological processes [39,40], these cells are not further addressed in this review article. Macroglial cells are generally categorized into astrocytes and oligodendrocytes. Due to upcoming knowledge about the functions of proteoglycan nerve-glial antigen 2 (NG2) expressing glial cells, NG2 glia are considered a further category of macroglia [41].

Approximately 40% of the human brain is considered to be white matter. It consists of (i) axons, the functional unit of neurons providing the basis for signal transduction and information, (ii) astrocytes, which are essential for structural and metabolic support to neurons, and (iii) myelin. In the CNS, myelin is imperative for the stabilization, protection, and electrical insulation of axons, enabling accelerated electrical signal propagation [34–36]. Myelin sheaths are generated by oligodendrocytes. These specialized glial cells either derive from oligodendroglial precursor cells (OPCs) or niche-located neural stem cells (NSCs) [37]. The structural integrity of myelin is of crucial importance for CNS function and restoration [38]. Unfortunately, pathological degeneration and inflammation [35] or genetic intervention [39] can result in myelin loss, which may lead to impaired neuronal signaling, functional deficits, and a shortened lifetime [40]. Hence, white matter deficits and myelin dysfunctions are considered to be a main contributing factor for neurodegenerative diseases and malfunctions of the CNS [41].

The major cell types of the CNS are produced by several spatiotemporal, partially overlapping generation and division waves of progenitor cells, which are guided by extrinsic and intrinsic cues [38,42], resulting in a well-defined brain anatomy and cytoarchitecture. In the oligodendrogenic context, it is important to briefly introduce OPCs/NG2 glia and their differentiation potency (Figure 1). These cells derive from radial glia, the primary progenitor cells at embryonic stages, and are produced in three waves following a ventral-dorsal temporal progression in the developing forebrain [38]. They populate the brain and spinal cord to generate oligodendrocytes that myelinate the entire CNS during postnatal life [34]. A small fraction of OPCs is maintained as an immature, slowly proliferative, or quiescent cell population in the adult CNS [43]. Noteworthy, accumulating evidence indicates that beyond generating oligodendrocytes, OPCs exhibit the potential to also give rise to astroglial cells in vitro [44] and in vivo [45–47]. As mentioned above, OPCs can additionally be generated postnatally and in the adult brain from transient amplifying cells (TAPs or C cells) derived from NSCs located in the subventricular zone (SVZ) [48], mainly from the dorsal part (facing the corpus callosum) [49]. For OPC differentiation and subsequent myelination to occur, various signals are necessary in order to stabilize oligodendroglial fate and to regulate extensive changes in cell shape and membrane architecture. Pro-oligodendroglial extracellular signals comprise several pathways, such as

those elicited by sonic hedgehog (SHH), Wnt/β-catenin, bone morphogenic protein (BMP), cytokines (LIF, Cxcl1), neurotransmitters (glutamate, ATP, adenosine), hormones (thyroid hormone T3, insulin), extracellular matrix molecules (fibronectin, laminin), metabolic signals (hypoxia), or in response to physical cues (spatial constrain, rigid substrate), and axonal receptors (Lingo-1, PSA-Ncam) [9,50,51]. Additionally, intrinsic regulators, such as the transcription factors basic helix-loop-helix oligodendrocyte lineage transcription factor 2 (Olig2) and sex determining region Y-Box 10 (Sox10), have also been implicated in OPC differentiation [52] in that, for example, exposure to SHH, expressed by the ventral telencephalon, instructs early progenitor cells to become OPCs, possibly via upregulation of Olig2 [53]. This induction is antagonized by the dorsally expressed Wnt/β-catenin and BMP pathways [54]. BMP4, on the other hand, has been shown to promote the expression of a family of inhibitor of DNA-binding (Id) proteins Id2 and Id4, which form complexes with Olig2. This interaction prevents Olig2 from binding to DNA, blocking its ability to act as a transcription factor and therefore inhibiting the differentiation along the oligodendroglial lineage but promoting astrogliogenesis [55]. Furthermore, post-translation processes, such as the regulation of the JAK/STAT3 activity by modulating STAT3's acetylation state, mediated by the histone deacetylase Hdac3, which has been shown to control Olig2 expression, are also needed to suppress astrogliogenesis [56].

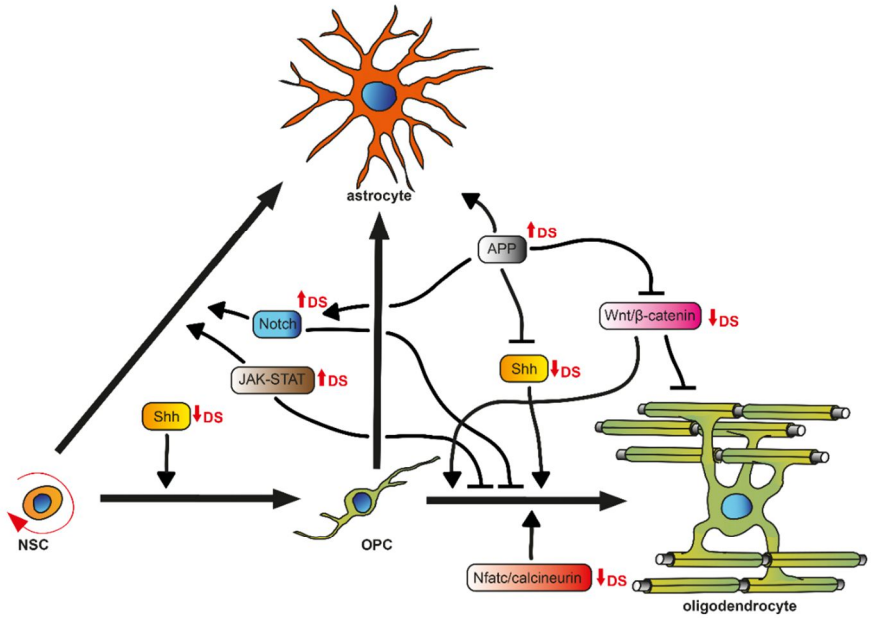

Figure 1. Representation of key signaling pathways involved in oligodendrogenesis. Neural stem cells (NSCs) exhibit astrogenic and oligodendrogenic potential. For oligodendroglial precursor cells (OPCs) derived from NSCs to successfully differentiate into myelinating oligodendrocytes, OPCs follow a highly regulated differentiation process that is affected by a fine-tuned network of signaling pathways. Within Down syndrome (DS) (red arrows), signaling pathways reveal aberrant dynamics.

Hence, based on this fine-tuned regulation of cell fate and differentiation mediators, it is likely that neurogenesis and gliogenesis are misguided in their responses to gene-dosage abnormalities caused by aneuploidy disorders. This holds true for DS brain development, where not only altered progenitor cell proliferation and apoptosis but also potential signaling pathways responsible for a neuro- to astrogenic shift are assumed to be responsible for observed neuronal hypocellularity and concurrent over-population of astroglial cells. However, so far, an oligodendrogenic to astrogenic shift has not been taken into account, although the number of oligodendrocytes and myelination rate are

decreased in DS [11,16,18]. Furthermore, the differentiation of OPCs to mature oligodendrocytes was shown to be negatively affected in the DS mouse model Ts65Dn [11].

4. Defective OPC Differentiation in DS—Possible Interfering Regulators

Overall brain volume reduction and hypocellularity are already present in fetuses and children with DS [57–60]. This fact indicates that defective neuro- and gliogenesis during early phases of brain development may be a major causal factor of DS-associated brain abnormalities, which might be a consequence of early apoptosis and impaired proliferation in DS [6,61]. Also, the comparison of hippocampal regions of DS fetuses between 17 and 21 weeks of gestation to age-matched controls showed a higher percentage of cells with astrocytic phenotypes, but a smaller percentage of cells with neuronal phenotypes [62]. A few studies demonstrated elevated numbers of Olig2 expressing cells (thus declared as OPCs) in DS fetal brains at 14 and 18 weeks of gestation [63], even up to 34 weeks [10], suggesting a cell-fate shift from neurogenesis to gliogenesis at early developmental stages. Of note, the number of Olig2 expressing cells in the DS mouse model Ts65Dn is increased at embryonic day 13.5 and 14 [64], but decreases thereafter [11] when compared to age-matched controls. Intriguingly, the percentage of mature oligodendrocytes was drastically diminished from postnatal days 15–60 [11], whereas a massive increase of astrocyte numbers and reactivity was shown at the age of 48 weeks in the same DS mouse model [65]. Considering the capacity of OPCs to generate astroglial cells instead of oligodendrocytes, a shift within the glial cell commitment in DS accompanied with a generally defective differentiation capacity of oligodendroglial progenitors might be suggested.

Several authors have already discussed the involvement of pathways essential for cell fate and differentiation within neurogenesis in DS, thereby giving strong evidence that therapeutic approaches targeting these pathways could improve aberrant brain cytoarchitecture, in particular the neuro- to astrogliogenic shift [4–7,61]. Hereinafter, we focus on pathways relevant for oligodendrogenesis (Figure 1) instead and highlight to what extent they might constitute new therapeutic avenues.

4.1. JAK-STAT Signaling

One of the most important signaling pathways for the gliogenic cascade in NSCs is the Janus kinase-signal transducer and activator of transcription (JAK-STAT) pathway, mediated by ligands such as interleukins (ILs), interferons (INFs), the glycoprotein (gp) 130 family, and the γ-chain (gC) family [6,66]. Common downstream targets, such as GFAP and S100β which specify glial cell fate, are transcriptionally activated by STATs [6,67]. STAT3 in particular plays an essential role in regulating astrogliogenesis during brain development [66]. In vivo studies showed that overexpression of STAT3 in the neocortex of DS mice (Ts1Cje) enhanced astrogliogenesis [68], whereas its knockout inhibited the astroglial fate in mouse NSCs [69]. Additionally, it was reported that IL-6 in DS children and IFN-γ in embryonic trisomy 16 mouse brains (Ts16, a model used for human trisomy 21 (DS)), were increased respectively [70,71], both of which are capable of activating the STAT3 pathway [72]. Indeed, neonate DS mice (Ts65Dn) exhibited hyperactivation of STAT3 in the hippocampus [73]. More importantly, four IFN receptors, IFN-α receptor 1 and 2 (IFNAR1, IFNAR2), IFN-γ R2 (IFNGR2), and interleukin 10 receptor β (IL10RB), are located on Hsa21 and overexpressed in DS with a mean ratio of ~1.5 proportional to the gene-dosage effect of trisomy 21 [74–76]. This disposition leads to a generally increased INF sensitivity in DS [74].

Overstimulation of the JAK-STAT signaling pathway can also be linked to dual-specificity tyrosine-(Y)-phosphorylation-regulated kinase 1A (DYRK1A), which is also overexpressed in DS due to the location on Hsa21 [77]. Overexpression of this protein was shown to result in elevated STAT3 activity, which promoted the astrocytic differentiation of neocortical progenitors in Ts1Cje mice [68].

Interestingly, the STAT3 pathway was also shown to be a crucial regulator of OPC differentiation by means of shifting oligodendroglia toward an astrocytic fate, thereby causing astrogliosis and insufficient remyelination in Theiler's murine encephalomyelitis [78]. Given that STAT3 pathway can be activated by IFN-γ, the expression of which is increased in DS mice, it needs to be pointed

out that IFN-γ was demonstrated to decrease rat OPC differentiation into oligodendrocytes [47]. Moreover, this study also indicated that IFN-γ might shift cell commitment toward the astrocytic lineage. Accordingly, transgenic mice overexpressing IFN-γ under control of the MBP promotor exhibited hypomyelination accompanied by an increase of astrocyte numbers, as well as reactive gliosis in white matter tracts [79]—a shift in brain cytoarchitecture that is strikingly similar to DS neuropathology. Therefore, overstimulation of JAK-STAT signaling caused by overexpressed levels of INFRs, ligands, and subsequent overactivation of the STAT3 pathway may promote an NSC/OPC fate toward an astrogliogenic pathway in the DS brain.

4.2. SHH Signaling

The spatiotemporal activity of Sonic Hedgehog (SHH) controls cell proliferation, migration, fate and differentiation of progenitor cell waves during brain development [80]. SHH is a well-known regulator that promotes oligodendroglial fate, OPC generation, differentiation, and myelin production in the spinal cord and forebrain during embryonic development [81,82], as well as OPC production and recruitment throughout adulthood [83] and in demyelination [84]. In the canonical SHH pathway, in the absence of SHH, the inhibitory transmembrane receptor Patched1 (Ptch1) suppresses the activity of the SHH signaling activator Smoothened (Smo) [85]. SHH binding to Ptch1 interrupts its inhibition on Smo, which triggers a complex intracellular signaling cascade including the transcription factors of the Glioma-associated oncogene (Gli) family to mediate downstream gene transcription, such as Mammalian achaetescute homolog-1 (Ascl1/Mash1), Olig2, or Nk2 homeobox 2 (Nkx2.2) [86–88]. Ptch1 was shown to be overexpressed in 17–21 week old fetuses and the DS mouse Ts65Dn [89], leading to the assumption that the SHH pathway is repressed in DS. Indeed, Gli 1 and 2, as well as Mash1, are downregulated in trisomic neuronal precursor cells (NPCs) of Ts65Dn mice, which could be restored by the maintenance of SHH signaling activity by Smoothened Agonist (SAG) treatment [73].

Of note, inhibition of Gli1 activity was previously shown to be important for NSC-dependent remyelination [90]. Furthermore, OPC differentiation was shown to be defective and diminished in $SHH^{-/-}$ mutants [87,91] and rat OPCs treated with the steroidal alkaloid cyclopamine, which inhibits SHH signaling by targeting Smo [92]. Thus, the increased inhibition of Smo due to elevated Ptch1 levels in DS, subsequently leading to repressed SHH activity, may contribute to the observed downregulation of a whole cluster of genes associated with OPC differentiation and myelination [11] and the delayed differentiation of OPCs, subsequently leading to hypomyelination in DS brains [18].

4.3. Notch Signaling

Notch signaling was shown to cross-talk with JAK-STAT [72] and SHH signaling pathways [93], thereby inducing gliogenic shift during brain development. Mediated by binding of ligands such as delta-like protein 1 (Dll1), cleavage of the transmembrane receptor Notch by γ-secretase is initiated. This liberates the Notch intracellular domain (NICD), which translocates to the nucleus to transcriptionally activate Notch effector proteins, such as hairy/enhancer of split 1 and 5 (Hes1, Hes5) [94], which are proteins that were shown to promote the activation of STAT3 [95]. Notch1, Notch2, and Dll1 expression were demonstrated to be significantly upregulated in adult DS fibroblasts and cortices [94]. This process may increase Hes protein activity, thus contributing to the activation of STAT3 and enhancing astroglial differentiation. Notably, Wu and colleagues demonstrated, independently of DS studies, that Notch1 overexpression in glial restricted precursor cells (GRPs) upregulated *Hes1* mRNA levels and that overexpression of Hes1 promoted astrocyte generation at the expense of oligodendrocytes [96]. Taken together, the upregulation of JAK-STAT and Notch signaling may synergistically contribute to astrogliogenesis, thereby suppressing neurogenesis [6] and oligodendrogenesis in the DS brain.

4.4. Wnt/β-Catenin Signaling

The wingless and integration site (Wnt) signaling pathway is another fundamental mechanism that directs cell proliferation, polarity, and fate determination during embryonic development and tissue homeostasis [97,98]. Activation of the canonical Wnt pathway is dependent on the nuclear translocation of β-catenin, which drives the expression of several target genes [99]. The canonical Wnt signaling consists of extracellular Wnt proteins/ligands, surface membrane frizzled receptors (Fzd), low density lipoprotein (LDL) receptor related protein-5 and 6 (LRP-5/6), cytoplasmic β-catenin, and intranuclear transcription factors of the T cell factor/lymphoid enhancer factor (TCF/LEF) family. Binding of a Wnt ligand to Fzd and Lrp5/6 causes the degradation of the β-catenin destruction complex, which consists of adenomatous polyposis coli (APC), axin, glycogen synthase kinase 3 β (Gsk3β), and casein kinase 1 (CK1). This leads to the accumulation of β-catenin in the cytoplasm, which then translocates to the nucleus where it induces the expression of downstream target genes, including cyclin Dl, which is mediated by binding to TCF4 [99]. Signaling via the Wnt/β-catenin pathway is also a key regulator of oligodendrocyte development, as it is transiently activated in OPCs concurrent with the initiation of terminal differentiation [100]. β-catenin activity is down-regulated in mature oligodendrocytes, which is necessary for accurate oligodendrocyte differentiation [100], as mutant mice with elevated Wnt/β-catenin signaling in the oligodendrocyte lineage display blocked differentiation and hypomyelination [101]. Paradoxically, however, deletion of the Wnt effector TCF4 does not cause precocious oligodendrocyte differentiation as may be expected, but rather blocks oligodendrocyte differentiation [100,102,103]. Interestingly, loss of β-catenin in NPCs was demonstrated to cause precocious specification and differentiation to astrocytes [104].

In the context of DS, general downregulation of the Wnt/β-catenin signaling pathway was demonstrated in human DS and the DS mouse Tc1 hippocampus [99]. In particular, free, and thus activated, β-catenin levels were dramatically diminished. Contrary to this finding, Li and colleagues observed elevated β-catenin signaling in gene perturbation studies targeting a specific Hsa21-endcoded gene that they suggested was implicated in DS pathogenesis, which nevertheless resulted in defective neurogenesis [105]. Taken together, the aberrant Wnt/β-catenin signaling observed in DS may also contribute to defective oligodendrogenesis and lead to a gliogenic cell-fate shift during early brain development and homeostasis.

4.5. Nfatc/Calcineurin Signaling

The nuclear factor of activated T cell (Nfat) pathway is an essential regulator of vertebrate development, which is necessary for the regulation of proliferation and differentiation of NPCs from the SVZ [106]. Activated by calcineurin, a calcium and calmodulin-dependent serine/threonine protein phosphatase, cytoplasmic Nfatc is dephosphorylated and subsequently translocated into the nucleus, where it regulates protein expression such as IL-2 [6]. Regulator of calcineurin 1 (RCAN1), formerly known as DS critical region 1 (DSCR1), inhibits the calcineurin-mediated activation of Nfatc. Interestingly, RCAN1 is located on Hsa21 and was shown to be overexpressed in the DS fetal brain and in Ts1Cje and Ts65Dn mice [107,108]. Accordingly, Nfatc4 was reported to be hyperphosphorylated in the human fetal DS brain at gestation week 20 [109]. In this context, it needs to be mentioned that DYRK1A and RCAN1 were shown to act synergistically to control phosphorylation levels of Nfatc [109,110]. DYRK1A increases RCAN1 inhibitory activity by phosphorylating it and is capable of reducing Nfatc transcriptional activity by directly phosphorylating Nfatc proteins.

Notably, Nfat/calcineurin signaling was shown to be required for oligodendroglial differentiation and myelination by transcription factor network tuning [111]. When Nfatc activation was inhibited by preventing calcineurin binding to Nfats, OPC maturation and differentiation was strongly reduced. This pathway may therefore contribute to aberrant oligodendrogenesis and hypomyelination in DS, as inhibition of Nfatc/calcineurin signaling is mediated by elevated RCAN1 and DYRK1A activities.

4.6. APP-Mediated Signaling

The Hsa21-encoded *Amyloid precursor protein* (*APP*) gene is involved in cell migration and cell-cycle progression in brain development [112], specifically influencing NPC proliferation, cell-fate specification, and maturation [113]. Depending on the APP processing pathway (non-/amyloidogenic), APP is cleaved by α-, β-, and γ-secretases, resulting in N-terminal soluble secreted APP (sAPP) and C-terminal fragments, such as Aβ and the APP intracellular domain (AICD). The dysregulation of APP due to triplication was suggested to result in early-onset AD-like pathology in DS. Indeed, APP protein levels were shown to be increased in homogenates from the temporal cortex of fetuses with DS [6,114], and neuritic Aβ plaque formation is present in the hippocampus and enthorinal cortex of almost all adults with DS and in some DS children [115–117]. Furthermore, the triplication of APP in Ts65Dn mice was demonstrated to impair NPC proliferation, differentiation and maturation due to increased levels of AICD [73,89,118].

Notably, elevated levels of AICD increased the Ptch1 expression in trisomic NPCs [89], hence the APP/AICD system may at least contribute to the derangement of SHH signaling, as outlined above. Moreover, increased AICD levels can promote Gsk3β activity, thereby reducing the translocation of β-catenin to the nucleus, which may contribute to the suppression of the Wnt/β-catenin pathway [118]. Interestingly, a study in the field of intraventricular hemorrhage (IVH), a common neurological complication of prematurity causing cognitive deficits and ID [119], which is accompanied by inhibited proliferation/maturation of OPCs and hypomyelination [120], demonstrated that Gsk3β activity interfered with OPC differentiation and myelination [121]. Furthermore, a cross-talk of Gsk3β and Notch signaling was shown, as inhibition of Gsk3β downregulated Notch signaling. Accordingly, it can be suggested that increased Gsk3β activity due to APP overexpression may contribute to increased Notch signaling, thus enhancing astrogliogenesis at the expense of oligodendrogenesis. Indeed, exposure to soluble APP was demonstrated to regulate human NPC differentiation through activation of JAK-STAT and Notch signaling and to induce astrocytic differentiation [122]. As Aβ itself was reported to increase apoptosis in oligodendroglia in vitro [123], a more widespread implication of this protein is suggested to lead to aberrant oligodendrogenesis in DS.

5. Regulators of Glia Cell Fate: Avenues to Adjust Aberrant White Matter?

Adjusting glia cell-fate imbalance, hence overcoming intrinsic defects in oligodendroglial cell maturation and subsequently developmental dysmyelination, will be a major target in order to improve white matter structures in DS. To this end, repurposing pre-existing modulators or compounds developed for the promotion of endogenous oligodendroglial cell maturation in demyelinating diseases such as multiple sclerosis (MS) [9,124–126] represents a possible strategy. In this context, currently evaluated drugs related to the development of myelin-repair therapies are discussed here.

Modulating the Wnt/β-catenin pathway by means of indometacin, a non-steroidal anti-inflammatory drug (NSAID) [127], or Gsk3β inhibitors, such as CHIR99021 or LY-294002, exhibited the potential to promote oligodendrogenesis in healthy and demyelinated paradigms [86,87]. Furthermore, the antifungal agent miconazole, which interferes with ergosterol synthesis, as well as corticosteroid betamethasone clobetasol, which suppresses inflammatory responses, were demonstrated as therapeutic compounds for enhancing (re)myelination in vivo and in human OPCs in vitro [128]. Moreover, modulation of histamine receptor signaling by means of GSK239512, a histamine H3 receptor antagonist, was demonstrated to boost oligodendroglial differentiation as indicated by phenotypic screening and genetic association of human demyelination lesion samples of patients with MS [129]. In this regard, magnetization transfer ratio (MTR)-based post-hoc analyses indicated a small mean improvement in myelin content in treated patients with relapsing remitting (RR) MS relative to placebo [130]. On the other hand, the first-generation histamine H1 receptor blocker clemastine was initially identified as a remyelinating drug in a high-throughput screening [131] and was further investigated in a RRMS clinical study demonstrating a reduction in P100 latency delay in visual evoked potentials (VEPs) [132]. This readout could be used to monitor myelination dependent signal

propagation in the visual system. In addition to these OPC-directed drugs, several experimental compounds have been described to trigger signaling pathways modulating oligodendrogenesis. The endothelin (ET) receptor antagonist BQ788 was demonstrated to block endothelin-B receptor activation on astrocytes, thereby rescuing oligodendrogenesis and promoting remyelination [133]. The flavonoid molecule quercetin leads to enhanced oligodendrogenesis and remyelination in several ways, as it suppresses Notch signaling by inhibiting γ-secretase activity and disrupts the binding of β-catenin to TCF4 [134]. In a recent study by Granno and colleagues, a major role of Wnt/β-catenin signaling in DS was implicated. They combined bioinformatics with RNA and protein analyses using post-mortem tissue from adult DS individuals. Among other molecules, they identified axin2 to be significantly decreased in DS [99]. As the small molecule XAV939 was previously shown to stabilize axin2 by inhibiting the poly-ADP-ribosylating enzymes tankyrase 1 and 2 in hypoxic and demyelinating injuries, thereby accelerating OPC differentiation and myelination [135], it might also constitute a possible treatment approach for white matter deficits in DS.

Moreover, small molecule approaches addressing transcriptional/epigenetic regulators affecting oligodendrogenesis could also provide additional therapeutic perspectives. In this regard, GANT61, a blocker of the transcription factor Gli1, was demonstrated to promote the generation of oligodendrocytes from adult NSCs [90]. In accordance, specific inactivation of SIRT1 by means of the small molecule inhibitor EX-527, a protein deacetylase implicated in energy metabolism, increased the production of new NSC-derived OPCs in the adult mouse brain [136]. Likewise, a similar promoting effect could also be attributed to this molecule in the OPC context [137]. Furthermore, activation of the fibroblast growth factor receptor-3 (FGFR3) signaling was recently shown to redirect the differentiation of SVZ-derived NSCs from neuronal to oligodendroglial lineage, hence, promoting remyelination [138]. In this context, the membrane-bound and the cleaved ectodomains of the klotho protein were observed to be associated with FGFR3 signaling. This protein acts as a co-receptor and was found to modulate the Wnt and IGF pathways, thereby enhancing remyelination in demyelinating animal models [139,140].

However, promoting oligodendroglial maturation and axonal ensheathment might not be sufficient for successful white matter restoration or rescue. Reprogramming or reconverting astroglial to oligodendroglial cells, as well as a preservation of the oligodendroglial lineage by means of genetic or pharmacological approaches, are most likely mandatory for white matter stabilization in DS [9,141]. In 2014, information on FDA-approved drugs/small molecules, suitable for rescuing cognitive impairment due to neurodevelopmental alterations, neurotransmitter imbalances, and neurodegeneration in the Ts65Dn DS mouse, was compiled [5]. Of note, the preclinical evaluations that emerged from this study need to be considered critically, as this mouse model did not reflect all trisomic orthologues in individuals with DS, hence an effective translation to human clinical trials is still unclear. However, beside neurogenic effects, some identified drugs are also likely to foster oligodendrogenesis, thus representing potential therapeutics for enhanced myelin development and stabilization. Among these listed drugs, the selective generic estrogen receptor (ER) β agonist diarylpropionitrile (DPN) could be of interest based on the observation that it confers functional neuroprotection in a chronic experimental autoimmune encephalomyelitis (EAE) mouse model of MS by stimulating endogenous remyelination [142]. The stimulation of glial progenitor cells (GPCs) derived from both the SVZ and white matter with memantine, a low-affinity antagonist of NMDA receptors used to treat AD, was found to promote oligodendrogenesis, and therefore myelin repair, upon ischemic periventricular leukomalacia (PVL) [143]. Moreover, fluoxetine, an antidepressant based on selective serotonin reuptake inhibition, also known as Prozac, was demonstrated to boost oligodendrocyte-related gene transcripts such as *CNPase*, *OLIG1*, and *MOG* when applied to rhesus monkeys with major depressive disorders [144]. Lithium chloride (LiCl), which was established for the treatment of bipolar disorder (BD), can stimulate oligodendrocyte morphological maturation and promote remyelination after toxin-induced demyelination of organotypic slice cultures [145]. In addition, melatonin, a sleep/wake-cycle regulating hormone, was shown to increase oligodendrocyte generation from NSCs [146]. Further to this, the vitamin E derivate TFA-12 was found to reduce astrogliosis and

to accelerate remyelination of toxin-induced demyelinated lesions [147]. Given the impact of SHH signaling in oligodendrogenesis, a recent study demonstrated that the small molecule Smo agonist SAG could alter SHH signaling in DS [148]. Notably, SAG modulates oligodendroglial differentiation and additionally steers commitment of NSCs to the oligodendroglial lineage [92]. Interestingly, the γ-secretase inhibitor DAPT (N-[N-(3,5-difluorophenacetyl)-1-alanyl]-S-phenyl-glycinet-butylester) is an effective inhibitor of the Notch signaling pathway and might also confer benefits to white matter, as it was found to promote differentiation of NSCs/NPCs into oligodendrocytes, astrocytes, and neurons in vitro [149]. Nevertheless, to what degree the balance between these two glial cell types is affected remains to be shown. In this context, such a preferred shift toward oligodendroglia could be mediated via the acetylcholine esterase inhibitor donepezil, an FDA-approved drug for Alzheimer's disease and dementia. Donepezil was shown to promote the differentiation of primary NSCs into mature oligodendrocytes at the expense of astrocytes [150], and it was also found to enhance myelin sheath generation in neuron/glia co-cultures [151]. The FDA-approved anti-seizure drug ethosuximide was described to be capable of inducing trans-differentiation of muscle-derived stem cells into Olig2-positive oligodendroglial cells [152]. Whether ethosuximide activity could also be used to re-establish the glial cell balance needs to be shown, keeping in mind that Olig2 expression itself is not restricted to oligodendroglial cells, but is also found in the cytoplasm of astroglia [153].

The histone deacetylase class I and II inhibitors trichostatin A and valproate (VPA) were previously demonstrated to promote the conversion of astrocytes to OPCs [154,155], and could thus be considered as potential regulators for the desired glial shift in DS. A similar mode of action was revealed in response to forced expression of the microRNA miR-302/367 cluster, thereby enhancing the generation of oligodendroglia from astrocytes [156]. Likewise, injection of Sox2 lentiviral particles into the corpus callosum following cuprizone-mediated demyelination in vivo as well as lentiviral transduction of astroglial cells in vitro resulted in a conversion of astrocytes to oligodendroglial cells [156]. Similarly, overexpression of pro-oligodendroglial transcription factors, such as Olig2 or Ascl1/Mash1, also resulted in reprogramming of NSCs toward an oligodendroglial fate [157–160]. Of note, *Olig2* is an Hsa21-encoded gene, which was shown to be overexpressed in DS and assumed to interfere with neurogenesis in DS [6]. However, we demonstrated here that oligodendrogenesis is negatively affected in DS.

Nevertheless, it appears that the drugs and transcriptional/epigenetic regulators described here could indeed provide new avenues for the experimental and clinical rescue of white matter deficits in DS. To what degree some of these candidates are applicable in the context of DS in terms of application and opportunity windows certainly needs additional experimental and pre-clinical research efforts.

6. Concluding Remarks

Given the importance of myelinating glial cells for axonal support, trophism, maintenance, and electrical insulation, an overall increase in the number of functional oligodendrocytes would likely confer an overall benefit on neuronal cell numbers and functionality, which in turn could ameliorate ID, even in light of known neurogenic deficits in DS. Strikingly, DS research has so far mainly focused on aberrant neurogenesis and the underlying signaling pathways leading to defective neuronal cell proliferation, differentiation, and progenitor cell fate in DS. In this review, the collected evidence suggests that many of these dysregulated signaling pathways may also be involved in defective DS-related NSC/OPC proliferation, differentiation, and fate commitment. Furthermore, we demonstrated that several drugs and molecules identified to restore brain developmental deficits in rodent DS models based on neurogenesis criteria [5] might also mediate beneficial effects on the oligodendroglial lineage.

Hsa21 is the smallest human chromosome, currently known to encode more than 400 genes. This number might increase over time due to the recognition of non-coding RNAs [161,162]. Nevertheless, the description of dosage-sensitive Hsa21 genes resulting in a specific phenotype by gene-copy number variations is currently limited to only a few. This may be due to the fact that

over 20 proteins encoded by Hsa21 are involved in signal transduction and more than 30 proteins are considered to belong to transcription factors, both of which most likely influence the expression of other genes in the genomes of DS patients [7]. By implication, this inevitably results in a genome-wide dysregulation of several networks at the same time, which could be demonstrated, for example, in the case of the gene cluster M43, which is related to oligodendroglial differentiation and myelination [11].

Interestingly, pharmacological approaches addressing neurogenic deficits were found to be successful in a broad age range (prenatal, perinatal, and adult) of treated Ts65Dn mice, suggesting that the prevention or amelioration of cognitive deficits in DS may indeed be possible. This paves the way toward clinical trials, some of which (donepezil, folate or memantine) are still in progress, but no differences in outcome between treated and placebo have occurred as yet [5]. In humans, however, prenatal treatments will be challenging due to specific safety requirements. Nevertheless, the window of opportunity to improve differentiation and homeostasis in the oligodendroglial lineage might stretch over several developmental phases, as myelination is mainly a postnatal event. In this regard, it is worth mentioning that dysregulation of the M43 gene cluster, which is related to oligodendroglial lineage, appears during late neonate's development and during the first years of postnatal life in DS [11], a period that coincides with massive upregulation of oligodendroglial and myelination genes [163], as well as oligodendrocyte expansion in the human brain [164].

A number of mouse models with DS-related features were generated and used to study Hsa21dosage-sensitive genes and to understand their roles leading to cognitive impairment (reviewed in [5,165,166]). Although well-established mouse models such as Ts65Dn, Ts1Cje, and Ts16 recapitulate the human neuropathological phenotype to a certain extent, modeling of DS in rodent system remains challenging because Hsa21 genes are distributed throughout mouse chromosomes 16, 17, and 10 (Mmu16/17/10). Therefore, mouse models may provide different outcomes, hence negatively affecting translation to humans.

Author Contributions: Conceptualization, L.R. and P.G.; writing—original draft preparation, L.R., P.K., and P.G.; writing—review and editing, L.R., P.K., and P.G.; supervision, P.G.

Funding: This study was supported by the Jürgen Manchot foundation, Düsseldorf. Research on white matter deficits, myelin repair, and neuroregeneration in the laboratory of P.K. was additionally funded by the Deutsche Forschungsgemeinschaft (DFG; grants KU1934/2-1, KU1934/5-1), Christiane and Claudia Hempel Foundation for clinical stem cell research, DMSG Ortsvereinigung Düsseldorf und Umgebung e.V., iBrain, Stifterverband/Novartisstiftung, and the James and Elisabeth Cloppenburg, Peek and Cloppenburg Düsseldorf Stiftung. The MS Center at the Department of Neurology is supported in part by the Walter and Ilse Rose Foundation.

Conflicts of Interest: The authors declare no conflict of interest.

References

1. Baburamani, A.A.; Patkee, P.A.; Arichi, T.; Rutherford, M.A. New approaches to studying early brain development in Down syndrome. *Dev. Med. Child Neurol.* **2019**, *61*, 867–879. [CrossRef] [PubMed]
2. Chapman, R.S.; Hesketh, L.J. Behavioral phenotype of individuals with Down syndrome. *Ment. Retard. Dev. Disabil. Res. Rev.* **2000**, *6*, 84–95. [CrossRef]
3. Dossi, E.; Vasile, F.; Rouach, N. Human astrocytes in the diseased brain. *Brain Res. Bull.* **2017**. [CrossRef] [PubMed]
4. Haydar, T.F.; Reeves, R.H. Trisomy 21 and early brain development. *Trends Neurosci.* **2012**, *35*, 81–91. [CrossRef]
5. Gardiner, K.J. Pharmacological approaches to improving cognitive function in Down syndrome: Current status and considerations. *Drug Des. Dev. Ther.* **2015**, *9*, 103–125. [CrossRef]
6. Stagni, F.; Giacomini, A.; Emili, M.; Guidi, S.; Bartesaghi, R. Neurogenesis impairment: An early developmental defect in Down syndrome. *Free Radic. Biol. Med.* **2017**. [CrossRef]
7. Antonarakis, S.E. Down syndrome and the complexity of genome dosage imbalance. *Nat. Rev. Genet.* **2017**, *18*, 147–163. [CrossRef]

8. Xu, R.; Brawner, A.T.; Li, S.; Liu, J.J.; Kim, H.; Xue, H.; Pang, Z.P.; Kim, W.Y.; Hart, R.P.; Liu, Y.; et al. OLIG2 Drives Abnormal Neurodevelopmental Phenotypes in Human iPSC-Based Organoid and Chimeric Mouse Models of Down Syndrome. *Cell Stem Cell* **2019**, *24*, 908–926.e908. [CrossRef]
9. Kremer, D.; Göttle, P.; Hartung, H.-P.; Küry, P. Pushing Forward: Remyelination as the New Frontier in CNS Diseases. *Trends Neurosci.* **2016**, *39*, 246–263. [CrossRef]
10. Kanaumi, T.; Milenkovic, I.; Adle-Biassette, H.; Aronica, E.; Kovacs, G.G. Non-neuronal cell responses differ between normal and Down syndrome developing brains. *Int. J. Dev. Neurosci.* **2013**, *31*, 796–803. [CrossRef]
11. Olmos-Serrano, J.L.; Kang, H.J.; Tyler, W.A.; Silbereis, J.C.; Cheng, F.; Zhu, Y.; Pletikos, M.; Jankovic-Rapan, L.; Cramer, N.P.; Galdzicki, Z.; et al. Down Syndrome Developmental Brain Transcriptome Reveals Defective Oligodendrocyte Differentiation and Myelination. *Neuron* **2016**, *89*, 1208–1222. [CrossRef]
12. Zdaniuk, G.; Wierzba-Bobrowicz, T.; Szpak, G.M.; Stepien, T. Astroglia disturbances during development of the central nervous system in fetuses with Down's syndrome. *Folia Neuropathol.* **2011**, *49*, 109–114.
13. Mito, T.; Becker, L.E. Developmental changes of S-100 protein and glial fibrillary acidic protein in the brain in Down syndrome. *Exp. Neurol.* **1993**, *120*, 170–176. [CrossRef]
14. Murphy, G.M., Jr.; Ellis, W.G.; Lee, Y.L.; Stultz, K.E.; Shrivastava, R.; Tinklenberg, J.R.; Eng, L.F. Astrocytic gliosis in the amygdala in Down's syndrome and Alzheimer's disease. *Prog. Brain Res.* **1992**, *94*, 475–483.
15. Takashima, S.; Becker, L.E. Basal ganglia calcification in Down's syndrome. *J. Neurol. Neurosurg. Psychiatry* **1985**, *48*, 61–64. [CrossRef]
16. Karlsen, A.S.; Pakkenberg, B. Total numbers of neurons and glial cells in cortex and basal ganglia of aged brains with Down syndrome—A stereological study. *Cereb. Cortex* **2011**, *21*, 2519–2524. [CrossRef]
17. Wisniewski, K.E.; Schmidt-Sidor, B. Postnatal delay of myelin formation in brains from Down syndrome infants and children. *Clin. Neuropathol.* **1989**, *8*, 55–62.
18. Abraham, H.; Vincze, A.; Veszpremi, B.; Kravjak, A.; Gomori, E.; Kovacs, G.G.; Seress, L. Impaired myelination of the human hippocampal formation in Down syndrome. *Int. J. Dev. Neurosci.* **2012**, *30*, 147–158. [CrossRef]
19. Koo, B.K.; Blaser, S.; Harwood-Nash, D.; Becker, L.E.; Murphy, E.G. Magnetic resonance imaging evaluation of delayed myelination in Down syndrome: A case report and review of the literature. *J. Child Neurol.* **1992**, *7*, 417–421. [CrossRef]
20. Fenoll, R.; Pujol, J.; Esteba-Castillo, S.; de Sola, S.; Ribas-Vidal, N.; Garcia-Alba, J.; Sanchez-Benavides, G.; Martinez-Vilavella, G.; Deus, J.; Dierssen, M.; et al. Anomalous White Matter Structure and the Effect of Age in Down Syndrome Patients. *J. Alzheimers Dis.* **2017**, *57*, 61–70. [CrossRef]
21. Romano, A.; Moraschi, M.; Cornia, R.; Bozzao, A.; Rossi-Espagnet, M.C.; Giove, F.; Albertini, G.; Pierallini, A. White matter involvement in young non-demented Down's syndrome subjects: A tract-based spatial statistic analysis. *Neuroradiology* **2018**, *60*, 1335–1341. [CrossRef]
22. Gunbey, H.P.; Bilgici, M.C.; Aslan, K.; Has, A.C.; Ogur, M.G.; Alhan, A.; Incesu, L. Structural brain alterations of Down's syndrome in early childhood evaluation by DTI and volumetric analyses. *Eur. Radiol.* **2017**, *27*, 3013–3021. [CrossRef]
23. Powell, D.; Caban-Holt, A.; Jicha, G.; Robertson, W.; Davis, R.; Gold, B.T.; Schmitt, F.A.; Head, E. Frontal white matter integrity in adults with Down syndrome with and without dementia. *Neurobiol. Aging* **2014**, *35*, 1562–1569. [CrossRef]
24. McKenzie, I.A.; Ohayon, D.; Li, H.; de Faria, J.P.; Emery, B.; Tohyama, K.; Richardson, W.D. Motor skill learning requires active central myelination. *Science* **2014**, *346*, 318–322. [CrossRef]
25. Liu, J.; Dietz, K.; DeLoyht, J.M.; Pedre, X.; Kelkar, D.; Kaur, J.; Vialou, V.; Lobo, M.K.; Dietz, D.M.; Nestler, E.J.; et al. Impaired adult myelination in the prefrontal cortex of socially isolated mice. *Nat. Neurosci.* **2012**, *15*, 1621–1623. [CrossRef]
26. Lanfranchi, S.; Jerman, O.; Dal Pont, E.; Alberti, A.; Vianello, R. Executive function in adolescents with Down Syndrome. *J. Intellect. Disabil. Res.* **2010**, *54*, 308–319. [CrossRef]
27. Baddeley, A.; Jarrold, C. Working memory and Down syndrome. *J. Intellect. Disabil. Res.* **2007**, *51*, 925–931. [CrossRef]
28. Rowe, J.; Lavender, A.; Turk, V. Cognitive executive function in Down's syndrome. *Br. J. Clin. Psychol.* **2006**, *45*, 5–17. [CrossRef]
29. Nelson, L.; Johnson, J.K.; Freedman, M.; Lott, I.; Groot, J.; Chang, M.; Milgram, N.W.; Head, E. Learning and memory as a function of age in Down syndrome: A study using animal-based tasks. *Prog. Neuro-Psychopharmacol. Biol. Psychiatry* **2005**, *29*, 443–453. [CrossRef]

30. Pennington, B.F.; Moon, J.; Edgin, J.; Stedron, J.; Nadel, L. The neuropsychology of Down syndrome: Evidence for hippocampal dysfunction. *Child Dev.* **2003**, *74*, 75–93. [CrossRef]
31. Lanfranchi, S.; Carretti, B.; Spano, G.; Cornoldi, C. A specific deficit in visuospatial simultaneous working memory in Down syndrome. *J. Intellect. Disabil. Res.* **2009**, *53*, 474–483. [CrossRef] [PubMed]
32. Lanfranchi, S.; Cornoldi, C.; Vianello, R. Verbal and Visuospatial Working Memory Deficits in Children With Down Syndrome. *Am. J. Ment. Retard.* **2004**, *109*, 456–466. [CrossRef]
33. Lanfranchi, S.; Jerman, O.; Vianello, R. Working Memory and Cognitive Skills in Individuals with Down Syndrome. *Child Neuropsychol.* **2009**, *15*, 397–416. [CrossRef] [PubMed]
34. Fields, R.D. White matter in learning, cognition and psychiatric disorders. *Trends Neurosci.* **2008**, *31*, 361–370. [CrossRef]
35. Simon, K.; Hennen, S.; Merten, N.; Blattermann, S.; Gillard, M.; Kostenis, E.; Gomeza, J. The Orphan G Protein-coupled Receptor GPR17 Negatively Regulates Oligodendrocyte Differentiation via Galphai/o and Its Downstream Effector Molecules. *J. Biol. Chem.* **2016**, *291*, 705–718. [CrossRef]
36. Wang, X.; Zhao, Y.; Zhang, X.; Badie, H.; Zhou, Y.; Mu, Y.; Loo, L.S.; Cai, L.; Thompson, R.C.; Yang, B.; et al. Loss of sorting nexin 27 contributes to excitatory synaptic dysfunction by modulating glutamate receptor recycling in Down's syndrome. *Nat. Med.* **2013**, *19*, 473–480. [CrossRef]
37. Meraviglia, V.; Ulivi, A.F.; Boccazzi, M.; Valenza, F.; Fratangeli, A.; Passafaro, M.; Lecca, D.; Stagni, F.; Giacomini, A.; Bartesaghi, R.; et al. SNX27, a protein involved in down syndrome, regulates GPR17 trafficking and oligodendrocyte differentiation. *Glia* **2016**, *64*, 1437–1460. [CrossRef]
38. Rowitch, D.H.; Kriegstein, A.R. Developmental genetics of vertebrate glial-cell specification. *Nature* **2010**, *468*, 214–222. [CrossRef]
39. Casano, A.M.; Peri, F. Microglia: Multitasking specialists of the brain. *Dev. Cell.* **2015**, *32*, 469–477. [CrossRef]
40. Michell-Robinson, M.A.; Touil, H.; Healy, L.M.; Owen, D.R.; Durafourt, B.A.; Bar-Or, A.; Antel, J.P.; Moore, C.S. Roles of microglia in brain development, tissue maintenance and repair. *Brain* **2015**, *138*, 1138–1159. [CrossRef]
41. Peters, A. A fourth type of neuroglial cell in the adult central nervous system. *J. Neurocytol.* **2004**, *33*, 345–357. [CrossRef] [PubMed]
42. Kriegstein, A.; Alvarez-Buylla, A. The glial nature of embryonic and adult neural stem cells. *Annu. Rev. Neurosci.* **2009**, *32*, 149–184. [CrossRef] [PubMed]
43. Dawson, M.R.; Polito, A.; Levine, J.M.; Reynolds, R. NG2-expressing glial progenitor cells: An abundant and widespread population of cycling cells in the adult rat CNS. *Mol. Cell. Neurosci.* **2003**, *24*, 476–488. [CrossRef]
44. Raff, M.C.; Miller, R.H.; Noble, M. A glial progenitor cell that develops in vitro into an astrocyte or an oligodendrocyte depending on culture medium. *Nature* **1983**, *303*, 390–396. [CrossRef] [PubMed]
45. Dimou, L.; Gotz, M. Glial cells as progenitors and stem cells: New roles in the healthy and diseased brain. *Physiol. Rev.* **2014**, *94*, 709–737. [CrossRef]
46. Nishiyama, A.; Boshans, L.; Goncalves, C.M.; Wegrzyn, J.; Patel, K.D. Lineage, fate, and fate potential of NG2-glia. *Brain Res.* **2016**, *1638*, 116–128. [CrossRef]
47. Tanner, D.C.; Cherry, J.D.; Mayer-Pröschel, M. Oligodendrocyte Progenitors Reversibly Exit the Cell Cycle and Give Rise to Astrocytes in Response to Interferon-γ. *J. Neurosci.* **2011**, *31*, 6235. [CrossRef]
48. Menn, B.; Garcia-Verdugo, J.M.; Yaschine, C.; Gonzalez-Perez, O.; Rowitch, D.; Alvarez-Buylla, A. Origin of oligodendrocytes in the subventricular zone of the adult brain. *J. Neurosci.* **2006**, *26*, 7907–7918. [CrossRef]
49. Ortega, F.; Gascon, S.; Masserdotti, G.; Deshpande, A.; Simon, C.; Fischer, J.; Dimou, L.; Chichung Lie, D.; Schroeder, T.; Berninger, B. Oligodendrogliogenic and neurogenic adult subependymal zone neural stem cells constitute distinct lineages and exhibit differential responsiveness to Wnt signalling. *Nat. Cell Biol.* **2013**, *15*, 602–613. [CrossRef]
50. Snaidero, N.; Simons, M. Myelination at a glance. *J. Cell Sci.* **2014**, *127*, 2999–3004. [CrossRef]
51. Snaidero, N.; Simons, M. The logistics of myelin biogenesis in the central nervous system. *Glia* **2017**, *65*, 1021–1031. [CrossRef] [PubMed]
52. Miron, V.E.; Kuhlmann, T.; Antel, J.P. Cells of the oligodendroglial lineage, myelination, and remyelination. *Biochim. Biophys. Acta* **2011**, *1812*, 184–193. [CrossRef] [PubMed]
53. Lu, Q.R.; Sun, T.; Zhu, Z.; Ma, N.; Garcia, M.; Stiles, C.D.; Rowitch, D.H. Common developmental requirement for Olig function indicates a motor neuron/oligodendrocyte connection. *Cell* **2002**, *109*, 75–86. [CrossRef]
54. El Waly, B.; Macchi, M.; Cayre, M.; Durbec, P. Oligodendrogenesis in the normal and pathological central nervous system. *Front. Neurosci.* **2014**, *8*, 145. [CrossRef]

55. Samanta, J.; Kessler, J.A. Interactions between ID and OLIG proteins mediate the inhibitory effects of BMP4 on oligodendroglial differentiation. *Development* **2004**, *131*, 4131–4142. [CrossRef]
56. Zhang, L.; He, X.; Liu, L.; Jiang, M.; Zhao, C.; Wang, H.; He, D.; Zheng, T.; Zhou, X.; Hassan, A.; et al. Hdac3 Interaction with p300 Histone Acetyltransferase Regulates the Oligodendrocyte and Astrocyte Lineage Fate Switch. *Dev. Cell* **2016**, *37*, 582. [CrossRef]
57. Golden, J.A.; Hyman, B.T. Development of the superior temporal neocortex is anomalous in trisomy 21. *J. Neuropathol. Exp. Neurol.* **1994**, *53*, 513–520. [CrossRef]
58. Winter, T.C.; Ostrovsky, A.A.; Komarniski, C.A.; Uhrich, S.B. Cerebellar and frontal lobe hypoplasia in fetuses with trisomy 21: Usefulness as combined US markers. *Radiology* **2000**, *214*, 533–538. [CrossRef]
59. Pinter, J.D.; Eliez, S.; Schmitt, J.E.; Capone, G.T.; Reiss, A.L. Neuroanatomy of Down's syndrome: A high-resolution MRI study. *Am. J. Psychiatry* **2001**, *158*, 1659–1665. [CrossRef]
60. Schmidt-Sidor, B.; Wisniewski, K.E.; Shepard, T.H.; Sersen, E.A. Brain growth in Down syndrome subjects 15 to 22 weeks of gestational age and birth to 60 months. *Clin. Neuropathol.* **1990**, *9*, 181–190.
61. Liu, B.; Filippi, S.; Roy, A.; Roberts, I. Stem and progenitor cell dysfunction in human trisomies. *EMBO Rep.* **2015**, *16*, 44–62. [CrossRef] [PubMed]
62. Guidi, S.; Bonasoni, P.; Ceccarelli, C.; Santini, D.; Gualtieri, F.; Ciani, E.; Bartesaghi, R. Neurogenesis impairment and increased cell death reduce total neuron number in the hippocampal region of fetuses with Down syndrome. *Brain Pathol.* **2008**, *18*, 180–197. [CrossRef] [PubMed]
63. Lu, J.; Lian, G.; Zhou, H.; Esposito, G.; Steardo, L.; Delli-Bovi, L.C.; Hecht, J.L.; Lu, Q.R.; Sheen, V. OLIG2 over-expression impairs proliferation of human Down syndrome neural progenitors. *Hum. Mol. Genet.* **2012**, *21*, 2330–2340. [CrossRef] [PubMed]
64. Chakrabarti, L.; Best, T.K.; Cramer, N.P.; Carney, R.S.; Isaac, J.T.; Galdzicki, Z.; Haydar, T.F. Olig1 and Olig2 triplication causes developmental brain defects in Down syndrome. *Nat. Neurosci.* **2010**, *13*, 927–934. [CrossRef] [PubMed]
65. Lockrow, J.; Fortress, A.; Granholm, A.-C. Age-Related Neurodegeneration and Memory Loss in Down Syndrome. *Curr. Gerontol. Geriatr. Res.* **2012**, *2012*, 463909. [CrossRef]
66. Bonni, A.; Sun, Y.; Nadal-Vicens, M.; Bhatt, A.; Frank, D.A.; Rozovsky, I.; Stahl, N.; Yancopoulos, G.D.; Greenberg, M.E. Regulation of gliogenesis in the central nervous system by the JAK-STAT signaling pathway. *Science* **1997**, *278*, 477–483. [CrossRef]
67. Hong, S.; Song, M.-R. STAT3 but not STAT1 is required for astrocyte differentiation. *PLoS ONE* **2014**, *9*, e86851. [CrossRef]
68. Kurabayashi, N.; Nguyen, M.D.; Sanada, K. DYRK1A overexpression enhances STAT activity and astrogliogenesis in a Down syndrome mouse model. *EMBO Rep.* **2015**, *16*, 1548–1562. [CrossRef]
69. Cao, F.; Hata, R.; Zhu, P.; Nakashiro, K.; Sakanaka, M. Conditional deletion of Stat3 promotes neurogenesis and inhibits astrogliogenesis in neural stem cells. *Biochem. Biophys. Res. Commun.* **2010**, *394*, 843–847. [CrossRef]
70. Corsi, M.M.; Dogliotti, G.; Pedroni, F.; Palazzi, E.; Magni, P.; Chiappelli, M.; Licastro, F. Plasma nerve growth factor (NGF) and inflammatory cytokines (IL-6 and MCP-1) in young and adult subjects with Down syndrome: An interesting pathway. *Neuro Endocrinol. Lett.* **2006**, *27*, 773–778.
71. Hallam, D.M.; Capps, N.L.; Travelstead, A.L.; Brewer, G.J.; Maroun, L.E. Evidence for an interferon-related inflammatory reaction in the trisomy 16 mouse brain leading to caspase-1-mediated neuronal apoptosis. *J. Neuroimmunol.* **2000**, *110*, 66–75. [CrossRef]
72. Lee, H.C.; Tan, K.L.; Cheah, P.S.; Ling, K.H. Potential Role of JAK-STAT Signaling Pathway in the Neurogenic-to-Gliogenic Shift in Down Syndrome Brain. *Neural Plasticity* **2016**, *2016*, 7434191. [CrossRef] [PubMed]
73. Trazzi, S.; Fuchs, C.; Valli, E.; Perini, G.; Bartesaghi, R.; Ciani, E. The amyloid precursor protein (APP) triplicated gene impairs neuronal precursor differentiation and neurite development through two different domains in the Ts65Dn mouse model for Down syndrome. *J. Biol. Chem.* **2013**, *288*, 20817–20829. [CrossRef] [PubMed]
74. Sullivan, K.D.; Lewis, H.C.; Hill, A.A.; Pandey, A.; Jackson, L.P.; Cabral, J.M.; Smith, K.P.; Liggett, L.A.; Gomez, E.B.; Galbraith, M.D.; et al. Trisomy 21 consistently activates the interferon response. *Elife* **2016**, *5*. [CrossRef]

75. Wilcock, D.M. Neuroinflammation in the aging down syndrome brain; lessons from Alzheimer's disease. *Curr. Gerontol. Geriatr. Res.* **2012**, *2012*, 170276. [CrossRef]
76. Ferrando-Miguel, R.; Shim, K.S.; Cheon, M.S.; Gimona, M.; Furuse, M.; Lubec, G. Overexpression of Interferon α/β Receptor β Chain in Fetal Down Syndrome Brain. *Neuroembryol. Aging* **2003**, *2*, 147–155. [CrossRef]
77. Guimera, J.; Casas, C.; Estivill, X.; Pritchard, M. Human minibrain homologue (MNBH/DYRK1): Characterization, alternative splicing, differential tissue expression, and overexpression in Down syndrome. *Genomics* **1999**, *57*, 407–418. [CrossRef]
78. Sun, Y.; Lehmbecker, A.; Kalkuhl, A.; Deschl, U.; Sun, W.; Rohn, K.; Tzvetanova, I.D.; Nave, K.A.; Baumgartner, W.; Ulrich, R. STAT3 represents a molecular switch possibly inducing astroglial instead of oligodendroglial differentiation of oligodendroglial progenitor cells in Theiler's murine encephalomyelitis. *Neuropathol. Appl. Neurobiol.* **2015**, *41*, 347–370. [CrossRef]
79. Corbin, J.G.; Kelly, D.; Rath, E.M.; Baerwald, K.D.; Suzuki, K.; Popko, B. Targeted CNS expression of interferon-gamma in transgenic mice leads to hypomyelination, reactive gliosis, and abnormal cerebellar development. *Mol. Cell. Neurosci.* **1996**, *7*, 354–370. [CrossRef]
80. Martí, E.; Bovolenta, P. Sonic hedgehog in CNS development: One signal, multiple outputs. *Trends Neurosci.* **2002**, *25*, 89–96. [CrossRef]
81. Alberta, J.A.; Park, S.-K.; Mora, J.; Yuk, D.-i.; Pawlitzky, I.; Iannarelli, P.; Vartanian, T.; Stiles, C.D.; Rowitch, D.H. Sonic Hedgehog Is Required during an Early Phase of Oligodendrocyte Development in Mammalian Brain. *Mol. Cell. Neurosci.* **2001**, *18*, 434–441. [CrossRef] [PubMed]
82. Danesin, C.; Agius, E.; Escalas, N.; Ai, X.; Emerson, C.; Cochard, P.; Soula, C. Ventral Neural Progenitors Switch toward an Oligodendroglial Fate in Response to Increased Sonic Hedgehog (Shh) Activity: Involvement of Sulfatase 1 in Modulating Shh Signaling in the Ventral Spinal Cord. *J. Neurosci.* **2006**, *26*, 5037. [CrossRef] [PubMed]
83. Loulier, K.; Ruat, M.; Traiffort, E. Increase of proliferating oligodendroglial progenitors in the adult mouse brain upon Sonic hedgehog delivery in the lateral ventricle. *J. Neurochem.* **2006**, *98*, 530–542. [CrossRef] [PubMed]
84. Ferent, J.; Zimmer, C.; Durbec, P.; Ruat, M.; Traiffort, E. Sonic Hedgehog Signaling Is a Positive Oligodendrocyte Regulator during Demyelination. *J. Neurosci.* **2013**, *33*, 1759. [CrossRef] [PubMed]
85. Taipale, J.; Cooper, M.K.; Maiti, T.; Beachy, P.A. Patched acts catalytically to suppress the activity of Smoothened. *Nature* **2002**, *418*, 892–896. [CrossRef] [PubMed]
86. Laouarem, Y.; Traiffort, E. Developmental and Repairing Production of Myelin: The Role of Hedgehog Signaling. *Front. Cell. Neurosci.* **2018**, *12*. [CrossRef] [PubMed]
87. Oh, S.; Huang, X.; Chiang, C. Specific requirements of sonic hedgehog signaling during oligodendrocyte development. *Dev. Dyn.* **2005**, *234*, 489–496. [CrossRef]
88. Yu, K.; McGlynn, S.; Matise, M.P. Floor plate-derived sonic hedgehog regulates glial and ependymal cell fates in the developing spinal cord. *Development* **2013**, *140*, 1594–1604. [CrossRef]
89. Trazzi, S.; Mitrugno, V.M.; Valli, E.; Fuchs, C.; Rizzi, S.; Guidi, S.; Perini, G.; Bartesaghi, R.; Ciani, E. APP-dependent up-regulation of Ptch1 underlies proliferation impairment of neural precursors in Down syndrome. *Hum. Mol. Genet.* **2011**, *20*, 1560–1573. [CrossRef]
90. Samanta, J.; Grund, E.M.; Silva, H.M.; Lafaille, J.J.; Fishell, G.; Salzer, J.L. Inhibition of Gli1 mobilizes endogenous neural stem cells for remyelination. *Nature* **2015**, *526*, 448–452. [CrossRef]
91. Tan, M.; Hu, X.; Qi, Y.; Park, J.; Cai, J.; Qiu, M. Gli3 mutation rescues the generation, but not the differentiation, of oligodendrocytes in Shh mutants. *Brain Res.* **2006**, *1067*, 158–163. [CrossRef] [PubMed]
92. Wang, L.C.; Almazan, G. Role of Sonic Hedgehog Signaling in Oligodendrocyte Differentiation. *Neurochem. Res.* **2016**, *41*, 3289–3299. [CrossRef] [PubMed]
93. Ravanelli, A.M.; Kearns, C.A.; Powers, R.K.; Wang, Y.; Hines, J.H.; Donaldson, M.J.; Appel, B. Sequential specification of oligodendrocyte lineage cells by distinct levels of Hedgehog and Notch signaling. *Dev. Biol.* **2018**, *444*, 93–106. [CrossRef] [PubMed]
94. Fischer, D.F.; van Dijk, R.; Sluijs, J.A.; Nair, S.M.; Racchi, M.; Levelt, C.N.; van Leeuwen, F.W.; Hol, E.M. Activation of the Notch pathway in Down syndrome: Cross-talk of Notch and APP. *FASEB J.* **2005**, *19*, 1451–1458. [CrossRef] [PubMed]
95. Kamakura, S.; Oishi, K.; Yoshimatsu, T.; Nakafuku, M.; Masuyama, N.; Gotoh, Y. Hes binding to STAT3 mediates crosstalk between Notch and JAK-STAT signalling. *Nat. Cell Biol.* **2004**, *6*, 547–554. [CrossRef]

96. Wu, Y.; Liu, Y.; Levine, E.M.; Rao, M.S. Hes1 but not Hes5 regulates an astrocyte versus oligodendrocyte fate choice in glial restricted precursors. *Dev. Dyn.* **2003**, *226*, 675–689. [CrossRef]
97. Logan, C.Y.; Nusse, R. The Wnt signaling pathway in development and disease. *Annu. Rev. Cell Dev. Biol.* **2004**, *20*, 781–810. [CrossRef]
98. Soomro, S.; Jie, J.; Fu, H. Oligodendrocytes Development and Wnt Signaling Pathway. *Int. J. Hum. Anat.* **2018**, *1*, 17–35. [CrossRef]
99. Granno, S.; Nixon-Abell, J.; Berwick, D.C.; Tosh, J.; Heaton, G.; Almudimeegh, S.; Nagda, Z.; Rain, J.C.; Zanda, M.; Plagnol, V.; et al. Downregulated Wnt/beta-catenin signalling in the Down syndrome hippocampus. *Sci. Rep.* **2019**, *9*, 7322. [CrossRef]
100. Emery, B. Regulation of oligodendrocyte differentiation and myelination. *Science* **2010**, *330*, 779–782. [CrossRef]
101. Fancy, S.P.; Baranzini, S.E.; Zhao, C.; Yuk, D.I.; Irvine, K.A.; Kaing, S.; Sanai, N.; Franklin, R.J.; Rowitch, D.H. Dysregulation of the Wnt pathway inhibits timely myelination and remyelination in the mammalian CNS. *Genes Dev.* **2009**, *23*, 1571–1585. [CrossRef] [PubMed]
102. Ye, F.; Chen, Y.; Hoang, T.; Montgomery, R.L.; Zhao, X.H.; Bu, H.; Hu, T.; Taketo, M.M.; van Es, J.H.; Clevers, H.; et al. HDAC1 and HDAC2 regulate oligodendrocyte differentiation by disrupting the beta-catenin-TCF interaction. *Nat. Neurosci.* **2009**, *12*, 829–838. [CrossRef] [PubMed]
103. Fu, H.; Qi, Y.; Tan, M.; Cai, J.; Takebayashi, H.; Nakafuku, M.; Richardson, W.; Qiu, M. Dual origin of spinal oligodendrocyte progenitors and evidence for the cooperative role of Olig2 and Nkx2.2 in the control of oligodendrocyte differentiation. *Development* **2002**, *129*, 681–693. [PubMed]
104. Sun, S.; Zhu, X.-J.; Huang, H.; Guo, W.; Tang, T.; Xie, B.; Xu, X.; Zhang, Z.; Shen, Y.; Dai, Z.-M.; et al. WNT signaling represses astrogliogenesis via Ngn2-dependent direct suppression of astrocyte gene expression. *Glia* **2019**, *67*, 1333–1343. [CrossRef] [PubMed]
105. Li, S.S.; Qu, Z.D.; Haas, M.; Ngo, L.; Heo, Y.J.; Kang, H.J.; Britto, J.M.; Cullen, H.D.; Vanyai, H.K.; Tan, S.S.; et al. The HSA21 gene EURL/C21ORF91 controls neurogenesis within the cerebral cortex and is implicated in the pathogenesis of Down Syndrome. *Sci. Rep.* **2016**, *6*, 14. [CrossRef] [PubMed]
106. Serrano-Pérez, M.C.; Fernández, M.; Neria, F.; Berjón-Otero, M.; Doncel-Pérez, E.; Cano, E.; Tranque, P. NFAT transcription factors regulate survival, proliferation, migration, and differentiation of neural precursor cells. *Glia* **2015**, *63*, 987–1004. [CrossRef] [PubMed]
107. Kurabayashi, N.; Sanada, K. Increased dosage of DYRK1A and DSCR1 delays neuronal differentiation in neocortical progenitor cells. *Genes Dev.* **2013**, *27*, 2708–2721. [CrossRef]
108. Baek, K.H.; Zaslavsky, A.; Lynch, R.C.; Britt, C.; Okada, Y.; Siarey, R.J.; Lensch, M.W.; Park, I.H.; Yoon, S.S.; Minami, T.; et al. Down's syndrome suppression of tumour growth and the role of the calcineurin inhibitor DSCR1. *Nature* **2009**, *459*, 1126–1130. [CrossRef]
109. Arron, J.R.; Winslow, M.M.; Polleri, A.; Chang, C.P.; Wu, H.; Gao, X.; Neilson, J.R.; Chen, L.; Heit, J.J.; Kim, S.K.; et al. NFAT dysregulation by increased dosage of DSCR1 and DYRK1A on chromosome 21. *Nature* **2006**, *441*, 595–600. [CrossRef]
110. Jung, M.S.; Park, J.H.; Ryu, Y.S.; Choi, S.H.; Yoon, S.H.; Kwen, M.Y.; Oh, J.Y.; Song, W.J.; Chung, S.H. Regulation of RCAN1 protein activity by Dyrk1A protein-mediated phosphorylation. *J. Biol. Chem.* **2011**, *286*, 40401–40412. [CrossRef]
111. Weider, M.; Starost, L.J.; Groll, K.; Kuspert, M.; Sock, E.; Wedel, M.; Frob, F.; Schmitt, C.; Baroti, T.; Hartwig, A.C.; et al. Nfat/calcineurin signaling promotes oligodendrocyte differentiation and myelination by transcription factor network tuning. *Nat. Commun.* **2018**, *9*, 899. [CrossRef] [PubMed]
112. Nalivaeva, N.N.; Turner, A.J. The amyloid precursor protein: A biochemical enigma in brain development, function and disease. *FEBS Lett.* **2013**, *587*, 2046–2054. [CrossRef] [PubMed]
113. Zhou, Z.D.; Chan, C.H.; Ma, Q.H.; Xu, X.H.; Xiao, Z.C.; Tan, E.K. The roles of amyloid precursor protein (APP) in neurogenesis: Implications to pathogenesis and therapy of Alzheimer disease. *Cell Adhes. Migr.* **2011**, *5*, 280–292. [CrossRef] [PubMed]
114. Guidi, S.; Emili, M.; Giacomini, A.; Stagni, F.; Bartesaghi, R. Neuroanatomical alterations in the temporal cortex of human fetuses with Down syndrome. In Proceedings of the 2nd International Conference of the Trisomy 21 Research Society, Chicago, IL, USA, 7–11 June 2017; p. 79.

115. Hof, P.R.; Bouras, C.; Perl, D.P.; Sparks, D.L.; Mehta, N.; Morrison, J.H. Age-related distribution of neuropathologic changes in the cerebral cortex of patients with Down's syndrome. Quantitative regional analysis and comparison with Alzheimer's disease. *Arch. Neurol.* **1995**, *52*, 379–391. [CrossRef] [PubMed]
116. Hyman, B.T.; West, H.L.; Rebeck, G.W.; Lai, F.; Mann, D.M. Neuropathological changes in Down's syndrome hippocampal formation. Effect of age and apolipoprotein E genotype. *Arch. Neurol.* **1995**, *52*, 373–378. [CrossRef] [PubMed]
117. Leverenz, J.B.; Raskind, M.A. Early amyloid deposition in the medial temporal lobe of young Down syndrome patients: A regional quantitative analysis. *Exp. Neurol.* **1998**, *150*, 296–304. [CrossRef] [PubMed]
118. Trazzi, S.; Fuchs, C.; De Franceschi, M.; Mitrugno, V.M.; Bartesaghi, R.; Ciani, E. APP-dependent alteration of GSK3β activity impairs neurogenesis in the Ts65Dn mouse model of Down syndrome. *Neurobiol. Dis.* **2014**, *67*, 24–36. [CrossRef]
119. Ballabh, P. Intraventricular hemorrhage in premature infants: Mechanism of disease. *Pediatr. Res.* **2010**, *67*, 1–8. [CrossRef]
120. Dummula, K.; Vinukonda, G.; Chu, P.; Xing, Y.; Hu, F.; Mailk, S.; Csiszar, A.; Chua, C.; Mouton, P.; Kayton, R.J.; et al. Bone morphogenetic protein inhibition promotes neurological recovery after intraventricular hemorrhage. *J. Neurosci.* **2011**, *31*, 12068–12082. [CrossRef]
121. Dohare, P.; Cheng, B.; Ahmed, E.; Yadala, V.; Singla, P.; Thomas, S.; Kayton, R.; Ungvari, Z.; Ballabh, P. Glycogen synthase kinase-3β inhibition enhances myelination in preterm newborns with intraventricular hemorrhage, but not recombinant Wnt3A. *Neurobiol. Dis.* **2018**, *118*, 22–39. [CrossRef]
122. Sugaya, K. Mechanism of glial differentiation of neural progenitor cells by amyloid precursor protein. *Neurodegener. Dis.* **2008**, *5*, 170–172. [CrossRef]
123. Roth, A.D.; Ramirez, G.; Alarcon, R.; Von Bernhardi, R. Oligodendrocytes damage in Alzheimer's disease: Beta amyloid toxicity and inflammation. *Biol. Res.* **2005**, *38*, 381–387. [CrossRef]
124. Kremer, D.; Akkermann, R.; Küry, P.; Dutta, R. Current advancements in promoting remyelination in multiple sclerosis. *Mult. Scler.* **2019**, *25*, 7–14. [CrossRef] [PubMed]
125. Küry, P.; Kremer, D.; Göttle, P. Drug repurposing for neuroregeneration in multiple sclerosis. *Neural Regen. Res.* **2018**, *13*, 1366–1367. [CrossRef] [PubMed]
126. Azim, K.; Angonin, D.; Marcy, G.; Pieropan, F.; Rivera, A.; Donega, V.; Cantu, C.; Williams, G.; Berninger, B.; Butt, A.M.; et al. Pharmacogenomic identification of small molecules for lineage specific manipulation of subventricular zone germinal activity. *PLoS Biol.* **2017**, *15*, e2000698. [CrossRef] [PubMed]
127. Preisner, A.; Albrecht, S.; Cui, Q.L.; Hucke, S.; Ghelman, J.; Hartmann, C.; Taketo, M.M.; Antel, J.; Klotz, L.; Kuhlmann, T. Non-steroidal anti-inflammatory drug indometacin enhances endogenous remyelination. *Acta Neuropathol.* **2015**, *130*, 247–261. [CrossRef]
128. Najm, F.J.; Madhavan, M.; Zaremba, A.; Shick, E.; Karl, R.T.; Factor, D.C.; Miller, T.E.; Nevin, Z.S.; Kantor, C.; Sargent, A.; et al. Drug-based modulation of endogenous stem cells promotes functional remyelination in vivo. *Nature* **2015**, *522*, 216–220. [CrossRef]
129. Chen, Y.; Zhen, W.; Guo, T.; Zhao, Y.; Liu, A.; Rubio, J.P.; Krull, D.; Richardson, J.C.; Lu, H.; Wang, R. Histamine Receptor 3 negatively regulates oligodendrocyte differentiation and remyelination. *PLoS ONE* **2017**, *12*, e0189380. [CrossRef]
130. Schwartzbach, C.J.; Grove, R.A.; Brown, R.; Tompson, D.; Then Bergh, F.; Arnold, D.L. Lesion remyelinating activity of GSK239512 versus placebo in patients with relapsing-remitting multiple sclerosis: A randomised, single-blind, phase II study. *J. Neurol.* **2017**, *264*, 304–315. [CrossRef]
131. Mei, F.; Fancy, S.P.J.; Shen, Y.A.; Niu, J.; Zhao, C.; Presley, B.; Miao, E.; Lee, S.; Mayoral, S.R.; Redmond, S.A.; et al. Micropillar arrays as a high-throughput screening platform for therapeutics in multiple sclerosis. *Nature Med.* **2014**, *20*, 954–960. [CrossRef]
132. Green, A.J.; Gelfand, J.M.; Cree, B.A.; Bevan, C.; Boscardin, W.J.; Mei, F.; Inman, J.; Arnow, S.; Devereux, M.; Abounasr, A.; et al. Clemastine fumarate as a remyelinating therapy for multiple sclerosis (ReBUILD): A randomised, controlled, double-blind, crossover trial. *Lancet* **2017**, *390*, 2481–2489. [CrossRef]
133. Hammond, T.R.; McEllin, B.; Morton, P.D.; Raymond, M.; Dupree, J.; Gallo, V. Endothelin-B Receptor Activation in Astrocytes Regulates the Rate of Oligodendrocyte Regeneration during Remyelination. *Cell Rep.* **2015**, *13*, 2090–2097. [CrossRef] [PubMed]

134. Wu, X.; Qu, X.; Zhang, Q.; Dong, F.; Yu, H.; Yan, C.; Qi, D.; Wang, M.; Liu, X.; Yao, R. Quercetin promotes proliferation and differentiation of oligodendrocyte precursor cells after oxygen/glucose deprivation-induced injury. *Cell Mol. Neurobiol.* **2014**, *34*, 463–471. [CrossRef] [PubMed]
135. Fancy, S.P.; Harrington, E.P.; Yuen, T.J.; Silbereis, J.C.; Zhao, C.; Baranzini, S.E.; Bruce, C.C.; Otero, J.J.; Huang, E.J.; Nusse, R.; et al. Axin2 as regulatory and therapeutic target in newborn brain injury and remyelination. *Nat. Neurosci.* **2011**, *14*, 1009–1016. [CrossRef] [PubMed]
136. Rafalski, V.A.; Ho, P.P.; Brett, J.O.; Ucar, D.; Dugas, J.C.; Pollina, E.A.; Chow, L.M.; Ibrahim, A.; Baker, S.J.; Barres, B.A.; et al. Expansion of oligodendrocyte progenitor cells following SIRT1 inactivation in the adult brain. *Nat. Cell Biol.* **2013**, *15*, 614–624. [CrossRef] [PubMed]
137. Prozorovski, T.; Ingwersen, J.; Lukas, D.; Göttle, P.; Koop, B.; Graf, J.; Schneider, R.; Franke, K.; Schumacher, S.; Britsch, S.; et al. Regulation of sirtuin expression in autoimmune neuroinflammation: Induction of SIRT1 in oligodendrocyte progenitor cells. *Neurosci. Lett.* **2019**, *704*, 116–125. [CrossRef]
138. Kang, W.; Nguyen, K.C.Q.; Hebert, J.M. Transient Redirection of SVZ Stem Cells to Oligodendrogenesis by FGFR3 Activation Promotes Remyelination. *Stem Cell Rep.* **2019**, *12*, 1223–1231. [CrossRef]
139. Kuro-o, M. Klotho. *Pflug. Arch.* **2010**, *459*, 333–343. [CrossRef]
140. Torbus-Paluszczak, M.; Bartman, W.; Adamczyk-Sowa, M. Klotho protein in neurodegenerative disorders. *Neurol. Sci.* **2018**, *39*, 1677–1682. [CrossRef]
141. Zare, L.; Baharvand, H.; Javan, M. In vivo conversion of astrocytes to oligodendrocyte lineage cells using chemicals: Targeting gliosis for myelin repair. *Regen. Med.* **2018**, *13*, 803–819. [CrossRef]
142. Khalaj, A.J.; Hasselmann, J.; Augello, C.; Moore, S.; Tiwari-Woodruff, S.K. Nudging oligodendrocyte intrinsic signaling to remyelinate and repair: Estrogen receptor ligand effects. *J. Steroid Biochem. Mol. Biol.* **2016**, *160*, 43–52. [CrossRef] [PubMed]
143. Li, W.J.; Mao, F.X.; Chen, H.J.; Qian, L.H.; Buzby, J.S. Treatment with UDP-glucose, GDNF, and memantine promotes SVZ and white matter self-repair by endogenous glial progenitor cells in neonatal rats with ischemic PVL. *Neuroscience* **2015**, *284*, 444–458. [CrossRef] [PubMed]
144. Rajkowska, G.; Mahajan, G.; Maciag, D.; Sathyanesan, M.; Iyo, A.H.; Moulana, M.; Kyle, P.B.; Woolverton, W.L.; Miguel-Hidalgo, J.J.; Stockmeier, C.A.; et al. Oligodendrocyte morphometry and expression of myelin—Related mRNA in ventral prefrontal white matter in major depressive disorder. *J. Psychiatr. Res.* **2015**, *65*, 53–62. [CrossRef] [PubMed]
145. Meffre, D.; Massaad, C.; Grenier, J. Lithium chloride stimulates PLP and MBP expression in oligodendrocytes via Wnt/beta-catenin and Akt/CREB pathways. *Neuroscience* **2015**, *284*, 962–971. [CrossRef] [PubMed]
146. Ghareghani, M.; Sadeghi, H.; Zibara, K.; Danaei, N.; Azari, H.; Ghanbari, A. Melatonin Increases Oligodendrocyte Differentiation in Cultured Neural Stem Cells. *Cell. Mol. Neurobiol.* **2017**, *37*, 1319–1324. [CrossRef]
147. Blanchard, B.; Heurtaux, T.; Garcia, C.; Moll, N.M.; Caillava, C.; Grandbarbe, L.; Klosptein, A.; Kerninon, C.; Frah, M.; Coowar, D.; et al. Tocopherol derivative TFA-12 promotes myelin repair in experimental models of multiple sclerosis. *J. Neurosci.* **2013**, *33*, 11633–11642. [CrossRef]
148. Das, I.; Park, J.-M.; Shin, J.H.; Jeon, S.K.; Lorenzi, H.; Linden, D.J.; Worley, P.F.; Reeves, R.H. Hedgehog agonist therapy corrects structural and cognitive deficits in a Down syndrome mouse model. *Sci. Transl. Med.* **2013**, *5*, 201ra120. [CrossRef]
149. Wang, J.; Ye, Z.; Zheng, S.; Chen, L.; Wan, Y.; Deng, Y.; Yang, R. Lingo-1 shRNA and Notch signaling inhibitor DAPT promote differentiation of neural stem/progenitor cells into neurons. *Brain Res.* **2016**, *1634*, 34–44. [CrossRef]
150. Imamura, O.; Arai, M.; Dateki, M.; Takishima, K. Donepezil promotes differentiation of neural stem cells into mature oligodendrocytes at the expense of astrogenesis. *J. Neurochem.* **2017**, *140*, 231–244. [CrossRef]
151. Cui, X.; Guo, Y.E.; Fang, J.H.; Shi, C.J.; Suo, N.; Zhang, R.; Xie, X. Donepezil, a drug for Alzheimer's disease, promotes oligodendrocyte generation and remyelination. *Acta Pharmacol. Sin* **2019**. [CrossRef]
152. Kang, M.L.; Kwon, J.S.; Kim, M.S. Induction of neuronal differentiation of rat muscle-derived stem cells in vitro using basic fibroblast growth factor and ethosuximide. *Int. J. Mol. Sci.* **2013**, *14*, 6614–6623. [CrossRef] [PubMed]
153. Setoguchi, T.; Kondo, T. Nuclear export of OLIG2 in neural stem cells is essential for ciliary neurotrophic factor-induced astrocyte differentiation. *J. Cell Biol.* **2004**, *166*, 963–968. [CrossRef] [PubMed]

154. Zare, L.; Baharvand, H.; Javan, M. Trichostatin A Promotes the Conversion of Astrocytes to Oligodendrocyte Progenitors in a Defined Culture Medium. *Iran J. Pharm. Res.* **2019**, *18*, 286–295. [PubMed]
155. Ghasemi-Kasman, M.; Zare, L.; Baharvand, H.; Javan, M. In vivo conversion of astrocytes to myelinating cells by miR-302/367 and valproate to enhance myelin repair. *J. Tissue Eng. Regen. Med.* **2018**, *12*, e462–e472. [CrossRef] [PubMed]
156. Farhangi, S.; Dehghan, S.; Totonchi, M.; Javan, M. In vivo conversion of astrocytes to oligodendrocyte lineage cells in adult mice demyelinated brains by Sox2. *Mult. Scler. Relat. Disord.* **2019**, *28*, 263–272. [CrossRef] [PubMed]
157. Hack, M.A.; Saghatelyan, A.; de Chevigny, A.; Pfeifer, A.; Ashery-Padan, R.; Lledo, P.M.; Gotz, M. Neuronal fate determinants of adult olfactory bulb neurogenesis. *Nat. Neurosci.* **2005**, *8*, 865–872. [CrossRef]
158. Maire, C.L.; Wegener, A.; Kerninon, C.; Nait Oumesmar, B. Gain-of-function of Olig transcription factors enhances oligodendrogenesis and myelination. *Stem Cells* **2010**, *28*, 1611–1622. [CrossRef]
159. Jessberger, S.; Toni, N.; Clemenson, G.D., Jr.; Ray, J.; Gage, F.H. Directed differentiation of hippocampal stem/progenitor cells in the adult brain. *Nat. Neurosci.* **2008**, *11*, 888–893. [CrossRef]
160. Braun, S.M.; Pilz, G.A.; Machado, R.A.; Moss, J.; Becher, B.; Toni, N.; Jessberger, S. Programming Hippocampal Neural Stem/Progenitor Cells into Oligodendrocytes Enhances Remyelination in the Adult Brain after Injury. *Cell Rep.* **2015**, *11*, 1679–1685. [CrossRef]
161. Gardiner, K.; Costa, A.C. The proteins of human chromosome 21. *Am. J. Med. Genet C Semin Med. Genet.* **2006**, *142C*, 196–205. [CrossRef]
162. Wiseman, F.K.; Alford, K.A.; Tybulewicz, V.L.J.; Fisher, E.M.C. Down syndrome-recent progress and future prospects. *Hum. Mol. Genet.* **2009**, *18*, R75–R83. [CrossRef] [PubMed]
163. Kang, H.J.; Kawasawa, Y.I.; Cheng, F.; Zhu, Y.; Xu, X.; Li, M.; Sousa, A.M.; Pletikos, M.; Meyer, K.A.; Sedmak, G.; et al. Spatio-temporal transcriptome of the human brain. *Nature* **2011**, *478*, 483–489. [CrossRef] [PubMed]
164. Yeung, M.S.; Zdunek, S.; Bergmann, O.; Bernard, S.; Salehpour, M.; Alkass, K.; Perl, S.; Tisdale, J.; Possnert, G.; Brundin, L.; et al. Dynamics of oligodendrocyte generation and myelination in the human brain. *Cell* **2014**, *159*, 766–774. [CrossRef] [PubMed]
165. Herault, Y.; Delabar, J.M.; Fisher, E.M.C.; Tybulewicz, V.L.J.; Yu, E.; Brault, V. Rodent models in Down syndrome research: Impact and future opportunities. *Dis. Model. Mech.* **2017**, *10*, 1165–1186. [CrossRef] [PubMed]
166. Gupta, M.; Dhanasekaran, A.R.; Gardiner, K.J. Mouse models of Down syndrome: Gene content and consequences. *Mamm. Genome* **2016**, *27*, 538–555. [CrossRef] [PubMed]

frontiers in Cellular Neuroscience

ORIGINAL RESEARCH
published: 16 March 2021
doi: 10.3389/fncel.2021.653075

C21orf91 Regulates Oligodendroglial Precursor Cell Fate—A Switch in the Glial Lineage?

*Laura Reiche[1], Peter Göttle[1], Lydie Lane[2,3], Paula Duek[2,3], Mina Park[1], Kasum Azim[1], Jana Schütte[1], Anastasia Manousi[1], Jessica Schira-Heinen[1] and Patrick Küry[1]**

[1]Department of Neurology, Medical Faculty, Heinrich-Heine-University Düsseldorf, Düsseldorf, Germany, [2]CALIPHO Group, SIB Swiss Institute of Bioinformatics, Geneva, Switzerland, [3]Department of Microbiology and Molecular Medicine, Faculty of Medicine, University of Geneva, Geneva, Switzerland

Neuropathological diseases of the central nervous system (CNS) are frequently associated with impaired differentiation of the oligodendroglial cell lineage and subsequent alterations in white matter structure and dynamics. Down syndrome (DS), or trisomy 21, is the most common genetic cause for cognitive impairments and intellectual disability (ID) and is associated with a reduction in the number of neurons and oligodendrocytes, as well as with hypomyelination and astrogliosis. Recent studies mainly focused on neuronal development in DS and underestimated the role of glial cells as pathogenic players. This also relates to C21ORF91, a protein considered a key modulator of aberrant CNS development in DS. We investigated the role of C21orf91 ortholog in terms of oligodendrogenesis and myelination using database information as well as through cultured primary oligodendroglial precursor cells (OPCs). Upon modulation of *C21orf91* gene expression, we found this factor to be important for accurate oligodendroglial differentiation, influencing their capacity to mature and to myelinate axons. Interestingly, C21orf91 overexpression initiates a cell population coexpressing astroglial- and oligodendroglial markers indicating that elevated C21orf91 expression levels induce a gliogenic shift towards the astrocytic lineage reflecting non-equilibrated glial cell populations in DS brains.

Keywords: white matter deficits, gliogenesis, cell fate, down syndrome, neuroregeneration

Abbreviations: ACSA-1/GLAST, astrocyte cell surface antigen-1; ACTB, ß-actin; aNSC(s), adult neural stem cell(s); APC/CC1, adenomatous polyposis coli protein (antibody clone CC1); BFGF, basic fibroblast growth factor; BSA, bovine serum albumin; CC, corpus callosum; CNS, central nervous system; CNPase, 2′,3′-cyclic-nucleotide 3′-phosphodiesterase; DIV, days *in vitro*; DS, Down syndrome; ENPP2/autotaxin, ectonucleotide pyrophosphatase/phosphodiesterase 2; EURL, early undifferentiated retina and lense; FB, forebrain; FBS, fetal bovine serum; GAPDH, glyceraldehyde 3-phosphate dehydrogenase; GEO, Gene Expression Omnibus; GFAP, glial fibrillary acid protein; GFP, green fluorescent protein; GM, gray matter; Gpr17, G protein-coupled receptor-17; Hes1, hairy and enhancer of split-1; HF, hippocampal formation; HOXD1, homeobox protein Hox-D1; HRP, horse radish peroxidase; HS, hemisphere; HSA21, human chromosome 21; HSPA2, heat shock protein family A (Hsp70) member 2; ID, intellectual disability; iPSC, induced pluripotent stem cell; MAG, myelin associated glycoprotein; MBP, myelin basic protein; MMU16, mouse chromosome 16; MOG, myelin oligodendrocyte glycoprotein; MS, multiple sclerosis; Myrf, myelin regulatory factor; NeuN, neuronal nuclei antigen; Nkx2.2, NK2 homeobox 2; Olig2, oligodendrocyte transcription factor 2; OPC(s), oligodendroglial precursor cell(s); PBS, phosphate buffered saline; pcw, post-conceptional weeks; PDGF, platelet-derived growth factor; PDGFR, platelet-derived growth factor receptor; PFA, paraformaldehyde; PKD1, polycystic kidney disease 1/polycystin 1; PLD1, phospholipidase D1; Plp1, proteolipid protein-1; PRRG1, proline rich and gla domain 1; PRR5L, proline rich 5 like; RNA, ribonucleic acid; RNAseq, RNA sequencing; RPKM, reads per kilo base per million mapped reads; RT, room temperature; SLC44A1, solute carrier family 44 member 1; Sox10, sex-determining region Y-box 10; SVZ, subventricular zone; TAP, transiently amplifying progenitor; TBS(-T), Tris-buffered saline (supplemented with Triton); TPM, transcripts per kilobase million; qRT-PCR, quantitative reverse transcription polymerase chain reaction; Wnt, wingless and integration site.

OPEN ACCESS

Edited by:
Christian Lohr,
University of Hamburg, Germany

Reviewed by:
Maria Cecilia Angulo,
Centre National de la Recherche Scientifique (CNRS), France
Yannick Poitelon,
Albany Medical College, United States
Marta Boccazzi,
University of Milan, Italy

***Correspondence:**
Patrick Küry
kuery@hhu.de

Specialty section:
This article was submitted to Non-Neuronal Cells, a section of the journal Frontiers in Cellular Neuroscience

Received: *13 January 2021*
Accepted: *22 February 2021*
Published: *16 March 2021*

Citation:
Reiche L, Göttle P, Lane L, Duek P, Park M, Azim K, Schütte J, Manousi A, Schira-Heinen J and Küery P (2021) C21orf91 Regulates Oligodendroglial Precursor Cell Fate—A Switch in the Glial Lineage? Front. Cell. Neurosci. 15:653075. doi: 10.3389/fncel.2021.653075

INTRODUCTION

White matter, which makes up approximately 40% of the human brain, consists of axons, astrocytes, and myelin, the latter of which is imperative for stabilization, protection, and electrical insulation of axons enabling accelerated electrical signal propagation. In the adult central nervous system (CNS), myelin is generated by oligodendrocytes, either deriving from oligodendroglial precursor cells (OPCs) or niche-located adult neural stem cells (aNSCs; Akkermann et al., 2017). The structural integrity of myelin is of crucial importance for CNS function and restoration (Snaidero and Simons, 2014), making it vulnerable to pathological degeneration and inflammation (Waxman, 1992) or genetic intervention (Nave, 1994). Myelin loss, therefore, leads to impaired neuronal signaling, functional deficits, and shortened lifetime (Wilkins et al., 2003). Moreover, axonal nutrition has recently been shown to depend on myelin and oligodendrocytes (Simons and Nave, 2015). Hence, white matter deficits and myelin dysfunctions are considered a main contributing factor for neurodegenerative diseases and malfunctions of the CNS (Bercury and Macklin, 2015).

Down syndrome (DS) results from a trisomy of human chromosome (HSA) 21 and represents the most common genetic cause for cognitive impairments and intellectual disability (ID). The neurological profile of DS patients is characterized by hypotrophy and hypocellularity of neurons (reviewed by Stagni et al., 2017; Baburamani et al., 2019) and oligodendrocytes (Karlsen and Pakkenberg, 2011) accompanied by hypomyelination in the hippocampal formation (Abraham et al., 2012), whereas astroglial cell numbers are increased (Mito and Becker, 1993; Zdaniuk et al., 2011). DS astrocytes also show alterations in the structure and intracellular protein expression (Dossi et al., 2018). Moreover, structural and functional abnormalities of DS white matter were described (Fenoll et al., 2017).

Several studies indicate that white matter malformation contributes to neurological impairment in DS patients (Powell et al., 2014; Fenoll et al., 2017) and that hypomyelination is caused by a cell-autonomous phenomenon in oligodendrocyte development (Olmos-Serrano et al., 2016)—a research focus that has, nevertheless, not been paid much attention so far (Reiche et al., 2019). Olmos-Serrano et al. (2016) revealed a module (termed as M43) enriched in genes associated with oligodendrocyte differentiation and myelination to exhibit a distinct downregulation in several DS brain regions such as the hippocampus throughout development. Among genes such as *CNP*, *PLP1*, *SOX10*, and *GPR17*, also *C21ORF91* is listed within this cluster. Also known as *early undifferentiated retina and lens* (*EURL*), *C21ORF91* is localized at the centromeric boundary of the DS critical region (DSCR; encompassing 21q21-21q22.3) and was initially described to play a role in defective DS neurogenesis (Li et al., 2016). There, it was shown that *C21ORF91*'s transcript levels within the tested DS brain regions exhibited a spatiotemporal increase compared to equivalent controls. Furthermore, in DS lymphoblastoid cells, *C21ORF91* is overexpressed with a mean ratio close to 1.5, which is proportional to the gene dosage effect of trisomy 21, thus implied to be involved in the DS phenotype (Ait Yahya-Graison et al., 2007). Indeed, *C21ORF91* has previously been suggested to be relevant for the observed neurodevelopmental disorder and ID arising from HSA21 triplication (Slavotinek et al., 2000; Rost et al., 2004; Korbel et al., 2009; Li et al., 2016). Although expressed ubiquitously in healthy human tissues, C21orf91 protein was shown to be enriched in oligodendrocytes along with other proteins important for their differentiation such as Olig2 (Cahoy et al., 2008). Moreover, *C21ORF91* expression in the healthy human brain peaks between birth and adulthood (Li et al., 2016), hence coinciding with the onset and progression of myelination. Interestingly, cognitive deficits and hypomyelinated patterns in DS are thought to arise during these early stages of life and increase during development (Pennington et al., 2003; Rowe et al., 2006; Lanfranchi et al., 2010; Abraham et al., 2012). Based on these parallels as well as on the here presented functional data, a possible correlation between elevated C21orf91 expression levels and myelination deficits as observed in DS can be suggested.

MATERIALS AND METHODS

Data Mining/Human C21ORF91 Correlations

RNA sequencing (RNAseq) and microarray data for humans were retrieved from Genevestigator (version 7.4.0; Hruz et al., 2008), a curated database that performs meta-analyses of gene expression data on a large panel of tissues and cell types of different experiments. For RNAseq data, 285 human tissues and cells were analyzed for their *C21ORF91* expression level. Gene expression was measured in transcripts per million (TMP). High expression as considered by Genevestigator corresponds to the log(2) of the average of the mean value higher than 3. For microarray data, 416 human tissues and cells were analyzed for their *C21ORF91* expression level. Gene expression is expressed as relative mean values. High expression as considered by Genevestigator corresponds to higher than 12.

C21ORF91 RNAseq expression data on the human developmental and adult brain for 26 different brain structures expressed as the mean of reads per kilobase million (RPKM) values was retrieved from the Allen Brain Atlas (October 2019 and November 2020). Brain structures were grouped in *allocortex* (hippocampus); *basal ganglia* (striatum); *neural plate* (dorsolateral prefrontal cortex, ventrolateral prefrontal cortex, anterior (rostral) cingulate (medial prefrontal) cortex, orbital frontal cortex, primary motor-sensory cortex, parietal neocortex, posterior (caudal) superior temporal cortex (area 22c), inferolateral temporal cortex (area TEv, area 20), occipital neocortex, amygdaloid complex, upper (rostral) rhombic lip, temporal neocortex, the primary motor cortex (area M1, area 4), the primary somatosensory cortex (area S1, areas 3, 1, 2), posteroventral (inferior) parietal cortex, primary auditory cortex (core), primary visual cortex (striate cortex, area V1/17), cerebellum, cerebellar cortex) and *thalamus* (dorsal thalamus, mediodorsal nucleus of the thalamus). These grouped brain structures were analyzed for the following grouped ages: 8 and

9 post-conception weeks (pcw), 12 and 13 pcw, 16 and 17 pcw, 19 and 21 pcw, 24–26 pcw (24, 25 and 26 pcw), 35–37 pcw, 4 and 10 months, 1–4 (1, 2, 3 and 4 years), 8–15 (8, 11, 13 and 15 years), 18–23 (18, 19, 21 and 23 years) and 30–40 (30, 36, 37 and 40 years). Data from the *ventricular zone* (lateral ganglionic eminence, medial ganglionic eminence, caudal ganglionic eminence) was available only for 8 and 9 pcw and was therefore omitted.

To obtain additional data on *C21ORF91* expression in the nervous system, we used the Brain EXPression Database (BrainEXP; Jiao et al., 2019), which performs a meta-analysis of microarray and RNAseq data in a subset of nervous system tissues consisting of 4567 samples from 2863 healthy individuals gathered from public databases and their data. The spinal cord, substantia nigra, hippocampus, hypothalamus, amygdala, putamen, caudate nucleus, nucleus accumbens, frontal cortex, BA9, anterior cingulate cortex, cerebellum, and cerebellar hemisphere could be analyzed and compared.

The heatmap displayed in the Allen Brain Atlas database (Sunkin et al., 2013) representing z-scores values of the microarray data for six adult donors was surveyed to identify structures with the highest *C21ORF91* expression. The four probes refer to *C21ORF91* sequences on the microarray chip: A_23_P211015 (GGT GAG GTA GAG CAA CTG AAT GCA AAG CTC CTA CAG CAA ATC CAG GAA GTT TTT GAA GAG); A_24_P125839 (AGT AGG GCG AAC AGG AAT GAA GTC GCA CCT ACC CAT AAA CAA CTG ACC TAA ACA GAC TT), CUST_5965_PI416261804 (ATT CGA TGA CTC TTG GTG AGG TAG AGC AAC TGA ATG CAA AGC TCC TAC AGC AAA TCC AG) and CUST_5966_PI416261804 (GAA AAA AGA AGA GAC AAT CTC TAG TCC AGA GGC TAA TGT CCA GAC CCA GCA TCC ACA TTA).

To characterize *C21ORF91* expression on a cellular level, single-nucleus RNAseq data (Allen Brain Atlas) was collected from two sets. The first covers multiple adult human cortical areas (MCA) including the middle temporal gyrus, anterior cingulate cortex, primary visual cortex, primary motor cortex, primary somatosensory cortex, and primary auditory cortex. The second experiment included specifically the adult primary motor cortex (M1). Single-nucleus RNAseq is expressed as counts per million (cpm) trimmed means.

To set-up a coexpressed gene cluster for *C21ORF91*, a list of genes whose expression positively correlates with *C21ORF91* in the adult brain was extracted using the "Correlate Gene Search" functionality appended to the microarray expression data from adult donors provided by the Allen Brain Atlas. Also, coexpression data from the BrainEXP database (Jiao et al., 2019) was retrieved with the default parameters. The genes coexpressing with *C21ORF91* were further analyzed to identify if they coexpress with each other.

Gene ontology (GO) enrichment analysis on the coexpression set from the adult brain microarray from Allen Brain Atlas was performed using PANTHER [(Thomas et al., 2003, 2006); RRID: SCR_004869; released 20190711] including GO biological process, molecular function and cellular component terms.

C21ORF91 homologs were searched by protein BLAST at NCBI. Reciprocal best hits were considered as orthologs. Homology in jawless fishes was searched by tBLASTn with human and zebrafish protein sequences as queries against RefSeq Genome and nucleotide collection databases.

Gene Expression Heatmap Generation

Bulk transcriptomic datasets assembled as done previously were used for defining the expression of *D16Ertd472* mouse *C21orf91* ortholog, further referred to as *C21orf91*) across multiple cell types that are present in the forebrain (Azim et al., 2017, 2018), and Gene Expression Omnibus (GEO) repository IDs are stated. These included substages of postnatal oligodendroglia (GSE9566; P16); early postnatal neural stem cells (NSCs) and transiently amplifying progenitors (TAPs; GSE60905); young adult substages of NSCs (GSE54653); young adult neuroblasts and ependymal cells (GSE18765); young adult choroid plexus cells (GSE82308); young adult and postnatal astrocytes (GSE35338, GSE9566); young adult microglia (GSE58483) and embryonic day 14 radial glial cells (vRGS; GSE40582). All analyses were performed in RStudio using publicly available packages installed directly from the Bioconductor consortium[1]. The LIMMA package was used to incorporate all datasets described above systematically which were then subsequently normalized using the standard RMA method. Known oligodendroglial, astrocyte, and NSC lineage markers were additionally studied for heatmap plotting purposes by taking the most significant probes for each gene (differential expression by <0.0001 False Discovery Rate between the individual cell types studied). The selected genes were visualized in an unsupervised heatmap using the pHeatmap package[2].

Brain Tissue Preparation, Sectioning, and Immunohistochemistry

For the analysis of transcript and protein levels of *RGD1563888* (rat *C21orf91* ortholog, further referred to as *C21orf91*), embryonic day 16 (E16), postnatal day 0 (P0), P7, P25, and adult (2–3 months) Wistar rats of either sex were deeply anesthetized and killed by an overdose of isoflurane (Piramal-Healthcare, Mumbai, India). Rat brains were isolated, shortly surface-washed with ice-cold Dulbecco's phosphate-buffered saline (PBS; Sigma-Aldrich, St. Louis, USA), and then frozen in −35°C to −50°C methyl butane and stored at −80°C until further processing. Regions of interest including whole hemisphere (HS), forebrain (FB), corpus callosum (CC), hippocampal formation (HF), and cerebellum (CB) were sectioned coronally using a cryostat (Leica CM3050S) at −28°C. Out of 50–100 μm thick slices, smaller regions (CC and HF) were isolated using a pre-cooled scalpel within the cryostat chamber. Note, that P0 tissue sections were used exclusively for Western blot analysis. Tissues were stored at −80°C.

For immunohistochemistry, P7 brains were directly processed, while adult rats were transcardially perfused with 150 ml ice-cold Dulbecco's phosphate-buffered saline (PBS; Sigma-Aldrich, St. Louis, MO, USA) followed by 400 ml 4% paraformaldehyde (PFA). Rat brains were harvested and

[1]https://www.bioconductor.org/packages/devel/workflows/vignettes/arrays/inst/doc/arrays.html

[2]https://cran.r-project.org/web/packages/pheatmap/index.html

post-fixed for 2 days (P7 brains) or overnight (adult brains) in 4% PFA at 4°C, followed by 48 h cryoprotective dehydration in 30% sucrose (in PBS) at 4°C. Brains were embedded in TissueTek OCT (Sakura Finetek Europe, Netherlands), frozen in −35°C to −50°C methyl butane, and stored at −80°C until preparation of 14 µm coronal sections using a cryostat (Leica CM3050S). Sections were stored at −80°C.

Immunohistochemical staining was performed as previously described (Beyer et al., 2020). Briefly, thawed brain sections were air-dried for at least 15 min at room temperature (RT), rehydrated in distilled water for 5 min, transferred to −20°C acetone for 5 min, and washed in 1× Tris-buffered saline (TBS; pH 7.6) and 1× TBS-T (TBS containing 0.02% Triton X-100) for 5 min each. Non-specific staining was blocked with 10% biotin-free bovine serum albumin (BSA; in TBS-T) for 1 h at RT, followed by application of the following antibodies (in 10% BSA in TBS) and incubation overnight at 4°C: rabbit anti-C21orf91 [1:1,000, Santa Cruz Biotechnology, Cat# sc-83610 (Li et al., 2016)], rabbit anti-C21orf91 (1:200, Bioss, Cat# bs-9983R), rabbit anti-C21orf91 (1:300, Sigma-Aldrich, Cat# HPA049030), mouse anti-neuronal nuclei antigen (NeuN; 1:1,000, Merck Millipore, Cat# MAB377), goat anti-PDGFR (alpha/CD140A, 1:250, Neuromics, Cat# GT15150), mouse anti-oligodendrocyte transcription factor 2 (Olig2; 1:500, Merck Millipore, Cat# MABN50), guinea pig anti-glial fibrillary acidic protein (GFAP; 1:2,000, Synaptic Systems, Cat# 173004), and mouse anti-adenomatous polyposis coli for oligodendrocytes (APC, CC1; 1:500, GeneTex, Cat# GTX16794). Sections were washed two times for 5 min in TBS and incubated with the species-appropriate fluorochrome-conjugated secondary antibodies (1:200 in PBS; donkey: anti-goat; goat: anti-rabbit, anti-mouse, anti-guinea pig; Alexa Fluor488- or Alexa Fluor594-conjugated) and DAPI (4,6-diamidino-2-phenylindole; nuclei labeling, 0.04 µl/ml; Roche Diagnostic GmbH) for 1 h at RT. Slices were mounted with Immu-Mount (Thermo Fisher Scientific, Darmstadt, Germany) and analyzed using a confocal laser scanning microscope 510 (CLSM 510, Zeiss, Jena, Germany) and the ImageJ BioVoxxel software (Schindelin et al., 2012). Z-stacked tile scans on average eight brain slices per marker and time-point (two slices per animal) were fused to a maximum intensity projection *via* ImageJ. C21orf91-positive cells within the whole tile scan projection were counted and normalized to its area [mm^2], distinguishing between CC and surrounding gray matter structures (GM). Then, on the one hand, the average distribution of C21orf91 expressing cells within the population of marker-positive cells (such as of all GFAP expressing cells within a tile scan) was calculated. To depict the marker-specific population size/density, pie charts vary in size. On the other hand, the mean percentage of marker expressing cells within the C21orf91-positive population was evaluated per animal. Rat brain preparations were approved by the ZETT (Zentrale Einrichtung für Tierforschung und Wissenschaftliche Tierschutzaufgaben; O69/11, V54/09).

Rat Oligodendroglial Cell Culture

Based on the procedure of McCarthy and de Vellis (1980), the generation of primary OPC cultures from postnatal day zero to one (P0–1) cerebral rat cortices of Wistar rats (either sex) was performed as previously described (Kremer et al., 2009; Göttle et al., 2018) whereas the cell culture medium was supplemented with fetal bovine serum (FBS) from a different company (Capricorn Scientific, Palo Alto, CA, USA). Primary OPCs (>97% pure) were either seeded onto 0.25 mg/ml poly-D-lysine coated (PDL, Sigma-Aldrich) glass coverslips (13 mm) in 24-well plates (for immunocytochemistry; 2.5×10^4 cells/well) or 0.25 mg/ml PDL coated 24-well plates (for quantitative reverse transcription-polymerase chain reaction (qRT-PCR); 5×10^4 cells/well) in high-glucose DMEM-based Sato medium. After 1.5 h, cell differentiation was induced by changing medium to differentiation medium (Sato medium supplemented with 0.5% FBS). The medium was exchanged every 3 days. The preparation of rodent primary oligodendroglial cell cultures was approved by the ZETT (O69/11, V54/09).

Plasmid Construction and OPC Transfection

Plasmid design and generation were conducted by Hybrigenics SA, Paris, France and kindly provided to our lab. Briefly, the complete coding sequence of the rat ortholog *C21orf91* (*RGD1563888*) was inserted into the company's pV22 vector, which is an equivalent vector to pHTN (Promega France; eucaryotic expression vector containing a HaloTag sequence) with slightly different polylinkers. OPCs were transfected *via* electroporation using the basic glia nucleofector kit and a nucleofector II device (both Lonza, Basel, Switzerland). In detail, $0.8–1 \times 10^6$ cells were transfected using the high-efficiency program A-033 resuspended in 100 µl nucleofection solution and a total amount of 2 µg plasmid per 1×10^6 cells. For visualization of short-term experiments, control (pHTN) and C21orf91 overexpression vectors were co-transfected with pmaxGFP (Lonza; a green fluorescent protein expression vector) and for visualization of transplanted cells, vectors were co-transfected with the pcDNA3-hyg-citrine vector (yellow fluorescent protein; Kremer et al., 2009) in a ratio of 10:1. Transfected OPCs were seeded onto 0.25 mg/ml PDL coated glass coverslips (13 mm) in 24-well plates (for immunocytochemistry; 7×10^4 cells/well) or 0.25 mg/ml PDL coated 24-well plates (for qRT-PCR; 1.5×10^5 cells/well) in expansion medium (Sato medium supplemented with 10 ng/ml recombinant human basic fibroblast growth factor (bFGF) and 10 ng/ml recombinant human platelet-derived growth factor-AA (PDGF-AA; both R&D Systems, Wiesbaden-Nordenstadt, Germany). After 4–5 h, the medium was exchanged to a differentiation medium (Kremer et al., 2009).

RNA Preparation, cDNA Synthesis, and Quantitative RT-PCR

Total RNA purification from tissues was done using Trizol reagent (Invitrogen) while cultured cells were lysed using 350 µl RLT lysis buffer (Qiagen) supplemented with β-mercaptoethanol (1:100, Sigma) and total RNA was purified by using RNeasy Mini Kit (Qiagen, Hilden, Germany) according to manufacturer instructions including DNase digestion. Before quantitative real-time polymerase chain reaction (qPCR), reverse

transcription with 250 ng RNA [measured using a NanoDrop ND 1000 (Peqlab, Erlangen, Germany)] was done using the High-Capacity cDNA Reverse Transcription Kit (ThermoFisher Scientific, Darmstadt, Germany). Gene expression levels were determined on a 7900HT sequence detection system (Applied Biosystems) applying SybrGreen universal master mix (ThermoFisher Scientific, Darmstadt, Germany). For sequence detection, the following forward (fwd) and reverse (rev) primers, generated *via* PrimerExpress 2.0 software (Applied Biosystems), were used, with β-actin (ACTB) and glyceraldehyde 3-phosphate dehydrogenase (GAPDH) serving as reference genes: ACTB_fwd: AACCCTAAGGCCAACCGTGAAA, ACTB_rev: AGTGGTACGACCAGAGGCAT, C21orf91_fwd: CTTCAGCAAGCGTCATCGAATT, C21orf91_rev: GTATCC TGGAAGACGCGGATG, CNPase_fwd: ATGCTGAGCTTG GCGAAGAA, CNPase_rev: GTACCCCGTGAAGATGGCC, GAPDH_fwd: GAACGGGAAGCTCACTGGC, GAPDH_rev: GCATGTCAGATCCACAACGG, MBP_fwd: CAATGGACCC GACAGGAAAC, MBP_rev: TGGCATCTCCAGCGTGTTC, MOG_fwd: CAGTTGTCACGCAGCTACGC, MOG_rev: AT GCCCTGGCCCTATCACTC. Relative gene expression levels were determined according to the ΔΔCt method (ThermoFisher Scientific, Darmstadt, Germany). All measurements were done in duplicates; generated from $n = 8$ independent experiments and data are shown as mean values ± SEM.

Immunocytochemistry and Assessment of Morphology

To evaluate marker expression and morphological maturation, the immunocytochemical analysis was performed after cells were fixed using 4% paraformaldehyde (PFA) at RT for 10 min. Non-specific binding of antibodies was prevented by incubation in blocking solution [10% normal goat serum (NGS); in PBS containing 0.1% Triton X-100] at RT for 45 min. Subsequently, cells were subjected to primary antibody solution (10% NGS, in PBS containing 0.01% Triton X-100), using the following dilutions overnight at 4°C: rabbit anti-GFAP (1:1,000, DAKO Agilent, Cat# Z0334), mouse anti-GFAP (1:1,000, Merck Millipore, Cat# MAB3402), mouse anti-2′, 3′-cyclic-nucleotide 3′-phosphodiesterase (CNPase; 1:1,000, Biolegend, Cat# 836402), rat anti-myelin basic protein (MBP; 1:250, Bio-Rad Laboratories, Cat# MCA409S), rabbit anti-C21orf91 (1:200, Bioss, Cat# bs-9983R), rabbit anti-C21orf91 (1:300, Sigma-Aldrich, Cat# HPA049030), mouse anti-CC1 (1:1,000, GeneTex, Cat# GTX16794), mouse anti-Olig2 (1:500, Merck Millipore Cat# MABN50), rabbit anti-Olig2 (1:500, Merck Millipore, Cat# AB9610), mouse anti-myelin oligodendrocyte glycoprotein (MOG; 1:500, Merck Millipore, Cat# MAB5680), goat anti-PDGFR (alpha/CD140A, 1:250, Neuromics, Cat# GT15150), mouse anti-astrocyte cell surface antigen-1 (ACSA-1/GLAST; 1:200, Miltenyi, Ca# 130-095-822), rabbit anti-hairy and enhancer of split-1 (HES1; 1:250, Invitrogen, Cat# PA5-28802), mouse anti-NK2 Homeobox 2 (NKX2.2; 1:100, R&D Systems, Cat# 883411), rabbit anti-sex-determining region Y-box 10 (Sox10; 1:100, S1058C002, DCS Immunoline, RRID: AB_2313583), chicken anti-green fluorescent protein/citrine (GFP; 1:1,000; Aves Labs, Cat# GFP-1020). Following three washing steps with PBS, secondary antibodies (anti-mouse, anti-rabbit, anti-goat) conjugated with either Alexa Fluor405, Alexa Fluor488, or Alexa Fluor594 (1:500; Thermo Fisher Scientific, Darmstadt, Germany) in PBS supplemented with DAPI (0.02 μg/ml; Roche Diagnostic GmbH, Mannheim, Germany) were applied for 90 min at RT. Cells were mounted with Citifluor (Cilifluor, Leicester, United Kingdom). For image acquisition, the Zeiss Axionplan2 microscope (Zeiss, Jena, Germany) was used and the analysis was performed with the ImageJ BioVoxxel software (Schindelin et al., 2012). Nine images per coverslip (2 coverslips/condition; mean of 2 coverslips generated from the same animal pool represents $n = 1$ independent experiment) were captured using 20× magnification and the same exposure times throughout each experiment and marker expression strength study. For quantification, the number of marker-positive cells in relation to DAPI-positive- (total number, for non-transfected cells) or GFP expressing cells (for transfected cells) was calculated and shown as a percentage. To assess the degree of morphological maturation, transfected (green fluorescent) OPCs were analyzed by fluorescence microscopy (Zeiss Axioplan, Jena, Germany) as previously described (Kremer et al., 2009; Göttle et al., 2010). Based on morphological cell parameters (processes, branches), cells were distinguished into 3 different categories for morphological maturation starting with a low number of processes in progenitor cells to multiple process-bearing cells (low, medium) up to more mature cells with a high degree of arborization or even sheath building (high). For classification of hybrid cells—cells with oligodendroglial- and astroglial marker coexpression—ubiquitous [indicating astrogenesis (Setoguchi and Kondo, 2004)] as well as nuclear Olig2-, Sox10-, Nkx2.2- and strong CC1 expression was correlated with GFAP- and GLAST expression.

Western Blotting

Isolated CC and HF tissues were lysed using an Ultra-turrax disperser (IKA®-Werke GmbH and Co. KG, Staufen, Germany) and radioimmunoprecipitation assay buffer (RIPA buffer, Cell Signaling Technology, Danvers, MA, USA) supplemented with HALT™ Protease-/Phosphatase inhibitor cocktail and EDTA (both Thermo Fisher Scientific). Afterward, sonication with an ultrasound homogenizer (SonopulsHD2070, 50% power, pulse 0.5 s on and 0.5 s off) was performed for 10 s and samples were centrifuged (14,000 rpm, 10 min, 4°C) to proceed with supernatants. Protein concentrations were determined using the DC Protein Assay (BioRad). Specimens were subjected to standard sodium dodecyl sulfate (SDS) gel electrophoresis and semi-dry western blotting using Bolt 12% Bis-Tris Plus gels and nitrocellulose membranes (both Thermo Fisher Scientific). Blocking was confirmed by total protein staining using the Pierce™ Reversible Protein Stain Kit (Thermo Fisher Scientific) also used for protein normalization. Afterward, membranes were blocked with Superblock (in TBS, Thermo Fisher Scientific) for 1 h at RT and applying the following primary antibodies: rabbit anti-C21orf91 [1:1,000, Santa Cruz Biotechnology, Cat# sc-83610 (Li et al., 2016)], rabbit anti-C21orf91 (1:300, Sigma-Aldrich, Cat# HPA049030), mouse

anti-GAPDH (1:5,000, Merck Millipore Cat# MAB374) and the secondary antibodies anti-rabbit IgG, HRP-linked (1:2,000, Cell Signaling Technology Cat# 7074,) and anti-mouse IgG (H + L), made in horse (1:5,000, Vector Laboratories, Burlingame, CA, USA Cat# PI-2000). For visualization, Super Signal West Pico Chemiluminescent Substrate (Thermo Fisher Scientific) was applied for 5 min. To ensure reliable quantification, membranes were stripped with 10 ml ReBlot Plus Strong Solution (1×, Merck Millipore) to detect C21orf91 and the housekeeping protein (GAPDH) sequentially on the same membrane. Protein bands were quantified using the Fusion FX software (Vilber Lourmat, Eberhardzell, Germany). The intensity for each band was determined and normalized to the total amount of the loaded protein amount and the intensity of the GAPDH band of the corresponding sample. Quantification was repeated two times for the published C21orf91 antibody (Li et al., 2016) and two times for the C21orf91 antibody from Sigma-Aldrich. Both antibodies marked a protein band of the same size and therefore the mean across all Western blot experiments (n = 3 animals) was calculated.

Myelinating Co-cultures, OPC Transplantation, and Assessment of Myelination Capacity

Dissociated neuron/oligodendrocyte co-cultures were obtained from E16 rat cerebral cortices (Wistar rats of either sex) as previously described in Göttle et al. (2015) and Göttle et al. (2018) with the only difference that 9×10^4 cortical cells were plated per well. After 15 days *in vitro* (DIV15), 10×10^4 transfected OPCs per coverslip were plated directly in the center of a co-culture. The medium was exchanged twice a week with freshly prepared myelination medium until DIV25. Then, co-cultures were fixed with 4% paraformaldehyde for 15 min at RT and processed for immunofluorescent staining. Blocking solution contained 2% NGS and 0.5% Triton X-100 in PBS, whereas the following primary antibodies were diluted in 2% NGS and 0.1% Triton X-100: mouse anti-MBP (1:250, Biolegend, San Diego, CA, USA, Cat# 836504), mouse anti-CC1 (1:800, GeneTex, Cat# GTX16794), rabbit anti-GFAP (1:800, DAKO Agilent, Cat# Z0334). After washing with PBS, secondary antibodies (anti-mouse and anti-rabbit) conjugated with either Alexa Fluor405 or Alexa Fluor594 (1:500; Thermo Fisher Scientific, Darmstadt, Germany) in PBS supplemented with DAPI (0.02 µg/ml; Roche Diagnostic GmbH, Mannheim, Germany) were applied for 90 min at RT. To assess the degree of cellular maturation, only transfected (green fluorescent) cells were scored by applying an evaluation tool based on morphological cell parameters (processes, branches). Moreover, expression and distribution of the MBP protein were assessed and led to the categorizations: MBP-positive cells with a high degree of arborization [pos], integrated and myelinating oligodendrocytes displaying T-shape structures (myelin; Göttle et al., 2015), non-organized MBP expressing [NOM] cells, characterized by a rather disorganized MBP accumulation and unusual morphologies as well as MBP-negative cells [neg]. For quantification, the number of protein marker-positive cells in relation to GFP expressing cells (transfected cells) was calculated and shown as percentage (n = 9 experiments). The generation of rodent myelinating co-cultures was approved by the LANUV (Landesamt für Natur, Umwelt und Verbraucherschutz; Az.81-02.04.2018.A388).

Statistical Analysis

Data are presented as mean values ± standard error of the mean (SEM). Graphs and statistical analysis were performed using Excel and the GraphPad Prism 8.0.2 software (GraphPad Prism, San Diego, CA, USA; RRID: SCR_002798). Shapiro-Wilk normality test was used to assess the absence of Gaussian distribution of all datasets. To determine statistical significance for normally distributed data sets, the Students t-test was applied for comparing two groups and one-way analysis of variance (ANOVA) with Turkey post-test for multiple comparisons was applied to compare three or more groups. For data sets not passing the Shapiro–Wilk normality test, Mann–Whitney U test for comparing two groups, and Kruskal–Wallis test with Dunn's post-test for multiple comparisons of three or more groups was applied. Statistical significance thresholds were set as follows: $^*p \leq 0.05$; $^{**}p \leq 0.01$; $^{***}p \leq 0.001$ and ns = not significant. "n" represents the number of independent experiments.

RESULTS

C21orf91 was previously shown to affect neurogenesis during fetal brain development and suggested to impact neuropathogenesis of HSA21-related disorders such as DS (Li et al., 2016). Interestingly, this study also revealed the highest *C21ORF91* mRNA expression levels in the adult corpus callosum (CC) which is considered as the largest white matter structure in the brain. This prompted us to investigate C21orf91's correlations and expression patterns in available databases and to study functional consequences upon forced overexpression in the oligodendroglial lineage.

The Human C21ORF91 Expression Profile Strongly Correlates With the Oligodendroglial Lineage

According to Genevestigator (Hruz et al., 2008), human *C21ORF91* is ubiquitously and highly expressed. Out of 285 human tissues and cells with available RNA sequencing (RNAseq) data, 167 tissues (60%) demonstrated high expression levels ($\log_{(2)} > 3$ of an average of the mean value of TPM). Based on these RNAseq data, hematopoietic cells and the nervous system including corpus callosum and different regions of the spinal cord belong to the 50 tissues and cells showing the highest expression of *C21ORF91* (**Figure 1A**). Microarray data from this platform, which encompasses a wider panel of brain structures than the RNAseq data, further indicated that within the nervous system; corpus callosum, diencephalon, and cerebral white matter belong to the most *C21ORF91* enriched regions (**Figure 1B**). In agreement with these observations, microarray expression data from 6 human adult donors from the Allen Brain Atlas (Sunkin et al., 2013) confirmed the highest expression levels in the corpus callosum and ventral thalamus and globus pallidus, both part of the diencephalon (**Figure 1C**). To obtain additional

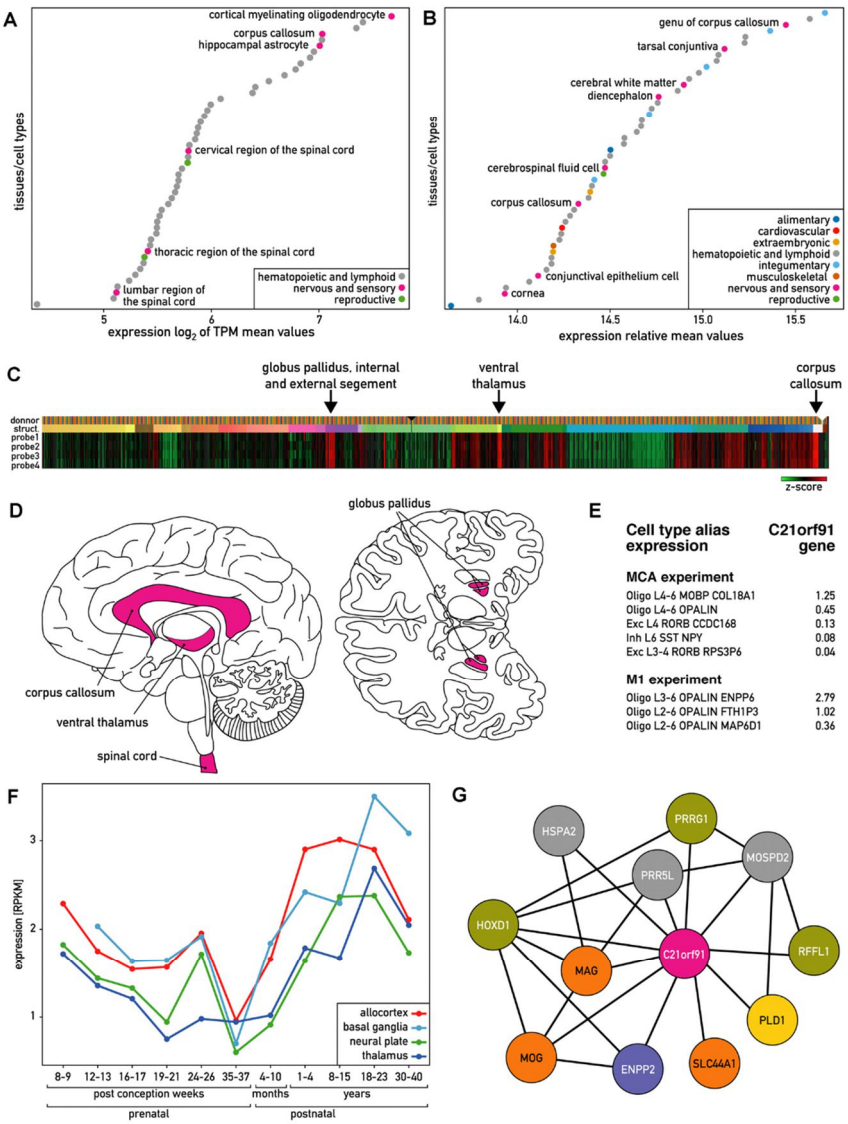

FIGURE 1 | Expression of human *C21ORF91* gene. **(A)** The 50 tissues and cell types with the highest *C21ORF91* expression according to Genevestigator measured with RNAseq and expressed as the log(2) of TPM (transcripts per kilobase million) mean values. Cortical myelinating oligodendrocytes and hippocampal astrocytes are the cell types, and corpus callosum and spinal cord are the tissues that are most enriched for *C21orf91*. **(B)** The 50 tissues and cell types with the highest C21ORF91 expression according to Genevestigator measured with microarrays and expressed as relative mean expression values. Corpus callosum, diencephalon, and cerebral white matter are the nervous system structures most enriched for *C21orf91*. **(C)** Heat map visualization of microarray expression data from six adult donors for the four available probes for *C21ORF91* from the Allen Brain Atlas. Indicated with arrows are the structures with the highest expression. Data is displayed as z-scores. Probe 1–4 correspond to *C21ORF91* sequence A_23_P211015, A_24_P125839, CUST_5965_PI416261804 and CUST_5966_PI416261804. **(D)** Schematic sagittal and inferior view of the human brain indicating the regions where *C21ORF91* gene is expressed according to Genevestigator and Allen Brain Atlas. **(E)** Single-nucleus RNAseq data from Allen Brain Atlas expressed as count per million (cpm) trimmed means.

(*Continued*)

FIGURE 1 | Continued
MCA stands for multiple cortex area set of experiments and M1 for primary motor cortex experiment. L4–6, L6, L3–4, L2–6, L3–6, L4 refer to cortex areas. Oligo stands for oligodendrocytes, Exc for excitatory neuron, and Inh for inhibitory neuron. **(F)** *C21ORF91* expression profile depicts a wave-like pattern, progressively increasing after birth to the age of 23 years. The expression is monitored for different brain structures at different ages. RNAseq data expressed as the mean of RPKM values. Ages vary from prenatal [8–37 post-conception weeks (pcw)] to postnatal stages from 4–10 months and 1–40 years. Brain structures were grouped as follows: *allocortex* (red) = hippocampus; *basal ganglia* (light blue) = striatum; *neural plate* (green) = 19 structures including frontal cortex and cerebellum; *thalamus* (dark blue) = dorsal thalamus, mediodorsal nucleus of thalamus. Data from the *ventricular zone* are not included. **(G)** Coexpression network of genes correlating with *C21ORF91* expression and each other generated from BrainEXP database. Nodes are colored according to protein function: orange: myelination, purple: oligodendrogenesis, yellow: dendrite spine morphogenesis, green: other expression evidence in the nervous system, and gray: other functions.

data on *C21ORF91* expression in the nervous system, we used the Brain EXPression Database (BrainEXP; Jiao et al., 2019). According to this database, *C21ORF91* expression is highest in the spinal cord, a structure that is absent in the panel analyzed by the Allen Brain atlas. The nervous system regions expressing *C21ORF91* (pink) are summarized in **Figure 1D**.

At the cellular level, RNAseq data from Genevestigator showed that *C21ORF91* is enriched in cortical myelinating oligodendrocytes and hippocampal astrocytes (**Figure 1A**). Single nucleus RNAseq data retrieved from the Allen Brain Atlas show that *C21ORF91* is preferentially expressed in oligodendroglial (Oligo) as compared to neuronal populations (Exc, Inh; **Figure 1E**). The oligodendroglial cell population Oligo derived from cortex areas L3–6 (Oligo L3–6 OPALIN ENPP6) which exhibits the highest *C21ORF91* expression also features both, high *OPALIN* transcript levels, encoding a protein involved in oligodendrocyte terminal differentiation (de Faria et al., 2019), as well as *ENPP6* transcripts, encoding a marker of newly forming oligodendrocytes (Xiao et al., 2016). RNAseq expression data from human brain structures at different ages indicate that *C21ORF91* expression is initiated at eight postconceptional weeks (pcw), then decreases until birth and increases progressively until the age of 23 years before it declines again (**Figure 1F**), thus approximately resembling the wave-like myelination process during brain development. Interestingly, the phylogenetic distribution of *C21ORF91*, shown to be conserved in various Gnathostomata (jawed vertebrates)—including mammals, chicken, Xenopus, or Zebrafish, but absent in jawless fish (**Supplementary Figure 1**)—closely mirrors the one of myelin (Baumann and Pham-Dinh, 2001).

Both, BrainEXP and the Allen Brain Atlas provide coexpression data. BrainEXP indicates that *C21ORF91* coexpresses with eleven genes (**Figure 1G**). The list includes *MOG*, *SLC44A1* and *MAG*, *HOXD1*, and *ENPP2/autotaxin* of which all were shown to be involved in oligodendrogenesis and myelination (Booth et al., 2007; Wheeler et al., 2015). It also includes *PRRG1* which is uncharacterized but is among the top 50 genes overexpressed in non-activated adult OPCs compared with activated adult OPCs (Moyon et al., 2015). The other coexpressed genes are *PLD1*, which promotes dendritic spine morphogenesis *via PKD1* activation (Li et al., 2019), *RFFL* which is reported to be expressed in the corpus callosum, brain stem, spinal cord and cerebellar white matter, and *HSPA2* and *PRR5L*, for which we did not find evidence for function in nervous system processes, oligodendrogenesis or myelination.

Additionally, the "Correlate Gene Search" of the Allen Brain Atlas was applied to adult brain microarray data indicating that C21ORF91 is coexpressed with 51 proteins, including ENPP2, HSPA2, MOG, PLD1, PRR5L, PRRG1, and SLC44A1 (with a Pearson's correlation >= 0.85). The analysis of GO terms associated with these 51 proteins revealed an enrichment of the following terms: myelination (GO:0042552), ensheathment of neurons (GO:0007272), axon ensheathment (GO:0008366), glial cell differentiation (GO:0010001), gliogenesis (GO:0042063), and myelin sheath (GO:0043209).

C21orf91 Ortholog Expression Is Enriched in White Matter Regions and Maturing Oligodendrocytes During Rodent Brain Development

To corroborate human findings, rodent *C21orf91* ortholog expression (*D16Ertd472e* for mouse, *RGD1563888* for rat) was examined using recently generated bulk transcriptomic datasets of numerous purified cell types and workflows for their analysis (Azim et al., 2015, 2018; **Figure 2**). This analysis confirmed the anticipated enrichment of *C21orf91*'s expression in myelinating oligodendrocytes. Note that *C21orf91* subclustered most with known mature oligodendrocyte markers, *MBP*, *Plp1*, and *Myrf*, and forming a larger cluster comprising pan oligodendrocyte or earlier stage lineage markers which include *Olig2, Sox10, Nkx2.2*, and *Gpr17*. As for a functional assessment we intended to use rat primary OPCs as previously established and published (Kremer et al., 2009; Göttle et al., 2010, 2015, 2018), we additionally examined *C21orf91* expression during rat CNS development. To this end, brains of postnatal day 0 (P0), P7, P25, and 2–3 months old (adult) rats were prepared and transcript and protein expression levels were analyzed in a region-specific way using tissues from the forebrain (FB), corpus callosum (CC), hippocampal formation (HF) and cerebellum (CB; **Figures 3A–C**). Real-time quantitative RT-PCR determination demonstrated that *C21orf91* gene expression was highest in adult CC compared to the other regions and revealed a clear transcript increase over time in all tested brain regions, again most apparent in CC (**Figure 3A**). This could be further verified *via* Western blot analysis, showing that C21orf91 protein expression was enriched during development in CC and HF (**Figures 3B,C**), peaking at P25 (observed with both tested antibodies, and shown as mean value).

As a next step, immunohistochemical staining of coronal P7 and adult rat CC brain sections was conducted. We assessed the antibody used by Li et al. (2016) as well as several other commercially available antibodies in our immunocytochemistry and confirmed that C21orf91 expression is correlating with neuronal marker NeuN expression in cortical sections for all of

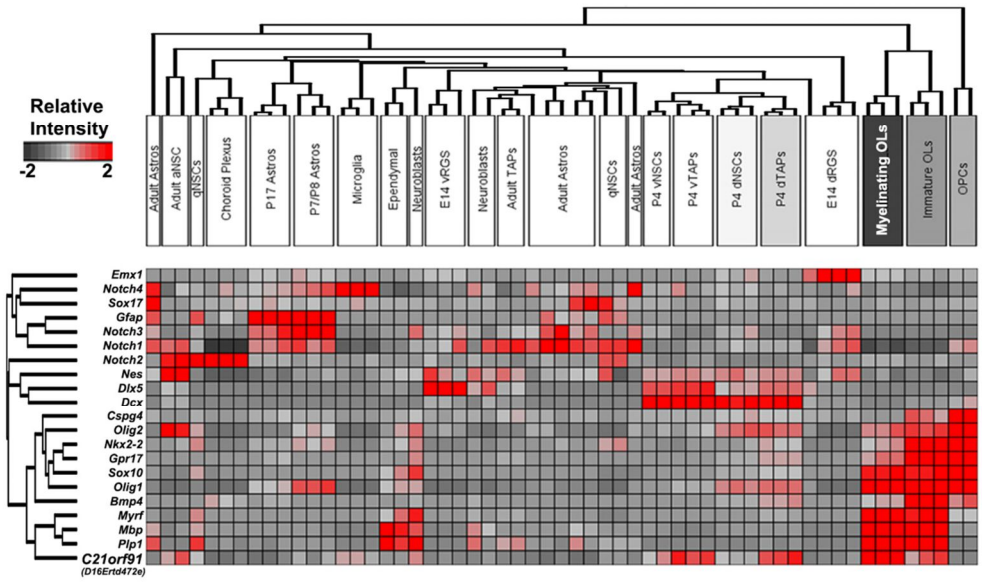

FIGURE 2 | Validation of enriched expression of mouse *C21orf91* ortholog in later stage oligodendroglial lineage cells compared to multiple cell types present in the forebrain. Bulk transcriptomic datasets assembled with essential hallmark constructed as a heatmap with known cell-specific hallmark genes and *C21orf91* ortholog (*D16Ertd472e*) clusters readily with later stage oligodendroglial markers and is highly expressed in myelinating oligodendrocytes (OL) as well as in transiently amplifying progenitors (TAPs) derived from region-specific early postnatal subventricular zone (SVZ) microdomains. Note: some datasets [e.g., adult astrocytes (Astros)] are not clustered together based on the genes lists for unsupervised clustering. The color legend represents the relative expression strength with red color indicating high values and gray color displaying lower values. Abbreviations: aNSC, activated neural stem cell; qNSC, quiescent NSC; Astros, astrocytes; vRGS/NSCs/TAPs, ventral radial glial cells/NSCs/TAPs; dNSCs/TAPs/RGS, dorsal NSCs/TAPs; OLs, oligodendrocytes; and OPCs, oligodendroglial precursor cells.

them (data not shown). Subsequent staining experiments were then nevertheless conducted using the published antibody (Li et al., 2016), to ensure comparability. Evaluation of staining patterns revealed that the density of C21orf91 expressing cells per mm^2 was enriched in adult CC compared to the surrounding gray matter (GM; **Figures 3D,D′**). In the next step, the distribution of C21orf91-positive cells within lineage-specific marker populations was assessed (**Figure 3E**). PDGFRα hereby represents the OPC population, CC1 accounts for mature oligodendrocytes, and GFAP was used as an astroglial marker. Interestingly, except for small populations in the early developmental stage P7 (see pie area; CC1-positive cells in the GM (gray pie) and GFAP-positive cells in CC (white pie) and GM), between 48–80% of oligodendroglial or astroglial lineage cells expressed C21orf91 in P7 and adult CC and GM. In a further survey, the distribution of nuclear Olig2- (**Figure 3F**), PDGFRα- (**Figure 3G**), CC1- (**Figure 3H**), and GFAP-positive cells (**Figure 3I**) within the C21orf91 expressing cell populations were analyzed. In CC, 80% of the C21orf91 expressing cells in P7 and 60% of the C21orf91 expressing cells in adult rats were also Olig2-positive (**Figures 3F,F′**). Furthermore, almost 40% of the C21orf91 expressing cells in P7 CC were PDGFRα-positive, declining in the adult CC along the course of white matter development (**Figures 3G,G′**). In parallel, the degree of CC1/C21orf91 expressing cells increased over time (**Figures 3H,H′**), additionally depicted by a proportional increase of C21orf91-positive cells within the CC1 population (compare CC1 in P7 and adult; **Figure 3E**). Interestingly, the percentage of C21orf91 expressing astrocytes also increased in the surrounding GM structures during development, comprising up to 40% of the C21orf91-positive cells (**Figures 3I,I′**). Furthermore, the proportional distribution of C21orf91 expressing cells within the GFAP-positive population doubled during development in both, CC and GM (**Figure 3E**).

C21orf91 Ortholog Expression Correlates With Differentiation and Maturation of Cultured OPCs

To investigate the role of C21orf91 in oligodendroglial differentiation, we first examined the expression of differentiation-associated markers and C21orf91 during spontaneous differentiation of cultured primary rat OPCs. Transcript levels of *C21orf91* (**Figure 4A**) were mildly downregulated at day 3, where *CNPase* expression (**Figure 4B**) is already significantly upregulated, but then upregulated at day 6, similar to the induction of *MBP* and *MOG* expression (**Figures 4C,D**). As oligodendroglial cell differentiation is

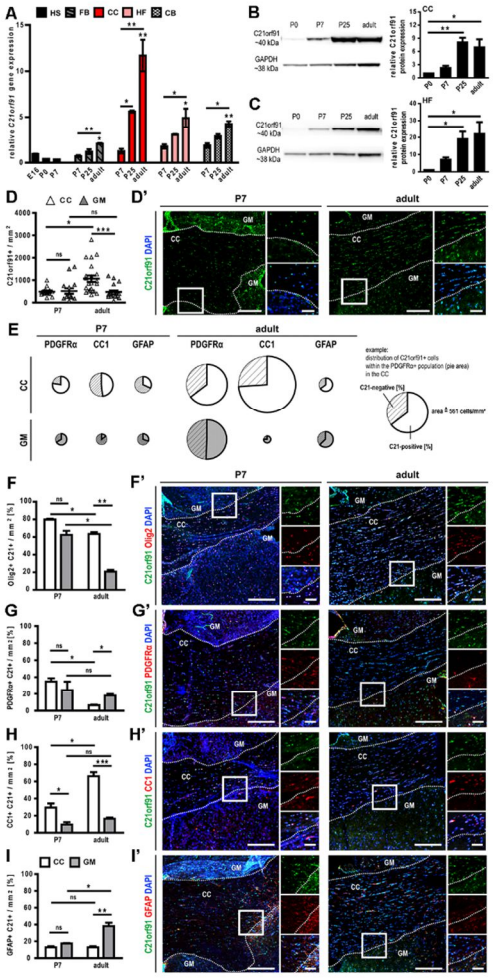

FIGURE 3 | C21orf91 ortholog expression is enriched in white matter structures and correlates with OPC differentiation markers during rat brain development. **(A)** Time- and region-specific qRT-PCR revealed enriched *C21orf91* ortholog (*RGD1563888*) transcript levels in the corpus callosum (CC, red bars) and hippocampal formation (HF, rose bars) compared to hemisphere (HS, black bars), forebrain (FB, gray dashed bars) and cerebellum (CB, chessboard bars), thereby showing an increasing pattern from embryonic day 16 (E16) over postnatal days (P7, P25) up to adult. Note, that stars without significance bars (adult bars) indicate a significant increase from E16 to adult. For a clear presentation, the indication of additional significance bars has been omitted. A similar correlation was depicted for C21orf91 ortholog protein abundance using Western blotting for CC **(B)** and HF **(C)**. Results derived from $n = 3$ animals **(A–C)** and measurements were repeated twice per lysate **(B,C)**. Note, that P0 tissue sections were used entirely for Western blot analysis. P7 and adult rat brain sections were immunostained for C21orf91 (RGD1563888; **D′**), and oligodendroglial markers **(F′–H′)**, and an astroglial marker **(I′)**. The number of C21orf91+ cells **(D)** was enriched in the adult corpus callosum (CC; white triangles) compared to the surrounding gray matter (GM; gray triangles) and CC of P7 rats. Panel **(D′)** shows representative tile scans for the analyzed region in P7 and adult rat brain sections stained for C21orf91 (green) with nuclei in blue (DAPI). The average distribution of C21orf91-positive cells within the PDGFRα-, CC1- or GFAP-positive cell population is shown in **(E)**. The marker-related population size/density is depicted by the size (=area) of the pie charts. White pies represent cells of the CC and gray pies refer to GM located cells. The whole circle area of the white PDGFRα pie chart (see example) equals 561 PDGFRα-positive cells/mm^2 and represents the scale for the other pie charts. C21orf91 expression is highly correlated with Olig2 **(F)**, PDGFRα **(G)** and CC1 **(H)** expression in the CC and GFAP **(I)** expression in adult GM. Representative images of tile scans and blow-ups are shown in **(F′)** for Olig2 (red), **(G′)** for PDGFRα (red), **(H′)** for CC1 (red) and **(I′)** for GFAP (red). Nuclei are shown in blue (DAPI). White dashed lines depict the border of CC and surrounding GM. Squares refer to blow-ups. Scale bars for tile scans: 200 μm, scale bars for blow-ups: 50 μm. Data are shown as mean values (±SEM) deriving from $n = 4$ animals; Kruskal-Wallis test with Dunn's post-test: $^*p \leq 0.05$, $^{**}p \leq 0.01$, $^{***}p \leq 0.001$, ns = not significant.

also reflected by the induction of specific myelin protein expression at particular time points (1d, 3d, 6d), double immunofluorescent staining with antibodies directed against C21orf91, CNPase (**Figures 4E,E′**), MBP (**Figures 4F,F′**) and MOG (**Figures 4G,G′**) were conducted. Discriminating between different C21orf91 expression strengths (strong: black bars, weak: dashed bars and cells without any positivity), it could be demonstrated that most oligodendroglial cells were expressing C21orf91, with the majority of them featuring strong C21orf91 expression levels (see representative images in **Figures 4E′,F′,G′**). Note that especially cells with strong C21orf91 signals (**Figures 4E–G**) also displayed expression of the stage-specific markers and that none of the myelin-positive cells was negative for C21orf91.

C21orf91 OIrtholog Overexpression Influences Rat OPC Differentiation

Given that the occurrence and strength of differentiation markers correlated with strong C21orf91 ortholog expression levels, it was of interest to find out whether C21orf91 ortholog modulation influences oligodendroglial differentiation, particularly in the context of increased C21orf91 levels in DS. To this end, C21orf91 ortholog (RGD1563888) was overexpressed leading to elevated transcript and protein levels (**Figures 5A–C**). Of note, transfection experiments were conducted with C21orf91 overexpression constructs (black bars) and the corresponding empty control vector (white bars) along with a green fluorescent protein (GFP) expression vector for detection of modulated cells. Morphological assessment of transfected cells was carried out according to our previously published schemes (Kremer et al., 2009; Göttle et al., 2010, 2015) and demonstrated that overexpression of C21orf91 accelerated the maturation process (in terms of process growth and arborization) resulting in a significantly increased number of cells with more mature morphologies (**Figures 5B–D**).

Although OPCs are generally determined to give rise to oligodendrocytes, they also exert a certain potential to generate astrocytes both *in vitro* (Rao and Mayer-Proschel, 1997; Nishiyama et al., 2009) as well as *in vivo* (Aguirre and Gallo,

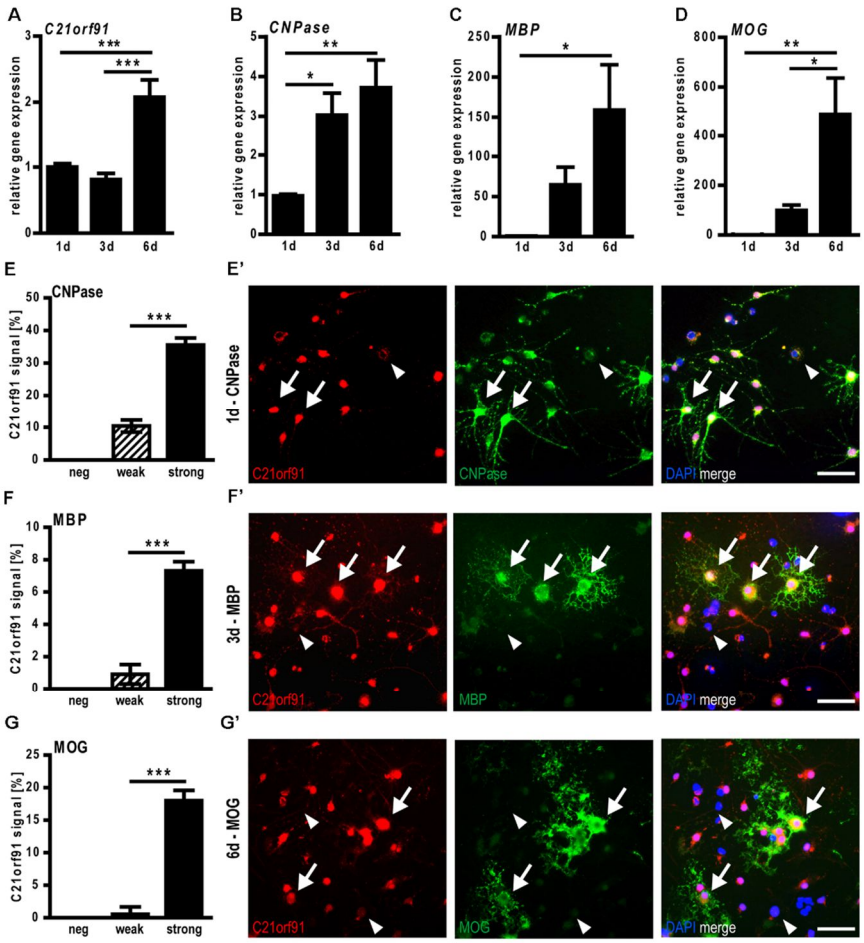

FIGURE 4 | C21orf91 ortholog expression correlates with myelin expression during spontaneous differentiation of cultured rat primary oligodendroglial precursor cells (OPCs). Determination of transcript levels using qRT-PCR indicated an upregulation of *C21orf91*ortholog (*RGD1563888*; **A**) concurrent with increased expression of *CNPase* **(B)**, *MBP* **(C)**, and *MOG* **(D)** for 6 days (1d-6d). Stage-specific analysis of C21orf91 ortholog (RGD1563888) protein expression (red, Bioss anti-C21orf91 antibody) *via* double immunostaining performed for CNPase at 1d **(E,E')**, MBP at 3d **(F,F')** and MOG at 6d **(G,G')** revealed that maturation/myelin marker expression during differentiation highly correlates with strong cellular C21orf91 expression levels (black bars). Arrows point to cells with a strong C21orf91 expression that are also myelin-positive, arrowheads point at weak/no expressors that are myelin-negative. Blue nuclei represent DAPI staining. Note, that there are no myelin-positive cells that lack C21orf91 expression. Scale bars: 50 μm. Data are shown as mean values (±SEM) deriving from $n = 8$ experiments **(A–D)** and $n = 5$ experiments **(E–G)**. Statistical significance was calculated using one-way ANOVA with Tukey post-test **(A–D)** and Mann-Whitney *U* two-tailed test **(E–G)**: $^{*}p \leq 0.05$, $^{**}p \leq 0.01$, $^{***}p \leq 0.001$.

2004; Guo et al., 2009; Tanner et al., 2011; see **Figure 5E**). Interestingly, an increased astrocyte generation (Mito and Becker, 1993; Zdaniuk et al., 2011) along with a diminished myelin formation is observed in DS (Abraham et al., 2012). We, therefore, investigated whether C21orf91 overexpression impacts the lineage fate by depicting the expression changes of several astroglial and oligodendroglial differentiation markers (**Table 1**). This analysis revealed that C21orf91 overexpression resulted in a distinct reduction of cells exhibiting oligodendroglial features such as nuclear Olig2- and strong Nkx2.2 expression. On the other hand, overexpressing cells increased the expression of PDGFRα compared to control transfected cells. However, CC1 expression appeared to be far appeared to be far less abundant (40% reduction) in modulated cells again. Additionally, Sox10 nuclear localization (Rehberg et al., 2002) appeared to be affected by C21orf91 overexpression as the number of

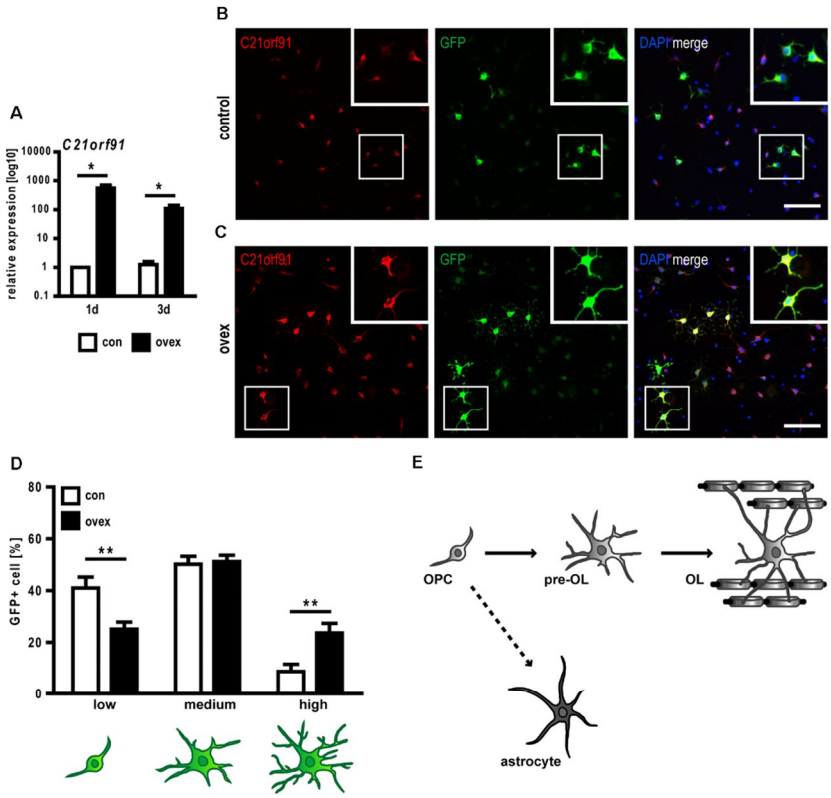

FIGURE 5 | C21orf91 ortholog overexpression accelerates morphological maturation of OPCs. OPCs were co-transfected with a GFP expression (for visualization, green) and an empty control vector (con, white bars) or a C21orf91 ortholog (RGD1563888) overexpression construct (ovex, black bars). Overexpression was confirmed using qRT-PCR **(A)** and immunostaining for C21orf91 (red, anti-C21orf91 antibody from Sigma-Aldrich) protein after 2 days of differentiation **(B,C)**. Squares show the blow-ups of representative transfected cells which indicate that overexpressing cells in **(C)** exhibited enriched C21orf91 protein abundance. Additionally, their distinct morphological maturation is highlighted (compare cell morphologies in **B,C**) which was further assessed using process- and branch-dependent categories (low-high), indeed revealing an accelerated morphological maturation **(D)**. Cell nuclei were labeled by DAPI (blue). Scale bars: 100 μm. Data are shown as mean values (±SEM) deriving from $n = 3$ experiments **(A)** and $n = 8$ experiments **(D)**. Statistical significance was calculated using Mann-Whitney U two-tailed test **(A)** and Student's two-sided, unpaired t-test **(B)**: $^{*}p \leq 0.05$, $^{**}p \leq 0.01$. OPCs, despite their primarily designated development into myelinating oligodendrocytes (OL), can also differentiate into astrocytes **(E)**.

cells with exclusively nuclear signals was decreased. On the other hand, an overall induction of astroglial markers was observed. Cytoplasmic translocation of Olig2 is known to account for astroglial differentiation (Setoguchi and Kondo, 2004), and indeed cell numbers with ubiquitous (nuclear and cytoplasmic) Olig2 expression were strongly increased throughout differentiation upon C21orf91 overexpression. Similarly, Hes1-positivity, a transcription factor known to induce astrogliogenesis at the expanse of oligodendrogenesis (Wu et al., 2003), was also elevated in cells with forced C21orf91 expression. Moreover, an overall upregulation of GFAP-positive cells at days 2, 3, and 5 of differentiation was observed leading to a 33%-increase in the number of GLAST expressing cells at day 5 (**Table 1**).

Overexpression of C21orf91 Ortholog Results in Aberrant Coexpression of Oligodendroglial and Astroglial Differentiation Markers

We next studied to what degree cellular coexpression of astroglial- and oligodendroglial markers could be observed. Immunocytofluorescent staining demonstrated that the forced expression of C21orf91 ortholog initiated aberrant combinations such as (nuclear) Olig2, Sox10, and CC1 expression in combination with GFAP signals at day 2 of differentiation (**Figures 6A′–C′**). Compared to control transfected cells, the numbers of Olig2/GFAP expressing cells were more than tripled (**Figure 6A**), whereas Sox10/GFAP expressing (**Figure 6B**)

TABLE 1 | C21orf91 ortholog (RGD1563888) overexpression results in a dysbalanced expression profile of glial differentiation markers during OPC differentiation.

	Marker	2d		3d		5d	
		Change ± SEM [%]	*p*	Change ± SEM [%]	*p*	Change ± SEM [%]	*p*
Oligodendroglial	Olig2 (nuclear)	−37.64 ± 2.22	**	−19.64 ± 2.45	*	−11.31 ± 1.86	ns
	Sox10 (nuclear)	−34.96 ± 2.60	**	–	–	−4.50 ± 7.07	ns
	Nkx2.2	−10.57 ± 6.60	ns	–	–	−34.45 ± 4.33	**
	PDGFRα	+16.07 ± 5.36	ns	+14.32 ± 3.03	*	–	–
	CC1	−10.62 ± 1.17	*	–	–	−32.34 ± 9.29	**
	MBP	–	–	+4.17 ± 1.37	0.07	+3.18 ± 5.69	ns
Astroglial	Sox10 (ubiquitous/cytoplasmic)	+38.04 ± 3.56	**	–	–	+16.21 ± 7.33	*
	Olig2 (ubiquitous)	+44.43 ± 5.76	**	+26.45 ± 4.26	*	+18.99 ± 5.50	*
	Hes1	+21.65 ± 1.46	**	–	–	–	–
	GFAP	+16.29 ± 3.88	*	+12.93 ± 2.15	*	+16.06 ± 2.44	**
	GLAST	+10.23 ± 7.15	ns	–	–	+33.10 ± 1.21	**

*Data are shown as mean changes to control transfected cells (% ± SEM). Blue color indicates a decreased marker expression, red color relates to increased marker expression. Data derived from n = 9 experiments for GFAP (2d), n = 5 experiments for Olig2 (nuclear and ubiquitous; 2d, 5d), Sox10 (nuclear and ubiquitous / cytoplasmic; 2d), PDGFRα (2d, 3d), CC1 (2d), MBP (3d, 5d) and GFAP (3d, 5d) and n = 4 for Olig2 (nuclear and ubiquitous; 3d), Sox10 (nuclear and ubiquitous / cytoplasmic; 5d), Nkx2.2 (2d, 5d), CC1 (5d), Hes1 (2d) and GLAST (5d). Statistical significance was calculated using Student's two-sided, unpaired t-test and Mann-Whitney U two-tailed test: *p ≤ 0.05, **p ≤ 0.01, ns = not significant.*

and CC1/GFAP-positive cells (**Figure 6C**) were doubled upon overexpression. In C21orf91 overexpressing cells, this mixed phenotype could occasionally still be found after 5 days in culture (data not shown). Furthermore, also coexpression of Nkx2.2 together with GFAP, as well as a few cells displaying a ubiquitous expression of Olig2 [indicating astrogenesis (Setoguchi and Kondo, 2004)] together with GLAST were found (**Figures 6D,E**).

Rat Oligodendroglial Cells Display Accelerated Maturation but Diminished Myelination Capacity Upon C21orf91 Ortholog Overexpression

As C21orf91 ortholog overexpression leads to dysregulated OPC differentiation and the acquisition of non-permissive marker combinations, their maturation capacity was evaluated. We first observed, that upon C21orf91 overexpression, cells did not show a significant difference for the positivity of maturation marker MBP (**Table 1**). However, the expression strength of MBP was increased after 3 days of differentiation when compared to control cells (**Figure 7A**). Following the observed accelerated morphological maturation at day 2 of differentiation (**Figure 5D**), C21orf91 overexpressing cells exhibited morphologically elaborated maturation (**Figure 7C**) also at day 3 compared to control transfected cells (**Figure 7B**). Furthermore, control cells displayed vesicle-like MBP signals (**Figure 7B**), indicating MBP expression is still at an earlier stage as compared to C21orf91 overexpressed cells. Next, C21orf91 overexpressing OPCs were evaluated in a more physiological environment allowing axon/oligodendrocyte interactions to occur and we assessed whether the produced MBP protein could contribute to the generation of functional myelin. For this purpose, we used myelinating neuron-oligodendrocyte co-cultures (Göttle et al., 2015, 2018, 2019) onto which transfected primary rat OPCs were applied during the myelination process. Transplanted cells were maintained in co-culture for another 10 days in presence of a myelination-inducing medium and then assessed for their potential to integrate and to ensheath axons (detectable as T-shaped MBP-positive structures) as previously established for p57kip2 suppressed OPCs in our former studies (Göttle et al., 2015). We distinguished between MBP-negative cells (neg), MBP expressing oligodendrocytes (pos), oligodendrocytes myelinating axons (myelin, T-shapes), and non-organized MBP expressing (NOM) cells. NOM cells were characterized by a rather disorganized MBP accumulation and by a somehow collapsed morphology (**Figures 7D,F**). We found that OPCs with enforced C21orf91 expression failed to ensheath axons when compared to control transfected cells (**Figure 7D**). Also, the number of NOM cells was substantially increased (**Figure 7D**). Of note, GFAP/MBP double staining revealed that some of these NOM cells exhibited non-permissive coexpression of these two proteins (**Figures 7E,F**).

DISCUSSION

There is an increasing acceptance of the fact that white matter composition and functionality contribute to a healthy and functional CNS and that respective deficiencies are therefore likely implicated in many if not all neurological manifestations (Kremer et al., 2016). And indeed, an unusual, aberrant glial composition has been observed in the CNS of DS patients which has been suggested to contribute to developmental deficiencies and subsequent cognitive impairments and ID (Haydar and Reeves, 2012; Kanaumi et al., 2013; Stagni et al., 2017; Dossi et al., 2018). However, the underlying reasons why the glial compartment is affected by chromosome 21 triplication and which of the dysregulated genes contribute to glial malformation remain to be understood.

The *C21ORF91* gene has so far not been investigated in the context of oligodendrogenesis and white matter, although it was listed within the dysregulated gene network M43 in DS which is associated with oligodendroglial development and myelination (Olmos-Serrano et al., 2016). Our here presented studies demonstrate that *C21ORF91* correlates with white matter formation and oligodendroglial lineage. Not only being conserved in various jawed vertebrates (**Supplementary Figure 1**), closely mirroring the phylogenetic distribution of

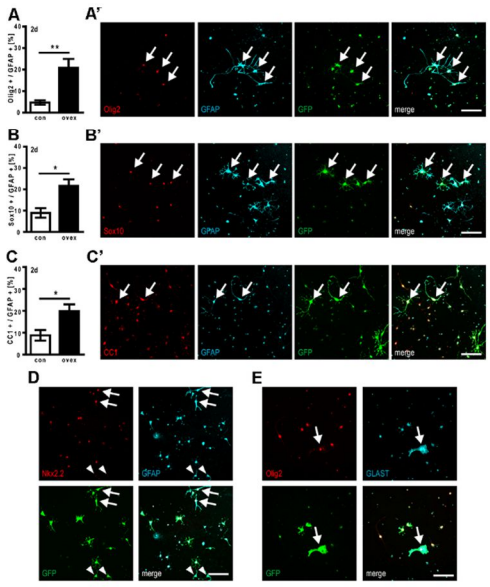

FIGURE 6 | C21orf91 ortholog overexpression results in aberrant OPC differentiation creating hybrid cells coexpressing astroglial and oligodendroglial markers. OPCs were co-transfected with a GFP expression (for visualization, green) and an empty control vector (con, white bars) or a C21orf91 ortholog (RGD1563888) overexpression construct (ovex, black bars). After 2 days (2d) of differentiation and C21orf91 overexpression, a significantly increased number of cells expressing GFAP (cyan) with oligodendroglial markers (red) Olig2 **(A)**, Sox10 **(B)**, and CC1 **(C)** were observed, representative images of which are shown in **(A'–C')**. Additional aberrant coexpression was also observed for GFAP (cyan) and Nkx2.2 (red; **D**) and for GLAST (cyan) with Olig2 (red; **E**). Arrows point at double-positive hybrid cells, arrowheads in **(D)** point to "normal" cells exhibiting a GFAP-positivity in the expected absence of oligodendroglial markers such as Nkx2.2. Scale bars: 100 μm. Data are shown as mean values (±SEM) deriving from n = 5–7 experiments. Mann-Whitney U two-tailed test: $^{*}p \leq 0.05$, $^{**}p \leq 0.01$.

myelin (Baumann and Pham-Dinh, 2001), our bioinformatical analyses independently revealed a coexpression network of genes including *PLD1*, *MOG*, *MAG*, *OPALIN*, *SLC44A1* and *ENPP2/autotaxin* (**Figure 1G**), all of which are associated with oligodendrogenesis, myelination, glial cell differentiation and axon ensheathment, and also being part of Olmos-Serrano et al.'s (2016) M43 gene cluster. Furthermore, we here confirmed this bioinformatics-based correlation of human expression data for rodents, demonstrating on the one hand that C21orf91 ortholog was indeed enriched in the CC, the largest white matter structure of the CNS while revealing on the other hand, that it was also clearly associated with oligodendroglial differentiation and maturation. Moreover, here we show that slight disturbances in the expression strength as introduced by overexpression, reproducing conditions of the developing CNS in DS (Ait Yahya-Graison et al., 2007; Li et al., 2016) appear to interfere with OPC maturation and the proper establishment of myelin sheaths while creating cells with aberrant expression profiles. Because forced overexpression led to faster OPC maturation (seen by MBP expression strength; **Figure 7**), yet defective myelination, complex patterns of hypomyelination in DS could be explained, with myelin markers MBP and MOG depicting non-significant differences in the expression in early periods of life, then being progressively downregulated in DS patients (Abraham et al., 2012; Olmos-Serrano et al., 2016). Based on these observations, we suggest that overexpression of this gene contributes to hypomyelination as described in DS.

In this regard, it is tempting to speculate that the glial disbalance, more precisely the overpopulation of astroglial cells, such as described in the hippocampus of infant and adult DS brains (Mito and Becker, 1993), is related to enriched *C21ORF91* expression. We confirmed increased levels of C21orf91 ortholog expression in the hippocampal formation (HF) during rat brain development and showed that in addition to myelinating oligodendrocytes, *C21ORF91* is also substantially expressed in hippocampal astrocytes. Furthermore, elevated levels of C21orf91 ortholog augmented the expression of astroglial markers in differentiating OPCs and even resulted in cells displaying both lineage features. To what degree C21orf91-dependent aberrant astrogenesis from OPCs contributes to a DS-related overpopulation of astrocytes and whether also glial precursor cells committed to the astroglial lineage are additionally dysregulated, remains to be addressed in future studies.

Related to the here described significantly increased combinations of astroglial and oligodendroglial markers in OPCs with elevated *C21orf91* ortholog expression levels, it is reasonable to assume that such cells are conflicted in their differentiation paths. It remains therefore to be shown in future studies to what extent this is a transient phenomenon with cells exhibiting a possible extension of early glial progenitor virtues. Consequently, whether and when progression into either astroglial or delayed oligodendroglial lineages occurs—possibly inflicting successful distribution, tissue integration, and axon interactions—or whether such cells die or become actively omitted within the developing CNS needs also to be investigated. Moreover, to understand how such aberrant expression patterns arise, it will be necessary to investigate responsible signaling pathways, thus allowing the identification of altered dynamics in DS. As summarized recently (Reiche et al., 2019), several signaling pathways are potentially involved in neural/glial fate decision and differentiation in DS. Of note, in terms of neurogenesis, Li et al. (2016) already demonstrated neural β-catenin upregulation in response to overexpression of *C21orf91*. Noteworthy, the Wnt/β-catenin signaling is also a key regulator of oligodendrocyte development, as it is transiently activated in OPCs concurrent with the initiation of terminal differentiation (Emery, 2010). It will therefore be of interest to see whether C21orf91-dependent β-catenin regulation also accounts for glial cells and which other suspected molecules are responding to elevated C21orf91 levels in OPCs. In this regard, studies on axin2/catenin are worth mentioning since these molecules are already investigated in the context of white matter lesions in

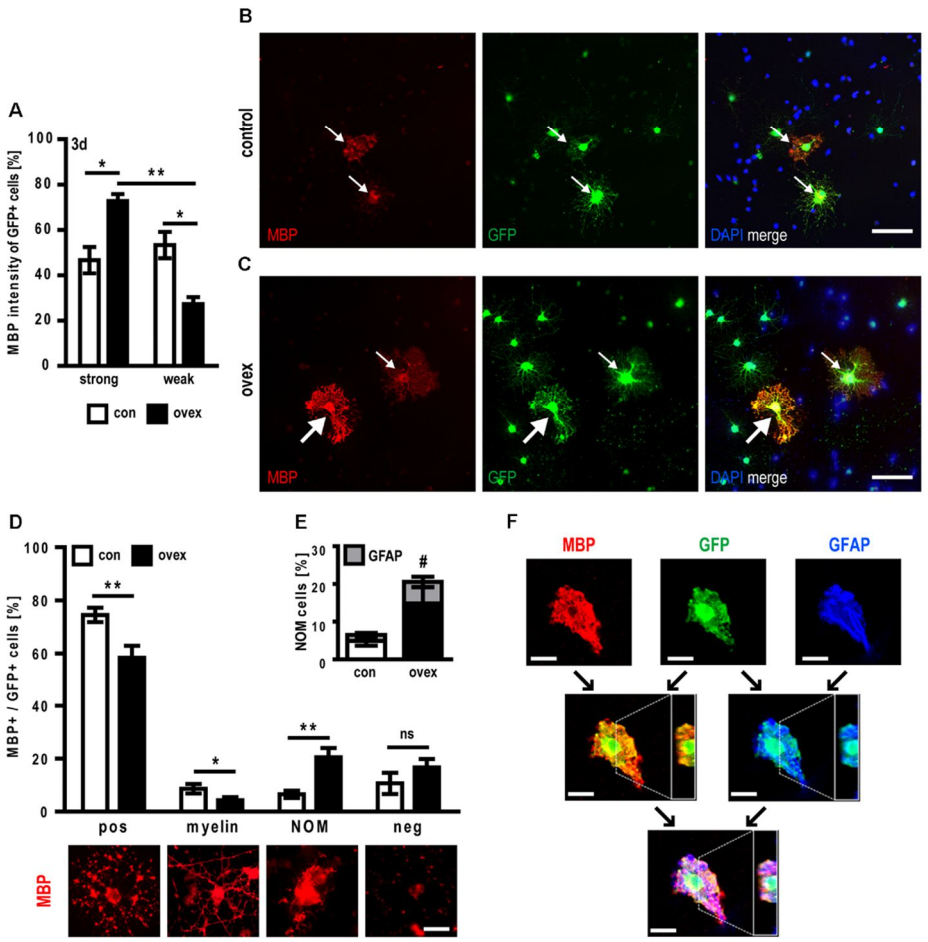

FIGURE 7 | C21orf91 ortholog overexpression leads to myelination failures and abnormal GFAP coexpression in myelin-producing oligodendrocytes. Immunofluorescence analysis of co-transfected OPCs with a GFP expression vector (for visualization, green) and an empty control vector (con, white bars) or a C21orf91 ortholog (RGD1563888) overexpression construct (ovex, black bars) revealed that after 3 days (3d) of differentiation the proportion of cells with strong MBP expression was increased upon C21orf91 overexpression **(A)**. While control transfected cells exhibited MBP vesicle-like signals (red; **B**) C21orf91 overexpression resulted in stronger MBP signals (bold arrows) and myelin protein presence in cell processes **(C)**. Thin arrows point at cells with weak MBP expression. Cell nuclei were labeled by DAPI (blue). To assess whether the observed elevated levels of produced MBP protein correlate with the establishment of functional myelin, transfected OPCs were transplanted onto and cultured for 10 days on dissociated co-cultures. By categorizing GFP-positive cells (green) into different MBP expression- and morphological-related stages **(D)**, it was shown that C21orf91 overexpression resulted in fewer MBP expressing (pos) cells and also diminished their capacity to ensheath axons (myelin). They rather exhibited strong but non-organized MBP expression (NOM). Double immunostaining for MBP and GFAP (gray bars, blue stain) exposed NOM cells also to aberrantly coexpress both markers **(E)** which were confirmed *via* the orthogonal projection of a confocal, z-stacked microscopy image **(F)**. Black arrows show which channels were merged; white dashed lines depict the y-axis cut through the z-stack which is shown in the white box on the right side of the images. Scale bars: 50 μm **(B,C)**; 25 μm **(D)** and 20 μm **(F)**. Data are shown as mean values (±SEM) deriving from $n = 5$ **(A)** and $n = 9$ experiments **(D,E)**. Statistical significance was calculated using Kruskal-Wallis test with Dunn's post-test **(A)** and Student's two-sided, unpaired *t*-test **(D,E)**: $^{*}p \leq 0.05$, $^{**}p \leq 0.01$, ns = not significant; $^{\#}p \leq 0.05$ for the statistical analysis of GFAP + /MBP+ cells (gray bars) in **(E)**.

human newborns with neonatal ischemic and gliotic brain damage. Axin2 is a target of Wnt and negatively feeds back on this pathway, thereby promoting degradation of β-catenin (Fancy et al., 2011).

Further investigations along this line will be the subject of upcoming studies and could indeed contribute to the identification of therapeutic approaches which would allow to support or protect white matter development in young DS

patients—a so far clinically unmet need. In this regard, it is worth mentioning that myelin repair studies in the context of multiple sclerosis (MS) or after hypoxia-ischemia mediated preterm brain injury have advanced in the last decade and that several modulating pharmacological agents are currently tested in clinical trials (Kremer et al., 2011, 2016; Reiche et al., 2019). Most promising substances emanating from demyelinating disease research should therefore be evaluated for their potential to correct the here described non-permissive cellular phenotype and to promote cells in their process to contact and myelinate axons.

Likewise, when it comes to the misexpression of MBP protein in *C21orf91* ortholog overexpressing cells in a more physiological context, it will also be of interest to study mechanisms of translational control in distal regions of oligodendrocyte processes. Regulated *via* ribonucleoprotein complexes referred to as RNA granules (Maggipinto et al., 2004) and with its mRNA residing in a translationally inactive state, the role of for example ribonucleoprotein types F and A2 (hnRNP_F, hnRNP_A2), both involved in post-transcriptional regulation of MBP expression (White et al., 2012) should be examined. Of note, fetal DS brains were found to possess increased protein levels of hnRNP_A2/B1 which was suggested to lead to impaired MBP expression (Kim et al., 2001). The here observed accumulation of MBP protein around oligodendroglial somata (NOM cells; **Figures 7D,F**) could therefore result from deficits in the transport of the mRNA-packed granules, suggesting that C21orf91 could be involved in specific transport processes. Such an extended functional role is supported by C21orf91's association with microtubules[3].

Finally, the here proposed influence of the C21orf91 protein on the establishment of mainly oligodendrocytes and white matter needs to be confirmed in suitable *in vivo* paradigms. Existing mouse models for DS such as the commonly used strains Ts65Dn and Ts1Cje comprise several HSA21 homologous genes located on mouse chromosome 16 (MMU16; Antonarakis, 2017; Herault et al., 2017) and are therefore likely not to support this strategy as they would not allow focusing exclusively on the functionality of the *C21ORF91* gene. Furthermore, Li et al. (2016) highlighted that this gene is also not represented within the modulated regions of those strains. Likewise, *C21orf91* ortholog knockout animals would also not be suitable, given that our data on oligodendroglia indicate that the observed cellular phenotype is a consequence of non-physiologically elevated gene expression levels. Such a constellation, therefore, needs to be mimicked by a *C21orf91* ortholog transgenic overexpression model, which needs yet to be generated. Here, an inducible expression might be considered to avoid too high protein levels as well as to provide the possibility to apply different time windows of gene induction. Nevertheless, a valuable alternative to such *in vivo* studies would be given by the generation of induced pluripotent stem cell (iPSC) generated neural cells that can be fostered to become oligodendrocytes [as shown by us in Jadasz et al. (2018)]. C21orf91 overexpression in such cells could be investigated in a tissue environment such as organoids and using DS patient-derived cells, it could then also be expanded towards humans. Of note, *C21ORF91* was classified as the second most induced gene among 71 genes overexpressed in DS iPSCs (Chou et al., 2012). If such increased levels are maintained in neural/oligodendroglial progeny cells molecular reverting/correcting strategies could be applied to assess the pathophysiological functionality of this gene.

[3]http://www.proteinatlas.org/ENSG00000154642-C21orf91/antibody

DATA AVAILABILITY STATEMENT

The datasets presented in this study can be found in online repositories. The names of the repository/repositories and accession number(s) can be found in the article/**Supplementary Material**.

ETHICS STATEMENT

The animal study was reviewed and approved by LANUV; Landesamt für Natur, Umwelt und Verbraucherschutz.

AUTHOR CONTRIBUTIONS

LR, PG, and PK contributed to the conception and design of the study. LL, PD, and KA analyzed and presented data from existing databases and websites. LR, MP, JS, and AM performed experiments. LR, MP, LL, PD, KA, JS-H, PG, AM, and PK contributed to data analysis and interpretation. LR, AM, and MP performed the statistical analysis. LR, LL, PD, KA, PG, and PK contributed to the data visualization. LL, PD, and KA contributed written sections of the manuscript. LR and PK wrote the manuscript. LR, PG, and PK contributed to funding acquisition. PK supervised the project. All authors contributed to the article and approved the submitted version.

FUNDING

LR was supported by the Jürgen Manchot Foundation, Düsseldorf and the iBrain Graduate School, Düsseldorf. This work was also supported by the Stifterverband/Novartisstiftung (to PK).

ACKNOWLEDGMENTS

We thank Brigida Ziegler and Birgit Blomenkamp for their technical assistance. Furthermore, we thank Hybrigenics SA for providing the C21orf91 expression vectors.

SUPPLEMENTARY MATERIAL

The Supplementary Material for this article can be found online at: https://www.frontiersin.org/articles/10.3389/fncel.2021.653075/full#supplementary-material.

SUPPLEMENTARY FIGURE 1 | Multiple sequence alignment of human *C21ORF91* and model organism orthologs performed with ClustalO and Jalview.

REFERENCES

Abraham, H., Vincze, A., Veszpremi, B., Kravjak, A., Gomori, E., Kovacs, G. G., et al. (2012). Impaired myelination of the human hippocampal formation in Down syndrome. *Int. J. Dev. Neurosci.* 30, 147–158. doi: 10.1016/j.ijdevneu.2011.11.005

Aguirre, A., and Gallo, V. (2004). Postnatal neurogenesis and gliogenesis in the olfactory bulb from NG2-expressing progenitors of the subventricular zone. *J. Neurosci.* 24, 10530–10541. doi: 10.1523/JNEUROSCI.3572-04.2004

Ait Yahya-Graison, E., Aubert, J., Dauphinot, L., Rivals, I., Prieur, M., Golfier, G., et al. (2007). Classification of human chromosome 21 gene-expression variations in Down syndrome: impact on disease phenotypes. *Am. J. Hum. Genet.* 81, 475–491. doi: 10.1086/520000

Akkermann, R., Beyer, F., and Küry, P. (2017). Heterogeneous populations of neural stem cells contribute to myelin repair. *Neural Regen. Res.* 12, 509–517. doi: 10.4103/1673-5374.204999

Antonarakis, S. E. (2017). Down syndrome and the complexity of genome dosage imbalance. *Nat. Rev. Genet.* 18, 147–163. doi: 10.1038/nrg.2016.154

Azim, K., Akkermann, R., Cantone, M., Vera, J., Jadasz, J. J., and Küry, P. (2018). Transcriptional profiling of ligand expression in cell specific populations of the adult mouse forebrain that regulates neurogenesis. *Front. Neurosci.* 12:220. doi: 10.3389/fnins.2018.00220

Azim, K., Angonin, D., Marcy, G., Pieropan, F., Rivera, A., Donega, V., et al. (2017). Pharmacogenomic identification of small molecules for lineage specific manipulation of subventricular zone germinal activity. *PLoS Biol.* 15:e2000698. doi: 10.1371/journal.pbio.2000698

Azim, K., Hurtado-Chong, A., Fischer, B., Kumar, N., Zweifel, S., Taylor, V., et al. (2015). Transcriptional hallmarks of heterogeneous neural stem cell niches of the subventricular zone. *Stem Cells* 33, 2232–2242. doi: 10.1002/stem.2017

Baburamani, A. A., Patkee, P. A., Arichi, T., and Rutherford, M. A. (2019). New approaches to studying early brain development in Down syndrome. *Dev. Med. Child Neurol.* 61, 867–879. doi: 10.1111/dmcn.14260

Baumann, N., and Pham-Dinh, D. (2001). Biology of oligodendrocyte and myelin in the mammalian central nervous system. *Physiol. Rev.* 81, 871–927. doi: 10.1152/physrev.2001.81.2.871

Bercury, K. K., and Macklin, W. B. (2015). Dynamics and mechanisms of CNS myelination. *Dev. Cell* 32, 447–458. doi: 10.1016/j.devcel.2015.01.016

Beyer, F., Jadasz, J., Samper Agrelo, I., Schira-Heinen, J., Groh, J., Manousi, A., et al. (2020). Heterogeneous fate choice of genetically modulated adult neural stem cells in gray and white matter of the central nervous system. *Glia* 68, 393–406. doi: 10.1002/glia.23724

Booth, J., Nicolay, D. J., Doucette, J. R., and Nazarali, A. J. (2007). Hoxd1 is expressed by oligodendroglial cells and binds to a region of the human myelin oligodendrocyte glycoprotein promoter *in vitro*. *Cell. Mol. Neurobiol.* 27, 641–650. doi: 10.1007/s10571-007-9150-4

Cahoy, J. D., Emery, B., Kaushal, A., Foo, L. C., Zamanian, J. L., Christopherson, K. S., et al. (2008). A transcriptome database for astrocytes, neurons, and oligodendrocytes: a new resource for understanding brain development and function. *J. Neurosci.* 28, 264–278. doi: 10.1523/JNEUROSCI.4178-07.2008

Chou, S. T., Byrska-Bishop, M., Tober, J. M., Yao, Y., Vandorn, D., Opalinska, J. B., et al. (2012). Trisomy 21-associated defects in human primitive hematopoiesis revealed through induced pluripotent stem cells. *Proc. Natl. Acad. Sci. U S A* 109, 17573–17578. doi: 10.1073/pnas.1211175109

de Faria, O., Jr., Dhaunchak, A. S., Kamen, Y., Roth, A. D., Kuhlmann, T., Colman, D. R., et al. (2019). TMEM10 promotes oligodendrocyte differentiation and is expressed by oligodendrocytes in human remyelinating multiple sclerosis plaques. *Sci. Rep.* 9:3606. doi: 10.1038/s41598-019-40342-x

Dossi, E., Vasile, F., and Rouach, N. (2018). Human astrocytes in the diseased brain. *Brain Res. Bull.* 136, 139–156. doi: 10.1016/j.brainresbull.2017.02.001

Emery, B. (2010). Regulation of oligodendrocyte differentiation and myelination. *Science* 330, 779–782. doi: 10.1126/science.1190927

Fancy, S. P., Harrington, E. P., Yuen, T. J., Silbereis, J. C., Zhao, C., Baranzini, S. E., et al. (2011). Axin2 as regulatory and therapeutic target in newborn brain injury and remyelination. *Nat. Neurosci.* 14, 1009–1016. doi: 10.1038/nn.2855

Fenoll, R., Pujol, J., Esteba-Castillo, S., de Sola, S., Ribas-Vidal, N., Garcia-Alba, J., et al. (2017). Anomalous white matter structure and the effect of age in down syndrome patients. *J. Alzheimers Dis.* 57, 61–70. doi: 10.3233/JAD-161112

Göttle, P., Forster, M., Gruchot, J., Kremer, D., Hartung, H. P., Perron, H., et al. (2019). Rescuing the negative impact of human endogenous retrovirus envelope protein on oligodendroglial differentiation and myelination. *Glia* 67, 160–170. doi: 10.1002/glia.23535

Göttle, P., Kremer, D., Jander, S., Odemis, V., Engele, J., Hartung, H. P., et al. (2010). Activation of CXCR7 receptor promotes oligodendroglial cell maturation. *Ann. Neurol.* 68, 915–924. doi: 10.1002/ana.22214

Göttle, P., Manousi, A., Kremer, D., Reiche, L., Hartung, H. P., and Küry, P. (2018). Teriflunomide promotes oligodendroglial differentiation and myelination. *J. Neuroinflammation* 15:76. doi: 10.1186/s12974-018-1110-z

Göttle, P., Sabo, J. K., Heinen, A., Venables, G., Torres, K., Tzekova, N., et al. (2015). Oligodendroglial maturation is dependent on intracellular protein shuttling. *J. Neurosci.* 35, 906–919. doi: 10.1523/JNEUROSCI.1423-14.2015

Guo, F., Ma, J., McCauley, E., Bannerman, P., and Pleasure, D. (2009). Early postnatal proteolipid promoter-expressing progenitors produce multilineage cells *in vivo*. *J. Neurosci.* 29, 7256–7270. doi: 10.1523/JNEUROSCI.5653-08.2009

Haydar, T. F., and Reeves, R. H. (2012). Trisomy 21 and early brain development. *Trends Neurosci.* 35, 81–91. doi: 10.1016/j.tins.2011.11.001

Herault, Y., Delabar, J. M., Fisher, E. M. C., Tybulewicz, V. L. J., Yu, E., and Brault, V. (2017). Rodent models in Down syndrome research: impact and future opportunities. *Dis. Models Mech.* 10, 1165–1186. doi: 10.1242/dmm.029728

Hruz, T., Laule, O., Szabo, G., Wessendorp, F., Bleuler, S., Oertle, L., et al. (2008). Genevestigator v3: a reference expression database for the meta-analysis of transcriptomes. *Adv. Bioinformatics* 2008:420747. doi: 10.1155/2008/420747

Jadasz, J. J., Tepe, L., Beyer, F., Samper Agrelo, I., Akkermann, R., Spitzhorn, L. S., et al. (2018). Human mesenchymal factors induce rat hippocampal- and human neural stem cell dependent oligodendrogenesis. *Glia* 66, 145–160. doi: 10.1002/glia.23233

Jiao, C., Yan, P., Xia, C., Shen, Z., Tan, Z., Tan, Y., et al. (2019). BrainEXP: a database featuring with spatiotemporal expression variations and co-expression organizations in human brains. *Bioinformatics* 35, 172–174. doi: 10.1093/bioinformatics/bty576

Kanaumi, T., Milenkovic, I., Adle-Biassette, H., Aronica, E., and Kovacs, G. G. (2013). Non-neuronal cell responses differ between normal and Down syndrome developing brains. *Int. J. Dev. Neurosci.* 31, 796–803. doi: 10.1016/j.ijdevneu.2013.09.011

Karlsen, A. S., and Pakkenberg, B. (2011). Total numbers of neurons and glial cells in cortex and basal ganglia of aged brains with Down syndrome--a stereological study. *Cereb. Cortex* 21, 2519–2524. doi: 10.1093/cercor/bhr033

Kim, S. H., Dierssen, M., Ferreres, J. C., Fountoulakis, M., and Lubec, G. (2001). Increased protein levels of heterogeneous nuclear ribonucleoprotein A2/B1 in fetal Down syndrome brains. *J. Neural Transm. Suppl.* 61, 273–280. doi: 10.1007/978-3-7091-6262-0_22

Korbel, J. O., Tirosh-Wagner, T., Urban, A. E., Chen, X. N., Kasowski, M., Dai, L., et al. (2009). The genetic architecture of Down syndrome phenotypes revealed by high-resolution analysis of human segmental trisomies. *Proc. Natl. Acad. Sci. U S A* 106, 12031–12036. doi: 10.1073/pnas.0813248106

Kremer, D., Aktas, O., Hartung, H. P., and Küry, P. (2011). The complex world of oligodendroglial differentiation inhibitors. *Ann. Neurol.* 69, 602–618. doi: 10.1002/ana.22415

Kremer, D., Göttle, P., Hartung, H.-P., and Küry, P. (2016). Pushing forward: remyelination as the new frontier in CNS diseases. *Trends Neurosci.* 39, 246–263. doi: 10.1016/j.tins.2016.02.004

Kremer, D., Heinen, A., Jadasz, J., Göttle, P., Zimmermann, K., Zickler, P., et al. (2009). p57kip2 is dynamically regulated in experimental autoimmune encephalomyelitis and interferes with oligodendroglial maturation. *Proc. Natl. Acad. Sci. U S A* 106, 9087–9092. doi: 10.1073/pnas.0900204106

Lanfranchi, S., Jerman, O., Dal Pont, E., Alberti, A., and Vianello, R. (2010). Executive function in adolescents with Down syndrome. *J. Intellect. Disabil. Res.* 54, 308–319. doi: 10.1111/j.1365-2788.2010.01262.x

Li, S. S., Qu, Z. D., Haas, M., Ngo, L., Heo, Y. J., Kang, H. J., et al. (2016). The HSA21 gene EURL/C21ORF91 controls neurogenesis within the cerebral

cortex and is implicated in the pathogenesis of Down syndrome. *Sci. Rep.* 6:29514. doi: 10.1038/srep29514

Li, W. Q., Luo, L. D., Hu, Z. W., Lyu, T. J., Cen, C., and Wang, Y. (2019). PLD1 promotes dendritic spine morphogenesis *via* activating PKD1. *Mol. Cell. Neurosci.* 99:103394. doi: 10.1016/j.mcn.2019.103394

Maggipinto, M., Rabiner, C., Kidd, G. J., Hawkins, A. J., Smith, R., and Barbarese, E. (2004). Increased expression of the MBP mRNA binding protein HnRNP A2 during oligodendrocyte differentiation. *J. Neurosci. Res.* 75, 614–623. doi: 10.1002/jnr.20014

McCarthy, K. D., and de Vellis, J. (1980). Preparation of separate astroglial and oligodendroglial cell cultures from rat cerebral tissue. *J. Cell Biol.* 85, 890–902. doi: 10.1083/jcb.85.3.890

Mito, T., and Becker, L. E. (1993). Developmental changes of S-100 protein and glial fibrillary acidic protein in the brain in Down syndrome. *Exp. Neurol.* 120, 170–176. doi: 10.1006/exnr.1993.1052

Moyon, S., Dubessy, A. L., Aigrot, M. S., Trotter, M., Huang, J. K., Dauphinot, L., et al. (2015). Demyelination causes adult CNS progenitors to revert to an immature state and express immune cues that support their migration. *J. Neurosci.* 35, 4–20. doi: 10.1523/JNEUROSCI.0849-14.2015

Nave, K. A. (1994). Neurological mouse mutants and the genes of myelin. *J. Neurosci. Res.* 38, 607–612. doi: 10.1002/jnr.490380602

Nishiyama, A., Komitova, M., Suzuki, R., and Zhu, X. (2009). Polydendrocytes (NG2 cells): multifunctional cells with lineage plasticity. *Nat. Rev. Neurosci.* 10, 9–22. doi: 10.1038/nrn2495

Olmos-Serrano, J. L., Kang, H. J., Tyler, W. A., Silbereis, J. C., Cheng, F., Zhu, Y., et al. (2016). Down syndrome developmental brain transcriptome reveals defective oligodendrocyte differentiation and myelination. *Neuron* 89, 1208–1222. doi: 10.1016/j.neuron.2016.01.042

Pennington, B. F., Moon, J., Edgin, J., Stedron, J., and Nadel, L. (2003). The neuropsychology of Down syndrome: evidence for hippocampal dysfunction. *Child Dev.* 74, 75–93. doi: 10.1111/1467-8624.00522

Powell, D., Caban-Holt, A., Jicha, G., Robertson, W., Davis, R., Gold, B. T., et al. (2014). Frontal white matter integrity in adults with Down syndrome with and without dementia. *Neurobiol. Aging* 35, 1562–1569. doi: 10.1016/j.neurobiolaging.2014.01.137

Rao, M. S., and Mayer-Proschel, M. (1997). Glial-restricted precursors are derived from multipotent neuroepithelial stem cells. *Dev. Biol.* 188, 48–63. doi: 10.1006/dbio.1997.8597

Rehberg, S., Lischka, P., Glaser, G., Stamminger, T., Wegner, M., and Rosorius, O. (2002). Sox10 is an active nucleocytoplasmic shuttle protein and shuttling is crucial for Sox10-mediated transactivation. *Mol. Cell. Biol.* 22, 5826–5834. doi: 10.1128/mcb.22.16.5826-5834.2002

Reiche, L., Küry, P., and Göttle, P. (2019). Aberrant oligodendrogenesis in down syndrome: shift in gliogenesis? *Cells* 8:1591. doi: 10.3390/cells8121591

Rost, I., Fiegler, H., Fauth, C., Carr, P., Bettecken, T., Kraus, J., et al. (2004). Tetrasomy 21pter-->q21.2 in a male infant without typical Down's syndrome dysmorphic features but moderate mental retardation. *J. Med. Genet.* 41:e26. doi: 10.1136/jmg.2003.011833

Rowe, J., Lavender, A., and Turk, V. (2006). Cognitive executive function in Down's syndrome. *Br. J. Clin. Psychol.* 45, 5–17. doi: 10.1348/014466505X29594

Schindelin, J., Arganda-Carreras, I., Frise, E., Kaynig, V., Longair, M., Pietzsch, T., et al. (2012). Fiji: an open-source platform for biological-image analysis. *Nat. Methods* 9, 676–682. doi: 10.1038/nmeth.2019

Setoguchi, T., and Kondo, T. (2004). Nuclear export of OLIG2 in neural stem cells is essential for ciliary neurotrophic factor-induced astrocyte differentiation. *J. Cell Biol.* 166, 963–968. doi: 10.1083/jcb.200404104

Simons, M., and Nave, K. A. (2015). Oligodendrocytes: myelination and axonal support. *Cold Spring Harb. Perspect. Biol.* 8:a020479. doi: 10.1101/cshperspect.a020479

Slavotinek, A. M., Chen, X. N., Jackson, A., Gaunt, L., Campbell, A., Clayton-Smith, J., et al. (2000). Partial tetrasomy 21 in a male infant. *J. Med. Genet.* 37:E30. doi: 10.1136/jmg.37.10.e30

Snaidero, N., and Simons, M. (2014). Myelination at a glance. *J. Cell Sci.* 127, 2999–3004. doi: 10.1242/jcs.151043

Stagni, F., Giacomini, A., Emili, M., Guidi, S., and Bartesaghi, R. (2017). Neurogenesis impairment: an early developmental defect in Down syndrome. *Free Radic. Biol. Med.* 114, 15–32. doi: 10.1016/j.freeradbiomed.2017.07.026

Sunkin, S. M., Ng, L., Lau, C., Dolbeare, T., Gilbert, T. L., Thompson, C. L., et al. (2013). Allen brain atlas: an integrated spatio-temporal portal for exploring the central nervous system. *Nucleic Acids Res.* 41, D996–D1008. doi: 10.1093/nar/gks1042

Tanner, D. C., Cherry, J. D., and Mayer-Pröschel, M. (2011). Oligodendrocyte progenitors reversibly exit the cell cycle and give rise to astrocytes in response to interferon-γ. *J. Neurosci.* 31, 6235–6246. doi: 10.1523/JNEUROSCI.5905-10.2011

Thomas, P. D., Campbell, M. J., Kejariwal, A., Mi, H., Karlak, B., Daverman, R., et al. (2003). PANTHER: a library of protein families and subfamilies indexed by function. *Genome Res.* 13, 2129–2141. doi: 10.1101/gr.772403

Thomas, P. D., Kejariwal, A., Guo, N., Mi, H., Campbell, M. J., Muruganujan, A., et al. (2006). Applications for protein sequence-function evolution data: mRNA/protein expression analysis and coding SNP scoring tools. *Nucleic Acids Res.* 34, W645–W650. doi: 10.1093/nar/gkl229

Waxman, S. G. (1992). Demyelination in spinal cord injury and multiple sclerosis: what can we do to enhance functional recovery? *J. Neurotrauma* 9, S105–S117.

Wheeler, N. A., Lister, J. A., and Fuss, B. (2015). The autotaxin-lysophosphatidic acid axis modulates histone acetylation and gene expression during oligodendrocyte differentiation. *J. Neurosci.* 35, 11399–11414. doi: 10.1523/JNEUROSCI.0345-15.2015

White, R., Gonsior, C., Bauer, N. M., Krämer-Albers, E.-M., Luhmann, H. J., and Trotter, J. (2012). Heterogeneous nuclear ribonucleoprotein (hnRNP) F is a novel component of oligodendroglial RNA transport granules contributing to regulation of myelin basic protein (MBP) synthesis. *J. Biol. Chem.* 287, 1742–1754. doi: 10.1074/jbc.M111.235010

Wilkins, A., Majed, H., Layfield, R., Compston, A., and Chandran, S. (2003). Oligodendrocytes promote neuronal survival and axonal length by distinct intracellular mechanisms: a novel role for oligodendrocyte-derived glial cell line-derived neurotrophic factor. *J. Neurosci.* 23, 4967–4974. doi: 10.1523/JNEUROSCI.23-12-04967.2003

Wu, Y., Liu, Y., Levine, E. M., and Rao, M. S. (2003). Hes1 but not Hes5 regulates an astrocyte versus oligodendrocyte fate choice in glial restricted precursors. *Dev. Dyn.* 226, 675–689. doi: 10.1002/dvdy.10278

Xiao, L., Ohayon, D., McKenzie, I. A., Sinclair-Wilson, A., Wright, J. L., Fudge, A. D., et al. (2016). Rapid production of new oligodendrocytes is required in the earliest stages of motor-skill learning. *Nat. Neurosci.* 19, 1210–1217. doi: 10.1038/nn.4351

Zdaniuk, G., Wierzba-Bobrowicz, T., Szpak, G. M., and Stepien, T. (2011). Astroglia disturbances during development of the central nervous system in fetuses with Down's syndrome. *Folia Neuropathol.* 49, 109–114.

Conflict of Interest: The authors declare that the research was conducted in the absence of any commercial or financial relationships that could be construed as a potential conflict of interest.

EBioMedicine 65 (2021) 103276

Contents lists available at ScienceDirect

EBioMedicine

journal homepage: www.elsevier.com/locate/ebiom

Research paper

Identification of novel myelin repair drugs by modulation of oligodendroglial differentiation competence

Anastasia Manousi[a,#], Peter Göttle[a,#], Laura Reiche[a], Qiao-Ling Cui[b], Luke M. Healy[b], Rainer Akkermann[a], Joel Gruchot[a], Jessica Schira-Heinen[a], Jack P. Antel[b], Hans-Peter Hartung[a,c], Patrick Küry[a,*]

[a] Department of Neurology, Medical Faculty, Heinrich-Heine-University Düsseldorf, 40225, Germany
[b] Department of Neurology and Neurosurgery, Montreal Neurological Institute, McGill University, Montreal, QC H4A 3K9, Canada
[c] Brain and Mind Centre, University of Sydney, Camperdown NSW 2050, Australia

ARTICLE INFO

Article History:
Received 7 December 2020
Revised 22 February 2021
Accepted 23 February 2021
Available online xxx

Keywords:
Remyelination
CDKN1C
Nuclear protein shuttling
Drug repurposing
Cell differentiation
Toxin-mediated demyelination

ABSTRACT

Background: In multiple sclerosis loss of myelin and oligodendrocytes impairs saltatory signal transduction and leads to neuronal loss and functional deficits. Limited capacity of oligodendroglial precursor cells to differentiate into mature cells is the main reason for inefficient myelin repair in the central nervous system. Drug repurposing constitutes a powerful approach for identification of pharmacological compounds promoting this process.
Methods: A phenotypic compound screening using the subcellular distribution of a potent inhibitor of oligodendroglial cell differentiation, namely p57kip2, as differentiation competence marker was conducted. Hit compounds were validated in terms of their impact on developmental cell differentiation and myelination using both rat and human primary cell cultures and organotypic cerebellar slice cultures, respectively. Their effect on spontaneous remyelination was then investigated following cuprizone-mediated demyelination of the corpus callosum.
Findings: A number of novel small molecules able to promote oligodendroglial cell differentiation were identified and a subset was found to foster human oligodendrogenesis as well as myelination *ex vivo*. Among them the steroid danazol and the anthelminthic parbendazole were found to increase myelin repair.
Interpretation: We provide evidence that early cellular processes involved in differentiation decisions are applicable for the identification of regeneration promoting drugs and we suggest danazol and parbendazole as potent therapeutic candidates for demyelinating diseases.
Funding: This work was supported by the Jürgen Manchot Foundation, Düsseldorf; Research Commission of the Medical Faculty of Heinrich-Heine-University Düsseldorf; Christiane and Claudia Hempel Foundation; Stifterverband/Novartisstiftung; James and Elisabeth Cloppenburg, Peek and Cloppenburg Düsseldorf Stiftung and International Progressive MS Alliance (BRAVEinMS).

1. Introduction

Multiple sclerosis (MS) is a disabling demyelinating disorder of the central nervous system (CNS) primarily arising from a misguided immune reaction. Specifically, immune cell infiltration in the CNS results in loss of myelin and oligodendrocytes, the myelin producing cells of the CNS [1,2]. Loss of myelin leads to impaired saltatory nerve conduction, neurodegeneration and eventually to irreversible neurological deficits [3,4]. In the adult CNS, a widespread population of resident oligodendroglial progenitor cells (OPCs) retains the capacity to generate myelinating oligodendrocytes throughout adulthood, thus contributing to myelin repair [5]. Despite this regenerative potential, the overall myelination capacity of these cells remains limited and further decreases over the course of the disease which is likely due to inhibitory signals and lack of stimulatory cues [6–9].

While the currently used MS therapies successfully address the autoimmune reaction no effective treatment in order to boost and stabilize existing remyelination activities yet exists – rendering neuroregeneration an unmet clinical need [10,11]. Oligodendrogenesis is dependent on many extrinsic and intrinsic cues the investigation of which is promising in opening new therapeutic avenues [12]. In our study, we focused on the p57kip2 protein, which we initially

* Corresponding author.
E-mail address: kuery@uni-duesseldorf.de (P. Küry).
# These authors have contributed equally to this study.

https://doi.org/10.1016/j.ebiom.2021.103276

Research in context

Evidence before this study

The currently used therapeutic approaches for multiple sclerosis are mainly focused on the immunological aspects of the pathology and they can slow down the progression of the disease, however, without inversion of the already existed damage. Compound screening and drug repurposing approaches led to the identification of compounds which promote oligodendroglial cell differentiation as means of myelin repair and neuroregeneration. And although some of them have already entered clinical trials, enhancement of regeneration still remains an unmet clinical need. Better understanding of the regulatory cues of regeneration processes might lead the way to new therapeutic approaches. In this respect, we previously described p57kip2 as potent nuclear inhibitor of oligodendroglial differentiation the subcellular re-localization of which allows maturation to proceed..

Added value of this study

This study used the capacity of p57kip2 protein's subcellular localization to serve as early differentiation competence marker. We identified four compounds with oligodendroglial differentiation promoting competence in the rat system, namely danazol, parbendazole, methiazole and nocodazole, with the first three also being able to promote human oligodendroglial cell maturation as well as developmental myelination of organotypic slice cultures. Moreover, danazol and parbendazole also promoted remyelination in the cuprizone-mediated mouse model of demyelination..

Implications of all of the available evidence

The use of p57kip2's subcellular localization as readout of our screening suggests its use as early oligodendroglial cell differentiation competence marker and supports the notion that early cellular processes involved in differentiation are applicable for the identification of myelin repair promoting drugs. In this context, we detected regenerative properties of the steroid danazol and the antihelminthic parbendazole. In addition, our study includes rat, mouse, and human systems as well as different brain regions, suggesting targeted mechanisms which are evolutionary conserved and are therefore suitable for biomedical translation

identified as intrinsic inhibitor of myelinating glial cell differentiation [13–15]. In a follow-up investigation we then demonstrated that the subcellular localization of this protein is associated with and necessary for the competence of OPCs to undergo differentiation [16]. Specifically, it was shown that p57kip2 translocation from the nucleus is critical for these cells to proceed in differentiation, maturation, and to generate myelin sheaths. Drug repurposing can serve as effective means for the treatment of yet unmet clinical conditions, including neurodegeneration [17–19]. This is exemplified by our recent demonstration that teriflunomide, an immunomodulatory disease-modifying treatment, which is approved as a first-line treatment for relapsing MS, can also promote p57kip2 shuttling, OPC differentiation as well as myelination *in vitro* [20].

During the past years, a number of studies aiming at identifying (small) molecules able to promote oligodendroglial cell differentiation and remyelination have emerged. Most of them are based on pharmacological compound screenings using myelin marker expression [21–24]. Many of these approaches revealed novel regulatory roles of known cellular mechanisms such as the cholesterol synthesis pathway [25], histamine receptor- [26], and muscarinic acetylcholine receptor signaling [21,22] and some substances already entered clinical trials, reviewed by [10,27,28]. Despite these recent developments a clinical application of an effective remyelinating treatment has still not been achieved. In order to provide an alternative approach for the identification of molecules that positively modulate myelin repair we performed a phenotypic compound screening based on p57kip2's protein subcellular distribution in primary rodent OPCs. This analysis was undertaken step-wise starting with primary rodent OPCs, then applying an *ex vivo* myelination model and using primary human OPCs with eventually testing active compounds in an *in vivo* de- and remyelination model.

2. Methods

2.1. Ethics statements for animal and human tissue experiments

The generation of rodent primary oligodendroglial cell and organotypic cerebellar slice cultures were approved by the ZETT (Zentrale Einrichtung für Tierforschung und wissenschaftliche Tierschutzaufgaben; O69/11, V54/09). Cuprizone mediated demyelination experiments were approved by the authorities at LANUV (Landesamt für Natur, Umwelt und Verbraucherschutz Nordrhein-Westfalen; Az.: 81–02.04.2019.A203) and carried out according to ARRIVE guidelines. These experimental procedures are characterised by mild severity grade and therefore no interventions to reduce pain, suffering and distress were needed. Human OPCs were isolated from second trimester (14–17 weeks) fetal samples obtained from the University of Washington Birth Defects Research Laboratory (MP-37–2014–540; 13–244-PED; eReviews_3345).

2.2. Rat oligodendroglial cell culture and immunocytochemistry

Primary OPC cultures from postnatal day zero or one cerebral rat cortices (Wistar rats of either sex) were generated as previously described [14,16,29]. Briefly, freshly removed cortices were cut in small pieces and placed in Minimum Essential Medium (MEM, Thermo Fisher Scientific, Darmstadt, Germany). After centrifugation at 2000 rpm for one minute the pellet was resuspended in 1 ml of digestion medium (MEM; 40 μg/ml DNAse; 0.24 mg/ml L-cystein; 30 U/ml papain, all Sigma–Aldrich, Taufkirchen, Germany). Following incubation (5% CO_2, 90% relative humidity, 37 °C) for 45 minutes, 1 ml of trypsin inhibitor solution [Leibvitz's medium L-15, Thermo Fisher Scientific; 1 mg/ml trypsin inhibitor, Sigma–Aldrich; 50 mg/ml biotin-free bovine serum albumin (BSA), Carl Roth, Karlsruhe, Germany; 40 μg/ml DNase I type IV, Sigma–Aldrich] was added. The solution was incubated for four minutes at room temperature (RT) and then the supernatant was removed. Subsequently, 1 ml of trypsin inhibitor solution was added to the pellet, followed by resuspension and addition of 10 ml Dulbecco's Modified Eagle Medium (DMEM, Thermo Fisher Scientific) containing 10% fetal bovine serum (Brazilian origin, Lonza, Basel, Switzerland; USA origin, Capricorn Scientific, Palo Alto, CA, USA); 4 mM L-glutamine; 100 U/ml penicillin/0.1 mg/ml streptomycin (both Thermo Fisher Scientific). The solution was centrifuged for five minutes at 1200 rpm and the supernatant was removed. In the next step, the pellet was resuspended in 1 ml of the same medium. Cell suspension from two animals was added to each uncoated T-75 cell culture flask (Greiner Bio-One, Kremsmünster, Austria). Mixed glial cultures were maintained for ten days (5% CO_2, 90% relative humidity, 37 °C) before OPC purification was performed. The medium was changed after the first four days and two times a week thereafter. Upon OPC purification, purity of the culture (~98%) was determined via anti–A2B5 staining (Merck Millipore, Darmstadt, Germany; data not shown). OPCs were seeded either onto 1 mg/ml poly-D-lysine coated (PDL, Sigma–Aldrich) 96-well plates (96-well

Black/Clear Flat Bottom TC-treated Imaging Microplate with Lid, Corning, Glendale, AZ, USA) for the compound screening or onto 0.25 mg/ml PDL coated glass coverslips (13 mm) in 24-well plates for each step of validation and initially kept in DMEM based Sato medium [5 μg/ml bovine insulin; 50 μg/ml human transferrin; 100 μg/ml bovine serum albumin fraction V (BSA, Thermo Fisher Scientific); 6.2 ng/ml progesterone; 16 μg/ml putrescine, 5 ng/ml sodium selenite; 400 ng/ml T3 (tri-iodo-thyronine); 400 ng/ml T4 (thyroxin; all Sigma–Aldrich unless stated otherwise); 4 mM L-glutamine; 100 U/ml penicillin/0.1 mg/l streptomycin (both Thermo Fisher Scientific)]. Cell differentiation was induced 1.5 h after plating by addition of Sato medium supplemented with 0.5% fetal bovine serum (referred to as differentiation medium hereafter). At the same time corresponding chemical compounds were applied.

Cells were fixed with 4% paraformaldehyde (PFA) for ten minutes at RT and non-specific staining was prevented by blocking with 10% normal goat serum (NGS, Sigma–Aldrich) for 45 min at RT. Rabbit anti-p57kip2 primary antibody (Sigma-Aldrich Cat# P0357, RRID: AB_260,850) diluted 1:250 in blocking solution was applied overnight at 4 °C. Staining with rat anti-myelin basic protein (MBP, 1:250, Bio-Rad, Hercules, CA, USA Cat# MCA409S, RRID:AB_325,004) was performed in blocking solution containing 0.02% Triton X-100 (Sigma–Aldrich) overnight at 4 °C. Cells stained using the mouse anti-myelin oligodendrocyte glycoprotein antibody (MOG, 1:500, Merck Millipore Cat# MAB5680, RRID:AB_1,587,278) were permeabilised with 0.1% Triton X-100 in blocking solution and 0.01% in antibody solution. Following washing steps with PBS, coverslips were incubated with the secondary antibodies goat anti-rabbit Alexa Fluor 594 (1:500, Thermo Fisher Scientific Cat# A-11,037, RRID:AB_2,534,095) or goat anti-rat Alexa Fluor 488 (1:500, Thermo Fisher Scientific Cat# A-11,006, RRID:AB_2,534,074) both diluted in PBS and incubated for two hours at RT. Nuclei were counterstained with 4′,6–diamidino–2–phenylindole (DAPI, 1:100, Roche, Basel, Switzerland). Finally, the coverslips were washed with PBS and mounted using Citifluor AF1 mountant solution (Electron Microscopy Sciences, Hatfield, PA, USA). Staining specificity was confirmed upon application of the same secondary antibodies without prior application of the corresponding primary antibodies (data not shown). For image acquisition the Zeiss Axionplan2 microscope (Carl Zeiss Microscopy, Jena, Germany) was used and the analysis was performed with the ImageJ BioVoxxel software (BioVoxxel Toolbox, RRID:SCR_015825). Nine images per coverslip were captured using 20x magnification and the same exposure times throughout each experiment. Two coverslips were analysed per condition. The total cell number per field was assessed via DAPI staining. For quantification, the number of protein marker-positive cells in relation to the total cell number was calculated and expressed as percentage.

2.3. Western blotting

For western blot analysis, 2.4×10^6 OPCs per well were seeded in 0.25 mg/ml PDL coated 6-well plates and after incubation in Sato medium for 1.5 h, cells were treated either with 0.1 μM parbendazole or DMSO for control in differentiation medium for one hour. Afterwards, cells were detached with pre-warmed trypsin-EDTA (Capricorn Scientific; 5% CO_2, 90% relative humidity, 37 °C, for three to five minutes). Prior to centrifugation (1500 rpm, ten minutes, 4 °C), the enzymatic reaction was stopped with differentiation medium. Cell pellets were immediately frozen on dry ice and stored at −80 °C. Cell lysis was carried out on ice with radioimmunoprecipitation assay buffer (RIPA buffer, Cell Signaling Technology, Danvers, MA, USA) supplemented with HALT™ Protease-/Phosphatase inhibitor cocktail and EDTA (both Thermo Fisher Scientific). Specimens were subjected to ten seconds of sonication with an ultrasound homogenizer (SonopulsHD2070; 50% power, pulse 0.5 seconds on and 0.5 seconds off) and subsequently centrifuged (14,000 rpm, ten minutes, 4 °C) to proceed with the supernatant. Protein concentrations were determined using the DC Protein Assay (BioRad, Cat# 5,000,112). Samples were subjected to standard sodium dodecyl sulfate (SDS) gel electrophoresis and semi-dry western blotting using Bolt 12% Bis-Tris Plus gels and nitrocellulose membranes (both Thermo Fisher Scientific). Proteins were stained using the Pierce™ Reversible Protein Stain Kit (Thermo Fisher Scientific, Cat# 24,580) for protein normalization prior blocking with 1% milk powder for one hour at RT and applying the following primary antibodies: rabbit anti-p38 (1:1000, Cell Signaling Technology Cat# 9212, RRID:AB_330,713), rabbit anti-p-p38 (1:1000, Cell Signaling Technology Cat# 9211, RRID:AB_331,641), mouse anti-GAPDH (1:5000, Merck Millipore Cat# MAB374, RRID: AB_2,107,445) and the secondary antibodies anti-rabbit IgG, HRP-linked (1:2000, Cell Signaling Technology Cat# 7074, RRID: AB_2,099,233) and anti-mouse IgG (*H + L*), made in horse (1:5000, Vector Laboratories, Burlingame, CA, USA Cat# PI-2000, RRID: AB_2,336,177). Signals were visualized using Super Signal West Pico Chemiluminescent Substrate (Thermo Fisher Scientific, Cat# 34,579) applied for five minutes. Membranes were first used to detect p-p38 and afterwards stripped with 10 ml ReBlot Plus Strong Solution (1x, Merck Millipore) for the detection of p38 and the housekeeping protein (GAPDH), all in a sequential manner on the same membrane to ensure reliable quantification. Protein bands were quantified using the Fusion FX software (Vilber Lourmat, Eberhardzell, Germany). The intensity for each band was determined and normalized to the total amount of the loaded protein amount and the intensity of the GAPDH band of the corresponding sample.

2.4. Chemical compound library screening

For the compound screening the Prestwick Chemical Library (Prestwick, Illkirch, France, Cat# PCL1280.10–50-G96), consisting of 1280 small molecules with high chemical and pharmacological diversity and 99% approved by the FDA, EMA and other agencies, was chosen and handled according to specifications from the providers. Compounds were tested on primary rat OPCs seeded onto PDL coated 96-well plates at a density of 5000 cells/well. All compounds were tested at a concentration of 10 μM and the cells were allowed to differentiate for 24 hours. As positive control 1 μM of the S1P agonist FTY720/Fingolimod [Echelon Biosciences, Salt Lake City, UT, USA, CAS 402,616–26–6; [30] and as negative controls differentiation medium +/- 0.5% DMSO were used. Each substance was tested in triplicates within each individual experiment and each experiment was repeated twice. For the determination of the subcellular localization the rabbit anti-p57kip2 primary antibody [p57kip2, 1:250, Sigma-Aldrich Cat# P0357, RRID:AB_260,850; [16] and the goat anti-rabbit Alexa Fluor 594 secondary antibody (1:500, Thermo Fisher Scientific Cat# A-11,037, RRID:AB_2,534,095) were used while nuclei were counterstained with DAPI. Nine images per well with a 20x magnification were automatically captured using the BD Pathway 855 High-Content Cell Analyzer (BD Biosciences, Rockville, MD, USA) and the signal intensity of the anti-p57kip2 staining was measured in each region of interest (nucleus vs. cytoplasm) using the Attovision v.1.7.1 software package (BD Biosciences Systems, RRID:SCR_014315). Analysis of the acquired data was conducted via an algorithm designed in house using the Matlab Software R2015a (Mathworks, Inc, RRID: SCR_001622), which provides the percentage of cells with prevailed nuclear p57kip2 localization in each well. As criterion for hit compound identification a $\geq$ 0.75 fold change in nuclear localization of the p57kip2 protein was used.

2.5. Organotypic cultures of cerebellar slices

For the preparation of slice cultures, a previously described protocol [31] with few adaptations was used. Briefly, freshly prepared intact cerebelli from Wistar rats aged seven days of both sexes, were

embedded in 4% agarose (UltraPure Low Melting Point, Thermo Fisher Scientific) and mounted vertically to the flat metal chuck of the HM 650 V microtome (Thermo Fisher Scientific) using superglue (UHU, Mannheim, Germany). Sagittal sections, 350 μm thick, were made (cutting frequency: 50 Hz, cutting amplitude: 1 mm, cutting speed: 12 mm/s) and plated onto cell culture inserts (hydrophilic PTFE, pore size: 0.4 μm, diameter 30 mm; Merck Millipore, Darmstadt, Germany) in 6−well plates upon addition of 1 ml of culture medium [50% MEM; 25% Hank's Balanced Salt Solution (HBSS) +/+; 25% heat inactivated horse serum; containing 100 U/ml penicillin/0.1 mg/ml streptomycin (all Thermo Fisher Scientific), and 5 mg/ml D−glucose monohydrate (Merck Millipore)] underneath the membrane. Compounds were diluted in the same medium and applied four hours later as medium change. A total number of six to eight slices per animal were plated onto two inserts and kept in culture for three days (5% CO_2, 90% relative humidity, 37 °C). Slices were then washed once with PBS both on the top and underneath the insert and fixed with 4% PFA for 20 minutes at RT.

For the immunofluorescence staining slices were permeabilised with 0.5% Triton X-100 in PBS and non-specific binding was prevented by incubation in blocking solution [10% NGS, 1% bovine serum albumin fraction V (BSA; Thermo Fisher Scientific), 0.2% Triton X-100 in PBS]. Primary antibodies rabbit anti-neurofilament (NF, 1:1000, Abcam, Cambridge, UK Cat# ab8135, RRID:AB_306,298), rat anti-MBP (1:250, Bio-Rad Cat# MCA409S, RRID:AB_325,004), and mouse anti-OLIG2 (OLIG2, 1:500, Merck Millipore Cat# MABN50, RRID:AB_10,807,410) were diluted in antibody solution [10% NGS, 1% BSA, 0.1% Triton X-100 in PBS]. Secondary antibodies goat anti-rabbit Alexa Fluor 405 (1:500, Thermo Fisher Scientific Cat# A-31,556, RRID:AB_221,605), goat anti-rat Alexa Fluor 488 (1:500, Thermo Fisher Scientific Cat# A-11,006, RRID:AB_2,534,074), and goat anti-mouse Alexa Fluor 647 (1:500, Thermo Fisher Scientific Cat# A32728, RRID:AB_2,633,277) were diluted in secondary antibody solution (1% NGS, 1% BSA, 0.1% Triton X-100 in PBS). All steps were performed overnight at 4 °C and slices were then mounted using Citifluor. Staining specificity was confirmed upon application of the same secondary antibodies without prior application of the corresponding primary antibodies (data not shown). Image acquisition was performed using a confocal microscope (CLSM 510, Carl Zeiss Microscopy) and analysed with the Zen 2 Blue Edition (Carl ZEISS Microscopy, ZEN Digital Imaging for Light Microscopy, RRID:SCR_013672) and ImageJ BioVoxxel software packages. Briefly, three images per field were obtained using 40x magnification via Z-stack scanning covering 2 μm depth in total and prior the analysis they were projected onto a single plane via orthogonal projection. To assess the number of myelinating oligodendrocytes in relation to the total number of OLIG2-positive cells 12−16 fields from similar structures were analysed for all conditions. The typical morphology of myelinating cells in organotypic slices is presented in Fig. 4a-a'''.

2.6. Human fetal oligodendroglial cell culture and immunocytochemistry

Human fetal second-trimester (14−17 weeks) telencephalon tissue samples collected from elective abortions were provided by the University of Washington Birth Defects Research Laboratory − an NIH supported program (MP-37−2014−540; 13−244-PED; eReviews_3345) (Seattle, Washington, USA). The tissue was digested with 0.25% trypsin (Thermo Fisher Scientific) and 25 μg/mL DNase I (Roche, Laval, Canada) to obtain dissociated cells. OPCs that comprise ~0.1% of the total cells were isolated using immunomagnetic beads coated with O4 antibody (Miltenyi Biotec, Bergisch Gladbach, Germany Cat# 130−096−670, RRID:AB_2,847,907) [32−34]. After selection, cells were plated in 96-wells plates coated with poly-L-lysine (Sigma-Aldrich) and extracellular matrix (ECM-gel from Engelbreth-Holm-Swarm murine sarcoma, Sigma-Aldrich) at a density of 1×10^4 cells per well. Cells were cultured in DMEM-F12 media supplemented with N1 (Sigma-Aldrich), B27 supplement (Sigma-Aldrich), PDGF-AA (10 ng/ml) and bFGF (10 ng/ml, both Sigma-Aldrich) for four days before treatment with reagents as triplicates for four and six days, media with reagents were changed every two days. Cells were live stained with mouse anti-O4 (1:200, R&D Systems, Minneapolis, MN, USA Cat# MAB1326, RRID:AB_357,617), and hybridoma anti-GalC IgG3 (GC, 1:50, Montreal Neurological Institute, McGill University, Montreal, Quebec, Canada) monoclonal antibodies for 15 minutes at 37 °C and then fixed with 4% PFA for ten minutes in RT. Secondary antibodies goat anti-mouse IgM-Alexa Fluor 647 (1:500, Southern-Biotech, Birmingham, AL, USA Cat# 1021−31, RRID:AB_2,794,254) to O4 and goat anti-mouse IgG3-Alexa Fluor 488 (1:500, Thermo Fisher Scientific Cat# A-21,151, RRID:AB_2,535,784) for GC were used for 30 minutes at RT. Cell nuclei were stained with Hoechst 33,258 (1:1000, Thermo Fisher Scientific Cat# H3569, RRID:AB_2,651,133). Cells were imaged and the O4- and GC-positive cells were counted.

2.7. Cuprizone mediated demyelination and remyelination

Eight-week-old female C57BL/6 mice (Janvier Labs, Le Genest Saint Isle, Mayenne, France) were used and all experiments were performed in the animal facility of the Heinrich-Heine-University (Zentrale Einrichtung für Tierforschung und wissenschaftliche Tierschutzaufgaben; ZETT) under pathogen-free conditions and in accordance with ethical care. Only mice of the same age and with body weight between 17 and 19 gr were included and as additional exclusion criterion >10% weight loss during the experiments was used. No animals were excluded from the analysis. Animals were distributed equally into cages (groups) upon delivery and were given one week as acclimatization period before the initiation of the experiments. Using the software G*Power a required size of six animals per group with effect size d 2.6 and confidence interval 95% was computed. Demyelination was induced by feeding 0.2% (w/w) cuprizone [bis(cyclohexanone)oxaldihydrazone]-containing diet [either from Envigo (Indianapolis, IN, USA Cat# TD.140803) or from SSNIFF Spezialdiäten GmbH (Soest, Germany; maintenance diet pellets 10 mm, V1534 implemented with 0.2% cuprizone, Sigma-Aldrich, CAS 370−81−0)] for six weeks. Thereafter animals were given standard rodent chow (SSNIFF, Cat# V1534). Parbendazole (MedChem Express, Monmouth Junction, NJ, USA, CAS 14,255−87−9) was applied at a concentration 1.14 mg/ml and using 20 mg/kg body weight as dose. Parbendazole stock concentration consisted of 13.33 mg/ml in DMSO which was further diluted using sterile saline solution with 2% Tween 80 (Sigma-Aldrich). A total volume of 350 μl of the parbendazole solution or the corresponding vehicle solution (8.6% DMSO in sterile saline solution with 2% Tween 80) was administered daily via intraperitoneal (i.p.) injections for the last 17 days of cuprizone treatment. Danazol (Sigma-Aldrich, CAS 17,230−88−5; stock concentration 30 mg/ml in DMSO) was diluted first 1:1 in Tween 80 in order to increase the stability in aqueous solutions and then further diluted down to a final concentration of 0.4 mg/ml in drinking water for oral application (5 ml per animal and per day, 100 mg/kg body weight to be applied daily). One week upon cuprizone withdrawal animals were deeply anesthetized using isoflurane inhalation and transcardially perfused with 20 ml PBS followed by 20 ml 4% PFA in PBS, brains were then removed and post-fixation was performed overnight in 4% PFA at 4 °C.

Following post-fixation, cryoprotection of mouse brains was performed in 30% sucrose (in PBS) at 4 °C for 48 hours. Brains were then embedded in Tissue-Tek OCT medium (Sakura Finetek Europe, Netherlands), frozen and stored at −80 °C until sectioning with cryostat (Leica CM3050S, Wetzlar, Germany). Coronal 10 μm sections were prepared and stored at −80 °C. Regions of interest, medial (Bregma −0.82 to −1.22 mm) and caudal (Bregma −1.94 to −2.34 mm) parts of corpus callosum, were assessed according to [35].

For immunohistochemical staining, sections were thawed and air-dried for at least ten minutes at RT. Rehydration was performed for five minutes in distilled water, followed by transfer to −20 °C acetone for five minutes and two consecutive washing steps first in 1x TBS (pH 7.6) and then 1x TBS-T (TBS implemented with 0.02% Triton X-100; pH 7.6) for five minutes each. Non-specific staining was blocked with 10% biotin-free bovine serum albumin (BSA, Carl Roth) in TBS-T or 10% normal donkey serum (NDS, Sigma−Aldrich) in TBS-T for 30 minutes at RT, followed by primary antibody solution application (10% BSA in 1x TBS or 10% NDS in 1x TBS) and incubation overnight at 4 °C. The following primary antibodies were used: mouse anti-APC (CC1, 1:500, GeneTex Cat# GTX16794, RRID:AB_422,404), rabbit anti-glutathione-S-transferase pi (GSTpi, 1:2000, Enzo Life Sciences, Farmingdale, NY, US Cat# ADI-MSA-101-E, RRID:AB_2,039,147), goat anti-PDGFR (alpha/CD140A, 1:250, Neuromics, Edina, MN, US Cat# GT15150, RRID:AB_2,737,233), and rat anti-PLP [PLP, 1:250, kind gift from B. Trapp and R. Dutta, Dept. of Neurosciences, Cleveland Clinic, OH, USA [36]. Slices were then washed twice in 1x TBS for five minutes each and secondary antibodies were diluted 1:200 and applied for 30 minutes along with DAPI (1:50) in PBS. The following secondary antibodies were used: goat anti-rabbit Alexa Fluor 594 (1:200, Thermo Fisher Scientific Cat# A-11,037, RRID:AB_2,534,095), goat anti-rat Alexa Fluor 488 (1:200, Thermo Fisher Scientific Cat# A-11,006, RRID:AB_2,534,074), goat anti-rabbit Alexa Fluor 488 (1:200, Thermo Fisher Scientific Cat# A-11,008, RRID:AB_143,165), goat anti-mouse Alexa Fluor 488 (1:200, Thermo Fisher Scientific Cat# A32728, RRID:AB_2,633,277), and donkey anti-goat Alexa Fluor 488 (1:200, Thermo Fisher Scientific Cat# A-11,055, RRID:AB_2,534,102). Two final washing steps were performed with 1x TBS-T and 1x TBS for five minutes prior to mounting with Shandon™ Immu-Mount (Thermo Fisher Scientific). Staining specificity was confirmed upon application of the same secondary antibodies without prior application of the corresponding primary antibodies (data not shown). For image acquisition and analysis a CLSM confocal microscope and the Zen 2 Blue edition and ImageJ BioVoxxel software packages were used, respectively. Animal handling and tissue processing were performed by the same person (AM) to ensure stability and control of all parameters and cofounders. Data analysis was conducted blindly.

2.8. Statistical analysis

Data are presented as mean ± standard error of the mean (SEM). Graph design and statistical analyses were performed using the GraphPad Prism 8.0.2 software (GraphPad Prism, San Diego, CA, RRID:SCR_002798). The absence of Gaussian distribution of our data was assessed via Shapiro-Wilk normality test and statistical significance via unpaired Mann-Whitney U test or Tukey's range test following one-way ANOVA. Data were considered statistically significant at $^{*}p < 0.05$, $^{**}p < 0.01$, $^{***}p < 0.001$. n represents the number of independent experiments. *A priori* sample size calculation for the in vivo experiments was performed using the G*Power 3.1.9.2 [37] software and the Wilcoxon-Mann-Whitney test (two groups).

2.9. Role of funders

The funding source had no role in study design, collection, analysis and interpretation of data or in manuscript writing.

3. Results

3.1. Phenotypic screening for compounds that promote nuclear exclusion of the p57kip2 protein

Nucleocytoplasmic shuttling of the p57kip2 protein is an early event during the course of spontaneous OPC differentiation and we could previously demonstrate that alteration of its gene expression or of its subcellular protein localization severely impacts cellular maturation [14,16]. We therefore chose the nuclear vs. cytoplasmic localization of this protein to establish a phenotypic screening for pharmacological compounds with the potential to promote oligodendrogenesis (Fig. 1a). As opposed to the majority of other screening approaches we decided to test compounds using primary OPC culture [16,20], which recapitulates closer the *in vivo* situation than cell lines or stem cell derivatives, in order to increase the translational potential of this study. The sphingosine-1-phosphate receptor FTY720P/Fingolimod (1 μM) was used as positive control and differentiation medium with or without 0.5% DMSO served as negative controls (Fig. 1c-c''). For determination of the subcellular localization of the p57kip2 protein, stained cells were automatically captured using the BD Pathway 855 High-Content Cell Analyzer. The staining protocol used for this study is well established [16,20] and staining specificity was regularly confirmed. In an automated way, signal intensities of the anti-p57kip2 staining in nucleus and cytoplasm were measured using the Attovision v.1.7.1 software and analysed with an algorithm designed in house. The output of the analysis is the percentage of cells with prevailed nuclear p57kip2 localization in each well, given that the p57kip2 signal intensity in the two regions (nuclear vs. cytoplasmic) is provided as input. Hit compounds were considered those which induced a $\geq$ 0.75 fold change in nuclear localization of the p57kip2 protein in comparison to the negative controls. This threshold corresponds to the maximum increase in nuclear exclusion between days one and three upon initiation of spontaneous differentiation that has been detected previously [16,20]. Of note, this is also the time frame when significant transition of OPCs to oligodendrocytes is taking place and importantly this threshold was kept constant throughout the whole screening.

Out of 1280 compounds tested on primary rat OPCs, 21 substances (Fig. 1d) were found to reproducibly boost p57kip2's nuclear shuttling (as represented for benzamil hydrochloride, CAS 161,804−20−2 in Fig. 1c'''). Of note, this analysis also revealed doxorubicin (CAS 25316-40-9) to induce an exclusive nuclear localization of the p57kip2 protein (data not shown). Whereas ifenprodil (CAS 23,210−56−2) [25,39,40] and isoxicam (CAS 34,552−84−6) [41] already emerged from other pro-oligodendroglial screenings, the majority of our confirmed hits were unknown in this context. However, some of the identified compounds are related to pathways that have previously been shown to regulate OPC differentiation and survival such as the histamine receptor-3 (H3R) inverse agonist GSK247246 [26] and benztropine acting on muscarinic receptors [21], respectively, thus proving the efficacy of our screening approach.

3.2. Secondary screening for compounds that promote OPC differentiation in vitro

For further validation of the confirmed hits their impact on OPC differentiation was determined by means of myelin protein expression. To this end, rat primary OPCs were cultured and stimulated using compound concentrations ranging from 10 to 0.001 μM. Cells were allowed to differentiate for three days upon compound stimulation and immunofluorescence staining against the late myelin marker MBP was performed. Potential cytotoxic effects were accessed via evaluation of total cell numbers (data not shown). From this secondary screening four substances emerged with the capacity to positively modulate OPC differentiation and the most efficient and well-tolerated concentrations were determined (Fig. 2f-i'; m-p).

Treatment with either 5 μM danazol, 0.02 μM parbendazole, or 0.1 μM methiazole (CAS 74,239−55−7) significantly induced the number of MBP-positive cells (Fig. 2m-o). Treatment with 0.1 μM nocodazole (CAS 31,430−18−9) induced only a non-significant increase in MBP-positive cells but reproducibly resulted in more complex morphological phenotypes (Fig. 2i-i'). Moreover, using

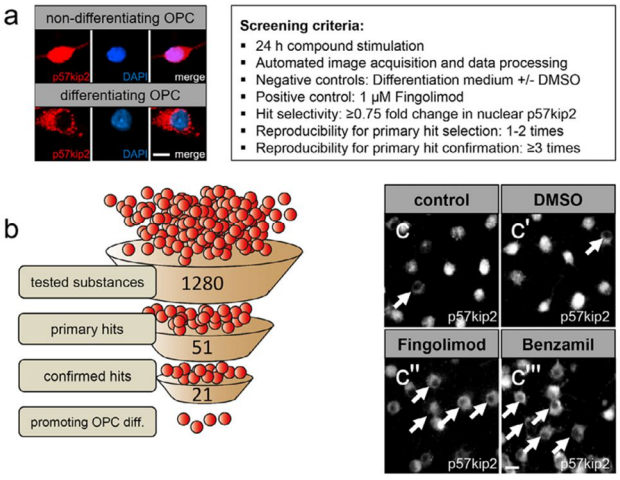

d

Confirmed primary hits: enhanced p57kip2 nuclear exclusion after 1d		
categories	**compounds**	**reproducibility**
Ion channels	Benzamil hydrochloride	(4 out of 5)
	Felodipine	(4 out of 5)
	Ifenprodil	(3 out of 5)
NSAIDs	Isoxicam	(3 out of 5)
	Fosfosal	(4 out of 4)
Anthelmintics	**Nocodazole**	(4 out of 4)
	Parbendazole	(4 out of 5)
	Methiazole	(4 out of 4)
Neurotransmitter receptor modulators	Alverine citrate salt	(4 out of 5)
	Pizotifen	(5 out of 5)
	Fluvoxamine maleate	(5 out of 5)
	Mianserine hydrochloride	(4 out of 5)
	Acetopromazine maleate salt	(4 out of 4)
	Doxepine	(4 out of 4)
	Cisapride	(4 out of 4)
	Tolcapone	(4 out of 4)
	Hexamethonium dibromide dihydrate	(3 out of 5)
	Mebeverine hydrocloride	(3 out of 5)
Others	Pentamidine isethionate	(5 out of 5)
	Danazol	(4 out of 4)
	Opipramol	(3 out of 5)

Fig. 1. *In vitro* phenotypic screening revealed compounds that promote nuclear exclusion of the p57kip2 protein in primary OPCs. Presentation of the readout and the experimental setup of the primary screening procedure (a). Funnel illustration showing the complete progression of the screening (b). Representative images taken using the BD Pathway 855 High-Content Cell Analyzer visualizing p57kip2's subcellular localization upon treatment with the negative controls, differentiation medium (control) and DMSO, the positive control Fingolimod (1 μM) and a profound primary hit benzamil hydrochloride (c-c'''). List of the confirmed primary hits (d). Arrows in c-c''' point at cells with cytoplasmic p57kip2 localization. Scale bars: 10 μm.

nocodazole a 31.43% decrease in the number of (DAPI positive) cells was observed, indicating that this substance might exert cytotoxicity and thus explaining the absence of statistically significant observations on myelin expression (Fig. 2p).

For those hits which promoted transition from OPCs to mature oligodendrocytes (excluding nocodazole due to cytotoxicity) we additionally investigated the time point day six using MOG as marker and we similarly detected a significant beneficial impact of parbendazole on cell maturation (Fig. 2s). Cells treated with danazol and methiazole induced similar changes in MOG protein expression, however, the effects were less prominent (Fig. 2q-r). Treatment with the benzimidazole derivatives, parbendazole and methiazole, not only led to increased numbers of MOG-positive cells but also accelerated morphological maturation (Fig. 2k-l'). At this point, our data provided therefore strong evidence that using the p57kip2 nuclear shuttling process as a screening read-out is efficient and successful for the identification of novel drugs that can positively modulate already early oligodendroglial cell stages.

3.3. Selected hit compounds promote oligodendroglial cell differentiation in primary human OPCs

As this study aimed at the identification of promyelinating drugs with a translational potential, it was of interest to explore the activities of selected compounds on human cells. For this purpose, we used human fetal brain-derived O4-selected oligodendroglial progenitor preparations [32–34,42] which were grown for four days in culture and then treated for another four or six days in the presence of 0.002 μM and 0.02 μM parbendazole, 0.01 μM and 0.1 μM methiazole, or 0.5 μM and 5 μM danazol. Due to the suspected toxic effect of nocodazole, this drug was excluded from the technically limited experiments with primary human cells. For technical reasons two completely different preparations from human donor tissues over a period of more than six months were used (HF601 and HF603) which resulted in quantitatively diverging expression levels. Nevertheless, double staining using anti-O4 and anti-galactocerebroside (GC) antibodies revealed that all three substances clearly elevated the

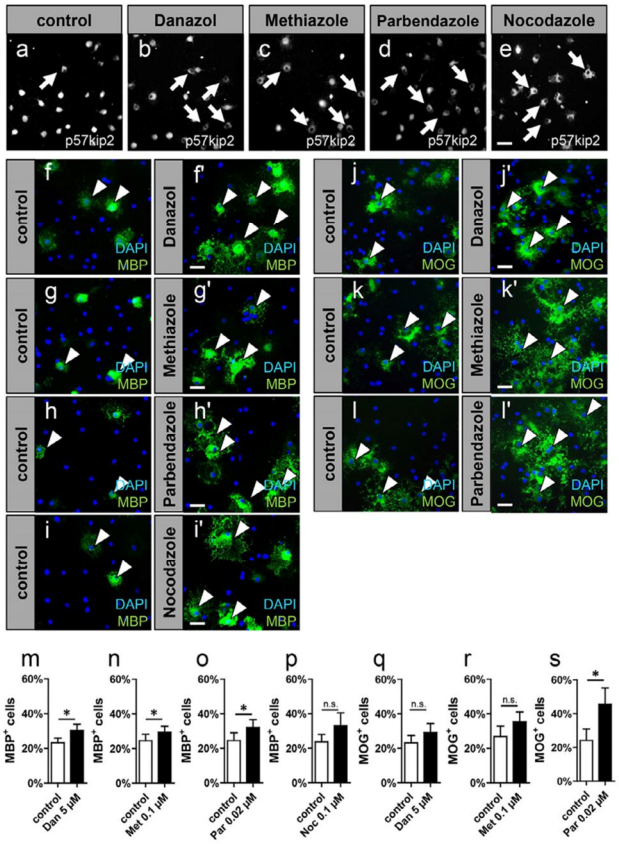

Fig. 2. Selected hit compounds promote p57kip2's protein nuclear exclusion and OPC differentiation *in vitro*. Representative images taken using the BD Pathway 855 High-Content Cell Analyzer visualizing the subcellular localization of the p57kip2 protein upon one-day long stimulation with 0.5% DMSO (a), danazol (b), methiazole (c), parbendazole (d), and nocodazole (e) each at a concentration of 10 μM. Immunocytochemical analysis for the mature myelin marker MBP upon a three-day long stimulation of primary rat OPCs with 5 μM danazol (m), 0.1 μM methiazole (n), 0.02 μM parbendazole (o), and 0.1 μM nocodazole (p). Immunocytochemical analysis for the mature myelin marker MOG upon a six-day long stimulation of primary rat OPCs with 5 μM danazol (q), 0.1 μM methiazole (r), and 0.02 μM parbendazole (s). For each substance medium with the corresponding DMSO concentration was used as control. Representative images for MBP (f-i') and MOG staining (j-l'). Arrows in representative pictures point at cells with cytoplasmic p57kip2 localization in a-e and arrowheads point to MBP-positive cells in f-i' or MOG-positive cells in j-l'. Nuclei were counterstained with DAPI. Scale bars: 20 μm. Data are shown as mean values and error bars represent SEM. Numbers of independent experiments $n = 6$ for (m), $n = 4$ for (n, p, q), $n = 5$ for (o, s), $n = 3$ for (r). Statistical significance was assessed using Mann-Whitney U test, unpaired data: $^{*}p < 0.05$; $^{**}p < 0.01$; $^{***}p < 0.001$. Dan, danazol; Par, parbendazole; Met, methiazole; Noc, nocodazole; MBP, myelin basic protein; MOG, myelin oligodendrocyte glycoprotein.

percentage of morphologically matured human oligodendroglial cells (compare Fig. 3e'',3f'',3g'',3h'') as well as their ability to express GC. Note that the most consistent effects were observed for 5 μM danazol at both time points, whereas the higher concentrations of parbendazole and methiazole resulted in declining values in cells of the second preparation (HF603), particularly at the later time point. This suggests additional titration and long-term toxicology investigations to be conducted along the course of a future biomedical translation process.

3.4. Members of the benzimidazole class of compounds promote ex vivo myelination

As a next step we investigated the impact of treatment with selected active compounds on endogenous developmental myelination. To this end, organotypic cerebellar slice cultures were prepared from postnatal day seven Wistar rats. Stimulation with either 0.1 μM parbendazole or 2 μM methiazole over three days induced a significant increase in the myelination capacity of the endogenous oligodendroglial cell population as shown by the improved potential of OLIG2-positive cells to make up MBP-positive myelin sheaths when compared to the control (DMSO) conditions (Fig. 4b-g). Danazol revealed to exert a similar trend regarding the generation of myelinated segments, however, no significant differences were found compared with controls (Fig. 4h).

3.5. Parbendazole and danazol enhance remyelination in vivo

To assess the impact on spontaneous remyelination of those compounds with strongest and most wide-spread activities the cuprizone mediated mouse model of de- and remyelination was applied [43]. We selected danazol and parbendazole for *in vivo* evaluation, as representatives of steroid and benzimidazole compound classes, respectively. To achieve demyelination of the corpus callosum mice were fed with 0.2% cuprizone diet for a total of six weeks. During the last 17 days of cuprizone treatment, animals were either receiving daily

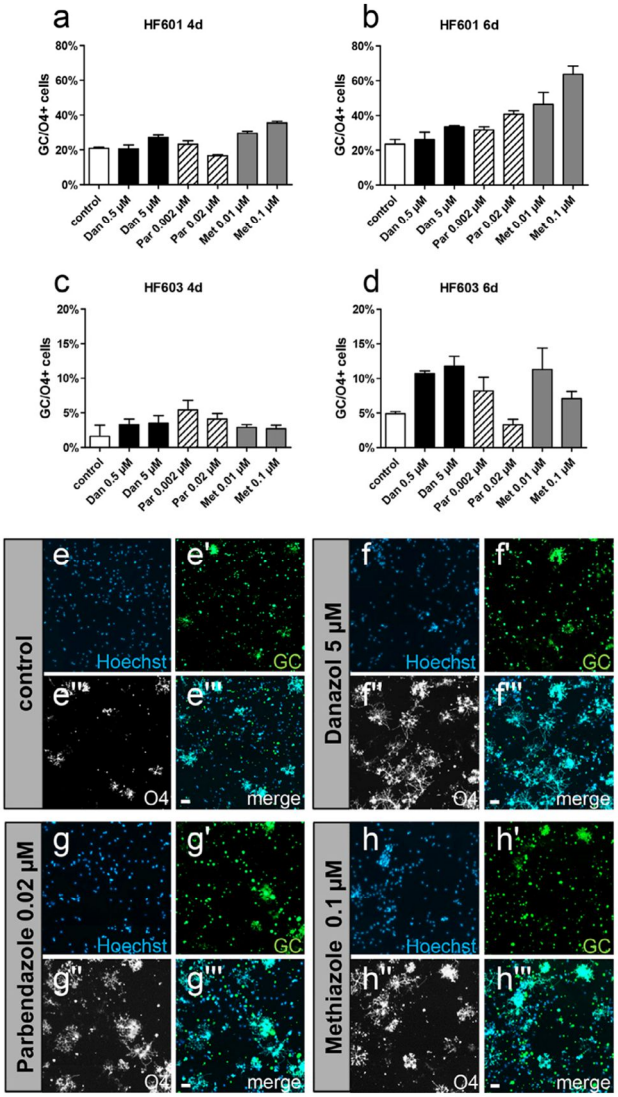

Fig. 3. Selected hit compounds enhance primary human OPC differentiation *in vitro*. Human OPCs of two different preparations (HF601, HF603) were cultured in the presence of 0.5 μM and 5 μM danazol, 0.002 μM, and 0.02 μM parbendazole, or 0.01 μM and 0.1 μM methiazole with DMSO-treated cells serving as controls. The results of each preparation are presented separately (HF601 in a, b and HF603 in c, d) and correspond in total to two independent experiments. Human OPCs of batch HF601 consistently showed increased degrees of anti-galactocerebroside (GC)-positivity at both time points and using all tested substance concentrations (a,b). Human OPCs of batch HF603 appeared generally less mature, showed increased GC-positivity after four days of treatment but appeared sensitive to high parbendazole and methiazole concentrations (c,d). Representative pictures of HF601 cells after six days of treatment (e-h'''). Note that all three substances evoked a clear morphological maturation of cells. Data are shown as means (derived from three wells per condition) but due to large variations and the still rather low number of technical replicates no statistical significance was calculated. Scale bars 20 μm.

intraperitoneal injections of parbendazole (20 mg/kg) or oral administration of danazol (100 mg/kg). For each substance the same number of cuprizone-treated animals were administered the corresponding vehicles. To assess the efficiency of both, cuprizone treatment and the extent of remyelination, naïve (non-cuprizone-treated) animals were also included in the analysis. The effect on remyelination was investigated one week upon cuprizone withdrawal (Fig. 5a). Immunohistochemical staining specificity was confirmed everywhere in order to exclude false positive signal detection.

Significant differences in the percentage of PLP-positive area (myelinated) within the region of interest were observed upon comparison of naïve with vehicle-treated groups, confirming the efficiency of cuprizone-dependent demyelination (Fig. 5b,b',f,g,g', h). Remarkably, parbendazole enhanced spontaneous remyelination as revealed by PLP density along the midline of the medial and caudal compartments of the corpus callosum, as compared with vehicle-treated counterparts (Fig. 5b-b'',f). This observation was supported by corresponding differences in the numbers of cells

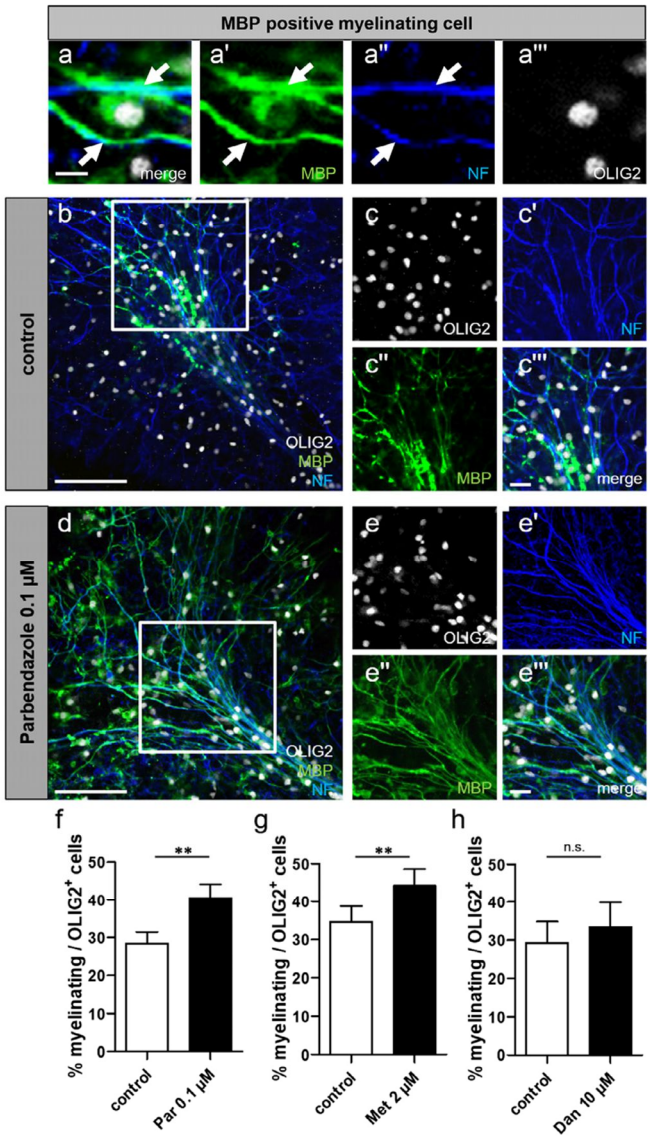

Fig. 4. Parbendazole and methiazole significantly promote *ex vivo* developmental myelination. Organotypic cerebellar slices from P7 rats were subjected to a three-day long substance application. For each substance medium with the corresponding DMSO concentration was used as control. Exemplary pictures of a myelinating oligodendrocyte revealing morphological criteria used for the analysis (a-a'''). Representative triple staining for OLIG2, MBP, and neurofilament for DMSO (b-c''') and parbendazole- (d-e''') treated slices. For the overview images (b,d) four images per field were obtained using 20x magnification via Z-stack scanning covering 3 μm depth in total and prior to the analysis they were projected onto a single plane via orthogonal projection. Scale bars for the exemplary images (a-a'''): 10 μm. Scale bars for the overview images (b,d): 100 μm. Scale bars for the detailed images (c-c'''; e-e'''): 20 μm. Immunohistochemical analysis assessing the number of MBP-positive, myelinating oligodendrocytes in relation to the total number of OLIG2-positive cells in slices treated with parbendazole (f), methiazole (g), danazol (h), and their corresponding DMSO concentrations (controls). Data are shown as means, and error bars represent SEM. Mann-Whitney U test, for unpaired data was used and data were considered statistically significant at $^{*}p < 0.05$, $^{**}p < 0.01$, $^{***}p < 0.001$. Number of experiments: $n = 5$ in all cases. Par, parbendazole; Met, methiazole; Dan, danazol; NF, neurofilament; MBP, myelin basic protein.

expressing mature oligodendroglial markers such as GSTπ (Fig. 5c-c'',f') and CC1 (Fig. 5d-d'',f''). In accordance, the early oligodendroglial marker PDGFRα exerted an opposite pattern, with the vehicle-treated group demonstrating significantly increased numbers of PDGFRα-positive cells as compared to the other two groups (naïve and parbendazole-treated mice, Fig. 5e-e'',f'''). Interestingly, oral administration of danazol also significantly enhanced the PLP-positive area hence remyelination in the same experimental setup (Fig. 5g-g'',h). However, only a small but statistically significant positive impact on the generation of GSTπ-positive cells was

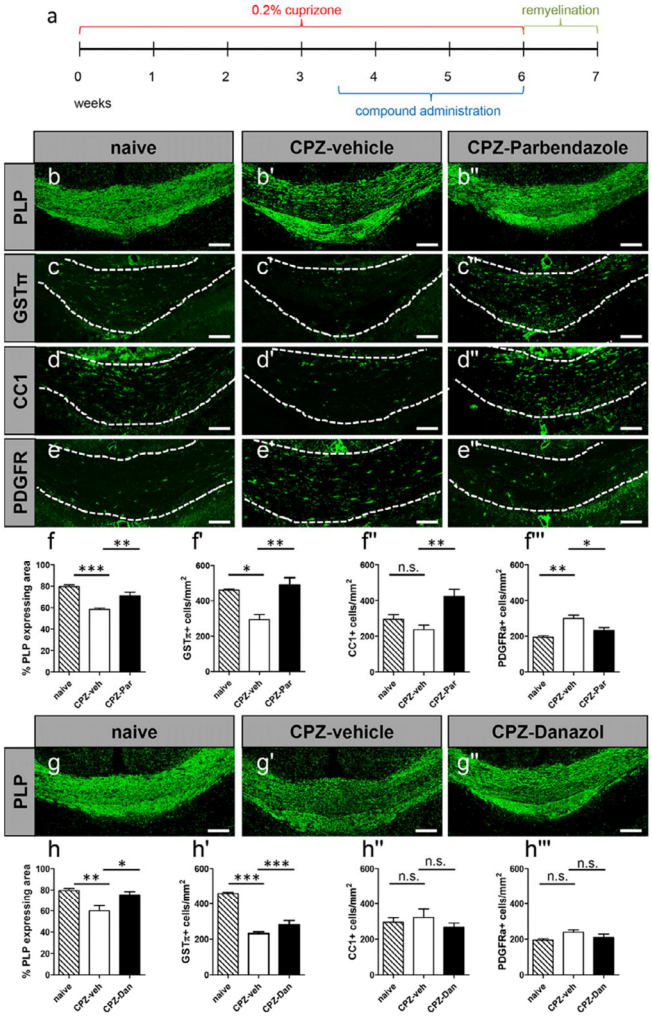

Fig. 5. Parbendazole and danazol positively affect spontaneous remyelination in a cuprizone-induced demyelination mouse model. Schematic representation of the experimental setup for cuprizone treatment and substance administration (a). Representative images of the oligodendroglial protein marker expression in corpus callosum after one week of remyelination (b-e''; g-g''). Image magnification 10x. The extent of remyelination was revealed as the percentage of PLP-expressing area in the defined region of interest between naïve, CPZ/vehicle-treated and CPZ/substance-treated groups. In a similar manner the impact of parbendazole and danazol on oligodendroglial cell differentiation and maturation was assessed as revealed by the number/mm^2 of mature (GSTπ, f',h'; CC1, f'',h'') and early (PGFRα, f''',h''') oligodendroglial protein marker-positive cells along the same area of the corpus callosum. Naïve group $n = 6$ ($n = 4$ for the GSTπ analysis); residual groups $n = 5$ each. For each mouse four coronal sections were analysed (two from the medial and two from the caudal region) and the data are shown as mean values while error bars represent SEM. Significance was assessed using Tukey's range test following one-way ANOVA. Data were considered statistically significant (95% confidence interval) at $^*p < 0.05$, $^{**}p < 0.01$, $^{***}p < 0.001$. CPZ, cuprizone; veh, vehicle; Par, parbendazole; Dan, danazol; PLP, myelin proteolipid protein; GSTπ, glutathione-S-transferase Pi; CC1, adenomatous polyposis coli protein (APC) clone CC1; PDGFRα, platelet-derived growth factor receptor alpha. Scale bars: 100 μm.

observed, whereas numbers of CC1- and PDGFRα-positive cells remained unaffected (Fig. 5h'-h''').

3.6. Parbendazole treatment activates p38MAPK in vitro

We then used available information on identified hit compounds to shed light onto the underlying mechanism of p57kip2 nuclear exclusion. p38MAPK activation is associated with regulation of nuclear protein export [44–46]. Moreover, omeprazole, another benzimidazole derivative, was shown to induce OPC differentiation involving p38MAPK and ERK1/2 activation [47]. In order to investigate whether p38MAPK is also activated in response to parbendazole, we stimulated primary OPCs with this substance for 60 minutes and indeed detected 2.3 times more phosphorylated p38MAPK (Fig. 6) protein in relation to the DMSO-treated control.

4. Discussion

We established and successfully performed a phenotypic drug screening based on the p57kip2 dependent regulation of OPC

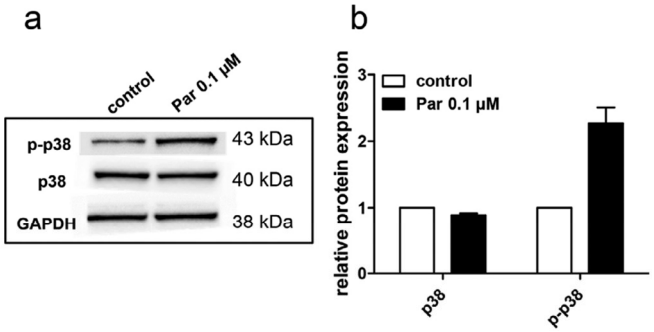

Fig. 6. Parbendazole treatment induces phosphorylation of p38MAPK. Rat primary OPCs were treated either with 0.01 μM parbendazole or the corresponding DMSO concentration (control) for one hour and harvested for Western blot analysis for the detection of p-p38, p38, and GAPDH proteins (a). Quantification of the relative protein expression (b). The relative protein expression of both the phosphorylated and non-phosphorylated forms of p38 was normalized over the total amount of the protein in the lysate and GAPDH levels. Data represent means of two independent experiments. Error bars represent SEM.

differentiation. On the one hand, this analysis provided information on new pharmacological compounds with the potential to boost myelin repair processes and on the other hand, we shed light on the upstream regulatory mechanisms. Up to now it was revealed that the intracellular p57kip2 shuttling process regulated gene expression (via Ascl1 and Hes5), cytoskeletal dynamics (via LIMK-1), cell cycle exit (CDK2; all described in [16]) as well as vascular ATPase activity [48], however, corresponding signaling cascades or involved surface receptors were not known.

We nevertheless took advantage of this potent mechanism in order to identify compounds that can modulate early oligodendroglial cell stages in contrast to the majority of other screenings which were mainly based on MBP expression and which also addressed later stages and larger time windows [21–26,38,39,49,50]. Moreover, the 1280 compounds tested here mainly consisted of either FDA/EMA- (US Food and Drug Administration/Europeans Medicines Agency) approved substances or substances with a clinical trial history, with 98% of them being predicted to have a high blood-brain-boundary (BBB) penetrance. In addition, we tested all substances using primary OPCs which creates a condition closer to the *in vivo* situation as compared to cell lines or stem cell derivates that were used in most related screenings [23–25,38,39,49–52]. Such unique selling points, however, included the backdrop of larger variations when using primary cells as well as the fact that p57kip2 translocation appears to be an early and fast process, the detection of which can be missed. Additional variations were likely deriving from the fact that in our study cells of three different species (rat, human, mouse) as well as OPCs deriving from cortex, cerebelli, or the corpus callosum were examined.

Among the hits we identified ion channel modulators (e.g. benzamil hydrocloride), nonsteroidal anti-inflammatory drugs (NSAIDs; e.g. fosfosal, CAS 6064–83–1) and neurotransmitter receptor modulators (e.g. alverine citrate salt, CAS 5560–59–8). Given that these mechanisms have previously been implicated in oligodendrogenesis [53–56] our screening procedure and the selected parameters could be validated. Moreover, a minor overlap with hits detected by other screenings, namely ifenprodil [25,39,40] and isoxicam [41], was observed. Of note, out of the identified hit compounds, only a small number was indeed able to promote transition of OPCs to mature oligodendrocytes. Possible explanations may include inappropriate concentrations or time-points of application/investigation or that additional, adverse pathways were elicited which interfered with cell differentiation.

Notably, three benzimidazoles were found to exert positive effects on several parameters of oligodendrogenesis. This compound family has been associated with anti-microbial, anti-viral, anti-cancer, anti-protozoal, anti-helminthic, anti-inflammatory, and analgesic activities [57]. Whereas their broad application in veterinary medicine has revealed drawbacks related to teratogenic and cytotoxic effects [58], their numerous pharmacological properties led to the development of drugs, such as the anti-ulcer medications pantoprazole and omeprazole, which are broadly subscribed in human medicine without the implication of severe side effects. Of note, omeprazole was recently proposed as promoter of oligodendroglial cell differentiation and remyelination [47].

We instead found parbendazole, methiazole, and nocodazole to clearly promote oligodendroglial cell differentiation and proceeded with parbendazole and methiazole, two less-characterized members of the compound family. As the methiazole cell cycle profile linked this compound to parbendazole and two other tubulin destabilizing agents [59] we believe that their similar effects could be attributed to alterations of the microtubule dynamics via a p38MAPK-related mechanism which was indeed substantiated by our observation of a parbendazole dependent induction of phosphorylated p38MAPK protein. Similar phosphorylation events were also shown to occur in response to omeprazole [47]. Nocodazole, on the other hand, a known microtubuli destabilizer, was described to act in a pro-oligodendroglial way and manner via increased microtubule arborization when applied acutely at nanomolar concentrations [60]. However, the authors reported increased cytotoxicity at micromolar levels, which is in accordance with our results, as well as deleterious effects on *in vitro* myelination even at low concentrations, thus justifying its exclusion from our further investigations.

Given their similar mode of action and based on the fact that *in vivo* experimentations are restricted parbendazole was selected for application on cuprizone demyelinated mice, taking into account that all three here investigated benzimidazole derivatives are predicted to be able to penetrate the BBB according to ADMET evaluation [61]. Moreover, teratogenic effects of parbendazole were only reported in sheep and cattle when administered at concentrations higher or equal to 60 mg/kg body weight [62], so the here administered daily doses of 20 mg/kg suggested a safe treatment, and finally confirmed a positive impact on the number of maturing oligodendroglial cells as well as on myelin reconstitution *in vivo*.

To what degree a similar positive impact of i.p. administered parbendazole on myelin lesion repair can also been observed in an inflammatory background (e.g. in experimental autoimmune encephalomyelitis) needs to be addressed in future experiments. Likewise, possible prolonged effects due to alternative dosing and application routes will also have to be determined.

The fourth studied substance, danazol, is an extensively studied testosterone derivative with anti-gonadotropic and anti-estrogenic

properties, which has initially been approved by the FDA for the treatment of endometriosis [63]. Danazol has been studied in cancer research in view of its potential to induce toxic effects on, among others, leukemic and multidrug-resistant cancer cells [64,65]. Recently, danazol was reported to rescue MBP gene expression in a zebrafish mutant featuring reduction or complete loss of MBP expression in the peripheral nervous system [66]. Here, we show prominent promotion of oligodendroglial cell differentiation using both rat and human primary OPCs, minor improvement of *ex vivo* myelination using rat tissue and significantly increased *in vivo* remyelination in cuprizone challenged mice. The latter of which appears to be restricted to a net positive effect on the size of the myelin-positive area and to a small significant increase in the number of GSTπ-positive cells, as opposed to the clear-cut changes on OPC and oligodendrocyte numbers upon parbendazole application. Nevertheless, it has to be taken into account that danazol was applied orally thus limiting control over the consumed doses. In addition, its limited effects on myelin repair could also result from its poor aqueous solubility and dissolution [67]. But given the advantage that it can be applied as oral drug, future *in vivo* tests are warranted. This could include either the use of direct drug delivery into the stomach (via gastric gavage), the application of higher concentration and/or of different surfactant and emulsifier solution in order to find out whether danazol's effect on spontaneous remyelination could be improved. The fact that other steroids have also been reported to exert a myelin repair potential additionally supports our findings. Specifically, progesterone and nestorone were shown to upkeep oligodendroglial cell maturation and myelin repair in cuprizone-induced chronic demyelinating regions [68]. Other studies highlight the prominent effect of testosterone and its synthetic analogue 7α-methyl-19-nortestosterone on myelin repair by oligodendrocytes in chronic and acute demyelinated lesions via the androgen receptor [69,70].

Given that substances were administrated while microgliosis, astrogliosis, OPC proliferation, and oligodendrocyte formation were still ongoing with the latter ones being vulnerable to cuprizone once they have reached a certain maturation state [71], we can therefore not fully exclude additional cytoprotective effects of parbendazole and danazol to occur *in vivo*. However, based on our cell- and tissue culture experiments we nevertheless suggest that the here observed positive effects on remyelination are mainly resulting from an increased OPC differentiation potential. Specific compound related cell proliferation effects were not determined i.e. animals were not killed at corresponding earlier time points. However, in the danazol- and parbendazole-treated mice we looked at the number of OLIG2-positive cells among the different groups and observed similar numbers in both substance and vehicle treated-mice (data not shown) thus speaking against a strong proliferation effect.

Finally, from a biological point of view, the here presented analysis has yielded important insights into signaling cascades controlling the p57kip2 dependent nuclear blockade of oligodendroglial differentiation. Our data suggest that external signals acting on ion channels and neurotransmitter receptors, microtubule dynamics (nocodazole, methiazole, parbendazole), steroid hormone receptors (danazol), sigma-1 receptors (opipramol, CAS 315–72–0), COX1/2, and STAT5 (isoxicam and fosfosal) are involved in the p57kip2 shuttling/OPC differentiation process, with most of the impact possibly resulting from microtubule modulation and activation of steroid hormone receptors (Fig. 1). It also revealed mitogen-activated protein kinases (MAPK) such as p38 to be implicated in the regulatory role in this process, which is additionally supported by our previous observations that CXCL12 chemokine stimulation resulted in MAPK phosphorylation and promoted oligodendroglial differentiation [72]. Moreover, p57kip2 nuclear exclusion and the subsequent promotion of cell differentiation were found to occur in an exportin 1 (CRM1) dependent manner [16]. And then, p38MAPK activation has previously been associated with nuclear export of different proteins such as E2F1, MAPK-activated protein kinase 5 (MK5), and NFAT, in all cases with the involvement of CRM1 [44–46].

Taken together, the here presented small scale library screening revealed to be a sensitive and powerful method for the detection of early promoters of the oligodendroglial cell differentiation process, which nevertheless fostered long-lasting impacts such as myelin production and axon wrapping. We applied a limited number of pharmacologically active compounds to primary oligodendroglia of three different species, of different CNS origins and in different environments thus looking for conserved molecular mechanisms. This alternative screening, particularly the short-term read-out based on protein translocation, proved to be applicable and successful, which is why application to larger compound libraries is suggested. Our findings on parbendazole and danazol are of great interest when it comes to white matter repair, particularly in light of them also being active in human oligodendroglial cells. Nevertheless, it must be considered that these hit compounds may only act as leading substances of which derivates shall be developed and tested.

Declaration of Competing Interest

Dr Healy reports consultancy fees from Merck, and funding from Canadian Stem Cell Network, CDQM, Quantum Leap and Bouchard Foundation outside of the submitted work. The rest of the authors declare that there is no conflict of interests regarding the publication of this article.

Contributors

Anastasia Manousi-Methodology; software; validation; formal analysis; investigation; data curation; writing-original draft; writing – review & editing; visualization; funding acquisition; data verification

Peter Göttle-Conceptualization; methodology; data curation; visualization; funding acquisition; resources

Laura Reiche-Methodology; formal analysis; investigation

Qiao-Ling Cui-Methodology; investigation

Luke M. Healy-Methodology; funding acquisition

Rainer Akkermann-Methodology

Joel Gruchot-Investigation; formal analysis

Jessica Schira-Heinen-Investigation

Jack P. Antel-Funding acquisition; resources

Hans-Peter Hartung-Supervision

Patrick Küry-Conceptualization; methodology; validation; data curation; writing-original draft; writing – review & editing; visualization; supervision; project administration; funding acquisition; resources, data verification

All authors read and approved the final version of the manuscript.

Acknowledgements

We thank Brigida Ziegler and Birgit Blomenkamp for technical assistance and Dr. Michael Dietrich for scientific consultancy and assistance. We thank Dr. David Kremer for logistical support. The anti-PLP antibody was kindly provided by the Department of Neurosciences at the Cleveland Clinic, OH.

AM was supported by the Jürgen Manchot Foundation, Düsseldorf. This work was also supported by a grant from the Research Commission of the Medical Faculty of Heinrich-Heine-University Düsseldorf (to PG), by the Christiane and Claudia Hempel Foundation for clinical stem cell research (to PK and PG), Stifterverband/Novartisstiftung (to PK) and the James and Elisabeth Cloppenburg, Peek and Cloppenburg Düsseldorf Stiftung (to PK and HPH). Work with human fetal oligodendroglial cells was supported by a grant from the International Progressive MS Alliance (BRAVEinMS, to LH and JPA).

Data and Code Availability

The code generated during this study is available at https://github.com/anastasiamanousi/p57kip2-translocation-Manousi-et-al.–2020. All other data are available upon request from the corresponding author.

Supplementary materials

Supplementary material associated with this article can be found, in the online version, at doi:10.1016/j.ebiom.2021.103276.

References

[1] Sospedra M, Martin R. Immunology of multiple sclerosis. Annu. Rev. Immunol. 2005;23(1):683–747.
[2] Becher B, Bechmann I, Greter M. Antigen presentation in autoimmunity and CNS inflammation: how T lymphocytes recognize the brain. J Mol Med (Berl) 2006;84(7):532–43.
[3] Lee JY, Taghian K, Petratos S. Axonal degeneration in multiple sclerosis: can we predict and prevent permanent disability? Acta Neuropathol Commun 2014;2(1):97.
[4] Lassmann H. Multiple sclerosis pathology. Cold Spring Harb Perspect Med 2018;8(3).
[5] Franklin RJM, Ffrench-Constant C. Regenerating CNS myelin - from mechanisms to experimental medicines. Nat Rev Neurosci 2017;18(12):753–69.
[6] Kotter MR, Stadelmann C, Hartung HP. Enhancing remyelination in disease–can we wrap it up? Brain 2011;134(Pt 7):1882–900.
[7] Kremer D, Göttle P, Hartung H-P, Küry P. Pushing forward: remyelination as the new frontier in CNS diseases. Trends Neurosci. 2016;39(4):246–63 a.
[8] Gruchot J, Weyers V, Göttle P, Förster M, Hartung H-P, Küry P, et al. The molecular basis for remyelination failure in multiple sclerosis. Cells 2019;8(8).
[9] Kremer D, Aktas O, Hartung H-P, Küry P. The complex world of oligodendroglial differentiation inhibitors. Ann. Neurol. 2011;69(4):602–18.
[10] Kremer D, Akkermann R, Küry P, Dutta R. Current advancements in promoting remyelination in multiple sclerosis. Multiple Sclerosis J 2018;25(1):7–14.
[11] Kremer D, Göttle P, Flores-Rivera J, Hartung H-P, Küry P. Remyelination in multiple sclerosis. Curr. Opin. Neurol. 2019;32(3):378–84.
[12] Zuchero JB, Barres BA. Intrinsic and extrinsic control of oligodendrocyte development. Curr. Opin. Neurobiol. 2013;23(6):914–20.
[13] Heinen A, Kremer D, Göttle P, Kruse F, Hasse B, Lehmann H, et al. The cyclin-dependent kinase inhibitor p57kip2 is a negative regulator of Schwann cell differentiation and in vitro myelination. Proc Natl Acad Sci U S A. 2008;105(25):8748–53.
[14] Kremer D, Heinen A, Jadasz J, Göttle P, Zimmermann K, Zickler P, et al. p57kip2 is dynamically regulated in experimental autoimmune encephalomyelitis and interferes with oligodendroglial maturation. Proc Natl Acad Sci U S A. 2009;106(22):9087–92.
[15] Jadasz JJ, Rivera FJ, Taubert A, Kandasamy M, Sandner B, Weidner N, et al. p57kip2 regulates glial fate decision in adult neural stem cells. Development 2012;139(18):3306–15.
[16] Göttle P, Sabo JK, Heinen A, Venables G, Torres K, Tzekova N, et al. Oligodendroglial maturation is dependent on intracellular protein shuttling. Journal of Neuroscience 2015;35(3):906–19.
[17] Tobinick EL. The value of drug repositioning in the current pharmaceutical market. Drug News Perspect 2009;22(2):119–25.
[18] Gasparini F, Di Paolo T. Drug repurposing: old drugs, new tricks to fast track drug development for the brain. Neuropharmacology 2019;147:1–3.
[19] Küry P, Kremer D, Göttle P. Drug repurposing for neuroregeneration in multiple sclerosis. Neural Regen Res 2018;13(8):1366–7.
[20] Göttle P, Manousi A, Kremer D, Reiche L, Hartung H-P, Küry P. Teriflunomide promotes oligodendroglial differentiation and myelination. J Neuroinflammation 2018;15(1).
[21] Deshmukh VA, Tardif V, Lyssiotis CA, Green CC, Kerman B, Kim HJ, et al. A regenerative approach to the treatment of multiple sclerosis. Nature 2013;502(7471):327–32.
[22] Mei F, Fancy SPJ, Shen Y-AA, Niu J, Zhao C, Presley B, et al. Micropillar arrays as a high-throughput screening platform for therapeutics in multiple sclerosis. Nat. Med. 2014;20(8):954–60.
[23] Guo YE, Suo N, Cui X, Yuan Q, Xie X. Vitamin C promotes oligodendrocytes generation and remyelination. Glia 2018;66(7):1302–16.
[24] Suo N, Guo YE, He B, Gu H, Xie X. Inhibition of MAPK/ERK pathway promotes oligodendrocytes generation and recovery of demyelinating diseases. Glia 2019;67(7):1320–32.
[25] Hubler Z, Allimuthu D, Bederman I, Elitt MS, Madhavan M, Allan KC, et al. Accumulation of 8,9-unsaturated sterols drives oligodendrocyte formation and remyelination. Nature 2018;560(7718):372–6.
[26] Chen Y, Zhen W, Guo T, Zhao Y, Liu A, Rubio JP, et al. Histamine Receptor 3 negatively regulates oligodendrocyte differentiation and remyelination. PLoS ONE 2017;12(12).
[27] Kremer D, Küry P, Dutta R. Promoting remyelination in multiple sclerosis: current drugs and future prospects. Multiple Sclerosis J 2015;21(5):541–9.
[28] Cunniffe N, Coles A. Promoting remyelination in multiple sclerosis. J. Neurol. 2019.
[29] McCarthy KD, de Vellis J. Preparation of separate astroglial and oligodendroglial cell cultures from rat cerebral tissue. J Cell Biol 1980;85(3):890–902.
[30] Miron VE, Jung CG, Kim HJ, Kennedy TE, Soliven B, Antel JP. FTY720 modulates human oligodendrocyte progenitor process extension and survival. Ann. Neurol. 2008;63(1):61–71.
[31] Jadasz JJ, Tepe L, Beyer F, Samper Agrelo I, Akkermann R, Spitzhorn LS, et al. Human mesenchymal factors induce rat hippocampal- and human neural stem cell dependent oligodendrogenesis. Glia 2018;66(1):145–60.
[32] Cui QL, Fragoso G, Miron VE, Darlington PJ, Mushynski WE, Antel J, et al. Response of human oligodendrocyte progenitors to growth factors and axon signals. J Neuropathol Exp Neurol 2010;69(9):930–44.
[33] Cui Q-L, D'Abate L, Fang J, Leong SY, Ludwin S, Kennedy TE, et al. Human fetal oligodendrocyte progenitor cells from different gestational stages exhibit substantially different potential to myelinate. Stem Cells Dev. 2012;21(11):1831–7.
[34] Leong SY, Rao VTS, Bin JM, Gris P, Sangaralingam M, Kennedy TE, et al. Heterogeneity of oligodendrocyte progenitor cells in adult human brain. Ann Clin Transl Neurol 2014;1(4):272–83.
[35] Franklin KBJ, Paxinos G. The mouse brain in stereotaxic coordinates. 3 ed. New York: Elsevier2008.
[36] Chen Z, Chen JT, Johnson M, Gossman ZC, Hendrickson M, Sakaie K, et al. Cuprizone does not induce CNS demyelination in nonhuman primates. Ann Clin Transl Neurol 2015;2(2):208–13.
[37] Faul F, Erdfelder E, Buchner A, Lang AG. Statistical power analyses using G*Power 3.1: tests for correlation and regression analyses. Behav Res Methods 2009;41(4):1149–60.
[38] Allimuthu D, Hubler Z, Najm FJ, Tang H, Bederman I, Seibel W, et al. Diverse chemical scaffolds enhance oligodendrocyte formation by inhibiting CYP51, TM7SF2, or EBP. Cell Chemical Biology 2019;26(4):593. -9.e4..
[39] Najm FJ, Madhavan M, Zaremba A, Shick E, Karl RT, Factor DC, et al. Drug-based modulation of endogenous stem cells promotes functional remyelination in vivo. Nature 2015;522(7555):216–20.
[40] Lariosa-Willingham KD, Rosler ES, Tung JS, Dugas JC, Collins TL, Leonoudakis D. A high throughput drug screening assay to identify compounds that promote oligodendrocyte differentiation using acutely dissociated and purified oligodendrocyte precursor cells. BMC Res Notes 2016;9(1).
[41] Buckley CE, Marguerie A, Roach AG, Goldsmith P, Fleming A, Alderton WK, et al. Drug reprofiling using zebrafish identifies novel compounds with potential pro-myelination effects. Neuropharmacology 2010;59(3):149–59.
[42] Kremer D, Cui Q-L, Göttle P, Kuhlmann T, Hartung H-P, Antel J, et al. CXCR7 is involved in human oligodendroglial precursor cell maturation. PLoS ONE 2016;11(1) b.
[43] Matsushima GK, Morell P. The neurotoxicant, cuprizone, as a model to study demyelination and remyelination in the central nervous system. Brain Pathol 2001;11(1):107–16.
[44] Seternes OM, Johansen B, Hegge B, Johannessen M, Keyse SM, Moens U. Both binding and activation of p38 mitogen-activated protein kinase (MAPK) play essential roles in regulation of the nucleocytoplasmic distribution of MAPK-activated protein kinase 5 by cellular stress. Mol. Cell. Biol. 2002;22(20):6931–45.
[45] Gómez del Arco P, Martínez-Martínez S, Maldonado JL, Ortega-Pérez I, Redondo JM. A role for the p38 MAP kinase pathway in the nuclear shuttling of NFATp. J Biol Chem 2000;275(18):13872–8.
[46] Ivanova IA, Dagnino L. Activation of p38- and CRM1-dependent nuclear export promotes E2F1 degradation during keratinocyte differentiation. Oncogene 2006;26(8):1147–54.
[47] Zhu K, Sun J, Kang Z, Zou Z, Wu X, Wang Y, et al. Repurposing of omeprazole for oligodendrocyte differentiation and remyelination. Brain Res. 2019;1710:33–42.
[48] Göttle P, Förster M, Gruchot J, Kremer D, Hartung HP, Perron H, et al. Rescuing the negative impact of human endogenous retrovirus envelope protein on oligodendroglial differentiation and myelination. Glia 2019;67(1):160–70.
[49] Porcu G, Serone E, De Nardis V, Di Giandomenico D, Lucisano G, Scardapane M, et al. Clobetasol and halcinonide act as smoothened agonists to promote myelin gene expression and RxRγ receptor activation. PLoS ONE 2015;10(12).
[50] Cui X, Guo Y-e, Fang J-h, Shi C-j, Suo N, Zhang R, et al. Donepezil, a drug for Alzheimer's disease, promotes oligodendrocyte generation and remyelination. Acta Pharmacol. Sin. 2019;40(11):1386–93.
[51] Joubert L, Foucault I, Sagot Y, Bernasconi L, Duval F, Alliod C, et al. Chemical inducers and transcriptional markers of oligodendrocyte differentiation. J. Neurosci. Res. 2010 n/a-n/a.
[52] Peppard JV, Rugg CA, Smicker MA, Powers E, Harnish E, Prisco J, et al. High-content phenotypic screening and triaging strategy to identify small molecules driving oligodendrocyte progenitor cell differentiation. J Biomol Screen 2014;20(3):382–90.
[53] Chen J, Zuo S, Wang J, Huang J, Zhang X, Liu Y, et al. Aspirin promotes oligodendrocyte precursor cell proliferation and differentiation after white matter lesion. Front Aging Neurosci 2014;6.
[54] Cheli VT, Santiago González DA, Spreuer V, Paez PM. Voltage-gated Ca++ entry promotes oligodendrocyte progenitor cell maturation and myelination in vitro. Exp Neurol 2015;265:69–83.
[55] Fan L-W, Bhatt A, Tien L-T, Zheng B, Simpson KL, Lin RCS, et al. Exposure to serotonin adversely affects oligodendrocyte development and myelinationin vitro. J Neurochem 2015;133(4):532–43.
[56] Preisner A, Albrecht S, Cui Q-L, Hucke S, Ghelman J, Hartmann C, et al. Non-steroidal anti-inflammatory drug indometacin enhances endogenous remyelination. Acta Neuropathol 2015;130(2):247–61.

[57] Salahuddin Shaharyar M, Mazumder A. Benzimidazoles: a biologically active compounds. Arabian J Chem 2017;10:S157–S73.
[58] Radostits O, Done S. Veterinary medicine: a textbook of the diseases of cattle, horses, sheep, pigs and goats. 10 ed. Elsevier London; 2007. p. 674–762.
[59] Lo Y-C, Senese S, France B, Gholkar AA, Damoiseaux R, Torres JZ. Computational cell cycle profiling of cancer cells for prioritizing FDA-approved drugs with repurposing potential. Sci Rep 2017;7(1).
[60] Lee BY, Hur EM. A role of microtubules in oligodendrocyte differentiation. Int J Mol Sci 2020;21(3).
[61] Dong J, Wang N-N, Yao Z-J, Zhang L, Cheng Y, Ouyang D, et al. ADMETlab: a platform for systematic ADMET evaluation based on a comprehensively collected ADMET database. J Cheminform 2018;10(1).
[62] Szabo KT. Congenital malformations in laboratory and farm animals /Kalman T. Szabo. San Diego: Academic Press; 1989.
[63] Dmowski WP, Scholer HFL, Mahesh VB, Greenblatt RB. Danazol—a synthetic steroid derivative with interesting physiologic properties *†. Fertil. Steril. 1971;22 (1):9–18.
[64] Podhorecka M, Macheta A, Chocholska S, Bojarska-Junak A, Szymczyk A, Goracy A, et al. Danazol induces apoptosis and cytotoxicity of leukemic cells alone and in combination with purine nucleoside analogs in chronic lymphocytic leukemia. Ann. Hematol. 2015;95(3):425–35.
[65] Chang Y-T, Teng Y-N, Lin K-I, Wang CCN, Morris-Natschke SL, Lee K-H, et al. Danazol mediates collateral sensitivity via STAT3/Myc related pathway in multidrug-resistant cancer cells. Sci Rep 2019;9(1).
[66] Diamantopoulou E, Baxendale S, de la Vega de León A, Asad A, Holdsworth CJ, Abbas L, et al. Identification of compounds that rescue otic and myelination defects in the zebrafish adgrg6 (gpr126) mutant. Elife 2019;8.
[67] Chen X, Vaughn JM, Yacaman MJ, Williams RO, Johnston KP. Rapid dissolution of high-potency danazol particles produced by evaporative precipitation into aqueous solution. J Pharm Sci 2004;93(7):1867–78.
[68] El-Etr M, Rame M, Boucher C, Ghoumari AM, Kumar N, Liere P, et al. Progesterone and nestorone promote myelin regeneration in chronic demyelinating lesions of corpus callosum and cerebral cortex. Glia 2015;63(1):104–17.
[69] Hussain R, Ghoumari AM, Bielecki B, Steibel J, Boehm N, Liere P, et al. The neural androgen receptor: a therapeutic target for myelin repair in chronic demyelination. Brain 2013;136(Pt 1):132–46.
[70] Bielecki B, Mattern C, Ghoumari AM, Javaid S, Smietanka K, Abi Ghanem C, et al. Unexpected central role of the androgen receptor in the spontaneous regeneration of myelin. Proc Natl Acad Sci 2016;113(51):14829–34.
[71] Vega-Riquer JM, Mendez-Victoriano G, Morales-Luckie RA, Gonzalez-Perez O. Five decades of cuprizone, an updated model to replicate demyelinating diseases. Curr Neuropharmacol 2019;17(2):129–41.
[72] Göttle P, Kremer D, Jander S, Ödemis V, Engele J, Hartung H-P, et al. Activation of CXCR7 receptor promotes oligodendroglial cell maturation. Ann. Neurol. 2010;68 (6):915–24.

Myelin repair is fostered by the corticosteroid medrysone specifically acting on astroglial subpopulations

Markley Silva Oliveira Junior,[a] Jessica Schira-Heinen,[a] Laura Reiche,[a] Seulki Han,[a] Vanessa Cristina Meira de Amorim,[b] Isabel Lewen,[a] Joel Gruchot,[a] Peter Göttle,[a] Rainer Akkermann,[a] Kasum Azim,[a,1] and Patrick Küry[a,1]*

[a]Department of Neurology, Neuroregeneration laboratory, Medical Faculty, Heinrich-Heine-University, Düsseldorf 40225, Germany
[b]Institute for Stem Cell Research and Regenerative Medicine, Medical Faculty, Heinrich-Heine-University, Düsseldorf 40225, Germany

eBioMedicine 2022;83: 104204
Published online xxx
https://doi.org/10.1016/j.ebiom.2022.104204

Summary

Background Multiple sclerosis is characterised by inflammation, oligodendrocyte loss and axonal demyelination and shows an additional impact on astrocytes, and their polarization. Although a certain degree of spontaneous myelin repair can be observed, disease progression, and aging impair regeneration efforts highlighting the need to better understand glial cell dynamics to establish specific regenerative treatments.

Methods Applying a chronic demyelination model, we here analysed demyelination and remyelination related effects on astrocytes and stem cell niches and studied the consequences of medrysone application on myelin repair, and astrocyte polarization.

Findings Medrysone induced recovery of mature oligodendrocytes, myelin expression and node formation. In addition, C3d/S100a10 co-expression in astrocytes was enhanced. Moreover, Timp1 expression in C3d positive astrocytes revealed another astrocytic phenotype with a myelination promoting character.

Interpretation Based on these findings, specific astrocyte subpopulations are suggested to act in a myelin regenerative way and manner the regulation of which can be positively modulated by this corticosteroid.

Funding This work was supported by the Jürgen Manchot Stiftung, the Research Commission of the medical faculty of the Heinrich-Heine-University of Düsseldorf, the Christiane and Claudia Hempel Foundation for clinical stem cell research and the James and Elisabeth Cloppenburg, Peek and Cloppenburg Düsseldorf Stiftung.

Keywords: Reactive astrogliosis; Multiple sclerosis; Corticosteroids; Cuprizone; Remyelination; Subventricular zone

Introduction

Oligodendrocyte loss and sustained myelin damage leading to axonal demyelination are main features of the inflammatory demyelinating disease Multiple sclerosis (MS). As a result, axonal nutrition and signal propagation are impaired eventually leading to irreversible functional deficits. Oligodendroglial precursor cells (OPCs) and neural stem cells (NSCs) can confer a certain degree of oligodendroglial cell replacement and myelin repair, the efficiency of which declines with disease progression and age.[1] Moreover, astrocyte activation and gliosis are observed additionally modulating endogenous repair processes.[2,3] This also holds true for nearby neurogenic stem cell niches, such as the subventricular zone (SVZ), with gliosis, and its upgrading inflammation leading to NSCs depletion.[3–5] As these NSCs contribute to neuronal, oligodendroglial and astroglial cell populations, thereby supporting axon integrity, neuronal communication and myelination this must be considered as a substantial impact.[6–8] Oligodendroglial cells are preferentially generated within the dorsal region (d-SVZ)[7–10] whereas astrocytes mainly develop from the lateral SVZ.[7,11] Nonetheless, under pathological conditions astrocytes can also be generated in the d-SVZ and populate nearby sites.[12,13] The d-SVZ can be further subdivided in 3 micro-niches: (i) medial-

*Corresponding author.
E-mail address: kuery@uni-duesseldorf.de (P. Küry).
[1] These authors contributed equally.

Research in context

Evidence before this study

At every 5 minutes, someone is diagnosed with Multiple sclerosis worldwide. Affecting young adults through neuroinflammation and demyelination episodes, this disease aggravates over ageing, imposing the patient to severe symptoms such as fatigue, loss of vision, numbness, mobility problems, pain, cognitive, and memory deficits. Drug-repurposing approaches can be of great help to find new treatments, particularly for the still unmet clinical need of fostering endogenous repair activities. By applying a preclinical model of chronic demyelination, we investigated the effects of medrysone, an ophthalmic anti-inflammatory corticosteroid, in the context of oligodendrocyte replacement, and axon remyelination *in vivo*.

Added value of this study

This study focused on the remyelinating potential of medrysone. We validated its activity in cultured primary oligodendroglial precursor cells by assessing pro-myelination gene activities, and myelin protein expression, which were, however, not directly affected by this drug. Nevertheless, TNF-α induced neurotoxic astrocytes treated with medrysone recovered a non-neurotoxic profile. Subsequently, chronically demyelinated mice fed with cuprizone, a copper chelator, were treated with this corticosteroid. Medrysone substantially promoted corpus callosum remyelination, and a number of beneficial features related to different astrocyte subpopulations were regulated by this drug. While therefore highlighting this drug's potential as a novel Multiple sclerosis treatment, this study also clearly demonstrates a functional involvement of astroglial cells in central nervous system repair - the successful pharmacological modulation of which has so far not been reported.

Implications of all the available evidence

Under *in vivo* circumstances, medrysone stimulated remyelination by boosting oligodendrocyte recruitment, axonal myelination, and nodes of Ranvier restoration. Nonetheless, effects were mediated in a non-direct way and an astrocyte heterogeneity signature particularly correlated to a regenerative potential was specifically modulated by medrysone. Our observations strongly support the notion that cellular processes others than those directly affecting oligodendroglia are indeed applicable for the identification of myelin repair promoting drugs. Our study includes a diversity of experimental methods with different cell subtypes identified and observing distinct brain structures evolutionary conserved between humans and mice, strengthening our suggestion of medrysone as a suitable molecule for biomedical translation.

dorsal SVZ (where the medial and dorsal wall are connected), (ii) middle-dorsal SVZ (the centre area of the d-SVZ), (iii) dorsal-horn SVZ (where the lateral and dorsal wall create a corner; see Figure 1C and 1C') all of which found to display differences in terms of progenitor generation in health and disease.[9,14–16]

Studies utilizing the demyelinating compound cuprizone (CPZ) have shown that SVZ dependent oligodendrogenesis, hence, myelin restoration/ cell replacement can be more efficient as from parenchymal OPCs,[2,17] highlighting the SVZ as critical structure for repair. Nevertheless, the involvement of reactive astrocytes in respect of their heterogeneity throughout the d-SVZ and within adjacent areas have not been well described so far. Initial reports relate to oligodendrocyte loss dependent on reactive astrocytes, up-regulating interleukins and complement factors[18–20] or to promote remyelination and OPCs/NSCs maturation depending on trophic factors released by resident astrocytes.[21,22] Reactive astrocytes were basically divided into neurotoxic/A1, and neuroprotective/A2 subtypes.[23] Whereas neurotoxic astrocytes regularly express complement factor 3d (C3d),[24,25] neuroprotective commonly express S100a10, known to be involved in tissue repair.[26–28] Moreover, transcriptomic evaluations have recently shown that some astroglial cells even express A1 and A2 molecules concomitantly, thereby leading to a "hybrid" phenotype that appears to contribute to brain regeneration,[29,30] hence, supporting the fact that A1/A2 labelling is outdated to define astrocytic function. More recently, Escartin and colleagues[31] published a consensus statement defining some key variables to proper characterize reactive astrogliosis such as protein co-expression, time, disease and region analysed (diseased or healed), and our study is based on these variables.

Fostering myelin repair in patients with demyelination diseases is still an unmet clinical need[32] and considering the here described cellular heterogeneity and the diverse and complex contributions of different phenotypes to successful tissue repair we investigated the impact of medrysone to white matter regeneration. This FDA-approved anti-inflammatory corticosteroid has recently been identified as potential neuroregenerative compound in the context of NSCs[33] and was applied here to mice suffering to sustained/chronic demyelination of the corpus callosum.

Methods

Ethics statement for animal experiment

Transgenic hGFAP-GFP promoter mice[34] [FVB/N-Tg (GFAPGFP) 14mes/J; Jax stock number: Cat#003257, female and male] provided by Prof. Dr. Nikolaj Klöcker (Medicine Faculty, Heinrich-Heine-University, Düsseldorf, Germany) mice were housed in a pathogen-free facility with 12 hours light/dark cycle and supplied with nutrition and hydration *ad libitum*. *In vivo* experiments were performed in adult mice of

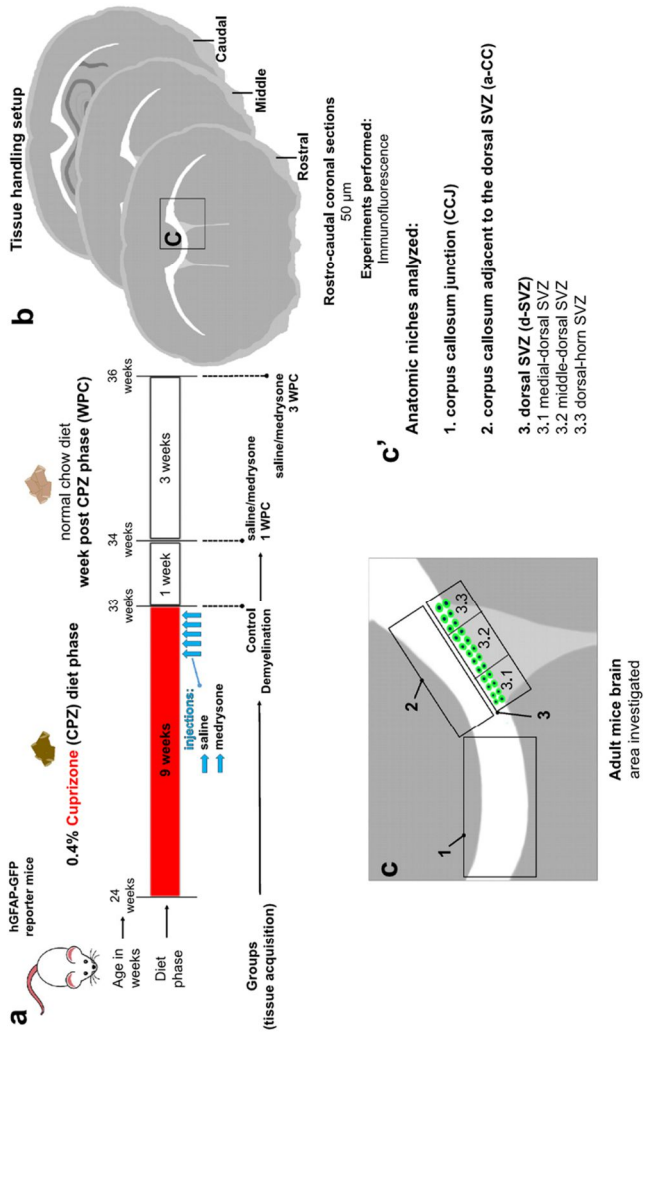

Figure 1. CPZ experimental setup. (a) Timeline of CPZ induced demyelination and of medrysone treatment in adult (24 weeks old) hGFAP-GFP reporter mice. CPZ treatment lasted for 9 weeks, then either medrysone- or saline solutions were applied intraperitoneally (i.p.) starting at five days before the end of the CPZ feeding period. Mice were sacrificed after one or three weeks post-CPZ. For additional controls, healthy mice and CPZ fed mice without treatment were sacrificed. (b) Rostrocaudal directed coronal brain slices were collected between 0.745mm to -1.25mm Bregma, and then analysed using immunofluorescence. (c,c') The corpus callosum junction (CCJ), corpus callosum adjacent to the dorsal-SVZ (a-CC) and dorsal-SVZ (divided in micro-domains: 1-medial dorsal SVZ, 2-middle dorsal SVZ, 3-dorsal horn SVZ) were the anatomic niches investigated.

either sex (from 24 weeks until 36 weeks of age). For primary astrocyte and OPC monocultures 0 or 1 day old neonatal Wistar rats of either sex were utilized. The Review Board for the Care of Animal Subjects of the district Government (LANUV, North-Rhine Westphalia, Germany) approved all research procedures under the following ethic approval numbers: Az.:8102.04.2019.A20 for *in vivo* experiments, O69/11 and V54/09 for *in vitro*. Any other details have been listed in the ARRIVE checklist.

Primary astrocyte monoculture

Primary astrocyte cultures were generated from postnatal rats (Wistar, 0-1 day old) according to McCarthy and de Vellis.[35] Brains were collected from the rat's skull and rinsed on MEM-Hepes medium (Life Technologies; Cat#123600038). The hemispheres were separated and cut off, meninges were removed, and the remaining cortices were cut into small pieces. The tissue was collected in centrifuge tubes containing 50 ml MEM-Hepes medium and spun down for 1 minute (min) at 2000 rpm. The tissue pellet was then triturated 10 times with a flame-polished Pasteur pipette and passed through a 40 μm cell strainer. Afterwards, the cell suspension was split onto 2 T-75 flasks and 20 ml of astrocyte medium [DMEM-low glucose (Life Technologies, Cat#D6046), 10% fetal calf serum (FCS; Gibco, Cat#10500-064), 2 ml of L-glutamine (Life Technologies, Cat#G7513), 50 units per ml of penicillin/streptomycin (Life Technologies, Cat#P4333)], each. The medium was changed 3 times a week, and after 10 days, flasks were placed onto a shaker (Excella E24 incubator, 4 h, 180 rpm, 37°C) to remove all microglial and dead cells. Afterwards, remaining astroglia were washed with Dulbecco's phosphate buffer solution (DPBS; Life Technologies, Cat#14190144), and subsequently 5 ml of trypsin was added for 5 min at 37°C and 5% CO_2. The reaction was stopped by adding astrocyte medium and the cell suspension collected into a 50 ml Falcon tube. Cells were centrifuged at 1200 rpm for 5 min, and the supernatant was completely aspirated afterwards. Afterwards, magnetic activated cell sorting (MACS; Miltenyi Biotec, Cat#130707677) was performed according to the manufacturer's protocol to purify the culture. Briefly, the cell pellet was resuspended in 80 uL of PB buffer (0.5% bovine serum albumin, Capricorn, Cat#FBS-16A in DPBS) and 20 uL of anti-Glast (ACSA-1; Miltenyi Biotec, Cat#130095822; RRID:AB_10829302) biotin antibodies were added, well mixed and incubated for 10 min at 2-8°C. 2 ml of cold PB buffer were added and the cells centrifuged at 1200 rpm for 5 min. The supernatant was removed, and cells were resuspended again in 80 μL of the cold PB buffer. 20 μL of anti-biotin microbeads were added, mixed, and incubated for another 15 min at 2-8°C. The cells were washed with 2 ml cold PB buffer and centrifuged at 1200 rpm for 5 min, the supernatant was removed, and cells were resuspended in 500 μL of buffer. For magnetic separation, the columns were placed in the magnetic field within 500 μL buffer per column. The cell suspension was disposed in it, and the columns were washed 3x with 500 μL of buffer; the magnetically labelled cells were flushed out by pressing the plunger within the column. The cell suspension was centrifuged for 5 min at 1200 rpm, and the supernatant was fully removed; the cells were resuspended in astrocyte medium. Purified astrocytes were cultured for 3 days onto 0.25 mg/ml poly-D-lysine coated (PDL, Sigma-Aldrich; N/A) glass coverslips (13 mm) in 24-well plates (for immunocytochemistry; 6.0×10^4 cells/well) or 0.25 mg/ml PDL coated 24-well plates for quantitative reverse transcription-polymerase chain reaction (qRT-PCR; 5×10^4 cells/well). Astrocytes were subjected to 0.1 % Dimethylsulfoxide (DMSO, Sigma Aldrich, Cat#D2650), 30ng/ml tumour necrosis factor-alpha (TNF-α, R&D System, Cat#510RT) or 2.5 μM medrysone (6α-methyl-11β-hydroxy-Progesterone; Cayman Chemical, Cat#19533) for 48 hours. Astrocyte monocultures were between 95 and 98% pure as revealed by Gfap/Glast double immunostaining (data not shown). The number of animals per analysis was at least n=10 per experiment for in vitro/cell culture experiments, given that primary cells are generally generated from 10 neonatal rats and then pooled. Nevertheless, reproduction and statistical evaluation of such experiments was then undertaken by performing 3-4 different and independent experiments. Sample sizes for our in vitro/cell culture experiments are based on our (published) experience with primary neural cell types.

Primary OPC monoculture

Primary OPC cultures were prepared from P0-1 Wistar rats according to McCarthy and de Vellis[35] with modifications by our group.[36–38] Primary OPCs (>97 % pure) were either seeded onto 0.25 mg/ml PDL coated glass coverslips (13 mm) in 24-well plates (for immunocytochemistry; 2.5×10^4 cells/well) or 0.25 mg/ml PDL coated 24-well plates for qRT-PCR (5×10^4 cells/well) in high-glucose DMEM-based Sato medium [(5 μg/ml bovine insulin; 50 μg/ml human transferrin; 100 μg/ml bovine serum albumin fraction V (BSA; Thermo Fisher Scientific); 6.2 ng/ml progesterone; 16 μg/ml putrescine, 5 ng/ml, sodium selenite; 400 ng/ml T3 (tri-iodo-thyronine); 400 ng/ml T4 (thyroxin; all Sigma–Aldrich unless stated otherwise); 4 mM L-glutamine; 100 U/ml penicillin/0.1 mg/l streptomycin (both Thermo Fisher Scientific)]. After 1.5 hours, cell differentiation was induced by changing to differentiation medium (Sato medium supplemented with 0.5 % FBS). The medium was exchanged every 3 days. OPCs were supplemented with 0.1 % DMSO or 5 μM medrysone for 72 hours without medium exchange. Primary OPC

cultures were on average 95% pure based on Gfap, Iba-1 staining for contaminating astrocytes and microglia, respectively (data not shown). The number of animals per analysis was at least n=10 per experiment for in vitro/cell culture experiments, given that primary cells are generally generated from 10 neonatal rats and then pooled. Nevertheless, reproduction and statistical evaluation of such experiments was then undertaken by performing 3-4 different and independent experiments. Sample sizes for our in vitro/cell culture experiments are based on our (published) experience with primary neural cell types.

Immunocytochemistry

Astrocytes were incubated with 0.5 % Triton X-100 (Sigma Aldrich) in DPBS for 30 minutes (min), followed by a 60 min incubation with blocking solution containing 10 % normal goat serum (NGS, Gibco, Cat#PCN5000) in DPBS supplemented with 0.5 % Triton X-100 (Sigma Aldrich, Cat#85111) and 10 % BSA. Primary antibodies for astrocytes were diluted in blocking buffer with following concentrations: Chicken anti-glial fibrillary acid protein (Gfap; 1:500, Aves labs, Cat#SKU:Gfap; RRID: AB_2307313); Rabbit anti-complement component 3d (C3d; 1:300, Dako, Cat#A0063; RRID: AB_578478). OPCs were blocked with 10% NGS in DPBS containing 0.1% Triton X-100 at RT for 45 min. Primary antibodies for OPCs were diluted in 10% NGS in DPBS containing 0.01% Triton X-100 with following concentrations: Rat anti-myelin basic protein (MBP; 1:250, Biorad, Cat#aa8287, RRID:AB_32500). Primary antibody incubations were performed overnight. Secondary antibodies were all used at 1:500 [anti-rabbit AlexaFluor 594 (Cat#A32740; RRID: AB_2762824); anti-chicken AlexaFluor 488 (Cat#A32931; RID:AB_2762843); anti-rat AlexaFluor 488 (Cat#A-11006; RRID:AB_2534074)]; all from Thermo Fisher Scientific). 4′,6′-diamino-2-phenylindole (Dapi, Roche diagnostic GmbH) was applied at a concentration of 5 μM nuclear dye. Secondary antibodies and dye incubation were performed for 120 min. Coverslips were mounted with Immu-mount (Thermo Fisher Scientific, Cat#1900331) on a glass-slide for subsequently confocal microscopy.

RNA preparation, cDNA synthesis and quantitative RT-PCR analysis

Total RNA purification from OPC and astrocyte monocultures was done using 350 μL of RLT lysis buffer (Qiagen, Cat#1015762) supplemented with β-mercaptoethanol (1:100, Sigma, Cat#M3148-25). The total RNA was purified by utilizing RNeasy Mini Kit according to manufacturer instructions including DNase digestion. Before quantitative real-time polymerase chain reaction (qPCR), reverse transcription with 250 ng RNA measured using a NanoDropND 1000 was done using the High-Capacity cDNA Reverse Transcription Kit (Thermo Fisher Scientific, Cat# N8080234). Gene expression levels were determined on a 7900HT sequence detection system (Applied Biosystems, Thermo Fisher Scientific), applying Sybr-Green universal master mix (Thermo Fisher Scientific, Cat#43676659). Following amplification primers were used: For OPCs rat (rt) Gapdh: fwd- GAA CGG GAA GCT CAC TGG C, rev- GCA TGT CAG ATC CAC AAC GG (as reference gene); rtMyrf: fwd- CCT GTG TCC GTG GTA CTG TG, rev- TCA CAC AGG CGG TAG AAG TG; rtPdgfrα: fwd- AGC TCT CTG TTC CCA ATG CC, rev- GCC TCC ATT CTG GAG CTT GT; rtSox10: fwd- GTC AGA TGG GAA CCC AGA GCA C, rev- CCC GTA GCC AGC TGC CGA G; rtCNPase: fwd- GCC GTT GTG GTA CTT CTC CA, rev- GCC CGA AAA AGC CAC ACA TT. For astrocytes rtHprt: fwd- CAG TCC CAG CGT CGT GAT TA, rev- ATG GCC TCC CAT CTC CTT CA (as reference gene); rtGfap: fwd- CTG GTG TGG AGT GCC TTC GT, rev- CAC CAA CCA GCT TCC GAG AG; rtSerpina3n: fwd-GGG CAG GTG CTT CGT, rev-AGC GCC TTT GTC TTT CTT TCT G; rtLcn2: fwd-TCT CAG GCC CAC CAT GAT AGA, rev-CAG GTT GTA GTC AGC AGA GAT GGA; rtSerping1: fwd-GAC AGC CTG CCC TCT GAC A, rev-GCA CTC AAG TAG ACG GCA TTG; rtC3: fwd- CCT TCC CGG GAG CAT CA, rev- GGG CAT ACC CAG CAA TGG; rtC1qa: fwd- CAG AAC CCA CCG ACG TAT GG, rev- TCC TGG TTG GTG AGG ACC TT; rtIL6: fwd- GTT GTG CAA TGG CAA TTC TGA, rev-TCT GAC AGT GCA TCA TCG CTG; rtPtx3: fwd- GGC CAA AAG TCA CCC TGT TC, rev- CCA TTC TTT TCT TGG CCA ATCT; rtCd14: fwd- ACA ACA GGC TGG ATA GGA AAC C, rev-TGA CAG GCT CCC CAC TTC AG; rtS100a10: fwd-GCC ATC CCA AAT GGA GCA T, rev- CCC CTG CAA ACC TGT GAA AT

(all primers manufactured by Eurofins genomics, Germany).

Cuprizone diet and drug-treatment procedure

To induce demyelination, 24 weeks old hGFAP-GFP reporter mice were exposed to a regular diet of 0.4 % CPZ (Sniff, Cat#V1534) for nine weeks. Animals were randomized into treatment arms, whilst making sure that the sex matched between groups. Our analyses were based on two arm-randomizations and two-tailed statistical tests to assess how medrysone affected spontaneous remyelination. During the last five days of CPZ feeding, mice received daily intraperitoneal injections of 500 μL of 0.5 % saline solution or of 5 mg/kg b.w. medrysone [first diluted in DMSO (20 mg/ml stock solution), thereafter diluted using saline to a 7.25 % final concentration of DMSO]. For recovery, mice received normal food for one or three weeks after CPZ feeding (see Figure 1A). Six groups were analysed: (i) control/non-CPZ fed; (ii) 9 weeks CPZ /demyelination; (iii-iv) 9 weeks CPZ, plus saline injection and one or

three weeks of normal food (saline 1/3 WPC respectively); (v-vi) 9 weeks CPZ, plus medrysone injection and one or three weeks of normal food (medrysone 1/3 WPC respectively). We measured the body weight of the animals since CPZ is known to have an impact on body weight. Immunohistochemical analysis was performed on rostrocaudal brain sections (bregma: 0.745μm to -1.25μm) analysing the corpus callosum junction (Figure 1C' area 1), adjacent corpus callosum (a-CC; Figure 1C' area 2) and the d-SVZ (Figure 1C' area 3; divided into three micro-domains: 3.1-medial dorsal-SVZ; 3.2-middle d-SVZ and 3.3-dorsal-horn SVZ). For *in vivo* investigations we used at least n=4 animals per experimental group. Experiments were previously determined using a G*power analysis. This analysis was also necessary to have animal experiments legally granted by the authorities (The Review Board for the Care of Animal Subjects of the district Government (LANUV, North-Rhine Westphalia, Germany).

Tissue processing and immunohistochemistry

For immunohistochemistry mice were transcardially perfused with 20 ml ice-cold DPBS and 20 ml 4 % PFA and dissected brains were post fixed with 4 % PFA 48 hours. Subsequently, brains were incubated with 30 % sucrose for 72 hours, embedded in 2 % agarose and cut into 50μm thick sections using a vibration microtome. Sections were permeabilised by incubation with 0.5 % Triton X-100 for 30 min, blocked with 10 % NGS supplemented with 5 % BSA and 1% Triton for 120 min and incubated with following antibodies overnight at 4° C: rat anti-MBP (rat; 1:300, Biorad, Cat#aa8287, RRID: AB_32500); mouse anti-adenomatous polyposis coli (CC1-APC; 1:300, anti-APC-Ab7-clone CC1, Merck millipore, Cat#OP80, RRID: AB_2057371); rabbit anti-glutathione S-transferase-pi (GSTπ; 1:500, Enzo, Cat#ADIMSA101, RRID: AB_10615079); rabbit anti-oligodendrocyte transcription factor 2 (Olig2; 1:500, Millipore, Cat#AB9610, RRID:AB_570666); mouse anti-contactin associated protein 1 (Caspr; 1:400, anti-Caspr-paranodin, neuroxin-IV, clone k65/35, Neuromab, Cat#75-001, RRID: AB_10671175); rabbit anti-sex-determining region Y-box 1- (Sox10; 1:100, DCS immunoline, Cat#S1058C002, RRID: AB_2313583); mouse anti-breast carcinoma-amplified sequence 1 (Bcas1/NaBC1; 1:200, Santa Cruz, Cat#sc-136342, RRID: AB_10839529); chicken anti-green fluorescent protein (GFP; 1:500, Aves labs, Cat#GFP1010, RRID: AB_2307313); rabbit anti-human C3d (1:500, Dako, Cat#A0063; RRID: AB_578478); mouse anti-signal transducer and activator of transcription 3 (Stat3; 1:400, Invitrogen, Cat#MA1-13042, RRID: AB_10985240); mouse anti-human S100 calcium-binding protein A10 (S100a10; 1:500, Thermo Fisher Scientific, Cat#MA5-15326, RRID: AB_2092361); rabbit anti-myelin proteolipid protein (PLP; 1:250, kind gift from Dr. B. Trapp, Department of Neurosciences, Cleveland Clinic, Ohio, United States; Chen et al., 2015); goat anti-tissue metallopeptidase inhibitor 1 (Timp1; 1:100, R&D System, Cat#AF580, RRID:AB_355455); goat anti-lipocalin-2/NGAL (Lcn2; 1:180, R&D System, Cat#AF1857, RRID: AB_355022); rabbit anti-nitric oxide synthase (iNOS; Abcam, Cat#ab95441, RRID:AB_10688716); rat anti-nuclear factor-erythroid factor 2-related factor 2 (Nrf2; 1:100, Cell Signalling Technology, Cat#14596, RRID: AB_2798531); rabbit anti-transcription factor Mafg (Mafg; 1:100, Genetex, Cat#GTX114541, RRID: AB_10619599); mouse anti-epidermal growth factor receptor (Egfr; 1:500, Anti-Egfr endoplasmic domain, Millipore, Cat#8662051047, RRID: AB_2096607). Antigen retrieval disrupts the GFP signal, thus, it was used only for anti-MBP, anti-Olig2 (Figure 1), anti-Sox10 (Figures 1 and 6) and anti-PLP (Figure 6) staining. For this purpose, sections were rinsed in 0.1 M phosphate buffer (pH 7.4) for 3×5 min, transferred to 10 mM sodium citrate buffer (pH 8.5) pre-heated to 80° C in a water bath for 20 min and rinsed 0.1 M phosphate buffer (pH 7.4) for 3×5 min before blocking and incubation with primary antibodies. After incubation with primary antibodies, sections were washed and incubated with secondary antibodies and Dapi for 120 min. All secondary antibodies were used at a concentration of 1:200 [anti-rat AlexaFluor 647 (Cat#A-11006; RRID: AB_2534074); anti-mouse AlexaFluor 594 (Cat#A32742; RRID:AB_2762825); anti-rabbit AlexaFluor 647 (Cat#A32733; RRID:AB_2633282); anti-chicken AlexaFluor 488 (Cat#A32931; RID:AB_2762843); anti-mouse AlexaFluor 647 (Cat#A32728; RRID:AB_2633277), Donkey anti-goat AlexaFluor 594 (Cat#A32758; RRID: AB_2762828), all Thermo Fisher Scientific]. Subsequently, sections were washed in DPBS and mounted onto glass slides (Superfrost Ultra Plus, Thermo Fisher Scientific).

All sections were analysed using a confocal laser scanning microscope (CLSM) 510 (Zeiss, 510, Carl Zeiss AG, Oberkirchen, Germany). Rostral, middle and coronal sections each 50 μm thick were utilized for cell quantification for each individual, totalizing an area of observation of 150 μm in a z-stack orientation. For quantification, areas corresponding to 150 μm of the junction corpus callosum and to 100μm of the d-SVZ were analysed per section. Z-stack orientation was performed and at least 35 slices per Z-stack file were taken for each sample. For MBP and PLP fluorescence at the CCJ and a-CC respectively (see Figure 1C') photomicrographs were analysed using the software Fiji-ImageJ version 1.47[39] using a virtual line traced around the region of interest (ROI) to determine fluorescence units. No normalization of ROIs was performed within the histogram algorithm. By using the ImageJ software, a square of 280 µm × 220 µm (standardised by using the ImageJ dimension rule) was drawn on each picture obtained for MBP and PLP quantification. Moreover, by using the histogram algorithm the

fluorescence intensity was quantified within the squared area – being aware that the corpus callosum at both CCJ and a-CC areas changes in thickness and size and that our evaluation was based on rostral, middle and caudal orientation.

Statistical analysis

Data are shown as mean values ± standard error of the mean (mean ± SEM). GraphPad Prism 7.0.2 (GraphPad Prism, San Diego, CA, RRID: rid_000081) was used for statistics and graphics collection. To assess the absence of Gaussian distribution, Shapiro–Wilk normality test was used for all datasets. Student's t-test was applied for comparing two groups and two-way analysis of variance (ANOVA) with Bonferroni post-test for multiple comparisons was applied to compare three or more groups. For data sets not passing the Shapiro-Wilk normality test, Kruskal–Wallis test with Dunn's post-test for multiple comparisons of three or more groups was applied. P values are defined as follows: * represents $p \leq 0.05$; ** represents $p \leq 0.01$; *** represents $p \leq 0.001$. Asterisks absence means no statistically significant difference was observed. Absent bars in certain groups indicate that the respective cell subtype was not found, these groups were not considered for the statistical analysis. A priori sample size calculation for the *in vivo* experiments was performed using the G*Power 3.1.9.2 software[40] (test family: t-tests; statistical test: means: Wilcoxon-Mann-Whitney test (two groups); tails: two; effect size d: 2.6; alpha error 0.05, power 0.95; allocation ratio N2/N1: 1; resulting max sample size: 6). This analysis was also necessary to have animal experiments legally granted by the authorities (The Review Board for the Care of Animal Subjects of the district Government (LANUV, North-Rhine Westphalia, Germany). The number of animals per analysis was at least n=10 per experiment for in vitro/cell culture analyses, given that primary cells are generally generated from 10 neonatal rats and then pooled. Nevertheless, reproduction and statistical evaluation of such experiments was then undertaken by performing 3-4 different and independent experiments. Sample sizes for our in vitro/cell culture experiments are based on our (published) experience with primary neural cell types.

Role of funders

The funding source had no role in study design, collection, analysis and interpretation of data or in manuscript writing

Results

In vivo demyelination and drug-treatment procedure

To induce demyelination, 24-week-old transgenic hGFAP-GFP reporter mice were exposed to 0.4 % CPZ for nine weeks. During the last five days of CPZ feeding, mice received daily intraperitoneal injections of 5 mg/kg of medrysone- or saline solution. Over the post cuprizone phase (WPC), mice received normal food for one or three weeks (Figure 1a). Six groups were analysed: (i) non-CPZ fed/control; (ii) 9 weeks CPZ diet/demyelination; (iii) 9 weeks CPZ, plus saline injection and one week of normal food (saline 1 WPC); (iv) 9 weeks CPZ, plus saline injection and three weeks of normal food (saline 3 WPC); (v) 9 weeks CPZ, plus medrysone injection and one week of normal food (medrysone 1 WPC); (vi) 9 weeks CPZ, plus medrysone injection and three weeks of normal food (medrysone 3 WPC). Immunofluorescence analysis was performed using 50 μm rostrocaudal coronal sections (1 rostral section, 1 middle section and 1 caudal section per n; Figure 1b) analysing the corpus callosum junction (CCJ; Figure 1c' area 1), the corpus callosum adjacent to d-SVZ (a-CC; Figure 1c' area 2) and the d-SVZ (Figure 1c' area 3; divided into three micro-domains: 3.1-medial dorsal-SVZ; 3.2-middle d-SVZ and 3.3-dorsal-horn SVZ). For cell counting 150 μm were analysed along the z-axis for all anatomic niches (Figure 1c'). For the CCJ an area of interest of 150 μm along the x/y-axis and, for d-SVZ an area of interest of 100 μm along the x/y-axis were analysed in terms of cell counts.

Remyelination and nodes of Ranvier recovery are improved by medrysone

We aimed at evaluating the potency of medrysone to improve remyelination in chronically demyelinated mice induced by a prolonged CPZ application. Looking at the CCJ (see Figure 1c) we found after 9 weeks of CPZ diet a diminished MBP expression (Figure 2s) as well as lower numbers of early-stage mature (GSTπ positive) oligodendrocytes (OL), mature (Olig2/CC1 double-positive) OL and of active myelinating OL (Sox10/Bcas1 double-positive cells; Figure 2t,2u,2v; see Figure 2x for OL maturation stages and representative markers). Adjacent localization of MBP and Caspr was used to identify nodes of Ranvier by their juxtaposition (Figure 2x'). Of note, the number of which was found to be reduced in response to demyelination (Figure 2w) confirming myelin loss. On the contrary, quantitative analysis revealed that medrysone significantly promoted the recovery of MBP expression (Figure 2s), of early-stage mature OL- (Figure 2t), of mature OL (Figure 2u) and of active myelinating OL numbers (Figure 2v), as well as of nodes of Ranvier numbers (Figure 2w) reaching levels similar to healthy controls at 1 and 3 weeks post CPZ, respectively.

Demyelination affects hGFAP-GFP cells at the corpus callosum and the d-SVZ

Throughout myelin damage and depending on the inflammatory stage astrocytes exert either detrimental

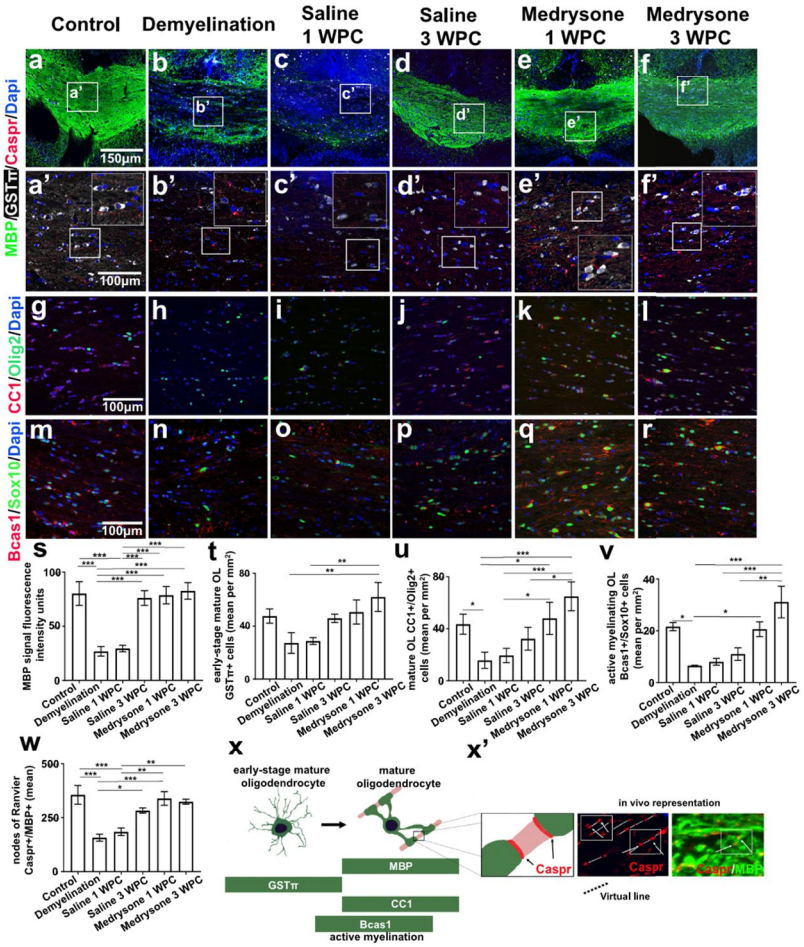

Figure 2. Medrysone promotes oligodendrocyte recovery and remyelination at the corpus callosum junction. Representative pictures of the corpus callosum junction (CCJ, Figure 1c) stained for MBP, GSTπ, Caspr (a-d, a'-d') Olig2 and CC1 (g-l), Sox10 and Bcas1 (m-r) protein expression. (s) Quantitative analysis of MBP stained structures revealed a decrease of myelin expression in the demyelination group with saline treatment leading to weak remyelination and medrysone significantly promoting MBP recovery at the early time point (1 WPC). (t, u, v) Similarly, the numbers of GSTπ positive, Olig2/CC1- and Sox10/Bcas1 double-positive cells recovered upon medrysone application accompanied by improved generation of nodes of Ranvier (w). (x) Oligodendrocyte maturation and representative markers (x') graphical and *in vivo* representation of nodes of Ranvier immunofluorescence (Caspr+/MBP+). Bars in (s) correspond to mean fluorescence intensity ± standard error of the mean (SEM), bars (t, u, v) correspond to mean cell numbers per mm^2 ± standard error of the mean (SEM), bars in (w) correspond to mean number of nodes ± standard error of the mean (SEM). Statistical significance was calculated using a two-way ANOVA with multiple comparison Bonferroni post-test (*$p < 0.05$, **$p < 0.01$, and ***$p < 0.001$). Number of animals per analysis: n=6 (s, t); n=5 (u, v, w). Exact p-values according to sequence from left to right: s: (p= 0.000000383874685, p=0.000000935915998, p=0.000001608060795, p=0.000000637203217, p=0.000001164768189, p=0.000004042884687, p=0.000001570954253, p=0.000000394110251). t: (p=0.001937648865078, p=0.003177866419346). u: p=0.045380409230564, p=0.012638408327068, p=0.00011622977178, p=0.036252296508041, p=0.000318271010733, p=0.011713553263055). v: (p=0.023166172011608, p=0.04065251019751, p=0.000116654567343, p=0.000261656183587, p=0.001371706447911). w: (p=0.000125063209522, p=0.000773952216255, p=0.018530905333733, p=0.000384534736556, p=0.001076299627656, p=0.002472602001283, p=0.007086659102636).

or beneficial effects which determines or influences remyelination efficacies.[41,42] After CPZ-mediated chronic demyelination, we found that the degree of GFP-positive cells at the CCJ did not change significantly between groups/pathophysiological stages (Figure 3g). However, when looking at the a-CC, a higher number of GFP-positive cells versus all groups was found in the demyelination, followed by still elevated levels in the medrysone 3 WPC group (Figure 3n), however, without difference to the control. Interestingly, in the d-SVZ, medrysone treated animals at 1 WPC displayed significantly elevated number of transgenic cells which sharply dropped below control levels at 3 WPC (Figure 3o).

Medrysone fosters Stat3 and S100a10 expression in C3d+ astrocytes in the remyelinated CCJ

Depending on the phenotype, astroglial cells can promote demyelination or remyelination.[25,43,44] Quantification of transgenic cells expressing C3d and signal transducer and activator of transcription 3 (Stat3), revealed that medrysone treatment leads to an increase of C3d+/Stat3+/GFP+ astroglial subpopulation at the CCJ (Figure 4n) and more exclusively at dorsal horn SVZ (Figure S3h). In contrast, demyelination led to an increased number of C3d expressing cells devoid of Stat3 (C3d+/Stat3-/GFP+) which were subsequently reduced or fully depleted in the recovery phase after both saline and medrysone treatment, respectively (Figure 4m). Senescence naturally induces astrocytes to express S100a10.[45] Nonetheless, during disease, S100a10 expression identifies astrocytes within remyelinated lesions in MS[26] as well as upon experimental demyelination.[47] We performed triple staining for C3d, S100a10 and GFP aiming at identifying reactive astrocytes at the CCJ (Figure 4g-4l). C3d+/S100a10-/GFP+ cells were significantly induced by demyelination (Figure 4o, 4h, 4h') with medrysone counteracting this effect leading to decreased numbers of C3d+/S100a10-/GFP+ cells at both investigated time points (Figure 4o). Our findings revealed that C3d+/S100a10+/GFP+ astrocytes (Figure 4p) appear after demyelination and saline or medrysone treatment but were not detectable in healthy control tissue. Medrysone treatment significantly promoted the C3d+/S100a10+/GFP+ phenotype at 1 WPC which further increased at 3 WPC. Furthermore, C3d-/S100a10+/GFP+ were identified at the CCJ of healthy controls which decreased by demyelination and were not found in saline treated 1 WPC mice, however, it re-appeared at 3 WPC independent of whether animals were saline or medrysone treated (data not shown).

C3d+/Stat3+ and C3d+/S100a10+ astrocytes were regulated at the a-CC throughout remyelination

As a next step, quantification of C3d/Stat3 double-positive, C3d+/S100a10+/GFP+ and C3d-/S100a10+/GFP+ astrocytes in the a-CC (see Figure 1c, 1c') was conducted. C3d+/Stat3-/GFP+ cell numbers were only induced during demyelination then decreasing at saline 1 WPC and being absent in all other groups (Figure 5m; red bars). C3d+/Stat3+/GFP+ cells were not present in control and demyelinated mice (Figure 5a, 5b, 5m), were moderately induced in saline treated animals (Figure 5c, 5d, 5m) and strongly induced upon medrysone treatment at both time points (Figure 5e, 5f, 5m; purple bars). C3d+/S100a10-/GFP+ astrocytes were strongly upregulated upon demyelination and at both remyelination timepoints in saline treated mice (Figure 5h, 5i, 5j, 5n; green bars). However, a robust reduction of this phenotype was observed in medrysone treated mice (Figure 5n). C3d+/S100a10+/GFP+ astrocytes rarely appeared over demyelination (blue bars; Figure 5h, 5n). Saline treated mice only showed low levels of this phenotype, whereas medrysone treatment led to a strong increase of C3d+/S100a10+/GFP+ astrocytes at the a-CC at both time points (Figure 5k, 5l, 5n; blue bars).

Demyelination at a-CC was accompanied by DRA or RRA throughout the recovery phase

Chronic demyelination can also decrease levels of myelin proteolipid protein (PLP) and of active myelinating OLs (Sox10+/Bcas1+) in the a-CC, with a weak recovery over saline-treatment (Figure 6e, 6j) and an enhanced recovery upon medrysone treatment (Figure 6d, 6e, 6i, 6j). Lipocalin 2 (Lcn2) it is known for its detrimental activities upon myelin disruption[46] which acts by controlling inducible nitric oxide synthase (iNOS) expression in glial cells.[48–50] We found astrocytes co-expressing Lcn2 and iNOS, identified as demyelination related astrocytes (DRA), which were only found at the a-CC (Figure 1c'). DRA (Lcn2+/iNOS+/GFP+) numbers were significantly increased upon demyelination (Figure 6l, 6m, 6o) with medrysone neutralizing this effect leading to a decreased DRA numbers at both investigated time points (Figure 6n, 6o). Timp1 is a metallopeptidase inhibitor that has been reported as one of the critical factors released by astrocytes able to promote white matter recovery after demyelination.[51–53] We therefore investigated whether reactive astrocytes expressed Timp1 during recovery phases. By means of Timp1/C3d/GFP triple staining we identified C3d-negative control astrocytes expressing Timp1 in healthy tissue. These astrocytes were exclusively found in the a-CC whereas no Timp1 positive cells were observed at d-SVZ and its micro-domains as well as the CCJ. Moreover, this phenotype was completely absent upon demyelination, during remyelination and in presence of medrysone (data not shown). C3d+ reactive astrocytes expressing Timp1, however, were absent in healthy and demyelinated tissues, appeared in saline treated animals at both recovery phases and were found to be increased in numbers in

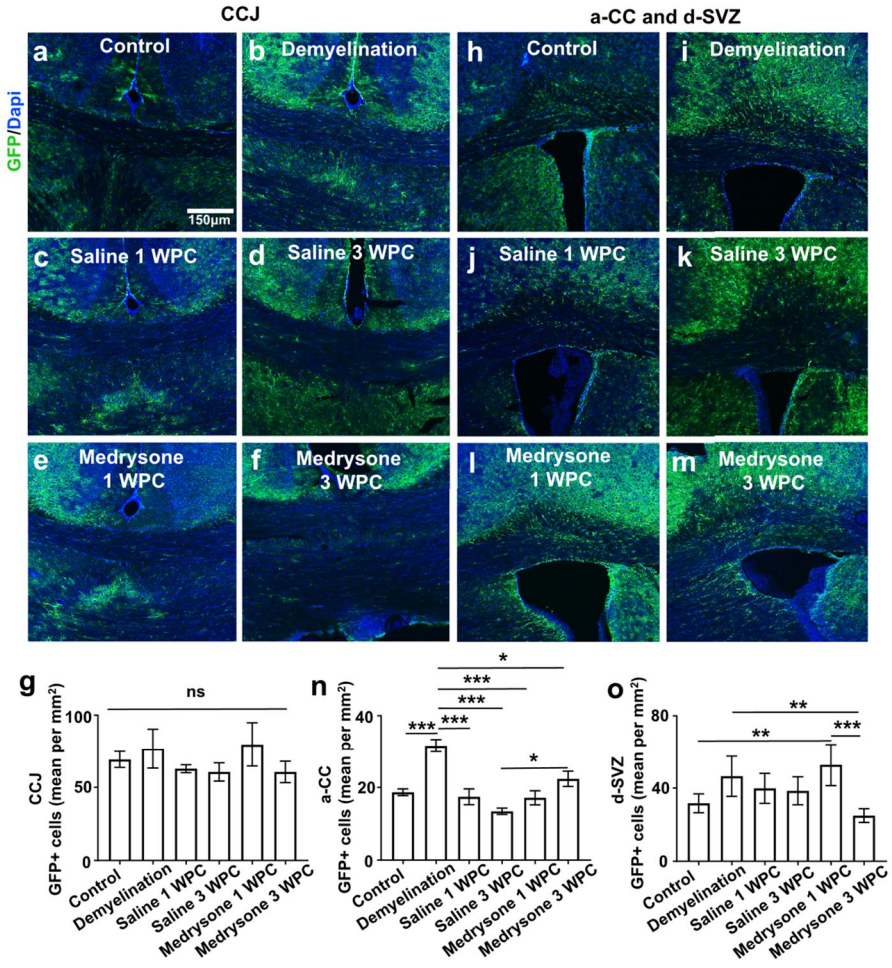

Figure 3. Quantification of hGFAP-GFP positive cells in the corpus callosum junction and dorsal SVZ. (a-m) Representative pictures of GFP-positive cells at the CCJ, a-CC and the d-SVZ with cell nuclei visualized using Dapi. (g) Quantification of GFP-positive cells revealed similar number of GFP expressing cells in all groups at the corpus callosum junction. (n) In the a-CC demyelination induced the degree of GFP-positive cells (versus control) and a mild induction between medrysone and saline groups was found at 3 WPC. Moreover, in the d-SVZ (o), GFP-positive cells were enriched upon medrysone treatment at 1 WPC (versus control), sharply dropping thereafter (3 WPC). Abbreviation: non-significant (ns). Bars correspond to mean cell numbers per mm^2 ± standard error of the mean (SEM). Statistical significance was calculated using Kruskal-Wallis test with Dunn's post-test (g) and two-way ANOVA with multiple comparisons Bonferroni post-test (n; o; $*p < 0.05$, $**p < 0.01$, and $***p < 0.001$). Number of animals $n=6$ (g, o), $n=7$ (n). Exact p-values according to sequence from left to right: n: ($p=0.000388398742168$; $p=0.000104914644292$, $p=0.000001511008705$, $p=0.000077138716235$, $p=0.019669035728742$, $p=0.028226088991489$). o: ($p=0.006937732126289$, $p=0.005565374980289$, $p=0.000255068999518$).

medrysone treated mice (Figure 6s, 6t). As this phenotype was exclusively observed over the recovery phase these cells were hence designated as remyelination related astrocytes (RRA). Of note, none of the C3d/Timp-1 double-positive cells expressed S100a10 (data not shown), indicating that C3d+/S100a10 +/GFP+ astrocytes were probably not participating at this trophic process.

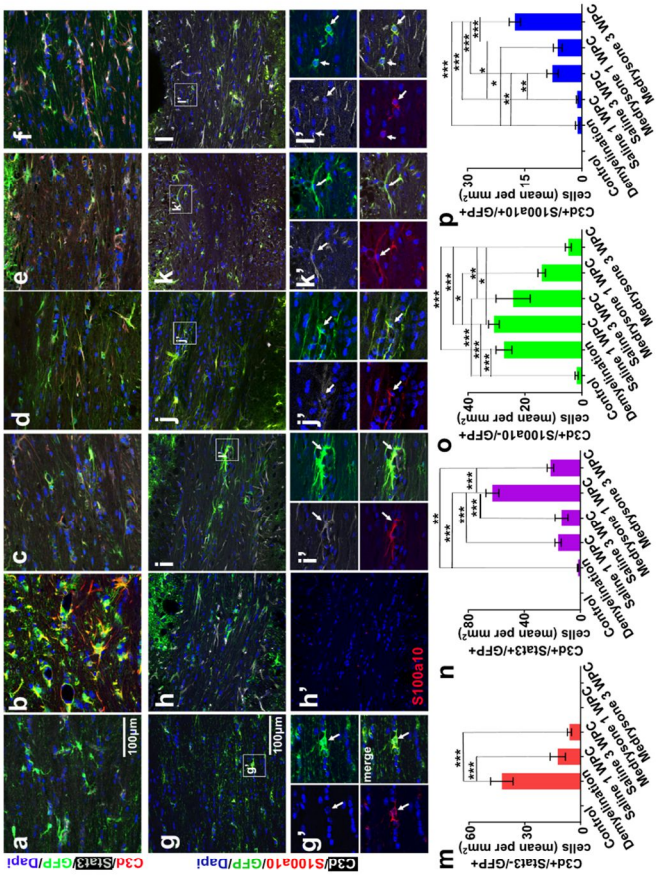

Figure 4. Dynamics of different astroglial subpopulations in the de- and remyelinating corpus callosum. (a-f) Representative pictures of the corpus callosum co-stained for C3d, Stat3 and GFP. (g-l, g'-l') Representative pictures of the corpus callosum co-stained for C3d, S100a10 and GFP. (m) Demyelination enhanced the number of C3d+/Stat3- astrocytes whereas in the recovery phase they were less present. Medrysone treated mice did not exhibit this astroglial phenotype. (n) Medrysone led to a transient increase of C3d+/Stat3+ astrocytes. (o) C3d +/S100a10- astrocytes increased after demyelination independent of the treatment, medrysone more effectively reduced this phenotype in both WPC phases. (p) Quantification of C3d +/S100a10+/GFP+ astrocytes revealed that medrysone promoted this phenotype. White arrows point to nuclei of representative cells (g'-l'). Abbreviations: Lateral ventricle (LV). Bars correspond to mean cell numbers per mm^2 ± standard error of the mean (SEM). Statistical significance was calculated using a two-way ANOVA with multiple comparisons Bonferroni post-test (*$p < 0.05$, **$p < 0.01$, and ***$p < 0.001$). Number of animals $n=5$ (m-p). Exact p-values according to sequence from left to right: m: ($p=0.000001939212634$, $p=0.000000093452992$. n: $p=0.000000001506$, $p=0.003533302378445$, $p=0.000000016322104$, 0.000000006736671, 0.000000013139942). o: ($p=0.000154193673$, $p=0.000026908283521$, $p=0.00080277543841$1, $p=0.000704424040409$, $p=0.015340507431056$, $p=0.000115145119193$, $p=0.003821079590641$). p: ($p=0.004044723153267$, $p=0.036174045580504$, $p=0.000000008760832$, $p=0.004716687589661$, $p=0.042115928088711$, $p=0.000000009715655$, $p=0.000027932768139$, $p=0.000004064840604$).

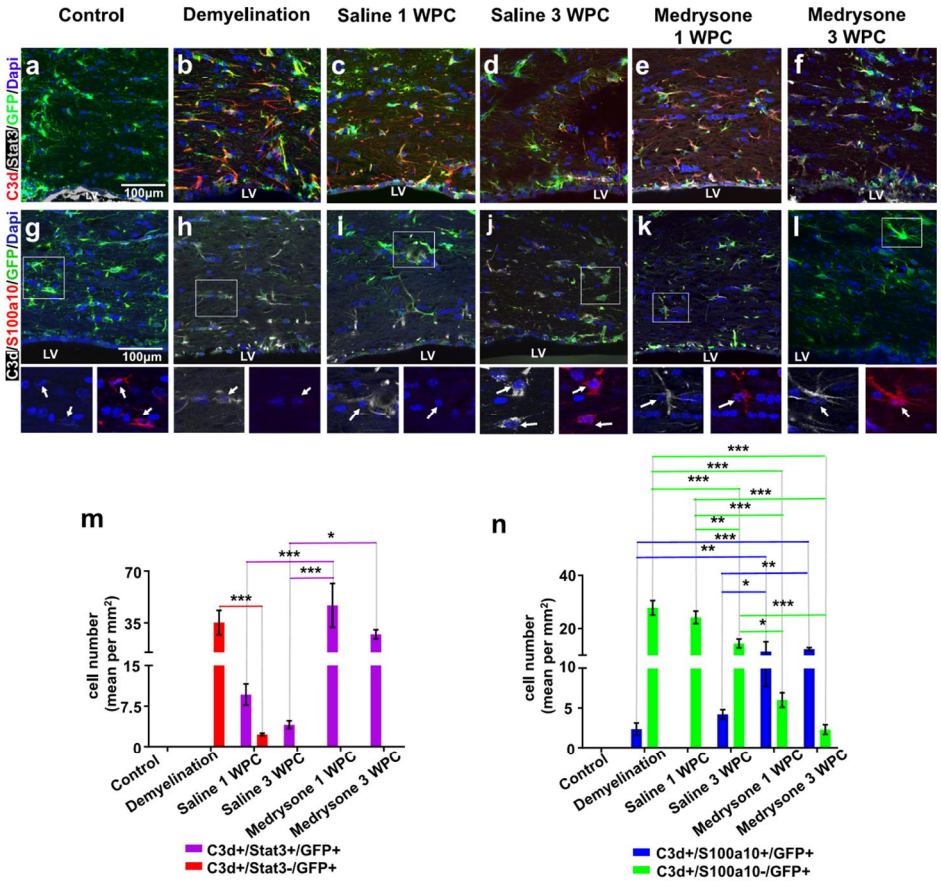

Figure 5. Numbers of C3d+/S100a10+ and C3d+/S100a10- astrocytes change in the adjacent corpus callosum over time and after medrysone treatment. Representative pictures of a-CC tissues sections stained for C3d, Stat3 and GFP (a-f) and stained for C3d, S100a10 and GFP (g-l). (M) Graphic representation of C3d and Stat3 co-expressing cells in the a-CC. (n) Graphic representation of the number of C3d+/S100a10+/GFP+ and C3d+/S100a10- astrocytes in the a-CC indicating temporal dynamics and changes induced upon medrysone treatment (red bars: C3d+/Stat3-/GFP+; purple bars C3d+/Stat3+/GFP+; blue bars: C3d+/S100a10+/GFP+ cells; green bars: C3d+/S100a10-/GFP+ cells). White arrows point to cell nuclei. Bars correspond to mean cell numbers per mm^2 ± standard error of the mean (SEM). Statistical significance was calculated using a two-way ANOVA with multiple comparisons Bonferroni post-test (*$p < 0.05$, **$p < 0.01$, and ***$p < 0.001$). Number of animals n=5 (m, n). Exact p-values according to sequence from left to right: m: red bars: (p=0.000410710343508). purple bars: (p=0.000056496386376, p=0.000003680985889, p=0.031174401322527). n: blue bars: (p=0.002451376341613, p=0.00060730463184, p=0.033987226291329, p=0.009878307898806). green bars: (p=0.000005242490508, p=0.000000000000286, p<0.000000000000001, p=0.00147922066168, p=0.000000000243146, p=0.00000000000024, p=0.015520259581564, p=0.000070506774492).

Discussion

Medrysone is an FDA-approved corticosteroid, designated as a topical anti-inflammatory agent for ophthalmic use.[54,55] Details on its activity in a neurological context are scarce and limited to a positively regulated MBP expression in cultured Oli-neu cells.[56] Nevertheless, medrysone was recently identified as an oligodendrogenesis promoting molecule in a pharmacogenomic study aiming at NSCs lineage manipulation.[33]

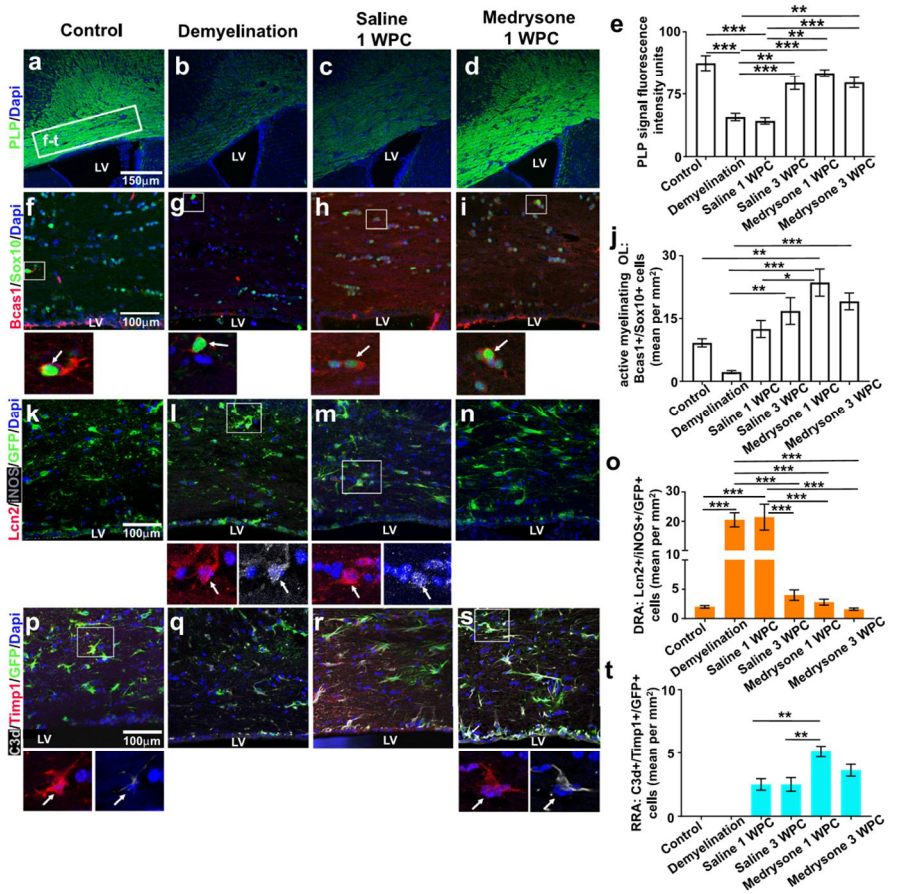

Figure 6. Medrysone treatment accompanies PLP recovery and remyelination-related astrogliosis at the corpus callosum adjacent to the dorsal SVZ. (a-d) Representative pictures showing PLP expression at the a-CC. (e) Quantification of PLP fluorescence intensity units revealed a demyelination induced decrease of PLP expression and a medrysone enhanced recovery of PLP levels. Representative photomicrographs of active myelinating OLs at the a-CC (Sox10+/Bcas1+). Quantification of active myelinating OLs at the a-CC (j) revealed a decrease of these cells during demyelination and medrysone to strongly counteract this effect. (k-n) Representative photomicrographs of DRAs (Lcn2+/iNOS+/GFP+) at the a-CC. (o) Quantification of DRA shows enhancement of this phenotype over demyelination and saline 1 WPC. (p-s) Representative photomicrographs of RRAs (C3d+/Timp1+/GFP+). (t) Quantification of RRA revealed that medrysone increased this phenotype at the early recovery phase. Abbreviations: Lateral ventricle (LV), demyelination related astrocytes (DRA), remyelination related astrocytes (RRA). Bars (e) correspond to PLP mean signal fluorescence intensity ± standard error of the mean (SEM), bars in (g, o, t) correspond to mean cell numbers per mm^2 ± standard error of the mean (SEM). Statistical significance was calculated using a two-way ANOVA with multiple comparisons Bonferroni post-test (*$p <$ 0.05, **$p < 0.01$, and ***$p < 0.001$). Number of animals n=5 (e, j, o), n=4 (t). Exact p-values according to sequence from left to right: e: (p=0.000006352482916, p=0.000002232001001, p=0.002400718707233, p=0.000115165255505, p=0.002114723859805, p=0.000711683124652, p=0.000036763007099, p=0.00062825077472). j: (p=0.003491161340599, p=0.003020739853541, p=0.000026903857775, p=0.000581789413022, p=0.03812643142709). o: (p=0.000012264417485, p=0.000006109495876, p=0.00006100471827, p=0.000023087347467, p=0.000008980415351, p=0.000029360883258, p=0.000011341827324, p=0.000004504968109). t: (p=0.006949092405986, p=0.006949092405986).

We here describe that medrysone application *in vivo* promotes myelin repair activities in a chronic demyelination set-up leading to an accelerated and more efficient restoration of mature cell numbers, nodal structures and myelin content. Of note medrysone also restored body weight of treated animals (data not shown). Although in most cases such a regenerative activity is linked to direct effects on resident OPCs, our investigations using primary OPCs failed in demonstrating any promotion of oligodendroglial maturation at different levels (morphology, gene expression, myelin protein production; see Figure S1) which contradicts earlier findings using the Oli-neu cell line population.[56] Moreover, medrysone did not affect cultured primary OPC cell numbers or proliferation rates (data not shown). Apart from providing evidence that the medrysone-mediated remyelinating effects are most likely not directly attributed to resident oligodendroglia these observations also question the validity of functional screening approaches performed using immortalized cell lines. It rather supports the notion that for a translational output primary cells derived from different species are better suited[56] as recently shown by us.[32,38]

We subsequently monitored astrocytes and SVZ-dependent astrogenic progeny at different sites within and adjacent to the corpus callosum and found a dynamic regulation of different cellular subpopulations to occur and to contribute to myelin repair. Our observations revealed that the numbers of GFP-positive cells (corresponding to either resident Gfap expressing astrocytes or stem cell derivates) did not change over time in CCJ, while at a-CC and d-SVZ sites (see Figure 1c for anatomic guidance), cell numbers were more variable (Figure 3), thus suggesting a prominent contribution from the niche. This is additionally confirmed by medrysone rescuing and enhancing type B cell numbers (Egfr+/GFP+) at the d-SVZ of demyelinated mice (Figure S5). Moreover, we set-out to understand the heterogeneity across reactive astrocyte subpopulations within these tissues and their possible co-relation with de- or remyelination. Prior to the here presented *in vivo* approach, we also investigated medrysone's effects on rat cortex astrocyte polarization and activation. This clearly revealed that astrocytes can sense medrysone, that there is no reaction in terms of cell numbers but that this corticosteroid effectively decreases the number of neurotoxic astrocytes (Gfap+/C3d+) in response to TNF-α (Figure S2e, S2f) accompanied by decrease of A1/neurotoxic transcripts such as C3, and IL-6 (Figure S2h), thus indicating that also *in vivo* astrocytes are key to its mode of action.

Indeed, reactive astrogliosis and myelin damage occur simultaneously during acute demyelination[57–60] and ablation of astrogliosis can be beneficial for remyelination[59] by either diminishing CPZ toxicity or via reduction of NF-kB activation in astrocytes.[61] However, over time reactive astrocytes were also found to be crucial for myelin clearance and hence facilitating oligodendrocyte and myelin replacement[43,62–65]; (Figures 4–6, S3). Of note, Lcn2 ablation in experimental autoimmune encephalomyelitis (EAE) animals was found to reduce demyelination, via diminishing metallopeptidases production.[66] We found that CPZ-diet also induced demyelination at the a-CC (Figure 6), which is recovered by medrysone earlier at 1 WPC. Over CPZ diet, demyelination related astrocytes (DRA; Lcn2+/iNOS+/GFP+) will exclusively populate the demyelinated a-CC (Figures 6g, 6j). Moreover, DRAs were strongly reduced upon medrysone treatment (Figure 6j). During the recovery phase, astrocytes were naturally losing such signatures or presented a hybrid phenotype simultaneously expressing neurotoxic and neuroprotective proteins (C3d, Stat3, S100a10 and Timp1, respectively.[28,29] Medrysone application, on the one hand, reduced numbers of neurotoxic-like astrocytes (C3d+/S100a10-) while it simultaneously enhanced cell numbers with a neuroprotective character described below.

Astrocytic Stat3 signalling appears to be mandatory for reactivity in a myriad of neurodegenerative diseases,[67,68] reducing inflammation and the spread of lesion during demyelination.[29,68–70] C3d/Stat3 co-expressing astrocytes were found to be enhanced by medrysone at the dorsal horn SVZ (Figure S3), CCJ (Figure 4) and a-CC (Figure 5m) during the early recovery phase. S100a10 is a key A2 marker, identifying pro-remyelinating astrocytes in MS lesions.[69] Nonetheless, neither in MS lesion astrocytes[26] nor in regenerated areas of the spinal cord[70] co-localization of C3d and S100a10 was reported, which is in contrast to the described presence of cells with a hybrid profile at CCJ, a-CC and middle d-SVZ in response to medrysone (Figure 5) indicating a strong and natural repair processes-exceeding effect of this corticosteroid. The recently published nuclear factor erythroid 2-related factor 2 (Nrf2) and transcription factor Mafg (Mafg), both being correlated to an anti- and pro-inflammatory signature in astrocytes, respectively,[2,74,76] were also investigated. Two subtypes, Mafg-/Nrf2+ and Mafg+/Nrf2-cells were found at the a-CC of control and saline 1 WPC groups, respectively (Figure S4). In the context of the anatomic domains investigated (see Figure 1c), these astrocyte subtypes were observed at the a-CC, only. Of note, this does not exclude the possibility that such astrocytes might also emerge from other brain areas.

An additional hybrid phenotype characterized by the presence of Timp1 (RRA; C3d+/Timp1+/GFP+) was identified and found to be enhanced in response to medrysone particularly at the a-CC (Figure 6t). Timp1 is naturally expressed by astrocytes,[31,45] was recently shown to induce a myelinating profile in transplanted NSCs[72,71], is expressed by astrocytes in demyelinated white matter MS lesions and revealed to be down-regulated during CPZ-dependent demyelination.[53]

Moreover, remyelination in acute and chronic demyelinated animals was shown to depend on astrocytic Timp1.[51,52] It is therefore conceivable that the here observed Timp1 expressing reactive astrocytes, yet in a minor number and only localized at the a-CC, can contribute to myelin repair as evoked by medrysone (Figures 6s, 6t). Further investigations will be necessary to describe additional trophic entities related to here-presented astrocyte subpopulations that are also involved in the overall repair process. Future investigations upon the microglia-astrocyte axis following medrysone-treatment could illuminate if astrocyte heterogeneity occurs in co- or interdependency of microglia stimulation.[25] This will also include investigations of medrysone acting directly on microglial cells as this has not being carried out so far. However, other corticosteroids have previously been shown to rescue an anti-inflammatory signature in these cells.[73–75] Likewise, a future investigation of medrysone on the EAE-clinical score [i.e., loss of tail tone, paralysis and cerebellar demyelination, which recapitulates MS disease features,[76,77] will be able to strengthen the inclusion of medrysone into upcoming clinical examinations.

Indeed, we here demonstrate that in a chronic demyelination set-up the application of the corticosteroid medrysone induces a robust myelin regeneration response marked by regulated astrocyte polarization and trophic factor expression. This study also suggests that this drug may be of use as a potential treatment for late-stage MS where regenerative processes increasingly fail.[1,32,77] Our study is currently limited to the fact that no interpretation of medrysone's anti-inflammatory effects on white matter repair could be considered. Additionally, it must be kept in mind that not all NSCs and astrocyte subtypes within the adult brain are fully covered by the GFAP-GFP driver. Finally, for a successful biomedical translation of these findings medrysone dependent responses of human brain cells need to be determined.

Contributors

Markley Silva Oliveira Junior performed the majority of all experiments, data analysis, data interpretation, text writing and figure design. Jessica Schira–Heinen has accessed and verified the data, in addition supported experimental design, data analysis, interpretation, text writing and figure design. Laura Reiche and Peter Göttle conducted primary OPC experiments and provided corresponding data analysis. Vanessa Cristina Meira de Amorim and Seulki Han provided support in data interpretation and data presentation. Isabel Lewen and Joel Gruchot executed primary astrocyte experiments and provided corresponding data analysis. Rainer Akkermann has accessed and verified the data and was involved in establishing the transgenic mouse strain and the cuprizone experiments. Kasum Azim was involved in experimental design, funding acquisition, data analysis and interpretation. Patrick Küry (PK) conceived the final project and manuscript and took the final decision for submission. PK was involved in experimental design, funding acquisition, data analysis and interpretation and in text writing and figure composition. All authors read and approved the final version of the manuscript.

Data sharing statement

Any additional information required to reanalyse the data reported in this paper is available from the lead contact upon request.

Declaration of interests

The authors declare no competing interest.

Acknowledgements

We are grateful to Birgit Blomenkamp, Brigida Ziegler and Julia Jadasz for their excellent technical support.

Supplementary materials

Supplementary material associated with this article can be found in the online version at doi:10.1016/j.ebiom.2022.104204.

References

1 McGinley MP, Goldschmidt CH, Rae-Grant AD. Diagnosis and treatment of multiple sclerosis: a review. *JAMA - J Am Med Assoc*. 2021;325(8):765–779.
2 Wheeler MA, Clark IC, Tjon EC, et al. MAFG-driven astrocytes promote CNS inflammation. *Nature*. 2020;176(3):139–148.
3 Lo CH, Skarica M, Mansoor M, Bhandarkar S, Toro S, Pitt D. Astrocyte heterogeneity in multiple sclerosis: current understanding and technical challenges. *Front Cell Neurosci*. 2021;15:1–8.
4 Xing YL, Röth PT, Stratton JAS, et al. Adult neural precursor cells from the subventricular zone contribute significantly to oligodendrocyte regeneration and remyelination. *J Neurosci*. 2014;34(42):14128–14146.
5 Liu Q, Sanai N, Jin WN, La Cava A, Van Kaer L, Shi FD. Neural stem cells sustain natural killer cells that dictate recovery from brain inflammation. *Nat Neurosci*. 2016;19(2):243–252.
6 Hillis JM, Davies J, Mundim MV, Al-Dalahmah O, Szele FG. Cuprizone demyelination induces a unique inflammatory response in the subventricular zone. *J Neuroinflammation*. 2016;13(1):1–15.
7 Kriegstein A, Alvarez-Buylla A. The glial nature of embryonic and adult neural stem cells. *Vol. 32, Ann Rev Neurosci*. 2009;32:149–184.
8 Lim DA, Alvarez-Buylla A. The adult ventricular–subventricular zone (V-SVZ) and olfactory bulb (OB) neurogenesis. *Cold Spring Harb Perspect Biol*. 2016;8(5):1–33.
9 Menn B, Garcia-Verdugo JM, Yaschine C, Gonzalez-Perez O, Rowitch D, Alvarez-Buylla A. Origin of oligodendrocytes in the subventricular zone of the adult brain. *J Neurosci*. 2006;26(30):7907–7918. 1.
10 Azim K, Fiorelli R, Zweifel S, et al. 3-dimensional examination of the adult mouse subventricular zone reveals lineage-specific microdomains. *PLoS One*. 2012;7(11).
11 Azim K, Akkermann R, Cantone M, Vera J, Jadasz JJ, Küry P. Transcriptional profiling of ligand expression in cell specific populations of the adult mouse forebrain that regulates neurogenesis. *Front Neurosci*. 2018;12:1–15.

12 Platel J-C, Gordon V, Heintz T, Bordey A. GFAP-GFP neural progenitors are antigenically homogeneous and anchored in their enclosed mosaic niche. *Glia*. 2008;57(1):66–78.
13 Benner EJ, Luciano D, Jo R, et al. Protective astrogenesis from the SVZ niche after injury is controlled by Notch modulator Thbs4. *Nature*. 2013;497(7449):369–373.
14 Faiz M, Sachewsky N, Gascón S, Bang KWA, Morshead CM, Nagy A. Adult neural stem cells from the subventricular zone give rise to reactive astrocytes in the cortex after stroke. *Cell Stem Cell*. 2015;17(5):624–634.
15 Butt AM, Rivera AD, Fulton D, Azim K. Targeting the subventricular zone to promote myelin repair in the aging brain. *Cells*. 2022;11(11):1809.
16 Brousse B, Magalon K, Durbec P, Cayre M. Region and dynamic specificities of adult neural stem cells and oligodendrocyte precursors in myelin regeneration in the mouse brain. *Biol Open Company Biol*. 2015;4:980–992.
17 Cebrian-Silla A, Nascimento MA, Redmond SA, et al. Single-cell analysis of the ventricular-subventricular zone reveals signatures of dorsal and ventral adult neurogenic lineages. *Elife*. 2021;10:1–34.
18 Moraga A, Pradillo JM, García-Culebras A, et al. Aging increases microglial proliferation, delays cell migration, and decreases cortical neurogenesis after focal cerebral ischemia. *J Neuroinflammation*. 2015;12(1):1.
19 Baxi EG, Debruin J, Jin J, et al. Lineage tracing reveals dynamic changes in oligodendrocyte precursor cells following cuprizone-induced demyelination. *Glia*. 2017;65(12):2087–2098.
20 Taraboletti A, Walker T, Avila R, et al. Cuprizone intoxication induces intrinsic alterations in oligodendrocyte metabolism independent of copper chelation. *Biochemistry*. 2017;56(10):1518–1528.
21 Pandur E, Pap R, Varga E, et al. Relationship of iron metabolism and short-term cuprizone treatment of c57bl/6 mice. *Int J Mol Sci*. 2019;20(9).
22 Butti E, Bacigaluppi M, Chaabane L, et al. Neural stem cells of the subventricular zone contribute to neuroprotection of the corpus callosum after cuprizone-induced demyelination. *J Neurosci*. 2019;39(28):5481–5492.
23 Lohrberg M, Winkler A, Franz J, et al. Lack of astrocytes hinders parenchymal oligodendrocyte precursor cells from reaching a myelinating state in osmolyte-induced demyelination. *Acta Neuropathol Commun*. 2020;8(1):224.
24 Liddelow SA, Barres BA. Reactive astrocytes: production, function, and therapeutic potential. *Immunity*. 2017;46(6):957–967.
25 Liddelow SA, Guttenplan KA, Clarke LE, et al. Neurotoxic reactive astrocytes are induced by activated microglia. *Nature*. 2017;541(7638):481–487.
26 Tassoni A, Farkhondeh V, Itoh Y, Itoh N, Sofroniew MV, Voskuhl RR. The astrocyte transcriptome in EAE optic neuritis shows complement activation and reveals a sex difference in astrocytic C3 expression. *Sci Rep*. 2019;9(1).
27 Harnis, Mairinger F, Fritsche L, Soub D, et al. Myelination in multiple sclerosis lesions is associated with regulation of bone morphogenetic protein 4 and its Antagonist Noggin. *Int J Mol Sci*. 2019;20(1):0–13.
28 Monteiro De Castro G, Deja NA, Ma D, Zhao C, Franklin RJM. Astrocyte activation via stat3 signaling determines the balance of oligodendrocyte versus schwann cell remyelination. *Am J Pathology*. 2015;185(9):2431–2440.
29 Das S, Li Z, Noori A, Hyman BT, Serrano-Pozo A. Meta-analysis of mouse transcriptomic studies supports a context-dependent astrocyte reaction in acute CNS injury versus neurodegeneration. *J Neuroinflammation*. 2020;17(1):1–17.
30 Hasel P, Rose IVL, Sadick JS, Kim RD, Liddelow SA. Neuroinflammatory astrocyte subtypes in the mouse brain. Vol. 24. *Nature Neuroscience*. Springer Science and Business Media LLC; 2021:1475–1487.
31 Escartin C, Galea E, Lakatos A, et al. Reactive astrocyte nomenclature, definitions, and future directions. *Nat Neurosci Nat Res*. 2021;24(3):312–325.
32 Manousi A, Küry P. Small molecule screening as an approach to encounter inefficient myelin repair. *Curr Opin Pharmacol*. 2021;61:127–135.
33 Azim K, Angonin D, Marcy G, et al. Pharmacogenomic identification of small molecules for lineage specific manipulation of subventricular zone germinal activity. *PLoS Biol*. 2017;15(3):1–27.
34 Zhuo L, Sun B, Zhang CL, Fine A, Chiu SY, Messing A. Live astrocytes visualized by green fluorescent protein in transgenic mice. *Dev Biol*. 1997;187(1):36–42.
35 McCarthy KD, de Vellis J. Preparation of separate astroglial and oligodendroglial cell cultures from rat cerebral tissue. *J Cell Biol Rockefeller University Press*. 1980;85:890–902.
36 Kremer D, Heinen A, Jadasz J, et al. P57Kip2 is dynamically regulated in experimental autoimmune encephalomyelitis and interferes with oligodendroglial maturation. *Proc Natl Acad Sci USA*. 2009;106(22):9087–9092.
37 Göttle P, Manousi A, Kremer D, Reiche L, Hartung HP, Küry P. Teriflunomide promotes oligodendroglial differentiation and myelination. *J Neuroinflammation*. 2018;15(1):1–12.
38 Manousi A, Göttle P, Reiche L, et al. Identification of novel myelin repair drugs by modulation of oligodendroglial differentiation competence. *EBioMedicine*. 2021;65:103276.
39 Schindelin J, Arganda-Carreras I, Frise E, et al. Fiji: An open-source platform for biological-image analysis. *Nat Methods*. 2012;9(7):676–682.
40 Faul F, Erdfelder E, Buchner A, Lang AG. Statistical power analyses using G*Power tests for correlation and regression analyses. *Behav Res Methods*. 2009;41(4):1149–1160.
41 Skripuletz T, Hackstette D, Bauer K, et al. Astrocytes regulate myelin clearance through recruitment of microglia during cuprizone-induced demyelination. *Brain*. 2013;136(1):147–167.
42 Schirmer L, Schafer PD, Bartels T, H. Rowitch D, A. Calabresi P. Diversity and function of glial cell types in multiple sclerosis. *Trends Immunol*. 2021;42(3):228–247.
43 Miyamoto N, Maki T, Shindo A, et al. Astrocytes promote oligodendrogenesis after white matter damage via brain-derived neurotrophic factor. *J Neurosci*. 2015;35(41):14002–14008.
44 Matias I, Morgado J, Gomes FCA. Astrocyte heterogeneity: impact to brain aging and disease. *Front Aging Neurosci*. 2019;11:1–18.
45 Clarke LE, Liddelow SA, Chakraborty C, Münch AE, Heiman M, Barres BA. Normal aging induces A1-like astrocyte reactivity. *Proc Natl Acad Sci U S A*. 2018;20(115(8)):E1896–E1905.
46 Allnoch L, Baumgärtner W, Hansmann F. Impact of astrocyte depletion upon inflammation and demyelination in a murine animal model of multiple sclerosis. *Int J Mol Sci*. 2019;20(16):3922.
47 Hou B, Zhang Y, Liang P, et al. Inhibition of the NLRP3-inflammasome prevents cognitive deficits in experimental autoimmune encephalomyelitis mice via the alteration of astrocyte phenotype. *Cell Death Dis*. 2020;11(5):1–16.
48 Lee S, Park JY, Lee WH, et al. Lipocalin-2 is an autocrine mediator of reactive astrocytosis. *J Neurosci Soc Neurosci*. 2009;29:234–249.
49 Al Nimer F, Elliott C, Bergman J, et al. Lipocalin-2 is increased in progressive multiple sclerosis and inhibits remyelination. *Neurol - Neuroimmunol Neuroinflammation*. 2016;3(1):e191.
50 Zhao N, Xu X, Jiang, et al., et al. Lipocalin-2 may produce damaging effect after cerebral ischemia by inducing astrocytes classical activation. *J Neuroinflammation*. 2019;16(1):1–15.
51 Ogier C, Creidy R, Boucraut J, Soloway PD, Khrestchatisky M, Rivera S. Astrocyte reactivity to Fas activation is attenuated in TIMP-1 deficient mice. An in vitro study. *BMC Neurosci*. 2005;6:1–12.
52 Moore CS, Milner R, Nishiyama A, et al. Astrocytic tissue inhibitor of metalloproteinase-1 (TIMP-1) promotes oligodendrocyte differentiation and enhances CNS myelination. *J Neurosci*. 2011;31(16):6247–6254.
53 Houben E, Janssens K, Hermans D, et al. Oncostatin M-induced astrocytic tissue inhibitor of metalloproteinases-1 drives remyelination. *Proc Natl Acad Sci U S A*. 2020;117(9):5028–5038.
54 Spaeth GL. Hydroxymethylprogesterone: an anti-inflammatory steroid without apparent effect on intraocular pressure. *Arch Ophthalmol*. 1966;75(6):783–787.
55 Bedrossian RH, Eriksen SP. The treatment of ocular inflammation with medrysone. *Arch Ophthalmol*. 1969;81(2):184–191.
56 Porcu G, Serone E, De Nardis V, et al. Clobetasol and halcinonide act as smoothened agonists to promote myelin gene expression and RxRγ receptor activation. *PLoS One*. 2015;10(12):1–22.
57 Bribián A, Medina-Rodríguez EM, Josa-Prado F, et al. Functional heterogeneity of mouse and human brain opcs: relevance for preclinical studies in multiple sclerosis. *J Clin Med*. 2020;9(6):1–21.
58 Steelman AJ, Thompson JP, Li J. Demyelination and remyelination in anatomically distinct regions of the corpus callosum following cuprizone intoxication. *Neurosci Res*. 2012;72(1):32–42.
59 Hibbits N, Yoshino J, Le TQ, Armstrong RC. Astrogliosis during acute and chronic cuprizone demyelination and implications for remyelination. *ASN Neuro*. 2012;4(6):393–408.

60 Orthmann-Murphy J, Call CL, Molina-Castro GC, et al. Remyelination alters the pattern of myelin in the cerebral cortex. *Elife*. 2020;9:1–61.
61 Madadi S, Pasbakhsh P, Tahmasebi F, et al. Astrocyte ablation induced by La-aminoadipate (L-AAA) potentiates remyelination in a cuprizone demyelinating mouse model. *Metab Brain Dis*. 2019;34:593–603.
62 Brück W, Pförtner R, Pham T, et al. Reduced astrocytic NF-κB activation by laquinimod protects from cuprizone-induced demyelination. *Acta Neuropathol*. 2012;124(3):411–424.
63 Clemente D, Ortega MC, Melero-Jerez C, de Castro F. The effect of glia-glia interactions on oligodendrocyte precursor cell biology during development and in demyelinating diseases. *Front Cell Neurosci*. 2013;7(DEC):1–15.
64 Wheeler MA, Jaronen M, Covacu R, et al. Environmental control of astrocyte pathogenic activities in CNS Inflammation. *Cell*. 2019;176(3):581–596.e18.
65 Tognatta R, Karl MT, Fyffe-Maricich SL, et al. Astrocytes are required for oligodendrocyte survival and maintenance of myelin compaction and integrity. *Front Cell Neurosci*. 2020;14:74.
66 Nam Y, Kim JH, Seo M, et al. Lipocalin-2 protein deficiency ameliorates experimental autoimmune encephalomyelitis: The pathogenic role of lipocalin-2 in the central nervous system and peripheral lymphoid tissues. *J Biol Chem*. 2014;289(24):16773–16789.
67 Haim I. Ben, Ceyzériat K, Sauvage MAC de, et al. The JAK/STAT3 pathway is a common inducer of astrocyte reactivity in Alzheimer's and Huntington's diseases. *J Neurosci*. 2015;35(6):2817–2829.
68 Herrmann JE, Imura T, Song B, et al. STAT3 is a critical regulator of astrogliosis and scar formation after spinal cord injury. *J Neurosci*. 2008;28(28):7231–7243.
69 Harnisch K, Teuber-Hanselmann S, Macha N, et al. Myelination in multiple sclerosis lesions is associated with regulation of bone morphogenetic protein 4 and its antagonist noggin. *Int J Mol Sci*. 2019;20(1):0–13.
70 Haindl MT, Köck U, Zeitelhofer-Adzemovic M, Fazekas F, Hochmeister S. The formation of a glial scar does not prohibit remyelination in an animal model of multiple sclerosis. *Glia*. 2019;67(3):467–481.
71 Samper-Agrelo I, Schira-Heinen J, Beyer F, et al. Secretome analysis of mesenchymal stem cell factors fostering oligodendroglial differentiation of neural stem cells in vivo. *Int J Mol Sci*. 2020;21(12):1–25.
72 Schira-Heinen J, Samper-Agrelo I, Estrada V, Küry P. Functional in vivo assessment of stem cell-secreted pro- oligodendroglial factors. *Neural Regen Res*. 2022;17(x):1–3.
73 Draheim T, Liessem A, Scheld M, Wilms F, Weissflog M, Denecke B, Clarner T. Activation of the astrocytic Nrf2/ARE system ameliorates the formation of demyelinating lesions in a multiple sclerosis animal model. *Glia*. 2016;64(12):2219–2230.
74 Harrison C. Steroids modulate microglia-mediated inflammation. *Nat Rev Drug Discov*. 2011;10(7):492–493.
75 Carrillo-De Sauvage MÁ, Maatouk L, et al. Potent and multiple regulatory actions of microglial glucocorticoid receptors during CNS inflammation. *Cell Death Differ*. 2013;20(11):1546–1557.
76 Cayre M, Falque M, Mercier O, Magalon K, Durbec P. Myelin repair: from animal models to humans. *Front Cell Neurosci*. 2021;15(04):1–20.
77 Greiner T, Kipp M. What guides peripheral immune cells into the central nervous system? *Cells*. 2021;10(8).

Göttle *et al. Journal of Neuroinflammation* (2023) 20:7
https://doi.org/10.1186/s12974-022-02686-6

Journal of Neuroinflammation

RESEARCH Open Access

Teriflunomide as a therapeutic means for myelin repair

Peter Göttle[1], Janos Groh[3], Laura Reiche[1], Joel Gruchot[1], Nicole Rychlik[1], Luisa Werner[1], Iria Samper Agrelo[1], Rainer Akkermann[1], Annika Zink[2], Alessandro Prigione[2], Hans-Peter Hartung[1,4,5], Rudolf Martini[3] and Patrick Küry[1*]

Abstract

Background Promotion of myelin repair in the context of demyelinating diseases such as multiple sclerosis (MS) still represents a clinical unmet need, given that this disease is not only characterized by autoimmune activities but also by impaired regeneration processes. Hence, this relates to replacement of lost oligodendrocytes and myelin sheaths—the primary targets of autoimmune attacks. Endogenous remyelination is mainly mediated via activation and differentiation of resident oligodendroglial precursor cells (OPCs), whereas its efficiency remains limited and declines with disease progression and aging. Teriflunomide has been approved as a first-line treatment for relapsing remitting MS. Beyond its role in acting via inhibition of de novo pyrimidine synthesis leading to a cytostatic effect on proliferating lymphocyte subsets, this study aims to uncover its potential to foster myelin repair.

Methods Within the cuprizone mediated de-/remyelination model teriflunomide dependent effects on oligodendroglial homeostasis and maturation, related to cellular processes important for myelin repair were analyzed in vivo. Teriflunomide administration was performed either as pulse or continuously and markers specific for oligodendroglial maturation and mitochondrial integrity were examined by means of gene expression and immunohistochemical analyses. In addition, axon myelination was determined using electron microscopy.

Results Both pulse and constant teriflunomide treatment efficiently boosted myelin repair activities in this model, leading to accelerated generation of oligodendrocytes and restoration of myelin sheaths. Moreover, teriflunomide restored mitochondrial integrity within oligodendroglial cells.

Conclusions The link between de novo pyrimidine synthesis inhibition, oligodendroglial rescue, and maintenance of mitochondrial homeostasis appears as a key for successful myelin repair and hence for protection of axons from degeneration.

Keywords Multiple sclerosis, Teriflunomide, Oligodendrocyte, Remyelination, Neuroregeneration

*Correspondence:
Patrick Küry
kuery@uni-duesseldorf.de
[1] Department of Neurology, Medical Faculty, Heinrich-Heine-University, Moorenstrasse 5, 40225 Düsseldorf, Germany
[2] Department of General Pediatrics, Neonatology and Pediatric Cardiology, Medical Faculty, Heinrich-Heine-University, Düsseldorf, Germany
[3] Department of Neurology, Section of Developmental Neurobiology, University Hospital, Würzburg, Germany
[4] Brain and Mind Center, University of Sydney, Sydney, Australia
[5] Department of Neurology, Palacky University Olomouc, Olomouc, Czech Republic

Background

The adult central nervous system (CNS) exhibits only limited regeneration capacities and impaired repair processes in patients with multiple sclerosis (MS) contribute to neurological disability and diminished quality of life on a long-term scale. While relapsing MS (RMS) is amenable to treatment by means of a number of well-established immunomodulatory drugs, the disease per se remains incurable and develops into progressive stages (PMS) with irreversible functional deficits. In this respect, the primary hallmark is the autoimmune mediated breakdown of myelin sheaths and the subsequent loss of mature oligodendrocytes associated with impaired axonal integrity and neurodegeneration [1]. Beyond immunomodulation the current focus lies on regenerative aspects and their potential for clinical translation. Partial replacement of lost oligodendrocytes and myelin sheaths following demyelination of the adult CNS can occur spontaneously as a result of activation of resident oligodendroglial precursor cells (OPCs) [2, 3]. Nevertheless, successful cell replacement and remyelination of denuded axons remain inefficient and should be supported via therapeutic intervention. In such a scenario an active promotion of axonal remyelination will lead to stabilization, electrical insulation, improved trophic and metabolic support thereby eventually preventing neurodegeneration and restoring axonal function [4, 5]. Hence, identification of substances exerting positive effects on oligodendroglial cell differentiation and boosting the endogenous remyelination capacity are of increasing biomedical interest as it represents an unmet clinical need [6, 7]. In addition to numerous drug screening approaches that have been conducted for this purpose (recently summarized in [8]) drug repurposing represents a promising alternative approach as it is thought to accelerate substance identification in a cost efficient manner [9]. Teriflunomide is an approved first line oral immunomodulatory medication for patients with RMS [10–12] acting via inhibition of pyrimidine biosynthesis in activated lymphocytes by selective and reversible blockade of the mitochondrial enzyme dihydroorotate dehydrogenase (DHODH) [13, 14]. DHODH is an inner mitochondrial membrane protein that catalyzes the oxidation of dihydroorotate to orotate, which is further converted into uridine monophosphate from which all other pyrimidine ribonucleotides arise [15]. Beyond its role as an immune modulator we previously described teriflunomide's potential role in neuroregeneration as it promoted primary OPC differentiation and internode formation, particularly when applied early and in pulses within myelinating neuron/glia co-cultures [16]. Subsequent studies further revealed an association with zymosterol accumulation and teriflunomide to exert promyelinating effects in demyelinated *Xenopus laevis* and mouse spinal cord [17]. We here provide additional evidence for the potential of teriflunomide as a regenerative compound as it was applied in a cuprizone mediated demyelination model suitable to study cellular and subcellular processes leading to axonal remyelination in vivo [18]. We revealed that oral teriflunomide application substantially promotes oligodendroglial differentiation, fosters myelin sheath restoration and restores mitochondrial integrities within the affected corpus callosum (CC).

Materials and methods

Ethics statements for animal experiments

Cuprizone mediated demyelination experiments were approved by the authorities at LANUV (Landesamt für Natur, Umwelt und Verbraucherschutz Nordrhein-Westfalen; Az.: 81-02.04.2019.A203) and were carried out according to ARRIVE guidelines. These experimental procedures are characterized by mild severity grade, and therefore, no interventions to reduce pain, suffering and distress were needed.

Cuprizone diet and drug-treatment

Eight-week-old female C57BL/6 mice (Janvier Labs, Paris, France) were used and all experiments were performed in the animal facility of the Heinrich-Heine-University (Zentrale Einrichtung für Tierforschung und wissenschaftliche Tierschutzaufgaben; ZETT) under pathogen-free conditions and in accordance with ethical care. Only mice of the same age and with body weight between 17 and 19 g (gr) were included and as additional exclusion criterion > 10% weight loss during the experiments was used. Upon delivery, animals were distributed equally into cages (groups) and were given 1 week as acclimatization period before the initiation of the experiments. Using the software G*Power a required size of maximal $n = 6$ animals per group was predicated (see further below for details). This analysis was also necessary to have animal experiments legally granted by the authorities (The Review Board for the Care of Animal Subjects of the district Government) (LANUV, North-Rhine Westphalia, Germany). For the here presented in vivo investigations we finally used at least $n = 4$ animals per experimental group.

Demyelination was induced by feeding 0.2% (w/w) cuprizone [bis(cyclohexanone)oxaldihydrazone]-containing diet from Envigo (Indianapolis, IN, US Cat# TD.140803) and SSNIFF Spezialdiäten GmbH (Soest, Germany; maintenance diet pellets 10 mm, V1534

implemented with 0.2% cuprizone, Sigma-Aldrich, CAS 370-81-0) for 6 weeks. Thereafter animals were given standard rodent chow (SSNIFF, Cat# V1534).

Teriflunomide (A-771726, Biorbyt, St Louis, US) was dissolved in autoclaved drinking water containing 0.6% Tween 80 at 60 µg per milligram and provided ad libitum. With an approximate consumption of 5 ml per day and 30 gr body weight, this corresponds to a dose of 10 mg/kg body weight per day. This concentration is based on previous animal experiments in other laboratories [19, 20] and comparable to doses used for human patients, when a dose conversion scaling is applied [21]. Non-treated controls received autoclaved drinking water with 0.6% Tween 80 only previously shown to exert no effect on neuroinflammation and neural damage [20]. No daily handling occurred; however, animals (control as well as teriflunomide treated groups) were handled twice a week for weight control. This occurred in parallel (for both groups) and also drinking water was changed twice a week (for both groups). Teriflunomide administration was performed as an early pulse during the fourth week of cuprizone challenge for 7 consecutive days (Fig. 1; pulse) or continuously for the final 18 days of cuprizone treatment (Fig. 1; constant). Following the 6-week demyelination period and teriflunomide treatment (see application scheme in Fig. 1) mice were fed standard rodent chow (SSNIFF, Cat# V1534) for another 7 days to allow newly formed oligodendrocytes (OLs) to remyelinate. Mice were then deeply anesthetized using isoflurane inhalation and transcardially perfused with 20 ml ice-cold PBS followed by 20 ml 4% paraformaldehyde (PFA) in PBS. Brains were then harvested and post-fixation was performed overnight in 4% PFA at 4 °C. Following post-fixation, cryo-protection of mouse brains was performed

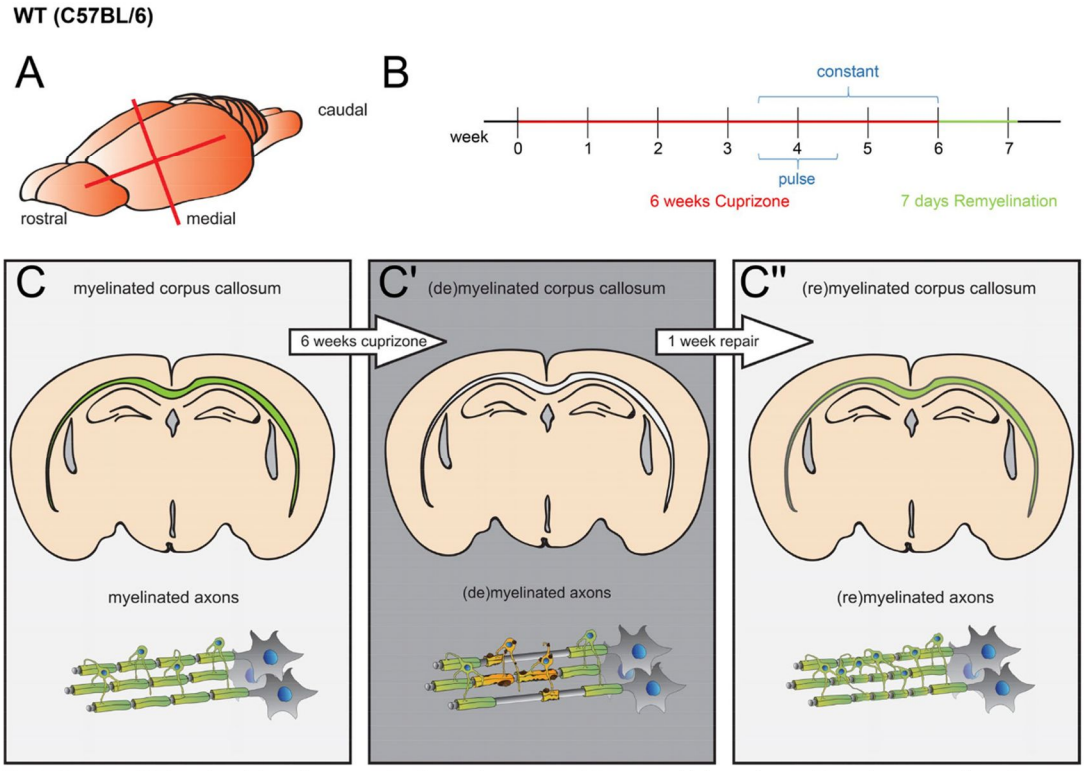

Fig. 1 Cuprizone (CPZ) mediated demyelination and teriflunomide treatment. **A** Rostro-caudal directed coronal brain slices were collected between − 1.94 and − 2.34 mm Bregma. **B** Timeline of (**C**–**C′′**) CPZ induced demyelination and of teriflunomide treatment in adult (8 weeks) mice. CPZ treatment lasted for 6 weeks. Teriflunomide was applied orally by means of two different application schemes: (1) early pulse during the fourth week of cuprizone challenge for 7 consecutive days (pulse) or (2) continuously for the final 20 days of cuprizone treatment (constant). Mice were sacrificed after 7 days of remyelination

in 30% sucrose (in PBS) at 4 °C for 24–48 h. Brains were embedded in Tissue-Tek OCT medium (Sakura Finetek Europe, Netherlands), frozen, and stored at − 80 °C until sectioning with a cryostat (Leica CM3050S, Wetzlar, Germany). Coronal 10 µm sections were prepared and stored at − 80 °C. As region of interest the caudal part of the corpus callosum (Bregma − 1.94 to − 2.34 mm) was assessed according to mouse brain atlas (Franklin and Paxinos, 2008).

Immunohistochemical staining

For immunohistochemical staining, sections were thawed and air-dried for at least 10 min at room temperature (RT). Rehydration was performed for 5 min in distilled water, followed by post fixation with 4% PFA for 10 min. Thereafter sections were transferred to 50% acetone for 2 min at RT, followed by 100% acetone for 2 min at RT, 50% acetone for 2 min and then washed 3 × with Tris-Buffered Saline supplemented with 0.02% Triton X-100; pH 7.6 (TBS-T) for 2 min each. Non-specific staining was blocked with 10% normal goat serum (NGS) (Biozol vector Cat# S-1000, Eching, Germany), 10% normal horse serum (NHS) (Biozol vector Cat# S-2000, Eching, Germany) or 10% normal donkey serum (NDS) (Sigma-Aldrich Cat# D9663, Taufkirchen, Germany) supplemented with 3% biotin-free bovine serum albumin [BSA (Carl Roth # 0163, Karlsruhe, Germany) in TBS w/o TX-100 for 30–60 min at RT, followed by primary antibody solution application and incubation overnight at 4 °C. The following primary antibodies were used: mouse anti-APC (CC1, 1:300, Sigma-Aldrich, Cat# OP80, RRID:AB_ 2057371); rabbit anti-sex determining region Y-Box 10 (Sox10; 1:100, DCS Immunoline, Hamburg, Germany Cat# S1058C002, RRID: AB_2313583) and goat anti-Sox10 (1:200, R&D System, Minneapolis, US Cat# AF2864; RRID: AB_442208); rat anti-proteolipid protein (PLP, 1:250, kind gift from B. Trapp and R. Dutta, Dept. of Neurosciences, Cleveland Clinic, OH, [22]), mouse anti-mammalian Achaete scute homolog-1 (Mash1, 1:200; [23, 24]) and rabbit anti-mitochondrial outer membrane marker (Tom20; Santa Cruz, Heidelberg, Germany Cat# sc-11415 (FL-145), RRID: AB_2207533). Slices were then washed twice in 1 × TBS for 5 min each and secondary antibodies were diluted 1:200 and applied for 30 min along with 4′,6-diamidino-2-phenylindol (DAPI, 1:50) in PBS. The following secondary antibodies were used: goat anti-rabbit Alexa Fluor 594 (1:200, Thermo Fisher Scientific Cat# A-11037, RRID:AB_2534095); goat anti-rat Alexa Fluor 488 (1:200, Thermo Fisher Scientific Cat# A-11006, RRID:AB_2534074); goat anti-rabbit Alexa Fluor 488 (1:200, Thermo Fisher Scientific Cat# A-11008, RRID:AB_143165); goat anti-mouse Alexa Fluor 488 (1:200, Thermo Fisher Scientific Cat# A32728, RRID:AB_2633277); donkey anti-goat Alexa Fluor 488 (1:200, Thermo Fisher Scientific Cat# A-11055, RRID:AB_2534102); horse anti-mouse IgG antibody, rat adsorbed (H + L) (1:200 Vector Scientific Cat# BA-2001, RRID:AB_2336180); goat anti-rabbit IgG antibody (H + L) (1:200 Vector Scientific Cat# BA-1000, RRID:AB_2313606); streptavidin, DyLight™ 594 (1:200 Vector Scientific Cat# SA-5594, RRID:AB_2336418); streptavidin, DyLight™ 488 (1:200 Vector Scientific Cat# SA-5488, RRID:AB_2336405). Two final washing steps were performed with 1 × TBS-T and 1 × TBS for 5 min prior to mounting with Shandon™ Immu-Mount (Thermo Fisher Scientific). For image acquisition and analysis, a Zeiss LSM 510 Confocal Microscope (Zeiss, RRID:SCR_018062) and the ZEN Digital Imaging software for Light Microscopy (Zeiss, RRID:SCR_013672) as well as ImageJ software (BioVoxxel, RRID:SCR_015825) were used, respectively.

Corpus callosum dissection and RNA extraction

Mice were deeply anesthetized using isoflurane inhalation and transcardially perfused with 20 ml PBS before decapitation and dissection of the brain. Serial 1 mm-thick coronal slices of the brain containing the CC were obtained by means of Brain Matrice Stainless Steel device coronal, 1 mm; Ted Pella, Cat# 15065). To minimize inclusion of tissue surrounding of the CC, the corpus callosum were isolated with direct visualization using a binocular dissecting microscope (Tritech Research Cat# S 217045664). Caudal samples of the CC were snap-frozen using liquid nitrogen and stored in RNAse free tubes (Fig. 2A).

RNA extraction from the corpus callosum samples was performed using TRIzol™ (Thermo Fisher Scientific, Cat# 15065) reagent according to [25]. Frozen tissue sections were thawed on ice before 700 µL of TRIzol™ reagent were added. Polytron PT2100 cell shredder was used

(See figure on next page.)

Fig. 2 Gene expression responses upon teriflunomide stimulation. **A** Schematic presentation of corpus callosum tissue isolation for gene expression analysis (as shown here for the rostral CC, which was not analyzed in this study). **B**–**G** Quantitative RT–PCR of the dissected caudal corpus callosum 7d after cuprizone withdrawal (remyelination) indicated that pulsed teriflunomide application led to a significant upregulation of *PLP*, *Myrf*, *Mash1* and *CNPase* transcript levels, whereas *MBP* and *BCAS1* transcript levels were only mildly or not affected. *GAPDH* was used as reference gene. Number of animals per analysis n = 6. Data are shown as mean values (horizontal lines), while error bars represent standard error of the mean (SEM; vertical lines). Plots also show all individual data points. Statistical significance was calculated using one-way ANOVA with Tukey post-test (**B**–**G**). Data were considered statistically significant (95% confidence interval) at $*p < 0.05$, $**p < 0.01$, $***p < 0.001$

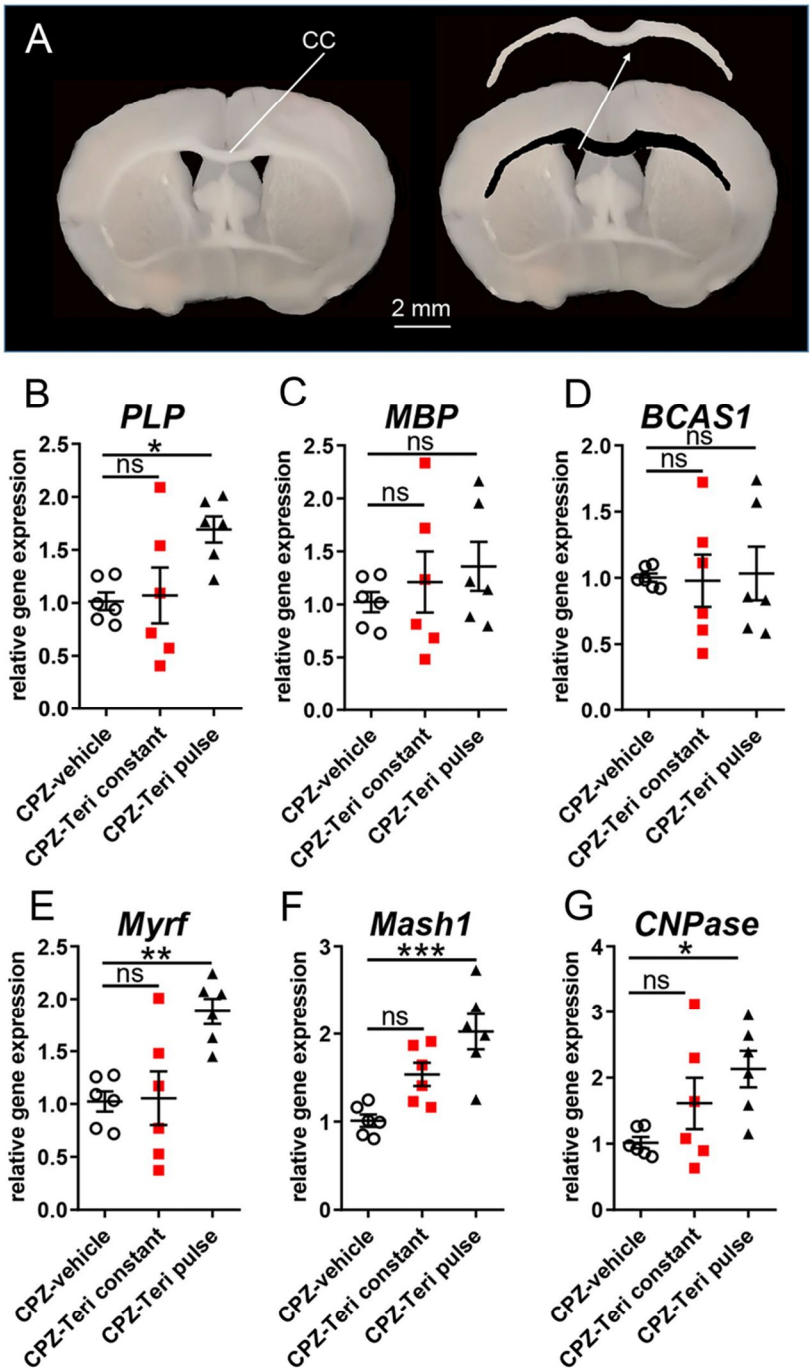

Fig. 2 (See legend on previous page.)

to break down cells. After an incubation of 5 min at RT 200 µL chloroform were added and the collection tube was shaken for 10–15 s (sec). Afterward, another incubation step of 5 min at RT followed, before samples were centrifuged for 15 min (4 °C, 12.000*g*). The RNA phase was carefully transferred to a new collection tube and 1 µL of glycogen was added for pellet visualization. In addition, 500 µL of isopropanol were added and the tubes were vortexed for about 5 s. Samples were then incubated for 15 min at RT and centrifuged for 10 min (4 °C, 12.000*g*). Isopropanol was carefully removed from the pellet. After washing with 1 mL 75% ethanol, tubes were vortexed and centrifuged for 5 min (4 °C, 12.000*g*). The supernatant was removed and samples were air-dried for 10–15 min until the rest of ethanol evaporated. Finally, RNA was eluted in 21.5 µL RNAse free water by incubating it on a heating shaker for 10 min (60 °C, 450 rpm). RNA concentration was determined using the NanoDrop ND-1000 spectral photometer (Thermo Fisher Scientific, RRID:SCR_016517) applying RNAse-free water as a blank. RNA was then stored at − 20 °C until cDNA synthesis was performed.

cDNA synthesis, and determination of gene expression levels by means of quantitative real-time RT-PCR were all performed as previously described [16]. Primer sequences were determined using PrimerExpress 2.0 software (Life Technologies) and tested for the generation of specific amplicons (sequences are available upon request). glyceraldehyde-3-phosphate dehydrogenase (GAPDH) and ornithine decarboxylase (ODC) were used as reference genes, and relative gene expression levels were determined according to the ΔΔCt method (Life Technologies). Each sample was measured in quadruplicate. Primer sequences: PLP_fwd: GGGCTCCCGGCCATATAA, PLP_rev: TCATCACCAGACAAGCAAAGAAA, MBP_fwd: ACAGAGACACGGGCATCCTT, MBP_rev: CACCCCTGTCACCGCTAAAG, BCAS1_fwd: CGCTGGGAAAGTTGTTTTGG, BCAS1_rev: TCTCCTCTGCACCTGTGGAAA, Myrf_fwd: GGACCCCAACTACCAATCCA, Myrf_rev: TGTCTTGACGTACTTGGGCT, Mash1_fwd: TCGTCCTCTCCGGAACTGAT, Mash1_rev: TAGCCGAAGCCGCTGAAGT, CNPase_fwd: CTGCCGCCGGGACAT, CNPase_rev: TCCCGCTCGTGGTTGGTAT, mfn1.1_fwd: GCAACCGAGAAGCTGCAGAT, mfn1.1_rev: CTGTACTTGGTGGCTGCAGTT T, mfn1.2_fwd: CAGTCCGGGCCAAGCA, mfn1.2_rev: GTGCAGGGAATCCATGATGAG, drp1_fwd: GCGCTGATCCCGGTCAT, drp1_rev: CCGCACCCACTGTGTTGA, pparg_fwd: CCCACCAACTTGGGAATCAG, pparg_rev: GGAATGGGAGTGGTCATCCA, ppargc1a_fwd: TGAAGAGCGCCGTGTGATT, ppargc1a_rev: TTCTGTCCGGGTTGTGTCA, ppargc1b_fwd: GGAAAAGGCCATCGGTGAA, ppargc1b _rev: GCTCATGTCACCGGAGAGATTT, pdpk1_fwd: AATGGTGAGGTCCCAGACTGA, pdpk1_rev: CCTGCTAACACCACTAGGAATGC, ldha_fwd: CTGTGTGGAGTGGTGTGAATGTC, ldha_rev: CAGCTGGGGGTTCAGAGACT.

Electron microscopy

For electron microscopy, mice were transcardially perfused with 4% PFA and 2% glutaraldehyde in cacodylate buffer, then brains were dissected and post-fixed with 4% PFA and 2% glutaraldehyde overnight according to [26]. Appropriate regions of the corpus callosum were dissected, tissue sections were osmicated and processed for light and electron microscopy by dehydration and embedding in Spurr's medium. Ultrathin section (70 nm) were mounted to copper grids, counterstained with lead citrate, and investigated using a ProScan Slow Scan CCD camera mounted to a Leo 906 E electron microscope (Zeiss) and corresponding software iTEM (Soft Imaging System). Using morphological criteria, identified myelinated axons were counted and related to the total number of quantified axons.

Analysis of mitochondrial dynamics

Changes in mitochondrial morphology were assessed from auto segmented images with an ImageJ macro "mitochondria analyzer" reporting several measures including mitochondrial count, length and mean form factor (FF; inverse "circularity" output value and defines a mitochondrial shape measure given by: perimeter^2/(4πarea)) according to [27, 28]. The value 1 indicates round objects and this value increases with mitochondrial elongation, hence, allowing to distinguish two different morphologies from low (form factor 1) to high complex (form factor > 1) mitochondrial networks.

Statistical analysis

Data are presented as mean ± standard error of the mean (SEM). Statistical analyses and graph design were performed using the GraphPad Prism 8.0.2 software (GraphPad Prism, San Diego, CA, RRID:SCR_002798). Shapiro–Wilk normality test was used to assess the absence of Gaussian distribution of all data sets. To determine statistical significance for normally distributed data sets one-way analysis of variance (ANOVA) with Turkey post-test for multiple comparisons was applied to compare three or more groups. For data sets not passing the Shapiro–Wilk normality test, Kruskal–Wallis test with Dunn's post-test for multiple comparisons of three or more groups was applied. Statistical significance thresholds were set as follows: $^{*}p \leq 0.05$; $^{**}p \leq 0.01$; $^{***}p \leq 0.001$ and ns = not significant. "*n*" represents the number of

independent experiments. A priori sample size calculation for the in vivo experiments was performed using the G*Power 3.1.9.2 software [29] (test family: *t* tests; statistical test: means: Wilcoxon–Mann–Whitney test (two groups); tails: two; effect size d: 2.6; alpha error 0.05, power 0.95; allocation ratio N2/N1: 1; resulting maximal sample size: 6).

Results

Since it was recently demonstrated that teriflunomide exerts direct effects on oligodendroglial cells in vitro and in vivo [16, 17] we further examined its potential for remyelination and restoration of subcellular structures.

Teriflunomide enhances oligodendroglial dynamics and remyelination in vivo

To assess the extent of fostered remyelination by teriflunomide the cuprizone mediated mouse model of de- and remyelination was used [18]. Demyelination of the corpus callosum was initiated by feeding mice with 0.2% cuprizone diet for a total of 6 weeks. Based on our previous in vitro work demonstrating that teriflunomide signaling only induces its pro-oligodendroglial effects on OPCs when administered as short and early pulse [16] we applied two different schemes of teriflunomide administration in vivo (Fig. 1). During cuprizone challenge proliferation of parenchymal OPCs begins around week 3 with OPC densities peaking around weeks 4 and 5 [18, 30]. In an attempt to target these newly forming OPCs we administered the drug orally within drinking water as an early pulse (during the fourth week of cuprizone challenge for 4 consecutive days; "pulse"; Fig. 1) and also for a longer period during the final 12 days of cuprizone treatment ("constant", Fig. 1).

Analysis and quantification of the proteolipid–protein (PLP)-positive area in the caudal region of the corpus callosum revealed that both teriflunomide stimuli (constant and pulse) enhanced spontaneous remyelination as compared with vehicle-treated counterparts (Fig. 3A, A″, F). Furthermore, oligodendroglial cell dynamics reflected by the percentage of (Sox10-positive) oligodendroglial cells expressing the mature oligodendroglial marker adenomatous polyposis coli protein (APC) clone CC1 (CC1) supported this finding (Fig. 3B, C″, G). Total numbers of oligodendroglial lineage cells (as quantified using Sox10 expression) did not change significantly between the groups (Fig. 3H). Oligodendroglial cells expressing the essential transcriptional regulator Mash1 [23], previously described to be involved in teriflunomide's pro-myelinating activity [16], were present in significantly increased numbers in treated animals as compared to vehicle control (Fig. 3D, E″, I).

Evaluated gene expression responses upon teriflunomide stimulation

In line with the previous analysis, transcript levels of oligodendroglial differentiation-associated markers were determined by means of quantitative real-time PCR (qRT-PCR) of dissected CC tissues of the caudal region 1 week after remyelination (Fig. 2). Of note, only an early teriflunomide pulse (Fig. 1, early pulse) exerted an effect on myelin genes in that *2′,3′-cyclic-nucleotide 3′-phosphodiesterase (CNPase)* and *PLP* transcript levels were significantly upregulated (Fig. 2B, G). *MBP* transcript levels were elevated too, but reached no statistical significance and no regulation was observed for *breast carcinoma-amplified sequence 1 (BCAS1)* transcript levels (Fig. 2C, D). This response was further accompanied by an upregulation in the expression of key oligodendroglial transcription regulators (Fig. 2E, F) required for proper differentiation and myelin induction, such as *Mash1* [23] and *myelin regulatory factor (Myrf)* [31].

Teriflunomide enhances axonal remyelination in vivo

To investigate whether the observed transcript and protein responses correlated with improved remyelination, the numbers of myelinated axons were quantified in electron micrographs from the caudal CC (Fig. 4A–E). One-week post-cuprizone application the corresponding quantification revealed a significant increase in the number of myelinated axons following both pulse and constant teriflunomide application as compared to control animals (Fig. 4E).

(See figure on next page.)

Fig. 3 Teriflunomide administration positively affects remyelination-related oligodendroglial dynamics. **A**–**E″** Representative images of oligodendroglial differentiation-associated protein markers in the caudal corpus callosum after 1 week of remyelination. **A**, **A″**, **F**) Degree of remyelination was determined as the percentage of PLP-positive area in the defined region of interest between CPZ-vehicle treated, CPZ with teriflunomide constant treatment (CPZ-Teri constant) and CPZ with teriflunomide pulse treatment (CPZ-Teri pulse) groups. The impact on oligodendroglial cell differentiation and maturation was assessed by the number/mm^2 of Sox10-positive cells and the relative percentage of double positive cells (Sox10 + /CC1 + ; **B**, **C″**,**G**, **H**), (Sox10 + /Mash1 + ; **D**, **E″**, **I**) along the same area of the corpus callosum. Number of animals per analysis n = 6. Data are shown as mean values (horizontal lines), while error bars represent standard error of the mean (SEM; vertical lines). Plots also show all individual data points. Statistical significance was calculated using Kruskal–Wallis test with Dunn's post-test (**F**, **G**, **H**) and Tukey's range test following one-way ANOVA (**I**). Data were considered statistically significant (95% confidence interval) at $*p < 0.05$, $**p < 0.01$, $***p < 0.001$. Scale bars: 50 µm, 20 µm

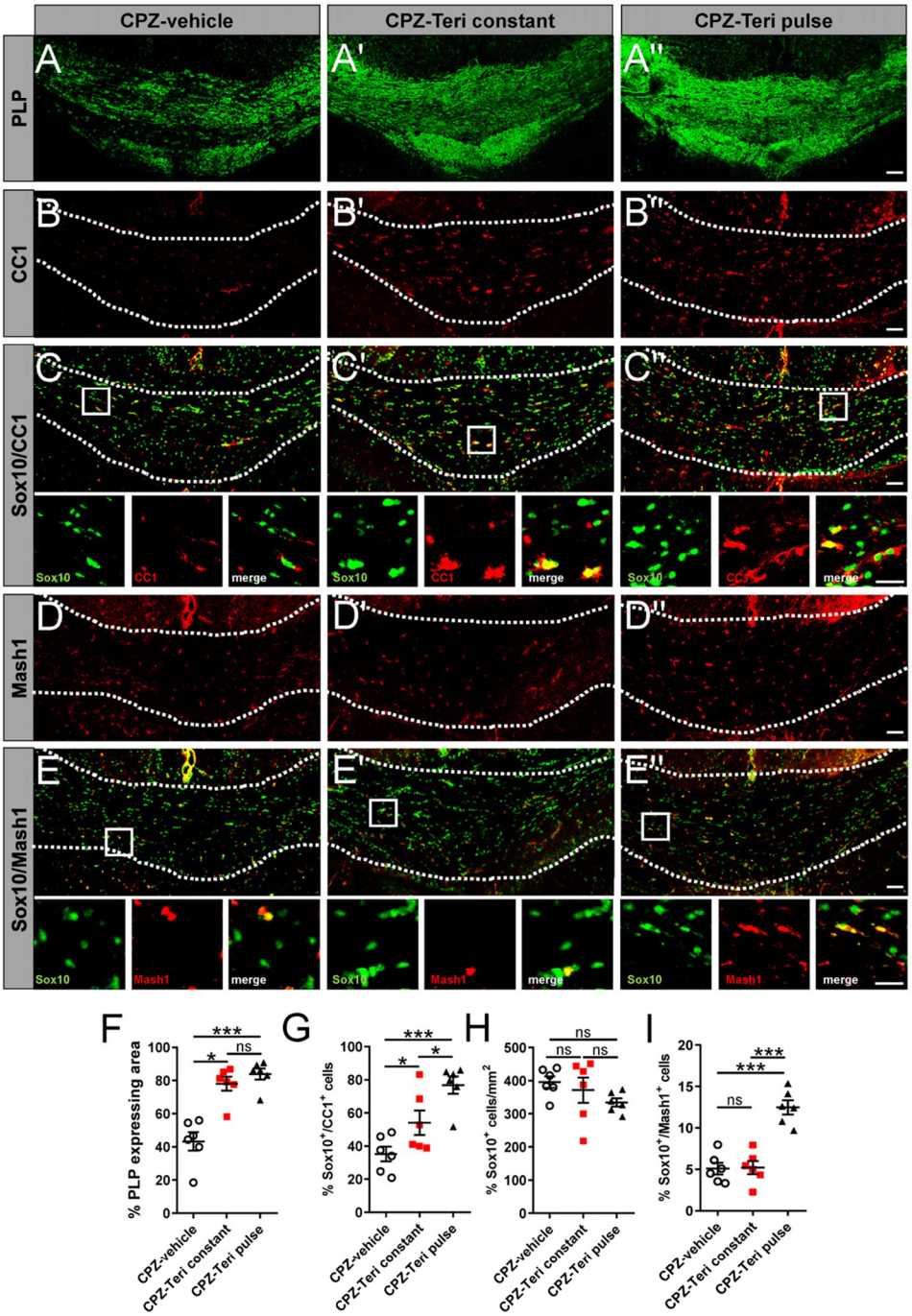

Fig. 3 (See legend on previous page.)

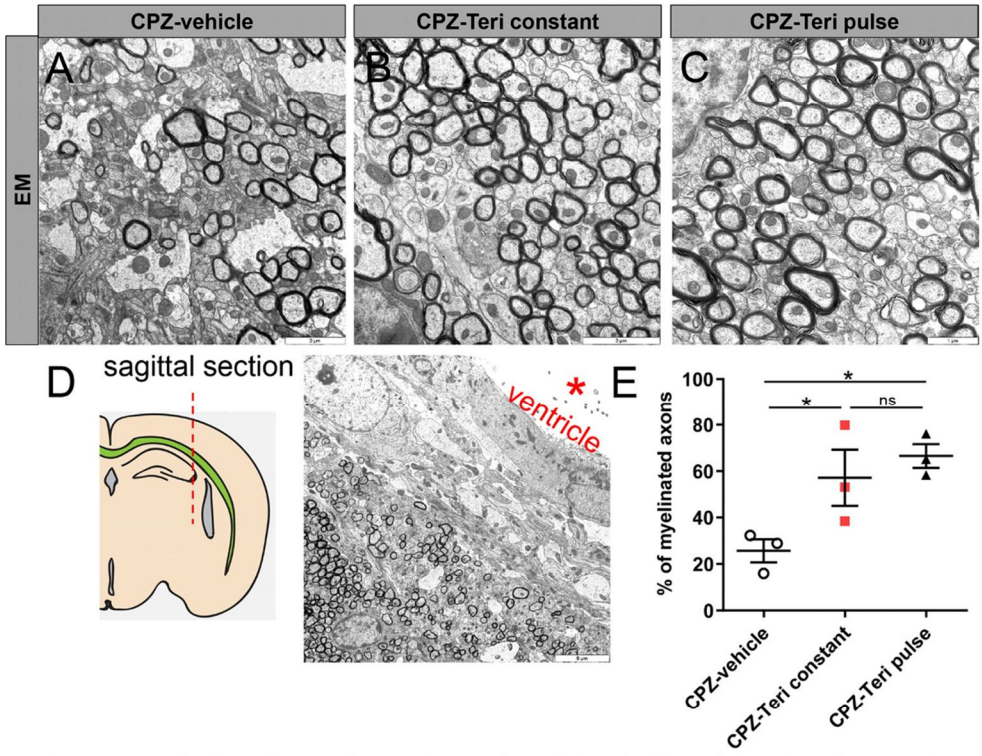

Fig. 4 **A**–**C** Electron micrographs of sagittal corpus callosum (CC) sections from vehicle- and teriflunomide-treated mice showing myelinated axons ($n = 3$ per group). **A**, **B** Scale bars: 2 µM and **C** scale bar (1 µM). **D** Region of interest: sagittal section of the CC hitting the axons in cross section. Scale bar 5 µM. **E** Quantification of myelinated axons in corpus callosum revealed a significant increase upon both stimulation schemes (pulse and constant teriflunomide application). Data are shown as mean values (horizontal lines), while error bars represent standard error of the mean (SEM; vertical lines). Plots also show all individual data points. Significance was assessed using Tukey's range test following one-way ANOVA (**E**). Data were considered statistically significant (95% confidence interval) at $^*p < 0.05$, $^{**}p < 0.01$, $^{***}p < 0.001$

Teriflunomide restores mitochondrial integrity in remyelinating oligodendroglial cells

All stages of oligodendroglial cell differentiation and especially the myelination process are characterized by an extensive mitochondrial demand related to biosynthesis and maintenance of myelin membranes [32]. We, therefore, examined whether mitochondrial homeostasis is affected in our model and in response to teriflunomide. We first investigated transcriptional changes in genes related to mitochondrial homeostasis

(See figure on next page.)

Fig. 5 Mitochondrial gene expression responses upon teriflunomide application. **A**–**H** Quantitative RT-PCR of the dissected corpus callosum 7 days after cuprizone withdrawal (remyelination) indicated that both teriflunomide pulse and constant stimulation schemes led to a significant upregulation of genes catalyzing mitochondrial fusion such as *mfn1.1*, *mfn1.2*, *ppargc1a*, *ppargc1b* and to downregulation of genes responsible for glycolytic pathway, e.g., *pdpk1* and *ldha* transcript levels, whereas *drp1* (mitochondrial fission) and *pparg* were not affected. *GAPDH* was used as reference gene. **I** Illustration depicts mitochondrial dynamics involved in oligodendroglial differentiation, cell maturation and myelin sheath generation according to [49]. Fragmented and condense mitochondrial morphology is linked to ROS production, mitochondrial DNA damage and lower ATP synthesis. An elongated mitochondrial network hints to active mitochondrial biogenesis, ATP synthesis and lipid metabolism necessary for cell differentiation and generation of myelin. Teriflunomide induced the upregulation of mitofusins, and also mitochondrial elongation by depletion of the cellular pyrimidine pool secondary to DHODH inhibition. Number of animals per analysis $n = 6$. Data are shown as mean values (horizontal lines), while error bars represent standard error of the mean (SEM; vertical lines). Plots also show all individual data points. Statistical significance was calculated using Kruskal–Wallis test with Dunn's post-test (**A**–**C**) and Tukey's range test following one-way ANOVA (**D**–**H**). Data were considered statistically significant (95% confidence interval) at $^*p < 0.05$, $^{**}p < 0.01$, $^{***}p < 0.001$

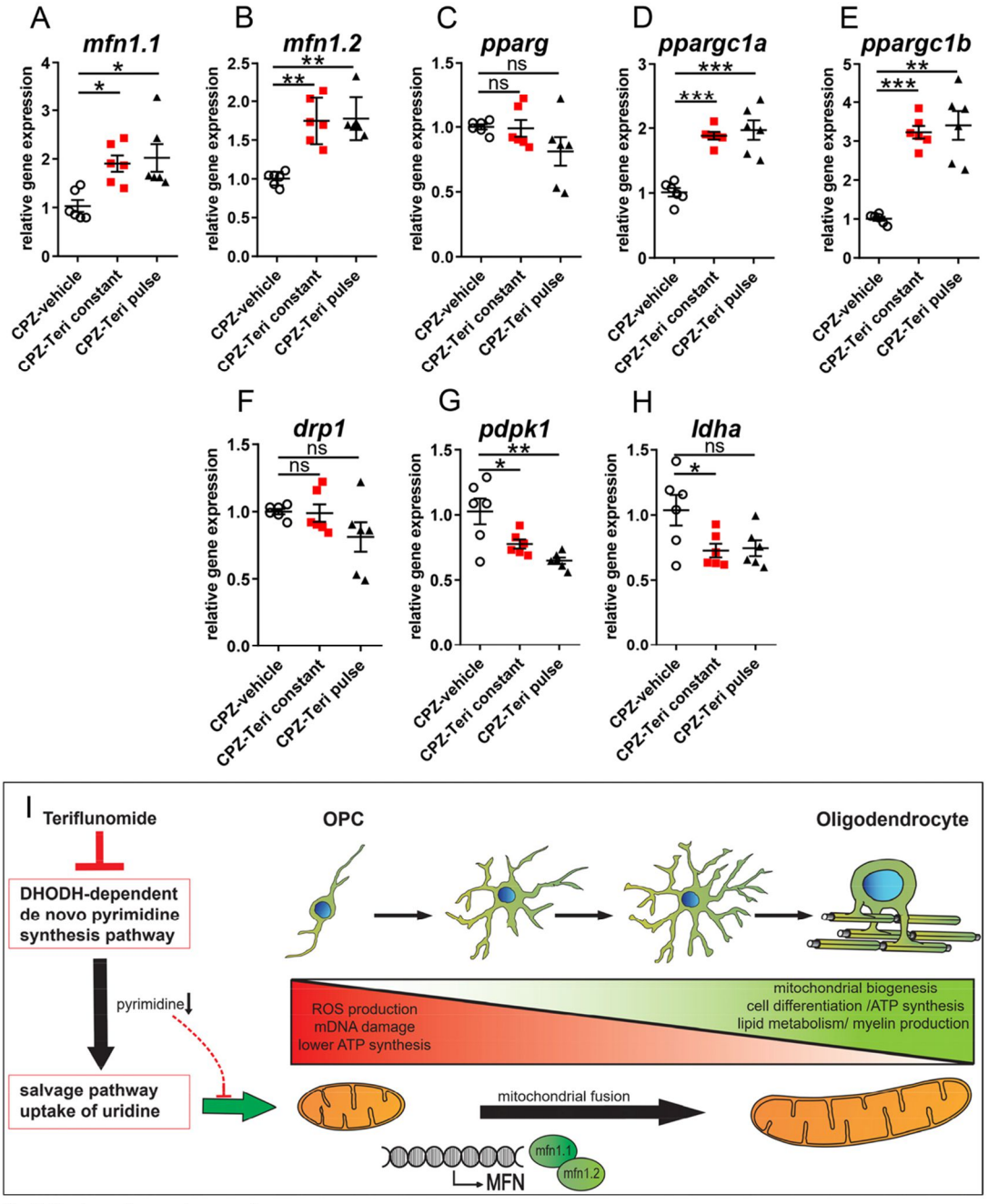

Fig. 5 (See legend on previous page.)

(Fig. 5A–H). It was observed that both pulse and constant teriflunomide stimulation schemes led to significant upregulation of *peroxisome proliferator activated receptor gamma coactivator 1 alpha (ppargc1a)* and *peroxisome proliferator activated receptor gamma coactivator 1 beta (ppargc1b)* transcript levels which encode major regulators of mitochondrial biogenesis [33, 34]. Both teriflunomide treatment schemes also increased the expression of genes *mitofusin 1 and 2 (mfn1.1 and 1.2)* which are responsible for inducing mitochondrial fusion (elongation) and for preservation of mitochondrial DNA essential for mitochondrial function [35]. Accordingly, transcript levels of *dynamin-related protein 1 (drp1)* which is needed to induce the opposite process of mitochondrial fission (fragmentation) [36] were slightly (although not significantly) lowered upon teriflunomide application. These findings suggest that teriflunomide treatment promotes mitochondrial biogenesis and mitochondrial fusion as processes known for being associated with oxidative metabolism and more mature and differentiated cell types [37].

In agreement with an induction of mitochondrial metabolism, we observed that teriflunomide reduced the expression of the glycolysis gatekeeper *3-phosphoinositide-dependent protein kinase (pdpk1)* [38] as well as of *lactate dehydrogenase A (ldha),* the terminal enzyme in the glycolytic pathway responsible for pyruvate to lactate conversion [39]. Both genes have been associated with high proliferation rates [40] and their levels need to be decreased to enable proper cell differentiation [41].

We next assessed the state of the mitochondrial network morphology in oligodendroglial cells of corpus callosum after 1 week of teriflunomide withdrawal by determining the expression of the mitochondrial outer membrane marker protein Tom20 (Fig. 6A, B″). Herein, teriflunomide treatment (pulse and constant) increased the overall Tom20 expression per area (Fig. 6A, B″, C). Furthermore, morphometric analysis according to [27, 28] indicated that both teriflunomide treatment schemes significantly increased mitochondrial branch length and form factor (FF) (Fig. 6D, F). The latter of which FF indicates an increase in mitochondrial elongation and interconnection, whereas no significant increase in the number of mitochondria could be observed (Fig. 6E). Furthermore, teriflunomide treatment decreased the fraction of Sox10-positive cells containing mitochondria with a fragmented shape (low), while elongated (complex) mitochondrial morphologies were enhanced (Fig. 6G, G″). Hence, these results indicate that teriflunomide promotes mitochondrial elongation which is in agreement with the observed upregulation of *mfn1.1/mfn1.2-* and downregulation *drp1* transcripts (Fig. 5A, B, F).

Discussion

Currently used disease-modifying therapies (DMTs) mainly act on the immune system and are clinically used to reduce relapse occurrence and hence to slow down progression to persistent disability in MS patients. Teriflunomide is an approved first-line DMT for RMS and acts via blocking de novo pyrimidine synthesis thereby exerting a cytostatic effect on proliferating B- and T-cells [42]. However, teriflunomide withholds the potential to be employed as a regenerative compound operating beyond immunomodulation due to recent findings revealing teriflunomide to promote oligodendroglial cell homeostasis and myelination in vitro [16] and based on promyelinating effects in *Xenopus laevis* and in mouse spinal cords [17]. Consistent with these observations, we here demonstrate that teriflunomide fosters myelin repair within a toxin-based de-/remyelination model leading to accelerated generation of oligodendrocytes, restoration of myelin sheaths and amelioration of mitochondrial integrity. Of note, along the boosted oligodendroglial marker expression teriflunomide also promoted the expression of the differentiation associated transcription factors *Mash1* (Fig. 2F), a gene regulation which was also demonstrated previously in a stroke model within cells of the subventricular zone [43]. The initially described teriflunomide

(See figure on next page.)

Fig. 6 Teriflunomide mediated mitochondrial changes in oligodendroglial cells within the corpus callosum. **A**, **B″** Representative images of Sox10 and Tom20 double positive cells in the caudal corpus callosum after 1 week of remyelination. **A**, **B″**, **C** Extent of mitochondrial changes was revealed as the percentage of Tom20-expressing area in the defined region of interest (white borders). Further morphometric quantifications were assessed to determine mitochondrial, **D** length, **E** number and **F** mean form factor (FF). FF = 1 indicates round object, hence low length of mitochondrial networks within cells (form factor 1; low) and increases with elongation, to multiple mitochondria exhibiting elongated tubules (form factor > 1 complex). **G**–**G″** Moreover, the relative percentage of double positive cells (Sox10+/Tom20+) containing few and less-elongated Tom20+ mitochondria categorized as "low" (blow up; asterix in B) where compared to Sox10-positive cells exhibiting Tom20+ mitochondria with elongated mitochondrial networks categorized as "complex" (blow ups; asterix in **B′**, **B″**. **G′** Individual data points related to the determination of double positive cells (Sox10 + /Tom20 +) categorized as "low" and (**G″**) individual data points for double positive cells (Sox10 + /Tom20 +) categorized as "complex". Number of animals per analysis $n = 6$. Data are shown as mean values (horizontal lines), while error bars represent standard error of the mean (SEM; vertical lines). Plots also show all individual data points. Significance was assessed using Tukey's range test following one-way ANOVA (**C**–**G**). Data were considered statistically significant (95% confidence interval) at $^{*}p < 0.05$, $^{**}p < 0.01$, $^{***}p < 0.001$. Scale bars: 50 µm, 20 µm, 10 µm

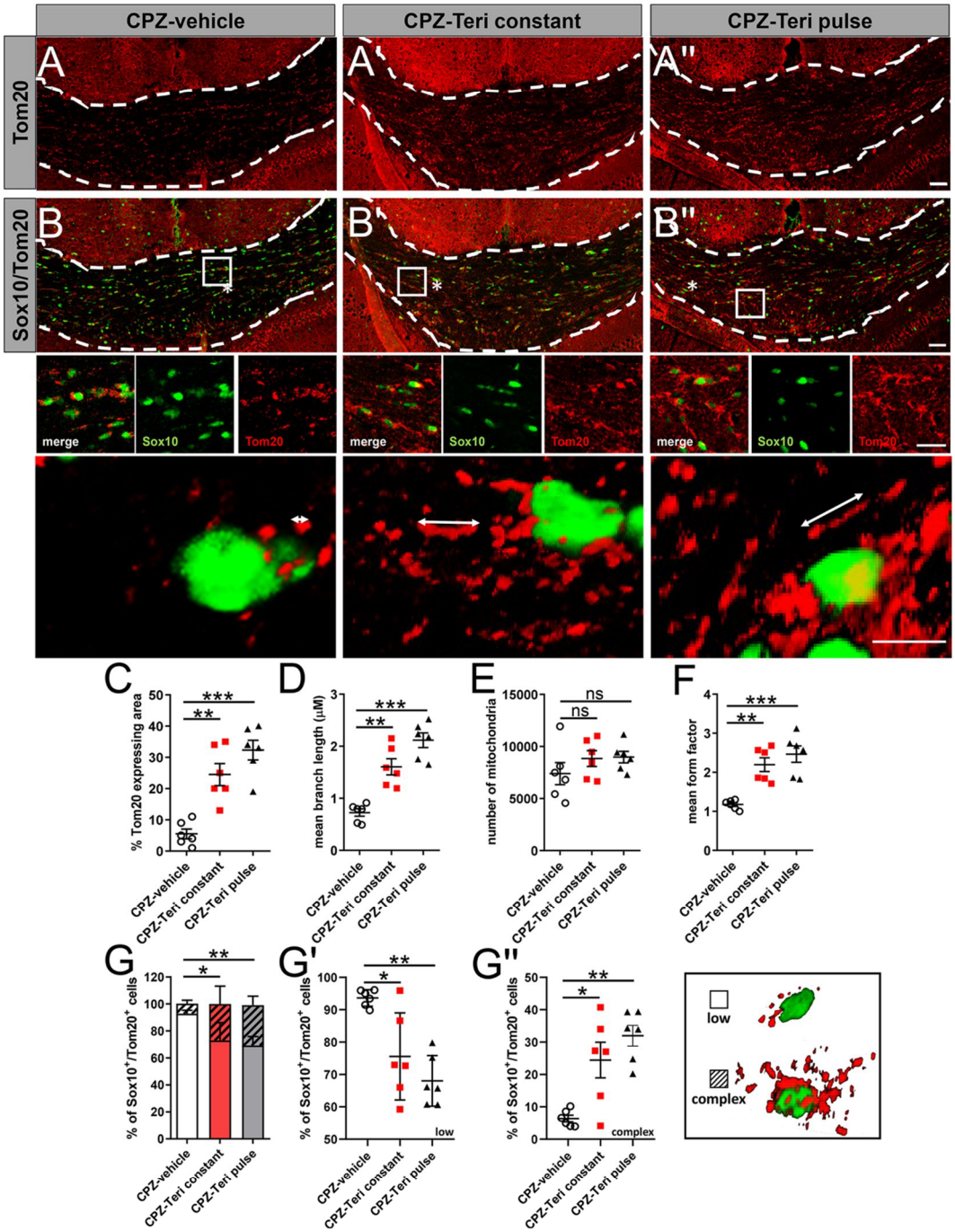

Fig. 6 (See legend on previous page.)

dependent pro-oligodendroglial effect via p73-signaling might, therefore, also be relevant in vivo [16].

Compared to previous in vitro studies [16] demonstrating promyelinating effects upon pulsed treatment only, it was of interest to examine that effects on spontaneous remyelination activities and gene expression responses as well as on mitochondrial dynamics occurred upon both pulsed and long-term teriflunomide application. Of note, the teriflunomide concentration used in this study [19, 20], resembles doses used in human patients and most importantly did not impact cell number/survival rates (see Fig. 3) as opposed to higher concentrations used in vitro [16]. Likewise, whereas in isolated OPCs, a prolonged teriflunomide application revealed to be counterproductive (as opposed to a maturation inducing pulsed stimulation), treatment of myelinating neuron/oligodendrocyte co-cultures appeared to be less sensitive in terms of timing [16]. Thus, this indicates that an increasingly complex environment supports a repair effect of this drug. And also, in the here presented in vivo paradigm long-term (constant) teriflunomide application did not negatively affect remyelination indicating that prolonged application as occurring in the context of the RMS therapy will not interfere with neuroregeneration. It is, therefore, tempting to speculate that the here described restoration of myelinated axons could in fact also contribute to the reduced disability progression in treated patients (TEMSO, ClinicalTrials.gov number NCT00134563; TOWER, ClinicalTrials.gov number NCT00751881) [44]. Nevertheless, it has to be taken into account that teriflunomide was applied orally thus limiting control over the consumed doses.

A growing number of studies suggest that lack of myelin repair and neurodegeneration are often attributed to a disturbance in mitochondrial homeostasis/metabolic function [45, 46]. Indeed, mitochondrial integrity has recently emerged as an essential modulator for neuronal and oligodendroglial cell differentiation [47, 48]. When compared with neurons and astrocytes, mitochondria length in oligodendroglia cell processes are between 0.8 and 2.3 µM and, therefore, approximately half as long as in astrocytes or neurons [49]. Indeed, in our analysis we measured mitochondrial lengths between 0.8 and 2.0 µM (Fig. 6D), hence, indicating oligodendroglial origin. An intact mitochondrial function is imperative for the increased energy demand during cell differentiation but also for lipid biosynthesis and the maintenance of myelin membranes [50, 51]. Assuring adenosine triphosphate (ATP) synthesis by means of oxidative phosphorylation (OXPHOS) [52, 53] is, therefore, critical for oligodendroglial cells to differentiate, mature and to build up myelin sheaths around axons [49]. Hence, these cells exhibit a high mitochondrial metabolism and contain increased densities of long, tubular (complex) mitochondria (Fig. 6D, F, G) [54]—a mitochondrial morphology that is thought to support high OXPHOS rates [55]. In the context of demyelination, mitochondria in both axons and OPCs are impaired, and lipid metabolism in OPCs within demyelinated lesions is disturbed [46]. Mitochondrial homeostasis and dynamics depend on two opposing processes, fission and fusion, the imbalance of which can result in cell damage, disturbed myelin repair and subsequent neurodegeneration [52, 56]. Fission, a mechanism promoted by drp1 (Fig. 5F), leads to shorter length, fewer cristae and fragmentation of mitochondria and is attributed to lower ATP rates in oligodendroglial cells [47]. Such mitochondria were mainly present within CPZ-vehicle treated animals following demyelination (Fig. 6B). Reduction of pyrimidine pools promoted by dihydroorotate dehydrogenase (DHODH) inhibition via teriflunomide not only triggers cell-cycle arrest [10, 16], but was also shown to modulate the expression of two highly conserved dynamin-related GTPases mfn1.1 and mfn1.2 (Fig. 5A, B) [57], thereby promoting mitochondrial fusion/elongation (Fig. 6B′, B″) [58–60]. Magalon and colleagues revealed that mitochondrial elongation is attributed to promoted oligodendrogenesis, as inhibition of mitochondrial fission/defragmentation fostered oligodendroglial cell maturation [61]. The underlying molecular mechanism of pyrimidine pool depletion resulting in altered mitofusin expression yet needs to be elucidated in future studies as it might be further explored therapeutically for sustained mitochondrial homeostasis and as an alternative approach to interfere with neurological dysfunction. Overall, our findings imply that teriflunomide promotes maturation and differentiation of OPCs also through a metabolic reprogramming that inhibits glycolysis and activates mitochondrial oxidative metabolism as well as mitochondrial biogenesis and fusion. Such modulated mitochondrial behavior might also be relevant for other neurological disorders, where mitochondrial fission is aberrant, such as, for example, Charcot–Marie–Tooth disease type 2A, a peripheral polyneuropathy caused by *mfn1.2* mutations [62]. Here, it could be of interest to examine the role of teriflunomide in suitable mouse models preceding clinical trials.

The applied toxin mediated demyelination model allows a precise and temporal analysis of neural cell responses to teriflunomide but lacks concomitant effects mediated to or via infiltrating immune cells. This apparent limitation, therefore, makes the translation of such regenerative effects to humans to be interpreted with caution. However, a previous study revealed teriflunomide to impair microglial activation in a mutant PLP mouse model [26], indicating that also resident immune cells are tamed further contributing to an overall beneficial effect.

Accordingly, a recent clinical study indicated that teriflunomide treatment is associated with favorable outcomes regarding functional optic nerve recovery following optic neuritis in early multiple sclerosis [63].

Due to the fact that teriflunomide was applied within the cuprizone-mediated demyelination phase, one cannot fully exclude additional cytoprotective effects of teriflunomide to occur in vivo. Specific teriflunomide-related demyelination effects were not determined as animals were not killed at corresponding earlier timepoints. Based on our previous in vitro study [16] demonstrating a direct pro-oligodendroglial effect by teriflunomide, we specifically aimed at endpoint 1 week after cuprizone treatment to directly study oligodendroglial effects in vivo. This timepoint is in agreement with many other studies using this toxin-mediated demyelination model [64]. Based on the same literature [64] it is also clear that during the teriflunomide application period most demyelination already occurred. Hence, the observed positive effects on remyelination most likely result from an increased OPC differentiation potential, while minor additional effects can currently not be fully excluded.

Whether beyond oligodendroglia and microglia also other neural cells respond along this line needs to be shown. Nevertheless, teriflunomide was demonstrated to shift the astrocytic bioenergetic profile from oxidative metabolism to glycolysis and to attenuate TNFα-induced inflammatory responses [65]. Future investigations will, therefore, address to what degree this drug also ameliorates neurotoxic profiles of astrocytes as recently shown in a related mouse model upon medrysone treatment [66].

Conclusions

The here presented study revealed that teriflunomide enhances endogenous myelin repair following cuprizone mediated demyelination. Hence, teriflunomide reflects an exciting translational candidate combining immunomodulatory and pro-regenerative properties. Moreover, this study revealed a novel link between de novo pyrimidine synthesis inhibition, stabilization of mitochondrial homeostasis and functional myelin repair. Thus, drugs affecting mitochondrial homeostasis could present further interesting approaches with clinical relevance for myelin repair and neuroregeneration.

Abbreviations

OPCs	Oligodendroglial precursor cells
NCS	Central nervous system
RMS	Relapsing MS
PMS	Progressive MS
MS	Multiple sclerosis
DHODH	Dihydroorotate dehydrogenase
CC	Corpus callosum
OLs	Oligodendrocytes
PFA	Paraformaldehyde
NGS	Normal goat serum
NHS	Normal horse serum
NDS	Normal donkey serum
Sox10	Sex determining region Y-Box 10
PLP	Proteolipid protein
Mash1	Mammalian achaete scute homolog-1
MBP	Myelin basic protein
BCAS1	Breast carcinoma amplified sequence 1
CNPase	2′,3′-Cyclic-nucleotide 3′-phosphodiesterase
Myrf	Myelin regulatory factor
Mfn1.1	Mitofusin 1
Mfn1.2	Mitofusin 2
Drp1	Dynamin-related protein 1
Pparg	Peroxisome proliferator activated receptor gamma
Ppargc1a	Peroxisome proliferator activated receptor gamma coactivator 1 alpha
Ppargc1b	Peroxisome proliferator activated receptor gamma coactivator 1 beta
Ldha	Lactate dehydrogenase A
DMTs	Disease-modifying therapies
OXPHOS	Oxidative phosphorylation
ATP	Adenosine triphosphate
GAPDH	Glyceraldehyde 3-phosphate dehydrogenase
gr	Grams
g	G force
FF	Form factor
rpm	Revolutions per minute
min	Minutes
TBS	Tris-Buffered Saline
RT	Room temperature
sec	Seconds
h	Hours
d	Days

Acknowledgements

We thank Brigida Ziegler, Julia Jadasz and Birgit Blomenkamp (all Düsseldorf) and Heinrich Blazyca (Würzburg) for their technical assistance.

Author contributions

PG performed the majority of all experiments, data analysis, data interpretation, text writing and figure design. JAG, and RM provided corresponding EM analysis, interpretation, text writing and figure design. LR, JOG, NR, IS and RA were involved in establishment of cuprizone experiments and provided corresponding data analysis. LR and NR provided support in data interpretation and data presentation. AZ and AP were involved in mitochondrial data analysis and interpretation. HPH was involved in data interpretation and text writing. P.K. was involved in experimental design, funding acquisition, data analysis and interpretation. PK conceived the final project and manuscript, was involved in experimental design, funding acquisition, data analysis and interpretation and in text writing and figure composition. All the authors read and approved the final manuscript.

Funding

Open Access funding enabled and organized by Projekt DEAL. This work was supported by the Christiane and Claudia Hempel Foundation for clinical stem cell research and the James and Elisabeth Cloppenburg, Peek and Cloppenburg Düsseldorf Stiftung.

Availability of data and materials

The data sets used and/or analysed during the current study are available from the corresponding author on reasonable request.

Declarations

Ethics approval and consent to participate

Cuprizone mediated demyelination experiments were approved by the authorities at LANUV (Landesamt für Natur, Umwelt und Verbraucherschutz Nordrhein-Westfalen; Az.: 81_02.04.2019.A203) and carried out according to

ARRIVE guidelines. These experimental procedures are characterized by mild severity grade, and therefore, no interventions to reduce pain, suffering and distress were needed.

Consent for publication
Not applicable.

Competing interests
The authors declare no competing interests.

Received: 16 September 2022 Accepted: 23 December 2022
Published online: 07 January 2023

References

1. Lassmann H. Multiple sclerosis pathology. Cold Spring Harb Perspect Med. 2018;8(3): a028936.
2. Franklin RJ, Ffrench-Constant C. Remyelination in the CNS: from biology to therapy. Nat Rev Neurosci. 2008;9(11):839–55.
3. Zawadzka M, Rivers LE, Fancy SP, Zhao C, Tripathi R, Jamen F, et al. CNS-resident glial progenitor/stem cells produce Schwann cells as well as oligodendrocytes during repair of CNS demyelination. Cell Stem Cell. 2010;6(6):578–90.
4. Gensert JM, Goldman JE. Endogenous progenitors remyelinate demyelinated axons in the adult CNS. Neuron. 1997;19(1):197–203.
5. Simons M, Nave KA. Oligodendrocytes: myelination and axonal support. Cold Spring Harb Perspect Biol. 2015;8(1): a020479.
6. Bezukladova S, Genchi A, Panina-Bordignon P, Martino G. Promoting exogenous repair in multiple sclerosis: myelin regeneration. Curr Opin Neurol. 2022;35(3):313–8.
7. Lubetzki C, Zalc B, Kremer D, Küry P. Endogenous clues promoting remyelination in multiple sclerosis. Curr Opin Neurol. 2022;35(3):307–12.
8. Manousi A, Küry P. Small molecule screening as an approach to encounter inefficient myelin repair. Curr Opin Pharmacol. 2021;61:127–35.
9. Küry P, Kremer D, Göttle P. Drug repurposing for neuroregeneration in multiple sclerosis. Neural Regen Res. 2018;13(8):1366–7.
10. Claussen MC, Korn T. Immune mechanisms of new therapeutic strategies in MS: teriflunomide. Clin Immunol. 2012;142(1):49–56.
11. O'Connor P, Wolinsky JS, Confavreux C, Comi G, Kappos L, Olsson TP, et al. Randomized trial of oral teriflunomide for relapsing multiple sclerosis. N Engl J Med. 2011;365(14):1293–303.
12. Confavreux C, O'Connor P, Comi G, Freedman MS, Miller AE, Olsson TP, et al. Oral teriflunomide for patients with relapsing multiple sclerosis (TOWER): a randomised, double-blind, placebo-controlled, phase 3 trial. Lancet Neurol. 2014;13(3):247–56.
13. Bruneau JM, Yea CM, Spinella-Jaegle S, Fudali C, Woodward K, Robson PA, et al. Purification of human dihydro-orotate dehydrogenase and its inhibition by A77 1726, the active metabolite of leflunomide. Biochem J. 1998;336(Pt 2):299–303.
14. Cherwinski HM, Cohn RG, Cheung P, Webster DJ, Xu YZ, Caulfield JP, et al. The immunosuppressant leflunomide inhibits lymphocyte proliferation by inhibiting pyrimidine biosynthesis. J Pharmacol Exp Ther. 1995;275(2):1043–9.
15. Zhang J, Teran G, Popa M, Madapura H, Ladds M, Lianoudaki D, et al. DHODH inhibition modulates glucose metabolism and circulating GDF15, and improves metabolic balance. iScience. 2021;24(5): 102494.
16. Göttle P, Manousi A, Kremer D, Reiche L, Hartung HP, Küry P. Teriflunomide promotes oligodendroglial differentiation and myelination. J Neuroinflammation. 2018;15(1):76.
17. Martin E, Aigrot MS, Lamari F, Bachelin C, Lubetzki C, NaitOumesmar B, et al. Teriflunomide promotes oligodendroglial 8,9-unsaturated sterol accumulation and CNS remyelination. Neurol Neuroimmunol Neuroinflamm. 2021. https://doi.org/10.1212/NXI.0000000000001091.
18. Matsushima GK, Morell P. The neurotoxicant, cuprizone, as a model to study demyelination and remyelination in the central nervous system. Brain Pathol. 2001;11(1):107–16.
19. Ringheim GE, Lee L, Laws-Ricker L, Delohery T, Liu L, Zhang D, et al. Teriflunomide attenuates immunopathological changes in the dark agouti rat model of experimental autoimmune encephalomyelitis. Front Neurol. 2013;4:169.
20. Groh J, Horner M, Martini R. Teriflunomide attenuates neuroinflammation-related neural damage in mice carrying human PLP1 mutations. J Neuroinflammation. 2018;15(1):194.
21. Nair AB, Jacob S. A simple practice guide for dose conversion between animals and human. J Basic Clin Pharm. 2016;7(2):27–31.
22. Chen Z, Chen JT, Johnson M, Gossman ZC, Hendrickson M, Sakaie K, et al. Cuprizone does not induce CNS demyelination in nonhuman primates. Ann Clin Transl Neurol. 2015;2(2):208–13.
23. Nakatani H, Martin E, Hassani H, Clavairoly A, Maire CL, Viadieu A, et al. Ascl1/Mash1 promotes brain oligodendrogenesis during myelination and remyelination. J Neurosci. 2013;33(23):9752–68.
24. Göttle P, Sabo JK, Heinen A, Venables G, Torres K, Tzekova N, et al. Oligodendroglial maturation is dependent on intracellular protein shuttling. J Neurosci. 2015;35(3):906–19.
25. Pavic G, Petzsch P, Jansen R, Raba K, Rychlik N, Simiantonakis I, et al. Microglia contributes to remyelination in cerebral but not spinal cord ischemia. Glia. 2021;69(11):2739–51.
26. Groh J, Friedman HC, Orel N, Ip CW, Fischer S, Spahn I, et al. Pathogenic inflammation in the CNS of mice carrying human PLP1 mutations. Hum Mol Genet. 2016;25(21):4686–702.
27. Chaudhry A, Shi R, Luciani DS. A pipeline for multidimensional confocal analysis of mitochondrial morphology, function, and dynamics in pancreatic beta-cells. Am J Physiol Endocrinol Metab. 2020;318(2):E87–101.
28. Hemel I, Engelen BPH, Luber N, Gerards M. A hitchhiker's guide to mitochondrial quantification. Mitochondrion. 2021;59:216–24.
29. Faul F, Erdfelder E, Buchner A, Lang AG. Statistical power analyses using G*Power 3.1: tests for correlation and regression analyses. Behav Res Methods. 2009;41(4):1149–60.
30. Xing YL, Roth PT, Stratton JA, Chuang BH, Danne J, Ellis SL, et al. Adult neural precursor cells from the subventricular zone contribute significantly to oligodendrocyte regeneration and remyelination. J Neurosci. 2014;34(42):14128–46.
31. Bujalka H, Koenning M, Jackson S, Perreau VM, Pope B, Hay CM, et al. MYRF is a membrane-associated transcription factor that autoproteolytically cleaves to directly activate myelin genes. PLoS Biol. 2013;11(8): e1001625.
32. Spaas J, van Veggel L, Schepers M, Tiane A, van Horssen J, Wilson DM 3rd, et al. Oxidative stress and impaired oligodendrocyte precursor cell differentiation in neurological disorders. Cell Mol Life Sci. 2021;78(10):4615–37.
33. Corona JC, Duchen MR. PPARgamma as a therapeutic target to rescue mitochondrial function in neurological disease. Free Radic Biol Med. 2016;100:153–63.
34. Yeligar SM, Kang BY, Bijli KM, Kleinhenz JM, Murphy TC, Torres G, et al. PPARgamma regulates mitochondrial structure and function and human pulmonary artery smooth muscle cell proliferation. Am J Respir Cell Mol Biol. 2018;58(5):648–57.
35. Sidarala V, Zhu J, Levi-D'Ancona E, Pearson GL, Reck EC, Walker EM, et al. Mitofusin 1 and 2 regulation of mitochondrial DNA content is a critical determinant of glucose homeostasis. Nat Commun. 2022;13(1):2340.
36. Gao F, Reynolds MB, Passalacqua KD, Sexton JZ, Abuaita BH, O'Riordan MXD. The mitochondrial fission regulator DRP1 controls post-transcriptional regulation of TNF-alpha. Front Cell Infect Microbiol. 2020;10: 593805.
37. Lisowski P, Kannan P, Mlody B, Prigione A. Mitochondria and the dynamic control of stem cell homeostasis. EMBO Rep. 2018;19(5):e45432.
38. Peng F, Wang JH, Fan WJ, Meng YT, Li MM, Li TT, et al. Glycolysis gatekeeper PDK1 reprograms breast cancer stem cells under hypoxia. Oncogene. 2018;37(8):1119.
39. Xie H, Hanai J, Ren JG, Kats L, Burgess K, Bhargava P, et al. Targeting lactate dehydrogenase–a inhibits tumorigenesis and tumor progression in mouse models of lung cancer and impacts tumor-initiating cells. Cell Metab. 2014;19(5):795–809.
40. Dupuy F, Tabaries S, Andrzejewski S, Dong Z, Blagih J, Annis MG, et al. PDK1-dependent metabolic reprogramming dictates metastatic potential in breast cancer. Cell Metab. 2015;22(4):577–89.
41. Prigione A, Rohwer N, Hoffmann S, Mlody B, Drews K, Bukowiecki R, et al. HIF1alpha modulates cell fate reprogramming through early

glycolytic shift and upregulation of PDK1-3 and PKM2. Stem Cells. 2014;32(2):364–76.
42. Bar-Or A, Pachner A, Menguy-Vacheron F, Kaplan J, Wiendl H. Teriflunomide and its mechanism of action in multiple sclerosis. Drugs. 2014;74(6):659–74.
43. Lu Z, Zhang D, Cui K, Fu X, Man J, Lu H, et al. Neuroprotective action of teriflunomide in a mouse model of transient middle cerebral artery occlusion. Neuroscience. 2020;428:228–41.
44. Freedman MS, Wolinsky JS, Comi G, Kappos L, Olsson TP, Miller AE, et al. The efficacy of teriflunomide in patients who received prior disease-modifying treatments: subgroup analyses of the teriflunomide phase 3 TEMSO and TOWER studies. Mult Scler. 2018;24(4):535–9.
45. Barcelos IP, Troxell RM, Graves JS. Mitochondrial dysfunction and multiple sclerosis. Biology (Basel). 2019;8(2):37.
46. Zhao JW, Wang DX, Ma XR, Dong ZJ, Wu JB, Wang F, et al. Impaired metabolism of oligodendrocyte progenitor cells and axons in demyelinated lesion and in the aged CNS. Curr Opin Pharmacol. 2022;64: 102205.
47. Rinholm JE, Vervaeke K, Tadross MR, Tkachuk AN, Kopek BG, Brown TA, et al. Movement and structure of mitochondria in oligodendrocytes and their myelin sheaths. Glia. 2016;64(5):810–25.
48. Bertholet AM, Delerue T, Millet AM, Moulis MF, David C, Daloyau M, et al. Mitochondrial fusion/fission dynamics in neurodegeneration and neuronal plasticity. Neurobiol Dis. 2016;90:3–19.
49. Meyer N, Rinholm JE. Mitochondria in myelinating oligodendrocytes: slow and out of breath? Metabolites. 2021;11(6):359.
50. Marangon D, Boccazzi M, Lecca D, Fumagalli M. Regulation of oligodendrocyte functions: targeting lipid metabolism and extracellular matrix for myelin repair. J Clin Med. 2020;9(2):470.
51. Poitelon Y, Kopec AM, Belin S. Myelin fat facts: an overview of lipids and fatty acid metabolism. Cells. 2020;9(4):812.
52. Tepavcevic V. Oligodendroglial energy metabolism and (re)myelination. Life. 2021;11(3):238.
53. Schoenfeld R, Wong A, Silva J, Li M, Itoh A, Horiuchi M, et al. Oligodendroglial differentiation induces mitochondrial genes and inhibition of mitochondrial function represses oligodendroglial differentiation. Mitochondrion. 2010;10(2):143–50.
54. Yazdankhah M, Shang P, Ghosh S, Bhutto IA, Stepicheva N, Grebe R, et al. Modulating EGFR-MTORC1-autophagy as a potential therapy for persistent fetal vasculature (PFV) disease. Autophagy. 2020;16(6):1130–42.
55. Tondera D, Grandemange S, Jourdain A, Karbowski M, Mattenberger Y, Herzig S, et al. SLP-2 is required for stress-induced mitochondrial hyperfusion. EMBO J. 2009;28(11):1589–600.
56. Mari M, Colell A. Mitochondrial oxidative and nitrosative stress as a therapeutic target in diseases. Antioxidants. 2021;10(2):314.
57. Rojo M, Legros F, Chateau D, Lombes A. Membrane topology and mitochondrial targeting of mitofusins, ubiquitous mammalian homologs of the transmembrane GTPase Fzo. J Cell Sci. 2002;115(Pt 8):1663–74.
58. Malla B, Liotta A, Bros H, Ulshofer R, Paul F, Hauser AE, et al. Teriflunomide preserves neuronal activity and protects mitochondria in brain slices exposed to oxidative stress. Int J Mol Sci. 2022;23(3):1538.
59. Miret-Casals L, Sebastian D, Brea J, Rico-Leo EM, Palacin M, Fernandez-Salguero PM, et al. Identification of new activators of mitochondrial fusion reveals a link between mitochondrial morphology and pyrimidine metabolism. Cell Chem Biol. 2018;25(3):268-78 e4.
60. Pellattiero A, Scorrano L. Flaming mitochondria: the anti-inflammatory drug leflunomide boosts mitofusins. Cell Chem Biol. 2018;25(3):231–3.
61. Magalon K, Le Grand M, El Waly B, Moulis M, Pruss R, Bordet T, et al. Olesoxime favors oligodendrocyte differentiation through a functional interplay between mitochondria and microtubules. Neuropharmacology. 2016;111:293–303.
62. Iwata K, Scorrano L. Finding a new balance to cure Charcot-Marie-Tooth 2A. J Clin Invest. 2019;129(4):1533–5.
63. Pfeuffer S, Kerschke L, Ruck T, Rolfes L, Pawlitzki M, Albrecht P, et al. Teriflunomide treatment is associated with optic nerve recovery in early multiple sclerosis. Ther Adv Neurol Disord. 2021;14:1756286421997372.
64. Zhan J, Mann T, Joost S, Behrangi N, Frank M, Kipp M. The cuprizone model: dos and do nots. Cells. 2020;9(4):843.
65. Kabiraj P, Grund EM, Clarkson BDS, Johnson RK, LaFrance-Corey RG, Lucchinetti CF, et al. Teriflunomide shifts the astrocytic bioenergetic profile from oxidative metabolism to glycolysis and attenuates TNFalpha-induced inflammatory responses. Sci Rep. 2022;12(1):3049.
66. Silva Oliveira M, Schira-Heinen J, Reiche L, Han S, de Amorim VCM, Lewen I, et al. Myelin repair is fostered by the corticosteroid medrysone specifically acting on astroglial subpopulations. EBioMedicine. 2022;83:104204.

Publisher's Note

International Journal of
Molecular Sciences

MDPI

Article

A Novel Ex Vivo Model to Study Therapeutic Treatments for Myelin Repair following Ischemic Damage

Luisa Werner [1,†], Michael Gliem [1,†], Nicole Rychlik [1], Goran Pavic [1], Laura Reiche [1], Frank Kirchhoff [2], Markley Silva Oliveira Junior [1], Joel Gruchot [1], Sven G. Meuth [1], Patrick Küry [1,‡] and Peter Göttle [1,*,‡]

[1] Department of Neurology, Medical Faculty, Heinrich Heine University, 40225 Düsseldorf, Germany; kuery@uni-duesseldorf.de (P.K.)
[2] Molecular Physiology, Center for Integrative Physiology and Molecular Medicine, University of Saarland, 66424 Homburg, Germany
* Correspondence: peter.goettle@uni-duesseldorf.de
† These authors contributed equally to this work.
‡ These authors also contributed equally to this work.

Abstract: Stroke is a major reason for persistent disability due to insufficient treatment strategies beyond reperfusion, leading to oligodendrocyte death and axon demyelination, persistent inflammation and astrogliosis in peri-infarct areas. After injury, oligodendroglial precursor cells (OPCs) have been shown to compensate for myelin loss and prevent axonal loss through the replacement of lost oligodendrocytes, an inefficient process leaving axons chronically demyelinated. Phenotypic screening approaches in demyelinating paradigms revealed substances that promote myelin repair. We established an ex vivo adult organotypic coronal slice culture (OCSC) system to study repair after stroke in a resource-efficient way. Post-photothrombotic OCSCs can be manipulated for 8 d by exposure to pharmacologically active substances testing remyelination activity. OCSCs were isolated from a NG2-CreERT2-td-Tomato knock-in transgenic mouse line to analyze oligodendroglial fate/differentiation and kinetics. Parbendazole boosted differentiation of $NG2^+$ cells and stabilized oligodendroglial fate reflected by altered expression of associated markers PDGFR-α, CC1, BCAS1 and Sox10 and GFAP. In vitro scratch assay and chemical ischemia confirmed the observed effects upon parbendazole treatment. Adult OCSCs represent a fast, reproducible, and quantifiable model to study OPC differentiation competence after stroke. Pharmacological stimulation by means of parbendazole promoted OPC differentiation.

Keywords: ischemic stroke; neuroregeneration; myelin repair; oligodendrocyte

check for updates

Citation: Werner, L.; Gliem, M.; Rychlik, N.; Pavic, G.; Reiche, L.; Kirchhoff, F.; Silva Oliveira Junior, M.; Gruchot, J.; Meuth, S.G.; Küry, P.; et al. A Novel Ex Vivo Model to Study Therapeutic Treatments for Myelin Repair following Ischemic Damage. *Int. J. Mol. Sci.* **2023**, *24*, 10972. https://doi.org/10.3390/ijms241310972

Academic Editor: Antonietta Bernardo

Received: 31 May 2023
Revised: 19 June 2023
Accepted: 26 June 2023
Published: 30 June 2023

1. Introduction

An ischemic stroke is caused by the acute disruption of blood supply. Treatment in ischemic stroke focuses on the early disease stages of lesion pathology, i.e., on restoring blood flow to the affected brain area (reperfusion). As time windows for reperfusion are narrow and treatment is sometimes not successful, persistent neurological deficits remain in the majority of patients. Disability is not only caused by neuronal and axonal degeneration but also by extensive loss of oligodendrocytes (OL) and their myelin sheaths [1]. Oligodendrocytes are highly vulnerable to ischemic damage and undergo necroptosis and apoptosis due to the release of toxic glutamate and ATP [2]. The latter, loss of oligodendroglial cells and their myelin sheaths (demyelination), was underestimated in the stroke field and mostly compromises axonal survival and correlates negatively with long-term clinical outcome and the disability degree [3,4]. Oligodendrocytes play a fundamental role in maintaining neuronal function and integrity through trophic and metabolic support [5,6]. Further studies indicated that remyelination is a major repair mechanism provoked by stroke-induced injury, whereby OPCs have a potential key function compensating for myelin loss and preventing additional axonal degeneration [7–9]. Herein, the infarct core represents an

irreparably damaged area, as almost all cells die within a few minutes after occlusion. On the other hand, the peri-infarct area, termed penumbra, exhibits an area of brain tissue that is damaged but rescued either via restoration of blood flow (short-term) or myelin repair (long-term) [10–13]. In this regard, it is known that OPC activation, proliferation, and recruitment to the infarct region are induced [14], whereby an increased number of oligodendroglial cells are found in the penumbra, adjacent to the infarct core. Nevertheless, brain damage progresses at later stages of stroke, correlating with increased failure of OPCs to successfully differentiate into myelinating oligodendrocytes and leading to inefficient myelin repair [15–17]. Hence, a reliable stroke model to study oligodendroglial cell differentiation and maturation kinetics in the context of stroke is needed in order to investigate the effects of possible therapeutics to enhance the process of remyelination and restore normal brain function following stroke. To save resources and reduce animal suffering (3R principles), we set out to establish a slice culture model to test these substances ex vivo.

2. Results

Within this study, we established a new ex vivo model of post-photothrombotic adult organotypic coronal slice culture (Figure 1) that provides an experimental design for the analysis of regenerative mechanisms of white matter damage after stroke. In terms of transferability, this ex vivo method is closer to the results of in vivo experiments compared to conventional in vitro cell culture studies, while at the same time, the number of animals compared to in vivo experiments is reduced. We used the transgenic NG2-CreERT2 td-Tomato knock-in mouse line [18] in order to pursue the response/fate of resident parenchymal oligodendroglial progenitor cells following stroke. NG2 (nerve/glia antigen-2) is a type I transmembrane glycoprotein (chondroitin sulfate proteoglycan 4) and expressed by resident parenchymal OPCs. This fraction of cells is widely accepted as a pool of resident precursor cells generating myelin-forming oligodendrocytes within adulthood that exhibit the potential target to promote cell-replacement therapies in the CNS [19,20].

2.1. Slice Culture Viability Following Photothrombotic Ischemia

In the first step, we tested tissue viability by various means. A macroscopic indicator for healthy brain slices is the absence of cuts and increasing levels of transparency during cultivation [21–23]. Furthermore, we identified apoptotic cells within the cultivated slices in order to evaluate their viability during cultivation by using a TUNEL Assay (Figure 2A,B,A′–A′′′′).). Of note, our results showed no increase in apoptotic TUNEL-positive cells over time in cultivation, comparing slices cultivated for four or eight days. We also found no significant difference in apoptosis rates comparing cells within the hemisphere that underwent photothrombosis, excluding the ischemically lesioned area, and the contralateral, healthy hemisphere (Figure 2A). In addition, no differences in apoptosis rates of $NG2^+$ cells at the border zone of the ischemic lesion over time (4 d–8 d) could be detected (Figure 2B). Moreover, we tested the viability of post-photothrombotic OCSCs following two, four, and eight days of cultivation by 2,3,5-triphenyl tetrazolium chloride (TTC) staining. The TTC is enzymatically reduced by living cells to a red dye produced by dehydrogenase [24]. This technique allowed us to check the overall viability of the organotypic slices after cultivation. Infarcted and damaged tissue stayed unstained while living tissue was stained red (Figure 2C) [24,25]. In general, our results suggest that the cells within the cultivated brain slices were mostly vital, with a moderate apoptosis rate under all conditions of below 20% (Figure 2). The analysis of the proliferation of $NG2^+$ cells using the marker Ki-67 demonstrated no detectable differences over time, while proliferation was around 5% (Figure 2D). Interestingly, the number of $NG2^+$ cells per mm^2 adjacent to the lesion site increased over time (2 d–8 d). Together with the low proliferation rate, this may imply the migration of $NG2^+$ cells to the border zone in the slices following stroke (Figure 2E).

Int. J. Mol. Sci. **2023**, *24*, 10972

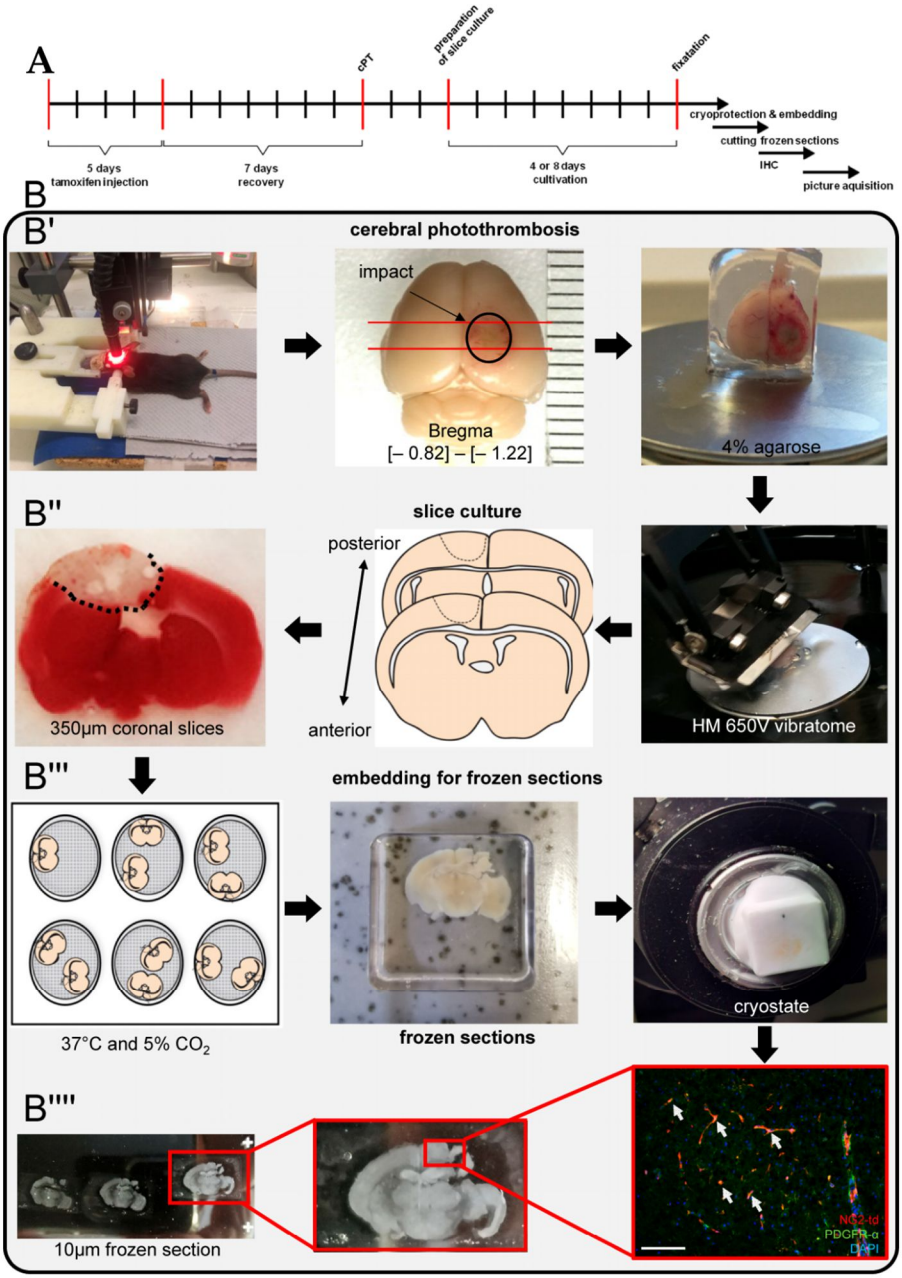

Figure 1. (**B**) Scheme of generating ischemic adult coronal slice cultures showing key steps in (**B′**) photothrombotic stroke, (**B″**–**B‴′**) dissection process, and (**A**) timelines for slice culture protocol. (**B‴′**) representative immunofluorecent staining, arrows indicating NG2+ cells positive for PDGFR-α. Scale bar (100 µM).

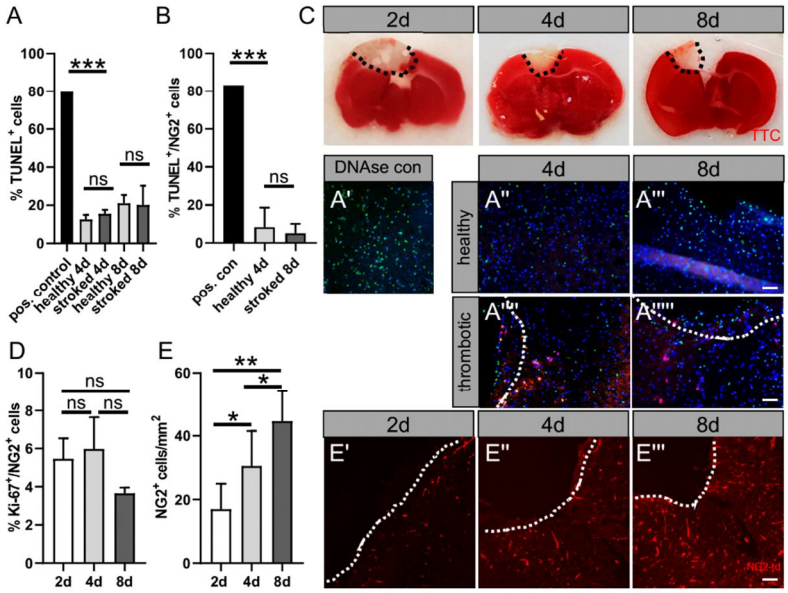

Figure 2. Representative data showing slice culture viability in culture post-photothrombosis. (**A**) TUNEL$^+$ cells (**A′**) were counted and the percentage was calculated in relation to the total cell number assessed by DAPI$^+$ cells for 4 d (**A′′**,**A′′′′**) and 8 d (**A′′′**,**A′′′′′**). (**B**) Determination of apoptosis rate of NG2$^+$ cells, double-positive cells for TUNEL and NG2 td-Tomato set in relation to the total number of NG2 td-Tomato$^+$ cells. (**C**) Tissue viability following cerebral photothrombosis (cPT) is exemplified by 2,3,5-Triphenyltetrazolium chloride (TTC) staining on 2 d, 4 d, and 8 d in culture by the distinction between infarcted (no staining) and living tissue (red staining). Within the border zone following stroke, (**D**) the proliferation of NG2$^+$ cells was determined by the quantification of Ki67 marker expression. (**E**) The number of NG2$^+$ cells per mm within the border zone was quantified for (**E′**–**E′′′**) 2 d, 4 d and 8 d in culture. Dashed lines indicate the border between photothrombotically lesioned tissue and border zone. Scale bar: 50 µm. Data are shown as mean values (±SD) and are derived from (**A**,**B**) n = 3, (**C**) n = 5, (**D**) n = 10 experiments. Statistical significance was calculated using Tukey's range test following one-way ANOVA (**A**–**E**). Data were considered statistically significant (95% confidence interval) at * $p < 0.05$, ** $p < 0.01$, *** $p < 0.001$, ns, not significant.

2.2. NG2 Glia within the Border Zone of Ischemic Lesion

After the induction of td-Tomato expression in NG2$^+$ cells by tamoxifen injection, one-week recovery and photothrombotic stroke as indicated in (Figure 1A), we analyzed the differentiation behavior/competence of NG2 glia at the border zone of the lesion site after 2, 4, and 8 days of cultivation. Given that the differentiation of adult NG2 glia in aged mice contributes to the generation of postnatal parenchymal OL lineage cells in the dorsal cortex and corpus callosum [18], we performed staining against different oligodendrocyte markers as well as the astrocytic lineage marker GFAP (glial fibrillary acidic protein) within the border zone of the lesion site (Figure 3A). Of note, almost all td-Tomato positive cells (tdT^+) were restricted to the OL lineage according to the expression of OL lineage marker SRY (sex determining region Y) Sox10 at day 2 but decreased to 32.5% at day 8 in cultivation (Figure 3B). At the same time, the number of NG2$^+$ cells coexpressing the astrocytic lineage marker GFAP significantly increased over time from only 17.3% at 2 d to 87% of cells being double-positive at 8 d (Figure 3C). In addition, we examined the differentiation competence of OPCs within OCSCs after 2, 4, and 8 d in culture by means of platelet-derived growth

factor receptor alpha (PDGFR-α), adenomatous polyposis coli (APC) clone (CC1), and breast carcinoma amplified sequence 1 (BCAS1) immunostaining. At day 2, 90.5% of tdT^+ in the border zone still expressed PDGFR-α, only expressed by immature OLs, whereas the percentage of PDGFR-α/tdT^+-positive cells decreased to 26.3% at day 8 (Figure 3E). In accordance with the loss of PDGFR-α expression, NG2 glia were differentiating into OL and started to express mature OL differentiation marker CC1. Furthermore, 9.5% of tdT^+ glia were already $CC1^+$ at day 4, whereas at day 8, the percentage of $CC1^+/tdT^+$ glia significantly increased to 13.8%. Furthermore, BCAS1 was examined, as this marker is particularly suitable to identify newly formed myelinating oligodendrocytes and indicates regions where new myelin has been actively formed [26]. Our results show that at 4 days after cultivation, 5.6% of tdT^+ glia were already BCAS1 positive cells, while the percentage of BCAS1/tdT^+ significantly increased to 21.0% at d 8 within the border zone of the infarction (Figure 3F). These results demonstrate that NG2-expressing cells at the border zone of the lesion site are committed to the OL lineage and able to differentiate into myelinating OLs. However, these cells increasingly expressed an astrocytic lineage marker over time in culture. Taken together, these results show that the differentiation dynamics of $NG2^+$ cells in OCSCs are comparable to known in vivo data [13,20].

2.3. Promotion of Oligodendroglial Differentiation within the Border Zone upon Parbendazole Exposition

Previous investigations using phenotypic compound screening revealed that, among other drugs, the anthelminthic drug parbendazole impacts OPC differentiation and myelin repair in the context of a cuprizone-mediated de(re)myelination mouse model for multiple sclerosis [27]. As parbendazole was shown, beyond its anthelmintic activity [28–30], to enhance OPC differentiation in the context of demyelination, we hypothesized that it could also show beneficial effects on remyelination after stroke. To this end, we used our new model (post-photothrombotic adult OCSCs) for stimulation experiments with parbendazole. To assess the effect of parbendazole, post-photothrombotic adult organotypic coronal slices were cultured with 0.02 µM parbendazole or DMSO as control for 4 or 8 days, respectively. Immunohistochemical staining was performed, to pursue the fate of $NG2^+$ glia that migrated to the border zone of the photothrombotic lesion (Figure 4A). By use of anti-Ki67 staining, we could not detect a significant impact of parbendazole treatment on proliferation in NG^+ cells at the infarction border zone at day 4 in culture (Figure 4B,D,G). To assess possible effects of parbendazole on apoptosis, a TUNEL assay was performed, showing no significant difference when OCSCs were treated with parbendazole (Figure 4F). Microgliosis is a dominant feature of stroke pathology impacting oligodendrogenesis; hence, Iba1 staining (Figure 4I–K) was performed. Herein, no differences in the distribution of microglia/myeloid cells positive for Iba1 upon parbendazole treatment could be detected. Given that OPCs have the potential to differentiate into oligodendrocytes or astrocytes [31,32] and an increment in the expression of GFAP was already seen in our OCSCs (Figure 3C), we were also interested in whether parbendazole exerts effects on astrocytes or the fate of OPCs. Therefore, GFAP staining was performed on the post-photothrombotic slice culture after 4 and 8 days in cultivation, and double-positive cells for tdT and GFAP at the border of the lesion were counted. Interestingly we found a high number of cells being double-positive (tdT^+; $GFAP^+$) under control conditions with 71.51%. This was significantly higher than in slices treated with parbendazole, with just around 27.11% (Figure 4C,E,H). These data suggest that parbendazole might stabilize the OPC lineage, rather than the astrocytic fate. To corroborate this finding, the state of oligodendrocyte differentiation was analyzed via immunofluorescence staining using anti-PDGFR-α antibodies, which are only expressed by immature precursors. Staining was performed on OCSCs cultivated for 4 days with or without parbendazole treatment. In addition, we conducted immunofluorescence staining using the late OL differentiation marker CC1 on slices cultivated to a maximum of 8 days to determine the number of further differentiated NG2 glia. Our results revealed that upon parbendazole treatment, the percentage of immature PDGFR-α positive NG2

cells was significantly lower at 31.1%, compared to control with 57.17% (Figure 5A). Correspondingly, we found that after 8 days of cultivation, the number of mature CC1-positive oligodendrocytes was significantly increased at 21.25% when comparing to control sections with 8.8% (Figure 5C). Consequently, the number of NG2/Sox10 double-positive cells increased from 45% to 81% (Figure 5B), and the number of NG2/CC1 cells increased from 8.9% to 21,2% (Figure 5C). Interestingly, our results also indicated a significant increase in the number of NG2/BCAS1 double-positive cells from 4.5% to 21.09% as well as of NG2/MBP double-positive cells from 3.5% to 10.6%, suggesting an increased remyelination potential. Of note, the overall cell number remained stable under parbendazole treatment (Figure 5E,F). Our data therefore indicate an enhanced oligodendroglial cell differentiation and enhanced potential for remyelination upon stimulation with the pharmacologically active compound parbendazole.

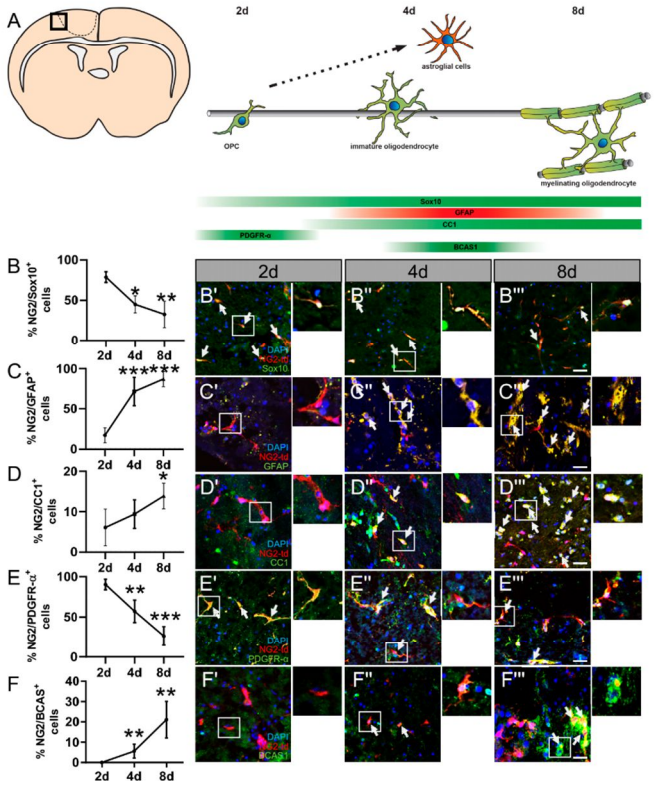

Figure 3. (**A**) Schematic overview of oligodendroglial marker expression kinetics within the border zone of the ischemic lesion by means of NG2-CreERT2-td-Tomato mice. (**B**–**F**) Quantification of confocal LSM micrographs within the border zone (**B′**–**F‴**) of NG2 td-Tomato (red) positive cells coexpressing (**B**) Sox10, (**C**) GFAP, (**D**) CC1, (**E**) PDGFR-α, and (**F**) BCAS1 (green) under the border zone and within the lesion site 2 d, 4 d, and 8 d in culture. Arrows indicate double-positive cells. Dashed lines indicate the border between thrombotic core region and penumbra. Scale bar: 20 µm. Data are shown as mean values (±SD) and are derived from (**B**) n = 6, (**C**) n = 4, (**D**) n = 5, (**E**) n = 6, and (**F**) n = 7 experiments. Statistical significance was calculated using Kruskal–Wallis test with Dunn's post-test (**B**) and Tukey's range test following one-way ANOVA (**C**–**F**). Data were considered statistically significant (95% confidence interval) at * $p < 0.05$, ** $p < 0.01$, *** $p < 0.001$.

Int. J. Mol. Sci. **2023**, *24*, 10972

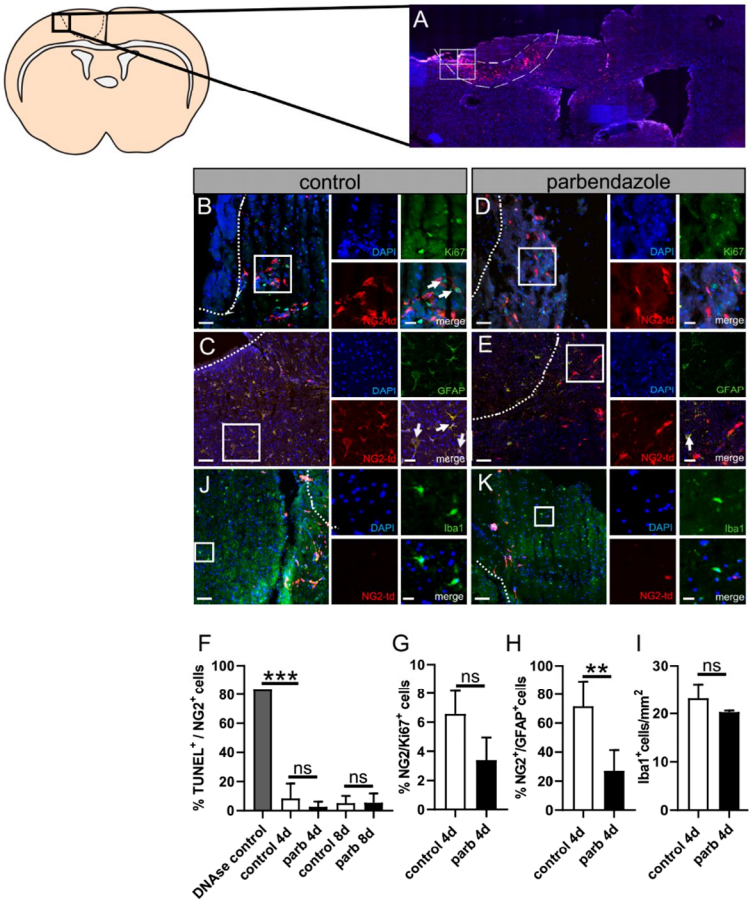

Figure 4. Effect of parbendazole on apoptosis, proliferation, microgliosis, and oligodendroglial cell fate of NG2$^+$ cells within the border zone of post-photothrombotic adult coronal organotypic slice cultures. (**A**) Laser scanning micrograph (LSM) image of a photothrombotically lesioned NG2-CreERT2 td-Tomato mice brain after 4 days of cultivation. Immunostaining of cell nuclei using DAPI. The composition of 4 images (1 image measures 2195 × 1949 pixel or 482 × 428 µm) indicates the ROIs. Dashed lines indicate the border zone. Arrows indicate double-positive cells. (**F**) Quantification of NG2$^+$ cells double positive cells for TUNEL indicating the apoptosis rate after 4 d and 8 d in culture. (**G**) Percentage of NG2$^+$ and Ki-67$^+$ double positive cells for DMSO control- (**B**) and parbendazole- (**D**) treated slice culture after 4 d. (**H**) Identification of astroglial lineage cells at the border zone of the photothrombotic lesion upon control (**C**) or parbendazole treatment (**E**) after 4 d. (**I**) Identification of Iba1 positive cells at the border zone upon control (**J**) or parbendazole (**K**) treatment after 4 d. Double-positive cells for NG2 td-Tomato and GFAP were counted and set in relation to the total amount of NG2$^+$ cells. Dashed lines indicate the border between photothrombotically lesioned tissue and the border zone. Scale bars: (**A**) 10× magnification, (**B**,**D**) 50 µm, 20 µm, (**C**,**E**) 100 µm, and 20 µm, (**J**,**K**) 100 µm, 20 µm. Data are shown as mean values (±SD) and are derived from (**F**) n = 3, (**G**) n = 3, (**H**) n = 4, and (**I**) n = 3 experiments. Statistical significance was calculated using the Kruskal–Wallis test with Dunn's post-test (**F**), and Mann–Whitney U test (**G**,**H**). Data were considered statistically significant (95% confidence interval) at ** $p < 0.01$, *** $p < 0.001$, ns, not significant.

Int. J. Mol. Sci. **2023**, *24*, 10972

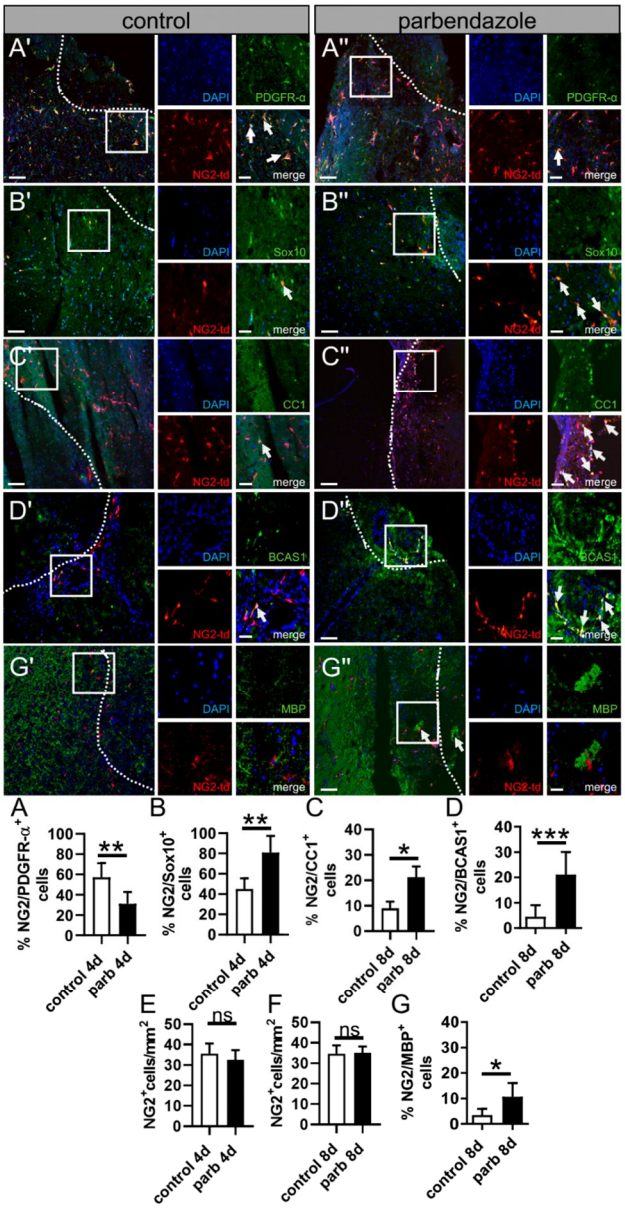

Figure 5. Promoting OPC differentiation within the border zone of post-photothrombotic adult coronal cultures following stimulation with parbendazole. (**A′**–**G′′**) Representative images of oligodendroglial differentiation-associated protein markers on slices treated with parbendazole (**A′′**–**D′′**,**G′′**) or DMSO, as control (**A′**–**D′**,**G′**). The impact on oligodendroglial cell differentiation and maturation was assessed by the number/mm^2 of NG2$^+$ cells and the relative percentage of double-positive cells (NG2$^+$/PDGFR-α$^+$ cells; (**A**–**A′′**)), (NG2$^+$/Sox10$^+$ cells; (**B**–**B′′**)), (NG2$^+$/CC1$^+$ cells; (**C**–**C′′**)), (NG2$^+$/BCAS1$^+$ cells; (**D**–**D′′**)), (NG2$^+$/MBP$^+$ cells; (**G**–**G′′**)) along the same area. Arrows in detailed

pictures indicate double-positive cells. Dashed lines indicate the border between ischemically lesioned tissue and the border zone. (**A′**–**G′′**) Scale bars: 100 µm, 20 µm. Data are shown as mean values (±SD) and are derived from (**A**) n = 7, (**B**) n = 5, (**C**) n = 7, (**D**) n = 7 and (**G**) n = 3 experiments. Statistical significance was calculated using Student's *t*-test (**A**,**C**) and Mann–Whitney U test (**B**,**D**,**E**–**G**). Data were considered statistically significant (95% confidence interval) at * $p < 0.05$, ** $p < 0.01$, *** $p < 0.001$, ns, not significant.

2.4. Characterization of Cells Invading the Scratch on Myelination Co-Culture

In order to reconfirm the effect of parbendazol on oligodendroglial's fate in the context of injury, we performed a scratch assay on myelinating co-cultures at 17 days in vitro (DIV17), a timepoint where mature OLs start to myelinate axons in this culture system [33]. To this end, we used dissociated neuron–oligodendrocyte (OL) co-cultures from embryonic day 16 (E16) cerebral cortex. The co-culture was maintained in a modified myelination medium that supports both OL and neuron differentiation and comprises on average 38.5% NeuN+ neurons, 28.3% Olig2+ OL lineage cells, 10% of Glial fibrillary acidic protein (GFAP)+ astrocytes, and 10% CD11b+ microglia/macrophage at DIV10 [34]. To this end, cells that migrated into the scratch were counted after 0, 24, and 48 h and were then further characterized by immunofluorescent staining using the oligodendroglial lineage marker oligodendrocyte transcription factor 2 (Olig2) and the astrocytic marker glial fibrillary acidic protein (GFAP). We found that after 48 h, significantly more cells migrated into the scratch after parbendazole stimulation (Figure 6A,B,E). Quantification revealed that significantly more Olig2 positive cells migrated into the scratch, while the number of GFAP positive cells was significantly reduced compared to control conditions (Figure 6C,D,F–G). The same experiments were carried out on co-cultures at DIV24, a time point that is characterized by the onset of myelination. At this time, significantly more cells also migrated into the scratch after parbendazole stimulation; however, the ratio between Olig2 and GFAP positive cells only slightly and not significantly differed between the conditions. Hence, these data show that parbendazole is able to promote oligodendroglial cell migration at earlier time points.

2.5. Rescue of Oligodendroglial Differentiation Competence by Means of Parbendazole Treatment Following Chemical Ischemia after 3 d In Vitro

In addition, our data were confirmed in a chemical ischemia model. We mimicked the effects of transient energy restriction in the ischemic penumbra by transiently removing glucose, blocking oxidative phosphorylation with sodium azide, and blocking glycolysis with 2-deoxy-D-glucose according to [35,36]. Those experiments were carried out on primary cultured OPCs, allowing us to confirm our data and investigate the effects of parbendazole directly on OLs, concerning energy deprivation, without other brain cells possibly interfering. To determine relevant cell-specific concentrations, total cell numbers as well as the expression of myelin basic protein (MBP), a marker that serves to monitor oligodendroglial differentiation, were investigated in a dose-dependent manner after 3 days in culture (Figure 7C,D,A–A′′′). Our data revealed that the total cell number is comparable to control conditions using concentrations ranging from 10 mM NaN_3 with 4 mM 2DG up to 40 mM NaN3 with 16 mM 2DG. However, using higher concentrations, cell numbers were drastically reduced. Furthermore, immunofluorescence staining for MBP indicated a significant reduction in the expression of MBP with increasing NaN_3 and 2DG concentrations. MBP expression was already diminished by about 50% using the lowest chemical ischemia concentrations, whereas MBP expression could not be detected using the highest concentration. Moreover, we investigated differentiation into mature oligodendrocytes by means of MBP (Figure 7E,B–B′′′) and CC1 (Figure 7G,F–F′′′) expression after stimulation with parbendazole. When cells were treated with parbendazole alone (without chemical ischemia), both MBP and CC1 expression was significantly higher compared to control conditions, confirming our findings above. Additionally, our data show that MBP as well as CC1 expression can be rescued by parbendazole stimulation after mild chemical ischemia (at low concentrations).

Int. J. Mol. Sci. **2023**, *24*, 10972

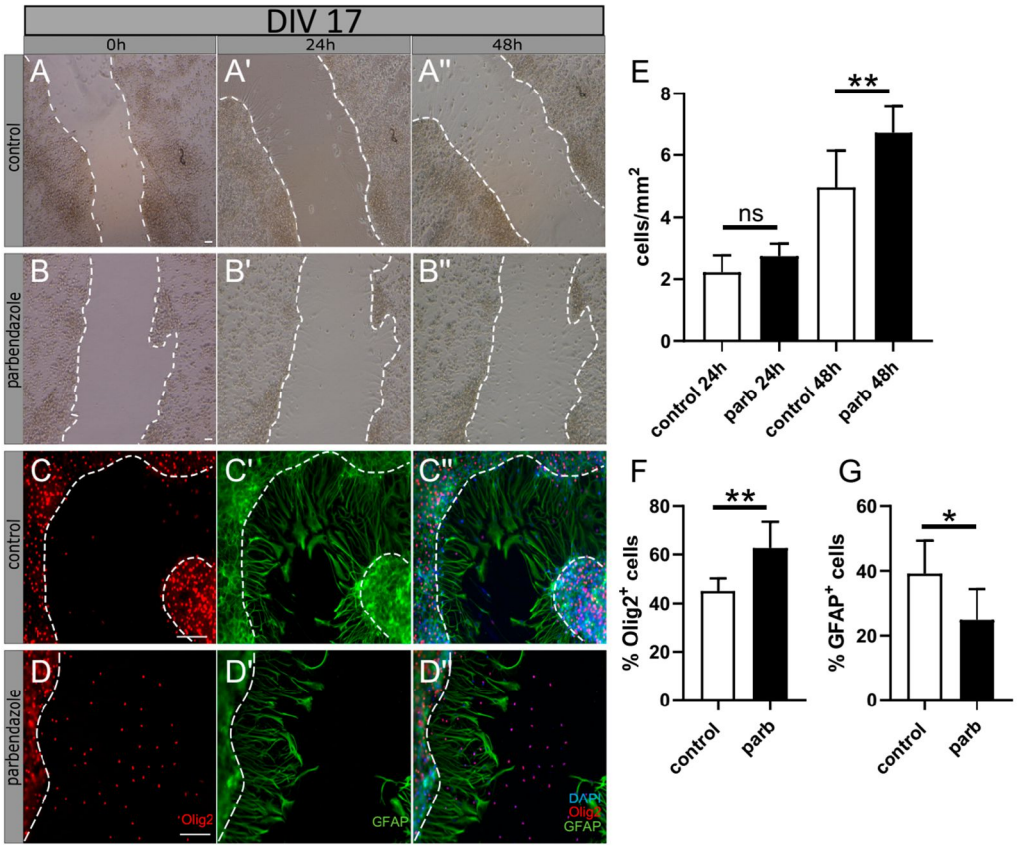

Figure 6. Identification and characterization of cells invading the scratch on myelination co-culture at 17 days in vitro (DIV). Representative bright field images of cells migrating into the scratch 24 and 48 h after stimulation with parbendazole (**B**–**B′′**) and DMSO (**A**–**A′′**) as control. Cells inside the scratch were counted, and the area of the scratch was calculated (**E**). Scale bar: 100 µm. After 48 h, the percentage of Olig2$^+$ cells (**C**,**D**,**F**) and GFAP$^+$ cells (**C′**,**D′**,**G**) was calculated in relation to the total number of cells, assessed by the number of DAPI$^+$ cells, as exemplified by merged pictures (**C′′**, **D′′**). Scale bar: 100 µm. Data are shown as mean values (±SD) and are derived from n = 7 experiments for bright field images and n = 6 for immunofluorescence staining. Statistical significance was calculated using (**E**) Mann–Whitney U and Student's *t*-test (**F**,**G**). Data were considered statistically significant (95% confidence interval) at * $p < 0.05$, ** $p < 0.01$, ns, not significant.

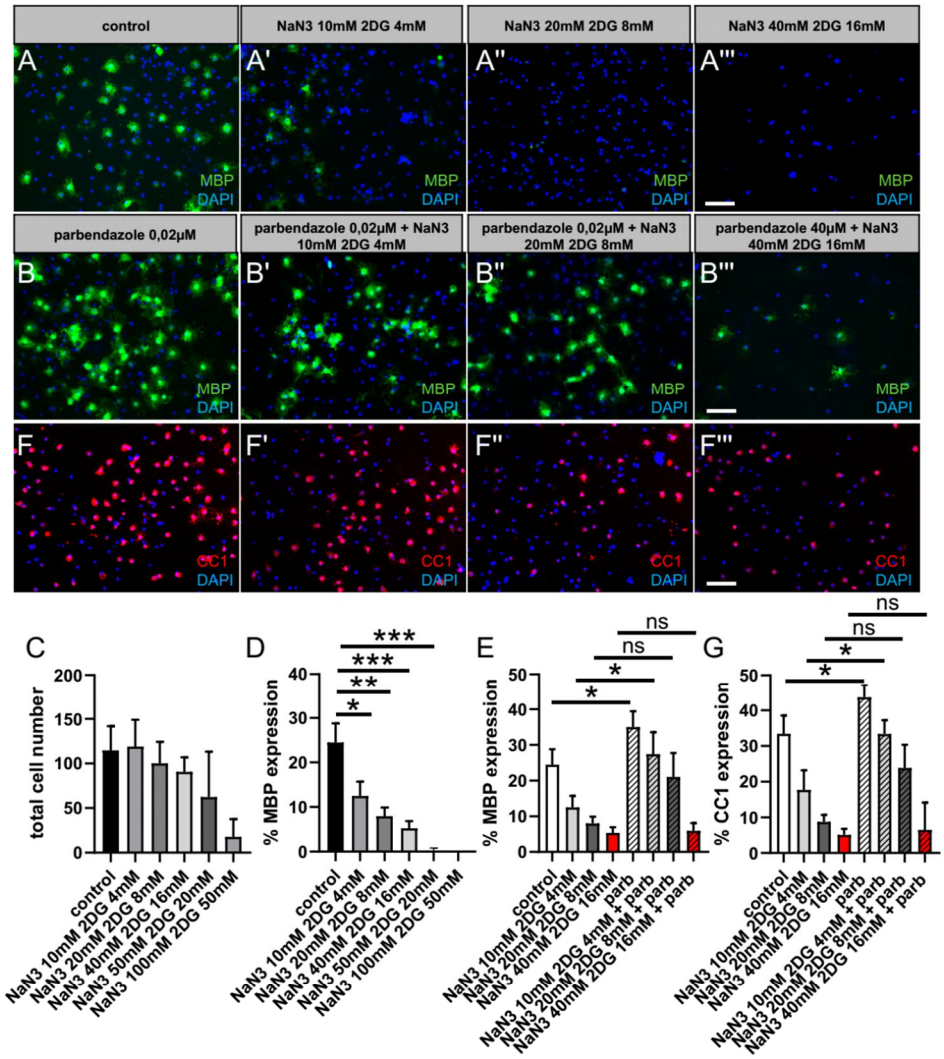

Figure 7. Rescue of oligodendroglial differentiation competence by means of parbendazole treatment following chemical ischemia after 3 d in vitro. Modification of oligodendroglial differentiation competence upon energy restriction removing glucose, blocking oxidative phosphorylation with sodium azide NaN_3, and blocking glycolysis with 2-deoxy-D-glucose (2DG). In order to determine functionally relevant cell-specific concentrations, (**C**) total cell number as well as (**D**) MBP expression of primary cultured OPCs was investigated in a dose-dependent manner after 3 days in culture (**A**–**A‴**). (**E**) In response to parbendazole treatment MBP (**B**–**B‴**) as well as (**G**) CC1 (**F**–**F‴**) expression can be rescued. Scale bar: 50 µm. Data are shown as mean values (±SD) and derive from n = 3 experiments. Statistical significance was calculated using Kruskal–Wallis test with Dunn's post-test (**C**–**E**). Data were considered statistically significant (95% confidence interval) at * $p < 0.05$, ** $p < 0.01$, *** $p < 0.001$ ns, not significant.

3. Discussion

This study demonstrates the capability of a new ex vivo model to study the differentiation kinetics of oligodendroglial cells within the peri-infarct region. Consistent with previous observations in demyelination models [27] and using two in vitro models, namely scratch assay and chemical ischemia, we here demonstrated that parbendazole treatment led to the accelerated generation of oligodendrocytes within the penumbra following stroke. Appropriate experimental animal models for cerebral ischemic damage in vivo such as cerebral photothrombosis or transient middle cerebral artery occlusion most closely reflect the molecular and cellular mechanisms after human stroke but encounter numerous challenges [37]. On the contrary, the 3R principles are guiding principles for more ethical use of animals "to avoid animal experiments altogether (Replacement), to limit the number of animals (Reduction) and their suffering (Refinement) to an absolute minimum" [38]. To this end, the ex vivo model of post-photothrombotic adult organotypic slice cultures established here offers the possibility of an experimental design for research on physiological, pathologic, and reparative mechanisms after cerebral damage following stroke that is close to animal studies but reduces the number of animals and their suffering and thereby addresses two Rs of the 3R principle. An experiment with n = 4 with two conditions and two time points requires at least 16 animals for experiments in vivo, whereas by means of our ex vivo model, significantly fewer animals (two animals) are required. At the same time, mechanisms can be studied more precisely in OCSCs than in vivo. OCSCs offer the opportunity to selectively and precisely add or remove cell populations, e.g., inflammatory cell populations, either by depletion paradigms or by modification of the time point for slice culture preparation, allowing or preventing the invasion of cells in vivo. They offer a greater temporal resolution (fixation/analysis at different time points within one probe) than in vivo models for fate mapping as exemplified for $NG2^+$ cells over short time periods (8 d). Nevertheless, its needs to be taken into account that the short time window of tamoxifen induction and photothrombosis can result in anti-inflammatory and neuroprotective effects of this drug, as previously described [39]. Moreover, the lack of a blood–brain barrier improves control of drug concentrations and makes them appropriate for drug screening, e.g., parbendazole. Furthermore, live imaging analysis will be possible. The advantage compared to in vitro studies is the continued existence of tissue's cell composition and connections in many respects. Nevertheless, slice culture thinning over time limits their temporal use in culture; hence, in vivo studies are more appropriate for long-term experimental investigation. Further limitations are that beside the analysis of mechanistic effects potential roles on disability, the clinical improvement and interaction of cells recruited in the in vivo situation from the organism after the time point of slice culture preparation cannot be assessed. Furthermore, emerging inflammation and trauma in OCSCs due to tissue slicing can generate a layer of astrocytic scar tissue onto the slice surface, altering mechanisms compared to the in vivo conditions [40]. As indicated above, this model has its limitations but can definitely serve as a prescreening platform for treatments, which can then be further validated in vivo, given that behavioral tests also cannot be assessed within this ex vivo model. With regard to brain injury, pathological analysis shows that demyelination or myelin loss is a main feature of ischemic stroke injury, suggesting that myelin repair is a major therapeutic target for functional recovery as demonstrated previously [11–13]. To this end, promoted myelin repair within the penumbra following stroke results in significant axonal regrowth and stabilization [41] and further improved neurological outcomes [3,8].

By means of NG2 td-Tomato knock-in mice, allowing us to monitor the fate, proliferation, migration, and differentiation of adult resident parenchymal OPCs, we were able to monitor the effect of the promyelination drug parbendazole on adult OPCs within the peri-infarct area following stroke. Of note, Sozmen and colleagues could demonstrate that the major response of OPCs after stroke arises from parenchymal progenitors as no recruitment of SVZ-derived cells in the OPC lineage post-stroke was found [13]. Given that oligodendroglial cell differentiation is inefficient in the environment of an ischemic lesion [17], the

finding that parbendazole promotes myelin repair [27] in our ex vivo ischemic stroke model was of considerable interest. The differentiation kinetics shown in Figure 3 were boosted upon parbendazole treatment and enhanced oligodendroglial cell maturation, as indicated by alterations in PDGFR-α, CC1, Sox10, BCAS1, and MBP expression by $NG2^+$ cells. Within this study, we focused on early time points and hence the generation of oligodendrocytes from OPCs and very early myelination indicators such as BCAS1 and MBP expression. Stretching the time in culture might give an idea of remylination. In the end, "the final aim" remyelination and the effect on the clinical score will have to be studied in vivo, which is behind the scope of this study. As parbendazole was administered within a pathophysiological scenario of ongoing inflammation, trauma, astrogliosis, and microgliosis, as well as OPC proliferation and migration, additional primary or secondary cytoprotective effects cannot be fully excluded. Given the restriction of Ki67 only providing a snapshot of proliferating cells at the very moment when slices were fixed, future studies regarding the role of proliferation during lesion expansion or drug treatment need to be performed by means of BrdU or EdU incorporation. However, we previously demonstrated OPC-specific effects of parbendazole in vitro and in vivo [27], and our current cell culture experiments (Figure 7) additionally suggested that OPC differentiation is the primarily targeted process. As resident OPCs are known to migrate towards the peri-infarct area before differentiating into mature oligodendrocytes [42], as indicated in Figure 2E–E‴), it was interesting to assess the migration of adult OPCs upon parbendazole treatment. Whereas migration seems to play a role in $NG2^+$ cell accumulation in the border zone of our slices over time, no difference in the number of $NG2^+$ cells at the peri-infarct zone could be detected upon parbendazole treatment. In contrast, juvenile (developmental) OPCs, as demonstrated in the scratch assays of embryonal cells of the neuron–oligodendrocyte in vitro myelination culture (Figure 6), showed increased migration behavior after parbendazole treatment. Their higher resistance to ischemic damage compared to adult OPCs and higher affinity to respond to injury [43] might explain this difference. On the other hand, considering that slices were prepared 3 days after the induction of cerebral photothrombosis to allow inflammatory cells to invade the tissue, the initiation of OPC migration might be missed by the parbendazole treatment of the ex vivo slice culture [12].

The plasticity of oligodendroglial cells upon acute brain injuries can evoke various response cascades directing the conversion of oligodendrocytes into astrocytes [44].

In this context, it is interesting to mention that miconazole, another imidazole derivative related to parbendazole (a group of heterocyclic compounds that have biological, chemical properties to treat parasitic illnesses produced by either protozoa or helminthes [45]), was found to promote the neuroregeneration and neurobehavioral recovery of rats after t-MCAO via a brain-derived growth factor (BDNF)-dependent mechanism [46]. In addition, BDNF was demonstrated to maintain and stabilize oligodendroglial lineage in a dose-dependent manner [47]. This is in accordance with the finding that parbendazole reduces GFAP expression within $NG2^+$ cells both ex vivo and in vitro (Figures 4H and 6G). Nevertheless, to what degree parbendazole initiates the same pathway and whether, further cells beyond oligodendroglia can also be addressed by this drug need to be investigated in future experiments. Moreover, the results and interpretation presented here need to be further evaluated in other anatomic regions as well as different stroke models prior to translation to humans.

4. Materials and Methods

4.1. Ethics Statements for Animal Experiments

Cerebral-photothrombosis-induced cortical ischemia experiments were approved by the authorities at LANUV (Landesamt für Natur, Umwelt und Verbraucherschutz NordrheinWestfalen; Az.: 81-02.04.2018.A275) and carried out according to ARRIVE guidelines. The animals were bred under defined conditions with access to food and water ad libitum in the animal facility (ZETT) of the Heinrich-Heine-University Düsseldorf. For preparation of rat myelinating co-culture and OPC mono-culture experiments, cerebral cortices of

Wistar rats of either sex were used—AZ.: 81-02.04.2018.A388. For adult organotypic cortical slice culture, ten- to twelve-week-old transgenic NG2-CreERT2 td-Tomato mice of either sex were used.

4.2. Mouse Line

Ten- to twelve week-old NG2-CreERT2 (Cspg4-CreERT2) td-Tomato mice generated as described elsewhere [18] were used for adult organotypic cortical slice culture 3 days after the induction of a cerebral photothrombosis. The NG2-CreERT2 knock-in mouse line, in which the open reading frame of the tamoxifen-inducible form of the Cre DNA recombinase (CreERT2) was inserted into the cspg4 (NG2; neural/glial antigen 2) locus via homologous recombination, was crossbred to a Rosa26-td-Tomato reporter line. In NG2-CreERT2/Rosa26-tdTomato mice, NG2 positive cells can be labeled and their fate map tracked in vivo upon induction of the Cre activity via tamoxifen. All mouse lines were maintained in the C57BL/6 N background, and only NG2 and reporter-heterozygous mice were used.

4.3. Oligodendroglial Cell Culture

Generation of primary OPCs from postnatal day zero (P0) cerebral rat cortices (Wistar rats of either sex) was performed as previously described [33]. The Institutional Review Board (IRB) of the ZETT (Zentrale Einrichtung für Tierforschung und wissenschaftliche Tierschutzaufgaben) at the Heinrich Heine University Düsseldorf has approved all animal procedures under licenses O69/11 and V54/09. Anti-A2B5 staining (Merck Millipore, Darmstadt, Germany; MAB312R RRID:AB_11213098) revealed that the cultures consisted of 98% oligodendroglial cells. OPCs were either seeded onto 0.25 mg/mL poly-D-lysine-coated (PDL, Sigma-Aldrich, St. Louis, MO, USA) glass coverslips (13 mm) in 24-well plates (for immunocytochemistry; 2.5×10^4 cells/well) or onto 0.25 mg/mL PDL coated 24-well plates (for quantitative reverse transcription polymerase chain reaction (qRT-PCR); 5×10^4 cells/well) in high-glucose DMEM-based Sato medium. After 1.5 h, oligodendroglial cell differentiation was initiated via Sato medium supplemented with 0.5% fetal bovine serum (FBS) (Capricorn Scientific, Palo Alto, CA, USA). The medium was exchanged every 3 days. To determine the physiological reaction from OPCs exposed to the substances, OPCs were treated in a dose-dependent manner using concentrations of 10 mM, 20 mM, 40 mM, 50 mM, and 100 mM for sodium azide (NaN_3; Sigma-Aldrich, St. Louis, MO, USA Cat# S2002-100G); 4 mM, 8 mM, 16 mM, 20 mM, and 50 mM for 2-Deoxy-D-Glucose (2-DG; Sigma-Aldrich, St. Louis, MO, USA Cat# D8375-5G); and 0.02 µM for parbendazole (MedChem Express, Monmouth Junction, NJ, USA, CAS 14255879). The 0.02 µM application dosage was found to be the most effective compared to the others [27]. Stock concentrations of NaN_3 (4.14 mM), 2-DG (10 mM) and parbendazole (10mM) were prepared using dimethyl sulfoxide (DMSO, Sigma-Aldrich, St. Louis, MO, USA) and this solvent was also used as control at equal dilutions. A 500 µL measure of prepared solutions was added to the cells containing either substances or DMSO, and final concentrations of substances were used.

4.4. Myelinating Co-Cultures

Dissociated neuron/oligodendrocyte co-cultures were obtained from embryonic day 16 (E16) rat cerebral cortices (Wistar rats of either sex) according to [33]. Cortical cells were plated on 15 mm poly-D-lysine (0.1 mg/mL) coated coverslips (65,000 cells per coverslip) and kept in myelination medium consisting of N2 and neurobasal medium (ThermoFisher Scientific, Waltham, MA, USA; ratio 1:1) including NGF (50 ng/mL) and NT-3 (10 ng/mL) (both R&D Systems, Minneapolis, MN, USA). The day of primary culture was defined as day one in vitro (DIV1). After 10 days in vitro (DIV10), insulin was excluded, and the ratio of the insulin-free N2 to neurobasal medium including the B27 supplement (ThermoFisher Scientific) was adjusted to 4:1. This myelination medium was further supplemented with 60 ng/mL tri-iodo-thyronine (T3, Sigma-Aldrich, St. Louis, MO, USA). Final concentrations

of individual N2 medium components (DMEM-F12 based, high glucose; ThermoFisher Scientific) were insulin (10 µg/mL), transferrin (50 µg/mL), sodium selenite (5.2 ng/mL), hydrocortisone (18 ng/mL), putrescine (16 µg/mL), progesterone (6.3 ng/mL), biotin (10 ng/mL), N-acetyl-L-cysteine (5 µg/mL) (all Sigma-Aldrich St. Louis, MO, USA), bovine serum albumin (0.1%, Roth, Karlsruhe, Germany), and penicillin–streptomycin (50 units/mL, ThermoFisher Scientific). Co-cultures were kept for 17 days (DIV17) or 24 days (DIV24) in vitro, respectively, until a scratch assay was performed. During that time, the medium was exchanged every three days with the myelination medium.

4.5. Scratch Assay of Myelinating Co-Cultures and Stimulation

A scratch assay within the myelinating co-culture was performed on either DIV 17 or DIV 24 according to [48], with a few modifications. To this end, a 20 µL sterile pipette tip was used to generate a scratch on the cell surface from the upper part of the cover slip vertically down to the lower part of the cover slip. During this procedure, constant speed, 60–80° angle and moderate pressure were kept equal to gain comparable scratches with a similar width on all coverslips. Directly afterward, the scratch medium was exchanged with the new medium additionally containing 0.02 µM parbendazole or DMSO as control. Afterward, pictures of the scratch were taken 3 days (t1 = 0 h, t2 = 24 h, t3 = 48 h) in a row until fixation. Pictures were taken using the Nikon eclipse TE200 microscope in 20× magnification at the upper and the lower edge of the scratch. In between the picture acquisition, cells were placed back into the incubator at 37 °C, 5% CO_2.

4.6. Tamoxifen Administration

To generate NG2-positive cells in the tissue, tamoxifen (10 mg/mL, T5648, Sigma-Aldrich, St. Louis, MO, USA) dissolved in corn oil (Sigma-Aldrich, St. Louis, MO, USA) was administered (100 mg/kg body weight) intraperitoneally once per day for 5 consecutive days in order to induce Cre activity according to [18].

4.7. Induction of Cerebral Photothrombosis (cPT)

After tamoxifen injection, NG2-CreERT2 td Tomato mice had 1 week of recovery in order to give cells time to successfully express the red fluorescent protein td-Tomato in NG2-cells/OPCs, before the introduction of cerebral photothrombosis. Cerebral photothrombosis was induced according to [21]. Briefly, a fiber optic bundle coupled to a cold light source (Schott EL 1500, Mainz, Germany) was centered 2 mm posterior and 2.4 mm lateral from Bregma. After the intraperitoneal injection of 1 mg Rose Bengal (Sigma Aldrich, St. Louis, MO, USA), the brain was illuminated through the intact skull for 15 min. The dye was photochemically activated and caused sendothelial damage and thrombosis in the brain supplying vessels in the light cone and thus resulted in a circumscribed cerebral infarction. After the illumination was stopped, the skin was readapted using tissue adhesive and the animal was allowed to wake.

4.8. Preparation of Organotypic Coronal Slice Culture (OCSCs)

In general, the entire procedure from slice generation and slice transfer to culture should take less than one hour in order to reduce stress and preserve viability. Briefly, eleven-week-old NG2-CreERT2 td-Tomato mice were used for OCSCs which were prepared 3 days after induction of cerebral photothrombosis (cPT) (Figure 1). The induction of td-Tomato in $NG2^+$ cells was performed via intraperitoneal injection of 0.1 mL tamoxifen per day/animal for five days to induce Cre activity according to [18]. After one week of a recovery phase, cPT was performed according to [21], inducing a well-reproducible, stereotactically targeted ischemic damage by means of photo-activation of a previously injected photoactivable dye through the intact skull. Three days after the induction of cerebral photothrombosis, adult organotypic slice cultures (350 µm) were generated, adapted from [49]. Mice were deeply anesthetised by means of isoflurane, decapitated, and their brain was removed. To remove blood and hair from the brain, the brain was washed with ice-cold

sterile Hank's balanced salt solution (HBSS) (Gibco, Waltham, MA, USA Cat# 14025-050). The cerebellum and the brain stem were removed with a scalpel. Under aseptic conditions, the remaining brain was embedded in 4% low-melting-point agarose (Sigma-Aldrich Ca# A9414) in plastic embedding molds (Sakura, Umkirch, Germany, Tissue-Tek Cryomold Intermediate 15 mm × 15 mm × 15 mm Cat# 4566). The embedding mold was placed on ice until the agarose became solid. Thereafter, the agarose brain was glued to the magnetic platform of the HM 650 V vibratome (Thermo Scientific, Waltham, MA, USA) and was submerged in a chamber filled with ice-cold HBSS. The brain was trimmed until the stroke lesion occurred—Bregma [−0.82]–[−1.22]. Then, brain sections were cut with a thickness of 350 µm (cutting frequency: 50 Hz, cutting amplitude: 1.0, cutting speed: 0.9 mm/s). Slices were collected in a Petri dish with ice-cold HBSS, and then they were placed on cell culture inserts. From each brain, 8 slices were obtained. After two, four, or eight days of cultivation, the slices were fixed with 4% PFA and embedded for cryo-sectioning, allowing to quantify the contribution/differentiation dynamics of $NG2^+$ cells via serial immunohistochemical staining per slice (Figure 1).

4.9. Slice Culture Conditions and Stimulation

Millicell cell culture inserts measuring 0.4 µm (hydrophilic PTFE, pore size: 0.4 µm, diameter 30 mm) (Millipore, Tullagreen, Carrigtwohill, Ireland Ref# PICM0RG50) were transferred under sterile conditions into a 6-well plate. Prior to the preparation of the slices, inserts were covered with 1.2 mL serum-supplemented medium (SSM, Table 1), and the membrane was incubated for 1 h in the incubator at 37 °C and 5% CO_2. This equilibration step ensures the membrane's alignment with media humidity, temperature, and pH. After a short washing step in SSM, brain slices were transferred on the membrane of Milicell cell culture inserts, with 2 slices per insert, using a spatula, and inserts were placed onto 1 mL of SSM medium. Excess medium on top of the membrane was removed to guarantee an air–medium interface for proper oxygenation and attachment to the slice [50]. They were then incubated with the SSM medium for 2 h at 37 °C and 5% CO_2 in order to confer recovery from mechanical injury. After the recovery period, the medium was changed to serum-free medium (SFM, Table 1), given SFM's beneficial properties for neuronal and glial viability, as well as the structural integrity of adult organotypic slice cultures [49,51,52]. SFM medium of slices was supplemented with 0.02 µM parbendazole (10 mM stock, MedChem Express Monmouth Junction, NJ, USA, CAS 14255-87-9) or DMSO as control. The parbendazole stock concentration (10 mM) consisted of 13.33 mg/mL in DMSO, which was further diluted in SFM. The slices were cultured to a maximum of 8 days at 37 °C and 5% CO_2. The medium was exchanged every 2 days.

Table 1. (Media used for slice culture).

Medium	Composition	Supplier
Serum-free medium (SFM)	Neurobasal medium	Gibco Cat# 21103-049
	2% B27 supplement	Gibco Cat# 17504-044
	1% N2 supplement	Gibco Cat#17502-048
	1% L-Glutamine (×100)	Gibco
	0.5% Glucose	Sigma-Aldrich, Cat# SLBF1738V
	1% Antibiotic/antimycotic (×100)	Sigma-Aldrich, Cat# A5955
Serum-supplemented medium (SSM)	Neurobasal medium	Gibco Cat# 21103-049
	10% Fetal bovine serum (FBS)	Roth, Cat# 8076.2
	0.5% Glucose	Sigma-Aldrich, Cat# SLBF1738V
	1% Antibiotic/antimycotic (×100)	Sigma-Aldrich, Cat# A5955

4.10. TTC Staining

To show the viability of organotypic slices following eight days of cultivation, 2,3,5-Triphenyltetrazolium chloride (TTC) stainings were performed to allow the differentiation between infarcted (no staining) and living tissue (red staining). TTC indicates tissue viability and reveals the infarct size [24,25] (Figure 1). After 8 days of cultivation, organotypic slice cultures were incubated for 30 min in a 1% TTC solution at 37 °C. The TTC is enzymatically reduced by living cells to a red dye produced by dehydrogenase. For the TTC solution, 8 parts of 1.4% di-sodium-hydrogen phosphate-dihydrate (Merck Cat# 1.06580.5000) solution, and 2 parts of 1.2% sodium hydrogen-phosphate-monohydrate (Merck Cat#. 1.06586.2500) were mixed and 1% TTC (Sigma-Aldrich, St. Louis, MO, USA Cat# BCCC3620) were added. The solution was preheated at 37 °C and protected from light before usage. After 30 min, slices were mounted onto objective slides, which were covered on both sides with CitiFluor ™ (science services).

4.11. Fixation

Both neuron-oligodendrocyte co-culture and oligodendroglial cell culture were washed three times with PBS to remove cell debris and afterward fixed with 500 µL of 4% paraformaldehyde (PFA) for 15 min at room temperature (RT). Another three steps of washing with PBS followed in order to remove PFA residues. Cells were kept in PBS at 4 °C until staining.

Slices from NG2-CreERT2 td Tomato mice were fixed for immunohistochemistry. To this end, slices were washed 1× with PBS and thereafter fixed with 4% PFA for 15 min. To cover the whole slice with liquid, 1 mL was added underneath the membrane and 1 mL was added on top of the slice and the membrane. Afterwards, slices were washed once with PBS and transferred from the membrane into a new six-well plate filled with 3–4 mL of 30% sucrose (Roth, Karlsruhe, Germany Cat# 4661.2), diluted in PBS. The slices were kept in sucrose for 24–48 h to dehydrate slices for cryoprotection before being frozen in liquid nitrogen.

4.12. Embedding of Slices for Frozen Sections

For quantification analysis, 10× serial 10 µm thick coronal sections were obtained from a single coronal slice. To this end, slices were incubated overnight in 30% sucrose for cryoprotection before embedding in Tissue Tek and blocked at −20 °C. Next, a drop of Tissue Tek (Sakura, Finetek, Umkirch, Germany Cat# 4583) was added into a plastic embedding mold (Sakura, Finetek, Umkirch, Germany Tissue-Tek Cryomold Intermediate 15 mm × 15 mm × 15 mm Cat. No. 4566). The slice was transferred with a spatula and was placed on the drop of Tissue Tek. Then, the plastic embedding mold was filled with Tissue Tek, and the position of the slice was adjusted to be planar using a brush. The mold was then shortly transferred into cooled 2-Methylbutane, and 10 µm frozen sections were performed with a cryostate (Leica CM30505). Three frozen serial sections were collected on microscope slides (Superfrost Plus, Thermo Scientific, Waltham, MA, USA Cat# 10149870), and slides were then stored at −20 °C until IHC was performed.

4.13. Immunocytochemistry (ICC)

Fixed cells from oligodendrocyte mono cultures were permeabilized with PBS containing 0.01% Triton X-100 (Sigma-Aldrich), and unspecific staining was blocked with 10% normal goat serum or donkey serum (Sigma-Aldrich) for 40 min as established previously [33]. Cells were then incubated with primary antibodies in PBS with 10% normal goat serum or donkey serum overnight at 4 °C using rat anti-myelin basic protein (MBP; 1:250, Bio Rad., Munich, Germany; Cat# MCA409S RRID:AB_325004). Fixed co-cultures were blocked with PBS containing 0.5% Triton X-100 and 2% normal goat serum and then incubated overnight in 0.1% Triton and 2% normal goat serum containing mouse anti-oligodendrocyte transcription factor 2 (Olig2; 1:500, Merck Millipore, Billerica, MA, USA; Cat# MABN50 RRID:AB_10807410) and rabbit anti-Glial Fibrillary Acidic Protein (GFAP; 1:500, DAKO Agilent, Hamburg, Germany; Cat# Z0334 RRID:AB_10013382). For both culture systems,

coverslips were washed with PBS 24 h later and then incubated with secondary antibodies in PBS (diluted 1:500) for 2 h conjugated to goat anti-rat Alexa Fluor 488 (ThermoFisher Scientific; Cat# A-11006 RRID:AB_2534074), goat anti-mouse Alexa Fluor 594 (ThermoFisher Scientific; Cat# A11005 RRID:AB_10561507), goat anti-rabbit (ThermoFisher Scientific; Cat# A11037 RRID:AB_10561549), or goat anti-rat (ThermoFisher Scientific Cat# A-11007, RRID:AB_10561522). Nuclei were stained with 4′,6-diamidin-2-phenylindol (DAPI, Roche, Basel, Switzerland). Images (20×; Zeiss Axionplan2 microscope) were captured using the same light intensity and filters for all images to be compared and processed with Axiovision 4.2 software (Zeiss, Jena, Germany; RRID:SciRes_000111). The analysis was performed using Java software Version 1.54e (ImageJ, RRID:nif-0000-30,467/Wright Cell Imaging Facility, RRID:nif-0000-30,471). When ICC was performed on mono-culture, immunopositive cells were counted in nine randomly chosen fields per coverslip. For co-culture experiments, two coverslips were used per condition. The total number of cells per field was determined via DAPI staining. For quantification, the number of immune-positive cells was compared to the total cell number and expressed as percentage [mean ± standard error of the mean (SEM)].

4.14. Immunohistochemistry

For immunohistochemistry, the defrosted brain sections were air-dried for 10 min at R.T. and then rehydrated in dH_2O for 5 min. The microscopy slides with the brain sections were post-fixated in 4% PFA for 5 min and transferred to −20 °C cold acetone for another 5 min, before being washed with first TBS and then TBS-T (TBS containing 0.02% Triton) again for 5 min each. In order to block unspecific staining, slides were blocked with 100 µL 4% BSA, 5% NGS, 0.2% Triton X-100 in TBS for 30 min at R.T. Primary antibodies were diluted in the same solution used for blocking and were incubated overnight at 4 °C. This blocking and antibody solution composition was used for all antibodies except for the goat anti PDGFR-α antibody, where a concentration of 3% BSA and 5% normal donkey serum (NDS) was used, as the secondary antibodies' host was donkey. Slices were incubated with primary antibodies using the following dilutions: mouse anti-adenomatosis polyposis coli (CC1; 1:250, GeneTex Cat# GTX16794 RRID:AB_422404), rabbit anti-glial fibrillary acidic protein (GFAP; 1:10.000, DAKO Agilent, Hamburg, Germany; Cat# Z0334 RRID:AB_10013382), mouse anti-myelin basic protein (MBP; 1:250, Biolegend, San Diego, CA, USA, Cat# 836504 RRID:AB_2616694), goat anti-platelet derived growth factor receptor alpha (PDGFR-α; 1:250, Neuromics, Minneapolis, MN, USA catalog #GT15150-100 RRID:AB_2737233), goat anti-sex determining region Y-box 10 (Sox10; 1:200, R&D System, Minneapolis, MN, USA, Cat#AF2864; RRID: AB_442208), mouse anti-breast carcinoma amplified sequence 1 (BCAS1; 1:250, Santa Cruz Cat# Cat# sc-136342, RRID:AB_10839529), and rabbit anti-ionized calcium binding adaptor molecule 1 (Iba1; 1:500, WAKO Pure Chemical Corporation, Osaka, Japan; RRID: AB_839504). After 24 h, slices were washed twice in 1xTBS for 5 min each, and secondary antibodies were diluted 1:200 and applied for 2 h at R.T. along with 4′,6-diamidino-2-phenylindol (DAPI, 1:50) in PBS. The following secondary antibodies were used: goat anti-rat Alexa Fluor 488 (1:200, Thermo Fisher Scientific Cat# A-11006, RRID:AB_2534074); goat anti-rabbit Alexa Fluor 488 (1:200, Thermo Fisher Scientific Cat# A-11008, RRID:AB_143165); goat anti-mouse Alexa Fluor 488 (1:200, Thermo Fisher Scientific Cat# A32728, RRID:AB_2633277), and donkey anti-goat Alexa Fluor 488 (1:200, Thermo Fisher Scientific Cat# A11055 RRID:AB_2534102). After this incubation step, slices were washed first in 0.2% TBS-T and subsequently in TBS for 5 min each. Finally, mounting was performed with Fluoromount g (Thermo Fisher Scientific, Waltham, MA, USA). Stained slides were kept at 4 °C until image acquisition.

4.15. Data Analysis

The immunostaining was analyzed with a Zeiss Axioplan 2 fluorescence microscope (Zeiss) and the software Axiovision 4.2 (Zeiss). Images of coronal cross-sections within the lesion location Bregma [−0.82]–[−1.22] were taken using 20× magnification. Regions

of interest (ROIs) were defined by an overlay micrograph comprising 4 images (1 image measures 2195 × 1949 pixel or 482 × 428 µm, with an overlay of boxes from 5%) within the penumbra at the border zone between intact and lesioned tissue at the right hemisphere (see Figure 4). All data were verified in this area. The number of cells that were positive for each marker was counted by using the Java software ImageJ Version 1.54e (ImageJ).

4.16. Statistical Analysis

Data are shown as mean values ± standard deviation (mean ± SD). GraphPad Prism 7.0.2 (GraphPad Prism, San Diego, CA, USA, RRID: rid_000081) was used for statistics and graphics collection. To assess the absence of Gaussian distribution, the Shapiro–Wilk normality test was used for all data sets. Student's *t*-test was applied for comparing two groups, and two-way analysis of variance (ANOVA) with Tukey post-test for multiple comparisons was applied to compare three or more groups. For data sets not passing the Shapiro–Wilk normality test, the Mann–Whitney U comparing two groups and the Kruskal–Wallis test with Dunn's post-test for multiple comparisons of three or more groups were applied. p values are defined as follows: * represents $p \leq 0.05$; ** represents $p \leq 0.01$; *** represents $p \leq 0.001$. The absence of asterisks means no statistically significant difference was observed. n represents the number of independent experiments.

5. Conclusions

Taken together, the study here presented introduces an ex vivo model that has the potential to improve and facilitate stroke research. Furthermore, we could identify parbendazole as a promising treatment to enhance post-stroke recovery.

Author Contributions: L.W. performed the majority of the experiments, data analysis, and interpretation. M.G. was involved in experimental design and data interpretation. N.R. performed parts of the slice culture experiments. G.P. was involved in the execution of photothrombosis. L.R. and M.S.O.J. provided support in data interpretation and data presentation. J.G. performed parts of immunohistochemical staining. F.K. and S.G.M. were involved in data interpretation and text writing. P.K. was involved in conceptualization and data interpretation, text review/editing, and funding acquisition. P.G. was involved in the conceptualization and direction of the study, experimental design, funding acquisition, data analysis, and interpretation. P.G. conceived the final project and wrote the manuscript. All authors have read and agreed to the published version of the manuscript.

Funding: This research was funded by the Christiane and Claudia Hempel Foundation for clinical stem cell research and the James and Elisabeth Cloppenburg, Peek and Cloppenburg Düsseldorf Stiftung.

Institutional Review Board Statement: Cerebral photothrombosis induced cortical ischemia experiments were approved by the authorities at LANUV (Landesamt für Natur, Umwelt und Verbraucherschutz NordrheinWestfalen; Az.: 81-02.04.2018.A275) and carried out according to ARRIVE guide-lines. The animals were bred under defined conditions with access to food and water ad libitum in the animal facility (ZETT) of the Heinrich-Heine-University Düsseldorf. For the preparation of rat myelinating co-cultures and OPC mono-culture experiments cerebral cortices of Wistar rats with either sex were used; AZ.: 81-02.04.2018.A388. For adult organotypic cortical slice culture, ten- to twelve-week-old transgenic NG2-CreERT2 td-Tomato mice of either sex were used.

Informed Consent Statement: Not applicable.

Data Availability Statement: The data sets used and/or analyzed during the current study are available from the corresponding author on reasonable request.

Acknowledgments: We thank Brigida Ziegler, Zippora Kohne, and Birgit Blomenkamp (all Düsseldorf) for their technical assistance.

Conflicts of Interest: Declare no conflict of interest. The funders had no role in the design of the study.

Abbreviations

2-DG	2-deoxy-D-glucose
BCAS1	Breast carcinoma amplified sequence 1
BDNF	Brain derived growth factor
BSA	Bovine serum albumin
CC1	Monoclonal antibody anti-adenomatous polyposis coli (APC) clone
CNS	Central nervous system
cPT	Cerebral photothrombosis
DAPI	4′,6-diamidin-2-phenylindol
DMSO	Dimethylsulfoxid
DOAJ	Directory of open access journals
DIV	Days in vitro
FBS	Fetal bovine serum
GFAP	Glial fibrillary acidic protein
HBSS	Hank's balanced salt solution
ICC	Immunocytochemistry
IHC	Immunohistochemistry
IRB	Institutional Review Board
LD	Linear dichroism
MBP	Myelin basic protein
MDPI	Multidisciplinary Digital Publishing Institute
NaN3	sodium azide
NDS	Normal donkey serum
NG2	Neural/glial antigen 2
NGF	Nerf growth factor
NGS	Normal goat serum
Olig2	Oligodendrocyte transcription factor 2
OL	Oligodendrocyte
OPC	Oligodendroglial precursor cell
OCSC	Organotypic coronal slice culture
PDGFR-α	Platelet-derived growth factor receptor alpha
PDL	Poly-D-lysine
PFA	Paraformaldehyde
PBS	Phosphate buffered saline
ROI	Region of interest
RT	Room temperature
SD	Standard deviation
SEM	Standard error of the mean
SFM	Serum-free medium
SSM	Serum-supplemented medium
SOX10	SRY (sex determining region Y) -Box Transcription Factor 10
T3	Tri-iodo-thyronine
tdT^+	td-Tomato positive cells
TLA	Three letter acronym
TTC	2,3,5-Triphenyltetrazolium chloride
wt	Wild type

References

1. Dewar, D.; Underhill, S.M.; Goldberg, M.P. Oligodendrocytes and ischemic brain injury. *J. Cereb. Blood Flow Metab.* **2003**, *23*, 263–274. [CrossRef]
2. Xu, S.; Lu, J.; Shao, A.; Zhang, J.H.; Zhang, J. Glial Cells: Role of the Immune Response in Ischemic Stroke. *Front. Immunol.* **2020**, *11*, 294. [CrossRef]
3. Zhou, J.; Zhuang, J.; Li, J.; Ooi, E.; Bloom, J.; Poon, C.; Lax, D.; Rosenbaum, D.M.; Barone, F.C. Long-term post-stroke changes include myelin loss, specific deficits in sensory and motor behaviors and complex cognitive impairment detected using active place avoidance. *PLoS ONE* **2013**, *8*, e57503. [CrossRef]
4. Garcia-Martin, G.; Alcover-Sanchez, B.; Wandosell, F.; Cubelos, B. Pathways Involved in Remyelination after Cerebral Ischemia. *Curr. Neuropharmacol.* **2022**, *20*, 751–765. [CrossRef] [PubMed]

5. Lassmann, H. Multiple Sclerosis Pathology. *Cold Spring Harb. Perspect. Med.* **2018**, *8*, a028936. [CrossRef]
6. Simons, M.; Nave, K.A. Oligodendrocytes: Myelination and Axonal Support. *Cold Spring Harb. Perspect. Biol.* **2015**, *8*, a020479. [CrossRef]
7. Tognatta, R.; Miller, R.H. Contribution of the oligodendrocyte lineage to CNS repair and neurodegenerative pathologies. *Neuropharmacology* **2016**, *110 Pt B*, 539–547. [CrossRef]
8. Zhang, R.; Chopp, M.; Zhang, Z.G. Oligodendrogenesis after cerebral ischemia. *Front. Cell. Neurosci.* **2013**, *7*, 201. [CrossRef] [PubMed]
9. Itoh, K.; Maki, T.; Lok, J.; Arai, K. Mechanisms of cell-cell interaction in oligodendrogenesis and remyelination after stroke. *Brain Res.* **2015**, *1623*, 135–149. [CrossRef] [PubMed]
10. Lo, E.H. A new penumbra: Transitioning from injury into repair after stroke. *Nat. Med.* **2008**, *14*, 497–500. [CrossRef] [PubMed]
11. Cheng, J.; Shen, W.; Jin, L.; Pan, J.; Zhou, Y.; Pan, G.; Xie, Q.; Hu, Q.; Wu, S.; Zhang, H.; et al. Treadmill exercise promotes neurogenesis and myelin repair via upregulating Wnt/beta-catenin signaling pathways in the juvenile brain following focal cerebral ischemia/reperfusion. *Int. J. Mol. Med.* **2020**, *45*, 1447–1463. [PubMed]
12. Bonfanti, E.; Gelosa, P.; Fumagalli, M.; Dimou, L.; Vigano, F.; Tremoli, E.; Cimino, M.; Sironi, L.; Abbracchio, M.P. The role of oligodendrocyte precursor cells expressing the GPR17 receptor in brain remodeling after stroke. *Cell Death Dis.* **2017**, *8*, e2871. [CrossRef]
13. Sozmen, E.G.; Rosenzweig, S.; Llorente, I.L.; DiTullio, D.J.; Machnicki, M.; Vinters, H.V.; Havton, L.A.; Giger, R.J.; Hinman, J.D.; Carmichael, S.T. Nogo receptor blockade overcomes remyelination failure after white matter stroke and stimulates functional recovery in aged mice. *Proc. Natl. Acad. Sci. USA* **2016**, *113*, E8453–E8462. [CrossRef] [PubMed]
14. Kang, S.H.; Fukaya, M.; Yang, J.K.; Rothstein, J.D.; Bergles, D.E. NG2+ CNS glial progenitors remain committed to the oligodendrocyte lineage in postnatal life and following neurodegeneration. *Neuron* **2010**, *68*, 668–681. [CrossRef] [PubMed]
15. Hernandez, I.H.; Villa-Gonzalez, M.; Martin, G.; Soto, M.; Perez-Alvarez, M.J. Glial Cells as Therapeutic Approaches in Brain Ischemia-Reperfusion Injury. *Cells* **2021**, *10*, 1639. [CrossRef] [PubMed]
16. Rosenzweig, S.; Carmichael, S.T. The axon-glia unit in white matter stroke: Mechanisms of damage and recovery. *Brain Res.* **2015**, *1623*, 123–134. [CrossRef]
17. Shi, H.; Hu, X.; Leak, R.K.; Shi, Y.; An, C.; Suenaga, J.; Chen, J.; Gao, Y. Demyelination as a rational therapeutic target for ischemic or traumatic brain injury. *Exp. Neurol.* **2015**, *272*, 17–25. [CrossRef]
18. Huang, W.; Zhao, N.; Bai, X.; Karram, K.; Trotter, J.; Goebbels, S.; Scheller, A.; Kirchhoff, F. Novel NG2-CreERT2 knock-in mice demonstrate heterogeneous differentiation potential of NG2 glia during development. *Glia* **2014**, *62*, 896–913. [CrossRef]
19. Chang, A.; Nishiyama, A.; Peterson, J.; Prineas, J.; Trapp, B.D. NG2-positive oligodendrocyte progenitor cells in adult human brain and multiple sclerosis lesions. *J. Neurosci.* **2000**, *20*, 6404–6412. [CrossRef]
20. Song, F.E.; Huang, J.L.; Lin, S.H.; Wang, S.; Ma, G.F.; Tong, X.P. Roles of NG2-glia in ischemic stroke. *CNS Neurosci.* **2017**, *23*, 547–553. [CrossRef]
21. Gliem, M.; Krammes, K.; Liaw, L.; van Rooijen, N.; Hartung, H.P.; Jander, S. Macrophage-derived osteopontin induces reactive astrocyte polarization and promotes re-establishment of the blood brain barrier after ischemic stroke. *Glia* **2015**, *63*, 2198–2207. [CrossRef]
22. Finley, M.; Fairman, D.; Liu, D.; Li, P.; Wood, A.; Cho, S. Functional validation of adult hippocampal organotypic cultures as an in vitro model of brain injury. *Brain Res.* **2004**, *1001*, 125–132. [CrossRef] [PubMed]
23. Humpel, C. Organotypic brain slice cultures: A review. *Neuroscience* **2015**, *305*, 86–98. [CrossRef] [PubMed]
24. Benedek, A.; Moricz, K.; Juranyi, Z.; Gigler, G.; Levay, G.; Harsing, L.G., Jr.; Matyus, P.; Szenasi, G.; Albert, M. Use of TTC staining for the evaluation of tissue injury in the early phases of reperfusion after focal cerebral ischemia in rats. *Brain Res.* **2006**, *1116*, 159–165. [CrossRef] [PubMed]
25. Hatfield, R.H.; Mendelow, A.D.; Perry, R.H.; Alvarez, L.M.; Modha, P. Triphenyltetrazolium chloride (TTC) as a marker for ischaemic changes in rat brain following permanent middle cerebral artery occlusion. *Neuropathol. Appl. Neurobiol.* **1991**, *17*, 61–67. [CrossRef] [PubMed]
26. Fard, M.K.; van der Meer, F.; Sanchez, P.; Cantuti-Castelvetri, L.; Mandad, S.; Jakel, S.; Fornasiero, E.F.; Schmitt, S.; Ehrlich, M.; Starost, L.; et al. BCAS1 expression defines a population of early myelinating oligodendrocytes in multiple sclerosis lesions. *Sci. Transl. Med.* **2017**, *9*, eaam7816. [CrossRef]
27. Manousi, A.; Göttle, P.; Reiche, L.; Cui, Q.L.; Healy, L.M.; Akkermann, R.; Gruchot, J.; Schira-Heinen, J.; Antel, J.P.; Hartung, H.P.; et al. Identification of novel myelin repair drugs by modulation of oligodendroglial differentiation competence. *EBioMedicine* **2021**, *65*, 103276. [CrossRef] [PubMed]
28. Havercroft, J.C.; Quinlan, R.A.; Gull, K. Binding of parbendazole to tubulin and its influence on microtubules in tissue-culture cells as revealed by immunofluorescence microscopy. *J. Cell Sci.* **1981**, *49*, 195–204. [CrossRef]
29. Lo, Y.C.; Senese, S.; France, B.; Gholkar, A.A.; Damoiseaux, R.; Torres, J.Z. Computational Cell Cycle Profiling of Cancer Cells for Prioritizing FDA-Approved Drugs with Repurposing Potential. *Sci. Rep.* **2017**, *7*, 11261. [CrossRef]
30. Foster, K.E.; Burland, T.G.; Gull, K. A mutant beta-tubulin confers resistance to the action of benzimidazole-carbamate microtubule inhibitors both in vivo and in vitro. *Eur. J. Biochem.* **1987**, *163*, 449–455. [CrossRef]
31. Raff, M.C.; Miller, R.H.; Noble, M. A glial progenitor cell that develops in vitro into an astrocyte or an oligodendrocyte depending on culture medium. *Nature* **1983**, *303*, 390–396. [CrossRef] [PubMed]

32. Noble, M.; Wolswijk, G.; Wren, D. The complex relationship between cell division and the control of differentiation in oligodendrocyte-type-2 astrocyte progenitor cells isolated from perinatal and adult rat optic nerves. *Prog. Growth Factor Res.* **1989**, *1*, 179–194. [CrossRef]
33. Göttle, P.; Sabo, J.K.; Heinen, A.; Venables, G.; Torres, K.; Tzekova, N.; Parras, C.M.; Kremer, D.; Hartung, H.P.; Cate, H.S.; et al. Oligodendroglial maturation is dependent on intracellular protein shuttling. *J. Neurosci.* **2015**, *35*, 906–919. [CrossRef]
34. Pang, Y.; Zheng, B.; Kimberly, S.L.; Cai, Z.; Rhodes, P.G.; Lin, R.C. Neuron-oligodendrocyte myelination co-culture derived from embryonic rat spinal cord and cerebral cortex. *Brain Behav.* **2012**, *2*, 53–67. [CrossRef] [PubMed]
35. Gasterich, N.; Bohn, A.; Sesterhenn, A.; Nebelo, F.; Fein, L.; Kaddatz, H.; Nyamoya, S.; Kant, S.; Kipp, M.; Weiskirchen, R.; et al. Lipocalin 2 attenuates oligodendrocyte loss and immune cell infiltration in mouse models for multiple sclerosis. *Glia* **2022**, *70*, 2188–2206. [CrossRef] [PubMed]
36. Engels, M.; Kalia, M.; Rahmati, S.; Petersilie, L.; Kovermann, P.; van Putten, M.; Rose, C.R.; Meijer, H.G.E.; Gensch, T.; Fahlke, C. Glial Chloride Homeostasis Under Transient Ischemic Stress. *Front. Cell. Neurosci.* **2021**, *15*, 735300. [CrossRef]
37. Tajiri, N.; Dailey, T.; Metcalf, C.; Mosley, Y.I.; Lau, T.; Staples, M.; van Loveren, H.; Kim, S.U.; Yamashima, T.; Yasuhara, T.; et al. In vivo animal stroke models: A rationale for rodent and non-human primate models. *Transl. Stroke Res.* **2013**, *4*, 308–321. [CrossRef]
38. Maestri, E. The 3Rs Principle in Animal Experimentation: A Legal Review of the State of the Art in Europe and the Case in Italy. *BioTech* **2021**, *10*, 9. [CrossRef]
39. Finney, C.A.; Shvetcov, A.; Westbrook, R.F.; Morris, M.J.; Jones, N.M. Tamoxifen offers long-term neuroprotection after hippocampal silent infarct in male rats. *Horm. Behav.* **2021**, *136*, 105085. [CrossRef]
40. Pineau, H.; Sim, V. POSCAbilities: The Application of the Prion Organotypic Slice Culture Assay to Neurodegenerative Disease Research. *Biomolecules* **2020**, *10*, 1079. [CrossRef]
41. Khodanovich, M.Y.; Gubskiy, I.L.; Kudabaeva, M.S.; Namestnikova, D.D.; Kisel, A.A.; Anan'ina, T.V.; Tumentceva, Y.A.; Mustafina, L.R.; Yarnykh, V.L. Long-term monitoring of chronic demyelination and remyelination in a rat ischemic stroke model using macromolecular proton fraction mapping. *J. Cereb. Blood Flow Metab.* **2021**, *41*, 2856–2869. [CrossRef]
42. Tanaka, K.; Nogawa, S.; Ito, D.; Suzuki, S.; Dembo, T.; Kosakai, A.; Fukuuchi, Y. Activation of NG2-positive oligodendrocyte progenitor cells during post-ischemic reperfusion in the rat brain. *Neuroreport* **2001**, *12*, 2169–2174. [CrossRef]
43. Ahrendsen, J.T.; Grewal, H.S.; Hickey, S.P.; Culp, C.M.; Gould, E.A.; Shimizu, T.; Strnad, F.A.; Traystman, R.J.; Herson, P.S.; Macklin, W.B. Juvenile striatal white matter is resistant to ischemia-induced damage. *Glia* **2016**, *64*, 1972–1986. [CrossRef] [PubMed]
44. Bai, X.; Zhao, N.; Koupourtidou, C.; Fang, L.P.; Schwarz, V.; Caudal, L.C.; Zhao, R.; Hirrlinger, J.; Walz, W.; Bian, S.; et al. In the mouse cortex, oligodendrocytes regain a plastic capacity, transforming into astrocytes after acute injury. *Dev. Cell* **2023**, *in press*. [CrossRef]
45. Belgodere, E.; Bossio, R.; Parrini, V.; Pepino, R. Imidazole derivatives with potential biological activity. *Arzneimittelforschung* **1980**, *30*, 1051–1056. [CrossRef]
46. Li, N.; Song, X.; Wu, L.; Zhang, T.; Zhao, C.; Yang, X.; Shan, L.; Yu, P.; Sun, Y.; Wang, Y.; et al. Miconazole stimulates post-ischemic neurogenesis and promotes functional restoration in rats. *Neurosci. Lett.* **2018**, *687*, 94–98. [CrossRef]
47. Langhnoja, J.; Buch, L.; Pillai, P. Potential role of NGF, BDNF, and their receptors in oligodendrocytes differentiation from neural stem cell: An in vitro study. *Cell Biol. Int.* **2021**, *45*, 432–446. [CrossRef] [PubMed]
48. Pinto, B.I.; Cruz, N.D.; Lujan, O.R.; Propper, C.R.; Kellar, R.S. In Vitro Scratch Assay to Demonstrate Effects of Arsenic on Skin Cell Migration. *J. Vis. Exp.* **2019**, *144*, e58838.
49. Tan, G.A.; Furber, K.L.; Thangaraj, M.P.; Sobchishin, L.; Doucette, J.R.; Nazarali, A.J. Organotypic Cultures from the Adult CNS: A Novel Model to Study Demyelination and Remyelination Ex Vivo. *Cell. Mol. Neurobiol.* **2018**, *38*, 317–328. [CrossRef]
50. Yoon, J.J.; Nicholson, L.F.; Feng, S.X.; Vis, J.C.; Green, C.R. A novel method of organotypic brain slice culture using connexin-specific antisense oligodeoxynucleotides to improve neuronal survival. *Brain Res.* **2010**, *1353*, 194–203. [CrossRef]
51. Hassen, G.W.; Tian, D.; Ding, D.; Bergold, P.J. A new model of ischemic preconditioning using young adult hippocampal slice cultures. *Brain Res. Brain Res. Protoc.* **2004**, *13*, 135–143. [CrossRef] [PubMed]
52. Kim, H.; Kim, E.; Park, M.; Lee, E.; Namkoong, K. Organotypic hippocampal slice culture from the adult mouse brain: A versatile tool for translational neuropsychopharmacology. *Prog. Neuropsychopharmacol. Biol. Psychiatry* **2013**, *41*, 36–43. [CrossRef] [PubMed]

NEURAL REGENERATION RESEARCH
www.nrronline.org

Review

Star power: harnessing the reactive astrocyte response to promote remyelination in multiple sclerosis

Markley Silva Oliveira Junior[1, #], Laura Reiche[1, #], Emerson Daniele[2, 3], Ines Kortebi[2, 3], Maryam Faiz[2, 3], Patrick Küry[1, *]

https://doi.org/10.4103/1673-5374.380879

Date of submission: January 27, 2023

Date of decision: May 5, 2023

Date of acceptance: May 23, 2023

Date of web publication: July 20, 2023

Abstract

Astrocytes are indispensable for central nervous system development and homeostasis. In response to injury and disease, astrocytes are integral to the immunological- and the, albeit limited, repair response. In this review, we will examine some of the functions reactive astrocytes play in the context of multiple sclerosis and related animal models. We will consider the heterogeneity or plasticity of astrocytes and the mechanisms by which they promote or mitigate demyelination. Finally, we will discuss a set of biomedical strategies that can stimulate astrocytes in their promyelinating response.

Key Words: astrocytes; demyelination; drug-based therapies; myelin repair; oligodendrocyte precursor cells; reactive astrogliosis

From the Contents

Introduction	578
Search Strategy and Selection Criteria	578
Reactive Astrocytes in Multiple Sclerosis: Friend or Foe?	578
Genes/Factors Associated with Diverse Astrocyte Subtypes in Multiple Sclerosis	579
Repairing Multiple Sclerosis: How to Modulate Repair via Reactive Astrocytes?	580
Concluding Remarks	581

Introduction

Multiple sclerosis (MS, **Box 1**) is a debilitating autoimmune disease characterized by chronic damage to myelin. Previous research has focused on the immune compartment in the development and progression of MS as reviewed in (Dendrou et al., 2015; Prinz and Priller, 2017); however, there is emerging evidence that central nervous system (CNS) resident cells also contribute to MS pathology (Healy et al., 2022). Specifically, astrocytes that become reactive in response to injury or disease, have been shown to influence diverse mechanisms involved in the pathology of MS (reviewed by Ponath et al., 2018), hence play also a crucial role in demyelination and remyelination (**Box 2**). Astrocytes can trigger demyelination through primary damage to myelin (Wan et al., 2022) or oligodendrocytes via the upregulation of for example apoptosis-related interleukins (Sanchis et al., 2020; Bretheau et al., 2022). In contrast, astrocytes can promote remyelination through the secretion of trophic factors that aid the maturation and/or differentiation of precursors (OPCs) (Butti et al., 2019; Lohrberg et al., 2020). An emerging question in neurobiology is: how many and how different are the astrocyte types that drive disease pathology? As per a recent consensus article (Escartin et al., 2021), the determination of reactive astrocyte diversity relies on identifying profiles according to a combined evaluation of the CNS region, tissue type (developing, healthy or diseased), sex, and species analyzed together with their functional profiles, multi-omic (transcriptomic, proteomic, epigenomic, etc.) signatures, and morphologies (Escartin et al., 2021).

Nonetheless, transcriptomic evaluations of astrocytes have begun to identify gene expression signatures that are associated with diverse functional types. For example - and in the absence of a new applicable classification - "A1" astrocytes whose gene signature includes complement component 3 (C3) expression have previously been associated with a neurotoxic phenotype (Zamanian et al., 2012; Liddelow et al., 2017; Guttenplan et al., 2021). These C3-expressing astrocytes are present in MS (Liddelow et al., 2017) and its animal model, experimental autoimmune encephalomyelitis (EAE, **Box 3**) (Tassoni et al., 2019). Another "A1" gene signature is depicted by high transcript levels of MAF bZIP transcription factor G (*Mafg*) and methionine adenosyltransferase 2 alpha (*Mat2α*) but concurrent low transcript expression for nuclear factor erythroid 2-related factor 2 (*Nrf2*), which is associated with a proinflammatory phenotype in EAE (Wheeler et al., 2020). These markers could recently also be identified in the chronic cuprizone (CPZ)-mediated animal model for MS (**Box 3**) (Silva Oliveira Junior et al., 2022). However, as defined by Escartin et al. (2021), astrocytes likely exist as a continuum of diverse states and functions, depending on context, hence do not polarize into simple binary phenotypes such as "good (A1)" or "bad (A2)", but can even show simultaneous features/signatures assigned to neuroprotective or neurotoxic functions (Das et al., 2020; Hasel et al., 2021; Silva Oliveira Junior et al., 2022).

Ultimately, the understanding of astrocyte diversity is important when considering (astrocyte-mediated) therapeutic strategies for MS. Interestingly, Gorter and Baron (2022) recently listed a few Food and Drug Administration (FDA)-approved agents for MS, such as siponimod, as well as novel promyelinating compounds that may exert their beneficial effects via astrocyte modulation. Whether their mode of action relies on the manipulation of diverse astrocyte types is an outstanding question.

In this review, we will examine astrocyte types in MS through the lens of de- and remyelination. We will also highlight current treatment strategies that alter the balance of astrocyte types to promote remyelination.

Search Strategy and Selection Criteria

The authors obtained their information from published articles collected using databases PubMed (NLM, National Library of Medicine), ScienceDirect (Elsevier), and Web of Science (Clarivate) until December 2022. Keywords and terms such as multiple sclerosis, astrocyte(s), white matter, de-/remyelination, pro-recovery, pro-inflammatory, and specific markers such as Lcn2, S100a10, and Mafg were either used individually or in combination to search appropriate information without limiting the year of publication. However, this review aimed at citing the most recent articles, whilst older original publications describing initial findings were also necessary to cite.

Reactive Astrocytes in Multiple Sclerosis: Friend or Foe?

Historically, reactive astrogliosis was interpreted as an unchangeable maladaptive response, and ablation of this mechanism was thought to be beneficial (Jäkel and Dimou, 2017). More recent studies have shown that astrocytes play roles in both demyelination ("pro-disease") and remyelination ("pro-recovery") processes. Note, those reactive astrocytes naturally compose the normal appearing white matter and grey matter areas in MS lesions (Schirmer et al., 2021; Trobisch et al., 2022), highlighting their contribution also in the early phases of MS.

[1]Department of Neurology, Neuroregeneration laboratory, Medical Faculty, Heinrich-Heine-University, Düsseldorf, Germany; [3]Institute of Medical Science, University of Toronto, Toronto, Canada; [3]Division of Anatomy, Department of Surgery, University of Toronto, Toronto, Canada

*__Correspondence to:__ Patrick Küry, PhD, kuery@uni-duesseldorf.de.

https://orcid.org/0000-0002-2654-1126 (Patrick Küry)

#Both authors contributed equally to this article.

Funding: *This work was supported by the Heart and Stroke Foundation and Ontario Institute of Regenerative Medicine (New Ideas Grant), Canada First Research Excellence Fund (Medicine by Design), the National Sciences and Engineering Research Council, the Jürgen Manchot Foundation, the Christiane and Claudia Hempel Foundation for Clinical Stem Cell Research and the James and Elisabeth Cloppenburg, Peek and Cloppenburg Düsseldorf Stiftung (to PK).*

How to cite this article: *Silva Oliveira Junior M, Reiche L, Daniele E, Kortebi I, Faiz M, Küry P (2024) Star power: harnessing the reactive astrocyte response to promote remyelination in multiple sclerosis. Neural Regen Res 19(4):578-582.*

Box 1 | Multiple sclerosis (MS) at a glance

The chronic, inflammatory, demyelinating, and neurodegenerative central nervous system (CNS) disorder multiple sclerosis (MS) is an immune-mediated disease caused by complex interactions between several cell types (leucocytes, CNS-resident innate cells) and gene-environment axis (extensively reviewed by Filippi et al., 2018 and Dobson and Giovannoni, 2019). Focal lesions/plaques, the regions of demyelination that are pathological hallmarks of all MS phenotypes, are found in the white and grey matter and can occur in the brain, optic nerve, and spinal cord (Gilmore et al., 2009; Green et al., 2010; Petrova et al., 2018).

The appearance and development of symptoms (wide-ranging, e.g., sensory-, motor- and or visual impairments, cognitive deficits, memory loss, and many more) can vary and also depend on the disease stages. While most patients experience a relapsing-remitting MS (RRMS) disease course, a minor fraction of patients suffers from primary-progressive MS (PPMS). RRMS is characterized by an abrupt onset of symptoms that fade over time, yet recovery of lesions varies between patients. Most symptoms arise during the relapsing stages when immune attacks occur. Here, cells of the innate and adaptive immune systems (myeloid cells, $CD4^+$ and $CD8^+$ T cells, and B cells) infiltrate the CNS parenchyma, distributing perivascularly around post-capillary venules of the blood-brain barrier (BBB). Through cell interactions and induced secretion of soluble factors [cytokines, lipids, reactive oxygen species (ROS), and others], infiltrating immune cells together with CNS-resident activated microglia and astrocytes contribute to oligodendrocyte injury, demyelination, and axonal damage (Filippi et al., 2018; Li et al., 2018). Eventually and over time, also in these patients a more progressive disease course is observed with no more apparent immune cell infiltration but ongoing and over taking neurodegenerative processes to occur.

Such other factors contributing to neurodegeneration and ongoing tissue injury (Filippi et al., 2018) include acute or chronic oxidative stress via innate and adaptive immune cell activation, loss of (myelin) trophic support, altered glutamate homeostasis, and a pro-inflammatory environment that may be driven by meningeal immune cell infiltrates and CNS-innate microglia and astrocytes in MS active lesions.

Over time, demyelinated tissues undergo scarification, which is organized by astrocytes, meningeal cells, and infiltrating peripheral immune cells. Scarification aims to decrease brain tissue destruction; however, it also enhances disability and disease progression.

Box 2 | Remyelination – regenerative but insufficient process in multiple sclerosis (MS)

Demyelination, or loss of myelin is followed by a spontaneous, regenerative response, called remyelination. Remyelination is a complicated multi-step process that can reverse deficits in conduction and aims to protect unsheathed axons from secondary degeneration. In the central nervous system (CNS), remyelination is mediated by newly generated oligodendrocytes. Both parenchymal oligodendrocyte precursor cells (OPCs), a population of widespread resident adult multipotent progenitors that comprise 5% of total brain cells (Franklin et al., 2021), and neural stem cells (NSCs) located within the germinal niche can generate such new oligodendrocytes. Moreover, even Schwann cells (SCs), the myelinating glia of the peripheral nervous system (PNS), were revealed to contribute to this CNS regenerative response (reviewed by Chen et al., 2021). Briefly, OPCs migrate to lesion sites (Levine and Reynolds, 1999), (eventually) proliferate (Choi et al., 2018) and predominantly differentiate into new myelin-forming oligodendrocytes. Nonetheless, extended myelin damage as well as a number of identified inhibitory components (Kremer et al., 2011) impede subventricular zone (SVZ)- and parenchymal-derived OPCs from maturating (see Figure 1), impairing a last-long reparative response of such progenitors (Xing et al., 2014; Brousse et al., 2015). In general, remyelination depends on several factors and steps, such as pivotal myelin debris clearance via e.g. microglia (Kotter, 2006; Lampron et al., 2015) or accurate OPC differentiation, easily disrupted via pro-inflammatory milieu induced by infiltrating leucocytes and CNS-innate glial cells (microglia, astrocytes), rendering it susceptible to an inadequate/insufficient process.

Box 3 | Short note on animal models used for multiple sclerosis (MS)

To investigate pathological mechanisms of MS and study therapeutic interventions, several animal models have been developed to mimic specific aspects of MS pathology, particularly the acute inflammatory stage (reviewed by Gharagozloo et al., 2022 and Leo and Kipp, 2022). The most commonly used (and within this review cited) models are the toxin-mediated oligodendrocyte death and demyelination inducing cuprizone (CPZ) model and the experimental autoimmune encephalomyelitis (EAE), which results in a T cell-mediated autoimmune attack against myelin sheaths via systemic injection of myelin peptides together with an adjuvant.

As Gorter and Baron (2022) highlighted, further complexity in studying MS is added by the indication that demyelinating and ongoing remyelination processes coexist. However, in experimental animal models for MS, demyelination, and remyelination are often considered to be separated processes occurring at different time points; hence none of the existing MS models can fully replicate the actual biology of chronic demyelination in MS. Nevertheless, these models showed to exhibit similarities in underlying pathways associated with immune and astroglial responses, neurodegeneration, oligodendroglial damage, and remyelination deficits some of which are described in more detail in this review.

Masvekar et al. (2019) identified several biomarkers via cerebrospinal fluid analysis of MS patients that possibly enable a correlation between MS progression, toxic astrogliosis, and microglial activation. Seen from a physiological point of view, astrocytes (together with endothelial cells and pericytes) mediate the controlled entrance of nutrients and ions from the periphery into the CNS while preventing the access of pathogens (blood-brain barrier; BBB). Via direct communication with T cells, astrocytes can either block or promote T cell migration into the CNS at the BBB (Williams et al., 2020). Dysregulation of BBB tight junctions such as observed in response to autoantibodies targeting aquaporin 4 (AQP4), in the disease neuromyelitis optica (Lennon et al., 2004) contributes to demyelination (Soerensen et al., 2021). Although Lennon and colleagues (2004) could not detect anti-AQP4 autoantibodies in the cerebrospinal fluid of MS patients, nor in the CPZ-dependent demyelination model (Rohr et al., 2020), altered AQP4 expression levels in MS lesions (Rohr et al., 2020) as well as upon CPZ application (Zhan et al., 2020) supports the assumption that astrocytes at the BBB may be involved in the initial stages of MS lesion formation (Gorter and Baron, 2022). In EAE, prior to immune cell infiltration into the parenchyma, reactive astrocytes seem to phagocyte myelin debris, resulting in the induction of nuclear factor kappa-light-chain-enhancer of activated B cells (NF-κB) signaling and secretion of cell-recruiting chemokines, hence triggering self-activation and resulting in an astroglial-mediated influx of leukocytes (Ponath et al., 2017). Thus, reactive astrocytes direct damage without a first interaction with leucocytes during demyelination, suggesting that the initial lesion observed in MS can be potentially co-regulated by astrocytes and not entirely/directly by leucocytes as once thought (Schirmer et al., 2021). For an even more detailed overview of the many demyelination-promoting roles, reactive astrocytes can acquire, see also (Ponath et al., 2018; Gorter and Baron, 2022; Salles et al., 2022).

On the other hand, key studies examining the role of astrocytes in MS have demonstrated that they are also essential for myelin repair. Depletion of reactive astrocytes in mice exposed to CPZ prevented remyelination due to microglial dysfunction and accumulation of myelin debris (Skripuletz et al., 2013). Similarly, in an osmolyte-induced demyelinating model, lack of astrocytes in lesions diminished OPC maturation, therefore impairing the generation of new oligodendrocytes and remyelination of denuded axons (Lohrberg et al., 2020). Moreover, in EAE glial scar formation was shown to be myelin protective and appeared to support the presence/accumulation of OPCs in normal appearing white matter areas, which in turn also promoted remyelination in the cerebellum and spinal cord (Haindl et al., 2019).

Genes/Factors Associated with Diverse Astrocyte Subtypes in Multiple Sclerosis

Although the spectrum of astrocyte types in MS has not been defined yet, it is clear that astrocytes play diverse roles and contribute to both disease progression and repair. Using single cell- and single nucleus RNA sequencing approaches, recent studies revealed marker genes that are enriched in specific astrocyte subtypes/states (Schirmer et al., 2019; Wheeler et al., 2020; Trobisch et al., 2022). Below, we will review these genes/pathways in the context of de- and remyelination in MS and preclinical models, focusing on CPZ-mediated demyelination and EAE (**Box 3**). Of note, most EAE studies focus on either spinal cord lesions (e.g., Wanner et al., 2013; Jin et al., 2022) or investigated whole brain isolates (e.g., Wheeler et al., 2020; Sanmarco et al., 2021), taking probably not fully into account that astrocytes show remarkable regional differences in their heterogeneity (Itoh et al., 2017; Silva Oliveira Junior et al., 2022; Trobisch et al., 2022). Using Ribotag technology, regional differences in astrocytes could already be described in EAE, with spinal cord-, cerebellar-, and cortical astrocytes displaying changes in genes related to cholesterol synthesis (e.g., Hmgcs1, Hmgcr, Msmo1), while such alterations were not observed in hippocampal astrocytes (Itoh et al., 2017).

Complement factors

The complement system is revealed to be implied in MS pathogenesis (Saez-Calveras and Stuve, 2022). Complement factor 1q (C1q) is activated and highly expressed following CPZ-mediated demyelination, in EAE, and is also upregulated in brain lesions of MS patients (Ingram et al., 2014; Watkins et al., 2016). C1q can induce the expression of yet another complement protein C3 in astrocytes (**Figure 1**; Liddelow et al., 2017). These C3-producing cells fail to provide metabolic support to neurons (Goetzl et al., 2018) and oligodendrocytes (Itoh et al., 2017; Tassoni et al., 2019), induce nodal loss, and impair myelin deposition (Ingersoll et al., 2010; Brennan et al., 2015). In addition, C3 can bind to myelin on oligodendrocytes and exacerbate EAE (Jégou et al., 2007). Of interest, increased astroglial production of C3 has also been linked to the progression of MS (Bhargava et al., 2021). Surprisingly, Guttenplan et al. (2021) demonstrated that C3 expression of cultured astrocytes did not result in the death of oligodendrocytes *in vitro*. Additionally, during both spontaneous- and drug-induced remyelination in a CPZ model, astroglial subpopulations expressing C3 in combination with possible myelin-beneficial/neuroprotective factors S100a10, Stat3, and Timp1 were observed (Silva Oliveira Junior et al., 2022), suggesting alternative roles for this complement protein, which may be context-dependent.

Sterile alpha and toll-interleukin receptor (TIR) motif containing 1

Sterile alpha and toll-interleukin receptor (TIR) motif containing 1 (Sarm1) is the key marker of axonal loss in Wallerian degeneration (Gerdts et al., 2015)

NEURAL REGENERATION RESEARCH
www.nrronline.org

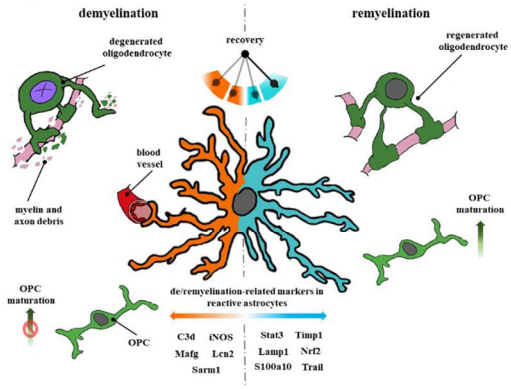

Figure 1 | Molecules expressed by reactive astrocytes during de- and remyelination of the central nervous system.
Reactive astrocytes are a heterogeneous cell population. This is highlighted by the distinct pattern of molecules these cells can express and release during disease. Such molecules can be either related to demyelination, oligodendrocyte degeneration, and impairment of OPC maturation (orange branch; e.g., C3/C3d, Mafg, iNOS, Lcn2, Sarm1) or to remyelination, OPC maturation and oligodendrocyte regeneration (blue branch; e.g. Stat3, Timp1, Lamp1 and Trail, Nrf2, S100a10). Future studies and therapies could focus on steering the pendulum of reactive astrocyte subpopulations towards a remyelinating- and overall more beneficial phenotype (blue branch) to promote recovery. Created using GIMP (GNU Image Manipulation Program, free and open-source editor), ArtFlow Studio App, and Microsoft PowerPoint. C3/C3d: Complement factor 3d; iNOS: inducible nitric oxide synthase; Lamp1: lysosome-associated membrane glycoprotein 1; Lcn2: lipocalin 2; Mafg: MAF bZIP transcription factor G; OPC: oligodendrocyte precursor cell; S100a10: S100 calcium-binding protein a10; Sarm1: sterile alpha and toll-interleukin receptor (TIR) motif containing 1; Stat3: signal transducer and activator of transcription 3; Timp1: tissue inhibitor of metalloproteinases 1; Trail: tumor necrosis factor-related apoptosis-inducing ligand. Green upward arrows: OPC maturation; orange circle with diagonal stroke: blocked/impaired due to demyelination-related markers.

and one of the fundamental enzymes that regulate demyelination in EAE (Jin et al., 2022) and neuromyelitis optica (Herwerth et al., 2022). Specific deletion of Sarm1 in astrocytes using GFAP and Aldh1L1 drivers, resulted in lower infiltration rates of $CD45^+$ cells into the spinal cord, in upregulation of glial cell line-derived neurotrophic factor and downregulation of NF-κB expression (Jin et al., 2022), all of which correlate with improved EAE outcomes. Interfering with glial cell line-derived neurotrophic factor expression in these knockout mice resulted in increased NF-κB protein levels, decreased myelin basic protein protein expression in the spinal cord, and overall worsened EAE clinical scores (Jin et al., 2022), hence strongly supporting a role of astrocytic Sarm1 expression in demyelination.

Lipocalin 2
Lipocalin 2 (Lcn2) is an inflammatory modulator, expressed by neurons, microglia, and astrocytes and suggested to be involved in demyelinating pathologies (Nam et al., 2014; Gasterich et al., 2022). Lcn2 is increased in progressive MS and is seen to inhibit remyelination *in vitro* (Al Nimer et al., 2016). Similarly, in EAE, full genetic ablation of Lcn2 reduced demyelination by decreasing the production of matrix metalloproteinases (Nam et al., 2014). In contrast, recent findings showed that Lcn2 deficient mice under acute CPZ-mediated demyelination exhibit a higher degree of T cell infiltration, loss of oligodendroglial lineage cells, and increased levels of demyelination (Gasterich et al., 2022). Lcn2-deficient EAE mice instead demonstrated no change in their clinical outcomes (Gasterich et al., 2022). These findings support a role for Lcn2 in early demyelination and lesion formation. While Lcn2 expression has been reported to be upregulated in astrocytes in optic neuritis in EAE (Chun et al., 2015; Tassoni et al., 2019), a specific role of astrocytic Lcn2 expression in demyelination or remyelination has, however, not been assigned yet.

Signal transducer and activator of transcription 3
Signal transducer and activator of transcription 3 (Stat3) is a key regulator of reactive astrocytes across different CNS pathologies (see **Figure 1**; Ben Haim et al., 2015; Sofroniew, 2020; Escartin et al., 2021; Abubakar et al., 2022; Choi et al., 2022) and its expression revealed to be important upon injury or disease. Seminal studies in spinal cord injury demonstrated that in *Stat3* knockout mice lesion spreading, demyelination, reduction in the border-forming response and impaired axonal regeneration occurred (Okada et al., 2006; Herrmann et al., 2008; Ben Haim et al., 2015; Anderson et al., 2016). Related to white matter, demyelination, and MS, a single study on lysolecithin-induced demyelination showed that astrocyte-specific ablation of *Stat3* decreased remyelination levels (Monteiro De Castro et al., 2015). Moreover, in EAE, proliferative border-forming reactive astrocytes were found to surround blood vessels and to prevent T cell and macrophage infiltration in the parenchyma (Spence et al., 2011; Wanner et al., 2013).

Lysosome-associated membrane glycoprotein 1 and tumor necrosis factor-related apoptosis-inducing ligand
Lysosome-associated membrane glycoprotein 1 (Lamp1) and tumor necrosis factor-related apoptosis-inducing ligand (Trail) were identified as important reactive astrocyte factors in EAE mice limiting disease progression induced via an interferon-gamma axis (Sanmarco et al., 2021). Both Lamp1 knockdown, as well as the absence of Trail expression in astrocytes, resulted in an increase in EAE severity by reducing $CD4^+$ T cell apoptosis. Trail expression, which is responsible for the induction of T cell apoptosis via the death receptor 5 was demonstrated to depend on natural killer cell-derived interferon-gamma expression (Johann and Waisman, 2021; Sanmarco et al., 2021). As this mechanism exhibits a positive impact on this subpopulation of reactive astrocytes, it is worth mentioning that interferon-gamma is also known to delay the differentiation of both grey and white matter OPCs (Lentferink et al., 2018) and to induce a proinflammatory/neurotoxic gene signature in astrocytes similar to the stimulation with C1q, IL1α, TNFα or in response to lipopolysaccharides (Hasel et al., 2021). Hence, depending on time and disease, the same factor can induce different responses of astrocytes, highlighting a heterogeneous yet also plastic feature of these cells during demyelination.

Mafg/Nrf2/Mat2a axis
Oxidative stress is one of the main processes behind oligodendrocyte loss in MS (Lassmann, 2019; Carlström et al., 2020). In astrocytes, Nrf2 and Mafg regulate the activation of the glutathione peroxidase (GPx) system (Hirotsu et al., 2012). The GPx system is crucial for antioxidant activity, metabolic transition, and DNA methylation in mammals (Nguyen et al., 2016; Carissimi et al., 2018) but was also found to control OPC maturation and survival of oligodendrocytes during demyelination (French et al., 2009; Hughes and Stockton, 2021). Astrocytic production of GPx4, a cofactor of the GPx system, prevents ROS overproduction and ferroptosis in EAE, thereby limiting cell loss (Hu et al., 2019). While Nrf2 was recently found to mark astrocytes with a non-neurotoxic activity in MS and EAE (Wheeler et al., 2020), Mafg upregulation is correlated with the production of proapoptotic molecules (Hirotsu et al., 2012; Wang et al., 2021). Wheeler et al. (2020) have shown that ablation of Mafg in astrocytes ameliorates the clinical course of EAE and directs astrocytes into a proremyelination state, as Mafg antagonizes the Nrf2 receptors in astrocytes, thereby blocking the activation of the GPx system. This mechanism is dependent on Mat2α, which controls DNA methylation, thereby preventing Nrf2 production that leads to aberrant Mafg expression. The authors concluded that the GPx system's reactivation in astrocytes depends on the GPx-Nrf2 pathway, which improves ROS catabolism in astrocytes, depriving oxidative stress and minimizing demyelination (Wheeler et al., 2020).

S100 calcium-binding protein a10
The calcium-binding protein S100 calcium-binding protein a10 (S100a10) has been reported to be expressed by a subset of "A2" reactive astrocytes that are associated with an anti-inflammatory gene signature (Zamanian et al., 2012; Liddelow et al., 2017). S100a10 expression in EAE was investigated and found to be reduced in the hippocampus mediated via the Nlr family pyrin domain containing 3 inflammasome (Hou et al., 2020). Of interest, treatment with MCC950, a selective inhibitor of Nlr family pyrin domain containing 3, resulted in increased levels of S100a10 expression, a concomitant reduction in numbers of C3-expressing (hence activated) astrocytes, and lead to overall improved EAE outcomes (Hou et al., 2020).

Tissue inhibitor of metalloproteinases 1
Tissue inhibitor of metalloproteinases 1 (Timp1) is an extracellular protein and endogenous regulator of matrix metalloproteinases. It is well documented that astrocytes secrete Timp1 in response to myelin injury (Pagenstecher et al., 1998; Nygårdas and Hinkkanen, 2002; Crocker et al., 2006; Moore et al., 2011), and global Timp1 ablation has been shown to impair spontaneous remyelination during EAE (Crocker et al., 2006). It has also been observed that OPCs treated with conditioned media from Timp1-deficient astrocytes are inhibited in their differentiation (Moore et al., 2011). It was furthermore shown that astrocyte-derived Timp1 promotes OPC maturation into oligodendrocytes and that astrocyte-specific ablation of this molecule impairs spontaneous myelin repair in demyelinated mice (Houben et al., 2020). More recently, Timp1-positive astrocytes were detected to occur specifically within white matter tracts following lipopolysaccharide application, a model mimicking bacterial infection, which suggests region-specific roles or manifestations of this astroglial phenotype (Hasel et al., 2021).

Repairing Multiple Sclerosis: How to Modulate Repair via Reactive Astrocytes?

It is clear that reactive astrogliosis is inherently heterogenic (Sofroniew, 2020; Escartin et al., 2021), and it is therefore of interest to develop strategies that target disease promoting cell types and direct them to a proregenerative state. Drug repurposing studies as well as small molecule therapies are possibly the most promising strategies to manipulate astrocyte types/states in MS (Gorter and Baron, 2022). Here we will discuss a few examples of drugs that can alter the balance of demyelinating and remyelinating astrocyte types.

Dimethyl fumarate induces Nrf2, which is essential for redox balance. In EAE, dimethyl fumarate treatment was shown to prevent axonal loss and demyelination (Yadav et al., 2021). Drug treatment reduced cytotoxic macrophages and was shown to diminish C3 protein deposition in the spinal cord as well as to limit the number of C3-expressing astrocytes (Yadav et al., 2021).

Siponimod is a functional agonist of the sphingosine-1 phosphate receptors (S1PR1 and S1PR5). In lysolecithin-induced demyelination, siponimod treatment was shown to attenuate demyelination (O'Sullivan et al., 2016). This effect was suggested to be astrocyte-dependent, as astrocytes showed internalization of S1PR1 and S1PR5 upon lipopolysaccharide treatment *in vitro* as well as during lysolecithin-dependent demyelination *in vivo* (O'Sullivan et al., 2016). Similar to dimethyl fumarate, siponimod also results in astrocyte-specific upregulation of Nrf2 and downregulation of NF-κB (Colombo et al., 2020), suggesting possible alteration of astrocyte types.

Finally, it was observed that the administration of the corticosteroid medrysone (hydroxymethylprogesterone) in mice subjected to CPZ-dependent demyelination resulted in improved oligodendrocyte recovery, node formation, and axonal remyelination. As a specific enhancement of reactive astrocytes that expressed C3 in combination with Stat3, S100a10 or Timp1 was observed, the drug, however, did not affect primary OPC maturation; hence myelin repair effects were directly assigned to medrysone's ability to modulate astrocyte profiles (Silva Oliveira Junior et al., 2022).

These few findings strongly suggest that drug-based therapies aiming at a direct modulation of reactive astrocyte types, indeed change their biochemical signatures towards more neuroprotective/neuroregenerative profiles and thus support tissues where repair is scarce. Other therapeutic strategies to promote CNS repair taking advantage of astrocytic plasticity and functional diversity constitute the direct transplantation of astroglial lineage cells (primary astrocytes, precursor- or induced pluripotent stem cell-derived astrocytes) or trans-differentiation approaches as reviewed by Hart and Karimi-Abdolrezaee (2021).

Concluding Remarks

Although the full spectrum of astrocyte types in MS has not been defined, a few studies have been conducted to link transcriptional and functional identity. Understanding the mechanisms leading to heterogeneity or plasticity among reactive astrocytes could be crucial to develop specific treatments that might be able to address the still clinically unmet need, fostering neuroregeneration in the injured and diseased CNS. Recent findings have shown that modulation of reactive astrogliosis is possible, at least by certain (repurposed) drugs, and that such a modulation is able to generate a repair outcome. This observation should therefore prompt additional investigations using broad substance libraries in order to fully explore the pharmacological potential of steering astrocytes specifically. Moreover, transcriptome and proteome responses of reactive astrocytes after drug exposure might help in aligning these molecular signatures with functional phenotypes – a correlation, which is still insufficiently understood.

Author contributions: *MSOJ and LR equally performed the majority of data search, data collection, and data analysis, and were equally involved in text writing, figure design, and manuscript revision. ED and IK contributed to text writing and data search. MF and PK supported the data search, discussed findings, conceived the final manuscript, took the final decision for submission, and were also responsible for funding acquisition, and revision of the text, content organization, and figure composition. All authors read and approved the final version of the manuscript.*
Conflicts of interest: *The authors declare no conflicts of interest.*
Data availability statement: *Not applicable.*

References

Abubakar MB, Sanusi KO, Ugusman A, Mohamed W, Kamal H, Ibrahim NH, Khoo CS, Kumar J (2022) Alzheimer's disease: an update and insights into pathophysiology. Front Aging Neurosci 14:742408.
Al Nimer F, Elliott C, Bergman J, Khademi M, Dring AM, Aeinehband S, Bergenheim T, Romme Christensen J, Sellebjerg F, Svenningsson A, Linington C, Olsson T, Piehl F (2016) Lipocalin-2 is increased in progressive multiple sclerosis and inhibits remyelination. Neurol Neuroimmunol Neuroinflamm 3:e191.
Anderson MA, Burda JE, Ren Y, Ao Y, O'Shea TM, Kawaguchi R, Coppola G, Khakh BS, Deming TJ, Sofroniew MV (2016) Astrocyte scar formation AIDS central nervous system axon regeneration. Nature 532:195-200.
Ben Haim L, Ceyzeriat K, Carrillo-de Sauvage MA, Aubry F, Auregan G, Guillermier M, Ruiz M, Petit F, Houitte D, Faivre E, Vandesquille M, Aron-Badin R, Dhenain M, Deglon N, Hantraye P, Brouillet E, Bonvento G, Escartin C (2015) The JAK/STAT3 pathway is a common inducer of astrocyte reactivity in Alzheimer's and Huntington's diseases. J Neurosci 35:2817-2829.
Bhargava P, Nogueras-Ortiz C, Kim S, Delgado-Peraza F, Calabresi PA, Kapogiannis D (2021) Synaptic and complement markers in extracellular vesicles in multiple sclerosis. Mult Scler 27:509-518.
Brennan FH, Gordon R, Lao HW, Biggins PJ, Taylor SM, Franklin RJ, Woodruff TM, Ruitenberg MJ (2015) The complement receptor C5aR controls acute inflammation and astrogliosis following spinal cord injury. J Neurosci 35:6517-6531.
Bretheau F, Castellanos-Molina A, Belanger D, Kusik M, Mailhot B, Boisvert A, Vallieres N, Lessard M, Gunzer M, Liu X, Boilard E, Quan N, Lacroix S (2022) The alarmin interleukin-1alpha triggers secondary degeneration through reactive astrocytes and endothelium after spinal cord injury. Nat Commun 13:5786.
Butti E, Bacigaluppi M, Chaabane L, Ruffini F, Brambilla E, Berera G, Montonati C, Quattrini A, Martino G (2019) Neural stem cells of the subventricular zone contribute to neuroprotection of the corpus callosum after cuprizone-induced demyelination. J Neurosci 39:5481-5492.
Carissimi A, Martinez D, Kim LJ, Fiori CZ, Vieira LR, Rosa DP, Pires GN (2018) Intermittent hypoxia, brain glyoxalase-1 and glutathione reductase-1, and anxiety-like behavior in mice. Braz J Psychiatry 40:376-381.
Carlström KE, Zhu K, Ewing E, Krabbendam IE, Harris RA, Falcão AM, Jagodic M, Castelo-Branco G, Piehl F (2020) Gsta4 controls apoptosis of differentiating adult oligodendrocytes during homeostasis and remyelination via the mitochondria-associated Fas-Casp8-Bid-axis. Nat Commun 11:4071.
Chen CZ, Neumann B, Forster S, Franklin RJM (2021) Schwann cell remyelination of the central nervous system: why does it happen and what are the benefits? Open Biol 11:200352.
Choi EH, Xu Y, Medynets M, Monaco MCG, Major EO, Nath A, Wang T (2018) Activated T cells induce proliferation of oligodendrocyte progenitor cells via release of vascular endothelial cell growth factor-A. Glia 66:2503-2513.
Choi HJ, Park JH, Jeong YJ, Hwang JW, Lee S, Lee H, Seol E, Kim IW, Cha BY, Seo J, Moon M, Hoe HS (2022) Donepezil ameliorates Abeta pathology but not tau pathology in 5xFAD mice. Mol Brain 15:63.
Chun BY, Kim JH, Nam Y, Huh MI, Han S, Suk K (2015) Pathological involvement of astrocyte-derived lipocalin-2 in the demyelinating optic neuritis. Invest Ophthalmol Vis Sci 56:3691-3698.
Colombo E, Bassani C, De Angelis A, Ruffini F, Ottoboni L, Comi G, Martino G, Farina C (2020) Siponimod (BAF312) activates Nrf2 while hampering NFkappaB in human astrocytes, and protects from astrocyte-induced neurodegeneration. Front Immunol 11:635.
Crocker SJ, Whitmire JK, Frausto RF, Chertboonmuang P, Soloway PD, Whitton JL, Campbell IL (2006) Persistent macrophage/microglial activation and myelin disruption after experimental autoimmune encephalomyelitis in tissue inhibitor of metalloproteinase-1-deficient mice. Am J Pathol 169:2104-2116.
Das S, Li Z, Noori A, Hyman BT, Serrano-Pozo A (2020) Meta-analysis of mouse transcriptomic studies supports a context-dependent astrocyte reaction in acute CNS injury versus neurodegeneration. J Neuroinflammation 17:227.
Dendrou CA, Fugger L, Friese MA (2015) Immunopathology of multiple sclerosis. Nat Rev Immunol 15:545-558.
Dobson R, Giovannoni G (2019) Multiple sclerosis- a review. Eur J Neurol 26:27-40.
Escartin C, Galea E, Lakatos A, O'Callaghan JP, Petzold GC, Serrano-Pozo A, Steinhäuser C, Volterra A, Carmignoto G, Agarwal A, Allen NJ, Araque A, Barbeito L, Barzilai A, Bergles DE, Bonvento G, Butt AM, Chen WT, Cohen-Salmon M, Cunningham C, et al. (2021) Reactive astrocyte nomenclature, definitions, and future directions. Nat Neurosci 24:312-325.
Filippi M, Bar-Or A, Piehl F, Preziosa P, Solari A, Vukusic S, Rocca MA (2018) Multiple sclerosis. Nat Rev Dis Primers 4:43.
Franklin RJM, Frisén J, Lyons DA (2021) Revisiting remyelination: towards a consensus on the regeneration of CNS myelin. Semin Cell Dev Biol 116:3-9.
French HM, Reid M, Mamontov P, Simmons RA, Grinspan JB (2009) Oxidative stress disrupts oligodendrocyte maturation. J Neurosci Res 87:3076-3087.
Gasterich N, Bohn A, Sesterhenn A, Nebelo F, Fein L, Kaddatz H, Nyamoya S, Kant S, Kipp M, Weiskirchen R, Zendedel A, Beyer C, Clarner T (2022) Lipocalin 2 attenuates oligodendrocyte loss and immune cell infiltration in mouse models for multiple sclerosis. Glia 70:2188-2206.
Gerdts J, Brace EJ, Sasaki Y, DiAntonio A, Milbrandt J (2015) SARM1 activation triggers axon degeneration locally via NAD+ destruction. Science 348:453-457.
Gharagozloo M, Mace JW, Calabresi PA (2022) Animal models to investigate the effects of inflammation on remyelination in multiple sclerosis. Front Mol Neurosci 15:995477.
Gilmore CP, Donaldson I, Bo L, Owens T, Lowe J, Evangelou N (2009) Regional variations in the extent and pattern of grey matter demyelination in multiple sclerosis: a comparison between the cerebral cortex, cerebellar cortex, deep grey matter nuclei and the spinal cord. J Neurol Neurosurg Psychiatry 80:182-187.
Goetzl EJ, Schwartz JB, Abner EL, Jicha GA, Kapogiannis D (2018) High complement levels in astrocyte-derived exosomes of Alzheimer disease. Ann Neurol 83:544-552.
Gorter RP, Baron W (2022) Recent insights into astrocytes as therapeutic targets for demyelinating diseases. Curr Opin Pharmacol 65:102261.
Green AJ, McQuaid S, Hauser SL, Allen IV, Lyness R (2010) Ocular pathology in multiple sclerosis: retinal atrophy and inflammation irrespective of disease duration. Brain 133:1591-1601.
Guttenplan KA, Weigel MK, Prakash P, Wijewardhane PR, Hasel P, Rufen-Blanchette U, Munch AE, Blum JA, Fine J, Neal MC, Bruce KD, Gitler AD, Chopra G, Liddelow SA, Barres BA (2021) Neurotoxic reactive astrocytes induce cell death via saturated lipids. Nature 599:102-107.
Hart CG, Karimi-Abdolrezaee S (2021) Recent insights on astrocyte mechanisms in CNS homeostasis, pathology, and repair. J Neurosci Res 99:2427-2462.
Hasel P, Rose IVL, Sadick JS, Kim RD, Liddelow SA (2021) Neuroinflammatory astrocyte subtypes in the mouse brain. Nat Neurosci 24:1475-1487.
Healy LM, Stratton JA, Kuhlmann T, Antel J (2022) The role of glial cells in multiple sclerosis disease progression. Nat Rev Neurol 18:237-248.
Herrmann JE, Imura T, Song B, Qi J, Ao Y, Nguyen TK, Korsak RA, Takeda K, Akira S, Sofroniew MV (2008) STAT3 is a critical regulator of astrogliosis and scar formation after spinal cord injury. J Neurosci 28:7231-7243.
Herwerth M, Kenet S, Schifferer M, Winkler A, Weber M, Snaidero N, Wang M, Lohrberg M, Bennett JL, Stadelmann C, Hemmer B, Misgeld T (2022) A new form of axonal pathology in a spinal model of neuromyelitis optica. Brain 145:1726-1742.

NEURAL REGENERATION RESEARCH
www.nrronline.org

Hirotsu Y, Katsuoka F, Funayama R, Nagashima T, Nishida Y, Nakayama K, Douglas Engel J, Yamamoto M (2012) Nrf2–MafG heterodimers contribute globally to antioxidant and metabolic networks. Nucleic Acids Research 40:10228-10239.
Hou B, Zhang Y, Liang P, He Y, Peng B, Liu W, Han S, Yin J, He X (2020) Inhibition of the NLRP3-inflammasome prevents cognitive deficits in experimental autoimmune encephalomyelitis mice via the alteration of astrocyte phenotype. Cell Death Dis 11:377.
Houben E, Janssens K, Hermans D, Vandooren J, van den Haute C, Schepers M, Vanmierlo T, Lambrichts I, van Horssen J, Baekelandt V, Opdenakker G, Baron W, Broux B, Slaets H, Hellings N (2020) Oncostatin M-induced astrocytic tissue inhibitor of metalloproteinases-1 drives remyelination. Proc Natl Acad Sci U S A 117:5028-5038.
Hu CL, Nydes M, Shanley KL, Morales Pantoja IE, Howard TA, Bizzozero OA (2019) Reduced expression of the ferroptosis inhibitor glutathione peroxidase-4 in multiple sclerosis and experimental autoimmune encephalomyelitis. J Neurochem 148:426-439.
Hughes EG, Stockton ME (2021) Premyelinating oligodendrocytes: mechanisms underlying cell survival and integration. Front Cell Dev Biol 9:714169.
Ingersoll SA, Martin CB, Barnum SR, Martin BK (2010) CNS-specific expression of C3a and C5a exacerbate demyelination severity in the cuprizone model. Mol Immunol 48:219-230.
Ingram G, Loveless S, Howell OW, Hakobyan S, Dancey B, Harris CL, Robertson NP, Neal JW, Morgan BP (2014) Complement activation in multiple sclerosis plaques: an immunohistochemical analysis. Acta Neuropathol Commun 2:53.
Itoh N, Itoh Y, Tassoni A, Ren E, Kaito M, Ohno A, Ao Y, Farkhondeh V, Johnsonbaugh H, Burda J, Sofroniew MV, Voskuhl RR (2017) Cell-specific and region-specific transcriptomics in the multiple sclerosis model: focus on astrocytes. Proc Natl Acad Sci U S A 115:E302-309.
Jégou JF, Chan P, Schouft MT, Griffiths MR, Neal JW, Gasque P, Vaudry H, Fontaine M (2007) C3d binding to the myelin oligodendrocyte glycoprotein results in an exacerbated experimental autoimmune encephalomyelitis. J Immunol 178:3323-3331.
Jin L, Zhang J, Hua X, Xu X, Li J, Wang J, Wang M, Liu H, Qiu H, Chen M, Zhang X, Wang Y, Huang Z (2022) Astrocytic SARM1 promotes neuroinflammation and axonal demyelination in experimental autoimmune encephalomyelitis through inhibiting GDNF signaling. Cell Death Dis 13:759.
Johann L, Waisman A (2021) The astrocyte LAMP lights a T cell TRAIL of death. Neuron 109:1423-1425.
Kotter MR (2006) Myelin impairs CNS remyelination by inhibiting oligodendrocyte precursor cell differentiation. J Neurosci 26:328-332.
Kremer D, Aktas O, Hartung HP, Küry P (2011) The complex world of oligodendroglial differentiation inhibitors. Ann Neurol 69:602-618.
Lampron A, Larochelle A, Laflamme N, Préfontaine P, Plante MM, Sánchez MG, Yong VW, Stys PK, Tremblay M-È, Rivest S (2015) Inefficient clearance of myelin debris by microglia impairs remyelinating processes. J Exp Med 212:481-495.
Lassmann H (2019) Pathogenic mechanisms associated with different clinical courses of multiple sclerosis. Front Immunol 9:3116.
Lennon VA, Wingerchuk DM, Kryzer TJ, Pittock SJ, Lucchinetti CF, Fujihara K, Nakashima I, Weinshenker BG (2004) A serum autoantibody marker of neuromyelitis optica: distinction from multiple sclerosis. Lancet 364:2106-2112.
Lentferink DH, Jongsma JM, Werkman I, Baron W (2018) Grey matter OPCs are less mature and less sensitive to IFNγ than white matter OPCs: consequences for remyelination. Sci Rep 8:2113.
Leo H, Kipp M (2022) Remyelination in multiple sclerosis: findings in the cuprizone model. Int J Mol Sci 23:16093.
Levine JM, Reynolds R (1999) Activation and proliferation of endogenous oligodendrocyte precursor cells during ethidium bromide-induced demyelination. Exp Neurol 160:333-347.
Li R, Patterson KR, Bar-Or A (2018) Reassessing B cell contributions in multiple sclerosis. Nat Immunol 19:696-707.
Liddelow SA, Guttenplan KA, Clarke LE, Bennett FC, Bohlen CJ, Schirmer L, Bennett ML, Münch AE, Chung WS, Peterson TC, Wilton DK, Frouin A, Napier BA, Panicker N, Kumar M, Buckwalter MS, Rowitch DH, Dawson VL, Dawson TM, Stevens B, et al. (2017) Neurotoxic reactive astrocytes are induced by activated microglia. Nature 541:481-487.
Lohrberg M, Winkler A, Franz J, van der Meer F, Ruhwedel T, Sirmpilatze N, Dadarwal R, Handwerker R, Esser D, Wiegand K, Hagel C, Gocht A, König FB, Boretius S, Möbius W, Stadelmann C, Barrantes-Freer A (2020) Lack of astrocytes hinders parenchymal oligodendrocyte precursor cells from reaching a myelinating state in osmolyte-induced demyelination. Acta Neuropathol Commun 8:224.
Masvekar R, Wu T, Kosa P, Barbour C, Fossati V, Bielekova B (2019) Cerebrospinal fluid biomarkers link toxic astrogliosis and microglial activation to multiple sclerosis severity. Mult Scler Relat Disord 28:34-43.
Monteiro De Castro G, Deja NA, Ma D, Zhao C, Franklin RJM (2015) Astrocyte activation via Stat3 signaling determines the balance of oligodendrocyte versus Schwann cell remyelination. Am J Pathol 185:2431-2440.
Moore CS, Milner R, Nishiyama A, Frausto RF, Serwanski DR, Pagarigan RR, Whitton JL, Miller RH, Crocker SJ (2011) Astrocytic tissue inhibitor of metalloproteinase-1 (TIMP-1) promotes oligodendrocyte differentiation and enhances CNS myelination. J Neurosci 31:6247-6254.
Nam Y, Kim JH, Seo M, Kim JH, Jin M, Jeon S, Seo JW, Lee WH, Bing SJ, Jee Y, Lee WK, Park DH, Kook H, Suk K (2014) Lipocalin-2 protein deficiency ameliorates experimental autoimmune encephalomyelitis: the pathogenic role of lipocalin-2 in the central nervous system and peripheral lymphoid tissues. J Biol Chem 289:16773-16789.
Nguyen A, Duquette N, Mamarbachi M, Thorin E (2016) Epigenetic regulatory effect of exercise on glutathione peroxidase 1 expression in the skeletal muscle of severely dyslipidemic mice. PLoS One 11:e0151526.
Nygårdas PT, Hinkkanen AE (2002) Up-regulation of MMP-8 and MMP-9 activity in the BALB/c mouse spinal cord correlates with the severity of experimental autoimmune encephalomyelitis. Clin Exp Immunol 128:245-254.
O'Sullivan C, Schubart A, Mir AK, Dev KK (2016) The dual S1PR1/S1PR5 drug BAF312 (Siponimod) attenuates demyelination in organotypic slice cultures. J Neuroinflammation 13:31.
Okada S, Nakamura M, Katoh H, Miyao T, Shimazaki T, Ishii K, Yamane J, Yoshimura A, Iwamoto Y, Toyama Y, Okano H (2006) Conditional ablation of Stat3 or Socs3 discloses a dual role for reactive astrocytes after spinal cord injury. Nat Med 12:829-834.
Pagenstecher A, Stalder AK, Kincaid CL, Shapiro SD, Campbell IL (1998) Differential expression of matrix metalloproteinase and tissue inhibitor of matrix metalloproteinase genes in the mouse central nervous system in normal and inflammatory states. Am J Pathol 152:729-741.
Petrova N, Carassiti D, Altmann DR, Baker D, Schmierer K (2018) Axonal loss in the multiple sclerosis spinal cord revisited. Brain Pathol 28:334-348.
Ponath G, Ramanan S, Mubarak M, Housley W, Lee S, Sahinkaya FR, Vortmeyer A, Raine CS, Pitt D (2017) Myelin phagocytosis by astrocytes after myelin damage promotes lesion pathology. Brain 140:399-413.
Ponath G, Park C, Pitt D (2018) The role of astrocytes in multiple sclerosis. Front Immunol 9:217.
Prinz M, Priller J (2017) The role of peripheral immune cells in the CNS in steady state and disease. Nat Neurosci 20:136-144.
Rohr SO, Greiner T, Joost S, Amor S, Valk Pvd, Schmitz C, Kipp M (2020) Aquaporin-4 expression during toxic and autoimmune demyelination. Cells 9:2187.
Saez-Calveras N, Stuve O (2022) The role of the complement system in multiple sclerosis: a review. Front Immunol 13:970486.
Salles D, Samartini RS, Alves MTS, Malinverni ACM, Stavale JN (2022) Functions of astrocytes in multiple sclerosis: a review. Mult Scler Relat Disord 60:103749.
Sanchis P, Fernández-Gayol O, Comes G, Escrig A, Giralt M, Palmiter RD, Hidalgo J (2020) Interleukin-6 derived from the central nervous system may influence the pathogenesis of experimental autoimmune encephalomyelitis in a cell-dependent manner. Cells 9:330.
Sanmarco LM, Wheeler MA, Gutiérrez-Vázquez C, Polonio CM, Linnerbauer M, Pinho-Ribeiro FA, Li Z, Giovannoni F, Batterman KV, Scalisi G, Zandee SEJ, Heck ES, Alsuwailm M, Rosene DL, Becher B, Chiu IM, Prat A, Quintana FJ (2021) Gut-licensed IFNγ+ NK cells drive LAMP1+TRAIL+ anti-inflammatory astrocytes. Nature 590:473-479.
Schirmer L, Velmeshev D, Holmqvist S, Kaufmann M, Werneburg S, Jung D, Vistnes S, Stockley JH, Young A, Steindel M, Tung B, Goyal N, Bhaduri A, Mayer S, Engler JB, Bayraktar OA, Franklin RJM, Haeussler M, Reynolds R, Schafer DP, et al. (2019) Neuronal vulnerability and multilineage diversity in multiple sclerosis. Nature 573:75-82.
Schirmer L, Schafer DP, Bartels T, Rowitch DH, Calabresi PA (2021) Diversity and function of glial cell types in multiple sclerosis. Trends Immunol 42:228-247.
Silva Oliveira Junior M, Schira-Heinen J, Reiche L, Han S, de Amorim VCM, Lewen I, Gruchot J, Gottle P, Akkermann R, Azim K, Kury P (2022) Myelin repair is fostered by the corticosteroid medrysone specifically acting on astroglial subpopulations. EBioMedicine 83:104204.
Soerensen SF, Wirenfeldt M, Wlodarczyk A, Moerch MT, Khorooshi R, Arengoth DS, Lillevang ST, Owens T, Asgari N (2021) An experimental model of neuromyelitis optica spectrum disorder–optic neuritis: insights into disease mechanisms. Front Neurol 12:703249.
Sofroniew MV (2020) Astrocyte reactivity: subtypes, states, and functions in CNS innate immunity. Trends Immunol 41:758-770.
Spence RD, Hamby ME, Umeda E, Itoh N, Du S, Wisdom AJ, Cao Y, Bondar G, Lama J, Ao Y, Sandoval F, Suriany S, Sofroniew MV, Voskuhl RR (2011) Neuroprotection mediated through estrogen receptor-α in astrocytes. Proc Natl Acad Sci U S A 108:8867-8872.
Tassoni A, Farkhondeh V, Itoh Y, Itoh N, Sofroniew MV, Voskuhl RR (2019) The astrocyte transcriptome in EAE optic neuritis shows complement activation and reveals a sex difference in astrocytic C3 expression. Sci Rep 9:10010.
Trobisch T, Zulji A, Stevens NA, Schwarz S, Wischnewski S, Öztürk M, Perales-Patón J, Haeussler M, Saez-Rodriguez J, Velmeshev D, Schirmer L (2022) Cross-regional homeostatic and reactive glial signatures in multiple sclerosis. Acta Neuropathol 144:987-1003.
Wan T, Zhu W, Zhao Y, Zhang X, Ye R, Zuo M, Xu P, Huang Z, Zhang C, Xie Y, Liu X (2022) Astrocytic phagocytosis contributes to demyelination after focal cortical ischemia in mice. Nat Commun 13:1134.
Wang M, Liu F, Fang B, Huo Q, Yang Y (2021) Proteome-scale profiling reveals MAFF and MAFG as two novel key transcription factors involved in palmitic acid-induced umbilical vein endothelial cell apoptosis. BMC Cardiovasc Disord 21:448.
Wanner IB, Anderson MA, Song B, Levine J, Fernandez A, Gray-Thompson Z, Ao Y, Sofroniew MV (2013) Glial scar borders are formed by newly proliferated, elongated astrocytes that interact to corral inflammatory and fibrotic cells via STAT3-dependent mechanisms after spinal cord injury. J Neurosci 33:12870-12886.
Watkins LM, Neal JW, Loveless S, Michailidou I, Ramaglia V, Rees MI, Reynolds R, Robertson NP, Morgan BP, Howell OW (2016) Complement is activated in progressive multiple sclerosis cortical grey matter lesions. J Neuroinflammation 13:161.
Wheeler MA, Clark IC, Tjon EC, Li Z, Zandee SEJ, Couturier CP, Watson BR, Scalisi G, Alkwai S, Rothhammer V, Rotem A, Heyman JA, Thaploo S, Sanmarco LM, Ragoussis J, Weitz DA, Petrecca K, Moffitt JR, Becher B, Antel JP, et al. (2020) MAFG-driven astrocytes promote CNS inflammation. Nature 578:593-599.
Williams JL, Manivasagam S, Smith BC, Sim J, Vollmer LL, Daniels BP, Russell JH, Klein RS (2020) Astrocyte-T cell crosstalk regulates region-specific neuroinflammation. Glia 68:1361-1374.
Yadav SK, Ito N, Soin D, Ito K, Dhib-Jalbut S (2021) Dimethyl fumarate suppresses demyelination and axonal loss through reduction in pro-inflammatory macrophage-induced reactive astrocytes and complement c3 deposition. J Clin Med 10:857.
Zamanian JL, Xu L, Foo LC, Nouri N, Zhou L, Giffard RG, Barres BA (2012) Genomic analysis of reactive astrogliosis. J Neurosci 32:6391-6410.
Zhan J, Mann T, Joost S, Behrangi N, Frank M, Kipp M (2020) The cuprizone model: dos and do nots. Cells 9:843.

C-Editors: Zhao M, Liu WJ, Qiu Y; T-Editor: Jia Y

C21ORF91 overexpression leads to glial differentiation misbalance in Down syndrome to be rescued by remyelination drugs

Laura Reiche[1], Cherie Anne Stringer[2], Kevin Camey[2], Brigida Ziegler[1], Luisa Werner[1], Peter Göttle[1], Elizabeth Head[2], David Kremer[3], and Patrick Küry[1,4]

[1] Department of Neurology, Medical Faculty and University Hospital Düsseldorf, Heinrich Heine University Düsseldorf, Germany

[2] Department of Pathology and Laboratory Medicine, University of California Irvine, UCI School of Medicine 1111 Gillespie Neuroscience Research Facility, Irvine, California, USA

[3] Department of Neurology and Neurorehabilitation, Hospital Zum Heiligen Geist, Academic Teaching Hospital of the Heinrich Heine University Düsseldorf, Kempen, Germany

[4] Department of Neurology, University of Bern, Bern, Switzerland

Correspondence: Patrick Küry, Moorenstrasse 5, D-40225 Düsseldorf, Germany, 0049 211 8117822, kuery@hhu.de

Conflict-of-interest statement

The authors have declared that no conflict of interest exists.

2.8 C21ORF91 Overexpression Leads to Glial Differentiation Misbalance in Down Syndrome to Be Rescued by Remyelination Drugs

Abstract

Down syndrome (DS), the most prevalent chromosomal condition causing cognitive impairments and intellectual disability, is hallmarked by brain anomalies, and white matter malformation. DS brains exhibit imbalanced glial cell populations, evident in hypomyelination and region-specific astrogliosis, and the C21ORF91 protein is a promising driver responsible for such a non-equilibrated glial development. Elevated levels of C21ORF91 disrupt oligodendroglial precursor cell (OPC) differentiation, favoring astroglial features at the expense of oligodendroglial development, resulting in hybrid cells with mixed glial properties. Using immunohistochemistry on human post-mortem tissue from DS, DS with Alzheimer's disease (DSAD), Alzheimer's disease (AD), and aged controls (AC), we correlated C21ORF91- with glial marker expression in the occipital and frontal cortex. Unique hybrid cells co-expressing oligodendroglial and astroglial markers were identified exclusively in DS/DSAD brains. C21ORF91 overexpression in rodent OPCs mimicked the generation of these atypical phenotypes. Recently identified myelin repair drugs effectively restored this abnormal hybrid population and concurrent myelination deficits by stabilizing OPC differentiation and by reducing pro-inflammatory, neurotoxic astroglial signatures. Our findings provide evidence that C21ORF91 overexpression contributes to DS neuropathogenesis. The observation that myelin repair drugs targeting OPC differentiation can efficiently rescue C21ORF91-dependent effects offers potential therapeutic strategies for DS-related brain abnormalities.

INTRODUCTION

Down syndrome (DS) is the most common chromosomal disorder and genetic contributor to intellectual disability (ID) and cognitive impairments, caused by either triplication (95% of cases), translocation (5% of cases), or mosaicism (2% of cases) of human chromosome 21 (Hsa21) (1). DS affects one in 700-1000 live newborns annually worldwide (2). People with DS exhibit a diverse range of phenotypic manifestations that impact the development and function of various organs. The most common characteristics of DS, including deficits in executive functions, learning, and memory ability, can significantly impair individual independence and quality of life (3), so far remain elusive for medical management. Typical developmental hallmarks are generally delayed in individuals with DS, and cognitive impairments can become progressively more severe with aging and the development of Alzheimer's disease (AD) (4-7). The complexity of the human brain and critical spatiotemporal processes during development, coupled with the unique genetic background of individuals with DS, complicate our understanding of ID-underlaying mechanisms (3). Yet, certain neurological phenotypes are consistently observed, such as smaller total brain volume (8, 9), impaired neurodevelopment (3), myelination deficits (10), and signs of accelerated brain aging, including neuropathological alterations similar to Alzheimer's disease (AD) patients, occurring by the age of 40 years (7). At the cellular level, DS is characterized by altered neurogenesis and neuronal hypotrophy, increased astrogliogenesis and astroglial reactivity, alongside oligodendroglial hypocellularity and perturbations in oligodendrocyte maturation, leading to hypomyelination (3, 10-12). Structural and functional white matter differences are typically observed in individuals with DS (8, 13, 14) that correlate with poorer performance in neuropsychological tests (15, 16). Indeed, ongoing myelin remodeling is considered important for behavior, cognition, and learning throughout adulthood (17, 18).

Given that myelination continues into early adulthood in humans (19), it may represent an accessible pharmacological target as compared to neurogenesis occurring prenatally. Understanding the etiology of DS-related changes in oligodendroglial differentiation and white matter integrity could, therefore, enable therapeutic strategies aimed at improving cognition,

quality of life, and independence. Oligodendroglial precursor cells (OPCs) are crucial for addressing these challenges, as their accurate differentiation is pivotal for myelination, saltatory signal propagation, and axonal nutrition. Focusing on this cell type is common in research on demyelinating diseases such as multiple sclerosis (MS), to which pharmacological interventions still represent an unmet clinical need (20-22). Excitingly, pharmacological approaches to improve oligodendroglial differentiation competence can foster remyelination and regain function in demyelinating animal models (23).

The gene *C21ORF91*, localized on human chromosome 21 (Hsa21), has emerged as a significant contributor to the neurological phenotypes observed in DS (24, 25). Overexpression of its ortholog protein impacts neurogenesis and cortical development in mice (24) and disturbs rat OPC differentiation, hindering their maturation into functional myelinating oligodendrocytes (25).

We here identify correlations between C21ORF91 expression and aberrant oligodendroglial phenotypes in different Hsa21 trisomic (DS) diagnostic classes. Additionally, we assessed the specific impact of C21ORF91 overexpression on cellular phenotype generation in rat primary cell cultures and explored strategies to stabilize OPC differentiation competence using recently discovered small molecule drugs for myelin repair (26-28). Our results support the role of C21ORF91 in glial specification and suggest potential therapeutic avenues for DS by leveraging insights from related neurological (demyelinating) conditions.

RESULTS

C21ORF91 expression correlates with aberrant glial hybrid phenotypes in Hsa21 trisomic diagnostic classes.

Previously, we demonstrated that C21ORF91 plays a pivotal role in oligodendroglial maturation and myelination, with possible implications in DS neuropathophysiology as its overexpression resulted in a misbalanced differentiation along the oligodendroglial lineage in rats (25). Existing studies for C21ORF91 protein expression have been limited to fetal DS tissues and have focused exclusively on neurons (24). Extending these findings, we here

examined its expression in the occipital- (OCC) and frontal cortex (FCX) of human DS, DS with Alzheimer's disease (DSAD), and sporadic AD as well as aged control tissues (Table 1). We correlated C21ORF91 expression with the oligodendroglial marker myelin basic protein (MBP) and astroglial marker glial fibrillary acidic protein (GFAP) in serial post-mortem tissue sections (Figure 1). However, evaluating and comparing signal intensities proved challenging due to sample heterogeneity, particularly age differences and variations in tissue preservation. This is specifically evident for MBP, resulting in the unexpected presentation of stronger signals in gray matter (GM) as compared to white matter (WM) regions across nearly all cases shown here (see and compare II in Figure 1A-D). Previous studies have noted that MBP signals tend to be better preserved in GM tracts during aging compared to WM (29). Despite these limitations, we observed that in the OCC, DS and DSAD sections displayed the weakest MBP signals in WM (Figure 1B,C; II) compared to AC and AD sections (Figure 1A,D, II). In DS and DSAD tissues, we could frequently identify single cell bodies expressing MBP protein (Figure 1B'',C''), whereas in AD and the aged control samples (Figure 1A'',D''), MBP signals were more diffuse and widespread, making it difficult to attribute the signals to single cells. This may reflect and be caused by hypomyelination and diminished mature oligodendrocyte population that have been described in other DS studies (13, 14). GFAP signals were confined to the subpial zone in controls, whereas in DS, DSAD, and AD, they appeared up-regulated and patchy indicating gliosis (see and compare (III) in Figure 1 A-D, A'''-D'''), typical for these diagnostic classes (7, 11). For C21ORF91 labeling, we observed a distinct intracellular localization (Figure 1A'-D', Table 1). Strong nuclear C21ORF91 signals were predominantly found in WM and correlated with both GFAP- and MBP-labeled cells, whereas cytoplasmic signals were more common in GM and mainly co-localized with GFAP signals in the serial sections. The most intriguing observation was the detection of a glial hybrid cellular phenotype co-expressing MBP and GFAP proteins exclusively in C21ORF91-positive cells, only found in DS (Figure 1B'-B''',E) and DSAD (Figure 1C'-C''',F) in OCC and FCX. This abnormal combination of markers was recently observed in rat oligodendroglial cells overexpressing C21ORF91, which were restricted in their capacity to ensheath axons (25). As we previously

described and termed the “non-organized MBP expressing (NOM)-phenotype” attributed to a collapsed cytoarchitecture (25), these MBP/GFAP-positive hybrids also exhibited an atrophied morphology in the human post-mortem tissues (see Figure 1E,F).

Immunofluorescence for C21ORF91 protein expression revealed a co-localization with oligodendroglial markers SOX10, nuclear OLIG2, and CC1 representing both immature and mature cells in the WM across all classes (data not shown). These correlations were observed in both brain regions (Figure 2), and C21ORF91 signals were prevalently detected in the nucleus (Table 1). C21ORF91 signals were also observed in GFAP-positive astrocytes revealing cytoplasmic protein localization (Figure 2C). As was observed in the MBP/GFAP/C21ORF91-expressing hybrid cells identified in serial sections (Figure 1), we confirmed the presence of OLIG2/GFAP/C21ORF91-positive cells within single tissue sections (Figure 2). This phenotype was observed exclusively in the Hsa21 trisomic cases, including DS (Figure 2A,B) and DSAD (Figure 2C) in FCX, and was more prominent in the OCC (Table 1). These cells showed strong, either nuclear (Figure 2B,B’) or cytoplasmic (Figure 2C,C’) C21ORF91 signals. Interestingly, the above-mentioned atrophied morphological feature was also characteristic of OLIG2/GFAP/C21ORF91-positive hybrid cells. They exhibited a small cellular expansion with an average area of 160.92 µm ± 17.85 µm in DS and 186 µm ± 33.57 µm in DSAD, with short and sparsely ramified processes, thus presenting a rather stunted morphology than other glial cells within the tissue (Figure 2, Table 1).

Myelin repair drugs foster rat oligodendroglial maturation and myelination capacity upon C21ORF91 overexpression

Artificially elevated C21ORF91 expression levels in rat OPCs restrict their maturation and myelination capacity *ex vivo* (25). Additionally, we observed the induction of MBP and GFAP co-expression upon C21ORF91 overexpression, indicative of a compromised differentiation competence. These cells appeared as NOM phenotype, similar to what we here observed in human DS and DSAD (Figures 1,2). Based on our established expertise to foster oligodendroglial differentiation competence and myelination in the context of myelin repair

155 studies (26-28, 30), we next tested the potential of some previously identified pro-
156 oligodendroglial molecules to rescue the C21ORF91-dependent differentiation failure.
157 To this end, rat OPCs were co-transfected with a C21ORF91 expression construct together
158 with a GFP expression vector and then applied to dissociated neuron/oligodendrocyte co-
159 cultures at 15 days *in vitro* (DIV, Figure 3A). Myelinating co-cultures with transplanted
160 C21ORF91-overexpressing cells were then cultivated for another 10 days and treated with
161 either danazol (Dan), parbendazole (Parb), methiazole (Met), teriflunomide (Teri), or
162 medrysone (Medry), as well as DMSO as control. Immunofluorescent staining with antibodies
163 directed against GFP, GFAP, MBP, and neurofilament (NF) revealed that the number of
164 myelinating cells among the C21ORF91 overexpressors (marked by GFP) is significantly
165 increased upon danazol, parbendazole, and medrysone stimulation when compared to DMSO-
166 treated cells (Figure 3B). Note that myelinating cells exhibited typical T-shaped structures and
167 were in contact with NF-positive axons (see Figure 3; Dan and Parb). Interestingly, the degree
168 of cells with a NOM phenotype – appearing collapsed or not accurately forming a cytoskeleton,
169 aligning but not ensheathing axons (Figure 3E, DMSO) – was reduced by all five pro-
170 oligodendroglial compounds, with danazol and parbendazole treatments showing statistically
171 significant effects (Figure 3C). Likewise, the aberrant co-expression of MBP and GFAP,
172 prominently found in this C21ORF91-induced NOM subpopulation (25), was also reduced by
173 these pro-myelinating drugs (Figure 3D). Here, danazol, parbendazole, and medrysone
174 significantly decreased the percentage of cells exhibiting this non-physiological phenotype
175 (Figure 3D).
176
177 **Aberrant C21ORF91-driven oligodendroglial differentiation competence is stabilized by**
178 **myelin repair drugs**
179 As danazol, parbendazole, and medrysone were shown to most efficiently restore C21ORF91
180 overexpression-related maturation defects in the advanced rat *ex vivo* myelination setup
181 (Figure 3), we were interested in exploring how dysbalanced OPC differentiation could be
182 recovered. This was tested in primary rat OPC monocultures, allowing us to exclude potential

183 secondary effects from cell-cell interactions and focus on the molecular mechanisms
184 underlying differentiation dynamics. Following transfection, C21ORF91-overexpressing OPCs
185 were cultured in differentiation medium supplemented with danazol, parbendazole,
186 medrysone, or DMSO (control) for five days before the expression of differentiation-associated
187 markers was evaluated (Figure 4).
188 Nuclear localization of OLIG2 (Figure 4A,A') indicative of increased oligodendroglial lineage
189 commitment (31), was elevated by danazol and medrysone treatment while expression of the
190 oligodendroglial maturation marker CC1 (Figure 4B,B') was restored by all three myelin repair
191 drugs (danazol, parbendazole, and medrysone). However, contrary to expectations from the
192 co-culture data (Figure 3), none of the drugs significantly increased the percentage of MBP-
193 positive cells. Yet, it appeared that MBP distribution patterns could be improved by danazol
194 and medrysone, evaluated by its morphological expansion (Figure 4C',D,D') and an overall
195 restored expression strength (see also Figure 8), thus indicating a qualitative enhancement of
196 oligodendrocyte maturation. Note that some restoration levels even exceeded levels of control
197 transfected cells as published before (see (25) and referring here to dotted baselines labeled
198 with con[25]).
199 We next assessed the potential of danazol, parbendazole, and medrysone to correct the
200 generation of hybrid cellular phenotypes at day two of differentiation. This was done by
201 evaluating the intracellular localization of OLIG2 and SOX10, as their translocation to the
202 cytosol has been shown to induce astrogliogenesis instead of oligodendrogenesis (31, 32),
203 along with concomitant GFAP expression. While all three myelin repair drugs reduced the
204 prevalence of cells exhibiting concomitant OLIG2 and GFAP co-expression, indicative of a
205 reduction in lineage ambivalence (Figure 5B,B'), the number of nuclear OLIG2 expressors was
206 only significantly restored by danazol and medrysone treatment (Figure 5A), which is in
207 accordance with observations at day five (Figure 4A). Nuclear translocation of SOX10, a
208 transcription factor acting downstream of OLIG2-mediated oligodendrogenesis (33, 34), was
209 rescued exclusively by danazol (Figure 5C). However, the number of OPCs co-expressing

SOX10 and GFAP cells was significantly reduced following danazol and medrysone application (Figure 5D,D').

C21ORF91 overexpression promotes neurotoxic astrocytic parameters in rat OPCs

Recent advances in the description of reactive astroglial phenotypes identified neurotoxic or beneficial subtypes along with additional marker proteins (35) worth investigating in the context of C21ORF91-modulated cell differentiation. Since astrocytes in DS brains show several functional abnormalities such as impaired neurotrophic support, perturbations in synaptogenesis and dendritic spinogenesis, and altered morphology (11) along with an inflammatory profile (36), we were interested in evaluating further astroglial parameters induced by C21ORF91 overexpression. This was achieved by comparing astroglial marker protein expression in control transfected vs. C21ORF91-overexpressing OPCs, after five days of differentiation (Figure 6). Note that we consistently observed a small minority of GFAP-positive cells arising from control transfection (as already presented in (25)), most likely resulting from nucleofection-induced stress. For the expression of glutamate aspartate transporter 1 (GLAST; Figure 6A,A'), seen as a more mature and functional marker of astrocytes, we observed a clear increment in GFAP-expressing cells in response to elevated C21ORF91 levels. This was accompanied by the reactive, neurotoxic astroglial marker induction of MAF bZIP transcription factor G (MAFG; Figure 6B,B') and Lipocalin 2 (LCN2, Figure 6C,C'). Supporting the generation of a neuroinflammatory stress condition, overexpressing cells were also found to secret significantly higher levels of the neurotoxic LCN2 protein (Figure 6E) and of the pro-inflammatory cytokine tumor necrosis factor alpha (TNFa, Figure 6F). Another astrocytic marker, presumed neuroprotective, tissue inhibitor of metalloproteinases 1 (TIMP1) was not significantly regulated (Figure 6D,D'). Likewise, our current staining protocols do not allow the concomitant detection of all reactive marker proteins, making it difficult to rule out the generation of several similar cellular subpopulations with varying levels of activation parameters.

Although astroglial morphological changes have yet to be confirmed as reliable indicators of reactivity and neurotoxicity (37, 38), it is worth mentioning that GFAP-positive C21ORF91 overexpressors displayed a reduction in both the number and length of fine cellular processes. Instead, these cells rather possess thick protrusions with an overall decreased territory volume compared to control cells (see for example Figure 6A',C',D').

The application of myelin repair drugs could significantly attenuate these effects in our rat primary cells (Figure 7). Both danazol and medrysone markedly reduced the percentage of GFAP-positive cells at day five of differentiation (Figure 7A; see also Figure 8 for cells after two days). Likewise, the appearance of strong GLAST signals was reduced by all three drugs (Figure 7B,B'). Neurotoxic features (Figure 7C,D) and secretion of TNFa (Figure 7G) and LCN2 (Figure 7G) were equally restored, most prominently by medrysone and danazol, while TIMP1 expression remained largely unaffected. Remarkably, danazol and medrysone were also found to restore fine arborization and morphological structure of cellular processes in monocultured C21ORF91-overexpressing cells (Figure 7B'), as well as shown in the few GFAP-positive cells arising from transplanted OPCs on myelinating co-cultures after 10 days of differentiation (Figure 7H).

DISCUSSION

In this study, we demonstrate the detrimental downstream effects of C21ORF91 protein overexpression on rat oligodendroglial precursor cell fate stability, leading to the induction of astroglial characteristics associated with a reactive, neurotoxic profile. This aberrant lineage commitment was effectively restored by danazol and medrysone, and, to a lesser extent by parbendazole, thereby fostering accurate maturation into functional, myelinating oligodendrocytes in our *ex vivo* models. While this pharmacological recovery is of considerable biomedical interest, it is important to note that the here presented pro-oligodendroglial compounds demonstrated heterogeneous dynamics in stabilizing glial parameters (Figure 8), indicating the involvement of multiple and yet unknown pathways. Hybrid glial phenotypes, aberrantly co-expressing oligodendroglial and astroglial markers, appear to be exclusively

265 related to human DS and DSAD brain tissues, but not in euploid-aged or AD brains (Figures
266 1,2). This underscores the potential of these molecules to mitigate neurodevelopmental deficits
267 associated with chromosome 21 aneuploidies and improve brain function, particularly in the
268 development of white matter (13, 14).
269 Interestingly, hybrid cells were more prevalent in occipital compared to frontal cortical tissues,
270 possibly reflecting distinct spatiotemporal *C21ORF91* expression patterns in DS brains,
271 elevated from birth on in the visual cortex (V1C, part of the OCC), but diminished after birth in
272 the dorsolateral prefrontal cortex (DFC, part of FCX) compared to euploid age-matched
273 controls (24). Note that the FCX generally ages faster than the OCC (39), and in a previous
274 study on C21ORF91, comparisons were made using the biological age, not the physiological
275 age, in DS and euploid controls (24), which contrasts with our approach here (Table 1).
276 Notably, similar MBP/GFAP-co-expressing cells were also observed in a phenylketonuria
277 mouse model, which is associated with central hypomyelination (40). Similar hybrid glia have
278 also beeen described in shiverer and quaking mouse strains, both of which exhibit elevated
279 levels of neurodegeneration (41). These studies hypothesized that myelinating
280 oligodendrocytes may switch to non-myelinating GFAP-positive oligodendrocytes under
281 pathological conditions, potentially contributing to white matter gliosis.
282 Due to the inability to conduct longitudinal studies in humans and the current lack of an
283 appropriate C21ORF91 mouse model, it remains unclear whether these hybrid cells are
284 continuously generated or if they can survive and integrate throughout development. If they do
285 persist, it is yet to be determined whether they eventually commit to a specific glial lineage or
286 maintain their aberrant state, possibly contributing to an inflamed, neurotoxic milieu and
287 hypomyelination. Therefore, more extensive developmental studies will be necessary to track
288 their spatiotemporal occurrence in greater detail.
289 In this context, it is noteworthy that DS astrocytes have been shown to exhibit elevated
290 expression of *GFAP*, *GLAST*, and *iNOS* as well as activated morphologies with thicker
291 branches compared to normal brain tissues (36). These pathological features resemble those
292 we observed in our primary C21ORF91-modulated cells of oligodendroglial origin (Figure 7B',H

293 and Figure 8). Additionally, significantly elevated LCN2 protein levels have been detected in
294 the sera of DS patients (42, 43), further supporting an indirect correlation with our *ex vivo*
295 model findings. LCN2, previously described as a neurotoxic marker (44), has since been
296 reconsidered as a pan-reactive astrocyte marker, expressed in both pro-
297 inflammatory/neurotoxic and neuroprotective astrocytes (45). Interestingly, it also supports
298 oligodendrocyte maintenance and survival in demyelinating disease models (46, 47). However,
299 insufficient remyelination mediated by LCN2 has been reported following subarachnoid
300 hemorrhage (48), suggesting that LCN2's effects are context-dependent and may exacerbate
301 neurodegenerative processes (49). The role of concurrent TIMP1 expression, whether as a
302 consequence of anomalous differentiation or of functional significance, remains to be
303 determined in future studies. These investigations will also need to clarify whether the astroglial
304 features induced by C21ORF91 overexpression in oligodendroglial cells result from a disease-
305 specific glial hybrid phenotype due to disrupted differentiation, or from a glial fate switch from
306 OPCs to mature astrocytes exhibiting functional abnormalities akin to DS astrocytes.
307 Our findings on the pharmacological reversal of the C21ORF91-mediated effects offer valuable
308 insights into its underlying mechanism of action. The steroid and pituitary gonadotropin
309 inhibitor danazol (50), the corticosteroid medrysone, and the antihelminthic parbendazole
310 could all ameliorate the myelination capacity of C21ORF91-overexpressing cells, with danazol
311 and medrysone showing the most robust restoring effects (Figure 8). Further research is
312 needed to elucidate how these drugs, previously reported to enhance remyelination (27, 28,
313 51), exert their beneficial effects on OPC fate stabilization and differentiation, and how
314 C21ORF91 is functionally involved. Although these drugs are approved for treating CNS-
315 unrelated pathologies, such as endometriosis (52), fibrocystic breast disease (53), or eye
316 inflammation (54, 55), or constituting a promising candidate drug for cancer treatments shown
317 in preclinical studies (56-58), their potential application in fostering white matter generation
318 during postnatal DS development requires further verification, including determining optimal
319 therapeutic windows.

The limitations of our study include focusing exclusively on the specific impact of C21ORF91 on oligodendroglia, without addressing the broader range of modulated cell/cell interactions and genome-wide alterations observed in DS. As previously mentioned, more specific, preferably inducible animal models that allow cell-specific C21ORF91 overexpression will be essential for understanding the temporal dynamics, as comparisons using only human samples are not feasible. While no model fully replicates all neuropathological aspects of human trisomy 21 in DS (3, 59, 60), such models are better suited for developing a comprehensive understanding of genome-wide alterations and interactions, rather than restricting tissue and cell effects to a single misexpressed ortholog.

As recently reviewed by the DS biobank research consortium (61), access to well-characterized brain samples from individuals with DS and DSAD remains limited. The scarcity of human post-mortem CNS material of comparable storage duration (which may influence tissue preservation), the lack of highly suitable controls, inherent challenges in marker histology and antibody selection further hinder our ability to gain a more detailed understanding of the mechanisms that impair white matter formation and functionality in DS. Given that DS brains age more rapidly and have a reduced life expectancy compared to the healthy population, identifying suitable age-matched controls is particularly challenging. Additionally, myelin preservation differs between GM and WM in the aging brain (29), and mature oligodendrocytes naturally decline with age (62), making it difficult to establish an optimal age for comparative investigation. Thus, more extensive histological investigations, potentially incorporating additional tissue resources, are urgently needed in the future. Ideally, these studies should include single-cell profiling of DS tissues, spanning from fetal development to late stages of life.

In conclusion, an imbalanced glial composition, disrupted neurodevelopment, and reduced white matter integrity contribute to developmental and cognitive impairments seen in DS. An emerging hypothesis suggests that, in DS, not only does a neuro-to-astroglial shift result in astroglial overpopulation, but a potentially dysregulated oligodendrogenesis may also contribute to this phenomenon (10). Our findings provide strong evidence for the functional

involvement of C21ORF91 in DS neuropathology. Given the current lack of medical treatments for intellectual disability and cognitive impairment in DS patients, the pharmacological strategies we describe here, which support oligodendrogenesis and/or reduce neurotoxic stress, should be considered. Additionally, future studies must explore other undifferentiated cell populations, such as neural stem cells or glial precursor cells committed to the astroglial lineage, to better understand the broader impact of C21ORF91 misexpression on neural network formation.

MATERIALS AND METHODS

Sex as a biological variable

Due to the limited availability of human DS, DSAD, and appropriate healthy aged control tissues, our study did not consider sex as a biological variable for human histology. Nevertheless, the sex of the post-mortem cases is listed in Table 1 for transparency. For primary rat co-cultures, the sex of embryos was not considered, while for postnatal OPC cultures, the sex variable was controlled by using equal numbers of male and female P0-1 pups.

Immunohistology of human post-mortem brain tissue

Human frontal and occipital cortical tissue of all diagnostic classes was sectioned at 30 µm using a Leica Vibratome (Model# VT 10005). Tissue sections were washed twice for five minutes with 1x Tris-buffer saline (TBS, Bioland Scientific LLC, Cat# TBS01-03). For immunofluorescent staining (IF), sections were incubated in citrate buffer (0.0147 g/ml sodium citrate; pH 6,0; Fisher Chemical Cat# S279-500) at 80°C for 30 minutes. The tissue was allowed to cool to room temperature (RT) for ten minutes, then was washed twice in 1x TBS. For diaminobenzidine (DAB) staining, sections were treated with 1x TBS with 3% hydrogen peroxide and 10% MeOH for 30 minutes before four subsequent TBS washing steps. Tissue was incubated once in TBS-A (1x TBS with 0.1% Triton-x; Fisher BioReagents, Cat# BP151-

100) for 15 minutes, then transferred to TBS-B (TBS-A with 5% bovine serum albumin; Gemini Bio, Cat# 700-100P) for 30 minutes. Tissue sections were then incubated in blocking solution (TBS-B with 5% normal horse/goat serum; Vector Laboratories, Cat# S-2000-20) at RT for one hour and subsequently primary antibody solutions were applied overnight at 4°C on an orbital shaker using the following dilutions in blocking solution: mouse anti-adenomatous polyposis coli protein (APC clone CC1; 1:100; GeneTex, Cat# GTX16794, RRID:AB_422404), rabbit anti-C21ORF91 (1:200; Santa Cruz, Cat# sc-83610, RRID:AB_2259263), goat anti-sex-determining region Y-box 10 (SOX10; 1:100; Thermo Fisher Scientific, Cat# PA5-47001, RRID:AB_2608449); mouse anti-glial fibrillary acidic protein (GFAP; 1:1000 (IF), 1:3000 (DAB); Abcam, Cat# ab4648, RRID:AB_449329), goat anti-oligodendrocyte transcription factor 2 (OLIG2; 1:50; R&D systems, Cat# AF2418, RRID:AB_2157554), and rat anti-myelin basic protein (MBP; 1:3000; Bio-Rad Laboratories, Cat# MCA409S, RRID:AB_32500). Tissue sections were washed in TBS-A twice for five minutes, incubated in TBS-B once for 15 minutes, and then incubated using secondary antibody-containing solutions for one hour at RT in the dark. Secondary antibodies for IF were prepared in blocking solution at a dilution of 1:10000 of either donkey anti-mouse Alexa Fluor 488 (Invitrogen, Cat# A21202), donkey anti-rabbit Alexa Fluor 555 (Invitrogen, Cat# A31572), or donkey anti-goat Alexa Fluor 647 (Invitrogen, Cat# A21447). Following incubation in secondary antibody solution for IF, tissue samples were washed in 1x TBS for five minutes and then in 1x PBS (Bioland Scientific LLC, Cat# PBS01-02) for two minutes. Tissue was incubated in 1x TrueBlack Lipofuscin Autofluorescence Quencher (diluted in 70% ethanol; Biotium, Cat# 23007) for four minutes then washed three times in 1x TBS before being mounted to glass slides (FisherBrand Super Frost Plus Microscope slides, Cat# 12-550-15) using mounting medium with 4′,6-diamidino-2-phenylindole (DAPI; Vector Laboratories, VECTASHIELD Vibrance antifade mounting medium Cat# H-1800). After covering with Fisherbrand Microscope Cover Glass (Fisher Scientific, Cat# 12-544-E), stained tissue slices were dried overnight in the dark before imaging. For DAB staining, biotinylated secondary antibodies were prepared in blocking solution at a dilution of 1:1000 of either horse anti-rabbit (Vector Laboratories, Cat# BA-1100), horse anti-mouse

(Vector Laboratories, Cat# BA-2000), or goat anti-rat (Vector Laboratories (Vector Laboratories, Cat# BA-9400). Following incubation in secondary antibodies, tissues were incubated in avidin-biotin complex reagent (Vector Laboratories, Vectastain Elite ABC Kit, Peroxidase, Standard Cat#PK-6100) for one hour at RT. Subsequently, tissue sections were washed three times in 1x TBS for five minutes before being incubated in DAB for seven minutes. The tissue was immediately placed in TBS to quench the DAB reaction and then mounted to glass slides (FisherBrand Super Frost Plus Microscope slides, Cat# 12-550-15) and dried overnight in the dark. Cresyl violet was used for counterstaining for three minutes. Following washing steps with distilled water, slides were submerged in 50% EtOH for 10 minutes, 70% EtOH for 10 minutes, 96% EtOH for 10 minutes, and 100% EtOH for 10 minutes. Slides were then incubated twice in Histoclear (Electron Microscopy Sciences, Cat# 64110-04) for 10 minutes. Finally, slides were embedded using DPX mounting media (Electron Microscopy Services, Cat# 13512) and then left to dry overnight in the dark before imaging.

Preparation, culture, and transfection of rat primary oligodendroglial precursor cells

Preparation of primary OPCs obtained from postnatal day zero to one (P0-1) cerebral cortices of Wistar rats of either sex was achieved as previously described (25, 27). After purification, primary OPCs (>97% pure based on GLAST, GFAP, and Iba-1 staining to determine astroglial or microglial contaminations, respectively; data not shown) were nucleofected with a pV22 plasmid containing the complete coding sequence of the rat ortholog *C21ORF91* gene (*RGD1563888*) or the equivalent control plasmid (pHTN, Promega France). Plasmids were designed and generated by Hybrigenics SA, Paris, France. As previously published (25), 0.8–1 × 10^6 cells were transfected with the Amaxa™ Basic Glial Cells Nucleofector™ Kit (Lonza, Basel, Switzerland) following the company's protocol. Briefly, a total amount of 2 µg plasmid per 1 × 10^6 cells was nucleofected with the high-efficiency program A-033. Control and C21ORF91 overexpression plasmids were co-transfected with pcDNA3-hyg-citrine vector for visualization. Transfected OPCs were seeded onto 0.25 mg/ml poly-D-lysine (PDL, Sigma-Aldrich, St. Louis, USA) coated glass coverslips (13 mm) in 24-well plates (for

immunocytochemistry; 7 × 10^4 cells/well) in expansion medium. To this end, Sato medium was supplemented with 10 ng/ml recombinant human basic fibroblast growth factor (bFGF; R&D Systems, Wiesbaden-Nordenstadt, Germany) and 10 ng/ml recombinant human platelet-derived growth factor-AA (PDGF-AA; R&D Systems, Wiesbaden-Nordenstadt, Germany). After 4–5 h, the expansion medium was replaced by a differentiation medium (Sato medium including 0.5% fetal bovine serum; Capricorn Scientific, Palo Alto, CA, USA). For stimulation with myelin repair drugs, differentiation medium was further supplemented with 5 µM danazol (Sigma-Aldrich, CAS 17,230-88-5), 0.02 µM parbendazole (MedChem Express, Monmouth Junction, NJ, USA, CAS 14255879), or 5 µM medrysone (6α-methyl-11β-hydroxy-Progesterone; Cayman Chemical, Cat#19533). All three molecules were dissolved in dimethyl sulfoxide (DMSO, Sigma-Aldrich) for stock solutions. Thus, DMSO served as a control, used at an equal dilution as in the highest treatment concentration (here 5 µM) after elucidating that DMSO itself exerted no concentration-dependent effects (data not shown, compare (27)). Note that DMSO treatment did also not affect the potential and morphological features of C21ORF91 overexpressing cells. Cells were cultivated for two or five days, washed once with PBS (Sigma-Aldrich), and then fixed using 4% PFA at room temperature (RT) for 10 min before two times washing with PBS and storing fixed cells at 4°C in the dark.

C21ORF91 overexpressing OPCs cultivated on rat myelinating co-cultures

For the generation of myelinating neuron/oligodendrocyte co-cultures, cerebral cortices of 16-day-old (E16) rat embryos of both sexes were processed (30, 63). According to the earlier published method (25), 10 × 10^4 transfected OPCs were centrally applied onto co-cultures grown for 15 days *in vitro* (DIV15, Figure 3a). The medium was exchanged twice a week with freshly prepared myelination medium supplemented with myelin repair drugs as follows: 5 µM danazol, 0.02 µM parbendazole, 5 µM medrysone, 5 µM teriflunomide (provided by Sanofi Genzyme, Waltham, USA) or 0.1 µM methiazole (BOC Sciences, CAS 74,239-55-7). Teriflunomide was only used in an early pulse stimulation (as described in (30); Figure 3a), and therefore, after three days, the medium was replaced with a non-supplemented

myelination medium. All molecules were dissolved in DMSO and the dilution of the highest treatment concentration (here 5 µM) served as control. For the teriflunomide control, the DMSO-containing medium was also exchanged for a non-supplemented myelination medium after three days according to the teriflunomide pulse. Note that there was no difference between three days of DMSO early pulse control and continuous DMSO treatment for 10 days (data not shown). To simplify data presentation, only the continuous DMSO application was used as a control condition for calculations. At DIV25, myelinating co-cultures were fixed with 4% PFA for 15 min at RT after two washing steps with PBS and processed for immunofluorescent staining. After final washing steps, fixed co-cultures were stored at 4°C in the dark.

Immunocytochemistry

In monocultured transfected cells, non-specific binding of antibodies was prevented by incubation in blocking solution [10% normal goat/donkey serum (NGS or NDS); in PBS containing 0.1% Triton X-100] at RT for 45 min. Subsequently, cells were subjected to primary antibody solution (10% NGS or NDS, in PBS containing 0.01% Triton X- 100), using the following dilutions overnight at 4°C: rabbit anti-GFAP (1:1000; DAKO Agilent, Cat# Z0334, RRID:AB_10013382), mouse anti-GFAP (1:1000; Millipore Cat# MAB3402, RRID:AB_94844), rat anti-MBP (1:250; Bio-Rad Laboratories, Cat# MCA409S, RRID:AB_32500), mouse anti-APC (clone CC1; 1:1000; GeneTex, Cat# GTX16794, RRID:AB_422404), rabbit anti-OLIG2 (1:500; Merck Millipore, Cat# AB9610, RRID:AB_570666), goat anti-platelet-derived growth factor receptor alpha (PDGFα/CD140A; 1:250, Neuromics, Cat# GT15150, RRID:AB_2737233), mouse anti-astrocyte cell surface antigen-1 (ACSA-1/GLAST; 1:200; Miltenyi Biotec, Cat# 130-095-822, RRID:AB_10829302), rabbit anti-SOX10 (1:100; DCS Immunoline, Cat#S1058C002, RRID:AB_2313583), rabbit anti-MAF bZIP transcription factor G (MAFG; 1:300; Genetex; Cat#GTX114541, RRID:AB_10619599), goat anti-lipocalin-2 (LCN2; 1:100; R&D Systems, Cat#AF1857, RRID:AB_35502), goat anti-tissue inhibitor of metalloproteinases 1 (TIMP1; 1:200; R&D System, Cat#AF580, RRID:AB_355455), and

chicken anti-green fluorescent protein/citrine (GFP; 1:1.000; Aves Labs, Cat# GFP-1020, RRID:AB_10000240). Following three washing steps with PBS, secondary antibodies (anti-mouse, anti-rabbit, anti-goat) conjugated with either Alexa Fluor405, Alexa Fluor488, or Alexa Fluor594 (1:500; Thermo Fisher Scientific, Darmstadt, Germany) in PBS supplemented with DAPI (0.02 µg/ml; Roche Diagnostic GmbH, Mannheim, Germany) were applied for 90 min at RT. Cells were mounted with Citifluor (Cilifluor, Leicester, United Kingdom). To analyze transfected cells in the myelinating co-culture system, the blocking solution contained 2% NGS and 0.5% Triton X-100 in PBS, whereas the following primary antibodies were diluted in 2% NGS and 0.1% Triton X-100: rat anti-MBP (1:250), mouse anti-GFAP (1:800), rabbit anti-neurofilament (NF, 1:1.000, Abcam, Cambridge, UK Cat# ab8135, RRID:AB_306,298), and chicken anti-GFP (1:1.000). After washing with PBS, secondary antibodies conjugated with either Alexa Fluor405, Alexa Fluor488, Alexa Fluor594 or Alexa Fluor 647 (1:500; Thermo Fisher Scientific, Darmstadt, Germany) in PBS supplemented with DAPI (0.02 µg/ml) were applied for 90 min at RT.

Enzyme-linked immunosorbent assay (ELISA)

To assess tumor necrosis factor alpha (TNFa) and LCN2 protein secretion, supernatants of stimulated cells were collected after five days of treatment, spun down to eliminate cell debris or floating cells (1.000 × g; 5 min; 4 °C), and pure supernatants were stored at −80 °C. Protein levels were quantified in duplets for each independent experiment using the colorimetric sandwich ELISA kits for rat TNFα (ab100785, Abcam) and rat LCN2 (ab119602, Abcam) according to the manufacturer's instructions. Measurements were performed with the Tecan INFinite M200 PRO Multimode Microplate Reader (Tecan, Männedorf, Switzerland).

Image acquisition and analysis

Whole slide images of DAB-stained human tissue sections were acquired via an Aperio Versa 200 digital slide scanner (23VER200BFX001, Leica Biosystems) at 20x and 40x magnification in brightfield. Images were processed using the Aperio Imagescope software (Leica

Biosystems) for further analysis of C21ORF91, MBP, and GFAP protein co-localization. A standard scale grid was applied to the whole slide images to pinpoint precise regions across sets of three serial sections stained with either MBP, GFAP, or C21ORF91. Unique pathological landmarks (e.g., vasculature and nuclei) were utilized during the image acquisition process to find and maintain consistent regional integrity among serial sections. Images were transferred to Google Slides, and aspect ratios were locked prior to analysis. Images were subsequently cropped and overlaid to assess the co-localization of the aforementioned markers by adjusting opacity.

For analysis of human sections, immunofluorescent slides were imaged using an LSM Airyscan 900 coNFocal microscope (Zeiss). Each image, at least two per case, was taken at 40x magnification as a Z-stack at 1 µm per slice for 10 µm within the total 30 µm thick post-mortem tissue sample. The Airyscan feature (increasing signal-to-noise ratio) was applied to each 1 µm-stack for a total of 10 µm to render the best resolution per slice and finally compressed via maximum orthogonal array projection. 3D rendering to assess the morphology and correlation of human C21ORF91 protein in OLIG2/GFAP -co-expressing glial hybrids was obtained using the IMARIS 10.1.0 software.

For image acquisition of transfected OPC monocultures, the Axionplan 2 microscope (Zeiss, Jena, Germany) was used and the analyses were performed using the ImageJ BioVoxxel software (64). Nine images per coverslip (two coverslips/condition; mean of two coverslips derived from the same animal pool representing an independent experiment (n=1)) were captured at 20x magnification, maintaining consistent exposure times across experiments. For image acquisition of transfected cells in co-cultures, consistent settings were applied using the Zeiss CLSM microscope 510 (CLSM 510, Zeiss) to maintain uniformity in exposure times, laser intensities, and digital gains. Transfected (GFP-positive) cells were assessed using a morphology-based scoring system as outlined in (25). This involved classifying the cells into three categories based on morphological criteria: MBP-positive cells with a high degree of arborization [pos], integrated and myelinating oligodendrocytes displaying T-shape structures enwrapping neurofilament (NF)-positive axons (63) [myelin], and the recently described non-

543 organized MBP expressing [NOM] cell phenotype. For quantification, the number of protein
544 marker-positive cells in relation to GFP-expressing cells (transfected cells) was calculated and
545 shown as a percentage. Note, that when marker-/GFP-positive subpopulations are displayed
546 (Figure 3d, Figure 6a-d, Figure 7a-e, Figure 8), the total number of cells for this dataset/marker
547 combination was set as 100%. This standardization allows the representation of co-expressing
548 marker distributions within these subpopulations, effectively highlighting cells that are triple-
549 positive.
550
551 **Statistical analysis**
552 Data are presented as mean values ± standard error of the mean (SEM) deriving from at least
553 three independent experiments. Graphs and statistical analysis were performed using Excel
554 and the GraphPad Prism 8.0.2 software (GraphPad Prism, San Diego, CA, USA; RRID:
555 SCR_002798). Shapiro-Wilk normality test was used to assess the absence of Gaussian
556 distribution of all datasets. To determine statistical significance for normally distributed data
557 sets, Students t-test was applied for comparing two groups and one-way analysis of variance
558 (ANOVA) with Dunnett's post-test for multiple comparisons was applied to compare three or
559 more groups. For data sets not passing the Shapiro-Wilk normality test, Kruskal-Wallis test
560 with Dunn's post-test for multiple comparisons of three or more groups was applied. Statistical
561 significance thresholds were set as follows: *$p \leq 0.05$; **$p \leq 0.01$; ***$p \leq 0.001$ and ns = not
562 significant.
563
564 **Study approval**
565 Frontal and occipital human post-mortem brain tissue was acquired from the Alzheimer's
566 Disease Research Center (ADRC) at the University of California, Irvine. Human tissue
567 collection and handling adhered to the University of California, Irvine International Review
568 Board guidelines. Diagnosis of Alzheimer's Disease neuropathology in human tissue was
569 performed in accordance with National Institute on Aging-Alzheimer's Association (NIA-AA)

guidelines. Human tissue was fixed in 4% paraformaldehyde (PFA) and then stored long-term at 4°C in 0.2% sodium azide in phosphate-buffered saline (PBS) solution.

Human brain tissues from four diagnostic classes were included in this study (Table 1): aged control (AC), Hsa21 trisomic classes: DS and DS with AD neuropathology (DSAD), and a positive control that included sporadic AD (AD). As DS brains demonstrate accelerated signs of aging (7), DS and DSAD cases could not be age-matched with AC or AD tissue but were matched according to pathology.

The preparation of neonatal rat primary oligodendroglial cell cultures was approved by the Institutional Review Board (IRB) of the Zentrale Einrichtung für Tierforschung und wissenschaftliche Tierschutzaufgaben (ZETT) at the Heinrich-Heine University Düsseldorf with the licenses O69/11 and V54/09. The review board of the state government Landesamt für Natur, Umwelt und Verbraucherschutz (LANUV), North-Rhine Westphalia, Germany, granted approval for generating embryonic rat myelinating co-cultures with license Az.81-02.04.2018.A388.

Data availability

Values for all data points in graphs are reported in the Supporting Data Values file.

Author Contributions

LR and PK: conceptualization and study design; LR and PK: methodology; LR, CAS, KC, BZ, and LW: experiments; LR, CAS, and KC: data analysis; LR, CAS, EH, and PK: data interpretation and verification; LR, CAS, KC, BZ, PG, and PK: data curation; LR: software; LR and PK: visualization; LR, CAS, and EH literature research; LR and PK: writing – original draft; LR, CAS, KC, LW, PG, EH, DK, and PK: review & editing; LR, DK and PK: funding acquisition; PK: supervision. All authors contributed to the manuscript revision and read and approved the submitted version.

Acknowledgments

We thank Birgit Blomenkamp-Radermacher and Julia Jadasz for their technical assistance. Furthermore, we thank Hybrigenics SA for providing the C21orf91 expression vectors. Some elements of the table of contents image and schematic presentation of the experimental design have been created with BioRender.com.

REFERENCES

1. Antonarakis SE, et al. Down syndrome. *Nat Rev Dis Primers*. Feb 6 2020;6(1):9. doi:10.1038/s41572-019-0143-7
2. de Graaf G, et al. Estimation of the number of people with Down syndrome in Europe. *Eur J Hum Genet*. Mar 2021;29(3):402-410. doi:10.1038/s41431-020-00748-y
3. Klein JA, Haydar TF. Neurodevelopment in Down syndrome: Concordance in humans and models. *Front Cell Neurosci*. 2022;16:941855. doi:10.3389/fncel.2022.941855
4. Pennington BF, et al. The neuropsychology of Down syndrome: evidence for hippocampal dysfunction. *Child development*. Jan-Feb 2003;74(1):75-93. doi:10.1111/1467-8624.00522
5. Rowe J, et al. Cognitive executive function in Down's syndrome. *The British journal of clinical psychology*. Mar 2006;45(Pt 1):5-17. doi:10.1348/014466505x29594
6. Lanfranchi S, et al. Executive function in adolescents with Down Syndrome. *Journal of intellectual disability research : JIDR*. Apr 2010;54(4):308-19. doi:10.1111/j.1365-2788.2010.01262.x
7. Lott IT, Head E. Dementia in Down syndrome: unique insights for Alzheimer disease research. *Nat Rev Neurol*. Mar 2019;15(3):135-147. doi:10.1038/s41582-018-0132-6
8. Fukami-Gartner A, et al. Comprehensive volumetric phenotyping of the neonatal brain in Down syndrome. *Cereb Cortex*. Jul 5 2023;33(14):8921-8941. doi:10.1093/cercor/bhad171
9. McCann B, et al. Structural magnetic resonance imaging demonstrates volumetric brain abnormalities in down syndrome: Newborns to young adults. *Neuroimage Clin*. 2021;32:102815. doi:10.1016/j.nicl.2021.102815
10. Reiche L, et al. Aberrant Oligodendrogenesis in Down Syndrome: Shift in Gliogenesis? *Cells*. Dec 7 2019;8(12)doi:10.3390/cells8121591
11. Ponroy Bally B, Murai KK. Astrocytes in Down Syndrome Across the Lifespan. *Front Cell Neurosci*. 2021;15:702685. doi:10.3389/fncel.2021.702685
12. Stagni F, Bartesaghi R. The Challenging Pathway of Treatment for Neurogenesis Impairment in Down Syndrome: Achievements and Perspectives. *Front Cell Neurosci*. 2022;16:903729. doi:10.3389/fncel.2022.903729
13. Abraham H, et al. Impaired myelination of the human hippocampal formation in Down syndrome. *Int J Dev Neurosci*. Apr 2012;30(2):147-58. doi:10.1016/j.ijdevneu.2011.11.005
14. Olmos-Serrano JL, et al. Down Syndrome Developmental Brain Transcriptome Reveals Defective Oligodendrocyte Differentiation and Myelination. *Neuron*. Mar 16 2016;89(6):1208-22. doi:10.1016/j.neuron.2016.01.042
15. Fenoll R, et al. Anomalous White Matter Structure and the Effect of Age in Down Syndrome Patients. *J Alzheimers Dis*. 2017;57(1):61-70. doi:10.3233/JAD-161112
16. Powell D, et al. Frontal white matter integrity in adults with Down syndrome with and without dementia. *Neurobiol Aging*. Jul 2014;35(7):1562-1569. doi:10.1016/j.neurobiolaging.2014.01.137
17. McKenzie IA, et al. Motor skill learning requires active central myelination. *Science*. Oct 17 2014;346(6207):318-22. doi:10.1126/science.1254960
18. Liu J, et al. Impaired adult myelination in the prefrontal cortex of socially isolated mice. *Nat Neurosci*. Dec 2012;15(12):1621-3. doi:10.1038/nn.3263

19. Lebel C, et al. Diffusion tensor imaging of white matter tract evolution over the lifespan. *NeuroImage*. Mar 2012;60(1):340-52. doi:10.1016/j.neuroimage.2011.11.094
20. Marangon D, et al. Oligodendrocyte Progenitors in Glial Scar: A Bet on Remyelination. *Cells*. Jun 12 2024;13(12)doi:10.3390/cells13121024
21. Dulamea AO. Role of Oligodendrocyte Dysfunction in Demyelination, Remyelination and Neurodegeneration in Multiple Sclerosis. *Advances in experimental medicine and biology*. 2017;958:91-127. doi:10.1007/978-3-319-47861-6_7
22. Tepavcevic V, Lubetzki C. Oligodendrocyte progenitor cell recruitment and remyelination in multiple sclerosis: the more, the merrier? *Brain*. Dec 19 2022;145(12):4178-4192. doi:10.1093/brain/awac307
23. Cayre M, et al. Myelin Repair: From Animal Models to Humans. *Front Cell Neurosci*. 2021;15:604865. doi:10.3389/fncel.2021.604865
24. Li SS, et al. The HSA21 gene EURL/C21ORF91 controls neurogenesis within the cerebral cortex and is implicated in the pathogenesis of Down Syndrome. Article. *Sci Rep*. Jul 2016;6:14. 29514. doi:10.1038/srep29514
25. Reiche L, et al. C21orf91 Regulates Oligodendroglial Precursor Cell Fate-A Switch in the Glial Lineage? *Frontiers in Cellular Neuroscience*. Mar 16 2021;15doi:ARTN 653075
10.3389/fncel.2021.653075
26. Göttle P, et al. Teriflunomide as a therapeutic means for myelin repair. *Journal of neuroinflammation*. Jan 7 2023;20(1):7. doi:10.1186/s12974-022-02686-6
27. Manousi A, et al. Identification of novel myelin repair drugs by modulation of oligodendroglial differentiation competence. *EBioMedicine*. Mar 2021;65:103276. doi:10.1016/j.ebiom.2021.103276
28. Silva Oliveira Junior M, et al. Myelin repair is fostered by the corticosteroid medrysone specifically acting on astroglial subpopulations. *EBioMedicine*. Sep 2022;83:104204. doi:10.1016/j.ebiom.2022.104204
29. Ahn JH, et al. Age-dependent differences in myelin basic protein expression in the hippocampus of young, adult and aged gerbils. *Lab Anim Res*. Sep 2017;33(3):237-243. doi:10.5625/lar.2017.33.3.237
30. Göttle P, et al. Teriflunomide promotes oligodendroglial differentiation and myelination. *Journal of neuroinflammation*. Mar 13 2018;15(1):76. doi:10.1186/s12974-018-1110-z
31. Setoguchi T, Kondo T. Nuclear export of OLIG2 in neural stem cells is essential for ciliary neurotrophic factor-induced astrocyte differentiation. *J Cell Biol*. Sep 27 2004;166(7):963-8. doi:10.1083/jcb.200404104
32. Rehberg S, et al. Sox10 is an active nucleocytoplasmic shuttle protein, and shuttling is crucial for Sox10-mediated transactivation. *Mol Cell Biol*. Aug 2002;22(16):5826-34. doi:10.1128/MCB.22.16.5826-5834.2002
33. Küspert M, et al. Olig2 regulates Sox10 expression in oligodendrocyte precursors through an evolutionary conserved distal enhancer. *Nucleic acids research*. Mar 2011;39(4):1280-93. doi:10.1093/nar/gkq951
34. Liu Z, et al. Induction of oligodendrocyte differentiation by Olig2 and Sox10: evidence for reciprocal interactions and dosage-dependent mechanisms. *Dev Biol*. Feb 15 2007;302(2):683-93. doi:10.1016/j.ydbio.2006.10.007
35. Silva Oliveira Junior M, et al. Star power: harnessing the reactive astrocyte response to promote remyelination in multiple sclerosis. *Neural regeneration research*. Mar 2024;19(3):578-582. doi:10.4103/1673-5374.380879
36. Chen C, et al. Role of astroglia in Down's syndrome revealed by patient-derived human-induced pluripotent stem cells. *Nat Commun*. Jul 18 2014;5:4430. doi:10.1038/ncomms5430
37. Escartin C, et al. Reactive astrocyte nomenclature, definitions, and future directions. *Nat Neurosci*. 2021;24(3):312-325. doi:10.1038/s41593-020-00783-4
38. Zhou B, et al. Astrocyte morphology: Diversity, plasticity, and role in neurological diseases. *CNS Neurosci Ther*. Jun 2019;25(6):665-673. doi:10.1111/cns.13123
39. Hedden T, Gabrieli JD. Insights into the ageing mind: a view from cognitive neuroscience. *Nat Rev Neurosci*. Feb 2004;5(2):87-96. doi:10.1038/nrn1323

40. Dyer CA, et al. Evidence for central nervous system glial cell plasticity in phenylketonuria. *J Neuropathol Exp Neurol*. Jul 1996;55(7):795-814. doi:10.1097/00005072-199607000-00005
41. Dyer CA, et al. GFAP-positive and myelin marker-positive glia in normal and pathologic environments. *J Neurosci Res*. May 1 2000;60(3):412-26. doi:10.1002/(SICI)1097-4547(20000501)60:3<412::AID-JNR16>3.0.CO;2-E
42. Dogliotti G, et al. Serum neutrophil gelatinase-B associated lipocalin (NGAL) levels in Down's syndrome patients. *Immun Ageing*. Dec 16 2010;7 Suppl 1(Suppl 1):S7. doi:10.1186/1742-4933-7-S1-S7
43. Naude PJ, et al. Serum NGAL is Associated with Distinct Plasma Amyloid-beta Peptides According to the Clinical Diagnosis of Dementia in Down Syndrome. *J Alzheimers Dis*. 2015;45(3):733-43. doi:10.3233/JAD-142514
44. Bi F, et al. Reactive astrocytes secrete lcn2 to promote neuron death. *Proc Natl Acad Sci U S A*. Mar 5 2013;110(10):4069-74. doi:10.1073/pnas.1218497110
45. Liddelow SA, et al. Neurotoxic reactive astrocytes are induced by activated microglia. *Nature*. 2017;541(7638):481-487. doi:10.1038/nature21029
46. Gasterich N, et al. Lipocalin 2 attenuates oligodendrocyte loss and immune cell infiltration in mouse models for multiple sclerosis. *Glia*. Nov 2022;70(11):2188-2206. doi:10.1002/glia.24245
47. Kalinin S, Feinstein DL. Astrocyte lipocalin-2 modestly effects disease severity in a mouse model of multiple sclerosis while reducing mature oligodendrocyte protein and mRNA expression. *Neurosci Lett*. Oct 15 2023;815:137497. doi:10.1016/j.neulet.2023.137497
48. Li Q, et al. Lipocalin-2-Mediated Insufficient Oligodendrocyte Progenitor Cell Remyelination for White Matter Injury After Subarachnoid Hemorrhage via SCL22A17 Receptor/Early Growth Response Protein 1 Signaling. *Neurosci Bull*. Dec 2022;38(12):1457-1475. doi:10.1007/s12264-022-00906-w
49. Dekens DW, et al. Lipocalin 2 as a link between ageing, risk factor conditions and age-related brain diseases. *Ageing Res Rev*. Sep 2021;70:101414. doi:10.1016/j.arr.2021.101414
50. Ashfaq S, et al. Danazol. *StatPearls*. 2024.
51. Werner L, et al. A Novel Ex Vivo Model to Study Therapeutic Treatments for Myelin Repair following Ischemic Damage. *Int J Mol Sci*. Jun 30 2023;24(13)doi:10.3390/ijms241310972
52. Dmowski WP, et al. Danazol--a synthetic steroid derivative with interesting physiologic properties. *Fertil Steril*. Jan 1971;22(1):9-18. doi:10.1016/s0015-0282(16)37981-x
53. Greenblatt RB, et al. The treatment of benign breast disease with danazol. *Fertil Steril*. Sep 1980;34(3):242-5.
54. Bedrossian RH, Eriksen SP. The treatment of ocular inflammation with medrysone. *Arch Ophthalmol*. Feb 1969;81(2):184-91. doi:10.1001/archopht.1969.00990010186008
55. Spaeth GL. Hydroxymethylprogesterone. An anti-inflammatory steroid without apparent effect on intraocular pressure. *Arch Ophthalmol*. Jun 1966;75(6):783-7. doi:10.1001/archopht.1966.00970050785014
56. Florio R, et al. The Benzimidazole-Based Anthelmintic Parbendazole: A Repurposed Drug Candidate That Synergizes with Gemcitabine in Pancreatic Cancer. *Cancers (Basel)*. Dec 17 2019;11(12)doi:10.3390/cancers11122042
57. Liang D, et al. Identification of anthelmintic parbendazole as a therapeutic molecule for HNSCC through connectivity map-based drug repositioning. *Acta Pharm Sin B*. May 2022;12(5):2429-2442. doi:10.1016/j.apsb.2021.12.005
58. Lo YC, et al. Computational Cell Cycle Profiling of Cancer Cells for Prioritizing FDA-Approved Drugs with Repurposing Potential. *Sci Rep*. Sep 12 2017;7(1):11261. doi:10.1038/s41598-017-11508-2
59. Moyer AJ, et al. All Creatures Great and Small: New Approaches for Understanding Down Syndrome Genetics. *Trends Genet*. May 2021;37(5):444-459. doi:10.1016/j.tig.2020.09.017
60. Ishihara K. Genes Associated with Disturbed Cerebral Neurogenesis in the Embryonic Brain of Mouse Models of Down Syndrome. *Genes (Basel)*. Oct 11 2021;12(10)doi:10.3390/genes12101598

757 61. Aldecoa I, et al. Down Syndrome Biobank Consortium: A perspective. *Alzheimer's &*
758 *dementia : the journal of the Alzheimer's Association*. Mar 2024;20(3):2262-2272.
759 doi:10.1002/alz.13692
760 62. Soreq L, et al. Major Shifts in Glial Regional Identity Are a Transcriptional Hallmark of
761 Human Brain Aging. *Cell Rep*. Jan 10 2017;18(2):557-570. doi:10.1016/j.celrep.2016.12.011
762 63. Göttle P, Küry P. Intracellular Protein Shuttling: A Mechanism Relevant for Myelin
763 Repair in Multiple Sclerosis? *International Journal of Molecular Sciences*. 07/03 05/29/received
764 06/25/accepted 2015;16(7):15057-15085. doi:10.3390/ijms160715057

765 64. Schindelin J, et al. Fiji: an open-source platform for biological-image analysis. *Nat*
766 *Methods*. Jun 28 2012;9(7):676-82. doi:10.1038/nmeth.2019

767

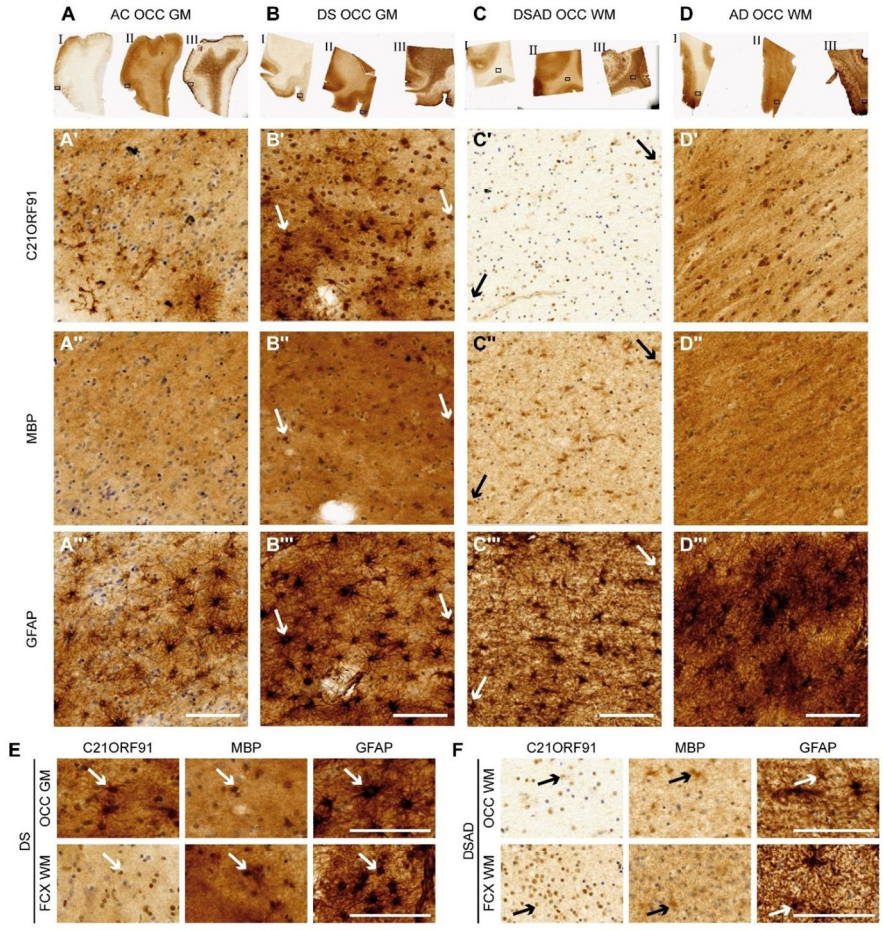

Figure 1: Co-expression of the oligodendroglial marker MBP, the astroglial marker GFAP, and C21ORF91 protein only occurs in human Hsa21 trisomic post-mortem tissues. Representative images of immunohistological staining (diaminobenzidine (DAB)) of occipital- and frontal cortex tissues (OCC, FCX, respectively) of Down syndrome (DS), DS with Alzheimer's disease (DSAD), AD, and aged control (AC) brains. By applying a grid-based assessment tool for orientation within the three serially sectioned brain slides that are shown in **(A-D)**, cells positive for all three stained proteins (arrows), namely C21ORF91 (I in **A-D**¸ **A'-D'**), MBP (II in **A-D**¸ **A''-D''**), and GFAP (III in **A-D**¸ **A'''-D'''**) were identified. This permissive glial hybrid phenotype was observed in both the OCC and FCX of DS **(E)** and DSAD **(F).** Scale bars: 100 µm

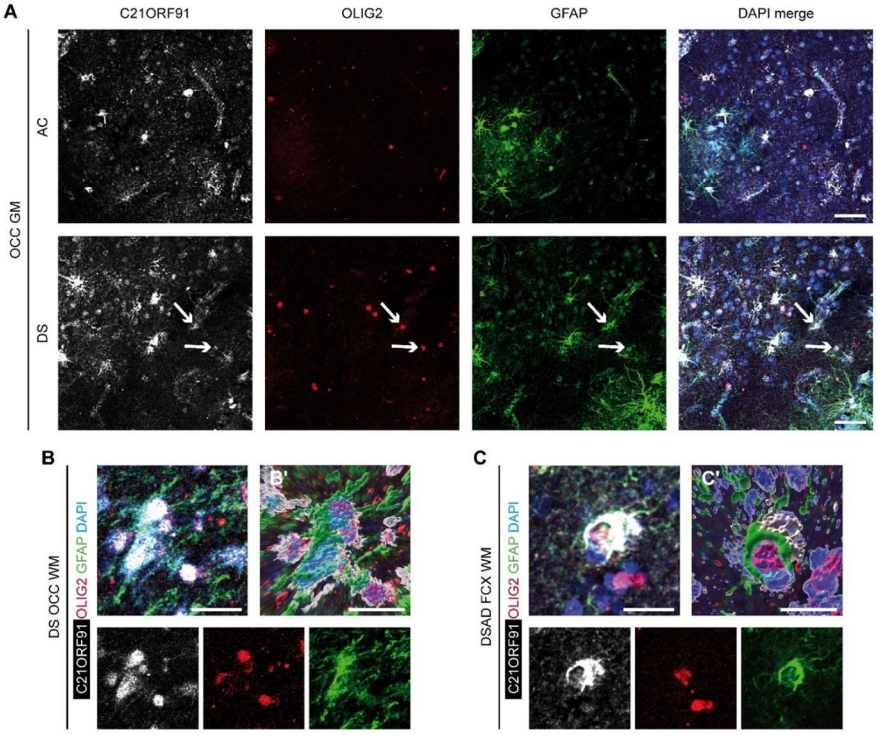

Figure 2: C21ORF91 protein shows a cell-specific expression pattern in human post-mortem tissues and correlates with OLIG2/GFAP co-expressing hybrid cells in Hsa21 trisomic conditions. Occipital - and frontal cortex tissues (OCC, FCX, respectively) of Down syndrome (DS), DS with Alzheimer's disease (DSAD), AD, and aged control (AC) brains were stained using antibodies against C21ORF91 (white), OLIG2 (red), and GFAP (green) **(A)**. Glial hybrid cells (arrows), with a clear nuclear OLIG2- and robust GFAP-signal, occurred exclusively in DS and DSAD in white and gray matter (WM, GM). Such cells showed a small morphological expansion and atrophied morphologies as representatively shown in the higher magnified images for DS OCC WM **(B)** and DSAD FCX GM **(C)** and their corresponding 3D rendered illustrations **(B',C')**. Note that for clearer presentation, in the 3D rendered images, DAPI (blue, nuclear staining) and C21ORF91 were selectively blurred as their signals masked/overlayed the nuclear OLIG2 signals. Scale bars: Scale bars: 50 µm **(A)** and 20 µm **(B-C')**.

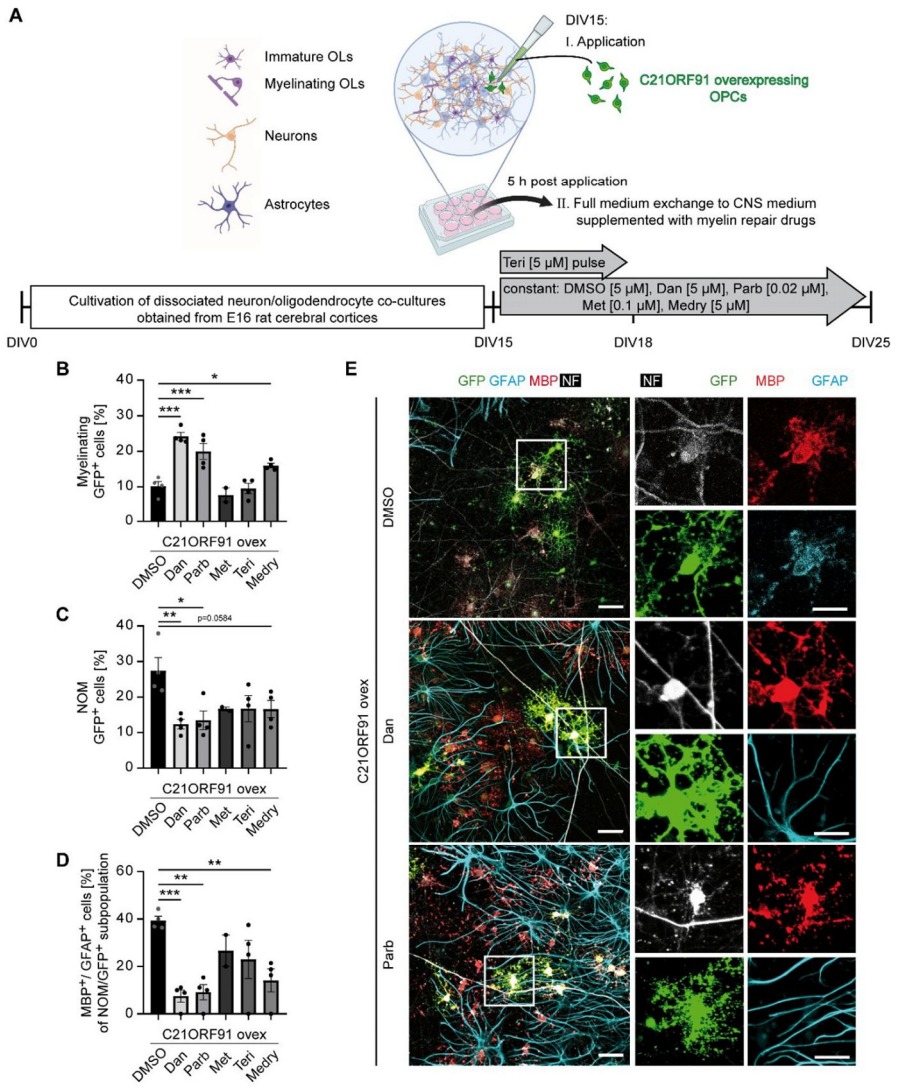

Figure 3: Restorative effects of myelin repair drugs on the myelination capacity of C21ORF91-overexpressing oligodendroglial cells. (A) Schematic presentation of the experimental set-up to evaluate the impact of myelin repair drug treatments (grey arrows and bars) on the differentiation and myelination capacity of C21ORF91-overexpressing rat oligodendroglial precursor cells (OPCs) (green, co-transfected with a GFP expression vector) applied onto dissociated neuron/oligodendrocyte co-cultures that have been cultivated 15 days *in vitro* (DIV). Ten days after application, immunofluorescence analysis of C21ORF91-overexpressing cells (ovex; GFP-positive cells) demonstrated that compared to dimethyl sulfoxide (DMSO, black bars, serving as control) danazol (Dan) and parbendazole (Parb) not only significantly increased the number of myelinating cells **(B)**, but also reduced the number of cells with a non-organized MBP expressing (NOM) phenotype **(C)**. The aberrant concurrent expression of MBP and GFAP within this NOM subpopulation **(D)** was not only diminished via danazol and parbendazole treatment but also by medrysone (Medry). Methiazole (Met) and teriflunomide (Teri)

805 treatment showed no significant effects compared to DMSO within this setup. Zoomed views (white
806 squares) of the immunostaining **(E)** for GFP (green), GFAP (cyan), MBP (red), and NF (grey)
807 representatively show an $MBP^+/GFAP^+$ NOM cell for the control (DMSO) treated group of C21ORF91-
808 overexpressing cells, while for danazol and parbendazole myelinating cells, depicting the typical T-
809 shaped structures of ensheathed axons are shown. Scale bars of overviews: 50 µm and for zoomed
810 view: 25 µm. Data are shown as mean values (±SEM) deriving from *n* = 4 experiments (for DMSO, dan,
811 parb, teri, medry in **B-D**) and *n* = 2 experiments (for met in **B-D**). Statistical significance was calculated
812 using one-way ANOVA with Dunnett's post-test (met excluded): *p ≤ 0.05, **p ≤ 0.01, ***p ≤ 0.001.

813

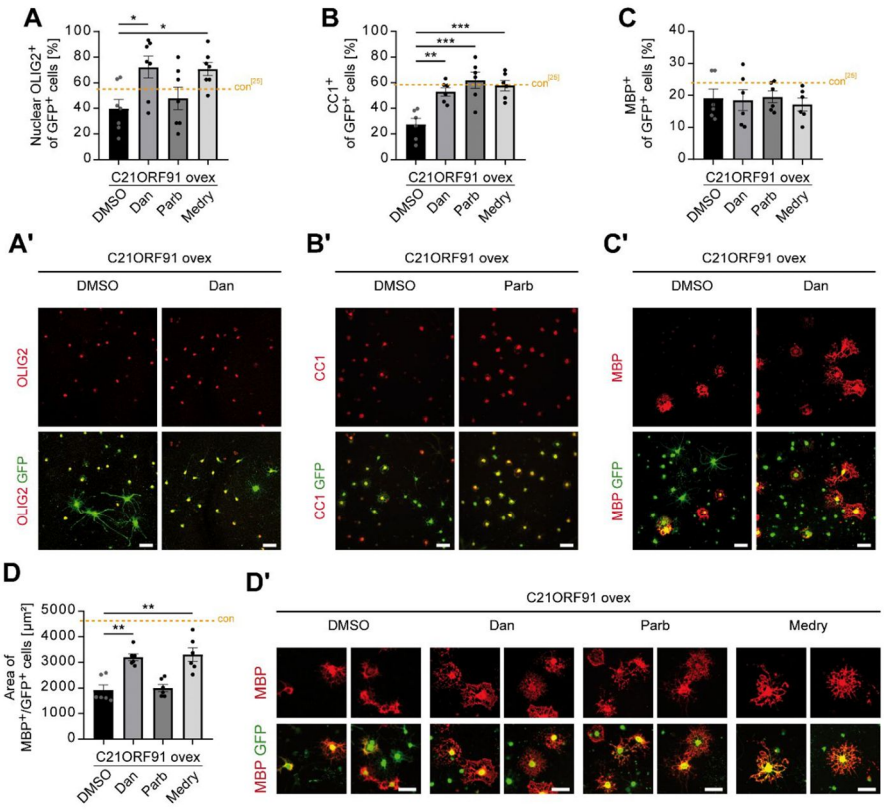

Figure 4: Myelin repair drugs foster rat OPC differentiation upon C21ORF91 overexpression. OPCs were co-transfected with a GFP expression vector (green) and a C21ORF91 overexpression construct (ovex) and treated with danazol (Dan), parbendazole (Parb), medrysone (Medry), or DMSO (black bars, control). After five days of differentiation upon elevated C21ORF91 expression, a significantly increased number of cells expressing oligodendroglial markers (red) OLIG2 **(A)** and CC1 **(B)** were observed via treatment with myelin repair drugs, representative images of which are shown in **(A', B')**. For MBP **(C)**, no change in the number of expressing cells was observed, but cell morphologies of danazol-treated cells appeared more complex **(C').** This was further assessed and confirmed utilizing area expansion analysis **(D, D')**. Note that the orange dashed lines within each graph indicate the mean values of control transfected OPCs (con; empty control vector). Recently published control values are indicated by [25]. Scale bars: 50 µm. Data are shown as means (±SEM). One-way ANOVA with Dunnett's post-hoc test (**A-C**, *n* = 5-7) for multiple comparison with control (DMSO) or Kruskal-Wallis test with Dunn's post-test (**D**, dot = mean of 10-15 cells/treatment for *n* = 6) was used to evaluate statistical significance: *p < 0.05, **p < 0 .01, ***p ≤ 0.001.

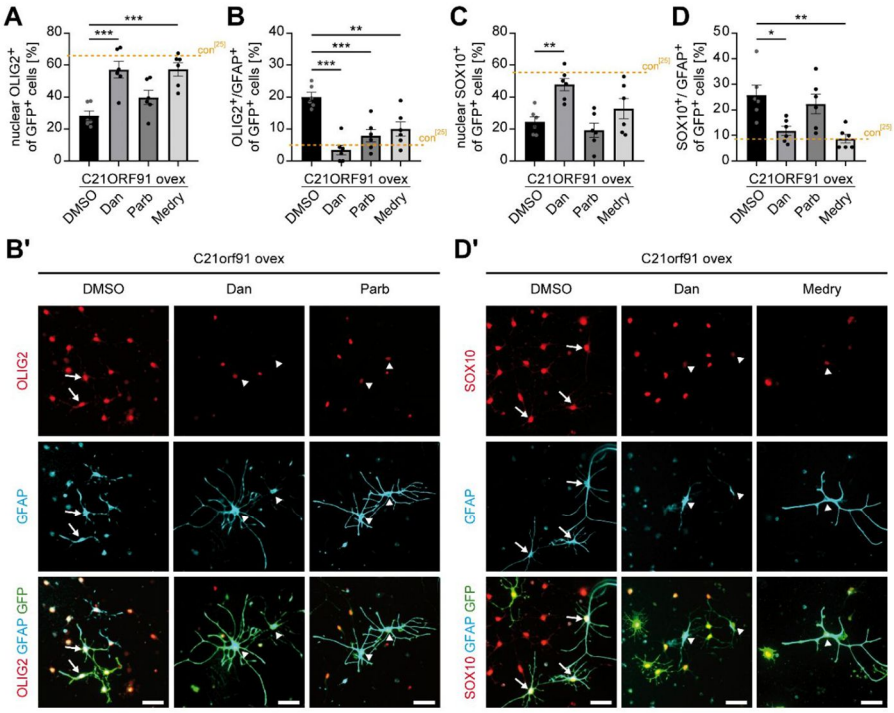

Figure 5: Early rat oligodendroglial lineage fate is promoted by myelin repair drugs while the proportion of glial cells with a hybrid phenotype resulting from elevated C21ORF91 expression was decreased. Immunofluorescence analysis of co-transfected OPCs with a GFP expression vector (green) and C21ORF91 overexpression construct (ovex) revealed that after two days of differentiation upon treatment with danazol (Dan), parbendazole (Parb), or medrysone (Medry), the proportion of cells with a nuclear OLIG2 expression **(A)** or cells co-expressing OLIG2 (red) and astroglial marker GFAP (cyan; **B, B'**) was shifted back towards levels of the published means of control transfected OPCs (orange dashed lines, con; empty control vector, see also [25] compared to DMSO (black bars, control treatment). For the number of nuclear SOX10-positive C21ORF91-overexpressing cells **(C)** this was observed for danazol, while the co-expression of SOX10 (red) and GFAP (cyan; **C, C'**) was significantly diminished for danazol and medrysone. Arrows point at double-positive hybrid cells, arrowheads indicate cells expressing GFAP in the expected absence (below-threshold intensities) of concurrent expression of oligodendroglial markers. Scale bars: 50 µm. Data are shown as mean values (±SEM) deriving from $n = 6$ experiments. Statistical significance was calculated using one-way ANOVA with Dunnett's post-test: *p ≤ 0.05, **p ≤ 0.01, ***p ≤ 0.001.

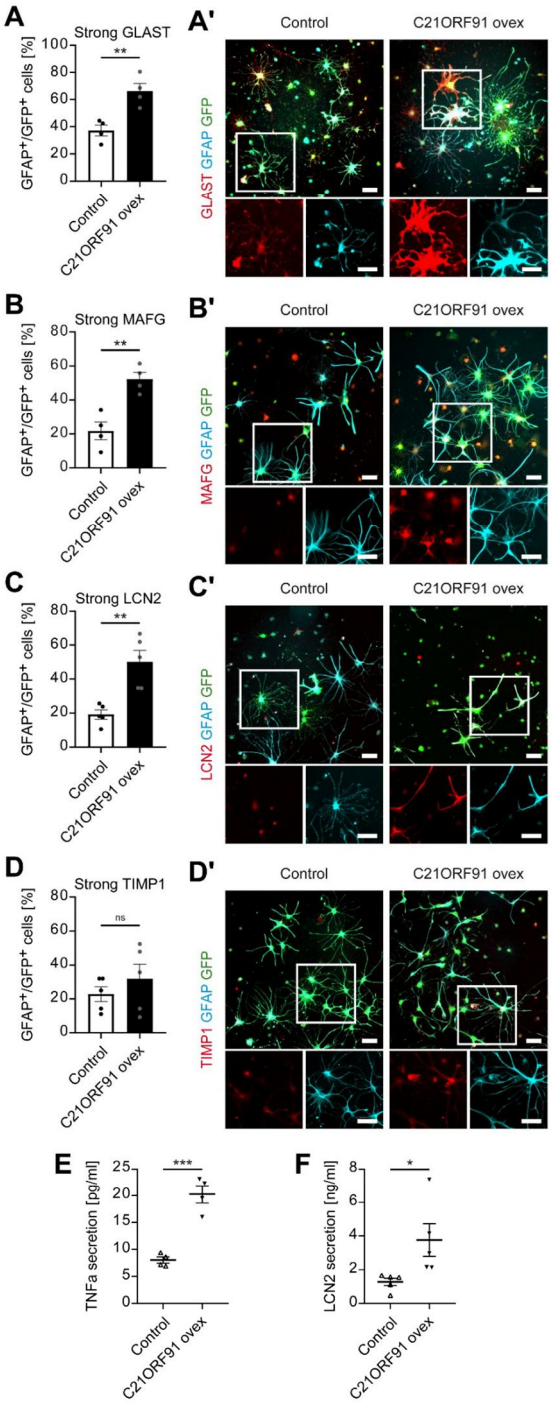

Figure 6: Elevated C21ORF91 expression drives rat OPC differentiation towards expression of astrocytic features with an inflammatory, neurotoxic profile. OPCs were co-transfected with a GFP expression vector (green) in combination with an empty control vector (control, white bars) or a C21ORF91 overexpression construct (ovex, black bars). After five days of differentiation, the effect of elevated C21ORF91 levels on the GFAP-expressing cell (cyan) subpopulation was examined by determining the percentage of strong co-expression of additional astroglial features by immunostaining for GLAST **(A, A')**, MAFG **(B, B')**, LCN2 **(C, C')**, and TIMP1 **(D, D')**, all shown in red. White squares indicate blow-ups, representatively demonstrating strong marker-/GFAP-positive cells upon C21ORF91 overexpression, while for control transfected cells no to only weak expression is shown. Scale bars: 50 µm. To further prove that C21ORF91 overexpression increases the expression of neurotoxic-related astrocytic features in differentiating OPC cultures, the protein concentration of two inflammation-associated markers, namely TNFa **(E)** and LCN2 **(F)** in the supernatant of transfected cultures at day five of differentiation was assessed via quantitative sandwich ELISAs. Triangles represent individual data points (white upward pointing: control transfection; black downward pointing: C21ORF91 overexpression). Data are shown as means (±SEM) deriving from n = 4-5 experiments. Statistical significance was calculated using Student's two-sided, unpaired t-test: *p < 0.05, **p < 0 .01, ***p ≤ 0.001, ns = not significant.

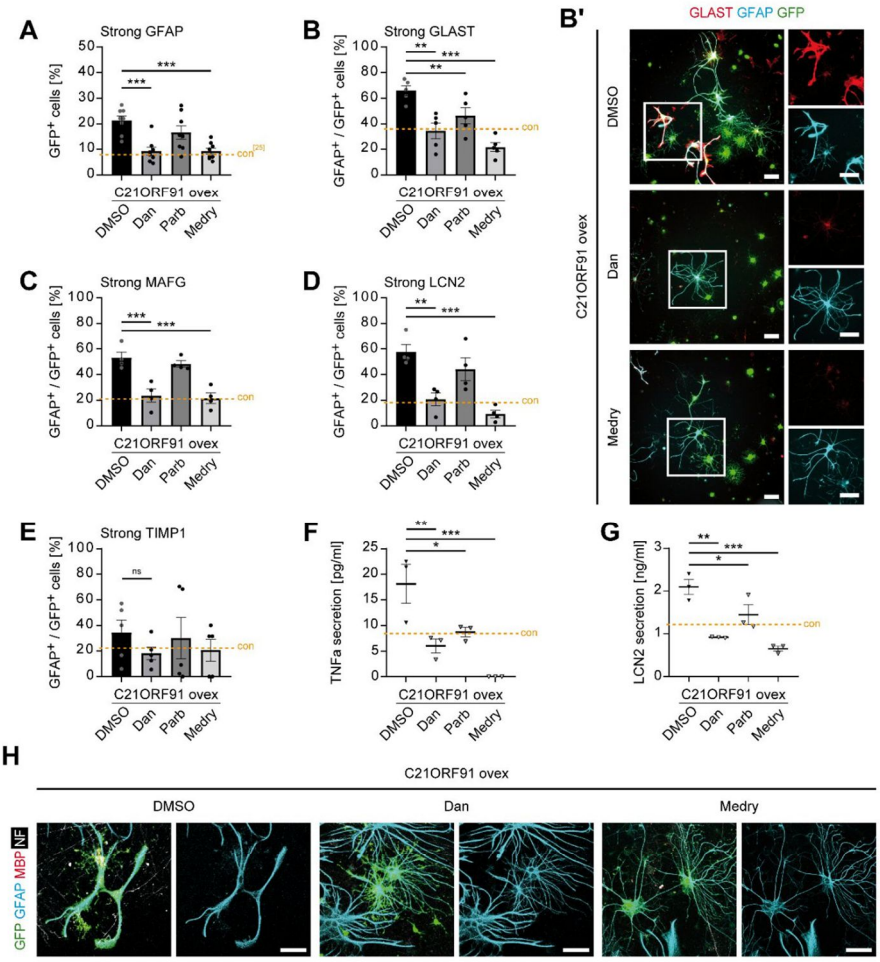

Figure 7: Restoring C21ORF91 overexpression-driven aberrant OPC differentiation of astrocytic features via myelin drugs. Five days after OPCs, co-transfected with a GFP expression vector (green) and a C21ORF91 overexpression construct (ovex), differentiated either treated with danazol (Dan), parbendazole (Parb), medrysone (Medry), or DMSO (control), immunofluorescence analysis demonstrated that the number of strong GFAP-expressing cells **(A)** was significantly decreased by danazol and medrysone compared to DMSO. Further evaluation on the degree of strongly expressing cells for astrocytic markers GLAST **(B,** red in **B')**, MAFG **(C)**, LCN2 **(D)**, and TIMP1 **(E)** within the GFAP/GFP-positive subpopulation (set as 100%) showed the same danazol- and medrysone-dependent reduction of activated astrocytic features. This was supported by quantitative sandwich ELISAs used to determine protein concentrations of TNFa **(F)** and LCN2 **(G)** in the supernatants. Triangles represent individual data points (*n* = 3 experiments). Note, that myelin repair drugs reached levels close to or even underneath the mean values of transfected OPCs with an empty control vector (orange dashed line, con) **(B-G)**. Recently published control values are indicated by [25]. As highlighted in **(B')**, GFAP-positive cells (cyan) appeared to exhibit thicker and fewer branches upon control (DMSO) treatment as compared to danazol- or medrysone-treated cells. Similar morphological features were also observed for GFAP-expressing cells (cyan) ten days after application of co-transfected C21ORF91-overexpressing OPCs on dissociated co-cultures **(H)**. In contrast to control (DMSO) treatment, danazol and medrysone treatments resulted in higher process-bearing cells with thinner branches. Scale bars:

914 50 µm. Data are shown as mean values (±SEM) deriving from *n* = 8 experiments **(A)**, *n* = 3-5
915 experiments **(B-E)**. Statistical significance was calculated using one-way ANOVA with Dunnett's post-
916 hoc test **(A-D,F,G)** for multiple comparison with control (DMSO) and Kruskal-Wallis test with Dunn's
917 post-test **(E)**: *p < 0.05, **p < 0 .01, ***p ≤ 0.001, ns = not significant.

918

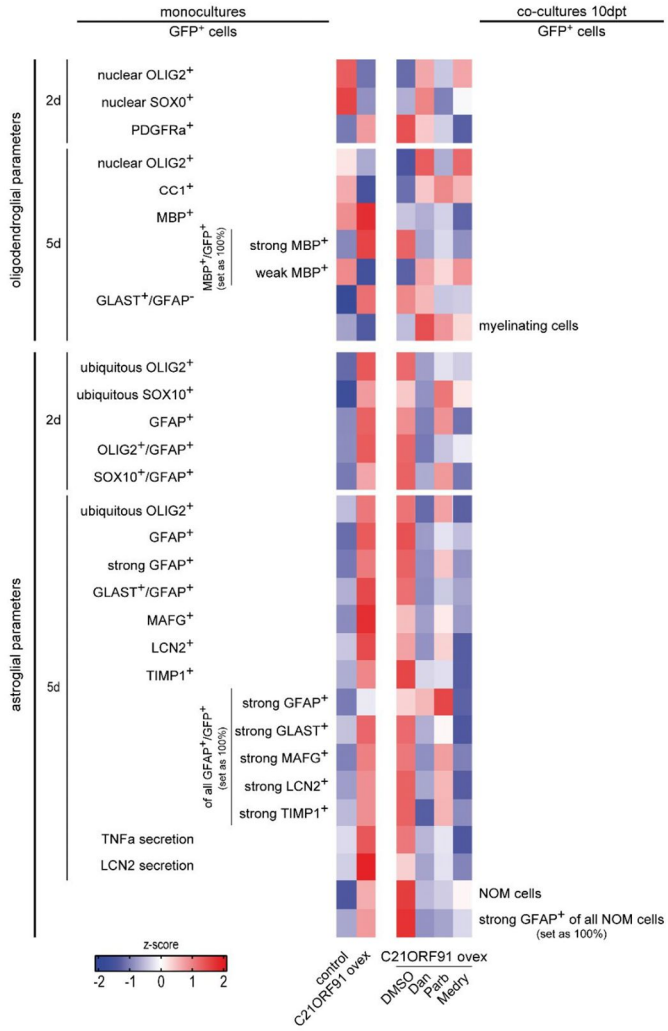

Figure 8: Heatmap-based summary of restoring effects mediated by myelin repair drugs in OPC differentiation upon elevated C21ORF91 expression. While C21-ORF91 over-expression results in a decrease of oligodendroglial parameters in both monocultures at day two (2d) or day five (5d) and OPCs applied and cultivated on co-cultures 10 days post-transfection (10 dpt), astroglial parameters were overall induced (compare control vs. C21ORF91 ovex columns). This dysregulated differentiation was rescued particularly by danazol (Dan), medrysone (Medry), and to a lesser extent by parbendazole (Parb) treatment when compared to DMSO-treated cells (compare columns designated as DMSO vs. Dan, Parb, Medry). MBP^+/GFP^+- as well as $GFAP^+/GFP^+$-cells account for specific subpopulations of transfected cells (indicated by vertical lines) to provide a clearer presentation of specific marker co-expression within the corresponding subpopulation. Data are presented as z-scores deriving from mean values of at least $n = 4$ experiments.

Table 1. C21ORF91 protein expression and glial hybrid cells in human post-mortem tissues

		AC	DS 1	DS 2	DSAD	AD
Age of death (years)		90	51	62	43	90
Sex		Male	Female	Female	Male	Male
Post-mortem index (hours)		5.8	2.72	7.03	3.87	3.75
FCX GM	Nuclear C21 [%]	27.27	69.44	72.64	77.67	63.21
	Cytoplasmic C21 [%]	10.02	30.85	16.33	12.26	22.5
	Total number of C21-/OLIG2+/GFAP+	0	0	0	0	0
	Total number of C21+/OLIG2+/GFAP+	0	0	1	2	0
	Cellular expansion of hybrids [µm^2]	-	-	47.77	278.69 ± 47.08	-
	Number of branches	-	-	2	7 ± 1.41	-
	Branch length [µm]	-	-	5.15 ± 3.29	12.73 ± 2.12	-
FCX WM	Nuclear C21 [%]	93.80	90.69	92.98	94.33	91.67
	Cytoplasmic C21 [%]	0	6.88	6.07	1.76	4.43
	Total number of C21-/OLIG2+/GFAP+	0	0	0	0	0
	Total number of C21+/OLIG2+/GFAP+	0	3	1	1	0
	Cellular expansion of hybrids [µm^2]	-	185.41 ± 38.22	183	345.278	-
	Number of branches	-	2.67 ± 0.72	1	9	-
	Branch length [µm]	-	6.70 ± 1.19	15.02	15.73 ± 1.59	-
OCC GM	Nuclear C21 [%]	52.42	67.34	84.03	76.21	70.03
	Cytoplasmic C21 [%]	14.09	24.72	10.41	12.74	21.96
	Total number of C21-/OLIG2+/GFAP+	0	0	0	0	0
	Total number of C21+/OLIG2+/GFAP+	0	2	3	1	0
	Cellular expansion of hybrids [µm^2]	-	199.73 ± 22.82	109.03 ± 17.25	155.21	-
	Number of branches	-	6	3.33 ± 0.27	3	-
	Branch length [µm]	-	14.93 ± 1.21	8.77 ± 2.55	15.60 ± 4.80	-
OCC WM	Nuclear C21 [%]	87.60	79.41	80.80	92.29	87.29
	Cytoplasmic C21 [%]	7.20	11.75	14.13	6.22	1.67
	Total number of C21-/OLIG2+/GFAP+	0	0	0	0	0
	Total number of C21+/OLIG2+/GFAP+	0	1	4	4	0
	Cellular expansion of hybrids [µm^2]	-	244.31	163.95 ± 35.95	147.30 ± 37.28	-
	Number of branches	-	4	4.75 ± 0.82	3.25 ± 0.65	-
	Branch length [µm]	-	13.07 ± 2.51	8.73 ± 1.19	9.76 ± 1.40	-

Immunofluorescent staining for C21ORF91 protein (here C21), oligodendroglial marker OLIG2, and astroglial marker GFAP in serially sectioned slides of frontal- (FCX) and occipital cortices (OCX) of Down syndrome (DS), DS with Alzheimer's disease (DSAD), AD, and aged control (AC) brains were further distinguished in gray or white matter (GM, WM, respectively) for assessments. Subcellular signal localization was calculated as a relative value to all DAPI-positive cells; hybrid = C21+/OLIG2+/GFAP+. Data are shown as mean values (±SEM) for more than one analyzed hybrid cell in the recorded area of 0.24 mm^2/image.

931

3 Discussion

Neurological disorders are among the most severe and complex diseases worldwide, often leading to lifelong impairments but offering only limited therapeutic options. DS exemplifies this unmet medical challenge. Profound cognitive impairments in individuals with DS significantly limit their ability to pursue personal goals, such as completing education with fewer difficulties, taking employment, or living independently. Despite the increasing recognition of the role glial cells play in brain development, homeostasis, and disease, research in DS has traditionally still focused on neuronal aspects. In particular, the contribution of oligodendroglial lineage deficits to DS neuropathology has received little attention. Moreover, there are currently no therapeutic strategies that effectively target intellectual disability in DS. One reason for this is that key processes such as cortical lamination and progenitor fate commitment – which may be disrupted and lead to a neuro-to-gliogenic shift – are mainly limited to embryonic development and thus relatively inaccessible to postnatal intervention (Stagni & Bartesaghi, 2022). However, neuronal circuit formation critically depends on the proper functioning of glial cells, such as oligodendroglial cells, not only for myelination but also for broader metabolic and structural functions.

This thesis, therefore, first aimed to determine whether hypomyelination and impaired oligodendrogenesis in DS are intrinsic features of the syndrome rather than secondary consequences of neuronal dysfunctions and loss. It further explored whether signalling pathways implicated in the neuro-to-gliogenic shift might also interfere with oligodendroglial lineage progression, thereby exacerbating astrogliogenesis and contributing to cognitive dysfunction. Furthermore, a central focus was placed on elucidating the role of the HSA21-encoded gene C21ORF91, hypothesising that it is essential for developmental myelination and that its overexpression disrupts accurate oligodendroglial differentiation, ultimately compromising white matter integrity.

In parallel, our research group has a longstanding interest in myelin repair strategies for demyelinating conditions such as the autoimmune disease MS or ischemic stroke, where remyelination and endogenous repair mechanisms remain largely ineffective, contributing to disease progression and worsening disabilities. Several promising pharmacological candidates have emerged from these efforts, as can be observed in the here presented studies. However, their applicability to genetically driven white matter pathologies like DS has not yet been explored – even though myelinogenesis is predominantly a postnatal process and thus theoretically accessible to intervention.

In this regard, this thesis also addressed whether pharmacological modulation of C21orf91-overexpressing rat OPCs, resulting in compromised glial fate specification and impaired myelination (Reiche et al., 2021), serving as a cellular model for observed glial

misdevelopment in DS, could restore lineage progression and promote myelination. Together, the presented studies provide new insights into oligodendroglial lineage dysregulation in DS and identify C21ORF91 as a novel driver of glial imbalance, differentiation, and myelination. Furthermore, this provides proof-of-concept that pharmacological targeting of oligodendroglial dysfunction via drug repurposing may represent a promising strategy to improve or restore white matter development – and potentially cognitive outcomes – in this genetically neurodevelopmental syndrome.

3.1 Oligodendroglial Cell Imbalance in DS and the Role of C21ORF91

The aetiology of intellectual disability and cognitive impairments in DS is unknown, but in fact, may result from structural and functional alterations in the brains of affected people (Klein & Haydar, 2022), so far best attributed to abnormalities in neurogenesis (Abukhaled et al., 2023). Recent neuroimaging studies demonstrate a profound decline in the total brain volume in individuals with DS, already evident in neonates (Fukami-Gartner et al., 2023) and young adults (McCann et al., 2021), especially affecting regions associated with DS-associated cognitive limitations such as executive functions (e.g., frontal lobe and cerebellum) and memory (hippocampus). DS brains are marked by a profoundly imbalanced cytoarchitecture (Fig. 2) comprising spatiotemporal anomalies in the development of all cortical cell populations, not only neurons (Olmos-Serrano et al., 2016; Russo et al., 2024). Particularly, oligodendrocytes and proper myelination are pivotal for higher brain functions (Fields, 2008; Hill et al., 2019; Miller, 1994; Mount & Monje, 2017), and deficits result in cognitive impairment (Chen et al., 2021b; Wang et al., 2020). However, its direct implications for the observed intellectual disability and decline in cognition in people with DS have not received much attention, which we aim to change.

As summarised in our review (section 2.1), DS brains are marked by various structural and functional changes in white matter in numerous regions, such as the hippocampus and the corpus callosum (Reiche et al., 2019). The myelination process is profoundly impaired, as it is not only generally delayed, averaging 12 months compared to typically developing euploid controls, but also decreased (Ábrahám et al., 2012; Wisniewski & Schmidt-Sidor, 1989). Furthermore, in DS brains, the density of myelinated axons is diminished (Ábrahám et al., 2012; Olmos-Serrano et al., 2016) and the characteristic grid-like structure of myelinated fibres is disrupted, accompanied by significantly decreased expression levels of the key myelin-associated proteins MBP, MAG (Olmos-Serrano et al., 2016), and CNP (Vlkolinsky et al., 2001). Indeed, the observed diminished white matter integrity correlates with reduced performance in neuropsychological assessments of people with DS (Fenoll et al., 2017; Powell et al., 2014). The new awareness of the importance of accurate white matter formation and its microstructure, as well as advances in imaging, enabled further correlations for white matter malformation and cognitive outcome in the DS population

(Cañete-Massé et al., 2022). Bazydlo et al. (2021) demonstrated that early decline in episodic memory before the onset of AD-associated dementia, which often occurs in adults with DS (DSAD), may be attributed to white matter degeneration, independently of chronological age. Notably, the onset and severity of deficits in cognition in individuals with DS coincide with the time pattern of myelination peaking in the first years of life till young adulthood (Reiche et al., 2019). Thus, indeed, cognitive impairments in DS are directly linked to alterations in white matter integrity.

Nevertheless, how is the oligodendroglial lineage affected despite altered myelination properties? On the one hand, Olmos-Serrano and colleagues (2016) demonstrated for the first time direct cell-autonomous deficits in oligodendroglial maturation and viability via multi-region transcriptome analysis in DS and healthy controls spanning from foetus to adults and further confirmed in a frequently used DS-mouse model Ts65Dn. On the other hand, when examining oligodendrocyte development in humans on a cellular level, temporal- and region-dependent changes in the numbers of OPCs, mostly traced by OLIG2-staining, can be observed in DS. In the germinal matrix, OLIG2-positive cell numbers were reduced in the earliest developmental embryonic waves (14-16 weeks of gestation), which normalised in the course of development (late gestation till birth). In contrast, in the temporal lobe white matter, the density of OLIG2-positive cells remained similar in normally developing controls and DS foetuses, though the rate of OPC accumulation over time was markedly higher in DS tissue (Kanaumi et al., 2013). In contrast, in the ventricular zone of frontal cortices of DS foetuses (14 and 18 weeks of gestation), significantly higher levels of OLIG2- and PDGFRα-positivity were observed (Lu et al., 2012). Thus, altered cell-autonomous lineage progression and dysbalanced progenitor pools may consequently contribute to the diminished myelination observed in postnatal and adult DS brains.

Interestingly, a growing body of evidence points toward a fundamental imbalance in cortical cell specification in DS, marked by a shift away from neurogenesis toward increased gliogenesis (Russo et al., 2024). Several studies indicated elevated numbers of astrocytes in foetal DS brains in regions such as the hippocampus (Guidi et al., 2008; Zdaniuk et al., 2011). However, we hypothesised that increased astrogliogenesis may be attributed to impaired oligodendrogenesis due to failed lineage specification, as OPCs, or OLIG2-positive progenitor cells, were shown to differentiate to glial fibrillary acidic protein (GFAP)-positive reactive astrocytes upon, e.g., injury (Chen et al., 2008; Lu et al., 2012). Further evidence can be drawn from observations in Ts65Dn mice, demonstrating that a decreased percentage of oligodendrocytes (Olmos-Serrano et al., 2016) is accompanied by elevated numbers of reactive astrocytes (Lockrow et al., 2012). Therefore, we summarised multiple pathways known to be implicated in disrupted neurogenesis in DS that may additionally underlie such an oligodendro-to-astroglial fate shift in NSCs and

OPCs, possibly altering their proliferation, differentiation, and fate commitment (Reiche et al., 2021, also see Fig. 2). Taken together, these findings support the view that glial lineage imbalance in DS is not merely secondary to neuronal loss but may reflect a primary developmental distortion in progenitor fate decisions and further disruption of intrinsic developmental lineage progression. Importantly, this shift has functional implications beyond myelin deficits. Astrocytes and oligodendrocytes play distinct and complementary roles in synaptic regulation, metabolic support, and axonal conduction. An excess of reactive astrocytes at the expense of mature oligodendrocytes may, therefore, disrupt neuronal circuit formation and plasticity, thereby additionally contributing to cognitive impairment. This glial imbalance may further be amplified by early inflammatory stimuli, oxidative stress, and metabolic challenges, which are increasingly recognised as part of the DS neuropathological landscape (Ponroy Bally & Murai, 2021; Russo et al., 2024).

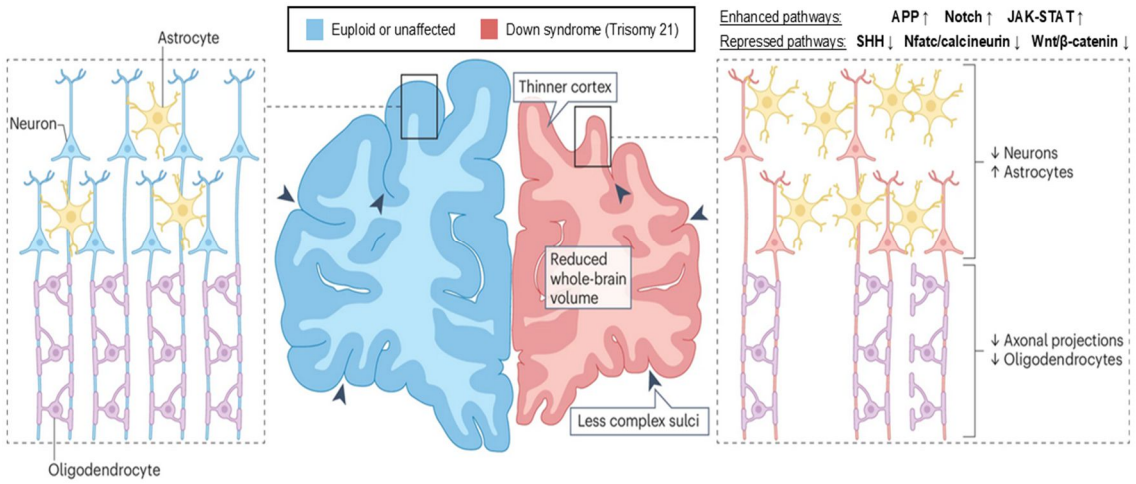

Figure 2. Schematic illustration of a coronal frontal lobe section of a neonatal human brain depicting the cytoarchitectural alterations in DS (red) compared to euploid, typical development (blue). Foetuses and infants with DS display significant anatomical abnormalities in brain structure, characterised by a reduced overall brain volume, a thinner cortex, and decreased complexity of gyri and sulci (highlighted by arrowheads). These structural differences reflect impaired and imbalanced brain development (insets). Particularly, the processes governing the generation and differentiation of neurons and astrocytes are impaired during neurodevelopment in DS, leading to a decreased number of neurons and an increased proportion of astrocytes relative to neurons. Furthermore, deficits in myelin formation and disturbances in oligodendrocyte production are also prominent features of DS neurodevelopment. Upward and downward arrows mark respective increases or decreases in specific cell populations. Enhanced and repressed pathways involved in this misbalanced cellular composition are indicated in bold. Adapted from (Russo et al., 2024) with permission license: 6017861412139.

In this context, it has to be mentioned that while neuroanatomical differences are pronounced in individuals with DS, there is variability among them, including variations in the severity and type of cognitive impairment and the presence of comorbidities (Russo et al., 2024). However, due to the restricted availability of human brain tissue, particularly from prenatal stages, research on postmortem DS brains often lacks sufficient power, which complicates reaching broadly applicable conclusions for the DS population

(Risgaard et al., 2022). Additionally, distinguishing alterations in cell fate commitment and/or differentiation in fixed postmortem tissue remains technically challenging. Furthermore, our awareness of the heterogeneity of oligodendroglia and astroglia has recently been enhanced, which has also led to the questioning of markers that were once widely accepted as lineage-specific. For instance, *OLIG2*, an HSA21-encoded gene, is well-known for its implication in lineage specification and is a highly important regulator for OPC differentiation (Zhou et al., 2000). It was recently also demonstrated to be implicated in interneuron specification and development (del Águila et al., 2022; Xu et al., 2019). Thus, claiming higher OLIG2-positive progenitors equal OPCs or oligodendroglial cells without additional lineage markers in the future will not be sufficient. Equally, GFAP, with our current knowledge, is, on the one hand, not the ideal marker for all astrocytes, especially when investigating reactive phenotypes (Escartin et al., 2021) and also marks radial glial cells (Choi, 1986). Thus, the cell populations investigated in previous studies, especially in foetal brains, need further clarification in future studies.

This also underscores the need to better understand the molecular drivers of glial fate specification, particularly in the context of gene dosage imbalance on HSA21. Remarkably, we demonstrated that the overexpression of C21orf91 in rat OPCs was sufficient to result in DS-characteristic hallmarks: impaired oligodendroglial differentiation, altered myelination capacity resulting in hypomyelination, and the induction of astroglial properties at the expense of oligodendroglial lineage commitment (see sections 2.2 and 2.8; (Reiche et al., 2021; Reiche et al., submitted)). Furthermore, we observed that elevated levels of this protein resulted in the concomitant expression of astroglial and oligodendroglial markers, not only restricted to mono- and co-culture levels or explained as a phenomenon in murine primary cultures, but indeed found OLIG2 or MBP along GFAP co-expressing C21ORF91-positive cells only in DS or DSAD cases, but not in aged euploid control or AD control (Reiche et al., submitted). This further underlined our hypothesis that, indeed, progenitor cells, usually committed to the oligodendroglial lineage, might shift their fate in DS. Interestingly, initial experiments conducted with rat SVZ-aNSCs overexpressing C21orf91 revealed that these cells also failed to commit to the oligodendroglial lineage, even when conditioned with mesenchymal stem cell-conditioned medium, which reliably promotes oligodendroglial lineage progression (Jadasz et al., 2018; Samper Agrelo et al., 2020). This was evidenced by a massive decline of Mbp-expressing cells compared to control-transfected NSCs (see Appendix 4.1.1, Fig. 3A,a). Instead, overexpression of C21orf91 was sufficient to inhibit or silence the mesenchymal stem cell-conditioned medium-induced cues and instead significantly induce GFAP expression (see Appendix 4.1.1, Fig. 3A,a).

We were interested to further elucidate which pathways might possibly be involved in this aberrant OPC differentiation induced via C21orf91 but attempts to enrich transfected cells

either via fluorescence-activated cell sorting (FACS) or antibiotic-resistance selection of the plasmid were not successful in OPCs (data not shown). Thus, we conducted qPCR analysis, which, however, has to be considered with caution, as the transfection efficiency of primary cells via nucleofection is generally low (here, we reached up to 30%), and transient transfection only allowed to analyse early developmental timepoints. As C21orf91 was recently described to interact with coiled-coil domain containing (CCdc) 85b, thereby modulating β-catenin (Li et al., 2016), transcript levels of genes involved in Wnt signalling (*Tcf4, Lrp1, Ctnnb1*) were investigated in both C21orf91 overexpressing NSCs and OPCs (see Appendix 4.1.2, Fig. 4). There was an overall aberrant regulation induced by C21orf91 overexpression. *Transcription factor* (*Tcf*) *4* and *catenin beta 1* (*Ctnnb1*), coding for the protein β-catenin, were downregulated in NSCs and OPCs with elevated C21orf91 expression (though *Ctnnb1* was initially upregulated at 1d in OPCs), while *low density lipoprotein receptor related protein* (*Lrp*) *1* was elevated in NSCs but decreased in OPCs. Note that the Wnt signalling is highly complex and needs tight regulation to guarantee accurate oligodendrocyte differentiation (Reiche et al., 2019). Lrp1 is downregulated in differentiating OPCs, thus, deletion of *Lrp1* in mouse OPCs increased the number of myelinating oligodendrocytes and enhanced remyelination in cuprizone-mediated demyelination (Auderset et al., 2020). However, another study suggests that Lrp1 is important for cholesterol homeostasis, and its ablation in OPCs results in metabolic deficits that inhibit differentiation (Lin et al., 2017). These contrary results demonstrate that there are possibly context-dependent factors for Lrp1-mediated OPC differentiation involving further upstream or downstream effectors. Nonetheless, β-catenin is transiently activated in OPCs, inducing terminal differentiation, and then downregulated again (Emery, 2010). Elevated levels in mutant mice display defective differentiation and hypomyelination (Fancy et al., 2009). Thus, overexpression of C21orf91 also affected Wnt signalling in both OPCs and NSCs, most likely disturbing correct timing for accurate oligodendroglial lineage progression and myelination onset, a process we already claimed to be important and affected in DS (Reiche et al., 2019).

Additionally, *hairy/enhancer of split* (*Hes*) *1* and *5* are upregulated in OPCs with increased *C21orf91* expression levels at day one, while only *Hes1* is induced in C21orf91 overexpressed NSCs. Interestingly, HES1 is also upregulated in the adult DS cortex (Fischer et al., 2005) and was demonstrated to induce an astroglial cell fate at the expense of oligodendroglial progression in glial restricted precursor cells (Wu et al., 2003).

G protein coupled receptor (*GPR*) *17* was implicated in the dysregulated gene cluster along *C21ORF91* identified in DS, associated with oligodendroglial development and myelination (Olmos-Serrano et al., 2016), and shown to indeed modulate OPC maturation, with any disruptions of its expression pattern causing myelination defects (reviewed by Lecca et al., 2020; Simon et al., 2016). GPR17 is directly linked with diminished sorting

nexin (SNX) 27 levels in DS (Wang et al., 2013) and was demonstrated to result in impaired OPC differentiation and myelination deficits in Ts65Dn mice (Meraviglia et al., 2016). Both genes, *Gpr17* and *Snx27*, were diminished in C21orf91 overexpressing OPCs compared to controls during differentiation on days one and three.

Thus, the overexpression of C21orf91 in NSCs and particularly in OPCs overall affects oligodendroglial lineage progression and capacity to mature to myelinating oligodendrocytes rather than intrinsically inducing astroglial marker expression.

Whether, in the end, OPCs or NSCs really differentiate to fully functioning astrocytes upon C21orf91 overexpression and occurring glial hybrids will remain in such a non-physiological stage or will progress into a specific lineage or eventually will undergo cell death will remain a topic for future studies. First efforts to transplant these transfected OPCs or NSCs into rodent brains to assess their ability to integrate or/and differentiate similar to previously established setups in our lab (Beyer et al., 2020; Samper Agrelo et al., 2020; Schira-Heinen et al., 2022a) were unsuccessful, as four days post-transplantation, only 10 GFP-positive cells were traceable in a brain, completely insufficient for meaningful interpretations (data not shown). This highlights the need for, on the one hand, stable transduction of C21orf91 overexpression into the genome of primary cells and, on the other hand, a suitable, ideally inducible, animal model for OPC fate mapping, such as modifying the NG2-CreERT2/Rosa26-tdTomato mouse strain used in our stroke study (Werner et al., 2023). Studying alterations due to C21orf91 overexpression in the common DS transgenic mice such as Ts65Dn is, for example, not suitable, as only the Dp(16)1Yey/Dp1Tyb, Dp9Tyb and Dp3Yah harbour the mouse orthologue gene of *C21orf91* on mouse chromosome 16 (Ishihara, 2021).

3.2 The Role of C21orf91 in Shaping the Nervous System

Among the genes on HSA21, C21ORF91 has emerged as a key modulator of neuronal and oligodendroglial lineage progression in DS, possibly attributed to interfering with Wnt signalling as mentioned above (Li et al., 2016; Reiche et al., 2021; Reiche et al., submitted). However, the exact underlying molecular pathways and functional role appear way more complex and need to be investigated further, as elevated expression of C21orf91 in OPCs did not result in a simple outcome of only shifting cells toward astroglial differentiation cues at the expanse of mature oligodendrocytes, but resulted in a subset of several differing cell phenotypes:

(1) undifferentiated OPCs,
(2) cells with hybrid co-expression,

(3) oligodendroglial cells exhibiting an increased morphological maturation and aberrantly enriched/accumulated Mbp-expression with a collapsed cytoarchitecture (referred to as non-organised Mbp-expressing (NOM) cells),
and (4) cells with astroglial properties of neurotoxic or neuroprotective reactive astrocyte phenotypes (see sections 2.2 (Reiche et al., 2021) and 2.8 (Reiche et al., submitted)).

Though we demonstrated that C21orf91 expression levels in OPCs were successfully elevated at gene transcript and protein levels in GFP-expressing cells (co-transfection for visualisation, see methods in 2.2), our chosen transfection method did not guarantee stable incorporation of the overexpression construct to the genome of the transfected cell, nor that every transfected cell is only harbouring only one extra copy of *C21orf91*, reflecting the observed 1.5-fold gene dosage effect observed in DS (Ait Yahya-Graison et al., 2007). Moreover, there were possibly differing levels of elevated C21orf91 protein levels. Thus, it would be interesting to determine the exact C21orf91 protein expression level (and correlating omics) within each of the four mentioned cell phenotypes to evaluate whether the different phenotypes relate to a certain dosage-dependent C21orf91 expression threshold that, in the end, modulates specification, fate switch, and/or differentiation progression.

Indeed, *C21ORF91* exhibits a spatiotemporal expression pattern in DS brains (Li et al., 2016). Under normally developing conditions, its expression follows a temporally dynamic pattern in both mouse and human brain development, with initially low levels that increase toward early adulthood, coinciding with the onset and progression of CNS myelination (Li et al., 2016; Reiche et al., 2021). Transcriptomic and bioinformatic analyses of both studies show high enrichment in myelin-rich regions such as the corpus callosum, diencephalon, spinal cord, and cerebral white matter, specifically in myelinating oligodendrocytes and hippocampal astrocytes. However, *C21ORF91* is ubiquitously expressed in various tissues and cell types (Reiche et al., 2021), thus most likely important for all cells in the body. On a cellular level, C21orf91 has been shown to influence both neurogenesis and oligodendrogenesis in a dosage-sensitive manner (Li et al., 2016; Reiche, 2017). In mice, forced overexpression or knockdown alters the proliferative capacity and differentiation of neural progenitors, with knockdown promoting differentiation but diminishing proliferation, while in contrast, overexpression promotes proliferation without affecting lineage progression. However, both gene modulations reduce dendritic spine density, more prominent in overexpression. This impaired neurogenesis is suggested to result from interactions with CCdc85b, which modulates β-catenin and thereby impacts Wnt signalling (Li et al., 2016).

Primary rat NSCs and OPCs show no altered proliferation capacity in response to C21orf91 modulations (data not shown). As described in the previous section, C21orf91 overexpression results in disrupted lineage specification in both cell pools: oligodendroglial

differentiation was impaired, while astroglial markers such as Hes1, Glast, Lcn2, and Mafg were upregulated (Reiche et al., submitted), Gfap, even under pro-oligodendroglial cues induced by mesenchymal stem cell-conditioned medium (see Appendix Fig. 4A). Conversely, C21orf91 knockdown promoted earlier OPC fate acquisition in NSCs treated with mesenchymal stem cell-conditioned medium compared to control-transfected NSCs (Park, 2020). However, these C21orf91-suppressed cells exhibited impaired differentiation (Appendix Fig. 3A,b), resulting in a diminished capacity to successfully integrate (Appendix Fig. 3C,F), and mature to myelinating cells (Appendix Fig. 3E), but rather stay quiescent (Appendix Fig. 3D) when transplanted into cerebellar slice cultures and further stimulated with mesenchymal stem cell-conditioned medium to promote their oligodendroglial lineage progression (Appendix Fig. 3F). Additionally, suppressed C21orf91 expression diminished morphological maturation in NSCs (Appendix Fig. 3B), what was also described in initial suppression experiments in OPCs (Reiche, 2017) suggesting that C21orf91 is essential not only for lineage commitment but also for functional maturation. NSCs with suppressed C21orf91 expression demonstrate diminished transcription levels for all studied genes, including *Ctnnb1* (Appendix Fig. 4B). Interestingly, transient β-catenin (encoded by *Ctnnb1*) signals in NSCs were demonstrated to result in cell death (Rosenbloom et al., 2020). Though we did not observe cell death induced by any C21orf91 modulation in OPCs nor NSCs, we only tested the very early timepoint (one day post-transfection, data not shown). Given the drastic loss of C21orf91-suppressed cells after transplantation in slice cultures (Appendix Fig. 3C) examined on day four, it seems reasonable to assume that prolonged diminished β-catenin signalling here induced cell death in this *ex vivo* system. Mechanistically, C21ORF91 modulation disrupted multiple regulatory pathways, including downregulation of *Tcf4* and *Ctnnb1* (Wnt signalling), altered *Lrp1* expression (lipid metabolism) and increased *Hes1*/*Hes5* expression (Notch targets). These mechanisms likely contribute to the defective oligodendroglial differentiation, hypomyelination, and increased astrogliogenesis observed in DS. However, the exact downstream cascade and temporal dynamics remain to be fully elucidated in future *in vivo* studies and analysis of omics.

Collectively, these findings position C21ORF91 as a dosage-sensitive regulator of neural lineage specification and progression. However, future studies will need to implement glial restricted precursors or radial glial cells to investigate astrogliogenesis to justify C21ORF91's currently suggested modulatory role in shaping the cytoarchitecture of the CNS. Besides, C21ORF91 might not only be involved in DS neuropathophysiology but could also constitute a new candidate for investigation in other neurological disorders affecting white matter and neuronal function.

Interestingly, impaired peripheral somatosensory function and aberrant nerve conduction velocity are described in children with DS (Brandt & Rosén, 1995). However, Schwann

cells, the myelinating cells of the PNS, have so far not received any attention in DS research. Remarkably, in Charcot-Marie-Tooth (CMT) disease, an inherited demyelinating peripheral neuropathy, dysfunction in Schwann cells – resulting in diminished myelination capacity – is the leading cause for observed motor and sensory deficits as well as slowed nerve conduction velocities (McLean et al., 2022). Thus, it was interesting to investigate whether C21orf91 may also affect Schwann cell behaviour (Schütte, 2022). Indeed, the expression pattern of C21orf91 in the PNS correlated with myelination during development (similar to the CNS) and, interestingly, in response to peripheral nerve injury and remyelination (Schütte, 2022). The modulation of C21orf91 did not affect the proliferation of Schwann cells, which in culture are known to give rise to typical bipolar-shaped, highly proliferative cells (reviewed by Monje, 2020). However, C21orf91-positive structures very impressively resembled the spindle apparatus and the cytokinetic bridge during mitotic phases (see Appendix Fig. 5A), possibly characterising it as a novel marker of the mitotic apparatus when compared to staining of α-tubulin and BRCA2 and CDKN1A interacting protein (BCCIP), a protein associated with spindle poles, centrosomes, and the mitotic cell cortex (Huhn et al., 2017). Interestingly, this is the first indirect proof of the assumption that C21ORF91 is localised to microtubules and the cytokinetic bridge (Human Protein Atlas), but this needs further examination via direct co-staining, e.g., with α-tubulin and BCCIP. Besides their important roles in cellular morphology and function (Huang et al., 2022), microtubules are also important for accurate myelination in Schwann cells (Kidd et al., 1994) and oligodendrocytes (Lee & Hur, 2020; Weigel et al., 2020). The fact that NSCs and OPCs were affected in their morphological maturation upon C21orf91 modulation might also be due to the interference of C21orf91 modulation with microtubule organisation. This interference might also affect their differentiation progression and defective myelination capacity, as observed in the collapsed cytoarchitecture in NOM cells unable to ensheath axons in co-cultures (Reiche et al., 2021).

Therefore, it is maybe not surprising that Schwann cells also exhibited morphological alterations upon C21orf91 overexpression (Appendix Fig. 5B-D'). Schwann cell phenotypes resulting from C21orf91 overexpression were distinguished by soma size, number and length of protrusions and web formation. In C21ORF91-overexpressing cells, the GFP-positive population was mainly categorised as Type 2 (large soma and at least three protrusions with web formation) and Type 3 (larger soma sizes with two or more protrusions but no web formation). Especially the morphological phenotype 3 might relate to myelinating Schwann cell phenotypes (Weiner et al., 2001). Deeper analysis of C21orf91-overexpressing Schwann cells highly enriched for C21orf91 signal intensities (Appendix Fig. 4C, D') showed that most Schwann cells belonged to phenotype 2. Note that control-transfected Schwann cells mainly belonged to the bipolar morphological Type 1. This observation leaves open questions, such as what causes these morphological

alterations, whether these phenotypes indeed relate to distinct functions, and prompts the need for further studies in myelin-promoting environments such as transplantation into lesion sides or co-cultures with neurons, as monocultured Schwann cells usually do not undergo (trans-)differentiation to repair or myelinating phenotypes without stimuli (Monje, 2020). This monoculture-attributed aspect also makes it difficult to interpret the induced transcriptional changes in Schwann cells with modulated *C21orf91* expression levels (Appendix Fig. 5.E). Overexpression seems to slightly promote a repair and differentiating Schwann cell phenotype seen in slight enrichment of myelin-associated genes (*Mag, P0, Mal*) at day four of cultivation, while suppression rather favours a repair phenotype by upregulation of *c-Jun* and *Gap43*, however, *Pdgf-BB* was reduced which eventually would impair repair functions (Sowa et al., 2019). Thus, more studies regarding Schwann cell behaviour upon C21orf91 modulations, for instance, in peripheral nerve injuries, are needed in the future.

However, in summary, all conducted observations in this thesis highlight that C21orf91 protein expression underlies possibly various signalling cues, itself interferes with at least Wnt and possibly Notch or Jak/Stat3 signalling (seen by Hes 1/5 modulation (for review, see Reiche et al., 2019), and needs precise temporal regulation to facilitate accurate neural progenitor cell specification, lineage progression, and terminal differentiation, exerting its modulatory role in a dosage-dependent manner.

3.3 Myelin Restoration – New Therapeutic Perspectives for Down Syndrome

The limited capacity of the CNS to repair white matter damage remains a major therapeutic challenge across neurological and neurodevelopmental conditions. While strategies to promote remyelination have recently been extensively studied in MS (Franklin et al., 2024; Lubetzki et al., 2022; Tepavcevic & Lubetzki, 2022), their application to DS has only recently gained attention. Crucially, a growing body of evidence suggests that impaired oligodendroglial differentiation, rather than irreversible cell loss, is a common and potentially targetable mechanism across distinct disease contexts (Fancy et al., 2011; Franklin et al., 2024; Simons et al., 2024; Stadelmann et al., 2019).

As clearly elucidated in this thesis, genome-wide gene dosage imbalances in DS disrupt oligodendroglial lineage maturation and result in hypomyelination (Olmos-Serrano et al., 2016; Reiche et al., 2019), with *C21ORF91* emerging as a promising candidate to be a driver gene responsible for the DS-characteristic neuropathological phenotype and contributing to cognitive impairments and intellectual disability (Li et al., 2016; Reiche et al., 2021; Reiche et al., submitted). As mentioned before, overexpression of this protein results in an overall defective OPC maturation, corrupting lineage specification and progression, producing aberrant and possibly unique DS-related disease cell phenotypes

such as hybrid cells co-expressing astrocytic markers or NOM cells with disrupted cytoarchitecture but elevated Mbp expression (Reiche et al., 2021; Reiche et al., submitted). C21ORF91 has been shown to interfere at least with Wnt/β-catenin signalling, but possibly also other multiple signalling pathways involved in fate specification, such as Notch (via Hes1/5) and GPR17-linked mechanisms, all of which have been implicated in the regulation of OPC differentiation and myelin formation (Li et al., 2016; Olmos-Serrano et al., 2016; Reiche et al., 2019; Simon et al., 2016). Against this mechanistic background, pharmacological rewiring of oligodendroglial fate and differentiation competence represents a promising therapeutic avenue.

Building on earlier work in MS and ischemic stroke, several repurposed compounds, such as danazol, parbendazole, medrysone, and teriflunomide (see section 2.3-2.6), have demonstrated the ability to enhance oligodendroglial differentiation and remyelination (Göttle et al., 2023; Göttle et al., 2018; Manousi et al., 2021; Silva Oliveira Junior et al., 2022; Werner et al., 2023). We hypothesised that these compounds could also rescue the intrinsically challenged OPC differentiation competence observed in DS. In section 2.8, we examine the effects of these myelin repair drugs on C21orf91-overexpressing OPCs, here serving as a model for dysregulated maturation of OPCs in DS. By evaluating their potential to restore oligodendroglial fate and promote functional myelination, we extend remyelination strategies beyond classical demyelinating disorders (Reiche et al., submitted).

Indeed, the steroid and pituitary gonadotropin inhibitor danazol (Ashfaq et al., 2024), the corticosteroid medrysone, and the anthelminthic parbendazole could all effectively restore the myelination capacity of C21orf91-overexpressing cells, with danazol and medrysone demonstrating the most efficient rescuing effects. All three myelin repair drugs could reverse cytoplasmic translocation of Olig2, hence stabilising oligodendroglial differentiation instead of the induction of astroglial differentiation (Setoguchi & Kondo, 2004). The exact mechanisms behind this translocation and the involvement of C21orf91 need to be further elucidated in upcoming studies. Given that microtubules and actin are potentially involved in nuclear translocation (Wu & Kengaku, 2018) and C21orf91 appears to be associated with microtubules (see Appendix Fig. 5A), analysing dyneins, myosins, and kinesins could not only be beneficial in understanding C21orf91's role in possibly altering nuclear trafficking and interfering with differentiation (Barbosa et al., 2024).

In this context, the positive impact of parbendazole, an active tubulin destabiliser, and methiazole (both anthelmintics similar to nocodazole) on OPC differentiation was previously attributed to microtubule modulation via a p38MAPK-related mechanism, as phosphorylated p38MAPK was induced via parbendazole in OPCs, resulting in more complex morphological phenotypes (Manousi et al., 2021). However, methiazole already failed to exert beneficial effects on C21orf91 overexpression-driven defective OPC

maturation in the co-culture system, while parbendazole failed to re-establish more complex morphological maturation of oligodendroglial cells when compared to danazol and medrysone (see section 2.8, (Reiche et al., submitted)). Overexpression resulted in an accelerated morphological maturation seen by process arborisation and MBP staining, yet failed to ensheath axons (Reiche et al., 2021), which might also be attributed to inhibited microtubule polymerisation. Thus, a fostered destabilisation, as induced by methiazole and parbendazole, in the end, is too much and results in an overall imbalanced maturation instead of promoting accurate OPC differentiation. For instance, nocodazole, a microtubule destabiliser that interacts with the mitotic spindle (Jordan et al., 1998), clearly showed dosage-dependent effects, only promoting morphological maturation of OPCs at nanomolar dosages and pulse stimulation (Lee & Hur, 2020). The promoted positive regulation of OPC maturation induced by parbendazole in C21orf91-overexpressing cells in the context of the co-culture system could, therefore, result from secondary effects of other innate co-culture cells, such as neurons or astrocytes, and should be further assessed in future studies. Which exact underlying pathways the here-tested myelin repair drugs regulate to promote OPC differentiation and how C21orf91 might be involved, whether as a primary or downstream target, remains to be addressed in the future. Note that none of the tested drugs were observed to reduce *C21orf91* transcript levels during spontaneous OPC differentiation (data not shown). Thus, it is unlikely that any of the tested compounds simply restored C21orf91 overexpression to physiological levels.

Danazol was found to inhibit STAT3 signalling in multidrug-resistant cancer cells (Chang et al., 2019). Interestingly, STAT3 is known to regulate OPC differentiation toward an astrocytic fate, resulting in astrogliosis and insufficient remyelination (Sun et al., 2015). Thus, C21orf91 overexpression could possibly promote Stat3 signalling in transfected OPCs, which is corrected by danazol and thereby stabilises oligodendroglial lineage progression. Therefore, Stat3 expression levels should be investigated in follow-up studies. As STAT3 overactivation in DS indeed resulted in enhanced astroglial production (Cao et al., 2010a; Kurabayashi et al., 2015), danazol becomes an even more attractive candidate for testing for correcting glial specification in DS.

Though demonstrated to have no direct effects on the spontaneous differentiation of primary rat OPCs, medrysone, an FDA-approved anti-inflammatory corticosteroid, robustly fostered remyelination in a chronic demyelination model by modulating the reactive profile of astrocytes (Silva Oliveira Junior et al., 2022). Here, pro-inflammatory and neurotoxic features in astrocytes were downregulated by medrysone administration, and a repair-beneficial astroglial phenotype was promoted, thereby fostering remyelination. Notably, DS astrocytes were demonstrated to exhibit increased transcript levels of *Gfap*, *Glast*, and *iNos,* as well as activated morphologies with thicker branches compared to euploid healthy

brain tissues (Chen et al., 2014). These pathological features resemble those we observed in our primary C21orf91-overexpressed OPCs (Reiche et al., submitted). Interestingly, elevated protein levels of LCN2 have been detected in the sera of DS patients (Dogliotti et al., 2010; Naude et al., 2015), additionally supporting an indirect correlation with our findings as C21orf91 overexpression induced Lcn2 secretion. Treatment with medrysone showed the most dominant reduction in restoring these neurotoxic astroglial features (Liddelow et al., 2017) along the elevated C21orf91-driven OPC differentiation (Reiche et al., submitted). However, there was no induction of Timp1, a marker for repair-attributed astrocytes (reviewed by Silva Oliveira Junior et al., 2024), within the cultured transfected cells, but a general decline in GFAP back to the level observed in control-transfected cells, hence restoring accurate OPC differentiation. Nonetheless, medrysone decreased the reactive state of astrocytes, which could not be observed for parbendazole treatment. Yet, it cannot be excluded that medrysone additionally directly affects the OPC fate guided by C21orf91-driven pathways. Thus, exploring the underlying pathways will have to be addressed in future studies.

While these medications are authorised to treat pathologies not associated with the CNS, including endometriosis (Dmowski et al., 1971), fibrocystic breast disease (Greenblatt et al., 1980), or eye inflammation (Bedrossian & Eriksen, 1969; Spaeth, 1966), and they also show potential as candidate drugs for cancer therapies according to preclinical studies (Florio et al., 2019; Liang et al., 2022; Lo et al., 2017), their possible role in promoting white matter development postnatally in DS requires further investigation, particularly in identifying the best therapeutic windows.

For future research in neurological diseases, identifying shared features and disease-specific mechanisms affecting white matter integrity will be key to unravelling the cellular phenotypes involved and developing targeted therapeutic strategies aimed at promoting (re-)myelination and ultimately improving cognitive function. In this regard, it should be emphasised that remyelination strategies may prove more effective in MS and ischemic stroke than in DS. In demyelinating diseases such as MS and stroke, OPC and NSC differentiation and remyelination are predominantly impaired due to acquired disruptions of CNS homeostasis, particularly involving astrocytes and microglia during disease progression (Liddelow et al., 2017; Marangon et al., 2024; Silva Oliveira Junior et al., 2024; Sofroniew, 2020). In contrast, while similar reactive glial states are observed in DS, presumably all cell types and progenitor pools may be intrinsically/cell-autonomously affected by genome-wide alterations resulting from HSA21 triplication. Consequently, responses to drugs promoting OPC differentiation in DS will likely differ substantially from those in MS or stroke, warranting further need for disease-specific testing and validation.

3.4 Conclusion

This thesis uncovered novel perspectives that contribute to white matter abnormalities in DS, focusing on aberrant oligodendroglial lineage progression, the role of the HSA21-encoded gene *C21ORF91*, and the potential of pharmacological intervention to restore oligodendroglial differentiation that is corrupted by C21orf91 orthologue overexpression in rat OPCs. The findings demonstrate that hypomyelination in DS reflects an intrinsic developmental disturbance, possibly favouring a shift from oligodendrogenesis toward astroglial differentiation of progenitors (OPCs, NSCs). This imbalance can be linked to the overexpression of C21ORF91, which was shown to disrupt oligodendroglial differentiation and myelination capacity and induce aberrant hybrid glial phenotypes with astro- and oligodendroglial properties *in vitro* and in postmortem DS brain tissue. Pharmacological screening revealed that several repurposed compounds, including danazol, parbendazole, and medrysone, can modulate C21orf91-disrupted OPC fate, promote oligodendroglial maturation, and/or enhance supportive astroglial cues. These findings extend beyond classical demyelinating disorders and suggest that myelin-promoting strategies may also benefit genetically driven conditions such as DS. In conclusion, this thesis identified oligodendroglial dysregulation as a central, targetable feature of DS neuropathology and established C21ORF91 as a novel contributor to white matter defects. It further proves that pharmacological modulation of progenitor fate progression is feasible to counteract myelination deficits, potentially improving brain development and cognitive function in DS and related disorders.

3.5 Future Perspectives

Advancing our understanding of glial cell specification and myelination in the context of DS will benefit substantially from using patient-derived induced pluripotent stem cell (iPSC) studies. These models provide a human-specific, developmentally relevant platform (Russo et al., 2024) to dissect the contribution of C21ORF91 to lineage fate and myelination. In contrast to most available animal models, which fail to recapitulate the nuanced features of human glial development as the HSA21 gene orthologues are located on three different mouse chromosomes, iPSC-derived systems allow for targeted investigation of the cellular and molecular mechanisms underlying the observed impairments- Furthermore, they facilitate personalised testing of the pharmacological approaches described in this thesis. Nonetheless, the Ts65Dn mouse model has emerged as a valuable *in vivo* tool, particularly due to its pronounced alterations in glial cell composition and overall defective OPC differentiation (Klein & Haydar, 2022). While it may not fully reflect the C21ORF91-driven pathology, it could serve as a suitable model to assess the efficacy of myelin repair drugs in a broader DS context.

Furthermore, future research should also explore the role of microglia, as their contribution, supportive and/or potentially detrimental, remains an underexplored yet possibly critical component of white matter integrity in DS. In this context, it would be exciting to elucidate whether C21ORF91 is possibly involved in specific microglial phenotypes or can disrupt their homeostatic functions. Moreover, the role of C21ORF91 in the onset and progression of other neurological disorders, such as MS or stroke, should be investigated in the future.

4 Appendix

4.1 Additional Information and Figures

4.1.1 C21orf91 Modulation in Rat aNSCs

4.1.1.1 Experimental Procedure

For the isolation of mesenchymal stem cells (MSCs) and SVZ-aNSCs, female 8–10 weeks old Wistar rats were used. Adult rat MSC cultures were prepared and cultivated as described by (Jadasz et al., 2013; Samper Agrelo et al., 2020). Adult rat NSC cultures from the SVZ were obtained and cultivated following the instructions of (Jadasz et al., 2018; Samper Agrelo et al., 2020). After the splitting of NSCs, cells were transfected via electroporation by using Amaxa® Rat Neural Stem Cell Nucleofector™ Kit. C21orf91 overexpression constructs are described in section 2.2 (Reiche et al., 2021). C21orf91 suppression constructs were generated by OriGene Technologies, choosing the shRNA cloning vector pGFP-V-RS with a TCAAGAG loop (control vector including a scrambled negative control non-effective shRNA cassette). For suppression, an equal 1:1:1 mixture of three different shRNA sequences of the rat *C21orf91* orthologue gene was used (AAT TGC CAA CCA GGA TTG TTC TCG ATC CA, AGT CGG CAT CTC AAG CTA TAC GCA GAG AA, and AGC AGC TCC TCA AGA ACT GTT CCA AGT TG). NSCs were transfected either with 1.5 µg/10^6 for overexpression (1:5 mix of citrine:overexpression construct) or with 2 µg/10^6 cells for suppression. Transfected cells were plated on pre-coated poly-L-ornithine/laminin (100 µg/mL and 12 µg/mL, Sigma-Aldrich) plates at a density of 75,000 cells/well for ICC and 1.5 x 10^5 cells/well for qRT-PCR. After 16 h, medium was exchanged with mesenchymal stem cell-conditioned medium (MSC-CM) to initiate oligodendroglial differentiation. ICC was performed as previously described by Jadasz et al. (2018). Organotypic brain slices were generated and stained as described in section 2.3 (Manousi et al., 2021) and by Jadasz et al. (2018). After 4 h of slice generation, 10,000 transfected vital cells (by means of staining Trypan blue) were transplanted onto each slice following a medium exchange to 1:1 slice medium and MSC-CM. Slices were cultivated for 4 days before fixation with 4% PFA. Data are shown as mean values (±SEM). To determine statistical significance, Student's *t*-test was applied: $*p < .05$; $**p < .01$; $***p < .001$. Note that NSC suppression experiments were conducted by Mina Park as part of her master's thesis (Park, 2020).

4.1.1.2 Results

C21orf91 overexpression resulted in the significant almost threefold induction of GFAP expression, while MBP was drastically decreased compared to control under seven days of MSC-CM conditioning (Fig. 2A, a.). The suppression of C21orf91 remarkably diminished both glial lineage markers, though more prominent for MBP (Fig. 2A, b.). Due to their huge morphological heterogeneity, this feature of elevated levels of C21orf91 was not analysed (data not shown). However, the suppression of C21orf91 delayed morphological maturation, as seen by process length and branching, three days in culture following MSC-CM conditioning compared to control cells (Fig. 2 B). Suppressed NSCs integrated less frequently into cerebellar slice cultures, as indicated by half the number of control transfected cells counted four days after transplantation (Fig. 2C), which is also illustrated in the representative images (Fig. 2F, (a)-(f)). Though the number of Olig2-positive cells showed no difference (Fig. 2D), the suppressed cells decreased MBP expression significantly compared to control cells (Fig. 2E). Also integrated into the slice culture environment, suppressed cells exhibited diminished morphological phenotypes (see Fig. 2F,(d-f)) than control transfected transplanted cells (see Fig. 2F (a-c)).

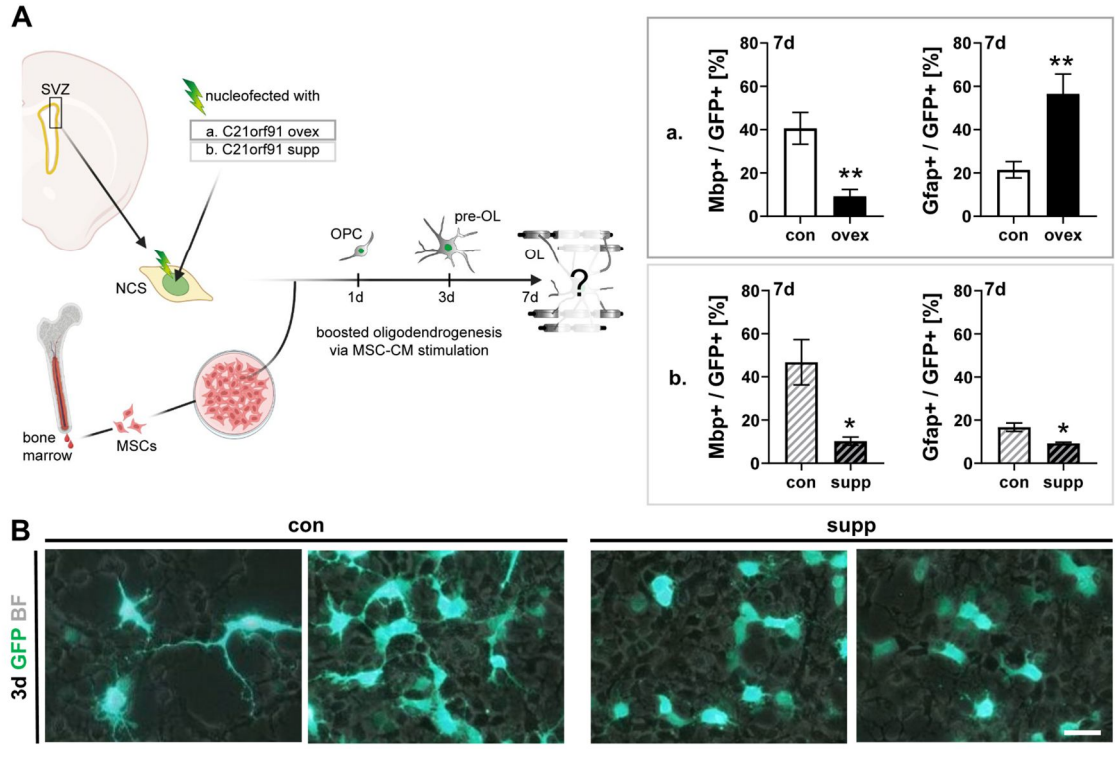

Continued

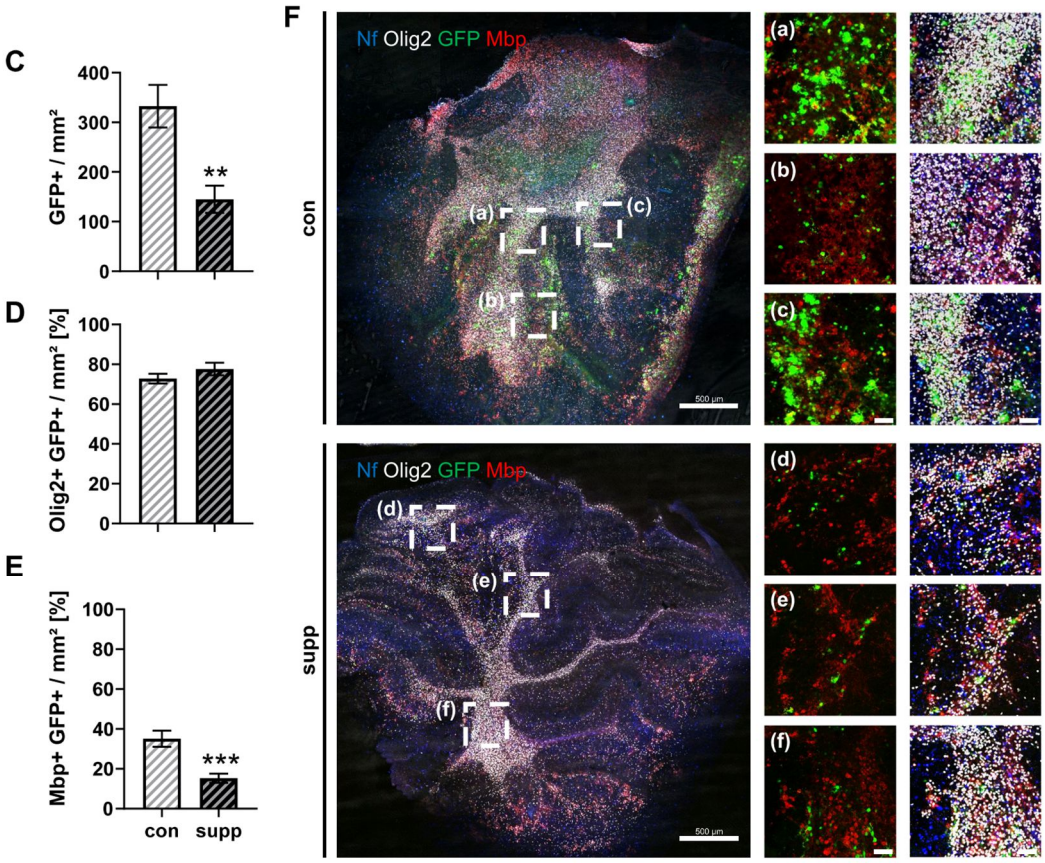

Figure 3. C21orf91 modulation inhibits pro-oligodendroglial cues of mesenchymal stem cell-conditioned medium in rat SVZ-aNSCs *in vitro* and *ex vivo*. Schematic presentation of experimental design (A, created with BioRender.com). NSCs were either transfected with a C21orf91 overexpression construct (a.; ovex; black bars) or a suppression mix (b., supp; black dashed bars) or the corresponding controls (con; white bars for ovex or white dashed bars for supp) and stimulated with MSC-CM to boost oligodendroglial lineage progression (estimated by Mbp staining) instead of astroglial cues (represented by Gfap staining) seven days (7 d) upon conditioning. Morphological presentation of transfected cells depicted by GFP signal (for visualisation of positively transfected cells) and brightfield (BF) cultured with MSC-CM for three days (3d) (B). Four days after transplantation of transfected cells onto cerebellar organotypic slice cultures conditioned with 1:1 slice culture medium and MSC-CM, GFP-positive cells per mm2 (C), Olig2-positive cells per mm2 (D), or Mbp-expressing cells per mm2 (E) were evaluated. Representative image of a whole slice (F) shows three randomly chosen areas for control transfected (a-c) or C21orf91 suppressed (e-d) integrated cells stained Nf (blue), Olig2 (white), and Mbp (red). GFP for visualisation of transfected cells. Data are shown as mean values (±SEM) and derived from n=3-5 experiments (A), or n=4 slices of one animal, with independent NSC pools/slice (C-E). Scale bar: 500 µm (F); 100 µm (a-f), t-test: *p < .05; ** p ≤0.01; *** p ≤ 0.001. Except for overexpression data and schematic illustration, data and images are adapted from (Park, 2020).

4.1.2 Changes in Transcript Levels in OPCs and aNSCs upon C21orf91 Modulation

4.1.2.1 Results

Analysis of mRNA transcript levels of modulated OPCs confirmed *C21orf91* was successfully overexpressed (ovex) at 1 d and 3 d, though decreasing over time (Fig. 3A, see also section 2.1; Reiche et al. 2021). *Tcf4*, *Lrp1*, *Ctnnb1* (also known as β-catenin), *Grp17*, and *Snx27* expression levels were induced along the differentiation from one to three days (1 d, 3 d) in control transfected cells (con), while inhibitors of oligodendrogenesis *Hes1*/*5* were downregulated. *C21orf91* overexpressing cells showed a drastic induction of *Ctnnb1* and *Hes1*, while *Lrp1* and *Hes5* were slightly upregulated compared to control at 1 d. The other transcript levels were diminished for the other specific time points compared to the controls. Instead of an increasing trend along lineage progression, *Snx27* and *Ctnnb1* transcript levels diminished at 3 d in C21orf91 protein overexpressing OPCs.

For aNSCs of the SVZ, described in 4.1.1, C21orf91-suppressed cells (supp) showed an overall downregulation of transcript levels at 1d of stimulation with MSC-CM (to induce and promote oligodendroglial lineage progression, see section 1.1.3 and Fig. 2A) (Fig. 3B). Upon its overexpression, except for *Ctnnb1* and *Hes5*, the other genes exhibited the same regulations as described for OPCs, most prominently diminishing *Tcf4* and inducing *Hes1* expression compared to control-transfected cells.

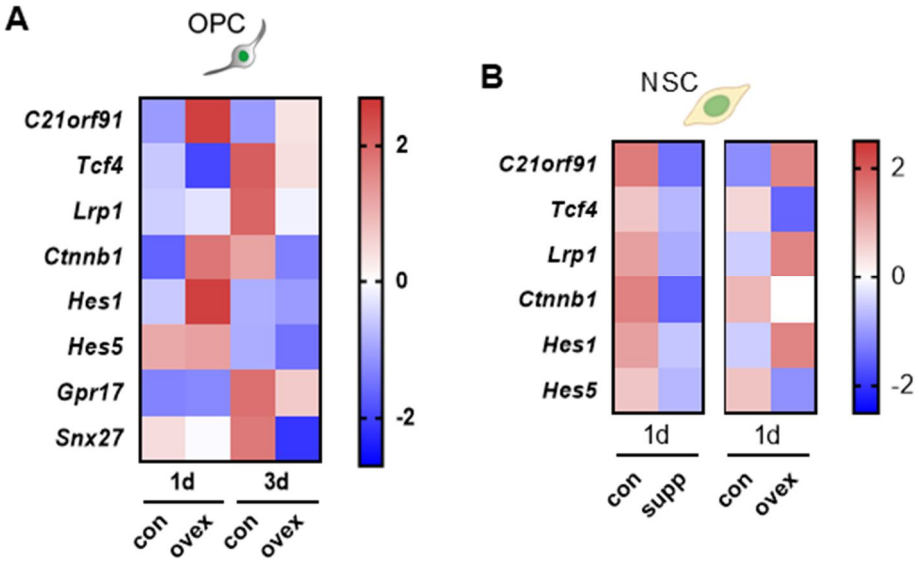

Figure 4. Modulations of C21orf91 expression levels result in an overall dysregulated pattern for various important regulatory transcript levels in rat oligodendroglial precursor cells. OPCs were transfected with an overexpression construct for C21orf91 (ovex) and control (con) and mRNA levels were measured at 1d and 3d of differentiation (A). For aNSCs, C21orf91 was either suppressed (supp) or overexpressed and conditioned with MSC-CM for 1d to promote oligodendroglial lineage progression (B). Data are presented as z-scores derived from mean values of n=2 experiments.

4.1.3 C21orf91 Modulation in Rat Schwann Cells

4.1.3.1 Experimental Procedure

Primary rat Schwann cells from p0-2 postnatal day-old pups were prepared and cultivated according to (Brockes et al., 1979; Schira-Heinen et al., 2022b). The Amaxa Basic Glial Cells Nucleofection™ Kit was used to nucleofect Schwann cells either with 2.5 µg/10^6 cells for the suppression construct mix (1:1:1) or 2 µg/10^6 cells for the overexpression construct of C21orf91 (with 10:1 co-transfection with citrine) and corresponding control plasmids. For ICC, 40,000 (native) or 50,000 (transfected) cells/well were plated, while for qPCR analysis 80,000 (native) or 120,000 (transfected) cells/well were seeded. Overexpressing Schwann cells and corresponding control transfected cells were further selected with hygromycin-supplemented medium (1:1000). Staining was performed as described in section 2.2 (Reiche et al., 2021) and additionally using mouse anti-S100 (1:500; Sigma-Aldrich), mouse anti-Ki-67 (1:500; Agilent Dako) and rabbit anti-C21orf91 (1:300; Sigma-Aldrich). Morphological analysis was assessed via cell size and shape of soma and protrusions. Data are shown as mean values (±SEM).

4.1.3.2 Results

In native Schwann cells, C21orf91 protein expression correlated with all mitotic phases two days in culture (Fig. 4A). Ki-67 and C21orf91 signal intensities increased in cells entering the mitotic cycle. During prophase, as chromosomes condense and the spindle apparatus assembles, a small C21ORF91-positive structure appears at the nucleus's centre, enlarging as spindle poles become visible in prometaphase and metaphase. Telophase describes the separation into two identical daughter cells, facilitated by a contractile ring, while C21ORF91 signals fade from the nuclear region. However, a C21ORF91-positive structure connecting the not fully separated cells (likely a chromatin bridge) remains. As cells transition from telophase to mitosis exit, the signals for both C21ORF91 and Ki-67 gradually decrease. However, strong C21ORF91 signals were detected for structures representing the spindle apparatus, especially the spindle poles and microtubules.

Overexpression of C21orf91 in Schwann cells led to distinct morphological changes compared to control-transfected cells, judged by S100 and C21orf91 staining, as well as GFP-expressing cells at day two of cultivation (Fig. 4B-D'). Three morphological phenotypes were identified based on cell size and protrusions: Type 1 cells (cross, most common in Schwann cell monocultures) are small with two opposing protrusions; Type 2 cells (star) have a large soma and at least three protrusions with web formation; Type 3 (triangle) cells have larger soma sizes with two or more protrusions but no web formation. In control cells, the majority were Type 1. However, in C21orf91-overexpressing cells, the

GFP+ population was mainly Type 2 and 3. Analysis of cells with high C21orf91 signals (Fig. 4C, D') showed that the majority of Schwann cells belonged to phenotype 2 upon elevated C21orf91 expression.

Gene expression analysis via qPCR (Fig. 4E) indicated that *C21orf91* transcript levels were stably suppressed for four days, while its overexpression was higher at day two compared to day four, though still elevated compared to control. Suppression and overexpression resulted in partially opposing gene expression dynamics, for instance *Gap43*, *cJun*, *Mag*, *Mal*, and *P0* transcript levels are induced in C21orf91-suppressed Schwann cells at day two, on the other hand these genes were diminished at the same timepoint in Schwann cells with elevated C21orf91 protein expression. However, *Ccdc8gb* expression is upregulated under both modulations of C21orf91.

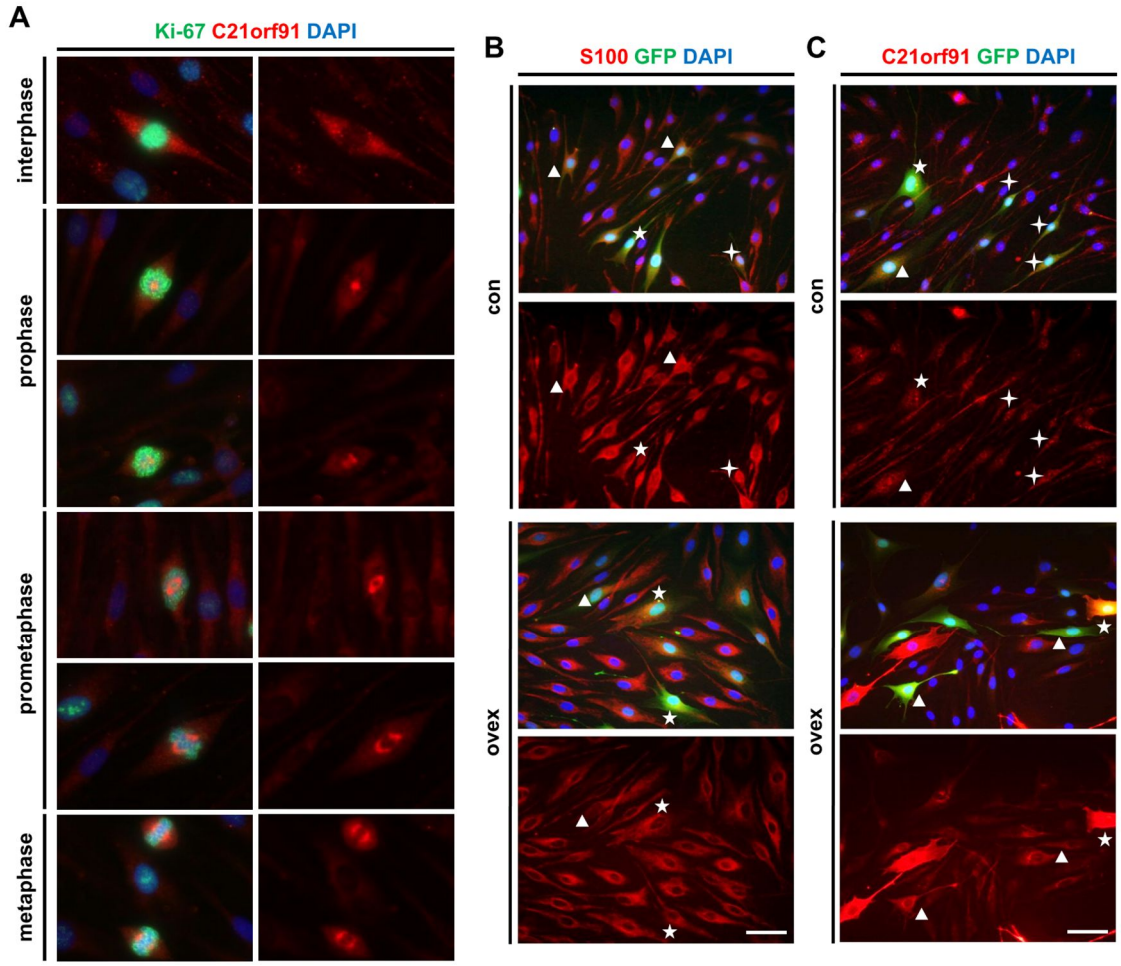

Continued

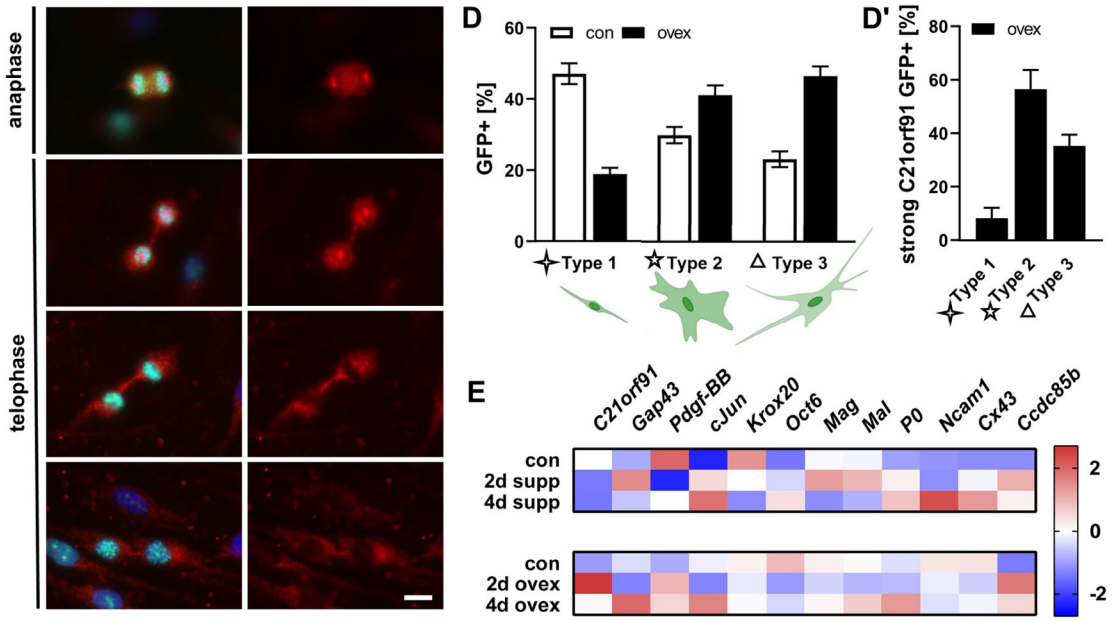

Figure 5. An overview of C21orf91's roles in rat Schwann cell mitosis, morphological presentation and transcript dynamics. C21ORF91 localisation during rat Schwann cell mitosis depicted by representative images for C21orf91 (red), Ki-67 (green), and DAPI (blue) two days in culture (A). Stained cells were distinguished for the different mitotic phases. Schwann cells were transfected with citrine (1:10) and either a control vector (con, white bars) or C21orf91 overexpression construct (ovex, black bars). Representative images for GFP (green), DAPI, and S100 (B) or C21orf91 (C) (both in red) indicate morphological heterogeneity induced by transfection after two days in culture. Morphological analysis for GFP-expressing cells depending on protrusions and cell sizes revealed that the cells categorised as phenotype 1 (cross, bipolar) make up the biggest proportion of control-transfected cells, but the smallest proportion of C21orf91-overexpressed cells (D). On the other hand, type 3 (triangle) occurs least in control transfected cells, while being most apparent in C21orf91 overexpressing cells. More defined analysis, focusing on only strongly C21orf91-expressing cells within the GFP-expressing population upon overexpression, demonstrated that most cells belong to phenotype 2 (star) (D'). Transcript level dynamics of C21orf91 suppressed (supp) or overexpressed (ovex) Schwann cells over the course of two and four days (2d, 4d) (E). Data are derived from n=1 (D, D') experiments (on average, 89 cells for control and 102 cells for ovex were counted in seven random pictures/condition) and presented as z-scores derived from mean values of n=3-5 experiments (E). Scale bars: 20 µm (A), 50 µm (B,C). Data and images are adapted from (Schütte, 2022).

4.2 List of Author Contributions for this Thesis

I. Aberrant Oligodendrogenesis in Down syndrome – Shift in Gliogenesis?

Laura Reiche, Patrick Küry*, Peter Göttle*

*these authors contributed equally

Published: Cells (2019); Impact factor: 5.656;

DOI: 10.3390/cells8121591

Contribution to conceptualisation, realisation, and publication

Approximated share of contribution: 60%

Co-conceptualisation, literature research, figure design, and preparation of the manuscript.

II. C21orf91 Regulates Oligodendroglial Precursor Cell Fate—A Switch in the Glial Lineage?

Laura Reiche, Peter Göttle, Lydie Lane, Paula Duek, Mina Park, Kasum Azim, Jana Schütte, Anastasia Manousi, Jessica Schira-Heinen and Patrick Küry

Published: Frontiers in Cellular Neuroscience (2021); Impact factor: 6.147;

DOI: 10.3389/fncel.2021.653075

Contribution to conceptualisation, realisation, and publication

Approximated share of contribution: 45%

Experimental conceptualisation and supervision of the characterisation of C21orf91 expression during rat brain development via qPCR, immunohistochemistry, and western blotting. Preparation and cultivation of primary cultures. Experimental conceptualisation and realisation of transfections of primary rat oligodendroglial cells examined via qPCR, immunocytochemistry, and assessment of myelination capacity after transplantation onto co-cultures. Co-conceptualisation and preparation of the manuscript and figure design.

III. Identification of Novel Myelin Repair Drugs by Modulation of Oligodendroglial Differentiation

Anastasia Manousi*, Peter Göttle*, **Laura Reiche**, Qiao-Ling Cui, Luke M. Healy, Rainer Akkermann, Joel Gruchot, Jessica Schira-Heinen, Jack P. Antel, Hans-Peter Hartung, Patrick Küry

*these authors contributed equally

Published: EBioMedicine (2021); Impact factor: 11.205;

DOI: 10.1016/j.ebiom.2021.103276

Contribution to conceptualisation, realisation, and publication

Approximated share of contribution: 15%

Preparation and cultivation of primary mixed cultures to obtain OPCs. Planning, realisation, and quantitative analysis of western blots, as well as preparation of the corresponding figure design and manuscript sections (materials and methods, results).

IV. Myelin Repair Is Fostered by the Corticosteroid Medrysone Specifically Acting on Astroglial Subpopulations

Markley Silva Oliveira Junior, Jessica Schira-Heinen, **Laura Reiche**, Seulki Han, Vanessa Cristina Meira de Amorim, Isabel Lewen, Joel Gruchot, Peter Göttle, Rainer Akkermann, Kasum Azim*, and Patrick Küry*

*these authors contributed equally

Published: EBioMedicine (2022); Impact factor: 11.1;

DOI: 10.1016/j.ebiom.2022.104204

Contribution to conceptualisation, realisation, and publication

Approximated share of contribution: 15%

Preparation and cultivation of primary mixed cultures to obtain astrocytes and OPCs. Planning, realization, immunostaining, and quantitative analysis of OPC experiments, as well as preparation of the corresponding figures and parts in the manuscript (especially material and methods).

V. Teriflunomide as a Therapeutic Means for Myelin Repair

Peter Göttle, Janos Groh, **Laura Reiche**, Joel Gruchot, Nicole Rychlik, Luisa Werner, Iria Samper Agrelo, Rainer Akkermann, Annika Zink, Alessandro Prigione, Hans-Peter Hartung, Rudolf Martini and Patrick Küry

Published: Journal of Neuroinflammation (2023); Impact factor: 9.3;

DOI: 10.1186/s12974-022-02686-6

Contribution to conceptualisation, realisation, and publication

Approximated share of contribution: 10%

Involved in establishing and realizing cuprizone animal experiments and performing immunohistological analysis. Supporting data interpretation and presentation.

VI. A Novel Ex Vivo Model to Study Therapeutic Treatments for Myelin Repair following Ischemic Damage

Luisa Werner*; Michael Gliem*, Nicole Rychlik, Goran Pavic, **Laura Reiche**, Frank Kirchhoff, Markley Silva Oliveira Junior, Joel Gruchot, Sven G. Meuth, Patrick Küry* and Peter Göttle*

*these authors contributed equally

Published: International Journal of Molecular Sciences (2023); Impact factor: 4.9;

DOI: 10.3390/ijms241310972

Contribution to conceptualisation, realisation, and publication

Approximated share of contribution: 10%

Preparation and cultivation of primary mixed cultures to obtain OPCs. Involved in initially establishing organotypic coronal slice cultures. Supporting data interpretation and presentation.

VII. Star Power: Harnessing the Reactive Astrocyte Response to Promote Remyelination in Multiple Sclerosis

Markley Silva Oliveira Junior*, **Laura Reiche***, Emerson Daniele, Ines Kortebi, Maryam Faiz, Patrick Küry

*these authors contributed equally

Published: Neural Regeneration Research (2023); Impact factor: 6.1;

DOI: 10.4103/1673-5374.380879

Contribution to conceptualisation, realisation, and publication

Approximated share of contribution: 30%

Co-conceptualisation, literature research, figure design, and preparation of the manuscript.

VIII. C21ORF91 Overexpression Leads to Glial Differentiation Misbalance in Down Syndrome to Be Rescued by Remyelination Drugs

Laura Reiche, Cherie Anne Stringer, Kevin Camey, Brigida Ziegler, Luisa Werner, Joel Gruchot, Peter Göttle, Elizabeth Head, David Kremer and Patrick Küry

Submitted

Contribution to conceptualisation, realisation, and publication

Approximated share of contribution: 50%

Conceptualization and study design. Performing histological staining in human postmortem tissues of Down syndrome patients. Preparation and cultivation of primary mixed cultures to obtain OPCs. Execution and analysis of transfected OPCs in mono- and transplanted onto co-cultures via immunocytochemistry and ELISA. Conceptualization and preparation of the manuscript, including figure design.

4.3 List of Other Author Contributions

Reiche L, Plaack B, Lehmkuhl M, Weyers V, Gruchot J, Picard D, Perron H, Remke M, Knobbe-Thomsen C, Reifenberger G, Küry P, Kremer D. HERV-W envelope protein is present in microglial cells of the human glioma tumor microenvironment and differentially modulates neoplastic cell behavior. Microbes Infect. 2024 Nov 20:105460. doi: 10.1016/j.micinf.2024.105460. Epub ahead of print. PMID: 39577621. **Contribution: 35%**

Gruchot J, **Reiche L**, Werner L, Herrero F, Schira-Heinen J, Meyer U, Küry P. Molecular dissection of HERV-W dependent microglial- and astroglial cell polarization. Microbes Infect. 2024 Jun 27:105382. doi: 10.1016/j.micinf.2024.105382. Epub ahead of print. PMID: 38944109. **Contribution: 15%**

Gruchot J, **Reiche L**, Chan A, Hoepner R, Küry P. Human endogenous retrovirus type-W and multiple sclerosis-related smoldering neuroinflammation. Neural Regen Res. 2025 Mar 1;20(3):813-814. doi: 10.4103/NRR.NRR-D-24-00121. Epub 2024 May 13. PMID: 38886951; PMCID: PMC11433918. **Contribution: 10%**

Gruchot J, Lewen I, Dietrich M, **Reiche L**, Sindi M, Hecker C, Herrero F, Charvet B, Weber-Stadlbauer U, Hartung HP, Albrecht P, Perron H, Meyer U, Küry P. Transgenic expression of the HERV-W envelope protein leads to polarized glial cell populations and a neurodegenerative environment. Proc Natl Acad Sci U S A. 2023 Sep 19;120(38):e2308187120. doi: 10.1073/pnas.2308187120. Epub 2023 Sep 11. PMID: 37695891; PMCID: PMC10515160. **Contribution: 10%**

Gruchot J, Lein F, Lewen I, **Reiche L**, Weyers V, Petzsch P, Göttle P, Köhrer K, Hartung HP, Küry P, Kremer D. Siponimod Modulates the Reaction of Microglial Cells to Pro-Inflammatory Stimulation. Int J Mol Sci. 2022 Oct 31;23(21):13278. doi: 10.3390/ijms232113278. PMID: 36362063; PMCID: PMC9655930. **Contribution: 10%**

Göttle P, Schichel K, **Reiche L**, Werner L, Zink A, Prigione A, Küry P. TLR4 Associated Signaling Disrupters as a New Means to Overcome HERV-W Envelope- Mediated Myelination Deficits. Front Cell Neurosci. 2021 Nov 23;15:777542. doi: 10.3389/fncel.2021.777542. PMID: 34887730; PMCID: PMC8650005. **Contribution: 20%**

Beyer F, Jadasz J, Samper Agrelo I, Schira-Heinen J, Groh J, Manousi A, Bütermann C, Estrada V, **Reiche L**, Cantone M, Vera J, Viganò F, Dimou L, Müller HW, Hartung HP, Küry P. Heterogeneous fate choice of genetically modulated adult neural stem cells in gray and white matter of the central nervous system. Glia. 2020 Feb;68(2):393-406. doi: 10.1002/glia.23724. Epub 2019 Oct 21. PMID: 31633850. **Contribution: 5%**

Göttle P, Manousi A, Kremer D, **Reiche L**, Hartung HP, Küry P. Teriflunomide promotes oligodendroglial differentiation and myelination. J Neuroinflammation. 2018 Mar 13;15(1):76. doi: 10.1186/s12974-018-1110-z. PMID: 29534752; PMCID: PMC5851312. **Contribution: 10%**

4.4 List of Co-Supervised Master Projects that Contributed to this Thesis

I. Immunohistological detection of C21orf91 expression in the central nervous system and investigation of its potential function upon gene suppression in neural stem cells

Mina Park; 2020
First reviewer: Prof. Dr. P. Küry; second reviewer: PD Dr. Carsten Berndt

Abstract

Down Syndrome (DS) is the most prevalent genetic disorder leading to intellectual disability and cognitive impairment. Neuropathological alterations in DS are characterized by reduced brain volume and impaired neuronal development which is represented by a diminished number of neurons and synaptic spines. White matter structures are also affected in DS, manifesting in an aberrantly increased number of astrocytes while the number of oligodendrocytes is decreased. Since observed hypomyelination and reduced white matter integrity in DS were demonstrated to correlate with intellectual disability, accurate oligodendrogenesis and myelin formation are recently gaining more attention as a cause for or outcome of DS-related neuropathology. C21orf91, a protein encoded at the centromeric boundary of the Down Syndrome Critical Region (DSCR), emerges as a potential regulator of abnormal CNS development in DS. Modulations of the C21orf91-coding gene showed its involvement in the regulation of neurogenesis and a recent study within the host laboratory further demonstrated that C21orf91 plays an important role in OPC differentiation. Nevertheless, which function C21orf91 has in the establishment of proper and functional white matter structures remains to be clarified.

This study aimed at further elucidating the role of C21orf91 in gliogenesis by revealing its expression profile during rodent brain development and by investigating the differentiation of C21orf91 suppressed neural stem cells (NSCs) upon exposure to astroglial or oligodendroglial cues. Through immunohistochemical staining of corpus callosum (CC) and surrounding gray matter structures of seven days postnatal and adult rat brains, it was depicted for the first time that C21orf91 is co-expressed with the astroglial- and/or NSC marker GFAP as well as with several oligodendroglial markers. Furthermore, C21orf91 gene suppression induced delayed morphological maturation and interfered with differentiation of NSCs – being more obvious under oligodendroglial cues as the number of maturation marker expressing cells was significantly reduced upon C21orf91 suppression. Transplanted on ex vivo cerebellar slice cultures, C21orf91 suppressed cells seemed to have integration difficulties and showed a reduced myelination capacity. Based on these findings, it can be concluded that appropriate C21orf91 expression plays a crucial role in oligodendrogenesis and myelin formation.

II. Functional role of C21orf91 in myelinating glial cells of the nervous system

Jana Schütte; 2022
First reviewer: Prof. Dr. P. Küry; second reviewer: Dr. Frank Bosse

Abstract

The nervous system is composed of a central (CNS) and a peripheral (PNS) part. It is susceptible to injury and different diseases such as Down syndrome (DS) or Charcot-Marie-Tooth disorder, which can lead to disrupted myelination and thereby greatly affect fast signal transmission and neuron function, and consequently lead to poorer quality of life. Myelination is carried out by two different glial cell types, namely oligodendrocytes (in the CNS) and Schwann cells (SCs) (in the PNS). To develop novel effective treatments aiming to support regeneration and remyelination, detailed knowledge of the mechanisms regulating cell differentiation is crucial. In 2016, Li and colleagues introduced C21orf91 (also termed EURL) as a gene being dynamically expressed during normal human and mouse cortical development with altered expression in DS patients. The study also showed that C21orf91 interacts with Ccdc85b, a modulator of β-catenin signaling, and is an important factor for proper neurogenesis. Recently, it was reported that C21orf91 might be correlated with myelination in the CNS and has been suggested to play an essential role for the common neuropathological abnormalities observed in DS brains (Reiche et al., 2021). C21orf91 overexpression in oligodendrocyte precursor cells (OPCs) and neural stem cells (NSCs) resulted in an aberrant differentiation and reduced myelination capacity of mature oligodendrocytes (Park, 2020; Reiche et al., 2021).

The present thesis aimed to provide a first characterization of C21orf91 in the PNS and to get insight into its putative functional role in SCs as analyzed by means of immunostaining, quantitative real-time PCR and Western blot. In vivo investigation in rats revealed that C21orf91 expression could be correlated with myelination during normal CNS and PNS development as well as in response to peripheral nerve injury. No clear statement can be made about the functional role of C21orf91 in the PNS after C21orf91 modulation experiments in SC monocultures, but it is suggested that C21orf91 might exert an impact on SC maturation into the myelinating phenotype in a time- and dosage-dependent manner, similarly to its role in the CNS. Interestingly, a correlation with both EPDR1 and p57kip2 expression is indicated. Therefore, further investigations using co-cultures and C21orf91/p57kip2 co-transfection should be conducted in addition to in vivo specific loss of function experiments in myelinating cells to clarify the importance of C21orf91 for normal nervous system development and regeneration after nerve injury.

5 References

Ábrahám, H., Vincze, A., Veszpremi, B., Kravjak, A., Gomori, E., Kovacs, G. G., & Seress, L. (2012). Impaired myelination of the human hippocampal formation in Down syndrome. *Int J Dev Neurosci*, *30*(2), 147-158. https://doi.org/10.1016/j.ijdevneu.2011.11.005

Abukhaled, Y., Hatab, K., Awadhalla, M., & Hamdan, H. (2023). Understanding the genetic mechanisms and cognitive impairments in Down syndrome: towards a holistic approach. *Journal of Neurology*, *271*(1), 87-104. https://doi.org/10.1007/s00415-023-11890-0

Ait Yahya-Graison, E., Aubert, J., Dauphinot, L., Rivals, I., Prieur, M., Golfier, G., Rossier, J., Personnaz, L., Creau, N., Blehaut, H., Robin, S., Delabar, J. M., & Potier, M. C. (2007). Classification of human chromosome 21 gene-expression variations in Down syndrome: impact on disease phenotypes. *Am J Hum Genet*, *81*(3), 475-491. https://doi.org/10.1086/520000

Akay, L. A., Effenberger, A. H., & Tsai, L. H. (2021). Cell of all trades: oligodendrocyte precursor cells in synaptic, vascular, and immune function. *Genes Dev*, *35*(3-4), 180-198. https://doi.org/10.1101/gad.344218.120

Akkermann, R., Beyer, F., & Küry, P. (2017). Heterogeneous populations of neural stem cells contribute to myelin repair. *Neural Regen Res*, *12*(4), 509-517. https://doi.org/10.4103/1673-5374.204999

Akkermann, R., Jadasz, J. J., Azim, K., & Küry, P. (2016). Taking Advantage of Nature's Gift: Can Endogenous Neural Stem Cells Improve Myelin Regeneration? *Int J Mol Sci*, *17*(11). https://doi.org/10.3390/ijms17111895

Álvarez-Lafuente, R., De las Heras, V., Bartolomé, M., Picazo, J. J., & Arroyo, R. (2004). Relapsing-Remitting Multiple Sclerosis and Human Herpesvirus 6 Active Infection. *Archives of Neurology*, *61*(10). https://doi.org/10.1001/archneur.61.10.1523

Ashfaq, S., Pellegrini, M. V., & Can, A. S. (2024). Danazol. In *StatPearls*. https://www.ncbi.nlm.nih.gov/pubmed/33232014

Assinck, P., Duncan, G. J., Plemel, J. R., Lee, M. J., Stratton, J. A., Manesh, S. B., Liu, J., Ramer, L. M., Kang, S. H., Bergles, D. E., Biernaskie, J., & Tetzlaff, W. (2017). Myelinogenic Plasticity of Oligodendrocyte Precursor Cells following Spinal Cord Contusion Injury. *J Neurosci*, *37*(36), 8635-8654. https://doi.org/10.1523/JNEUROSCI.2409-16.2017

Atlas, H. P. (cited 2025 May 06). https://www.proteinatlas.org/ENSG00000154642-C21orf91.

Auderset, L., Pitman, K. A., Cullen, C. L., Pepper, R. E., Taylor, B. V., Foa, L., & Young, K. M. (2020). Low-Density Lipoprotein Receptor-Related Protein 1 (LRP1) Is a Negative Regulator of Oligodendrocyte Progenitor Cell Differentiation in the Adult Mouse Brain. *Front Cell Dev Biol*, *8*. https://doi.org/10.3389/fcell.2020.564351

Back, A. M., Connor, B., & McCaughey-Chapman, A. (2024). Oligodendrocytes in Huntington's Disease: A Review of Oligodendrocyte Pathology and Current Cell Reprogramming Approaches for Oligodendrocyte Modelling of Huntington's Disease. *Journal of Neuroscience Research*, *102*(12). https://doi.org/10.1002/jnr.70010

Bacmeister, C. M., Huang, R., Osso, L. A., Thornton, M. A., Conant, L., Chavez, A. R., Poleg-Polsky, A., & Hughes, E. G. (2022). Motor learning drives dynamic patterns of intermittent myelination on learning-activated axons. *Nat Neurosci*, *25*(10), 1300-1313. https://doi.org/10.1038/s41593-022-01169-4

Barbosa, D. J., Carvalho, C., Costa, I., & Silva, R. (2024). Molecular Motors in Myelination and Their Misregulation in Disease. *Molecular Neurobiology*, *62*(4), 4705-4723. https://doi.org/10.1007/s12035-024-04576-9

Barradas, P. C., Ferraz, A. S., Ferreira, A. A., Daumas, R. P., & Moura, E. G. (2001). 2'3'cyclic nucleotide 3'phosphodiesterase immunohistochemistry shows an impairment on myelin compaction in hypothyroid rats. *International Journal of Developmental Neuroscience*, *18*(8), 887-892. https://doi.org/10.1016/s0736-5748(00)00028-9

Baumann, N., & Pham-Dinh, D. (2001). Biology of oligodendrocyte and myelin in the mammalian central nervous system. *Physiol Rev*, *81*(2), 871-927. https://www.ncbi.nlm.nih.gov/pubmed/11274346

Baydyuk, M., Morrison, V. E., Gross, P. S., & Huang, J. K. (2020). Extrinsic Factors Driving Oligodendrocyte Lineage Cell Progression in CNS Development and Injury. *Neurochemical Research*, *45*(3), 630-642. https://doi.org/10.1007/s11064-020-02967-7

Bazydlo, A., Zammit, M., Wu, M., Dean, D., Johnson, S., Tudorascu, D., Cohen, A., Cody, K., Ances, B., Laymon, C., Klunk, W., Zaman, S., Handen, B., Alexander, A., Christian, B., & Hartley, S. (2021). White matter microstructure associations with episodic memory in adults with Down syndrome: a tract-based spatial statistics study. *Journal of Neurodevelopmental Disorders*, *13*(1). https://doi.org/10.1186/s11689-021-09366-1

Bechler, M. E., Byrne, L., & Ffrench-Constant, C. (2015). CNS Myelin Sheath Lengths Are an Intrinsic Property of Oligodendrocytes. *Curr Biol*, *25*(18), 2411-2416. https://doi.org/10.1016/j.cub.2015.07.056

Bechler, M. E., Swire, M., & ffrench-Constant, C. (2017). Intrinsic and adaptive myelination—A sequential mechanism for smart wiring in the brain. *Developmental Neurobiology*, *78*(2), 68-79. https://doi.org/10.1002/dneu.22518

Bedrossian, R. H., & Eriksen, S. P. (1969). The treatment of ocular inflammation with medrysone. *Arch Ophthalmol*, *81*(2), 184-191. https://doi.org/10.1001/archopht.1969.00990010186008

Benes, F. M. (1994). Myelination of a Key Relay Zone in the Hippocampal Formation Occurs in the Human Brain During Childhood, Adolescence, and Adulthood. *Archives of General Psychiatry*, *51*(6). https://doi.org/10.1001/archpsyc.1994.03950060041004

Bergles, D. E., & Richardson, W. D. (2016). Oligodendrocyte Development and Plasticity. *Cold Spring Harbor Perspectives in Biology*, *8*(2). https://doi.org/10.1101/cshperspect.a020453

Beyer, F., Jadasz, J., Samper Agrelo, I., Schira-Heinen, J., Groh, J., Manousi, A., Butermann, C., Estrada, V., Reiche, L., Cantone, M., Vera, J., Vigano, F., Dimou, L., Muller, H. W., Hartung, H. P., & Küry, P. (2020). Heterogeneous fate choice of genetically modulated adult neural stem cells in gray and white matter of the central nervous system. *Glia*, *68*(2), 393-406. https://doi.org/10.1002/glia.23724

Beyer, F., Samper Agrelo, I., & Küry, P. (2019). Do Neural Stem Cells Have a Choice? Heterogenic Outcome of Cell Fate Acquisition in Different Injury Models. *International Journal of Molecular Sciences*, *20*(2). https://doi.org/10.3390/ijms20020455

References

Bezukladova, S., Genchi, A., Panina-Bordignon, P., & Martino, G. (2022). Promoting exogenous repair in multiple sclerosis: myelin regeneration. *Current Opinion in Neurology*, *35*(3), 313-318. https://doi.org/10.1097/wco.0000000000001062

Bjornevik, K., Münz, C., Cohen, J. I., & Ascherio, A. (2023). Epstein–Barr virus as a leading cause of multiple sclerosis: mechanisms and implications. *Nature Reviews Neurology*. https://doi.org/10.1038/s41582-023-00775-5

Bögler, O., Wren, D., Barnett, S. C., Land, H., & Noble, M. (1990). Cooperation between two growth factors promotes extended self-renewal and inhibits differentiation of oligodendrocyte-type-2 astrocyte (O-2A) progenitor cells. *Proceedings of the National Academy of Sciences*, *87*(16), 6368-6372. https://doi.org/10.1073/pnas.87.16.6368

Boison, D., Bussow, H., D'Urso, D., Muller, H. W., & Stoffel, W. (1995). Adhesive properties of proteolipid protein are responsible for the compaction of CNS myelin sheaths. *J Neurosci*, *15*(8), 5502-5513. https://doi.org/10.1523/JNEUROSCI.15-08-05502.1995

Bonfanti, E., Gelosa, P., Fumagalli, M., Dimou, L., Viganò, F., Tremoli, E., Cimino, M., Sironi, L., & Abbracchio, M. P. (2017). The role of oligodendrocyte precursor cells expressing the GPR17 receptor in brain remodeling after stroke. *Cell Death & Disease*, *8*(6), e2871-e2871. https://doi.org/10.1038/cddis.2017.256

Brandt, B., & Rosén, I. (1995). Impaired Peripheral Somatosensory Function in Children with Down Syndrome. *Neuropediatrics*, *26*(06), 310-312. https://doi.org/10.1055/s-2007-979780

Breton, J. M., Long, K. L. P., Barraza, M. K., Perloff, O. S., & Kaufer, D. (2021). Hormonal Regulation of Oligodendrogenesis II: Implications for Myelin Repair. *Biomolecules*, *11*(2). https://doi.org/10.3390/biom11020290

Brockes, J. P., Fields, K. L., & Raff, M. C. (1979). Studies on cultured rat Schwann cells. I. Establishment of purified populations from cultures of peripheral nerve. *Brain Research*, *165*(1), 105-118. https://doi.org/10.1016/0006-8993(79)90048-9

Brown, T. L., & Macklin, W. B. (2019). The Actin Cytoskeleton in Myelinating Cells. *Neurochemical Research*, *45*(3), 684-693. https://doi.org/10.1007/s11064-019-02753-0

Cahoy, J. D., Emery, B., Kaushal, A., Foo, L. C., Zamanian, J. L., Christopherson, K. S., Xing, Y., Lubischer, J. L., Krieg, P. A., Krupenko, S. A., Thompson, W. J., & Barres, B. A. (2008). A transcriptome database for astrocytes, neurons, and oligodendrocytes: a new resource for understanding brain development and function. *J Neurosci*, *28*(1), 264-278. https://doi.org/10.1523/JNEUROSCI.4178-07.2008

Cañete-Massé, C., Carbó-Carreté, M., Peró-Cebollero, M., Cui, S.-X., Yan, C.-G., & Guàrdia-Olmos, J. (2022). Altered spontaneous brain activity in Down syndrome and its relation with cognitive outcome. *Scientific Reports*, *12*(1). https://doi.org/10.1038/s41598-022-19627-1

Cao, F., Hata, R., Zhu, P., Nakashiro, K., & Sakanaka, M. (2010a). Conditional deletion of Stat3 promotes neurogenesis and inhibits astrogliogenesis in neural stem cells. *Biochem Biophys Res Commun*, *394*(3), 843-847. https://doi.org/10.1016/j.bbrc.2010.03.092

Cao, Q., He, Q., Wang, Y., Cheng, X., Howard, R. M., Zhang, Y., DeVries, W. H., Shields, C. B., Magnuson, D. S. K., Xu, X.-M., Kim, D. H., & Whittemore, S. R. (2010b). Transplantation of Ciliary Neurotrophic Factor-Expressing Adult Oligodendrocyte Precursor Cells Promotes Remyelination and Functional Recovery after SpinalCord Injury. *The Journal of Neuroscience*, *30*(8), 2989-3001. https://doi.org/10.1523/jneurosci.3174-09.2010

Chang, Y.-T., Teng, Y.-N., Lin, K.-I., Wang, C. C. N., Morris-Natschke, S. L., Lee, K.-H., & Hung, C.-C. (2019). Danazol mediates collateral sensitivity via STAT3/Myc related pathway in multidrug-resistant cancer cells. *Scientific Reports*, *9*(1). https://doi.org/10.1038/s41598-019-48169-2

Chen, C., Jiang, P., Xue, H., Peterson, S. E., Tran, H. T., McCann, A. E., Parast, M. M., Li, S., Pleasure, D. E., Laurent, L. C., Loring, J. F., Liu, Y., & Deng, W. (2014). Role of astroglia in Down's syndrome revealed by patient-derived human-induced pluripotent stem cells. *Nat Commun*, *5*, 4430. https://doi.org/10.1038/ncomms5430

Chen, C. Z., Neumann, B., Forster, S., & Franklin, R. J. M. (2021a). Schwann cell remyelination of the central nervous system: why does it happen and what are the benefits? *Open Biol*, *11*(1), 200352. https://doi.org/10.1098/rsob.200352

Chen, J.-F., Liu, K., Hu, B., Li, R.-R., Xin, W., Chen, H., Wang, F., Chen, L., Li, R.-X., Ren, S.-Y., Xiao, L., Chan, J. R., & Mei, F. (2021b). Enhancing myelin renewal reverses cognitive dysfunction in a murine model of Alzheimer's disease. *Neuron*, *109*(14), 2292-2307.e2295. https://doi.org/10.1016/j.neuron.2021.05.012

Chen, Y., Miles, D. K., Hoang, T., Shi, J., Hurlock, E., Kernie, S. G., & Lu, Q. R. (2008). The Basic Helix-Loop-Helix Transcription Factor Olig2 Is Critical for Reactive Astrocyte Proliferation after Cortical Injury. *The Journal of Neuroscience*, *28*(43), 10983-10989. https://doi.org/10.1523/jneurosci.3545-08.2008

Choi, B. H. (1986). Glial Fibrillary Acidic Protein in Radial Glia of Early Human Fetal Cerebrum. *Journal of Neuropathology and Experimental Neurology*, *45*(4), 408-418. https://doi.org/10.1097/00005072-198607000-00003

Chou, S. T., Byrska-Bishop, M., Tober, J. M., Yao, Y., Vandorn, D., Opalinska, J. B., Mills, J. A., Choi, J. K., Speck, N. A., Gadue, P., Hardison, R. C., Nemiroff, R. L., French, D. L., & Weiss, M. J. (2012). Trisomy 21-associated defects in human primitive hematopoiesis revealed through induced pluripotent stem cells. *Proc Natl Acad Sci U S A*, *109*(43), 17573-17578. https://doi.org/10.1073/pnas.1211175109

Coetzee, T., Fujita, N., Dupree, J., Shi, R., Blight, A., Suzuki, K., Suzuki, K., & Popko, B. (1996). Myelination in the absence of galactocerebroside and sulfatide: normal structure with abnormal function and regional instability. *Cell*, *86*(2), 209-219. https://doi.org/10.1016/s0092-8674(00)80093-8

Correale, J., Marrodan, M., & Ysrraelit, M. C. (2019). Mechanisms of Neurodegeneration and Axonal Dysfunction in Progressive Multiple Sclerosis. *Biomedicines*, *7*(1). https://doi.org/10.3390/biomedicines7010014

Crawford, Abbe H., Tripathi, Richa B., Richardson, William D., & Franklin, Robin J. M. (2016). Developmental Origin of Oligodendrocyte Lineage Cells Determines Response to Demyelination and Susceptibility to Age-Associated Functional Decline. *Cell Reports*, *15*(4), 761-773. https://doi.org/10.1016/j.celrep.2016.03.069

Davis, A. A., & Temple, S. (1994). A self-renewing multipotential stem cell in embryonic rat cerebral cortex. *Nature*, *372*(6503), 263-266. https://doi.org/10.1038/372263a0

Dawson, M. R., Polito, A., Levine, J. M., & Reynolds, R. (2003). NG2-expressing glial progenitor cells: an abundant and widespread population of cycling cells in the adult rat CNS. *Mol Cell Neurosci*, *24*(2), 476-488. https://www.ncbi.nlm.nih.gov/pubmed/14572468

de Graaf, G., Buckley, F., & Skotko, B. G. (2021). Estimation of the number of people with Down syndrome in Europe. *Eur J Hum Genet*, *29*(3), 402-410. https://doi.org/10.1038/s41431-020-00748-y

del Águila, Á., Adam, M., Ullom, K., Shaw, N., Qin, S., Ehrman, J., Nardini, D., Salomone, J., Gebelein, B., Lu, Q. R., Potter, S. S., Waclaw, R., Campbell, K., & Nakafuku, M. (2022). Olig2 defines a subset of neural stem cells that produce specific olfactory bulb interneuron subtypes in the subventricular zone of adult mice. *Development*, *149*(5). https://doi.org/10.1242/dev.200028

Dendrou, C. A., Fugger, L., & Friese, M. A. (2015). Immunopathology of multiple sclerosis. *Nat Rev Immunol*, *15*(9), 545-558. https://doi.org/10.1038/nri3871

Dewar, D., Underhill, S. M., & Goldberg, M. P. (2003). Oligodendrocytes and Ischemic Brain Injury. *Journal of Cerebral Blood Flow & Metabolism*, *23*(3), 263-274. https://doi.org/10.1097/01.Wcb.0000053472.41007.F9

Dimou, L., Simon, C., Kirchhoff, F., Takebayashi, H., & Götz, M. (2008). Progeny of Olig2-expressing progenitors in the gray and white matter of the adult mouse cerebral cortex. *Journal of Neuroscience*, *28*(41), 10434-10442. https://doi.org/10.1523/JNEUROSCI.2831-08.2008

Dmowski, W. P., Scholer, H. F., Mahesh, V. B., & Greenblatt, R. B. (1971). Danazol--a synthetic steroid derivative with interesting physiologic properties. *Fertil Steril*, *22*(1), 9-18. https://doi.org/10.1016/s0015-0282(16)37981-x

Dogliotti, G., Galliera, E., Licastro, F., Porcellini, E., & Corsi, M. M. (2010). Serum neutrophil gelatinase-B associated lipocalin (NGAL) levels in Down's syndrome patients. *Immun Ageing*, *7 Suppl 1*(Suppl 1), S7. https://doi.org/10.1186/1742-4933-7-S1-S7

Domingues, H. S., Portugal, C. C., Socodato, R., & Relvas, J. B. (2016). Oligodendrocyte, Astrocyte, and Microglia Crosstalk in Myelin Development, Damage, and Repair. *Front Cell Dev Biol*, *4*, 71. https://doi.org/10.3389/fcell.2016.00071

Dossi, E., Vasile, F., & Rouach, N. (2017). Human astrocytes in the diseased brain. *Brain Res Bull*. https://doi.org/10.1016/j.brainresbull.2017.02.001

Duncan, I. D., Radcliff, A. B., Heidari, M., Kidd, G., August, B. K., & Wierenga, L. A. (2018). The adult oligodendrocyte can participate in remyelination. *Proceedings of the National Academy of Sciences*, *115*(50). https://doi.org/10.1073/pnas.1808064115

El Waly, B., Macchi, M., Cayre, M., & Durbec, P. (2014). Oligodendrogenesis in the normal and pathological central nervous system. *Front Neurosci*, *8*, 145. https://doi.org/10.3389/fnins.2014.00145

Elbaz, B., & Popko, B. (2019). Molecular Control of Oligodendrocyte Development. *Trends Neurosci*, *42*(4), 263-277. https://doi.org/10.1016/j.tins.2019.01.002

Emery, B. (2010). Regulation of oligodendrocyte differentiation and myelination. *Science*, *330*(6005), 779-782. https://doi.org/10.1126/science.1190927

Emery, B., & Wood, T. L. (2024). Regulators of Oligodendrocyte Differentiation. *Cold Spring Harbor Perspectives in Biology*, *16*(6). https://doi.org/10.1101/cshperspect.a041358

Escartin, C., Galea, E., Lakatos, A., O'Callaghan, J. P., Petzold, G. C., Serrano-Pozo, A., Steinhäuser, C., Volterra, A., Carmignoto, G., Agarwal, A., Allen, N. J., Araque, A., Barbeito, L., Barzilai, A., Bergles, D. E., Bonvento, G., Butt, A. M., Chen, W.-T., Cohen-Salmon, M., . . . Verkhratsky, A. (2021). Reactive astrocyte nomenclature, definitions, and future directions. *Nat Neurosci*, *24*(3), 312-325. https://doi.org/10.1038/s41593-020-00783-4

Fancy, S. P., Baranzini, S. E., Zhao, C., Yuk, D. I., Irvine, K. A., Kaing, S., Sanai, N., Franklin, R. J., & Rowitch, D. H. (2009). Dysregulation of the Wnt pathway inhibits timely myelination and remyelination in the mammalian CNS. *Genes Dev*, *23*(13), 1571-1585. https://doi.org/10.1101/gad.1806309

Fancy, S. P. J., Chan, J. R., Baranzini, S. E., Franklin, R. J. M., & Rowitch, D. H. (2011). Myelin Regeneration: A Recapitulation of Development? *Annual Review of Neuroscience*, *34*(1), 21-43. https://doi.org/10.1146/annurev-neuro-061010-113629

Fang, L.-P., & Bai, X. (2023). Oligodendrocyte precursor cells: the multitaskers in the brain. *Pflügers Archiv - European Journal of Physiology*, *475*(9), 1035-1044. https://doi.org/10.1007/s00424-023-02837-5

Fenoll, R., Pujol, J., Esteba-Castillo, S., de Sola, S., Ribas-Vidal, N., Garcia-Alba, J., Sanchez-Benavides, G., Martinez-Vilavella, G., Deus, J., Dierssen, M., Novell-Alsina, R., & de la Torre, R. (2017). Anomalous White Matter Structure and the Effect of Age in Down Syndrome Patients. *J Alzheimers Dis*, *57*(1), 61-70. https://doi.org/10.3233/JAD-161112

Ferrara, N., Ousley, F., & Gospodarowicz, D. (1988). Bovine brain astrocytes express basic fibroblast growth factor, a neurotropic and angiogenic mitogen. *Brain Research*, *462*(2), 223-232. https://doi.org/10.1016/0006-8993(88)90550-1

Ferrari Bardile, C., Radulescu, C. I., & Pouladi, M. A. (2023). Oligodendrocyte pathology in Huntington's disease: from mechanisms to therapeutics. *Trends Mol Med*, *29*(10), 802-816. https://doi.org/10.1016/j.molmed.2023.07.010

Fields, R. D. (2008). White matter in learning, cognition and psychiatric disorders. *Trends Neurosci*, *31*(7), 361-370. https://doi.org/10.1016/j.tins.2008.04.001

Filippi, M., Bar-Or, A., Piehl, F., Preziosa, P., Solari, A., Vukusic, S., & Rocca, M. A. (2018). Multiple sclerosis. *Nat Rev Dis Primers*, *4*(1), 43. https://doi.org/10.1038/s41572-018-0041-4

Fischer, D. F., van Dijk, R., Sluijs, J. A., Nair, S. M., Racchi, M., Levelt, C. N., van Leeuwen, F. W., & Hol, E. M. (2005). Activation of the Notch pathway in Down syndrome: cross-talk of Notch and APP. *Faseb j*, *19*(11), 1451-1458. https://doi.org/10.1096/fj.04-3395.com

Fitzpatrick, J. M., Anderson, R. C., & McDermott, K. W. (2015). MicroRNA: Key regulators of oligodendrocyte development and pathobiology. *Int J Biochem Cell Biol*, *65*, 134-138. https://doi.org/10.1016/j.biocel.2015.05.021

References

Florio, R., Veschi, S., di Giacomo, V., Pagotto, S., Carradori, S., Verginelli, F., Cirilli, R., Casulli, A., Grassadonia, A., Tinari, N., Cataldi, A., Amoroso, R., Cama, A., & De Lellis, L. (2019). The Benzimidazole-Based Anthelmintic Parbendazole: A Repurposed Drug Candidate That Synergizes with Gemcitabine in Pancreatic Cancer. *Cancers (Basel)*, *11*(12). https://doi.org/10.3390/cancers11122042

Franklin, R. J. M., & Blakemore, W. F. (2003). Requirements for schwann cell migration within cns environments: A viewpoint. *International Journal of Developmental Neuroscience*, *11*(5), 641-649. https://doi.org/10.1016/0736-5748(93)90052-f

Franklin, R. J. M., Bodini, B., & Goldman, S. A. (2024). Remyelination in the Central Nervous System. *Cold Spring Harb Perspect Biol*, *16*(3). https://doi.org/10.1101/cshperspect.a041371

Franklin, R. J. M., Frisén, J., & Lyons, D. A. (2021). Revisiting remyelination: Towards a consensus on the regeneration of CNS myelin. *Semin Cell Dev Biol*, *116*, 3-9. https://doi.org/10.1016/j.semcdb.2020.09.009

Fukami-Gartner, A., Baburamani, A. A., Dimitrova, R., Patkee, P. A., Ojinaga-Alfageme, O., Bonthrone, A. F., Cromb, D., Uus, A. U., Counsell, S. J., Hajnal, J. V., O'Muircheartaigh, J., & Rutherford, M. A. (2023). Comprehensive volumetric phenotyping of the neonatal brain in Down syndrome. *Cereb Cortex*, *33*(14), 8921-8941. https://doi.org/10.1093/cercor/bhad171

Funfschilling, U., Supplie, L. M., Mahad, D., Boretius, S., Saab, A. S., Edgar, J., Brinkmann, B. G., Kassmann, C. M., Tzvetanova, I. D., Mobius, W., Diaz, F., Meijer, D., Suter, U., Hamprecht, B., Sereda, M. W., Moraes, C. T., Frahm, J., Goebbels, S., & Nave, K. A. (2012). Glycolytic oligodendrocytes maintain myelin and long-term axonal integrity. *Nature*, *485*(7399), 517-521. https://doi.org/10.1038/nature11007

Gaesser, J. M., & Fyffe-Maricich, S. L. (2016). Intracellular signaling pathway regulation of myelination and remyelination in the CNS. *Experimental Neurology*, *283*, 501-511. https://doi.org/10.1016/j.expneurol.2016.03.008

Gil, M., & Gama, V. (2023). Emerging mitochondrial-mediated mechanisms involved in oligodendrocyte development. *J Neurosci Res*, *101*(3), 354-366. https://doi.org/10.1002/jnr.25151

Godbout, R., Andison, R., Katyal, S., & Bisgrove, D. A. (2003). Isolation of a novel cDNA enriched in the undifferentiated chick retina and lens. *Dev Dyn*, *227*(3), 409-415. https://doi.org/10.1002/dvdy.10310

Golden, J. A., & Hyman, B. T. (1994). Development of the superior temporal neocortex is anomalous in trisomy 21. *J Neuropathol Exp Neurol*, *53*(5), 513-520. http://www.ncbi.nlm.nih.gov/pubmed/8083693

Gorter, R. P., & Baron, W. (2022). Recent insights into astrocytes as therapeutic targets for demyelinating diseases. *Curr Opin Pharmacol*, *65*, 102261. https://doi.org/10.1016/j.coph.2022.102261

Göttle, P., Groh, J., Reiche, L., Gruchot, J., Rychlik, N., Werner, L., Samper Agrelo, I., Akkermann, R., Zink, A., Prigione, A., Hartung, H. P., Martini, R., & Küry, P. (2023). Teriflunomide as a therapeutic means for myelin repair. *J Neuroinflammation*, *20*(1), 7. https://doi.org/10.1186/s12974-022-02686-6

Göttle, P., Manousi, A., Kremer, D., Reiche, L., Hartung, H. P., & Küry, P. (2018). Teriflunomide promotes oligodendroglial differentiation and myelination. *J Neuroinflammation*, *15*(1), 76. https://doi.org/10.1186/s12974-018-1110-z

Gradisnik, L., & Velnar, T. (2023). Astrocytes in the central nervous system and their functions in health and disease: A review. *World J Clin Cases*, *11*(15), 3385-3394. https://doi.org/10.12998/wjcc.v11.i15.3385

Greenblatt, R. B., Nezhat, C., & Ben-Nun, I. (1980). The treatment of benign breast disease with danazol. *Fertil Steril*, *34*(3), 242-245. https://www.ncbi.nlm.nih.gov/pubmed/7409245

Gruchot, J., Herrero, F., Weber-Stadlbauer, U., Meyer, U., & Küry, P. (2023a). Interplay between activation of endogenous retroviruses and inflammation as common pathogenic mechanism in neurological and psychiatric disorders. *Brain Behav Immun*, *107*, 242-252. https://doi.org/10.1016/j.bbi.2022.10.007

Gruchot, J., Lewen, I., Dietrich, M., Reiche, L., Sindi, M., Hecker, C., Herrero, F., Charvet, B., Weber-Stadlbauer, U., Hartung, H. P., Albrecht, P., Perron, H., Meyer, U., & Küry, P. (2023b). Transgenic expression of the HERV-W envelope protein leads to polarized glial cell populations and a neurodegenerative environment. *Proc Natl Acad Sci U S A*, *120*(38), e2308187120. https://doi.org/10.1073/pnas.2308187120

Guest, J. D., Santamaria, A. J., Solano, J. P., de Rivero Vaccari, J. P., Dietrich, W. D., Pearse, D. D., Khan, A., & Levi, A. D. (2025). Challenges in advancing Schwann cell transplantation for spinal cord injury repair. *Cytotherapy*, *27*(1), 36-50. https://doi.org/10.1016/j.jcyt.2024.08.005

Guidi, S., Bonasoni, P., Ceccarelli, C., Santini, D., Gualtieri, F., Ciani, E., & Bartesaghi, R. (2008). Neurogenesis impairment and increased cell death reduce total neuron number in the hippocampal region of fetuses with Down syndrome. *Brain Pathol*, *18*(2), 180-197. https://doi.org/10.1111/j.1750-3639.2007.00113.x

Hackett, A. R., Yahn, S. L., Lyapichev, K., Dajnoki, A., Lee, D.-H., Rodriguez, M., Cammer, N., Pak, J., Mehta, S. T., Bodamer, O., Lemmon, V. P., & Lee, J. K. (2018). Injury type-dependent differentiation of NG2 glia into heterogeneous astrocytes. *Experimental Neurology*, *308*, 72-79. https://doi.org/10.1016/j.expneurol.2018.07.001

Han, S., Gim, Y., Jang, E.-H., & Hur, E.-M. (2022). Functions and dysfunctions of oligodendrocytes in neurodegenerative diseases. *Frontiers in Cellular Neuroscience*, *16*. https://doi.org/10.3389/fncel.2022.1083159

Haydar, T. F., & Reeves, R. H. (2012). Trisomy 21 and early brain development. *Trends Neurosci*, *35*(2), 81-91. https://doi.org/10.1016/j.tins.2011.11.001

Hernández, I. H., Villa-González, M., Martín, G., Soto, M., & Pérez-Álvarez, M. J. (2021). Glial Cells as Therapeutic Approaches in Brain Ischemia-Reperfusion Injury. *Cells*, *10*(7). https://doi.org/10.3390/cells10071639

Hill, R. A., Li, A. M., & Grutzendler, J. (2018). Lifelong cortical myelin plasticity and age-related degeneration in the live mammalian brain. *Nat Neurosci*, *21*(5), 683-695. https://doi.org/10.1038/s41593-018-0120-6

Hill, R. A., Nishiyama, A., & Hughes, E. G. (2024). Features, Fates, and Functions of Oligodendrocyte Precursor Cells. *Cold Spring Harbor Perspectives in Biology*, *16*(3). https://doi.org/10.1101/cshperspect.a041425

Hill, W. D., Marioni, R. E., Maghzian, O., Ritchie, S. J., Hagenaars, S. P., McIntosh, A. M., Gale, C. R., Davies, G., & Deary, I. J. (2019). A combined analysis of genetically correlated traits identifies 187 loci and a role for neurogenesis and myelination in intelligence. *Mol Psychiatry*, *24*(2), 169-181. https://doi.org/10.1038/s41380-017-0001-5

Huang, L., Peng, Y., Tao, X., Ding, X., Li, R., Jiang, Y., Zuo, W., & Camara, A. (2022). Microtubule Organization Is Essential for Maintaining Cellular Morphology and Function. *Oxidative Medicine and Cellular Longevity*, *2022*, 1-15. https://doi.org/10.1155/2022/1623181

Huang, W., Guo, Q., Bai, X., Scheller, A., & Kirchhoff, F. (2019). Early embryonic NG2 glia are exclusively gliogenic and do not generate neurons in the brain. *Glia*, *67*(6), 1094-1103. https://doi.org/10.1002/glia.23590

Hughes, E. G., Orthmann-Murphy, J. L., Langseth, A. J., & Bergles, D. E. (2018). Myelin remodeling through experience-dependent oligodendrogenesis in the adult somatosensory cortex. *Nat Neurosci*, *21*(5), 696-706. https://doi.org/10.1038/s41593-018-0121-5

Hughes, E. G., & Stockton, M. E. (2021). Premyelinating Oligodendrocytes: Mechanisms Underlying Cell Survival and Integration. *Front Cell Dev Biol*, *9*(July), 714169. https://doi.org/10.3389/fcell.2021.714169

Huhn, S. C., Liu, J., Ye, C., Lu, H., Jiang, X., Feng, X., Ganesan, S., White, E., & Shen, Z. (2017). Regulation of spindle integrity and mitotic fidelity by BCCIP. *Oncogene*, *36*(33), 4750-4766. https://doi.org/10.1038/onc.2017.92

Ishihara, K. (2021). Genes Associated with Disturbed Cerebral Neurogenesis in the Embryonic Brain of Mouse Models of Down Syndrome. *Genes (Basel)*, *12*(10). https://doi.org/10.3390/genes12101598

Jadasz, J. J., Kremer, D., Göttle, P., Tzekova, N., Domke, J., Rivera, F. J., Adjaye, J., Hartung, H.-P., Aigner, L., & Küry, P. (2013). Mesenchymal Stem Cell Conditioning Promotes Rat Oligodendroglial Cell Maturation. *PLoS One*, *8*(8). https://doi.org/10.1371/journal.pone.0071814

Jadasz, J. J., Tepe, L., Beyer, F., Samper Agrelo, I., Akkermann, R., Spitzhorn, L. S., Silva, M. E., Oreffo, R. O. C., Hartung, H. P., Prigione, A., Rivera, F. J., Adjaye, J., & Küry, P. (2018). Human mesenchymal factors induce rat hippocampal- and human neural stem cell dependent oligodendrogenesis. *Glia*, *66*(1), 145-160. https://doi.org/10.1002/glia.23233

Jäkel, S., Agirre, E., Mendanha Falcão, A., van Bruggen, D., Lee, K. W., Knuesel, I., Malhotra, D., ffrench-Constant, C., Williams, A., & Castelo-Branco, G. (2019). Altered human oligodendrocyte heterogeneity in multiple sclerosis. *Nature*, *566*(7745), 543-547. https://doi.org/10.1038/s41586-019-0903-2

Jessen, K. R., & Mirsky, R. (2005). The origin and development of glial cells in peripheral nerves. *Nature Reviews Neuroscience*, *6*(9), 671-682. https://doi.org/10.1038/nrn1746

Jessen, K. R., & Mirsky, R. (2016). The repair Schwann cell and its function in regenerating nerves. *The Journal of Physiology*, *594*(13), 3521-3531. https://doi.org/10.1113/jp270874

Jia, W., Kamen, Y., Pivonkova, H., & Káradóttir, R. T. (2019). Neuronal activity-dependent myelin repair after stroke. *Neuroscience Letters*, *703*, 139-144. https://doi.org/10.1016/j.neulet.2019.03.005

Jordan, A., Hadfield, J. A., Lawrence, N. J., & McGown, A. T. (1998). Tubulin as a target for anticancer drugs: Agents which interact with the mitotic spindle. *Medicinal Research Reviews*, *18*(4), 259-296. https://doi.org/10.1002/(sici)1098-1128(199807)18:4<259::Aid-med3>3.0.Co;2-u

Kanaumi, T., Milenkovic, I., Adle-Biassette, H., Aronica, E., & Kovacs, G. G. (2013). Non-neuronal cell responses differ between normal and Down syndrome developing brains. *Int J Dev Neurosci*, *31*(8), 796-803. https://doi.org/10.1016/j.ijdevneu.2013.09.011

Kang, S. H., Fukaya, M., Yang, J. K., Rothstein, J. D., & Bergles, D. E. (2010). NG2+ CNS Glial Progenitors Remain Committed to the Oligodendrocyte Lineage in Postnatal Life and following Neurodegeneration. *Neuron*, *68*(4), 668-681. https://doi.org/10.1016/j.neuron.2010.09.009

Kent, S. A., & Miron, V. E. (2023). Microglia regulation of central nervous system myelin health and regeneration. *Nature Reviews Immunology*, *24*(1), 49-63. https://doi.org/10.1038/s41577-023-00907-4

Kessaris, N., Fogarty, M., Iannarelli, P., Grist, M., Wegner, M., & Richardson, W. D. (2005). Competing waves of oligodendrocytes in the forebrain and postnatal elimination of an embryonic lineage. *Nat Neurosci*, *9*(2), 173-179. https://doi.org/10.1038/nn1620

Kidd, G. J., Andrews, S. B., & Trapp, B. D. (1994). Organization of microtubules in myelinating Schwann cells. *J Neurocytol*, *23*(12), 801-810. https://doi.org/10.1007/bf01268092

Kiray, H., Lindsay, S. L., Hosseinzadeh, S., & Barnett, S. C. (2016). The multifaceted role of astrocytes in regulating myelination. *Exp Neurol*, *283*(Pt B), 541-549. https://doi.org/10.1016/j.expneurol.2016.03.009

Kirby, L., Jin, J., Cardona, J. G., Smith, M. D., Martin, K. A., Wang, J., Strasburger, H., Herbst, L., Alexis, M., Karnell, J., Davidson, T., Dutta, R., Goverman, J., Bergles, D., & Calabresi, P. A. (2019). Oligodendrocyte precursor cells present antigen and are cytotoxic targets in inflammatory demyelination. *Nature Communications*, *10*(1). https://doi.org/10.1038/s41467-019-11638-3

Kirdajova, D., Valihrach, L., Valny, M., Kriska, J., Krocianova, D., Benesova, S., Abaffy, P., Zucha, D., Klassen, R., Kolenicova, D., Honsa, P., Kubista, M., & Anderova, M. (2021). Transient astrocyte-like NG2 glia subpopulation emerges solely following permanent brain ischemia. *Glia*, *69*(11), 2658-2681. https://doi.org/10.1002/glia.24064

Klein, J. A., & Haydar, T. F. (2022). Neurodevelopment in Down syndrome: Concordance in humans and models. *Front Cell Neurosci*, *16*, 941855. https://doi.org/10.3389/fncel.2022.941855

Koch-Henriksen, N., Thygesen, L. C., Stenager, E., Laursen, B., & Magyari, M. (2018). Incidence of MS has increased markedly over six decades in Denmark particularly with late onset and in women. *Neurology*, *90*(22). https://doi.org/10.1212/wnl.0000000000005612

Komitova, M., Serwanski, D. R., Richard Lu, Q., & Nishiyama, A. (2011). NG2 cells are not a major source of reactive astrocytes after neocortical stab wound injury. *Glia*, *59*(5), 800-809. https://doi.org/10.1002/glia.21152

References

Korbel, J. O., Tirosh-Wagner, T., Urban, A. E., Chen, X. N., Kasowski, M., Dai, L., Grubert, F., Erdman, C., Gao, M. C., Lange, K., Sobel, E. M., Barlow, G. M., Aylsworth, A. S., Carpenter, N. J., Clark, R. D., Cohen, M. Y., Doran, E., Falik-Zaccai, T., Lewin, S. O., . . . Korenberg, J. R. (2009). The genetic architecture of Down syndrome phenotypes revealed by high-resolution analysis of human segmental trisomies. *Proc Natl Acad Sci U S A*, *106*(29), 12031-12036. https://doi.org/10.1073/pnas.0813248106

Kotter, M. R., Stadelmann, C., & Hartung, H. P. (2011). Enhancing remyelination in disease--can we wrap it up? *Brain*, *134*(7), 1882-1900. https://doi.org/10.1093/brain/awr014

Kremer, D., Aktas, O., Hartung, H. P., & Küry, P. (2011). The complex world of oligodendroglial differentiation inhibitors. *Ann Neurol*, *69*(4), 602-618. https://doi.org/10.1002/ana.22415

Kurabayashi, N., Nguyen, M. D., & Sanada, K. (2015). DYRK1A overexpression enhances STAT activity and astrogliogenesis in a Down syndrome mouse model. *EMBO Rep*, *16*(11), 1548-1562. https://doi.org/10.15252/embr.201540374

Kurtzke, J. F. (2000). Multiple sclerosis in time and space--geographic clues to cause. *J Neurovirol*, *6 Suppl 2*, S134-140. https://www.ncbi.nlm.nih.gov/pubmed/10871801

Küry, P., Nath, A., Creange, A., Dolei, A., Marche, P., Gold, J., Giovannoni, G., Hartung, H. P., & Perron, H. (2018). Human Endogenous Retroviruses in Neurological Diseases. *Trends Mol Med*, *24*(4), 379-394. https://doi.org/10.1016/j.molmed.2018.02.007

Küspert, M., Hammer, A., Bosl, M. R., & Wegner, M. (2011). Olig2 regulates Sox10 expression in oligodendrocyte precursors through an evolutionary conserved distal enhancer. *Nucleic Acids Res*, *39*(4), 1280-1293. https://doi.org/10.1093/nar/gkq951

Lanfranchi, S., Jerman, O., Dal Pont, E., Alberti, A., & Vianello, R. (2010). Executive function in adolescents with Down Syndrome. *J Intellect Disabil Res*, *54*(4), 308-319. https://doi.org/10.1111/j.1365-2788.2010.01262.x

Lassmann, H. (2019). Pathogenic mechanisms associated with different clinical courses of multiple sclerosis. *Front Immunol*, *9*(JAN), 3116. https://doi.org/10.3389/fimmu.2018.03116

Lebel, C., Gee, M., Camicioli, R., Wieler, M., Martin, W., & Beaulieu, C. (2012). Diffusion tensor imaging of white matter tract evolution over the lifespan. *Neuroimage*, *60*(1), 340-352. https://doi.org/10.1016/j.neuroimage.2011.11.094

Lecca, D., Raffaele, S., Abbracchio, M. P., & Fumagalli, M. (2020). Regulation and signaling of the GPR17 receptor in oligodendroglial cells. *Glia*, *68*(10), 1957-1967. https://doi.org/10.1002/glia.23807

Lee, B. Y., & Hur, E. M. (2020). A Role of Microtubules in Oligodendrocyte Differentiation. *Int J Mol Sci*, *21*(3). https://doi.org/10.3390/ijms21031062

Lee, H.-G., Wheeler, M. A., & Quintana, F. J. (2022). Function and therapeutic value of astrocytes in neurological diseases. *Nature Reviews Drug Discovery*, *21*(5), 339-358. https://doi.org/10.1038/s41573-022-00390-x

Leong, S. Y., Rao, V. T. S., Bin, J. M., Gris, P., Sangaralingam, M., Kennedy, T. E., & Antel, J. P. (2014). Heterogeneity of oligodendrocyte progenitor cells in adult human brain. *Annals of Clinical and Translational Neurology*, *1*(4), 272-283. https://doi.org/10.1002/acn3.55

Letourneau, A., Santoni, F. A., Bonilla, X., Sailani, M. R., Gonzalez, D., Kind, J., Chevalier, C., Thurman, R., Sandstrom, R. S., Hibaoui, Y., Garieri, M., Popadin, K., Falconnet, E., Gagnebin, M., Gehrig, C., Vannier, A., Guipponi, M., Farinelli, L., Robyr, D., . . . Antonarakis, S. E. (2014). Domains of genome-wide gene expression dysregulation in Down's syndrome. *Nature*, *508*(7496), 345-350. https://doi.org/10.1038/nature13200

Li, C., Tropak, M. B., Gerlai, R., Clapoff, S., Abramow-Newerly, W., Trapp, B., Peterson, A., & Roder, J. (1994). Myelination in the absence of myelin-associated glycoprotein. *Nature*, *369*(6483), 747-750. https://doi.org/10.1038/369747a0

Li, S. S., Qu, Z. D., Haas, M., Ngo, L., Heo, Y. J., Kang, H. J., Britto, J. M., Cullen, H. D., Vanyai, H. K., Tan, S. S., Chan-Ling, T., Gunnersen, J. M., & Heng, J. I. T. (2016). The HSA21 gene EURL/C21ORF91 controls neurogenesis within the cerebral cortex and is implicated in the pathogenesis of Down Syndrome [Article]. *Scientific Reports*, *6*, 14, Article 29514. https://doi.org/10.1038/srep29514

Li, X.-y., Kong, X.-m., Yang, C.-h., Cheng, Z.-f., Lv, J.-j., Guo, H., & Liu, X.-h. (2024). Global, regional, and national burden of ischemic stroke, 1990–2021: an analysis of data from the global burden of disease study 2021. *eClinicalMedicine*, *75*. https://doi.org/10.1016/j.eclinm.2024.102758

Liang, D., Yu, C., Ma, Z., Yang, X., Li, Z., Dong, X., Qin, X., Du, L., & Li, M. (2022). Identification of anthelmintic parbendazole as a therapeutic molecule for HNSCC through connectivity map-based drug repositioning. *Acta Pharm Sin B*, *12*(5), 2429-2442. https://doi.org/10.1016/j.apsb.2021.12.005

Liddelow, S. A., Guttenplan, K. A., Clarke, L. E., Bennett, F. C., Bohlen, C. J., Schirmer, L., Bennett, M. L., Münch, A. E., Chung, W. S., Peterson, T. C., Wilton, D. K., Frouin, A., Napier, B. A., Panicker, N., Kumar, M., Buckwalter, M. S., Rowitch, D. H., Dawson, V. L., Dawson, T. M., . . . Barres, B. A. (2017). Neurotoxic reactive astrocytes are induced by activated microglia. *Nature*, *541*(7638), 481-487. https://doi.org/10.1038/nature21029

Lin, J.-P., Mironova, Y. A., Shrager, P., & Giger, R. J. (2017). LRP1 regulates peroxisome biogenesis and cholesterol homeostasis in oligodendrocytes and is required for proper CNS myelin development and repair. *Elife*, *6*. https://doi.org/10.7554/eLife.30498

Linker, R. A., Mäurer, M., Gaupp, S., Martini, R., Holtmann, B., Giess, R., Rieckmann, P., Lassmann, H., Toyka, K. V., Sendtner, M., & Gold, R. (2002). CNTF is a major protective factor in demyelinating CNS disease: A neurotrophic cytokine as modulator in neuroinflammation. *Nat Med*, *8*(6), 620-624. https://doi.org/10.1038/nm0602-620

Lo, E. H. (2008). A new penumbra: transitioning from injury into repair after stroke. *Nat Med*, *14*(5), 497-500. https://doi.org/10.1038/nm1735

Lo, Y. C., Senese, S., France, B., Gholkar, A. A., Damoiseaux, R., & Torres, J. Z. (2017). Computational Cell Cycle Profiling of Cancer Cells for Prioritizing FDA-Approved Drugs with Repurposing Potential. *Scientific Reports*, *7*(1), 11261. https://doi.org/10.1038/s41598-017-11508-2

Lockrow, J., Fortress, A., & Granholm, A.-C. (2012). Age-Related Neurodegeneration and Memory Loss in Down Syndrome. *Current gerontology and geriatrics research*, *2012*, 463909. https://doi.org/10.1155/2012/463909

Long, K. L. P., Breton, J. M., Barraza, M. K., Perloff, O. S., & Kaufer, D. (2021). Hormonal Regulation of Oligodendrogenesis I: Effects across the Lifespan. *Biomolecules*, *11*(2). https://doi.org/10.3390/biom11020283

Lott, I. T., & Head, E. (2019). Dementia in Down syndrome: unique insights for Alzheimer disease research. *Nat Rev Neurol*, *15*(3), 135-147. https://doi.org/10.1038/s41582-018-0132-6

Lu, J., Lian, G., Zhou, H., Esposito, G., Steardo, L., Delli-Bovi, L. C., Hecht, J. L., Lu, Q. R., & Sheen, V. (2012). OLIG2 over-expression impairs proliferation of human Down syndrome neural progenitors. *Human Molecular Genetics*, *21*(10), 2330-2340. https://doi.org/10.1093/hmg/dds052

Lu, Q. R., Sun, T., Zhu, Z., Ma, N., Garcia, M., Stiles, C. D., & Rowitch, D. H. (2002). Common developmental requirement for Olig function indicates a motor neuron/oligodendrocyte connection. *Cell*, *109*(1), 75-86. http://www.ncbi.nlm.nih.gov/pubmed/11955448

Lubetzki, C., Zalc, B., Kremer, D., & Küry, P. (2022). Endogenous clues promoting remyelination in multiple sclerosis. *Current Opinion in Neurology*, *35*(3), 307-312. https://doi.org/10.1097/wco.0000000000001064

Ma, Z., Zhang, W., Wang, C., Su, Y., Yi, C., & Niu, J. (2024). A New Acquaintance of Oligodendrocyte Precursor Cells in the Central Nervous System. *Neuroscience Bulletin*, *40*(10), 1573-1589. https://doi.org/10.1007/s12264-024-01261-8

Manousi, A., Göttle, P., Reiche, L., Cui, Q. L., Healy, L. M., Akkermann, R., Gruchot, J., Schira-Heinen, J., Antel, J. P., Hartung, H. P., & Küry, P. (2021). Identification of novel myelin repair drugs by modulation of oligodendroglial differentiation competence. *EBioMedicine*, *65*, 103276. https://doi.org/10.1016/j.ebiom.2021.103276

Marangon, D., Castro, E. S. J. H., Cerrato, V., Boda, E., & Lecca, D. (2024). Oligodendrocyte Progenitors in Glial Scar: A Bet on Remyelination. *Cells*, *13*(12). https://doi.org/10.3390/cells13121024

Marin-Padilla, M. (1976). Pyramidal cell abnormalities in the motor cortex of a child with Down's syndrome. A Golgi study. *J Comp Neurol*, *167*(1), 63-81. https://doi.org/10.1002/cne.901670105

Marques, S., Zeisel, A., Codeluppi, S., van Bruggen, D., Mendanha Falcao, A., Xiao, L., Li, H., Haring, M., Hochgerner, H., Romanov, R. A., Gyllborg, D., Munoz-Manchado, A. B., La Manno, G., Lonnerberg, P., Floriddia, E. M., Rezayee, F., Ernfors, P., Arenas, E., Hjerling-Leffler, J., . . . Castelo-Branco, G. (2016). Oligodendrocyte heterogeneity in the mouse juvenile and adult central nervous system. *Science*, *352*(6291), 1326-1329. https://doi.org/10.1126/science.aaf6463

Matsas, R., Lavdas, A., Papastefanaki, F., & Thomaidou, D. (2008). Schwann Cell Transplantation for CNS Repair. *Current Medicinal Chemistry*, *15*(2), 151-160. https://doi.org/10.2174/092986708783330593

McCann, B., Levman, J., Baumer, N., Lam, M. Y., Shiohama, T., Cogger, L., MacDonald, A., Ijner, P., & Takahashi, E. (2021). Structural magnetic resonance imaging demonstrates volumetric brain abnormalities in down syndrome: Newborns to young adults. *Neuroimage Clin*, *32*, 102815. https://doi.org/10.1016/j.nicl.2021.102815

McIver, S. R., Muccigrosso, M., Gonzales, E. R., Lee, J. M., Roberts, M. S., Sands, M. S., & Goldberg, M. P. (2010). Oligodendrocyte degeneration and recovery after focal cerebral ischemia. *Neuroscience*, *169*(3), 1364-1375. https://doi.org/10.1016/j.neuroscience.2010.04.070

McKenzie, I. A., Ohayon, D., Li, H., de Faria, J. P., Emery, B., Tohyama, K., & Richardson, W. D. (2014). Motor skill learning requires active central myelination. *Science*, *346*(6207), 318-322. https://doi.org/10.1126/science.1254960

McLean, J. W., Wilson, J. A., Tian, T., Watson, J. A., VanHart, M., Bean, A. J., Scherer, S. S., Crossman, D. K., Ubogu, E., & Wilson, S. M. (2022). Disruption of Endosomal Sorting in Schwann Cells Leads to Defective Myelination and Endosomal Abnormalities Observed in Charcot-Marie-Tooth Disease. *The Journal of Neuroscience*, *42*(25), 5085-5101. https://doi.org/10.1523/jneurosci.2481-21.2022

Meraviglia, V., Ulivi, A. F., Boccazzi, M., Valenza, F., Fratangeli, A., Passafaro, M., Lecca, D., Stagni, F., Giacomini, A., Bartesaghi, R., Abbracchio, M. P., Ceruti, S., & Rosa, P. (2016). SNX27, a protein involved in down syndrome, regulates GPR17 trafficking and oligodendrocyte differentiation. *Glia*, *64*(8), 1437-1460. https://doi.org/10.1002/glia.23015

Mezydlo, A., Treiber, N., Ullrich Gavilanes, E. M., Eichenseer, K., Ancău, M., Wens, A., Ares Carral, C., Schifferer, M., Snaidero, N., Misgeld, T., & Kerschensteiner, M. (2023). Remyelination by surviving oligodendrocytes is inefficient in the inflamed mammalian cortex. *Neuron*, *111*(11), 1748-1759.e1748. https://doi.org/10.1016/j.neuron.2023.03.031

Miller, D. J., Duka, T., Stimpson, C. D., Schapiro, S. J., Baze, W. B., McArthur, M. J., Fobbs, A. J., Sousa, A. M. M., Šestan, N., Wildman, D. E., Lipovich, L., Kuzawa, C. W., Hof, P. R., & Sherwood, C. C. (2012). Prolonged myelination in human neocortical evolution. *Proceedings of the National Academy of Sciences*, *109*(41), 16480-16485. https://doi.org/10.1073/pnas.1117943109

Miller, E. M. (1994). Intelligence and brain myelination: A hypothesis. *Personality and Individual Differences*, *17*(6), 803-832. https://doi.org/10.1016/0191-8869(94)90049-3

Milo, R., & Kahana, E. (2010). Multiple sclerosis: Geoepidemiology, genetics and the environment. *Autoimmunity Reviews*, *9*(5), A387-A394. https://doi.org/10.1016/j.autrev.2009.11.010

Mitew, S., Hay, C. M., Peckham, H., Xiao, J., Koenning, M., & Emery, B. (2014). Mechanisms regulating the development of oligodendrocytes and central nervous system myelin. *Neuroscience*, *276*, 29-47. https://doi.org/10.1016/j.neuroscience.2013.11.029

Molina-Gonzalez, I., Miron, V. E., & Antel, J. P. (2022). Chronic oligodendrocyte injury in central nervous system pathologies. *Communications Biology*, *5*(1). https://doi.org/10.1038/s42003-022-04248-1

Monje, P. V. (2020). Schwann Cell Cultures: Biology, Technology and Therapeutics. *Cells*, *9*(8). https://doi.org/10.3390/cells9081848

Monk, K. R., Trevisiol, A., Kusch, K., Steyer, A. M., Gregor, I., Nardis, C., Winkler, U., Köhler, S., Restrepo, A., Möbius, W., Werner, H. B., Nave, K.-A., & Hirrlinger, J. (2020). Structural myelin defects are associated with low axonal ATP levels but rapid

recovery from energy deprivation in a mouse model of spastic paraplegia. *PLoS Biol*, *18*(11). https://doi.org/10.1371/journal.pbio.3000943

Moulson, A. J., Squair, J. W., Franklin, R. J. M., Tetzlaff, W., & Assinck, P. (2021). Diversity of Reactive Astrogliosis in CNS Pathology: Heterogeneity or Plasticity? In (Vol. 15): Frontiers Media S.A.

Mount, C. W., & Monje, M. (2017). Wrapped to Adapt: Experience-Dependent Myelination. *Neuron*, *95*(4), 743-756. https://doi.org/10.1016/j.neuron.2017.07.009

Murphy, G. M., Jr., Ellis, W. G., Lee, Y. L., Stultz, K. E., Shrivastava, R., Tinklenberg, J. R., & Eng, L. F. (1992). Astrocytic gliosis in the amygdala in Down's syndrome and Alzheimer's disease. *Prog Brain Res*, *94*, 475-483. http://www.ncbi.nlm.nih.gov/pubmed/1287731

Muzio, L., Viotti, A., & Martino, G. (2021). Microglia in Neuroinflammation and Neurodegeneration: From Understanding to Therapy. *Front Neurosci*, *15*. https://doi.org/10.3389/fnins.2021.742065

Naude, P. J., Dekker, A. D., Coppus, A. M., Vermeiren, Y., Eisel, U. L., van Duijn, C. M., Van Dam, D., & De Deyn, P. P. (2015). Serum NGAL is Associated with Distinct Plasma Amyloid-beta Peptides According to the Clinical Diagnosis of Dementia in Down Syndrome. *J Alzheimers Dis*, *45*(3), 733-743. https://doi.org/10.3233/JAD-142514

NCBI, N. C. f. B. I. (cited 2025 Apr 18). *Bethesda (MD): National Library of Medicine (US), National Center for Biotechnology Information, PubMed*. https://pubmed.ncbi.nlm.nih.gov/.

Neely, S. A., Williamson, J. M., Klingseisen, A., Zoupi, L., Early, J. J., Williams, A., & Lyons, D. A. (2022). New oligodendrocytes exhibit more abundant and accurate myelin regeneration than those that survive demyelination. *Nat Neurosci*, *25*(4), 415-420. https://doi.org/10.1038/s41593-021-01009-x

Nicaise, A. M., Johnson, K. M., Willis, C. M., Guzzo, R. M., & Crocker, S. J. (2018). TIMP-1 Promotes Oligodendrocyte Differentiation Through Receptor-Mediated Signaling. *Molecular Neurobiology*, *56*(5), 3380-3392. https://doi.org/10.1007/s12035-018-1310-7

Nicolay, D. J., Doucette, J. R., & Nazarali, A. J. (2007). Transcriptional control of oligodendrogenesis. *Glia*, *55*(13), 1287-1299. https://doi.org/10.1002/glia.20540

Nishiyama, A., Chang, A., & Trapp, B. D. (1999). NG2+ glial cells: a novel glial cell population in the adult brain. *J Neuropathol Exp Neurol*, *58*(11), 1113-1124. https://www.ncbi.nlm.nih.gov/pubmed/10560654

Nishiyama, A., Komitova, M., Suzuki, R., & Zhu, X. (2009). Polydendrocytes (NG2 cells): multifunctional cells with lineage plasticity. *Nat Rev Neurosci*, *10*(1), 9-22. https://doi.org/10.1038/nrn2495

Nishiyama, A., Lin, X. H., Giese, N., Heldin, C. H., & Stallcup, W. B. (1996). Co-localization of NG2 proteoglycan and PDGF α-receptor on O2A progenitor cells in the developing rat brain. *Journal of Neuroscience Research*, *43*(3), 299-314. https://doi.org/10.1002/(SICI)1097-4547(19960201)43:3<299::AID-JNR5>3.0.CO;2-E

Nishiyama, A., Watanabe, M., Yang, Z., & Bu, J. (2002). Identity, distribution, and development of polydendrocytes: NG2-expressing glial cells. *J Neurocytol*, *31*(6/7), 437-455. https://doi.org/10.1023/a:1025783412651

O'Brien, J. S. (1965). Stability of the Myelin Membrane. *Science*, *147*(3662), 1099-1107. https://doi.org/10.1126/science.147.3662.1099

Olmos-Serrano, J. L., Kang, H. J., Tyler, W. A., Silbereis, J. C., Cheng, F., Zhu, Y., Pletikos, M., Jankovic-Rapan, L., Cramer, N. P., Galdzicki, Z., Goodliffe, J., Peters, A., Sethares, C., Delalle, I., Golden, J. A., Haydar, T. F., & Sestan, N. (2016). Down Syndrome Developmental Brain Transcriptome Reveals Defective Oligodendrocyte Differentiation and Myelination. *Neuron*, *89*(6), 1208-1222. https://doi.org/10.1016/j.neuron.2016.01.042

Osorio, M. J., Mariani, J. N., Zou, L., Schanz, S. J., Heffernan, K., Cornwell, A., & Goldman, S. A. (2022). Glial progenitor cells of the adult human white and grey matter are contextually distinct. *Glia*, *71*(3), 524-540. https://doi.org/10.1002/glia.24291

Pantoni, L., Sarti, C., Alafuzoff, I., Jellinger, K., Munoz, D. G., Ogata, J., & Palumbo, V. (2006). Postmortem Examination of Vascular Lesions in Cognitive Impairment. *Stroke*, *37*(4), 1005-1009. https://doi.org/10.1161/01.STR.0000206445.97511.ae

Park, M. (2020). *Immunohistological detection of C21orf91 expression in the central nervous system and investigation of its potential function upon gene suppression in neural stem cells*

Pease-Raissi, S. E., & Chan, J. R. (2021). Building a (w)rapport between neurons and oligodendroglia: Reciprocal interactions underlying adaptive myelination. *Neuron*, *109*(8), 1258-1273. https://doi.org/10.1016/j.neuron.2021.02.003

Pérez-Cerdá, F., Sánchez-Gómez, M. V., & Matute, C. (2015). Pío del Río Hortega and the discovery of the oligodendrocytes. *Frontiers in Neuroanatomy*, *9*. https://doi.org/10.3389/fnana.2015.00092

Perlman, S. J., & Mar, S. (2012). Leukodystrophies. In *Neurodegenerative Diseases* (pp. 154-171). https://doi.org/10.1007/978-1-4614-0653-2_13

Petit, T. L., LeBoutillier, J. C., Alfano, D. P., & Becker, L. E. (1984). Synaptic development in the human fetus: a morphometric analysis of normal and Down's syndrome neocortex. *Exp Neurol*, *83*(1), 13-23. http://www.ncbi.nlm.nih.gov/pubmed/6228436

Pinter, J. D., Eliez, S., Schmitt, J. E., Capone, G. T., & Reiss, A. L. (2001). Neuroanatomy of Down's syndrome: a high-resolution MRI study. *Am J Psychiatry*, *158*(10), 1659-1665. https://doi.org/10.1176/appi.ajp.158.10.1659

Plemel, J. R., Keough, M. B., Duncan, G. J., Sparling, J. S., Yong, V. W., Stys, P. K., & Tetzlaff, W. (2014). Remyelination after spinal cord injury: Is it a target for repair? *Progress in Neurobiology*, *117*, 54-72. https://doi.org/10.1016/j.pneurobio.2014.02.006

Ponroy Bally, B., & Murai, K. K. (2021). Astrocytes in Down Syndrome Across the Lifespan. *Front Cell Neurosci*, *15*, 702685. https://doi.org/10.3389/fncel.2021.702685

Powell, D., Caban-Holt, A., Jicha, G., Robertson, W., Davis, R., Gold, B. T., Schmitt, F. A., & Head, E. (2014). Frontal white matter integrity in adults with Down syndrome with and without dementia. *Neurobiology of Aging*, *35*(7), 1562-1569. https://doi.org/10.1016/j.neurobiolaging.2014.01.137

Pringle, N., Collarini, E. J., Mosley, M. J., Heldin, C. H., Westermark, B., & Richardson, W. D. (1989). PDGF A chain homodimers drive proliferation of bipotential (O-2A) glial progenitor cells in the developing rat optic nerve. *The EMBO Journal*, *8*(4), 1049-1056. https://doi.org/10.1002/j.1460-2075.1989.tb03472.x

Prinz, M., & Priller, J. (2017). The role of peripheral immune cells in the CNS in steady state and disease. *Nat Neurosci*, *20*(2), 136-144. https://doi.org/10.1038/nn.4475

Purger, D., Gibson, E. M., & Monje, M. (2016). Myelin plasticity in the central nervous system. *Neuropharmacology*, *110*, 563-573. https://doi.org/10.1016/j.neuropharm.2015.08.001

Raff, M. C., Barres, B. A., Burne, J. F., Coles, H. S., Ishizaki, Y., & Jacobson, M. D. (1993). Programmed Cell Death and the Control of Cell Survival: Lessons from the Nervous System. *Science*, *262*(5134), 695-700. https://doi.org/10.1126/science.8235590

Raff, M. C., Miller, R. H., & Noble, M. (1983). A glial progenitor cell that develops in vitro into an astrocyte or an oligodendrocyte depending on culture medium. *Nature*, *303*(5916), 390-396. https://www.ncbi.nlm.nih.gov/pubmed/6304520

Redwine, J. M., & Evans, C. F. (2002). Markers of Central Nervous System Glia and Neurons In Vivo During Normal and Pathological Conditions. In *Protective and Pathological Immune Responses in the CNS* (pp. 119-140). https://doi.org/10.1007/978-3-662-09525-6_6

Reich, D. S., Longo, D. L., Lucchinetti, C. F., & Calabresi, P. A. (2018). Multiple Sclerosis. *New England Journal of Medicine*, *378*(2), 169-180. https://doi.org/10.1056/NEJMra1401483

Reiche, L. (2017). *C21orf91: a novel regulator of glial cell differentiation*

Reiche, L., Göttle, P., Lane, L., Duek, P., Park, M., Azim, K., Schutte, J., Manousi, A., Schira-Heinen, J., & Küry, P. (2021). C21orf91 Regulates Oligodendroglial Precursor Cell Fate-A Switch in the Glial Lineage? *Frontiers in Cellular Neuroscience*, *15*. https://doi.org/ARTN 65307510.3389/fncel.2021.653075

Reiche, L., Küry, P., & Göttle, P. (2019). Aberrant Oligodendrogenesis in Down Syndrome: Shift in Gliogenesis? *Cells*, *8*(12). https://doi.org/10.3390/cells8121591

Reiche, L., Stringer, C. A., Camey, K., Ziegler, B., Werner, L., Göttle, P., Head, E., Kremer, D., & Küry, P. (submitted). C21ORF91 overexpression leads to glial differentiation misbalance in Down syndrome to be rescued by remyelination drugs.

Risgaard, K. A., Sorci, I. A., Mohan, S., & Bhattacharyya, A. (2022). Meta-Analysis of Down Syndrome Cortical Development Reveals Underdeveloped State of the Science. *Frontiers in Cellular Neuroscience*, *16*. https://doi.org/10.3389/fncel.2022.915272

Rivera, F. J., Couillard-Despres, S., Pedre, X., Ploetz, S., Caioni, M., Lois, C., Bogdahn, U., & Aigner, L. (2009). Mesenchymal Stem Cells Instruct Oligodendrogenic Fate Decision on Adult Neural Stem Cells. *Stem Cells*, *24*(10), 2209-2219. https://doi.org/10.1634/stemcells.2005-0614

Rivers, L. E., Young, K. M., Rizzi, M., Jamen, F., Psachoulia, K., Wade, A., Kessaris, N., & Richardson, W. D. (2008). PDGFRA/NG2 glia generate myelinating oligodendrocytes and piriform projection neurons in adult mice. *Nat Neurosci*, *11*(12), 1392-1401. https://doi.org/10.1038/nn.2220

Roach, A., Takahashi, N., Pravtcheva, D., Ruddle, F., & Hood, L. (1985). Chromosomal mapping of mouse myelin basic protein gene and structure and transcription of the partially deleted gene in shiverer mutant mice. *Cell*, *42*(1), 149-155. https://doi.org/10.1016/s0092-8674(85)80110-0

Rosenbloom, A. B., Tarczynski, M., Lam, N., Kane, R. S., Bugaj, L. J., & Schaffer, D. V. (2020). beta-Catenin signaling dynamics regulate cell fate in differentiating neural stem cells. *Proc Natl Acad Sci U S A*, *117*(46), 28828-28837. https://doi.org/10.1073/pnas.2008509117

Rosenzweig, S., & Carmichael, S. T. (2015). The axon–glia unit in white matter stroke: Mechanisms of damage and recovery. *Brain Research*, *1623*, 123-134. https://doi.org/10.1016/j.brainres.2015.02.019

Rost, I., Fiegler, H., Fauth, C., Carr, P., Bettecken, T., Kraus, J., Meyer, C., Enders, A., Wirtz, A., Meitinger, T., Carter, N. P., & Speicher, M. R. (2004). Tetrasomy 21pter-->q21.2 in a male infant without typical Down's syndrome dysmorphic features but moderate mental retardation. *J Med Genet*, *41*(3), e26. http://www.ncbi.nlm.nih.gov/pubmed/14985397

Rowitch, D. H., & Kriegstein, A. R. (2010). Developmental genetics of vertebrate glial-cell specification. *Nature*, *468*(7321), 214-222. https://doi.org/10.1038/nature09611

Rupareliya, V. P., Singh, A. A., Butt, A. M., A, H., & Kumar, H. (2023). The “molecular soldiers” of the CNS: Astrocytes, a comprehensive review on their roles and molecular signatures. *European Journal of Pharmacology*, *959*. https://doi.org/10.1016/j.ejphar.2023.176048

Russo, M. L., Sousa, A. M. M., & Bhattacharyya, A. (2024). Consequences of trisomy 21 for brain development in Down syndrome. *Nature Reviews Neuroscience*, *25*(11), 740-755. https://doi.org/10.1038/s41583-024-00866-2

Saab, A. S., & Nave, K.-A. (2017). Myelin dynamics: protecting and shaping neuronal functions. *Current Opinion in Neurobiology*, *47*, 104-112. https://doi.org/10.1016/j.conb.2017.09.013

Saha, P., Sarkar, S., Paidi, R. K., & Biswas, S. C. (2020). TIMP-1: A key cytokine released from activated astrocytes protects neurons and ameliorates cognitive behaviours in a rodent model of Alzheimer’s disease. *Brain, Behavior, and Immunity*, *87*, 804-819. https://doi.org/10.1016/j.bbi.2020.03.014

Salzer, J., Feltri, M. L., & Jacob, C. (2024). Schwann Cell Development and Myelination. *Cold Spring Harbor Perspectives in Biology*, *16*(9). https://doi.org/10.1101/cshperspect.a041360

Sampaio-Baptista, C., & Johansen-Berg, H. (2017). White Matter Plasticity in the Adult Brain. *Neuron*, *96*(6), 1239-1251. https://doi.org/10.1016/j.neuron.2017.11.026

Samper Agrelo, I., Schira-Heinen, J., Beyer, F., Groh, J., Bütermann, C., Estrada, V., Poschmann, G., Bribian, A., Jadasz, J. J., Lopez-Mascaraque, L., Kremer, D., Martini, R., Müller, H. W., Hartung, H. P., Adjaye, J., Stühler, K., & Küry, P. (2020). Secretome Analysis of Mesenchymal Stem Cell Factors Fostering Oligodendroglial Differentiation of Neural Stem Cells In Vivo. *International Journal of Molecular Sciences*, *21*(12). https://doi.org/10.3390/ijms21124350

References

Santos, E. N., & Fields, R. D. (2021). Regulation of myelination by microglia. *Science Advances*, *7*(50). https://doi.org/10.1126/sciadv.abk1131

Scherer, S. S., & Arroyo, E. J. (2009). Myelin: Molecular Architecture of CNS and PNS Myelin Sheath. In *Encyclopedia of Neuroscience* (pp. 1169-1180). https://doi.org/10.1016/b978-008045046-9.01019-6

Schira-Heinen, J., Agrelo, I. S., Estrada, V., & Küry, P. (2022a). Functional in vivo assessment of stem cell-secreted pro-oligodendroglial factors. *Neural Regen Res*, *17*(10), 2194-2196. https://doi.org/10.4103/1673-5374.335800

Schira-Heinen, J., Wang, L., Akgün, S., Blum, S., Ziegler, B., Heinen, A., Hartung, H.-P., & Küry, P. (2022b). Modulation of Specific Sphingosine-1-Phosphate Receptors Augments a Repair Mediating Schwann Cell Phenotype. *International Journal of Molecular Sciences*, *23*(18). https://doi.org/10.3390/ijms231810311

Schütte, J. (2022). *Functional role of C21orf91 in myelinating glial cells of the nervous system*

Seeker, L. A., & Williams, A. (2021). Oligodendroglia heterogeneity in the human central nervous system. *Acta Neuropathologica*, *143*(2), 143-157. https://doi.org/10.1007/s00401-021-02390-4

Setoguchi, T., & Kondo, T. (2004). Nuclear export of OLIG2 in neural stem cells is essential for ciliary neurotrophic factor-induced astrocyte differentiation. *J Cell Biol*, *166*(7), 963-968. https://doi.org/10.1083/jcb.200404104

Shi, H., Hu, X., Leak, R. K., Shi, Y., An, C., Suenaga, J., Chen, J., & Gao, Y. (2015). Demyelination as a rational therapeutic target for ischemic or traumatic brain injury. *Experimental Neurology*, *272*, 17-25. https://doi.org/10.1016/j.expneurol.2015.03.017

Silva Oliveira Junior, M., Reiche, L., Daniele, E., Kortebi, I., Faiz, M., & Küry, P. (2024). Star power: harnessing the reactive astrocyte response to promote remyelination in multiple sclerosis. *Neural Regen Res*, *19*(3), 578-582. https://doi.org/10.4103/1673-5374.380879

Silva Oliveira Junior, M., Schira-Heinen, J., Reiche, L., Han, S., de Amorim, V. C. M., Lewen, I., Gruchot, J., Göttle, P., Akkermann, R., Azim, K., & Küry, P. (2022). Myelin repair is fostered by the corticosteroid medrysone specifically acting on astroglial subpopulations. *EBioMedicine*, *83*, 104204. https://doi.org/10.1016/j.ebiom.2022.104204

Simon, K., Hennen, S., Merten, N., Blattermann, S., Gillard, M., Kostenis, E., & Gomeza, J. (2016). The Orphan G Protein-coupled Receptor GPR17 Negatively Regulates Oligodendrocyte Differentiation via Galphai/o and Its Downstream Effector Molecules. *J Biol Chem*, *291*(2), 705-718. https://doi.org/10.1074/jbc.M115.683953

Simons, M., Gibson, E. M., & Nave, K. A. (2024). Oligodendrocytes: Myelination, Plasticity, and Axonal Support. *Cold Spring Harb Perspect Biol*, *16*(10). https://doi.org/10.1101/cshperspect.a041359

Slavotinek, A. M., Chen, X. N., Jackson, A., Gaunt, L., Campbell, A., Clayton-Smith, J., & Korenberg, J. R. (2000). Partial tetrasomy 21 in a male infant. *J Med Genet*, *37*(10), E30. http://www.ncbi.nlm.nih.gov/pubmed/11015462

Snaidero, N., & Simons, M. (2017). The logistics of myelin biogenesis in the central nervous system. *Glia*, *65*(7), 1021-1031. https://doi.org/10.1002/glia.23116

Sofroniew, M. V. (2020). Astrocyte Reactivity: Subtypes, States, and Functions in CNS Innate Immunity. *Trends Immunol*, *41*(9), 758-770. https://doi.org/10.1016/j.it.2020.07.004

Sowa, Y., Kishida, T., Tomita, K., Adachi, T., Numajiri, T., & Mazda, O. (2019). Involvement of PDGF-BB and IGF-1 in Activation of Human Schwann Cells by Platelet-Rich Plasma. *Plastic & Reconstructive Surgery*, *144*(6), 1025e-1036e. https://doi.org/10.1097/prs.0000000000006266

Sozmen, E. G., Rosenzweig, S., Llorente, I. L., DiTullio, D. J., Machnicki, M., Vinters, H. V., Havton, L. A., Giger, R. J., Hinman, J. D., & Carmichael, S. T. (2016). Nogo receptor blockade overcomes remyelination failure after white matter stroke and stimulates functional recovery in aged mice. *Proceedings of the National Academy of Sciences*, *113*(52). https://doi.org/10.1073/pnas.1615322113

Spaeth, G. L. (1966). Hydroxymethylprogesterone. An anti-inflammatory steroid without apparent effect on intraocular pressure. *Arch Ophthalmol*, *75*(6), 783-787. https://doi.org/10.1001/archopht.1966.00970050785014

Spitzer, S. O., Sitnikov, S., Kamen, Y., Evans, K. A., Kronenberg-Versteeg, D., Dietmann, S., de Faria, O., Agathou, S., & Káradóttir, R. T. (2019). Oligodendrocyte Progenitor Cells Become Regionally Diverse and Heterogeneous with Age. *Neuron*, *101*(3), 459-471.e455. https://doi.org/10.1016/j.neuron.2018.12.020

Stadelmann, C., Timmler, S., Barrantes-Freer, A., & Simons, M. (2019). Myelin in the central nervous system: Structure, function, and pathology. *Physiological Reviews*, *99*(3), 1381-1431. https://doi.org/10.1152/physrev.00031.2018

Stagni, F., & Bartesaghi, R. (2022). The Challenging Pathway of Treatment for Neurogenesis Impairment in Down Syndrome: Achievements and Perspectives. *Front Cell Neurosci*, *16*, 903729. https://doi.org/10.3389/fncel.2022.903729

Stagni, F., Giacomini, A., Emili, M., Guidi, S., & Bartesaghi, R. (2017). Neurogenesis impairment: An early developmental defect in Down syndrome. *Free Radic Biol Med*. https://doi.org/10.1016/j.freeradbiomed.2017.07.026

Stankoff, B., Aigrot, M.-S., Noël, F., Wattilliaux, A., Zalc, B., & Lubetzki, C. (2002). Ciliary Neurotrophic Factor (CNTF) Enhances Myelin Formation: A Novel Role for CNTF and CNTF-Related Molecules. *The Journal of Neuroscience*, *22*(21), 9221-9227. https://doi.org/10.1523/jneurosci.22-21-09221.2002

Stöckli, K. A., Lillien, L. E., Näher-Noé, M., Breitfeld, G., Hughes, R. A., Raff, M. C., Thoenen, H., & Sendtner, M. (1991). Regional distribution, developmental changes, and cellular localization of CNTF-mRNA and protein in the rat brain. *J Cell Biol*, *115*(2), 447-459. https://doi.org/10.1083/jcb.115.2.447

Sun, Y., Lehmbecker, A., Kalkuhl, A., Deschl, U., Sun, W., Rohn, K., Tzvetanova, I. D., Nave, K. A., Baumgartner, W., & Ulrich, R. (2015). STAT3 represents a molecular switch possibly inducing astroglial instead of oligodendroglial differentiation of oligodendroglial progenitor cells in Theiler's murine encephalomyelitis. *Neuropathol Appl Neurobiol*, *41*(3), 347-370. https://doi.org/10.1111/nan.12133

Takashima, S., & Becker, L. E. (1985). Basal ganglia calcification in Down's syndrome. *J Neurol Neurosurg Psychiatry*, *48*(1), 61-64. http://www.ncbi.nlm.nih.gov/pubmed/3156213

Takashima, S., Becker, L. E., Armstrong, D. L., & Chan, F. (1981). Abnormal neuronal development in the visual cortex of the human fetus and infant with down's syndrome. A quantitative and qualitative Golgi study. *Brain Res*, *225*(1), 1-21. http://www.ncbi.nlm.nih.gov/pubmed/6457667

Tanner, D. C., Cherry, J. D., & Mayer-Pröschel, M. (2011). Oligodendrocyte Progenitors Reversibly Exit the Cell Cycle and Give Rise to Astrocytes in Response to Interferon-γ [10.1523/JNEUROSCI.5905-10.2011]. *The Journal of Neuroscience*, *31*(16), 6235. http://www.jneurosci.org/content/31/16/6235.abstract

Tepavcevic, V., & Lubetzki, C. (2022). Oligodendrocyte progenitor cell recruitment and remyelination in multiple sclerosis: the more, the merrier? *Brain*, *145*(12), 4178-4192. https://doi.org/10.1093/brain/awac307

Tiane, A., Schepers, M., Rombaut, B., Hupperts, R., Prickaerts, J., Hellings, N., van den Hove, D., & Vanmierlo, T. (2019). From OPC to Oligodendrocyte: An Epigenetic Journey. *Cells*, *8*(10). https://doi.org/10.3390/cells8101236

Trapp, B. D., Andrews, S. B., Cootauco, C., & Quarles, R. (1989). The myelin-associated glycoprotein is enriched in multivesicular bodies and periaxonal membranes of actively myelinating oligodendrocytes. *J Cell Biol*, *109*(5), 2417-2426. https://doi.org/10.1083/jcb.109.5.2417

Trapp, B. D., Nishiyama, A., Cheng, D., & Macklin, W. (1997). Differentiation and Death of Premyelinating Oligodendrocytes in Developing Rodent Brain. *J Cell Biol*, *137*(2), 459-468. https://doi.org/10.1083/jcb.137.2.459

Tripathi, R. B., Rivers, L. E., Young, K. M., Jamen, F., & Richardson, W. D. (2010). NG2 Glia Generate New Oligodendrocytes But Few Astrocytes in a Murine Experimental Autoimmune Encephalomyelitis Model of Demyelinating Disease. *The Journal of Neuroscience*, *30*(48), 16383-16390. https://doi.org/10.1523/jneurosci.3411-10.2010

Tsai, H.-H., Niu, J., Munji, R., Davalos, D., Chang, J., Zhang, H., Tien, A.-C., Kuo, C. J., Chan, J. R., Daneman, R., & Fancy, S. P. J. (2016). Oligodendrocyte precursors migrate along vasculature in the developing nervous system. *Science*, *351*(6271), 379-384. https://doi.org/10.1126/science.aad3839

Valdés-Tovar, M., Rodríguez-Ramírez, A. M., Rodríguez-Cárdenas, L., Sotelo-Ramírez, C. E., Camarena, B., Sanabrais-Jiménez, M. A., Solís-Chagoyán, H., Argueta, J., & López-Riquelme, G. O. (2022). Insights into myelin dysfunction in schizophrenia and bipolar disorder. *World Journal of Psychiatry*, *12*(2), 264-285. https://doi.org/10.5498/wjp.v12.i2.264

Viganò, F., Möbius, W., Götz, M., & Dimou, L. (2013). Transplantation reveals regional differences in oligodendrocyte differentiation in the adult brain. *Nat Neurosci*, *16*(10), 1370-1372. https://doi.org/10.1038/nn.3503

Vlkolinsky, R., Cairns, N., Fountoulakis, M., & Lubec, G. (2001). Decreased brain levels of 2',3'-cyclic nucleotide-3'-phosphodiesterase in Down syndrome and Alzheimer's disease. *Neurobiology of Aging*, *22*(4), 547-553. http://www.ncbi.nlm.nih.gov/pubmed/11445254

von Bartheld, C. S., Bahney, J., & Herculano-Houzel, S. (2016). The search for true numbers of neurons and glial cells in the human brain: A review of 150 years of cell counting. *Journal of Comparative Neurology*, *524*(18), 3865-3895. https://doi.org/10.1002/cne.24040

Wagner, H. J., Munger, K. L., & Ascherio, A. (2004). Plasma viral load of Epstein–Barr virus and risk of multiple sclerosis. *European Journal of Neurology*, *11*(12), 833-834. https://doi.org/10.1111/j.1468-1331.2004.00871.x

Walton, C., King, R., Rechtman, L., Kaye, W., Leray, E., Marrie, R. A., Robertson, N., La Rocca, N., Uitdehaag, B., van der Mei, I., Wallin, M., Helme, A., Angood Napier, C., Rijke, N., & Baneke, P. (2020). Rising prevalence of multiple sclerosis worldwide: Insights from the Atlas of MS, third edition. *Multiple Sclerosis Journal*, *26*(14), 1816-1821. https://doi.org/10.1177/1352458520970841

Wang, F., Ren, S.-Y., Chen, J.-F., Liu, K., Li, R.-X., Li, Z.-F., Hu, B., Niu, J.-Q., Xiao, L., Chan, J. R., & Mei, F. (2020). Myelin degeneration and diminished myelin renewal contribute to age-related deficits in memory. *Nat Neurosci*, *23*(4), 481-486. https://doi.org/10.1038/s41593-020-0588-8

Wang, X., Zhao, Y., Zhang, X., Badie, H., Zhou, Y., Mu, Y., Loo, L. S., Cai, L., Thompson, R. C., Yang, B., Chen, Y., Johnson, P. F., Wu, C., Bu, G., Mobley, W. C., Zhang, D., Gage, F. H., Ranscht, B., Zhang, Y. W., . . . Xu, H. (2013). Loss of sorting nexin 27 contributes to excitatory synaptic dysfunction by modulating glutamate receptor recycling in Down's syndrome. *Nat Med*, *19*(4), 473-480. https://doi.org/10.1038/nm.3117

Weigel, M., Wang, L., & Fu, M. m. (2020). Microtubule organization and dynamics in oligodendrocytes, astrocytes, and microglia. *Developmental Neurobiology*, *81*(3), 310-320. https://doi.org/10.1002/dneu.22753

Weiner, J. A., Fukushima, N., Contos, J. J. A., Scherer, S. S., & Chun, J. (2001). Regulation of Schwann Cell Morphology and Adhesion by Receptor-Mediated Lysophosphatidic Acid Signaling. *The Journal of Neuroscience*, *21*(18), 7069-7078. https://doi.org/10.1523/jneurosci.21-18-07069.2001

Weitzdoerfer, R., Dierssen, M., Fountoulakis, M., & Lubec, G. (2001). Fetal life in Down syndrome starts with normal neuronal density but impaired dendritic spines and synaptosomal structure. *J Neural Transm Suppl*(61), 59-70. http://www.ncbi.nlm.nih.gov/pubmed/11771761

Werner, L., Gliem, M., Rychlik, N., Pavic, G., Reiche, L., Kirchhoff, F., Silva Oliveira Junior, M., Gruchot, J., Meuth, S. G., Küry, P., & Göttle, P. (2023). A Novel Ex Vivo Model to Study Therapeutic Treatments for Myelin Repair following Ischemic Damage. *Int J Mol Sci*, *24*(13). https://doi.org/10.3390/ijms241310972

Windrem, M. S., Nunes, M. C., Rashbaum, W. K., Schwartz, T. H., Goodman, R. A., McKhann, G., 2nd, Roy, N. S., & Goldman, S. A. (2004). Fetal and adult human oligodendrocyte progenitor cell isolates myelinate the congenitally dysmyelinated brain. *Nat Med*, *10*(1), 93-97. https://doi.org/10.1038/nm974

Wisniewski, K. E., & Schmidt-Sidor, B. (1989). Postnatal delay of myelin formation in brains from Down syndrome infants and children. *Clin Neuropathol*, *8*(2), 55-62. http://www.ncbi.nlm.nih.gov/pubmed/2524302

Wu, Y., Liu, Y., Levine, E. M., & Rao, M. S. (2003). Hes1 but not Hes5 regulates an astrocyte versus oligodendrocyte fate choice in glial restricted precursors. *Dev Dyn*, *226*(4), 675-689. https://doi.org/10.1002/dvdy.10278

References

Wu, Y. K., & Kengaku, M. (2018). Dynamic Interaction Between Microtubules and the Nucleus Regulates Nuclear Movement During Neuronal Migration. *J Exp Neurosci*, *12*, 1179069518789151. https://doi.org/10.1177/1179069518789151

Xiao, J., Yang, R., Biswas, S., Zhu, Y., Qin, X., Zhang, M., Zhai, L., Luo, Y., He, X., Mao, C., & Deng, W. (2017). Neural Stem Cell-Based Regenerative Approaches for the Treatment of Multiple Sclerosis. *Molecular Neurobiology*, *55*(4), 3152-3171. https://doi.org/10.1007/s12035-017-0566-7

Xu, R., Brawner, A. T., Li, S., Liu, J. J., Kim, H., Xue, H., Pang, Z. P., Kim, W. Y., Hart, R. P., Liu, Y., & Jiang, P. (2019). OLIG2 Drives Abnormal Neurodevelopmental Phenotypes in Human iPSC-Based Organoid and Chimeric Mouse Models of Down Syndrome. *Cell Stem Cell*, *24*(6), 908-926 e908. https://doi.org/10.1016/j.stem.2019.04.014

Xu, S., Lu, J., Shao, A., Zhang, J. H., & Zhang, J. (2020). Glial Cells: Role of the Immune Response in Ischemic Stroke. *Frontiers in Immunology*, *11*. https://doi.org/10.3389/fimmu.2020.00294

Xu, X.-M. (2009). Transplantation of Schwann Cells. In *Encyclopedia of Neuroscience* (pp. 4120-4124). https://doi.org/10.1007/978-3-540-29678-2_6096

Yamada, M., Iwase, M., Sasaki, B., & Suzuki, N. (2022). The molecular regulation of oligodendrocyte development and CNS myelination by ECM proteins. *Front Cell Dev Biol*, *10*. https://doi.org/10.3389/fcell.2022.952135

Yeung, M. S., Zdunek, S., Bergmann, O., Bernard, S., Salehpour, M., Alkass, K., Perl, S., Tisdale, J., Possnert, G., Brundin, L., Druid, H., & Frisen, J. (2014). Dynamics of oligodendrocyte generation and myelination in the human brain. *Cell*, *159*(4), 766-774. https://doi.org/10.1016/j.cell.2014.10.011

Yeung, M. S. Y., Djelloul, M., Steiner, E., Bernard, S., Salehpour, M., Possnert, G., Brundin, L., & Frisén, J. (2019). Dynamics of oligodendrocyte generation in multiple sclerosis. *Nature*, *566*(7745), 538-542. https://doi.org/10.1038/s41586-018-0842-3

Zawadzka, M., Rivers, L. E., Fancy, S. P. J., Zhao, C., Tripathi, R., Jamen, F., Young, K., Goncharevich, A., Pohl, H., Rizzi, M., Rowitch, D. H., Kessaris, N., Suter, U., Richardson, W. D., & Franklin, R. J. M. (2010). CNS-Resident Glial Progenitor/Stem Cells Produce Schwann Cells as well as Oligodendrocytes during Repair of CNS Demyelination. *Cell Stem Cell*, *6*(6), 578-590. https://doi.org/10.1016/j.stem.2010.04.002

Zdaniuk, G., Wierzba-Bobrowicz, T., Szpak, G. M., & Stepien, T. (2011). Astroglia disturbances during development of the central nervous system in fetuses with Down's syndrome. *Folia Neuropathol*, *49*(2), 109-114. https://www.ncbi.nlm.nih.gov/pubmed/21845539

Zhou, B., Zuo, Y. X., & Jiang, R. T. (2019). Astrocyte morphology: Diversity, plasticity, and role in neurological diseases. *CNS Neurosci Ther*, *25*(6), 665-673. https://doi.org/10.1111/cns.13123

Zhou, J., Zhuang, J., Li, J., Ooi, E., Bloom, J., Poon, C., Lax, D., Rosenbaum, D. M., & Barone, F. C. (2013). Long-Term Post-Stroke Changes Include Myelin Loss, Specific Deficits in Sensory and Motor Behaviors and Complex Cognitive Impairment Detected Using Active Place Avoidance. *PLoS One*, *8*(3). https://doi.org/10.1371/journal.pone.0057503

Zhou, Q., Wang, S., & Anderson, D. J. (2000). Identification of a Novel Family of Oligodendrocyte Lineage-Specific Basic Helix–Loop–Helix Transcription Factors. *Neuron*, *25*(2), 331-343. https://doi.org/10.1016/s0896-6273(00)80898-3

Zhou, Y., & Zhang, J. (2023). Neuronal activity and remyelination: new insights into the molecular mechanisms and therapeutic advancements. *Front Cell Dev Biol*, *11*. https://doi.org/10.3389/fcell.2023.1221890

Zhu, H., Hu, E., Guo, X., Yuan, Z., Jiang, H., Zhang, W., Tang, T., Wang, Y., & Li, T. (2024). Promoting remyelination in central nervous system diseases: Potentials and prospects of natural products and herbal medicine. *Pharmacological Research*, *210*. https://doi.org/10.1016/j.phrs.2024.107533

Zhu, X., Zuo, H., Maher, B. J., Serwanski, D. R., LoTurco, J. J., Lu, Q. R., & Nishiyama, A. (2012). Olig2-dependent developmental fate switch of NG2 cells. *Development*, *139*(13), 2299-2307. https://doi.org/10.1242/dev.078873

Zlomuzica, A., Plank, L., Kodzaga, I., & Dere, E. (2023). A fatal alliance: Glial connexins, myelin pathology and mental disorders. *Journal of Psychiatric Research*, *159*, 97-115. https://doi.org/10.1016/j.jpsychires.2023.01.008

6 Danksagung

Mein Dank richtet sich an alle, die Teil meiner Promotionszeit waren, mich stets für Wissenschaft und kritische Fragen begeistern konnten und letztendlich bei der Anfertigung dieser Thesis unterstütz und motiviert haben.

Besonderer Dank gilt hierbei natürlich Herrn Prof. Dr. Patrick Küry, meinem Doktorvater, der mir ermöglichte, dieses für mich faszinierende Forschungsthema und Herzensprojekt in seinem Team zu verfolgen. Patrick, danke, dass Du mich nie davon abgehalten hast über den Tellerrand hinauszublicken und mir zugetraut und mich ermutigt hast, mich in nahezu alle möglichen Forschungsschwerpunkte unserer Gruppe einzubringen. Ich freue mich auch weiterhin ohne Scheuklappen das große Ganze zu betrachten und bin Dir wohlgleich dankbar, dass Du mich an den nötigen Stellen auch bremsen konntest.

An dieser Stelle bedanke ich mich auch bei Frau Prof. Dr. Christine R. Rose, dass Sie Sich bereit erklärten meine Mentorin für dieses Doktorprojekt zu werden und das Gutachten dieser Dissertation übernehmen. Vielen Dank auch für die Gratisgetränke (Wertmarken) bei GLIA.

Natürlich gilt ein großer Dank der gesamten Forschungsgruppe, ob ehemalige Mitglieder oder noch das Zepter hochhaltend: ohne Euch wäre die Promotionszeit nicht die gewesen, die sie für mich war! Besonders Brigida Ziegler, Frank Bosse, Jessica Schira und Birgit Blomenkamp-Radermacher möchte ich an dieser Stelle erwähnen! Was ich von Euch gelernt habe und noch mit Euch teile, geht über das berufliche hinaus!

Besonderer Dank gilt auch dem ehemaligen Doktoranden-Team: PhD-Geschwister bis zum Ende und darüber hinaus! Ich bin unglaublich dankbar, dass aus unserer gemeinsamen Zeit so wunderbare Freundschaften gewachsen sind! Mögen wir bis ans Ende unserer Tage in alten und neuen Erinnerungen schwelgen. #GliaGang

Darüber hinaus gilt mein besonderer Dank allen meinen Freunden und Bekannten, die mich durch diese Zeit begleitet haben und immer zu mir standen – egal ob im engsten Kreis (meine 6 Ankersteine), im Laufe der Zeit eher in den Hintergrund gerückt (unsere Zeit wird wiederkommen) oder auf dem Weg verloren (man sieht sich immer zweimal im Leben): ich vergesse Euch nie und jeder Moment war/ist kostbar!

Meinen Dank Dir gegenüber, Michael, kann ich hier gar nicht in Worte fassen. Aber dafür haben wir zum Glück noch ein ganzes Leben gemeinsam vor uns, wo ich es versuchen kann!

Nicht zuletzt gebührt meinen Eltern, Katrin und Mario, der größte Dank. Ihr habt mir das Fundament gelegt, Mut zugesprochen, stets auf allen Ebenen unterstütz und immer an mich geglaubt. Danke, für Alles!

7 Eidesstattliche Erklärung

Ich, Laura Reiche, versichere an Eides Statt, dass die vorliegende Dissertation von mir selbständig und ohne unzulässige fremde Hilfe unter Beachtung der „Grundsätze zur Sicherung guter wissenschaftlicher Praxis an der Heinrich-Heine-Universität Düsseldorf“ erstellt worden ist. Die wörtlich oder inhaltlich entnommenen Stellen sowie Abbildungen aus anderen Werken wurden als solche kenntlich gemacht. Die Dissertation wurde weder vollständig noch in Teilen einer anderen Fakultät zur Erlangung eines akademischen Grades vorgelegt. Des Weiteren erkläre ich, dass ich keinen vorausgegangenen Promotionsversuch unternommen habe, und dass kein Promotionsversuch an einer anderen wissenschaftlichen Einrichtung läuft.

Ich bin mir bewusst, dass eine falsche Erklärung rechtliche Folgen haben wird.

Ort, Datum	Laura Reiche